

117 9/30

UC-1652

**LA-6030-C**

Conference Proceedings

CONF-750631--(abstr)

UC-34c

Issued: August 1975

**NOTICE**

PORIONS OF THIS REPORT AND INFORMATION It has been reproduced in this form to provide a copy to permit the broadest possible availability.

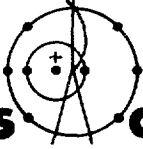
**Abstracts of  
Contributed Papers**

**Sixth International Conference on  
High-Energy Physics and  
Nuclear Structure**

**Santa Fe and Los Alamos, NM  
June 9-14, 1975**

Compiled by

- R. Mischke
- C. Hargrove
- C. Hoffman



**los alamos  
scientific laboratory**

**of the University of California**

**LOS ALAMOS, NEW MEXICO 87545**

An Affirmative Action/Equal Opportunity Employer

**MASTER**

UNITED STATES  
ENERGY RESEARCH AND DEVELOPMENT ADMINISTRATION  
CONTRACT W-7405-ENG. 36

DISTRIBUTION OF THIS DOCUMENT IS UNLIMITED

In the interest of prompt distribution, this report was not edited by the Technical Information staff.

Printed in the United States of America. Available from  
National Technical Information Service  
U.S. Department of Commerce  
5285 Port Royal Road  
Springfield, VA 22151  
Price: Printed Copy \$10.60 Microfiche \$2.25

This report was prepared as an account of work sponsored by the United States Government. Neither the United States nor the United States Energy Research and Development Administration, nor any of their employees, nor any of their contractors, subcontractors, or their employees, makes any warranty, express or implied, or assumes any legal liability or responsibility for the accuracy, completeness, or usefulness of any information, apparatus, product, or process disclosed, or represents that its use would not infringe privately owned rights.

NOTICE

This report was prepared as an account of work sponsored by the United States Government. Neither the United States nor the United States Energy Research and Development Administration, nor any of their employees, nor any of their contractors, subcontractors, or their employees, makes any warranty, express or implied, or assumes any legal liability or responsibility for the accuracy, completeness or usefulness of any information, apparatus, product or process disclosed, or represents that its use would not infringe privately owned rights.

The present conference is the sixth of a series of biannual conferences on High-Energy Physics and Nuclear Structure under the auspices of IUPAP. The preceding one occurred at Uppsala in 1973.

The conference was organized by an international advisory committee. As is detailed in the program, various other committees handled local arrangements. Proceedings of the sessions will be published by the AIP as one of their conference series.

This volume contains all abstracts submitted to the conference as of 1 May 1975. The abstracts are grouped according to subjects similar to those chosen for the sessions of contributed papers.

Financial support of the conference from the following organizations is gratefully acknowledged: International Union of Pure and Applied Physics, U. S. Energy Research and Development Administration, and the National Science Foundation.

The organizers thank H. Agnew for the Los Alamos Scientific Laboratory's essential support, and President Richard Weigle of St. John's for making available the facilities of the College.

Darragh E. Nagle  
Conference Secretary

8 May 1975  
Los Alamos, New Mexico

# TABLE OF CONTENTS

## I

### PION INTERACTIONS

#### I.A $\pi p$ and $\pi d$ Interactions

- .1 Corrections to the Glauber Model at Medium Energies in the Scattering off Two Potential Centres - M. Błeszyński and T. Jaroszewicz
- .2 Can One Recognize Resonance Poles from an Argand Diagram? -  
I. R. Afnan and A. W. Thomas
- .3 Relativistic 3-Body Calculation of  $\pi d$  Scattering - R. Aaron, E. J. Moniz and R. M. Woloshyn
- .4 Low Energy Pion Nucleon Scattering - P. Bertin, B. Coupat, J. Duclos, A. Gérard, D. Isabelle, A. Magnon, J. Miller, J. Morgens-  
stern, J. Picard, R. J. Powers and P. Vernin
- .5 The Elastic Scattering of Low Energy Pions on Protons - J. S. Frank,  
R. H. Heffner, K. A. Klare, R. E. Mischke, D. E. Nagle and D. C. Moir
- .6 The  $\pi^- d$  Breakup Reaction and  $\Delta$ 's in the Deuteron - R. Beurtey, C.  
Cvijanovich, J. C. Duchazeaubeneix, H. H. Duhm, J. C. Faivre, L.  
Goldzahl, J. C. Lugol, J. Saudinos, L. Dubal and C. F. Perdrisat
- .7 Incident-Energy Dependence of  $\pi^\pm$ -p Bremsstrahlung in the Region of  
the  $P_{33}(1232)$  Resonance - P. F. Glodis, H. C. Ballagh, R. P.  
Haddock, K. C. Leung, B. M. K. Nefkens, D. E. Smith, and D. I.  
Sober
- .8 An Experimental Study of the  $\pi^+ d \rightarrow p + p$  Reaction at Pion Energies of  
40, 50, and 60 MeV - B. M. Freedom, C. W. Darden, R. D. Edge, T.  
Marks, M. J. Saitmarsh, E. E. Gross, C. A. Ludemann, K. Gabethuler,

M. Blecher, K. Gotow, P. Y. Bertin, J. Alster, R. L. Burman, J. P. Perroud and R. P. Redwine

- .9 A Measurement of the Cross Section for the Reaction  $\pi^- + p \rightarrow \pi^+ + \pi^- + n$  at 350 and 300 MeV - C. A. Bordner, P. A. M. Gram, W. V. Hassenzahl, H. H. Howard, T. R. King, A. T. Oyer, G. A. Rebka and F. T. Shively
- .10 The Kroll-Ruderman Term in the OPE Contribution to the Electromagnetic Exchange Current - A. F. Yano and F. B. Yano

### I.B $\pi$ Nucleus Theory

- .1 The Effect of Fermi Motion on Inelastic Pion Nucleus Scattering - O. Nalcioglu and D. S. Koltun
- .2 Pion Charge-Exchange Reactions with Nuclei - G. A. Miller and J. E. Spencer
- .3 On the Optical Potential for Particle-Nucleus Scattering - A. N. Kamal
- .4 Single Charge Exchange Scattering  $^{13}\text{C}(\pi^+, \pi^0)^{13}\text{N}$  - L. C. Liu and V. Franco
- .5 Nuclear Matter Theory for Pion Scattering from Nuclei - H. A. Bethe and M. Johnson
- .6 New Estimate for Threshold Pion Production in Pion-Nucleus Collisions - R. Rockmore
- .7 First Order Optical Potential - D. J. Ernst, M. A. Nagarajan, R. M. Thaler and W. L. Wang
- .8 Correlation Expansion of the Optical Potential - D. J. Ernst, J. T. Londergan, G. A. Miller and R. M. Thaler
- .9 A Hole Line Expansion of the Pion-Nucleus Optical Potential - C. B. Dover and R. H. Lemmer

- 1.B .10 Resonances in Eikonal Models - J. R. Gillespie
- .11 Corrections to Glauber Theory in the Optical Limit - D. R. Harrington
- .12 Electric Form Factor and Three-Body Force in  ${}^3\text{H}$  and Nuclear Matter No. 4.130 - A. Kallio, P. Toropainen and C. Ciofi Degli Atti
- .13 Comparison of the Covariant and Non-Covariant Pion-Nucleus Optical Potentials - I. Celenza, L. C. Liu and C. M. Shakin
- .14 Is Levinson's Theorem a Node-Counting Device? - H. S. Picker
- .15 The Pion as a Probe for Studying Nuclear Structure - M. K. Gupta and G. E. Walker
- .16 Dependence of the Off-Energy-Shell T-Matrix on the Total Three-Momentum - L. Heller, G. E. Bohannon and F. Tabakin
- .17 The Effect of Short-ranged Unitary Transformations on the Rate of the Reaction  $\pi^-d \rightarrow \gamma nn$  - W. R. Gibbs, B. F. Gibson and G. J. Stephenson Jr.
- .18 Pion Charge-Exchange Scattering from Light Nuclei - W. R. Gibbs, B. F. Gibson, A. T. Hess, G. J. Stephenson, Jr. and W. B. Kaufmann
- .19 The A Dependence of the Pion-Nucleus Scattering Lengths - B. F. Gibson and C. K. Scott
- .20 On Pionic Degrees of Freedom in Nuclei - E. Vogt
- .21 Inelastic Two-Body Contributions to Pion Multiple Scattering - J. T. Londergan and E. J. Moniz
- .22 Glauber Type Representation for Nonlocal Potentials - B. S. Bhakar
- .23 Ambiguity in Pi-Nucleus Optical Potential - J. Haak, A. Lande, and F. Iachello
- .24 Pion-Nucleus Multiple Scattering and Nuclear  $\Delta$ -h States - M. Hirata, F. Lenz and K. Yazaki
- .25 A DWIA Calculation of the  ${}^{13}\text{C}(\pi^+, \pi^0) {}^{13}\text{N}(g.s)$  Cross Section - T-S. H. Lee, K. Kubodera and J. D. Vergados

- I.B .26 Pion Elastic and Charge Exchange Scattering on  $^3\text{He}$  - D. A. Sparrow
- .27 Pion Elastic Scattering from Aligned Targets - M. S. Iverson and E. Rost
- .28 Geometrical Indication of Dips in Diffraction Pattern - N. Nakamura, T. Kohmura and T. Negishi
- .29 Pion Scattering at Resonance Energies and Nuclear Correlations within Nuclei - T. Negishi and T. Kohmura
- .30 Pion Scattering from a Bound Nucleon - Y. Nogami and K. K. Bajaj
- .31 Serious Ambiguities in Inelastic Phase Shift Analysis - H. Burkhardt
- .32 Effective Isospin Potential in Nuclear Excitations - R. Leonardi
- .33 On the Interaction of Slow  $\pi$ -Mesons with Nuclei - G. G. Bunatian

I.C Intermediate Isobar Calculations

- .1 Calculation for the Reaction  $K^-d \rightarrow \pi^- \Lambda p$  with Two-Step Process - T. Ishihara, Y. Iwamura, Y. Takahashi and E. Satoh
- .2 The Role of  $\Delta_{33}$  - Isobars in Pion Condensation and Pion Scattering - G. E. Brown and W. Weise
- .3 The  $(p, \pi^-)$  Reaction and  $\Delta^{++}$  Components of Nuclei - L. S. Kisslinger and G. A. Miller
- .4 On the Excitation of the  $N^*(1236)$  in Nuclei - M. Dillig and M. G. Huber
- .5  $NN^*$  Admixtures in the Deuteron - E. Rost
- .6 Nuclear Modification of  $\pi$ -N Resonance - W. A. Friedman
- .7 Modification of the  $\Delta$ -Propagator in Nuclear Matter - F. Lenz, E. J. Moniz and K. Yazaki
- .8 Origin of the  $N^*(1200)$  Enhancement and the  $D^*$  Effect - R. Baldini-Celio, F. L. Fabbri, G. La Rosa and P. Picozza

## I.D $\pi$ -Nucleus Interactions

- .1 ( $\pi^\pm, {}^{12}\text{C}$ ) Backward Elastic Scattering at Intermediate Energies -  
F. Balestra, L. Busso, R. Garfagnini, G. Piragino, R. Barbini,  
C. Guaraldo, R. Scrimaglio and F. Cannata
- .2 ( $\pi^\pm, {}^{12}\text{C}$ ) Backward Inelastic Scattering at Intermediate Energies:  
Low Excited States - R. Barbini, C. Guaraldo, R. Scrimaglio,  
F. Balestra, L. Busso, R. Garfagnini and G. Piragino
- .3 ( $\pi^\pm, {}^{12}\text{C}$ ) Backward Inelastic Scattering at Intermediate Energies:  
Virtual States and Quasi-Free Scattering - R. Barbini, C. Guaraldo,  
R. Scrimaglio, F. Balestra, L. Busso, P. Garfagnini and G. Piragino
- .4 ( $\pi^+, {}^4\text{He}$ ) Inelastic Scattering at 110 MeV - F. Balestra, L. Busso,  
R. Garfagnini, G. Piragino, A. Zanini, R. Barbini, C. Guaraldo and  
R. Scrimaglio
- .5 ( $\pi^+, {}^4\text{He}$ ) Inelastic Scattering at 160 MeV - F. Balestra, L. Busso,  
R. Garfagnini, G. Piragino, A. Zanini, R. Barbini, C. Guaraldo and  
R. Scrimaglio
- .6 Measurements of  $\pi^\pm$  Nucleus Total Cross Sections at Energies Below  
200 MeV - G. Burleson, K. Johnson, J. Calarco, M. Cooper, D.  
Hagerman, H. Meyer, R. Redwine, I. Halpern, L. Knutson, R. Marrs,  
M. Jakobson and R. Jeppesen
- .7 The ( $\pi^+, \pi^0$ ) Reaction for Light Nuclei in the (3,3) Resonance Region  
- Y. Shamaï, J. Alster, E. D. Arthur, D. Ashery, S. Cochavi, D. M.  
Drake, M. A. Moinester and A. I. Yavin
- .8 The ( $\pi, d$ ) Reaction - R. A. Eisenstein and G. A. Miller
- .9 Forward Elastic Scattering Amplitudes for  $\pi^+$  from  ${}^{12}\text{C}$  and  ${}^{40}\text{Ca}$  -  
M. Warneke, L. Y. Lee, B. W. Mayes, E. V. Hungerford, J. C. Allred,  
N. Gabitzsch, J. Hudomalj-Gabitzsch, D. Mann, T. Witten, T.  
Williams, G. S. Mutchler and G. C. Phillips



- I.D .10 Alpha and Multinucleon Removal from  $^{58}\text{Ni}$  and  $^{60}\text{Ni}$  by Fast Pions -  
H. E. Jackson, D. G. Kovar, L. Meyer-Schützmeister, J. P. Schiffer,  
S. Vigdor, T. P. Wangler, R. E. Segel, R. L. Burman, P. A. M. Gram,  
D. M. Drake, R. B. Clark, B. C. Cook, V. G. Lind, E. N. Hatch,  
O. H. Otteson and R. E. McAdams
- .11 Systematics of Fast Pion Induced Processes in Complex Nuclei - R. E.  
Segel, H. E. Jackson, D. G. Kovar, L. Meyer-Schützmeister, S.  
Vigdor, T. P. Wangler, J. P. Schiffer, V. G. Lind, E. N. Hatch,  
O. H. Otteson, R. E. McAdams, R. L. Burman, P. A. M. Gram, D. M.  
Drake and B. C. Cook
- .12 Charged Pion Scattering on  $^4\text{He}$  Nuclei in the Energy Range from 68  
to 208 MeV - L. Alexandrov, T. Angelescu, I. V. Falomkin, M. M.  
Kulyukin, V. I. Lyashenko, R. Mach, A. Mihul, N. M. Kao, F.  
Nichitiu, G. B. Pontecorvo, V. K. Saricheva, M. Semergieva, Yu. A.  
Shcherbakov, N. I. Trosheva, T. M. Troshev, F. Balestra, L. Busso,  
R. Garfagnini and G. Piragino
- .13  $\pi^\pm$  Elastic Scattering on  $^3\text{He}$  Nuclei in the Energy Range from 68 to  
208 MeV - T. Angelescu, I. V. Falomkin, M. M. Kulyukin, V. I.  
Lyashenko, R. Mach, A. Mihul, N. M. Kao, F. Nichitiu, G. B. Ponte-  
corvo, V. K. Saricheva, M. Semergieva, Yu. A. Shcherbakov, N. I.  
Trosheva, T. M. Troshev, F. Balestra, L. Busso, R. Garfagnini and  
G. Piragino
- .14 Production of  $^{24}\text{Na}$  from the Irradiation of Phosphorus, Sulfur and  
Calcium by 70 - MeV  $\pi^\pm$  - N. Yanaki, D. Ashery, S. Cochavi and  
A. I. Yavin
- .15 The Reaction  $^{16}\text{O}(\pi^+, p)^{15}\text{O}$  at 70 MeV - D. Bachelier, J. L. Boyard,  
T. Hennino, J. C. Jourdain, P. Radvanyi and M. Roy-Stéphan

- I.D .16 Charged Particle Emission from Nuclei Bombarded with 235 MeV Pions and 800 MeV Protons - J. F. Amann, P. D. Barnes, M. Doss, S. A. Dytman, R. A. Eisenstein, J. A. Penkrot and A. C. Thompson
- .17 Elastic Scattering of 50 MeV  $\pi^+$  from  $^{12}\text{C}$  - J. F. Amann, P. D. Barnes, M. Doss, S. A. Dytman, R. A. Eisenstein, J. Penkrot, and A. C. Thompson
- .18 Recoil Momenta Distributions and  $\gamma$  Ray Yields from Pion Reactions with C, N, Na, S, and Ca - C. E. Stronach, C. M. Dennis, W. J. Kossler, H. O. Funsten, B. J. Lieb, W. F. Lankford and H. S. Plendl
- .19 Pion-Nucleus Total Cross Sections in the (3,3) Resonance Region - A. S. Carroll, I-H. Chiang, C. B. Dover, T. F. Kycia, K. K. Li, P. O. Mazur, D. N. Michael, P. M. Mockett, D. C. Rahm and R. Rubinstein
- .20  $\pi^-$ - $^4\text{He}$  Scattering Around the 3/2,3/2 Resonance - F. Binon, P. Duteil, M. Gouanère, L. Hugon, J. Jansen, J.-P. Lagnaux, H. Palevsky, J.-P. Peigneux, M. Spighele and J.-P. Stroot
- .21 Activation Studies of Pion-Induced Reactions on C, N, O, F, Al and Cu - G. W. Butler, B. J. Dropesky, A. E. Norris, C. J. Orth, R. A. Williams, G. Friedlander, G. D. Harp, J. Hudis, N. P. Jacob, Jr., S. S. Markowitz, S. Kaufman and M. A. Yates
- .22 The Elastic Scattering of Positive Pions by Carbon at 147 MeV - C. A. Bordner, P. A. M. Gram, W. V. Hassenzahl, H. H. Howard, T. R. King, A. T. Oyer, G. A. Rebka, and F. T. Shively
- .23 Single Proton Emission from  $\pi^-$  Absorption at Rest in Light Nuclei - B. Coupat, P. Y. Bertin, D. B. Isabelle, G. Kawadry, P. Vernin, A. Gérard, J. Miller, J. Morgenstern, J. Picard and B. Saghai

- I.D .24 The 1s and 1p Shells of Light Nuclei Studied in (p,d) at 185 MeV  
- B. Fagerström, J. Källne, O. Sundberg and G. Tibell
- .25 Fission of Heavy Nuclei Induced by Stopped Negative Pions - Yu. A. Batusov, D. Chultem, Dz. Ganzorig and O. Otgonsuren

## II

### STOPPING MUONS

- II .1 Coulomb Capture and X-Ray Cascades of Muons in Metal Halides -  
A. Brandao d'Oliveira, H. Daniel and T. von Egidy
- .2 Recent Experimental Results of the Mesic Chemistry Program at  
LAMPF - J. D. Knight, C. J. Orth, M. E. Schillaci, R. A. Naumann,  
H. Daniel, K. Springer and H. B. Knowles
- .3 Asymmetry and Energy Spectrum of High Energy Neutrons Emitted in  
Polarized Muon Capture - K. Kume, N. Ohtsuka, H. Ohtsubo and M.  
Morita
- .4 Muonic X-Ray Series in Metallic Al, Fe and In - R. Bergmann, H.  
Daniel, T. von Egidy, F. J. Hartmann, H.-J. Pfeiffer and K.  
Springer
- .5 Atomic Capture of Negative Mesons; the Fuzzy Fermi-Teller Model -  
M. Leon and J. Miller
- .6 The  $\alpha^2(Z\alpha)^2$  Contribution of Vacuum Polarization to Level Shifts in  
High Z Muonic Atoms - M. K. Sundaresan and P. J. S. Watson
- .7 E2(E1) Parity Mixing in Muonic Atoms - L. M. Simons
- .8 Effects of Non-Statistical Hyperfine Populations in Muon Capture  
by Polarized Nuclei - N. C. Mukhopadhyay and L. Hambro

- II
- .9 Migdal's Quasiparticle Approach and Its Implications of Allowed Muon Capture Strength in  $^{12}\text{C}$  - J. D. Immele and N. C. Mukhopadhyay
  - .10 Quantum Electrodynamics Tests with Muonic Atoms - C. K. Hargrove, E. P. Hincks, H. Mes, R. J. McKee, M. S. Dixit, A. L. Carter, D. Kessler, J. S. Wadden and H. L. Anderson
  - .11 Partial Muon Capture Rates in  $^{12}\text{C}$  - V. Devanathan, P. R. Subramanian, R. D. Graves and H. Überall
  - .12 Charge Parameters, Isotope Shifts, Quadrupole Moments, and Nuclear Excitation in Muonic  $^{170,171,172,173,174,176}\text{Yb}$  - A. Zehnder, F. Boehm, W. Dey, R. Engfer, H. K. Walter and J. L. Vuilleumier
  - .13 Muon Capture in Atoms, Crystals and Molecules - P. Vogel, P. K. Haff, V. Akylas and A. Winther
  - .14 Muonic x-Ray Studies in Sm - R. J. Powers, P. Barreau, B. Bihoreau, J. Miller, J. Morgenstern, J. Picard, L. Roussel and P. Bertin
  - .15 Negative Muon Spin Rotation at Oxygen Site in Paramagnetic MnO - S. Nagamiya, K. Nagamine, O. Hashimoto and T. Yamazaki
  - .16 Lifetimes of Negative Muons Bound to Actinide Nuclei - O. Hashimoto, S. Nagamiya, K. Nagamine and T. Yamazaki
  - .17 Strange Depolarization of Negative Muon in Transition Metals - K. Nagamine, S. Nagamiya, O. Hashimoto, S. Kobayashi and T. Yamazaki
  - .18 Probing the Giant Moment in a Dilute PdFe Alloy by Positive Muons at Very Low Temperatures - K. Nagamine, S. Nagamiya, O. Hashimoto, N. Nishida and T. Yamazaki
  - .19 Hyperfine Field on Positive Muon in Nickel in the Temperature Range of 0.12-300 K - K. Nagamine, S. Nagamiya, O. Hashimoto, T. Yamazaki and B. D. Patterson
  - .20 Statistical Theory of Muon Capture I - Y. Kohyama and A. Fujii

- II .21 Statistical Theory of Muon Capture II - Y. Kohyama and A. Fujii
- .22 Muonium Chemistry in the Gas Phase - D. G. Fleming, J. H. Brewer,  
D. M. Garner, A. E. Pifer, T. Bowen, D. Delise and K. M. Crowe
- .23 Nuclear Structure Studies in Heavy Deformed Nuclei Using Muonic  
Atoms - D. A. Close, J. J. Malanify and J. P. Davidson
- .24 An Investigation of Chemical Effects on Negative Muon Capture -  
L. F. Mausner, R. A. Naumann, J. A. Monard and S. N. Kaplan
- .25 Precision Measurement of Ground State Muonium Hyperfine Structure  
Interval  $\Delta\nu$  - D. E. Casperson, T. W. Crane, V. W. Hughes, P. A.  
Souder, R. D. Stambaugh, P. A. Thompson, H. F. Kaspar, H-W. Reist,  
H. Orth, G. zu Putlitz and A. B. Denison
- .26 High-Order Vacuum Polarization in Exotic Atoms - G. A. Rinker, Jr.  
and L. Wilets
- .27 Muonic X-Ray Measurements of Nuclear Charge Radii in the Mass-60  
Region - E. B. Shera, E. T. Ritter, R. B. Perkins, L. K. Wagner,  
H. D. Wohlfahrt, G. Fricke and R. M. Steffen
- .28 Deformed Hartree-Fock Description of the Fe, Ni, and Zn Isotopes -  
G. A. Rinker, Jr. and J. W. Negele
- .29 Microscopic Calculations of Isotopic Shifts in Deformed Nuclei -  
D. Zawischa and J. Speth
- .30 Muonium and Free-Muon Precession Components in Noble Gases at Low  
Pressure - A. E. Pifer, T. Bowen, D. A. Delise, J. H. Brewer and  
D. G. Fleming
- .31 Shape Isomer Excitation by Mu-Minus Capture - S. N. Kaplan, J. A.  
Monard and S. Nagamiya
- .32 Precise Muonic X-Ray Energies and the Vacuum Polarization - G.  
Backenstoss, H. Koch, A. Nilsson and L. Tauscher

- II .33 Observation of the Larmor Precession of the Muonic Helium Atom,  
 $\alpha\mu^-e^-$  - P. A. Souder, D. E. Casperson, T. W. Crane, V. W. Hughes,  
 D. C. Lu, M. H. Yam, H. Orth, G. zu Putlitz and H-W. Reist
- .34 Emission of the Auger Electrons in  $\mu$ -Mesic Atoms and Escape of  
 Charged Particles in  $\mu$ -Meson Capture by Light (C,N,O) and Heavy  
 (Ag, Br) Nuclei - Yu. A. Batusov, S. A. Bunyatov, L. Vizireva,  
 G. R. Gulkanyan, F. Mirsalikhova, V. M. Sidorov and Kh. Chernev
- .35 Search for Radiation Transitions from the Mesic Molecular  
 States - K. Andert, V. S. Evseev, H. G. Ortlepp, V. S. Roganov,  
 B. M. Sabirov, H. Haupt, H. Schneuwly and R. Engfer
- .36 Dependence of Muonic X-Ray Spectral Structure Upon Atomic Valency  
 - K. Andert, V. S. Evseev, H-G. Ortlepp, V. S. Roganov, B. M.  
 Sabirov, H. Haupt, H. Schneuwly and R. Engfer
- .37 Study of the Reaction  $\mu^-^{12}\text{C} \rightarrow {}^4\text{He} \quad {}^4\text{He} \quad {}^3\text{H} \quad n\nu$  - Yu. A. Batusov, S. A.  
 Bunyatov, L. Vizireva, G. R. Gulkanyan, F. Mirsalikhova, V. M.  
 Sidorov, Kh. Chernev, R. A. Eramzhyan
- .38 Negative Muon Depolarization in Hydroxides and Acids - V. I.  
 Goldansky, V. S. Evseev, T. N. Mamedov, Yu. V. Obukhov, V. S.  
 Roganov, M. V. Frontasyeva and N. I. Kholodov
- .39 Negative Muon Depolarization in the Benzene and Carbon Tetra-  
 chloride Mixtures - V. I. Goldansky, V. S. Evseev, T. N. Mamedov,  
 Yu. V. Obukhov, V. S. Roganov, M. V. Frontasyeva and N. I. Kholodov
- .40 Shifted Electronic X-Rays from Muonic Heavy Atoms - W. D. Fromm,  
 Dz. Gansorig, T. Krogulski, H. G. Ortlepp, S. M. Polikanov, B. M.  
 Sabirov, U. Schmidt and R. Arlt
- .41 Studies of Muonium Interactions in Monocrystalline Germanium - V. G.  
 Firsov, G. G. Myasishceva, Yu. V. Obukhov, V. S. Roganov

- II .42 Investigation of Atomic Capture of Muons and Structure of Muonic X-Ray Series in Magnesium Oxides - V. N. Pokrovsky, L. I. Ponomarev, V. G. Zinov and I. A. Yutlandov
- .43 Calculation of Quasi-Stationary State Characteristics of Hydrogen Mesic Molecules - L. I. Ponomarev, I. V. Puzyrin, and T. P. Puzyrina
- .44 The Polarization Measurement of Stopped Muons by Hanle Signals - A. Possoz, L. Grenacs, J. Lehmann, D. Meda, L. Palfy, J. Julien and C. Samour

### III

#### EXOTIC ATOMS AND CONDENSED NUCLEAR STATES

- III .1 Mesonic Polarizabilities - F. Cannata
- .2 The Lorentz-Lorenz Correction in Pionic Atoms and Pion Condensates - G. Baym and G. E. Brown
- .3 Negative Pion Capture by  ${}^4\text{He}$  - K. Kubodera
- .4 Pion Capture in  ${}^3\text{H}$  and  ${}^3\text{He}$  - A. C. Phillips and F. Roig
- .5 Nuclear Resonances in Hadronic Atoms - M. Leon
- .6  $\alpha$ -Particle Emission Following  $\pi^-$  Capture in  ${}^{12}\text{C}$  - K. O. H. Ziock, J. Comiso, T. Meyer and F. Schlepuetz
- .7 Kaon Absorption and Alpha Cluster - H. Nishimura and A. Arima
- .8 An Optical Model Analysis and the Effect of L·S Force Due to Strong Interactions in  $\bar{p}$ -Atoms - H. Nishimura and T. Fujita
- .9 Panofsky Ratio in  ${}^3\text{He}$  - M. Mizuta, Y. Kohyama and A. Fujii
- .10 Comparison of Pion-Induced Nuclear Reactions with Spallation Reactions - H. Ullrich, H. D. Engelhardt and C. W. Lewis

- III .11 Nuclear  $\gamma$ -Rays from Kaons Stopped in  $^{27}\text{Al}$  - C. J. Batty, S. F. Biagi, R. A. J. Riddle, A. Roberts, B. L. Roberts, D. H. Worledge, N. Berovic, G. J. Pyle, G. T. A. Squier, A. S. Clough, P. Coddington and R. E. Hawkins
- .12 Strong Interaction Effects in Kaonic Atoms - C. J. Batty, S. F. Biagi, R. A. J. Riddle, A. Roberts, B. L. Roberts, D. H. Worledge, N. Berovic, G. J. Pyle, G. T. A. Squier, A. S. Clough, P. Coddington and R. E. Hawkins
- .13 Quadrupole Hyperfine Structure Effects in Exotic Atoms - C. J. Batty, S. F. Biagi, R. A. J. Riddle, A. Roberts, B. L. Roberts, D. H. Worledge, N. Berovic, G. J. Pyle, G. T. A. Squier, A. S. Clough, P. Coddington and R. E. Hawkins
- .14 Photon Spectrum in Pion Capture on Tritium - H. W. Baer, J. A. Bistirlich, S. Cooper, K. M. Crowe, J. P. Perroud, R. H. Sherman, F. T. Shively and P. Truöl
- .15 Studies of Strong Interaction Effects in Antiprotonic Atoms - C. Cox, M. Eckhause, J. Kane, M. Rushton, W. Vulcan, R. Welsh, J. Miller, R. Powers, P. Barnes, R. Eisenstein, R. Sutton, W. Lam, D. Jenkins, T. King, R. Kunselman and P. Roberson
- .16 Fundamental Properties of  $K^-$ ,  $\bar{p}$  and  $\Sigma^-$  from Exotic Atoms - G. Dugan, Y. Asano, M. Y. Chen, S. Cheng, E. Hu, L. Lidofsky, W. Patton, C. S. Wu, V. Hughes and D. Lu
- .17 Nuclear Spectroscopic Quadrupole Moments from Muonic and Pionic Atoms - W. Dey, P. Ebersold, B. Aas, R. Eichler, H. J. Leisi, W. W. Sapp and F. Scheck
- .18 Observation of Nuclear Rotational Spectra in Pion Capture on  $^{175}\text{Lu}$  and  $^{165}\text{Ho}$  - P. Ebersold, B. Aas, W. Dey, R. Eichler, H. J. Leisi, W. W. Sapp and H. K. Walter



- III .19 Isotopic Effects in Antiprotonic Atoms - H. Koch, G. Backenstoss, P. Blüm, W. Fetscher, R. Hagedberg, A. Nilsson, P. Pavlopoulos, H. Poth, I. Sick, L. Simons and L. Tauscher
- .20 The  $K^-$  Nucleus Optical Potential - S. Y. Lee
- .21 The Study of the Relative Change of the Charge by Hydrogene Atoms in Transition Metal Hydrides - M. F. Kost, V. I. Mikheeva, L. N. Panurets, A. A. Chertkov, Z. V. Krumshtein, V. I. Petrukhin, V. M. Suvorov and I. Yutlandov
- .22 The Study of Negative Pion Transfer in  $C_m H_n + Z$  Mixtures - V. M. Bystritsky, V. A. Vasiljev, I. Galm, V. I. Petrukhin, V. E. Risin, V. M. Suvorov and B. A. Khomenko
- .23 The Study of the Negative Pion Transfer to Carbon in Organic Molecules - V. I. Petrukhin, V. V. Risin, I. F. Samenkova and V. M. Suvorov
- .24 Negative Pion Capture by Heavy Nuclei - S. R. Avramov, V. S. Butsev, D. Chultem, Yu. K. Gavrilov, Dz. Ganzorig and S. M. Polikanov
- .25 Radiative Pion Capture by  ${}^6\text{Li}$  - R. A. Sakaev and R. A. Eramzhyan
- .26 Experimental Search for Condensed Nuclear States - S. Frankel, W. Frati, O. Van Dyck, R. Werbeck and V. Highland
- .27 Instability of Neutron Star Matter for Pion Condensation - Y. Futami, Y. Takahashi and A. Suzuki
- .28 On Abnormal Nuclear Matter - E. Nyman and M. Rho

## IV

### NUCLEON INTERACTIONS

#### IV.A Nucleon-Nucleus Interactions

- .1 P-D Elastic Scattering at Large Angle - H. Tezuka and M. Yamazaki
- .2 Non-Eikonal Corrections to the Glauber Model and Proton-He<sup>4</sup> Scattering at 1 GeV - M. Błeszyński and T. Jaroszewicz
- .3 On the Modified Kerman, McManus, and Thaler Optical Potential and Its Applicability to the Scattering from Light Nuclei - M. Błeszyński and T. Jaroszewicz
- .4 Two-Component Model of High-Energy Hadron Scattering from Nuclei - R. Dymarz, A. Małecki and P. Picchi
- .5 Test of 1 GeV NN Matrix on Elastic Scattering Glauber Model Calculation - I. Brissaud, L. Bimbot, Y. LeBornec, B. Tatischeff and N. Willis
- .6 Proton Production in Nuclei by 600 MeV Protons - H. D. Orr, III, R. D. Edge and T. A. Filippas
- .7 Nuclear Induced Bremsstrahlung G. L. Strobel and K. C. Lam
- .8 The Individual Nucleons and Their Clustering in <sup>6</sup>Li as Probed in (p,d) and (p,2p) Reactions - J. Källne
- .9 Pion Production Through the Reaction d(p,dπ<sup>+</sup>)n at 600 MeV - E. V. Hungerford, J. C. Allred, K. Koester, L. Y. Lee, B. W. Mayes, T. Witten, J. Hudomalj-Gabitzsch, N. Gabitzsch, T. M. Williams, J. Clement, G. S. Mutchler and G. C. Phillips
- .10 Quasi-Elastic Deuteron Production - A. P. Sathe and E. A. Ressler
- .11 Elastic Scattering of 0.72 GeV Protons from <sup>4</sup>He for  $0.15 \text{ GeV}^2/c^2 \leq -t \leq 0.55 \text{ GeV}^2/c^2$  - J. C. Fong, G. J. Igo, S. L. Verbeck,

C. A. Whitten, Jr., D. L. Hendrie, V. Perez-Mendez, Y. Therrien  
and G. W. Hoffman

- IV.A .12 p -  $^3\text{He}$  Elastic Scattering at Intermediate Energies and the NN  
Interaction - R. Frascaria, N. Marty, V. Comparat, M. Morlet, A.  
Willis, D. Legrand, D. Garreta, R. Beurtey, G. Bruge, P. Couvert,  
H. Catz, A. Chaumeaux, J. C. Faivre, Y. Terrien and R. Bertini
- .13 Measurement of the Neutron Flux Generated by the LAMPF 800 MeV  
Proton Beam Stop - D. G. Perry
- .14 Scattering of Protons on Helium Between 348 and 1154 MeV - E.  
Aslanides, T. Bauer, R. Bertini, R. Beurtey, A. Boudard, F.  
Brochard, G. Bruge, A. Chaumeaux, H. Catz, J. M. Fontaine, R.  
Frascaria, P. Gorodetzky, J. Guyot, F. Hibou, M. Matoba, Y.  
Terrien and J. Thirion
- .15 1 GeV-Proton Scattering from  $^{40}\text{Ca}$ ,  $^{42}\text{Ca}$ ,  $^{44}\text{Ca}$ ,  $^{48}\text{Ca}$  and  $^{48}\text{Ti}$  -  
G. Alkhazov, T. Bauer, R. Beurtey, A. Boudard, G. Bruge, A.  
Chaumeaux, P. Couvert, G. Cvijanovich, H. H. Duhm, J. M. Fontaine,  
D. Garreta, A. Kulikov, D. Legrand, J. C. Lugol, J. Saudinos,  
J. Thirion and A. Vorobyov
- .16 PWBA (p,d) Calculations at Intermediate Beam Energies - D. G.  
Fleming, J. W. Grabowski and E. W. Vogt
- .17 Glauber Calculations for p- $^4\text{He}$  Elastic Scattering - J. P. Auger,  
J. R. Gillespie and R. J. Lombard
- .18 Effects of Antisymmetrization in Elastic Scattering of High-  
Energy Protons from Nuclei - A. Majewski and P. Picchi
- .19 Investigation of Pion and Kaon Production on Nuclei - M. Dillig  
and M. G. Huber
- .20  $\text{K}^+$  and  $\pi^+$  Momentum Spectra at  $0^\circ$  from 2.5-3.1 GeV/c Protons - T.  
Bowen, D. A. DeLise, and A. E. Pifer

- IV.A .21 Search for Spectral Peaks from  $(p, K^+)$  and  $(p, \pi^+)$  Reactions - T. Bowen, D. A. DeLise and A. E. Pifer
- .22 Characteristics of Low Z Fragments Produced in the Interaction of 800-MeV Protons with Uranium - G. W. Butler, D. G. Perry, A. M. Poskanzer, J. B. Natowitz and F. Plasil
- .23 Elastic and Inelastic Scattering of 1 GeV Protons by Nuclei - E. Boridy and H. Feshbach
- .24 Calculation of the Reaction  $pd \leftrightarrow {}^3\text{He} \gamma$  at Intermediate Energies - H. W. Fearing
- .25 High-Energy Proton-Nucleus Scattering and Correlations - R. D. Viollier
- .26 The Clinton P. Anderson Meson Physics Facility Radioisotope Program - H. A. O'Brien, Jr., A. E. Ogard, P. M. Grant, J. W. Barnes and B. R. Erdal
- .27 Proton-Nucleus Scattering at Intermediate Energies - G. A. Miller and J. E. Spencer
- .28 Analysis of  $\sim 1$  GeV Proton-Scattering on D and He in a Non-Eikonal Approach - A. S. Rinat, S. A. Gurvitz and Y. Alexander
- .29 Low Energy Scattering from a Complex Target - A. Deloff
- .30 Asymmetry Measurement of Quasi-Elastic Scattering of Polarized 637 MeV Protons by  ${}^{12}\text{C}$  and  ${}^6\text{Li}$  Nuclei - V. S. Nadezhdin, N. I. Petrov and V. I. Satarov
- .31 Large Angle  $pd$  Scattering, the D Form Factor and the Isobar Content of the D - S. A. Gurvitz and A. S. Rinat

#### IV.B Nuclear Structure and Hypernuclei

- .1 Momentum-Cutoff Sensitivity in Faddeev Calculations of Trinucleon Properties - R. A. Brandenburg, Y. E. Kim and A. Tubis
- .2 Lifetime of Nuclear Hole States Caused by Phonon-Hole Coupling - G. J. Wagner, P. Doll, K. T. Knöpfle and G. Mairle
- .3 Self-Consistent Hypernuclei with the Skyrme Interaction - M. Rayet
- .4 On the Production of Hypernuclei in Strangeness-Exchange Reactions - G. C. Bonazzola, T. Bressani, E. Chiavassa, G. Dellacasa, A. Fainberg, M. Gallio, N. Mirfakhrai, A. Musso and G. Rinaudo
- .5 On a Possibility to Research Hypernuclear Properties in the  $K^+$  - Meson Electroproduction Reactions - V. N. Fetisov and M. I. Kozlov
- .6 Hypercharge Exchange Reactions on Nuclei - W. Brückner, M. A. Faessler, K. Kilian, U. Lynen, B. Pietrzyk, B. Povh, H. G. Ritter, B. Schürlein, H. Schröder and A. H. Walenta
- .7 The Investigation of the  $\gamma$ -Transitions in Light Hypernuclei - M. Bedjidian, A. Filipkowski, I. Y. Grossiord, A. Guichard, M. Gusakow, S. Majewski, H. Piekarz, J. Piekarz and J. R. Pizzi

#### IV.C Nucleon Nucleon Interactions

- .1 Neutron-Proton Bremsstrahlung - G. E. Bohannon, L. Heller and R. H. Thompson
- .2 Three Body Break Up of the Deuteron by 800 MeV Protons - T. R. Witten, T. M. Williams, M. Furić, D. B. Mann, J. Hudomalj-Gabitzsch, N. D. Gabitzsch, G. S. Mutchler, J. M. Clement, R. D. Felder, G. C. Phillips, B. W. Mayes, E. V. Hungerford, L. Y. Lee, M. Warneke and J. C. Allred

- IV.C .3 Pion Production in the  ${}^1\text{H}(p,\pi^+p)n$  Reaction at  $E_p \approx 800$  MeV -  
 J. Hudomalj-Gabitzsch, T. Witten, N. D. Gabitzsch, G. S. Mutchler,  
 T. Williams, J. Clement, G. C. Phillips, E. Hungerford, L. Y. Lee,  
 M. Warneke, B. W. Mayes and J. C. Allred
- .4 Study of the Reaction  $pp \rightarrow \pi d$  at 398, 455 and 572 MeV - D. Aebischer,  
 B. Favier, G. Greeniaus, R. Hess, A. Junod, C. Lechanoine, J.-C.  
 Niklès, D. Rapin and D. W. Werren
- .5 Meson Theoretical Description of the Short-Range Repulsion in the  
 Nucleon-Nucleon Interaction - G. E. Brown, J. Durso and A. D.  
 Jackson
- .6 np Total Cross Section Between 50 and 150 MeV - D. M. Asbury, A. S.  
 Clough, J. A. Edgington, R. C. Brown, Y. Onel, U. von Wimmersperg,  
 I. M. Blair and N. M. Stewart
- .7 Neutron Production at  $0^\circ$  from the Reaction  $pp \rightarrow np\pi^+$  at Medium  
 Energies - G. Glass, M. E. Evans, M. Jain, R. A. Kenefick, L. C.  
 Northcliffe, C. G. Cassapakis, C. W. Bjork, P. J. Riley, B. E.  
 Bonner and J. E. Simmons
- .8 (n,p), (n,d), and (n,t) Reactions on  ${}^9\text{Be}$  and  ${}^{12}\text{C}$  at 800 MeV - P.  
 Riley, C. Bjork, C. Newsom, R. Kenefick, M. Evans, G. Glass, J.  
 Hiebert, M. Jain, L. C. Northcliffe, B. Bonner, J. Simmons, N.  
 Stein and C. Cassapakis
- .9 Measurements and Analysis with a One Pion Exchange Model of the  
 $np \rightarrow pX$  Inclusive Reaction Between 1.4 and 1.9 GeV/c and Differential  
 Cross Section Measurements of the  $np \rightarrow p\Delta_{33}^0$  Reaction - G. Bizard,  
 F. Bonthonneau, J. L. Laville, F. Lefebvres, J. C. Malherbe,  
 R. Regimbart, J. Duflo and F. Plouin

- IV.C .10 Absolute Differential Cross Section Measurements for Proton-Proton Elastic Scattering at 647 and 800 MeV - H. B. Willard, P. R. Bevington, R. J. Barrett, B. D. Anderson, F. Cverna, H. W. Baer, A. N. Anderson, H. Willmes and N. Jarmie
- .11 Proton-Proton Bremsstrahlung in the Inelastic Region - B. M. K. Nefkens, O. R. Sander and D. I. Sober
- .12 A Model of the  $pp \rightarrow pn\pi^+$  Reaction at 764 MeV - W. R. Gibbs, B. F. Gibson and G. J. Stephenson, Jr.
- .13 Small Angle Scattering of Hadrons by Deuterium and Extraction of Hadron-Neutron Amplitudes - G. K. Varma and V. Franco
- .14 Quasifree  $NN \rightarrow d\pi$  as Seen in the  $nd \rightarrow dN\pi$  Reaction - R. R. Silbar
- .15 Energy and Angular Distribution of Neutrons Produced by 800 MeV Proton-Proton Collisions - J. Pratt, R. Bentley, H. Bryant, R. Carlini, C. Cassapakis, B. Dieterle, C. Leavitt, T. Rupp and D. Wolfe
- .16 An Exact Treatment of  $\sigma$ -Meson Decay Effects in the Exchange Contribution to Nuclear Forces - E. L. Lomon
- .17 Polarization Effects in Pd Backward Scattering - B. Z. Kopeliovich and I. K. Potashnikova
- .18 Charge Form Factors of Nuclei in the Alpha-Cluster Model - E. V. Inopin, V. S. Kinchakov, V. K. Lukyanov and Yu. S. Pol'!
- .19 One-Boson-Exchange Relativistic Amplitudes as Quantum Mechanical Potentials in Lobachevsky Space - N. B. Skachkov
- .20 A Cascade-Exciton Marriage Model - K. K. Gudima and V. D. Toneev
- .21 On the Role of Nucleon-Nucleon Resonant Forces in the  $nd$ -Interaction - V. N. Efimov and E. G. Tkachenko

- .22 Pion Production from Nuclei Bombarded by Protons of 1, 2, and 3 BeV - R. D. Edge, D. H. Tompkins and J. W. Glenn
- .23 Pion Production at Threshold Induced by 154 MeV Protons - Y. Le Bornec, B. Tatischeff, L. Bimbot, I. Brissaud, H. D. Holmgren, J. Källne, F. Reide and N. Willis
- .24 First Results of  $(p, \pi^+)$  Reactions at 600 MeV - T. Bauer, R. Beurtey, A. Boudard, G. Bruge, A. Chaumeaux, P. Couvert, H. H. Duhm, D. Garreta, M. Matoba, Y. Terrien, L. Bimbot, Y. Le Bornec, B. Tatischeff, E. Aslanides, R. Bertini, F. Brochard, P. Gorodetzky and F. Hibou

V

ELECTROMAGNETIC AND WEAK INTERACTIONS

V.A e- and  $\gamma$ -Nucleus Interactions

- .1 Correlations and Binding Energy Sum Rules - A. E. L. Dieperink and T. de Forest, Jr.
- .2 Electron Scattering from  $\text{Sm}^{144,148,150}$  - N. Haik, J. Alster, S. Cochavi, M. A. Moinester, J. B. Bellicard, P. Leconte, Phan-Xuan-Ho and S. Turck
- .3 Rescattering Effects in the  $\gamma + D \rightarrow p + p + \pi^-$  Reaction - J. M. Laget and I. Blomqvist
- .4 The  $D(\gamma, p\pi^-)$  and the  ${}^4\text{He}(\gamma, p\pi^-)$  Reactions for High Values of the Recoil Momentum - P. E. Argan, G. Audit, N. de Botton, J. L. Faure, J. M. Laget, J. Martin, C. Schuhl and G. Tamas
- .5  ${}^{16}\text{O}$  Form Factors Interpreted by the Generalized Helm Model - B. A. Lamers, R. D. Graves and H. Überall



- V.A .6 Pion Photoproduction and Radiative Pion Capture in Flight from  $^{16}\text{O}$   
 - A. Nagl and H. Uberall
- .7 Experimental Study of Single Charged Pion Photoproduction from  
 Complex Nuclei - K. Baba, I. Endo, M. Fujisaki, S. Kadota, Y. Sumi,  
 H. Fujii, Y. Murata, S. Noguchi and A. Murakami
- .8 Threshold Pion Photoproduction from  $^{12}\text{C}$  - A. Nagl and H. Uberall
- .9 The  $^{11}\text{B}(\gamma, \pi^-)^{11}\text{C}$  Reaction Near Threshold - E. J. Winhold, L. J.  
 McVay, K. Min, P. Pella, D. Rowley, P. Stoler, S. Trentalange,  
 P. F. Yergin, K. S. R. Sastry and W. Turchinetz
- .10 Measurement of Electron-Deuteron Scattering at Large Momentum  
 Transfer - R. G. Arnold
- .11 The Neutron Charge Form Factor and Electrodisintegration of Triton  
 - B. A. Craver and Y. E. Kim
- .12 Electroexcitation of  $J^\pi = 6^+$  States in  $^{50}\text{Cr}$  and  $^{52}\text{Cr}$  - J. B.  
 Bellicard, B. Frois, M. Huet, Ph. Leconte, A. Nakada, Phan Xuan  
 Ho, S. Turck, P. deWitt Huberts and J. W. Lightbody, Jr.
- .13 Extraction of Nuclear Form Factor from  $(e, e')$  Cross Section -  
 H. C. Lee and F. C. Khanna
- .14 Nuclear Transition Form Factor and Transition Density in Inelastic  
 Electron Scattering - H. C. Lee and F. C. Khanna
- .15 Pion Photoproduction in  $\text{C}^{12}$  Just Above Threshold - A. M. Bernstein,  
 N. Paras, W. Turchinetz, E. C. Booth and B. Chasan
- .16 Renormalization of the Pion Photoproduction Hamiltonian in Nuclei  
 - J. Delorme, M. Ericson and G. Faldt
- .17 Angular Momentum Transfer in the  $\text{Au}^{197}(\gamma, \pi^-)\text{Hg}^{197}$  Reaction - H. A.  
 Medicus and R. Smalley

- V.A .18  ${}^3\text{He}(\gamma, 2p)n$  - B. F. Gibson and D. R. Lehman
- .19 Hole Strength and Momentum Distributions from  $(e, e'p)$  Reactions  
- M. Bernheim, A. Bussière, A. Gillebert, J. Mougey, M. Priou,  
D. Royer, I. Sick and G. J. Wagner
- .20 Helium Charge Form Factors at Large Momentum Transfer - B. T.  
Chertok
- .21 High Momentum Transfer e-D Scattering as a Probe of the Relativistic  
Structure of the Deuteron - C. Carlson and F. Gross
- .22 Connection of Muon Capture at Large Energy Transfer to Pion  
Absorption - J. Bernabeu, T. E. O. Ericson and C. Jarlskog
- .23 The  ${}^{16}\text{O}(\gamma, p){}^{15}\text{N}$  Reaction for  $E_\gamma = 40 - 200$  MeV - J. L. Matthews,  
W. Bertozzi, M. J. Leitch, C. P. Sargent, W. Turchinets, D. J. S.  
Findlay and R. O. Owens
- .24 A Measurement of the Longitudinal and Transverse  $\pi^+$  Electroproduction  
Cross Section - G. Bardin, J. Duclos, A. Magnon, B. Michel and  
J. C. Montret
- .25  $\alpha$ -Clustering Effects in the Photodisintegration of  ${}^{197}\text{Au}$  at  
Intermediate Energies - J-O Adler, G. Andersson and H-Å Gustafsson
- .26 The New Mesons as Members of a Nonet - K. Just
- .27 Electro- and Photoproduction of  $\pi^+$  on  ${}^{27}\text{Al}$  - I. Blomqvist, P.  
Janevek, G. G. Jonsson, H. Dinter and K. Tesch
- .28 Knock-Out Mechanisms in  $(\gamma, \text{Nucleon})$  Reactions at Intermediate  
Energies - J-O Adler, G. G. Jonsson and K. Lindgren
- .29 Analysis of Charge Density Variations in Nuclei - V. V. Burov,  
V. K. Lukyanov and Yu. S. Pol'

V.B Weak Interactions

- .1 A Study of Background for Neutrino Electron Elastic Scattering at LAMPF - H. H. Chen and J. F. Lathrop
- .2 A Statistical Theory of  $\hat{C}\hat{P}$  Violation - H. J. Kreuzer and C. G. Kuper
- .3 Asymmetry of Beta-Ray Angular Distribution in Polarized Nuclei and G-Parity Nonconservation - M. Morita and H. Ohtsubo
- .4 Parity-Nonconservation and the Photon Circular Polarization in  $n + p \rightarrow d + \gamma$  - B. A. Craver, E. Fischbach, Y. E. Kim and A. Tubis
- .5 Neutrino Absorption in  $^{16}\text{O}$  - J. B. Langworthy, B. A. Lamers and H. Überall
- .6 Beta-Decay Asymmetries in Polarized  $^{12}\text{B}$  and  $^{12}\text{N}$ , and the G-Parity Nonconserving Weak Interaction - K. Sugimoto, I. Tanihata and J. Göring
- .7 Tests for Neutrino Helicity-Flip in Elastic  $\nu_{\mu}$ -p and  $\nu_{\mu}$ -e Scattering - E. Fischbach, J. T. Gruenwald, S. P. Rosen, H. Spivack and B. Kayser
- .8 Charge Asymmetry by Isotensor Currents - S. Furui
- .9 Energy Dependence of Beta-Ray Asymmetries and Second Class Current - H. Ohtsubo, K. Kubodera and Y. Horikawa
- .10 Parity Violating Asymmetry in  $n+p \rightarrow d+\gamma$  and the Isospin Structure of the  $\Delta S = 0$  Nonleptonic Weak Interactions - B. A. Craver, Y. E. Kim, A. Tubis, P. Herczeg and P. Singer
- .11 Pionic Effects in the Weak Axial Current for Nuclei - J. Delorme, M. Ericson, A. Figureau and C. Thevenet
- .12 Determination of the Axial-Vector Form Factor in the Radiative Decay of the Pion - A. Stetz, J. Carroll, D. Ortendahl, V. Perez-Mendez, G. Igo, N. Chirapatpimol and M. A. Nasser

- V.B .13 Double  $\beta$ -Decay Nuclear ME for  $^{48}\text{Ca}$ ,  $^{130}\text{Te}$  and  $^{128}\text{Te}$  - J. D. Vergados
- .14 Nonconservation of Muon Number and CP Noninvariance - S. Barshay
- .15 Radiative Decay  $\pi^+ \rightarrow e^+ \nu_e \gamma$  - F. Scheck and A. Wulschlegler
- .16 Electron Polarization in Polarized Muon Decay, Radiative Corrections - W. E. Fischer and F. Scheck
- .17 Search for Second Class Currents in the  $\beta$ -Decay of A=12 Isobars - M. Steels, L. Grenacs, J. Lehmann, L. Palfy and A. Possoz

## VI

### HIGH ENERGY AND HEAVY IONS

#### VI.A High Energy Collisions

- .1 In-Elastic Interactions of 69 GeV/c Protons with Emulsion Nucleons - O. E. Badawy, A. A. El-Naghy, A. Hussein, N. Mettwali and M. I. Sherif
- .2 Coherent Production of Particles by 69 GeV/c Protons in Nuclear Emulsion - O. E. Badawy, A. A. El-Naghy, A. Hussein, N. Mettwali and M. I. Sherif
- .3 Nuclear Interactions of 200 and 300 GeV Protons in Emulsion - Collaboration Barcelona, Batavia, Belgrade, Bucharest, Lund, Montreal, Nancy, Ottawa, Paris, Rome, Strasbourg and Valencia
- .4 A Phenomenological Model for High Energy Proton-Nucleus Interactions - B. Andersson and I. Otterlund
- .5 Search for Ultra-High Momentum Transfer Scattering of Protons by Nuclei - L. M. Lederman and L. E. Price

- VI.A .6 Charged and Neutral Pion Production in  $\pi^-$ Ne Collisions at 200 GeV/c  
- J. S. Loos, J. R. Elliott, L. R. Fortney, A. T. Goshaw, J. W. Lamsa, W. J. Robertson, W. D. Walker and W. M. Yeager
- .7 A Study of 10.5 GeV/c  $\pi^+$  and  $\pi^-$  with Neon Nuclei - W. D. Walker, J. R. Elliott, L. R. Fortney, A. T. Goshaw, J. W. Lamsa, J. S. Loos, W. J. Robertson, W. M. Yeager, C. R. Sun and S. Dhar
- .8 p -  $^4\text{He}$  Elastic Scattering at 24 GeV/c - J. Berthot, G. Douhet, J. Gardès, L. Méritet, M. Querrou, A. Têtefort, F. Vazeille, J. P. Burq, M. Chemarin, M. Chevallier, B. Ille, M. Lambert, J. P. Marin, J. P. Gerber and C. Voltolini
- .9 Two-step Analysis of Nuclear Coherent  $3\pi$  Production in the  $J^P=0^-$  State - P. Osland
- .10 Finite Energy Corrections and Multiplicity Fluctuations in Gottfried's Model of Hadron Nucleus Interactions - B. Andersson
- .11 Excitation of the 15.1 MeV Level of Carbon by BeV Protons and Pions - D. Scipione, W. Mehlhop, O. Piccioni, P. Bowles, P. Caldwell, J. Sebek, R. Garland, B. Babcock, I. Kostoulas
- .12 Stripping and Dissociation of 6 BeV Deuterons and Tagged Neutron Beams - P. Bowles, C. Leemann, W. Mehlhop, H. Grunder, O. Piccioni, R. Thomas, D. Scipione, R. Garland and J. Sebek
- .13 Search for Delayed High Energy Radiation from Pb Target Irradiated by 45 GeV Protons - G. D. Alexeev, A. M. Zaitsev, N. A. Kalinina, V. V. Kruglov, V. N. Kuznetsov, A. V. Kulikov, A. V. Kuptsov, L. L. Nemenov, B. M. Pontecorvo, D. M. Khazins and I. N. Churin

## VI.B Heavy Ions

- .1 Inelastic Interactions of 17 GeV/c  $\alpha$  Particles with Nuclei -  
Collaboration Dubna, Moscow, Leningrad, Koshice, Tashkent and  
Warsaw
- .2 Analysis of Quasi-Elastic Knockout of Alpha Particles from  $^{16}\text{O}$  and  
 $^{28}\text{Si}$  by 0.65 and 0.85 GeV Alpha Particles - N. Chirapatpimol, J. C.  
Fong, M. M. Gazzaly, G. J. Igo, A. D. Liberman, S. L. Verbeck,  
C. A. Whitten, J. Arvieux, V. Perez-Mendez, M. Matoba, N. Chant  
and P. Roos
- .3  $^{16}\text{O}$ -Emulsion Nucleus Interactions at 0.15-0.2 and 2 GeV/n - B.  
Jakobsson, K. Kristiansson, R. Kullberg, B. Lindkvist and I.  
Otterlund
- .4 Pion Production in Nucleus-Nucleus Collisions - L. S. Schroeder
- .5 Multiple-Diffraction Expansion for Intermediate-Energy Reactions  
C. W. Wong and S. K. Young
- .6  $(\alpha, \alpha')$  Scattering on  $^{12}\text{C}$  at 1.37 GeV - T. Bauer, R. Bertini,  
A. Boudard, G. Bruge, H. Catz, A. Chaumeaux, H. Duhm, J. M.  
Fontaine, D. Garetta, V. Layly, J. G. Lugol and R. Schaeffer
- .7 Heavy Ion Collisions at ISR Energies: Possibilities for Experi-  
mental Study - H. G. Pugh
- .8 Observation of Double Spectator Process in the D + D Reaction -  
B. Th. Leemann, H. G. Pugh, N. S. Chant and C. C. Chang
- .9 Fragmentation of Relativistic Nuclei - B. Cork
- .10  $^6\text{Li}(\alpha, 2\alpha)$  at 700 MeV and the  $\alpha$ -d Momentum Distribution - W.  
Dollhopf, C. F. Perdrisat, P. Kitching and W. C. Olsen
- .11 Fragmentation of Relativistic Heavy Ions - H. Feshbach
- .12 Effects of the Coulomb Field on the Scattering of Hadrons and Heavy  
Ions by Nuclei - G. K. Varma and V. Franco

- VI.B .13 Deuteron Break-up on Proton at 2.95 GeV/c - J. Banaigs, J. Berger, L. Goldzahl, L. Vu-Hai, M. Cottureau, C. Le Brun, F. L. Fabbri and P. Picozza
- .14  ${}^3\text{He}$  Production from 6.9 GeV/c  ${}^4\text{He}$  Break up on Hydrogen Target - J. Berger, J. Duflo, L. Goldzahl, J. Oostens, F. Plouin, M. Van den Bossche, L. Vu Hai, G. Bizard, C. Le Brun, F. L. Fabbri, P. Picozza and L. Satta
- .15 Preliminary Study of  $\text{He}^4+p \rightarrow {}^3\text{He}+d$  at 4.0 GeV/c - J. Berger, J. Duflo, L. Goldzahl, F. Plouin, J. Oostens, M. Van den Bossche, L. Vu Hai, G. Bizard, C. Le Brun, F. L. Fabbri, P. Picozza and L. Satta
- .16 Alpha-Proton Elastic Scattering in the Forward Hemisphere in the Momentum Range from 4.0 to 6.9 GeV/c - J. Berger, J. Duflo, L. Goldzahl, F. Plouin, J. Oostens, M. Van den Bossche, L. Vu Hai, G. Bizard, C. Le Brun, F. L. Fabbri, P. Picozza and L. Satta
- .17 Alpha-Proton Elastic Scattering in the Backward Hemisphere in the Momentum Range from 3.2 to 5.08 GeV/c - J. Berger, J. Duflo, L. Goldzahl, J. Oostens, F. Plouin, M. Van den Bossche, L. Vu Hai, G. Bizard, C. Le Brun, F. L. Fabbri, P. Picozza and L. Satta
- .18 Alpha-Proton Interaction at 4 GeV/c - F. L. Fabbri, P. Picozza, L. Satta, J. Berger, J. Duflo, L. Goldzahl, F. Plouin, J. Oostens, M. Van den Bossche, L. Vu Hai, G. Bizard and C. Le Brun
- .19 Shock Waves in Colliding Nuclei - P. J. Siemens, J. P. Bondorf, M. I. Sobel and H. A. Bethe
- .20 Propagation of "Heat" in Nuclear Matter (N.M.) - R. Weiner and M. Weström

- VI.B .21 On the High-Momentum Tail of the Spectator Nucleon - B. S. Aladashvili, V. V. Glagolev, R. M. Lebedev, M. S. Nioradze, I. S. Saitov, V. N. Streltsov, B. Badelek, G. Odyniec, A. Sandacz, T. Siemiarczuk, J. Stepaniak and P. Zieliński
- .22 On a Fragmentation Mechanism of Relativistic Heavy Ions - V. K. Lukyanov and A. I. Titov

## VII

### INSTRUMENTATION

- VII .1 The Status of SC2 - B. W. Allardyce and E. G. Michaelis
- .2 The Omicron Spectrometer at SC2 - Collaboration Turin, Oxford, Amsterdam, Birmingham and CERN
- .3 Status of the SIN High Resolution Pion Spectrometer (SUSI) - Collaboration ETH, Grenoble, Heidelberg, Karlsruhe, Neuchatel and SIN
- .4 Double Arm Spectrometer System for Measuring Electron-Deuteron Elastic Scattering - F. Martin
- .5 A High Stopping Density  $\mu^+$  Beam - A. E. Pifer, T. Bowen and K. R. Kendall
- .6 Coincidence Experiments at Intermediate Energies - J. E. Spencer and H. A. Thiessen
- .7 Nuclear Scattering Applied to Radioscopy - J. Saudinos, G. Charpak, F. Sauli, D. Townsend and J. Vinciarelli
- .8 Timing with Plastic Scintillator Detectors - C. Cernigoi, N. Grion, G. Pauli and M. Russi



## VIII

### LATE ABSTRACTS

- VIII .1 Yields of 25 GeV/c  $K^-$  -Mesons, Antiprotons and Antideuterons from the Interactions of 70 GeV Protons with Nuclei - B. Yu. Baldin, G. Chemnitz, Ya. V. Grishkevich, B. A. Khomenko, N. N. Khovansky, Z. V. Krumshstein, V. G. Lapshin, R. Leiste, Yu P. Merekov, V. I. Petrukhin, D. Pose, A. I. Ronzhin, V. I. Rykalin, I. F. Samenkova, J. Schuler, G. A. Shelkov, V. I. Solianik, V. M. Suvorov, M. Szawlowsky, L. S. Vertogradov, N. K. Vishnevsky
- .2 The Momentum Characteristics of Secondary Particles from the Interactions of 50 GeV/c  $\pi^-$  -Meson with Nuclei, Irradiated Under a Strong Magnetic Field - A. A. El-Naghy, R. Khoshmukhamedov, J. Salomov, K. D. Tolstov, G. S. Shabratova, S. A. Azimov, R. A. Bondarenko, K. G. Gulyamov, V. I. Petrov, T. P. Trofimova, L. P. Tchernova, G. M. Tchernov
- .3 On the Total Binding Energy of Spherical Nuclei - F. A. Gareev, G. M. Vagradov
- .4 Decay Characteristics of the States of Giant Dipole Resonance on Isotopes  $^{58}\text{Ni}$  and  $^{60}\text{Ni}$  - B. S. Ishkhanov, I. M. Kapitonov, V. G. Shevchenko, V. V. Varlamov
- .5 Excited States of Virtual Clusters in Nucleus and Quasi-Elastic Knock-Out of Clusters at High Energies - N. F. Golovanova, I. M. H'in, V. G. Neudatchin, Yu. F. Smirnov, Yu. M. Tchuvil'sky
- .6 Effective Namiltonian and Angular Correlations in Radiative Pion Capture - G. Ya. Korenman and V. P. Popov
- .7 To the Theory of Quasielastic Knock-Out of Nuclear Clusters - V. V. Balashov and V. N. Mileev

- VIII .8 Two-Step Mechanism of the Nuclear Excitation in Coherent Particle Production - V. V. Balashov, V. I. Korotkikh, and V. N. Mileev
- .9 Propagation of Unstable Hadronic System Through Nuclear Matter in Coherent Production Processes - V. I. Korotkikh
- .10 A Study of the Isobar (I236) Production in the Reaction  $\pi^- + d \rightarrow p + \Delta^-$  ( $\Delta^-$  - backward) from 1,03 to 1,68 GeV/c. - B. M. Abramov, I. A. Dukhovskoy, V. S. Fedoretz, V. V. Kishkurne, A. P. Krutenkova, V. V. Kulikov, I. A. Radkevich
- .11 Study of the Reaction  $\pi^- + d \rightarrow p + \pi^- + n$  with Large Momentum Transfer in Incident Momenta Interval from 1,25 to 2,64 GeV/c. - B. M. Abramov, I. A. Dikhovskoy, V. S. Fedoretz, A. P. Krutenkova, V. V. Kulikov, I. A. Radkevich, V. V. Kishkurne
- .12 1 GeV Proton Scattering and Nuclear Sizes - G. D. Alkhazov, S. L. Belostotsky, O. A. Domchenkov, Yu. V. Dotsenko, N. P. Kuropatkin, M. A. Schuvsev, and A. A. Vorobyov
- .13 Fragments Production in the Interaction of 1.0 GeV Protons with Medium and Heavy Weight Nuclei - E. N. Volnin, A. A. Vorobyov, and D. M. Seleverstov
- .14 Measurements of  $^{12}\text{C}(\pi^\pm, \pi N)^{11}\text{C}$  Cross-Sections in the Region of (3/2 3/2) Resonance - L. H. Batist, V. D. Vitman, V. P. Koptev, M. M. Makarov, A. A. Naberezhnov, V. V. Nelyubin, G. Z. Obrant, V. V. Sarantsev, and G. V. Scherbakov
- .15 Note on the Optical Potential for Pion-Nucleus Scattering in ( 3,3 ) Resonance Region - A. V. Stepanov

- VIII .16 The Investigation of Magnetic Moments of  $^{39}\text{K}$  and  $^{49}\text{Ti}$  Nuclei in Elastic Electron Scattering - V. F. Likhachev, N. G. Afanas'ev, A. A. Nemashkalo, G. A. Savitskij, and V. M. Khvastunov
- .17 Proton Energy Dependence of the (e,e'p) Reaction Cross Section for  $^2\text{H}$ ,  $^4\text{He}$  and  $^6\text{Li}$  Nuclei - Yu. P. Antoufiev, V. L. Agranovich, S. V. Dementiy, V. S. Kuzmenko, V. I. Ogurtsov and P. V. Sorokin
- .18 Total Hadronic Photoabsorption Cross-Sections of Nuclei for Photons with Energies 150-500 MeV - V. G. Vlasenko, V. A. Goldstein, A. V. Mitrofanova, V. I. Noga, Yu. N. Danyuk, V. I. Startsev, P. V. Sorokin, Yu. N. Telegin

I

PION INTERACTIONS

I.A

$\pi$ P AND  $\pi$ D INTERACTIONS

CORRECTIONS TO THE GLAUBER MODEL AT MEDIUM ENERGIES  
IN THE SCATTERING OFF TWO POTENTIAL CENTRES

I.A.1

M. Błeszyński and T. Jaroszewicz  
Institute of Nuclear Physics, 31-342 Kraków, Poland

Scattering off two partially overlapping fixed potential centres is calculated in the first order eikonal expansion<sup>1</sup>. The amplitude obtained is the exact /up to terms of order  $1/k$ ,  $k$  being the projectile laboratory momentum/ Watson series

$$T = t_1 + t_2 + t_1 G_0 t_2 + t_2 G_0 t_1 + t_1 G_0 t_2 G_0 t_1 + \dots \quad (1)$$

This amplitude is then compared with the simple-minded approximation including the single and double scattering only,

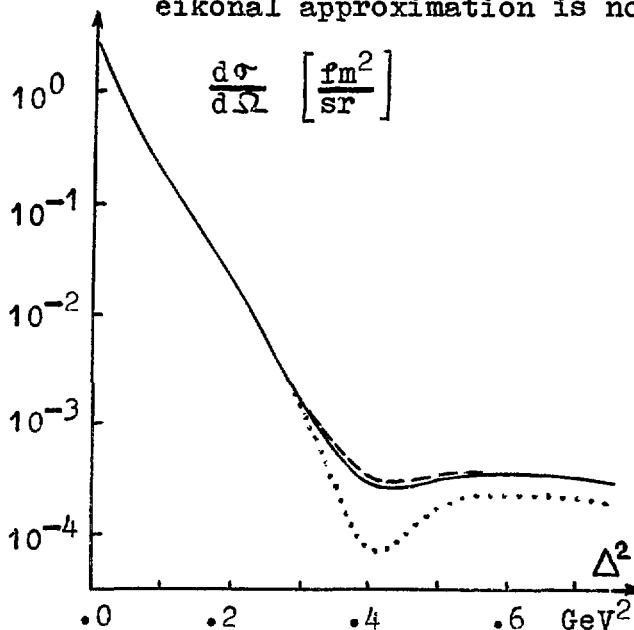
$$T = t_1 + t_2 + t_1 G_0 t_2 + t_2 G_0 t_1, \quad (2)$$

where a very simple off-shell continuation is assumed,  $\langle \vec{k}' | t | \vec{k} \rangle = t(\vec{k} - \vec{k}')$ . The comparison is made for the amplitudes corresponding to a fixed distance of the scatterers and for the amplitudes averaged over some density distribution.

In the figure below the cross-sections corresponding to (1) /solid curve/ and (2) /broken curve/ are plotted for parameters describing rather realistically pion deuteron scattering with  $k=1$  GeV/c; the deuteron D-wave is not included. The dotted curve is the Glauber result, i.e. single + double on-shell scattering only, with the eikonal free propagator

$$T^{GL} = t_1 + t_2 + t_1 G_0^{on} t_2 + t_2 G_0^{on} t_1,$$

to which both (1) and (2) converge at high energy. It is seen from these results that the formula (2) is a very good approximation to the exact result (1), both giving a significant correction to the Glauber formula at medium energies, where the eikonal approximation is no longer valid.



1. S.J. Wallace, Phys. Rev. Lett. 27, 622 (1971).

Fig.1. The differential cross-section for the scattering off a model system of two centres. See the text for details.

## "CAN ONE RECOGNIZE RESONANCE POLES FROM AN ARGAND DIAGRAM?"

I.R. Afnan,\* A.W. Thomas

Department of Physics, U.B.C., Vancouver, B.C. Canada V6T 1W5

The existence of a resonance pole is, in the most favourable cases, established by the observation of a circular trajectory in the Argand diagram, together with a Breit-Wigner peak in the "speed".<sup>1)</sup> By considering the case of pion scattering from the deuteron (in the (3,3) resonance region), we show that these conditions are not sufficient. In particular, Figures 1 and 2 show the behaviour of the  $J^\pi = 2^+$  scattering amplitude, calculated within the nonrelativistic Faddeev formalism.<sup>2)</sup> Note that even the single scattering (S-S) term, which one can easily show has no resonance pole, satisfies both the criteria mentioned earlier. Although this behaviour has been established before within Glauber theory,<sup>3)</sup> we note that (because of factorisation), this does have a pole! Because of three-body kinematics our amplitude has a cut, but no pole in the pion energy variable. (For completeness, we show the effect of summing the multiple scattering series, which is to narrow the peak, and shift it to lower energy. Preliminary results using relativistic kinematics for the pion, confirm the behaviour of the S-S amplitude - although higher order rescattering is much less important in that case.) In conclusion, we emphasize that similar problems may arise whenever a correct description of a (two-body) scattering process, requires consideration of more than two particles.

\* Permanent address - School of Physical Sciences, Flinders University, Bedford Park, South Australia, 5042. Australia.

- 1) R.D. Tripp, "Baryon Resonances", International School of Physics, Enrico Fermi, Course 33 (Academic Press, 1966).
- 2) I.R. Afnan, A.W. Thomas, Phys. Rev. C10, 109 (1974).
- 3) M. Hoenig, A.S. Rinat, Phys. Rev. C10, 2102 (1974).

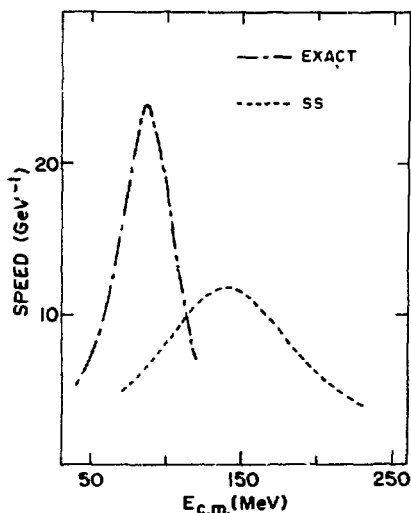


Figure 1: Speed in the  $J^\pi = 2^+$   $\pi d$  channel.

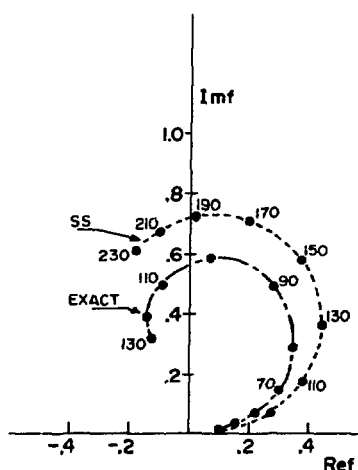


Figure 2: Argand diagram for the  $2^+$  amplitude.

R. Aaron, Northeastern University

and

E. J. Moniz and R. M. Woloshyn, M.I.T.

We study " $\pi d$ " elastic scattering in the vicinity of the 3-3 resonance using a relativistic 3-body model.<sup>1</sup> Our starting point is an elementary or bare isobar coupled to the p-wave  $\pi N$  channel (spin and isospin ignored). We first evaluate the isobar self-energy (i.e., the  $\pi N$  "bubble" graph) and fit the phase of the  $\Delta$  propagator to the  $\pi N$  3-3 phase shift, the free parameters being the isobar bare mass (we take 1350 MeV) and the  $\Delta\pi N$  coupling constant and interaction range. The 3-body equations for the  $\pi d$  amplitude (s-wave deuteron) can then be summarized diagrammatically as:

$$\pi \text{ --- } \text{[shaded block]} \text{ --- } \bar{\pi} = \text{[wavy line]} \text{ --- } \text{[shaded circle]} \text{ --- } \text{[solid line with circle]} \text{ --- } d \quad (1)$$

$$\Delta \text{ --- } \text{[shaded circle]} \text{ --- } \pi = \text{[wavy line]} \text{ --- } \text{[solid line with circle]} + \text{[wavy line]} \text{ --- } \text{[shaded circle]} \text{ --- } \text{[solid line with circle]} + \text{[wavy line]} \text{ --- } \text{[shaded circle]} \text{ --- } \text{[solid line with circle]} \text{ --- } \text{[shaded circle]} \text{ --- } \text{[solid line with circle]} \text{ --- } \pi \quad (2)$$

Circles on the intermediate isobar and deuteron propagators imply that all  $\pi N$  and  $NN$  bubbles, respectively, must be summed. The problem reduces to numerically solving the uncoupled integral equation for the  $\pi d \rightarrow N\Delta$  amplitude.

We use the model as a theoretical laboratory for investigating several questions which arise in pion scattering:

- (i) binding and Fermi motion effects on the  $\pi N$  amplitude;
- (ii) comparison to fixed scatterer calculations (Brueckner model);
- (iii) effect of nucleon-nucleon rescattering (last diagram in Eq. (2));
- (iv) effect of different  $\pi N$  and  $NN$  interaction parameters (e.g., narrow width isobar and strongly bound deuteron).

The binding and rescattering effects raise the energy at which the total cross section peaks and substantially reduces the backward differential cross section. The total elastic cross section is strongly affected by  $NN$  rescattering.

\* Work supported in part by the National Science Foundation and in part by the Atomic Energy Commission.

1. R. Aaron, R. D. Amado, and J. E. Young, Phys. Rev. **174** (1968) 2022.



## LOW ENERGY PION NUCLEON SCATTERING

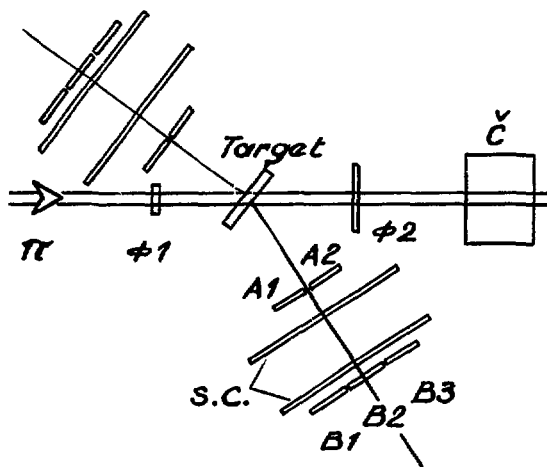
P. Bertin, B. Coupat, J. Duclos, A. Gérard, D. Isabelle, A. Magnon  
J. Miller, J. Morgenstern, J. Picard, R. J. Powers\*, P. Vernin

(C.E.N. Saclay Université de Clermont-Ferrand - France)

By using the low energy pion channel of the Saclay Linac, we made a systematic measurement of the differential cross-sections of  $\pi^+$  and  $\pi^-$  scattering on hydrogen from 20 to 100 MeV, in the angular range from 55 to 145 degrees.

The incoming pions were counted by a plastic scintillator ( $\phi 1$ ) in the beam. The electron contamination was eliminated by a threshold on  $\phi 1$  and by a gas Cerenkov counter ( $\check{c}$ ) in anticoincidence. The muon contamination was computed by a Monte Carlo program. The protons, in the  $\pi^+$  beam, were absorbed in a thin aluminium screen.

The scattered pions were detected by two sets of telescopes including plastic scintillators ( $A_i, B_j$ ) with an amplitude analysis and spark chambers (s.c) to define the origin of the particle. A good scattering event was defined by a coincidence between an incident pion and a scattered particle ( $\phi_1 \phi_2 A_i B_j$ ) with the proper amplitude.



Experimental set-up

An on line computer was used to record the data and to perform a pretreatment during the run.

The energy calibration of the pion channel was obtained with an accuracy of  $\pm 5\%$  by measuring the energy of the protons in the  $\pi^+$  beam with a calibrated solid state detector. The thickness of the liquid hydrogen target was precisely measured ( $\pm 5\%$ ) by comparing the range curves of 30 MeV pions with full and

empty target.

We obtained the differential cross-sections for 20.8, 30.5, 39.3, 51.5, 67.4, 81.7 and 95.9 MeV. From the analysis of the  $\pi^+$  data we are able to extract the  $\delta_3$ ,  $\delta_{33}$  and  $\delta_{31}$  phase shifts for these seven energies. The analysis of the  $\pi^-$  data is in progress (April 1975). The results will be available at the time of the Conference.

\* California Institute of Technology, Pasadena.

THE ELASTIC SCATTERING OF  
LOW ENERGY PIONS ON PROTONS<sup>†</sup>

I.A.5

J. S. Frank, R. H. Heffner, K. A. Klare, R. E. Mischke, and D. E. Nagle  
University of California, Los Alamos Scientific Laboratory  
Los Alamos, New Mexico 87544

and

D. C. Moir  
Arizona State University, Tempe, Arizona 85281

An experiment has been performed at the Clinton P. Anderson Meson Physics Facility (LAMPF) to measure the elastic differential cross section ( $d\sigma/d\Omega$ ) of low energy pions on protons. Data were taken at incident pion energies of 30, 40, 50, and 70 MeV for both positive and negative pions. The gas target, run at  $\sim 30^{\circ}\text{K}$  and  $\sim 1.2$  atmospheres pressure, was viewed with a system of multiwire proportional chambers and scintillation counters. The incident pion flux was measured by two independent systems: a  $\pi \rightarrow \mu\nu$  decay monitor and a scintillation counter energy-loss system to measure the total flux and composition of the beam.

Scattered particle trajectories were extrapolated onto the target plane and fiducial cuts within the gas target were made. Particle identification on the scattered pions was made with the system of energy-loss and total energy counters. Data were taken with the target empty to allow the subtraction of all residual backgrounds.

More than 10,000 events consistent with elastic  $\pi$ -p scattering were observed for each energy and polarity in the laboratory angular range  $45^{\circ}$  to  $135^{\circ}$ . Data analysis is underway at this time and preliminary results will be presented.

<sup>†</sup>Work supported by the U. S. Energy Research & Development Administration.

THE  $\pi^-d$  BREAKUP REACTION AND  $\Delta$ 's IN THE DEUTERON

R. Beurtey, G. Cvijanovich,<sup>\*</sup> J. C. Duchazeaubeneix, H. H. Dukm,<sup>\*\*</sup> J. C. Faivre, L. Goldzahl, J. C. Lugol and J. Saudinos, C.E.N. Saclay, France and L. Dubal, S.I.N. Villigen, Switzerland, and C. F. Perdrisat, College of William and Mary, Williamsburg, Virginia

Several experiments have been reported recently, which can be interpreted in terms of the existence of a  $\Delta\Delta$ -component in the deuteron ground state. These experiments involved 2-pion production with several projectiles,<sup>1,2</sup> and single pion photoproduction.<sup>3</sup>

Based on a paper by Nath, Kabir and Weber,<sup>4</sup> the emission of forward protons in the break-up reaction  $\pi^-d \rightarrow \pi^-pn$  at 1-2 GeV could be dominated by direct absorption of the  $\pi^-$  on a  $\Delta^{++}$ , rather than quasi-elastic back-scattering of the pion. The cross section for forward proton emission would then be directly related to the probability that the 2 nucleons in the deuteron be  $\Delta$ 's.

An experiment designed to investigate deuteron break-up resulting in forward proton emission has been performed in Saclay. A 0.98 GeV  $\pi^-$  beam was used because in elastic scattering on hydrogen, the differential cross section for forward protons has a distinct minimum at that energy.<sup>5</sup> The contribution to forward proton emission from single scattering on a deuteron target, had been calculated before the experiment by Monte Carlo, including Fermi momentum; the minimum in elastic  $\pi^-p$  was seen to produce a similar, but less deep minimum in  $\pi^-d$ . In the present experiment, the ratio of the  $0^\circ$  proton cross sections in  $\pi^-d \rightarrow pX$  and in elastic  $\pi^-p$  is found to be significantly larger than predicted if single scattering alone did occur. Furthermore, the angular distribution of the proton in the two reactions are different: with the deuteron target the distribution is flat, whereas on hydrogen it has a minimum at  $0^\circ$ , as seen in other experiments.<sup>6</sup>

Both features, the large deuterium-to-hydrogen ratio, and the characteristic angular distributions, are in excellent agreement with the predictions in ref. 5 and may be interpreted as independent evidence for the existence of a  $\Delta\Delta$ -component in the deuteron.

1. M. Goldhaber, Proceedings of the International Conference on Nuclear Structure (Munich, 1973), vol. 2, p. 14  
C. P. Horne e.a. Phys. Rev. Lett. 33, 380 (1974)
2. H. Braun e.a. Phys. Rev. Lett. 33, 312 (1974)  
M. J. Emms e.a. Phys. Lett. 52 B, 372 (1974)
3. P. Benz and P. Söding, Phys. Lett. 52, B 367 (1974)
4. N. R. Nath, H. J. Weber, P. K. Kabir, Phys. Rev. Lett. 26, 1404 (1971)
5. R. E. Rotschild e.a. Phys. Rev. D 5, 499 (1972)  
T. J. Richards e.a. Phys. Rev. D 10, 45 (1974)
6. P. J. Duke e.a. Phys. Rev. 149, 1077 (1966)  
J. M. Abillou e.a. Phys. Lett 32 B, 712 (1970).

<sup>\*</sup> Permanent address: Dept. of Physics, Upsala College, East Orange, N.J. 07019

<sup>\*\*</sup> Permanent address: Max-Planck-Institut fuer Kernphysik, Heidelberg.

INCIDENT-ENERGY DEPENDENCE OF  $\pi^\pm$ -p BREMSSTRAHLUNG  
IN THE REGION OF THE  $P_{33}(1232)$  RESONANCE\*

P. F. Glodis, H. C. Ballagh, R. P. Haddock, K. C. Leung,  
B. M. K. Nefkens, D. E. Smith, D. I. Sober  
UCLA, Los Angeles, Ca. 90024

ABSTRACT

The angular distributions of the photon spectra for  $\pi^\pm p \rightarrow \pi^\pm p \gamma$  have been measured for 325 MeV incident pion energy. Together with our previous results for 298<sup>1,2</sup> and 265<sup>2</sup> MeV incident pion energy, we can make a detailed investigation of the s-dependence of pion-proton bremsstrahlung in the region of the  $P_{33}(1232)$  resonance.

We present excitation functions for the differential bremsstrahlung cross section at 17 angles for both  $\pi^+$  and  $\pi^-$ . We concentrate on the backward direction where a destructive interference in  $\pi^+ p \rightarrow \pi^+ p \gamma$  results in a very low cross section and where possible structure effects and deviations from soft-photon-approximation calculations show up most readily.

---

\* Work supported in part by U.S. Atomic Energy Commission.

<sup>1</sup>D. I. Sober et al., Phys. Rev. D, March 1, 1975.

<sup>2</sup>K. C. Leung et al., to be published.

AN EXPERIMENTAL STUDY OF THE  $\pi^+d \rightarrow p+p$   
REACTION AT PION ENERGIES OF 40, 50, and 60 MeV\*

B. M. Freedom, C. W. Darden, R. D. Edge, T. Marks, Univ. of South Carolina, M. J. Saltmarsh, E. E. Gross, C. A. Ludemann, K. Gabethuler<sup>+</sup>, Oak Ridge National Laboratory, M. Blecher, K. Gotow, P. Y. Bertin<sup>++</sup>, Virginia Polytechnic Institute & State Univ., J. Alster<sup>+++</sup>, R. L. Burman, J. P. Perroud<sup>++++</sup>, R. P. Redwine<sup>+++++</sup> Los Alamos Scientific Laboratory.

ABSTRACT

The pion absorption reaction  $\pi^+d \rightarrow p+p$  has been measured at pion energies of 40, 50, and 60 MeV using a  $CD_2$  target and the low energy pion beams from the LEP channel at LAMPF. The protons were detected in coincidence using plastic scintillator detectors. Angular distributions were obtained at 10 angles from  $15^\circ$  to  $110^\circ$  (lab) with absolute errors of approximately  $\pm 3\%$  and relative errors of approximately  $\pm 2\%$ . Preliminary angular distributions are shown in FIG. 1. The curves are of the form  $K[A + \cos^2\theta_{cm}]$ . The preliminary values of the coefficients K and A and the integrated cross sections are presented in TABLE I. The integrated cross-sections agree rather well with previous data<sup>1</sup> and with recent calculations<sup>2</sup> whereas the value of A is somewhat larger than previously obtained.

FIGURE 1

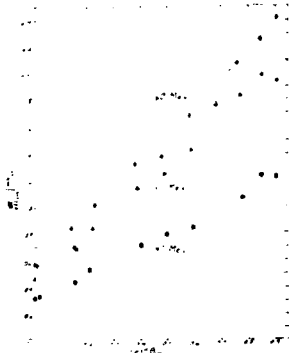


TABLE I

$T_\pi$	K	A	$\sigma_\pi$ (mb)
40	0.99	0.32	4.0
50	1.72	0.27	6.5
60	1.95	0.28	7.5

<sup>1</sup> A. M. Sach-H. Winick, and B. A. Wooten, Phys. Rev. 109, 1733 (1958).

<sup>2</sup> B. Goplen, W. R. Gibbs, and E. L. Lomon, Phys. Rev. Letters 32, 1012 (1974).

\* Supported by the O.N.R., the N.S.F. and the U.S.A.E.C.

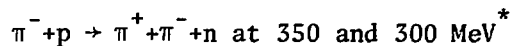
<sup>+</sup> Present address: S.I.N., Villagen, Switzerland.

<sup>++</sup> Present address: Univ. de Clermont F<sup>d</sup>, Clermont-Ferrand, France.

<sup>+++</sup> Present address: Univ. of Tel Aviv, Tel Aviv, Israel.

<sup>++++</sup> Present address: Univ. of Lausanne, Switzerland.

<sup>+++++</sup> Present address: Univ. of Bern, Bern, Switzerland.



C. A. Bordner,\*\* P. A. M. Gram,‡ W. V. Hassenzahl,‡  
H. H. Howard,‡ T. R. King,† A. T. Oyer,† G. A. Rebka,† F. T. Shively††

We will present measurements of the cross section,  $\frac{d^2\sigma}{d\Omega_c dP}$ , for the reaction  $\pi^- + p \rightarrow \pi^+ + \pi^- + n$  performed at two energies, 350 and 300 MeV, by detecting the outgoing  $\pi^+$  with a magnetic spectrometer. Angles and momenta of the  $\pi^+$  were selected to sample the doubly differential cross section at 18 points spread nearly uniformly over the accessible part of the center-of-mass phase space for each of the two energies. Approximately 1500 net events were recorded at each energy. These data represent the first steps in a program to determine the energy dependence of the total cross section down to 200 MeV. Knowledge of this energy dependence bears on the selection of the proper form of soft pion theory and on the s-wave  $\pi$ - $\pi$  scattering length.

\* Supported in part by AEC Contract AT(11-1)-2197 and W-7405-ENG-36.

\*\* Colorado College, Colorado Springs, Colorado 80903.

‡ University of California, Los Alamos Scientific Laboratory, Los Alamos, New Mexico 87544.

† University of Wyoming, Laramie, Wyoming 82071.

†† University of California, Lawrence Berkeley Laboratory, Berkeley, California 94720.

THE KROLL-RUDERMAN TERM IN THE OPE CONTRIBUTION TO  
THE ELECTROMAGNETIC EXCHANGE CURRENT

A. F. Yano and F. B. Yano\*

Department of Physics, California State University  
Long Beach, Calif. 90840

\* Department of Physics, California State University  
Los Angeles, Calif. 90032

We use two models for the  $\pi N$  vertex, namely PS and PV coupling, and show that the Kroll-Ruderman term is obtained in both cases from the Low theorem. In PS coupling, it arises from the derivative on the positive energy projection operator, whereas it arises from the derivative on the two body amplitude in PV coupling.

I.B  
71 NUCLEUS THEORY



O. Nalcioglu\*

University of Wisconsin, Madison, WI 53706

D.S. Koltun\*\*

University of Rochester, Rochester, NY 14627

The effect of Fermi motion of nucleons on the inelastic scattering of pions by nuclei is studied in the Distorted Wave Impulse Approximation. We assume the pion-nucleon  $t$ -matrix to have the non-local, separable form suggested by Kisslinger.<sup>1</sup> Transformation of this  $t$ -matrix from the pion-nucleon c.m. to the pion-nucleus c.m. introduces terms into the transition amplitude which are proportional to the nucleon momentum (recoil terms).<sup>2</sup> These recoil terms are usually neglected, but we have previously found<sup>2</sup> that they contribute significantly to the excitation of elastic dipole states, in the Plane Wave Impulse Approximation.

For the Distorted Wave study, we have used two forms of optical potential: a non-local (Kisslinger) potential<sup>1</sup> derived from the non-local  $t$ -matrix above,

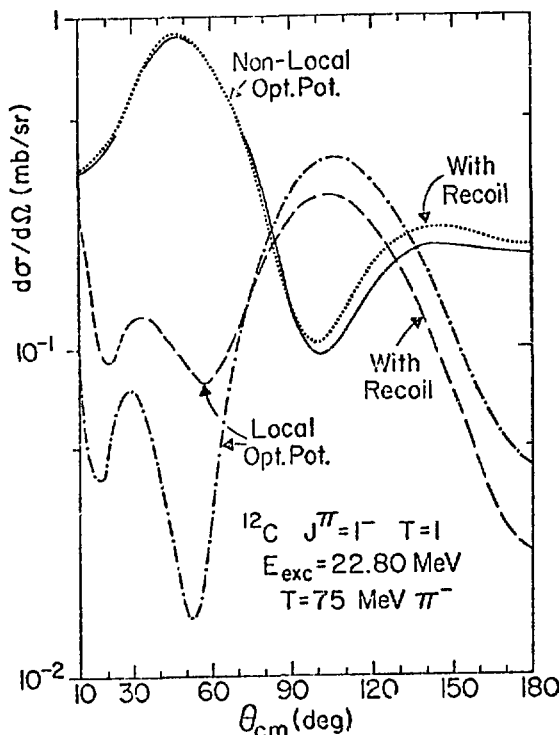


Fig.1 Inelastic Differential Cross Section

local potential. Further results for various nuclei and different energies will be presented.

\*Supported in part by the National Science Foundation.

\*\*Supported in part by the U. S. Atomic Energy Commission.

<sup>1</sup>L. S. Kisslinger, Phys. Rev. 98, 761 (1955).

<sup>2</sup>D. S. Koltun and O. Nalcioglu, Phys. Lett. 51B, 19 (1974).

<sup>3</sup>H. K. Lee and H. McManus, Nucl. Phys. A167, 257 (1972).

# PION CHARGE-EXCHANGE REACTIONS WITH NUCLEI

I.B.2

Gerald A. Miller  
Carnegie-Mellon University, Pittsburgh, Pa. 15213

James E. Spencer  
Los Alamos Scientific Laboratory, Los Alamos, N. M. 87544

## ABSTRACT

A comprehensive study<sup>1</sup> of the elastic charge-exchange reactions is presented in which the cross sections are evaluated in a coupled-channels framework.

Our main conclusions are:

- 1) For energies below the (3,3)  $\pi$ -nucleon resonance, there are considerable differences between the charge-exchange cross-sections predicted with the Kisslinger and local Laplacian models. There is a sharp dip at about 80 MeV predicted by the Laplacian model for the total SCE and DCE cross-sections to the analog and double analog which does not occur for the Kisslinger potential. Hence, accurate charge-exchange data, taken together with the corresponding elastic data, provide a very good means of differentiating between competing potential models.
- 2) In all models which we have tested, including variants of the Laplacian such as the Silbar-Sternheim potential, the charge-exchange cross-sections dip at energies in the vicinity of the  $\pi$ -nucleon resonance because of strong absorption. However, this is mediated by specific nuclear structure effects as well as nucleon number.
- 3) Charge-exchange data does not seem to provide any unique input for discussions concerning the so-called "angle transformation" since the effects of including this are comparable in all channels.
- 4) For energies around the  $\pi$ -nucleon resonance, effects which push neutrons into the nuclear surface are important for determining the size of the cross-sections and must be considered before any conclusions can be drawn about other possible effects.
- 5) The DWIA may be used in place of the full coupled channel calculation with negligible loss in accuracy.
- 6) The effect of Coulomb distortion on the charge exchange reactions is very small for pion energies greater than or equal to 100 MeV. Thus relations supplied by charge independence which give the charge-exchange T-matrices in terms of differences of elastic T-matrices for  $\pi$ 's of different charges may be used.
- 7) At energies of about 100 MeV, the effect of two-nucleon correlations, as predicted with a second-order optical potential, are expected to dominate the charge-exchange process.

## REFERENCE

1. G. A. Miller and J. E. Spencer, Phys. Letters 53B, 329 (1974), and Nucl. Phys. to be published.

On the Optical Potential for  
Particle-Nucleus Scattering

I.B.3

Abstract

A term by term analysis of the optical potential series is made using a separable scattering amplitude in a single partial wave. The Ericson-Ericson potential is shown to emerge on summation of a subset of the terms in the series. The high energy limit of the optical potential series is obtained.

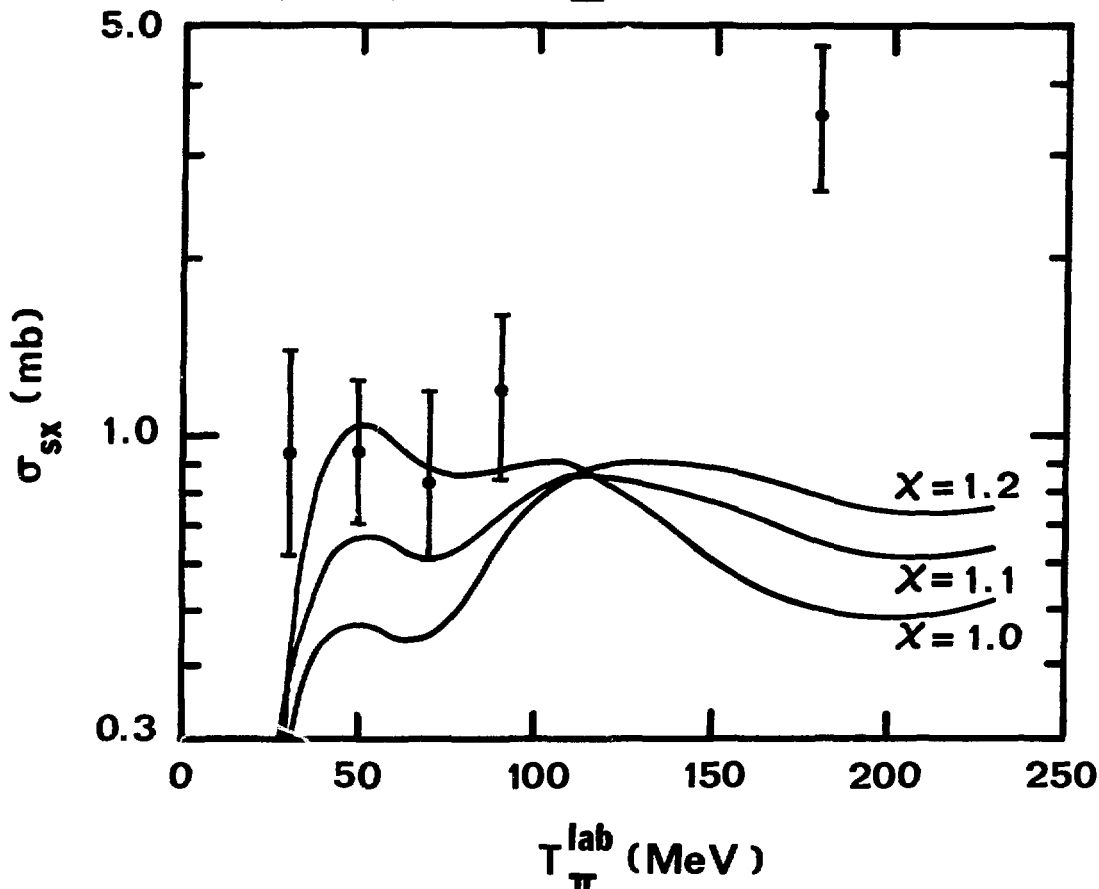
L. C. Liu and V. Franco\*

Physics Department, Brooklyn College of City University of New York,  
Brooklyn, New York 11210

The total cross sections of the single charge exchange reaction  $^{13}\text{C}(\pi^+, \pi^0)^{13}\text{N}(\text{g.s.})$  are calculated using a distorted wave eikonal approximation<sup>1</sup>. The charge exchange between the pion and the  $1p_{1/2}$  valence neutron is taken as the fundamental interaction in this DWEA calculation. To simulate the deformation of the nuclei, we allow the valence nucleon and the core nucleons to move in different harmonic oscillator wells in such a way that the mean square radius of the whole nucleus stays unchanged. The degree of overlap between the valence nucleon and core nucleus wave functions is represented in this simple model by the ratio  $\chi = a_v/a_0$ . Here,  $a_0$  and  $a_v$  are respectively the original h.o. parameters of the  $^{13}\text{C}$ , determined by electron scattering, and the modified h.o. parameter of the valence nucleon, introduced above. Our results show that the energy dependence of the cross sections is sensitive to  $\chi$ . The calculations are compared with the published data<sup>2</sup> in the figure.

\*Work supported in part by the National Science Foundation.

1. L. C. Liu and V. Franco, Phys. Rev. C11, 760 (1974).
2. D. T. Chivers, et al., Nucl. Phys. A126, 129 (1969).  
M. A. Moinsler, et al., Phys. Rev. C8, 2039 (1973).



Hans A. Bethe  
Cornell University, Ithaca, N.Y. 14850

Mikkel Johnson<sup>\*</sup>  
University of California, Los Alamos Scientific Laboratory

We present results relevant to pion scattering in the vicinity of the 33 resonance. Here the nucleus is black except in the surface, and we are therefore concerned mainly with the low density interaction; in the lowest order in the nuclear density  $\rho$  the theory is relatively simple, but in order  $\rho^2$  and higher it gets progressively more complicated. We have made two different calculations of the  $\rho^2$  term, both based on the Kisslinger off-shell assumption for the pion-nucleon amplitude. Various nuclear effects are considered but one calculation is less model dependent, as shown by Hüfner,<sup>(1)</sup> because we include nucleon correlations following Ericson and Ericson.<sup>(2)</sup> Hüfner's result is known more generally as Beg's theorem; although it applies only under certain restrictive conditions we believe these are sufficiently satisfied in the realistic case. Then the result is insensitive to the off-shell pion-nucleon amplitude. Although we prefer the calculation which includes correlations, we present results for both.<sup>(3)</sup>

For one application of our theory, we consider the location of the 33 resonance, which is most conveniently defined as the energy at which the real part of the forward amplitude vanishes. This is determined experimentally by coulomb-nuclear interference. In our theory we find three mechanisms which can influence the position of the resonance: a) the second order (i.e.,  $\rho^2$ ) Lorentz-Lorenz-Ericson effect, b) the small phases, c) the Fermi motion of the nucleons. All these effects go in the same direction and result in a downward shift of approximately 10 MeV.

Important experimental information may be obtained from a phase shift analysis of experiments. This is easily done at very low energy and energy near resonance. In the former case only several partial waves are involved and these can be obtained relatively unambiguously. Near resonance the nucleus can be described as a black disc up to some radius  $b_1$  (or equivalently up to some angular momentum); again only a few waves need to be learned directly from the data. The partial wave analysis is thus easier for heavy nuclei than light ones. The radius  $b_1$  and the residual phases are predicted by our theory.

- (1) J. Hüfner, Nucl. Phys. B 58 (1973) 55.
- (2) M. Ericson and T. E. O. Ericson, Ann. of Phys. 36 (1966) 323.
- (3) Results for the other calculation are found in H. A. Bethe and M. B. Johnson, Los Alamos report LA-5842-MS.

\*

Work supported by the U.S. Energy Research and Development Administration.

NEW ESTIMATE FOR THRESHOLD PION PRODUCTION IN PION-NUCLEUS COLLISIONS

Ronald Rockmore  
 Rutgers, The State University, New Brunswick, N.J. 08903

ABSTRACT

The Goldhaber-Teller model generalized to spin-isospin vibrations is used to provide a simple estimate for the total cross section for threshold pion production in pion-nucleus collisions ( $\pi^- A_Z \rightarrow \pi^- \pi^+ A_{Z-1}$ ) in the case of nuclei with  $N=Z$ . Cross sections are calculated using the threshold approximant to the production amplitude for single nucleons consisting of pion pole plus contact terms alternately derived from the phenomenological Lagrangian theory and the current-commutator theory of multiple-pion production. The threshold approximant in the latter theory fits the experimental pion-production data on protons poorly, and in the case of  ${}^4\text{He}$ , the lightest target nucleus considered, that theory predicts cross sections about a factor of 2 smaller than those similarly calculated with phenomenological Lagrangian input. In the case of the current-commutator theory, the Goldhaber-Teller predictions are consistent with those of the particle-hole model for  ${}^4\text{He}$  and  ${}^{16}\text{O}$  obtained earlier by Eisenberg after quadrupling his calculated values to compensate for an omitted factor of 2 in his production amplitude. While the cross sections for the  $(\pi, 2\pi)$  reaction in nuclei are still expected to be quite small, the prospect for their accessibility seems reasonably improved.

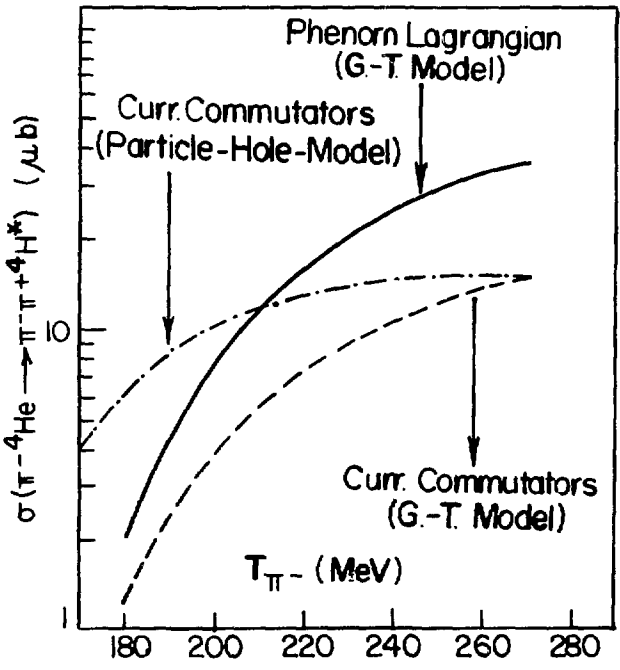


FIGURE  
 Theoretical threshold  ${}^4\text{He}(\pi^-, \pi^+){}^4\text{He}^*$  cross sections in the particle-hole and generalized Goldhaber-Teller models as a function of  $T_{\pi^-}$ .

## FIRST ORDER OPTICAL POTENTIAL

D. J. Ernst

Case Western Reserve University, Cleveland, Ohio 44106

M. A. Nagarajan

Daresbury Laboratory, Daresbury, Warrington, England

R. M. Thaler

Case Western Reserve University, Cleveland, Ohio 44106

W. L. Wang

Argonne National Laboratory, Argonne, Illinois 60439

The theory of Kerman, McManus and Thaler proceeds through a pseudo-optical potential operator  $U'$ , defined such that  $T' = \frac{A-1}{A} T$  is the solution of a Lippmann-Schwinger equation of the form  $T' = U' + \frac{1}{A} U' g P T'$ , where  $P$  is the projector onto the nuclear ground state. In the lowest order this optical potential is conventionally given by  $U' = (A-1)tP$ . This approximation is different from the approximation in which the true optical potential  $U$  is given by  $U = AtP$ . These two approximations are significantly different for energies below several GeV and for targets lighter than  $A \sim 50$ . Numerical differences between these two approximations for some cases of physical interest will be presented. Formal relations between the two approaches are given which demonstrate that the use of  $U' = (A-1)tP$  is to be preferred.

CORRELATION EXPANSION OF THE OPTICAL POTENTIAL

I.B.8

D. J. Ernst  
Case Western Reserve University, Cleveland, Ohio 44106

J. T. Londergan  
Indiana University, Bloomington, Indiana 74701

G. A. Miller  
Carnegie Mellon University, Pittsburgh, Pennsylvania 15206

R. M. Thaler  
Case Western Reserve University, Cleveland, Ohio 44106

The multiple scattering theory for the optical potential is arranged according to the number of target particles struck. The term which involves two target particles is summed as a three-body problem. Both the Kerman, McManus, and Thaler and Watson formalisms are treated in this manner. A technique using sum rules to estimate the corrections to the use of the closure propagator is presented. The approach of Foldy and Walecka is critically analyzed and additional corrections for the case of a nonlocal two-body interaction are given.



C. B. Dover

Brookhaven National Laboratory, Upton, New York 11973

R. H. Lemmer

Rand Afrikaans University, Johannesburg, South Africa

The simplest first order approximation to the pion optical potential  $V_{\text{opt}}(r)$ , proportional to the nuclear density  $\rho(r)$  times the free space  $\pi N$  amplitude  $f$ , is inadequate for describing the energy dependence of pion-nucleus total cross sections (for instance) in the (3,3) resonance region. In the presence of a resonance in the elementary  $\pi N$  amplitude, it is important to include the effects of the nuclear medium on the  $\pi N$  amplitude, such as the Pauli principle, off-shell nucleon propagation in the nuclear potential, and collision damping.

We have developed a systematic expansion of  $V_{\text{opt}}(r)$  in terms of an effective density dependent  $\pi N$  amplitude  $\tilde{f}$ , which registers these Pauli principle and binding energy effects. In this expansion, contributions to  $V_{\text{opt}}(r)$  are ordered according to the number of independent hole lines. This expansion assumes the form

$$-2\omega_q V_{\text{opt}}(q) = 4\pi \sum_k n(k) \tilde{f}(k, q; k, q) + \dots \quad (1)$$

where  $n(k)$  is the nucleon occupation number, and  $\omega_q$  is the pion energy. If we Fermi average over nucleon momenta  $k$ ,  $\tilde{f}(q, q) = \langle \tilde{f}(k, q; k, q) \rangle$  satisfies a modified Chew-Low equation of the form

$$\tilde{f}(q, q) = \tilde{f}_B(q, q) + 4\pi \sum_p \frac{1}{2\omega_p} \frac{F(q-p)}{\omega_p - \omega - i\epsilon} \tilde{f}^+(q, p) \tilde{f}(q, p) + \text{crossing term} \quad (2)$$

where  $\tilde{f}_B(q, q)$  is given<sup>1,2</sup> by the free Born term times a Pauli blocking factor  $F(q)$ . We have solved Eq. (2) numerically as a function of density, and compared the results to various approximate analytical solutions.<sup>1</sup> The main effect of the Pauli principle is to damp the Born term at low energies; higher order  $\pi N$  scattering graphs are not much affected, consistent with ref. (3). We have also compared these results with ref. (4), in which the Chew-Low graphs are summed to all orders in the density. This gives us an idea how fast the hole line expansion converges.

The method discussed here is very general; its application in a Hartree-Fock or shell model basis provides a tractable approach to the finite nucleus problem. The potential (1) must be supplemented by terms involving heavy meson exchange. In the hole line expansion, these contributions appear as an off-shell effective NN interaction (G-matrix), summed over the two nucleon legs. Such contributions have also been estimated.<sup>2</sup>

## REFERENCES

- \* Work supported, in part, by Energy Research and Development Administration.
1. H.A. Bethe, Phys. Rev. Lett. 30, 105 (1973); J. Eisenberg and H. Weber, Phys. Lett. 45B, 110 (1973); Phys. Rev. C10, 925 (1974).
  2. C.B. Dover, BNL Report 19359.
  3. C.B. Dover, D. Ernst and R.M. Thaler, Phys. Rev. Lett. 32, 557 (1974).
  4. C.B. Dover and R.H. Lemmer, Phys. Rev. C7, 2312 (1973).

## RESONANCES IN EIKONAL MODELS

J.R. Gillespie\*

Institut des Sciences Nucléaires, BP 257, Grenoble 38044, France

The use of eikonal amplitudes for optical potentials or for multiple scattering models such as Glauber's in the vicinity of a resonance (e.g. pion-nucleus scattering near the 3-3 resonance) is open to several uncertainties. The usual derivation of eikonal amplitudes is inconsistent with the conditions near a resonance : the amplitudes and wavefunctions vary rapidly, the angular distribution is uniquely determined by a single value of  $\ell$ , which like the energy, is not necessarily large.

Likewise propagator expansions in inverse powers of the momentum will fail to reproduce the resonance pole if truncated at any finite order.

The Fourier-Bessel (FB) representation may be obtained without approximation from the partial wave series. We show that continuing the FB amplitude in complex  $\ell$  one obtains the exact amplitude near a resonance. The non-resonant background may be treated by perturbation theory.

\*On leave of absence, Dept. of Physics, Boston University.

## IN THE OPTICAL LIMIT

David R. Harrington  
Department of Physics  
Rutgers University  
New Brunswick, New Jersey 08903

In the optical limit uncorrected Glauber theory gives a scattering amplitude equal to that for scattering from an elementary system via an optical potential proportional to the nuclear density. The lowest order finite-energy corrections to Glauber theory in the fixed-target approximation have the same form as corrections due to three-body interactions. In the optical limit these corrections can be taken into account by adding to the optical potential a correction quadratic in the optical potential and its derivative. This correction is identical to that for an elementary system except for an extra term proportional to the square of the optical potential. Estimates of the size of the extra term indicate that the corrected potentials for elementary and composite systems will differ appreciably only in the nuclear interior where, for a heavy nucleus, the absorption due to the leading term is already so strong that the size of the correction is unimportant. It should be possible, therefore, except perhaps at large angles, to calculate the finite energy corrections to scattering from a heavy nucleus by treating it as an elementary system interacting via an optical potential.

ELECTRIC FORM FACTOR AND THREE-BODY  
FORCE IN  $^3\text{H}$  AND NUCLEAR MATTER No 4.130

A.Kallio, P.Toropainen

Department of Theoretical Physics, University of Oulu, Finland  
and

C.Ciofi Degli Atti

Istituto Superiore di Sanita, Rome, Italy

The high-energy electric form factor and the binding energy of  $^3\text{H}$  and  $^{3,4}\text{He}$  are used to determine a 3-nucleon force purely phenomenologically. When three nucleons come close together this force becomes strongly repulsive much more so than with a pure two-body force, which is chosen to fit two-body scattering data and the binding energy. At large distances the three-body force becomes attractive. The saturation curve of nuclear matter is calculated by employing the same interaction. In all calculations the Jastrow method including the 3<sup>rd</sup> order terms is employed. Determination of this force enables one to compare the ranges and the strengths with meson theoretical models.

COMPARISON OF THE COVARIANT AND NON-COVARIANT  
 PION-NUCLEUS OPTICAL POTENTIALS

I.B.13

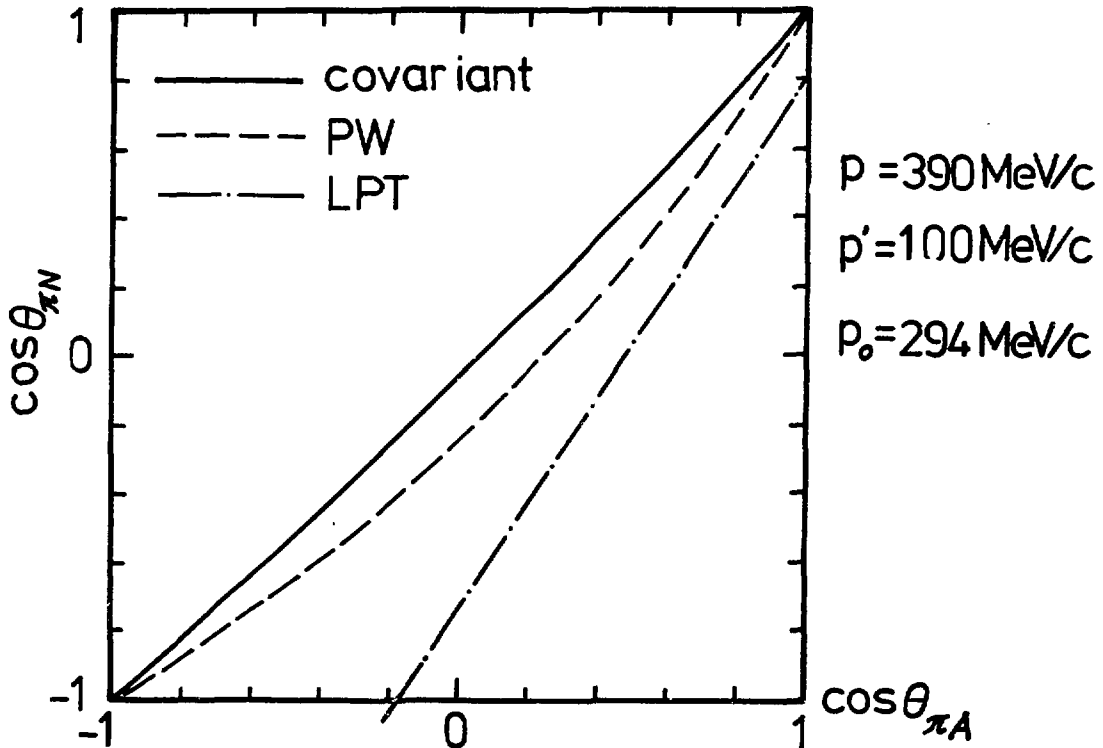
L. Celenza, L. C. Liu, and C. M. Shakin

Physics Department, Brooklyn College of City University of New York,  
 Brooklyn, New York 11210

We have compared a covariant optical potential<sup>1</sup> with several non-covariant analyses appearing in the literature<sup>2,3</sup>. The comparison was made using the fixed scatterer approximation and using the  $\pi N$  interaction of Londergan et al.<sup>4</sup> Using a special definition of the spinor for an off-mass-shell nucleon<sup>5</sup>, we resolved unambiguously the kinematical transformation of the off-shell pion-nucleon scattering amplitude. We have constructed an optical potential containing only true dynamical off-shell effects. Owing to the limited space, the full effect on the differential cross section of a covariant calculation will be reported elsewhere.

The covariant angle transformation is illustrated in the figure and compared with other ad-hoc transformations<sup>2,3</sup> for a case of off-shell ( $p \neq p'$ ) scattering of pion from  $^{12}\text{C}$  at  $T_\pi$  (lab)  $\sim 190$  MeV.

1. L. Celenza, L. C. Liu and C. M. Shakin, "Covariant pion-nucleus optical potential", to be published in Physical Review C.
2. R. H. Landau, S. C. Phatak and F. Tabakin, Ann. Phys.(N.Y.) 78,299 (1973)
3. M. G. Piepho and G. E. Walker, Phys. Rev. C9, 1352 (1974)
4. J.T.Londergan, K.W.McVoy and E.J. Moniz, Ann.Phys.(N.Y.)86, 147 (1974)
5. L. C. Liu, Nucl. Phys. A223, 523 (1974)



## IS LEVINSON'S THEOREM A NODE-COUNTING DEVICE?

H. S. Picker

Trinity College, Hartford, Connecticut 06106

## ABSTRACT

It has been suggested that medium-energy N-N and  $\pi$ - $\pi$  scattering data indicate the composite structure of these hadrons<sup>1</sup>). An essential ingredient of the argument of ref. 1 is the assumption that the underlying compositeness manifests itself by the appearance of a single node in the medium-energy elastic scattering wave functions at short distances. I note that in general, contrary to the implication of ref. 1, neither Levinson's theorem nor its subsequent generalizations for nonlocal potentials justify the inference that the number of such short-range nodes is equal to  $(\delta(0) - \delta(\infty))/\pi$ , where  $\delta(k)$  is the usual partial-wave phase shift. This assertion is demonstrated transparently through the example of a particularly simple nonlocal potential devised by Heller<sup>2</sup>). Heller's potential gives zero phase shift at all energies. I show that its parameters may be adjusted to produce scattering wave functions with or without short-range nodes.

1. D. D. Brayshaw, Phys. Rev. D 10, 2827 (1974).
2. L. Heller, in The Two-Body Force in Nuclei, ed. S. M. Austin and G. M. Crawley, Plenum, New York (1972).

## THE PION AS A PROBE FOR STUDYING NUCLEAR STRUCTURE\*

M. K. Gupta  
and

G. E. Walker

Indiana University, Bloomington, Indiana 47401

## ABSTRACT

Using a fixed scatterer separable pion-nucleon interaction as input in a microscopic theory of pion-nucleus reactions, we have studied pion-nucleus inelastic scattering, charge exchange and quasi-elastic scattering from light closed shell nuclei.

We have concentrated on the energy range  $T_{\pi} = 70 - 200$  MeV. The distorted wave impulse approximation, with a half-off shell pion-nucleon t-matrix has been adopted. As a result of these studies, we predict that the pion probe (at energies below 100 MeV) will excite strongly nuclear states not easily seen using other probes such as photons, electrons and protons. In particular, odd parity  $T = 0$  spin-flip states appear prominently in the nuclear response spectrum. Representative results supporting this conclusion will be shown. In addition the sensitivity of the results to the particular optical potential used to generate the distorted waves, the off-shell extrapolation of the pion nucleon t-matrix and the dependence of the nuclear response on the initial pion kinetic energy will be discussed.

\*Work supported in part by the National Science Foundation.

Dependence of the Off-Energy-Shell T-Matrix on the Total Three-Momentum\*

L. HELLER and G.E. BOHANNON, Los Alamos Scientific Laboratory, and  
F. TABAKIN, University of Pittsburgh.

Using a potential theory which satisfies the requirements of Lorentz invariance, the exact dependence of half-off-energy-shell T-matrix elements on the total 3-momentum,  $\vec{Q}$ , is presented for two spinless particles. This is used to obtain a formula for the dependence of fully-off-energy-shell T-matrix elements on  $\vec{Q}$ . Comparison is made with other procedures for transforming T-matrix elements from one frame to another, such as pion-nucleon center-of-mass to pion-nucleus center-of-mass.

\* Work performed under the auspices of the Energy Research and Development Administration.



W. R. GIBBS, B. F. GIBSON, and G. J. STEPHENSON JR.

Theoretical Division, Los Alamos Scientific Laboratory, Los Alamos, New Mexico 87544

Recently we have discussed the dependence in a kinematically complete geometry of the spectral shape observed on the model assumptions used in a calculation of the photo-absorption of negative pions from the atomic orbitals of deuterium.<sup>1</sup> We observed that the largest uncertainty arose from the treatment of the short distance behavior of the nucleon-nucleon relative wave functions in the initial and final states, but that, for variations which we consider reasonable, one should be able to extract the neutron-neutron scattering length to a few tenths of a fermi. On the other hand, Sotona and Truhlik<sup>2</sup> report a large effect on the  $\mu^-d$  capture rate and Sauer<sup>3</sup> demonstrated a large effect in the extraction of the Coulomb corrected proton-proton scattering length when short-ranged unitary transformations are applied to the nucleon-nucleon scattering wave functions. Consequently, we have investigated the effect of short-ranged unitary transformations on the rate of the  $\pi^-$  photo-absorption, including that transformation which gave Sauer's largest effect. Following Sauer, we use a transform of the type

$$U = 1 - 2|g\rangle\langle g|, \quad |r\rangle\langle r| = Cr(1 - \beta r)e^{-\alpha r},$$

where C is a normalization constant. Our standard wave functions are described in Ref. 1, being the Reid Soft Core deuteron, a PHS wave function model for the scattering state, and an atomic s-wave orbital modified by the Born term of the multiple scattering series for the pion on the deuteron. The operator was taken from Baer and Crowe.<sup>4</sup> Two features emerge from the results presented in the Table. First, large effects can be produced for the case in which Sauer sees a large effect ( $\alpha = 3$ ,  $\beta = 2$ ) if the transformation is applied only in one or the other state. When the same transformation is applied to both states, the two operations nearly commute, due to the effective long range of the operator compared to the unitary transformation, thus removing the effect. Second, the individual effects disappear when the range of the transform is decreased. We estimate a 15% uncertainty due to the neglect of higher order terms in the multiple scattering series and a 10% uncertainty due to our knowledge of the transition operator. Hence, while measurement of this rate can distinguish between models in which the two states are treated similarly or very differently, it is not very promising for distinguishing among cases where the states are transformed equivalently.

<sup>†</sup> Work done under the auspices of the U. S. ERDA

1. W. R. Gibbs, B. F. Gibson, and G. J. Stephenson Jr., Phys. Rev. **C11**, 90 (1975).

2. M. Sotona and E. Truhlik, Phys. Lett. **43B**, 362 (1973).

3. P. U. Sauer, Phys. Rev. Lett. **32**, 29 (1974).

4. H. W. Baer and K. M. Crowe, Proc., Int'l Conf. on Photonuclear Reactions and Applications, 1973.

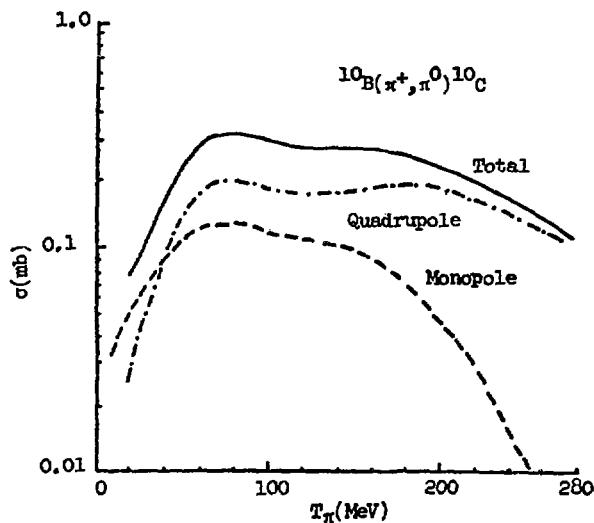
Total radiative capture rate for different wave-function models

Model	Standard	$\alpha = 3$			$\alpha = 5$		
		Scattering	Deuteron	Both	Scattering	Deuteron	Both
Rate x 10 <sup>-14</sup>	1.53	1.00	0.85	1.56	1.50	1.50	1.53

We have examined the reaction  $^{10}\text{B}(\pi^+, \pi^0)^{10}\text{C}$  as a means of studying nuclear structure properties and the charge-exchange mechanism. A full multiple-scattering treatment was used with a separable form of the pion-nucleon t-matrix describing the  $\pi$ -N interaction. Spin-flip contributions were included. Because the initial state is  $J^\pi = 3^+$  and the two final particle-stable states are  $J^\pi = 0^+$  and  $J^\pi = 2^+$ , the reaction can proceed by both the monopole and the quadrupole nuclear form factors. We find that the quadrupole, spin-flip transition to the  $2^+$  final state dominates the reaction; the lack of strong forward peaking of the basic  $\pi$ -N charge-exchange amplitude leads to the quadrupole dominance over the monopole as may be seen from the figure. The calculation is in excellent agreement with the data<sup>(1)</sup>. We have also examined the pion charge-exchange reaction for  $^7\text{Li}$  and  $^{13}\text{C}$ . We find that these cross sections, which do include the analogue transitions, are about the same size as the  $^{10}\text{B}$  cross section above  $T_\pi = 100$  MeV implying that analogue transitions are not dominant in pion charge-exchange scattering.

<sup>\*</sup>Work supported in part by the U.S. ERDA.

1. J. Alster, D. Ashery, S. Cochavi, M. A. Moinester, Y. Shamai, A. I. Yavin, M. Zaider, E. D. Arthur and D. M. Drake to be published.



B. F. GIBSON and C. K. SCOTT

Theoretical Division, Los Alamos Scientific Laboratory

The s-wave  $\pi^-$ -nucleus scattering lengths have been analyzed to separate the isoscalar and isovector contributions as a function of mass number. The scattering lengths determined by Hufner, Tauscher, and Wilkin<sup>1</sup> (HW) were used. A natural choice of a parametric form for the scattering lengths is

$$a[\pi^-(N,Z)] = a_0 A + a_1(N-Z) + b_0 A + b_1(N-Z)/A,$$

where  $a_0 = -5 \times 10^{-3} \mu^{-1}$  and  $a_1 = -87 \times 10^{-3} \mu^{-1}$  ( $\mu$  is the pion mass) are the isoscalar and isovector components of the free  $\pi$ -N scattering lengths.<sup>2</sup> Excluding  ${}^6\text{Li}$  and  ${}^{11}\text{B}$  from the analysis, we found

$$b_0 = (-20.7 + 17.2) \times 10^{-3} \mu^{-1} \quad \text{and} \quad b_1/A^2 = (+4.9 - 11.4) \times 10^{-3} \mu^{-1}.$$

A comparison of the fit with experiment is given in the Table. A typical discrepancy is that for  ${}^{12}\text{C}$ ,  $-(16 \pm 9) + i(11 \pm 9)$ , where the theoretical uncertainty in  $a_{\text{exp}}$  is probably underestimated. The quality of the fit implies that the parameters contain the essential features of  $\pi$ -nucleus scattering lengths for  $N-Z \leq 1$  nuclei. Data for  $N-Z \geq 2$  nuclei are required to determine the isotensor term.

From the present phenomenology of  $N-Z = 0, 1$  nuclei there are several tentative conclusions which suggest further experimental and theoretical work: (a) The  ${}^6\text{Li}$  and  ${}^{11}\text{B}$  scattering lengths do not fit the mass number systematics. (b) The value of  $b_1$  indicates a substantial contribution from pairwise interactions. (c)  $\text{Re}(a_1 + b_1/A)$  vanishes in the vicinity of  $A_0 = 170$ , with the obvious consequences for  $\pi^+$  and  $\pi^-$  scattering length relations above and below  $A_0$ . (d) For charge exchange scattering to the isobaric analogue state the real part of the scattering length vanishes near  $A = A_0$ . (e) The present fit casts doubt upon the validity of the cluster hypothesis of HW.

<sup>†</sup> Work performed under the auspices of the U. S. Energy Research and Development Administration.

<sup>1</sup> J. Hufner, L. Tauscher, and C. Wilkin, Nuclear Physics A231 (1974) 455.

<sup>2</sup> D. V. Bugg, A. A. Carter, and J. R. Carter, Physics Letters 44B (1973) 278.

Table. The s-wave  $\pi^-$ -nucleus scattering lengths in units of  $10^{-3} \mu^{-1}$ . The  $a_{\text{exp}}$  were taken as the average of the values quoted by HW. The  $a_{\text{calc}}$  are the values resulting from the present fit.

(N,Z)	$a_{\text{exp}}$	$a_{\text{calc}}$	(N,Z)	$a_{\text{exp}}$	$a_{\text{calc}}$
${}^4\text{He}$	-100 + 131	-103 + 129	${}^{20}\text{Ne}$	-492 + 1125	-514 + 1144
${}^6\text{Li}$	-132 + 140	-154 + 143	${}^7\text{Li}$	-230 + 141	-233 + 141
${}^{10}\text{B}$	-275 + 180	-257 + 172	${}^9\text{Be}$	-281 + 156	-274 + 152
${}^{12}\text{C}$	-324 + 197	-308 + 186	${}^{11}\text{B}$	-357 + 194	-316 + 164
${}^{14}\text{N}$	-362 + 190	-360 + 1101	${}^{19}\text{F}$	-481 + 1105	-482 + 1110
${}^{16}\text{O}$	-391 + 1106	-411 + 1115			

## ON PIONIC DEGREES OF FREEDOM IN NUCLEI

Erich Vogt  
University of British Columbia  
Vancouver, Canada

Many authors have recently speculated on the possibility that a pion forms  $N^*$  doorway states before it is absorbed in a nucleus. Perhaps the pion may also form other doorway states, more intrinsically nuclear, in which it is associated with many nucleons rather than a single nucleon. This possibility could be explored in studying the excitation function of partial absorption cross sections for final states in which only two fragments occur. Kinematically such states are easily distinguished from those in which fragment emission occurs as the second step in pion absorption by two nucleons: in the latter case a single fast nucleon will normally accompany the fragments. The two-fragment process<sup>1</sup>, though probably small in their partial yield, should be especially sensitive to any pion-many-nucleon doorways. These could manifest themselves as resonances, superimposed on the primary  $N^*$  doorway resonance, in the excitation functions. The presence of such resonances in several two-fragment exit channels could establish them as pion doorways and not cross section fluctuations. They would be a direct way of exhibiting pionic degrees of freedom in the nucleus. As in many other areas of nuclear physics one should look for doorway states in those partial cross sections most likely to exhibit them. An experiment at TRIUMF is underway<sup>1</sup> to search for resonances in fragment emission.

<sup>1</sup>P.W. Martin, et al, (private communication)

INELASTIC TWO-BODY CONTRIBUTIONS TO PION MULTIPLE SCATTERING--  
 J.T. Londergan, Indiana University, and E.J. Moniz, MIT.

The pion-nucleon scattering amplitudes are highly inelastic, indicating a strong coupling to production channels, mainly  $\pi N \rightarrow \pi\pi N$ . Because the inelastic component of the basic two-body interaction is large, a consistent multiple scattering theory for pions should include effects arising from the coupling of inelastic  $\pi N$  channels. We show how to generalize the conventional multiple scattering theory to calculate pion elastic scattering from nuclei, using a multichannel separable potential for the pion-nucleon scattering amplitude and employing the fixed-nucleon approximation. This procedure yields extra terms, not present in the conventional formalism, which we separate into two types: (1) excitation of the pion, both above and below inelastic threshold, and subsequent propagation through the nucleus. We refer to this process as inelastic shadowing. This includes the contributions from processes such as  $\pi N \rightarrow \rho N$  and  $\pi N \rightarrow \epsilon N$ . (2) isobar production, e.g.  $\pi N \rightarrow \pi\Delta$ . We examine both the qualitative and quantitative effects of both processes on pion multiple scattering. For the inelastic shadowing term, we show that qualitative estimates of this effect can be obtained from a knowledge of the pion-nucleon elastic scattering phase shifts plus specification of the inelastic threshold energy, that is, without any detailed information about the inelastic channels. We also show that the inelastic shadowing contribution is similar to the contribution from two-nucleon correlations, and we compare the size of these effects for pion scattering. We show the modification of the first-order optical potential necessary to account for inelastic shadowing effects. The isobar production contribution to pion elastic scattering involves the calculation of inelastic rescattering terms. We evaluate these terms for scattering of pions on very light nuclei and investigate this effect for energies near, and above, the  $\pi N P_{33}$  resonance.

## Glauber Type Representation For Nonlocal Potentials

B.S. BHAKAR

University of Manitoba , Winnipeg , Canada .

It is wellknown that a Glauber representation<sup>1</sup> for the scattering amplitude is quite successful in explaining the data in the high energy domain . The main results of the formalism has been obtained assuming a local potential . As it is a common practice to incorporate effects of inelasticity , various exchanges , and energy dependence near a resonance by means of a phenomenological nonlocal potential , it should be of considerable interest to extend the Glauber representation for a nonlocal potential . Earlier attempts in this direction have been made by Malenka<sup>2</sup> and Abarbanel<sup>3</sup> who have extended the formalism for spinorbit and  $L^2$  type potentials . But these potentials depend on the velocity to a finite power . In the present study , we have attempted to generalize the formalism for a nonlocal potential which may be written as

$$V\psi = \int d^3z' v(\underline{z}, \underline{z}') \psi(\underline{z}')$$

Such a potential is equivalent to introduction of all powers of momentum in the interaction . Following Glauber<sup>1</sup> , we assume the scattered wave of the form

$$\psi_k(\underline{z}) = e^{i\mathbf{k}\cdot\underline{z}} \rho(\underline{z})$$

The amplitude is derived by neglecting higher order derivatives of  $\rho(\underline{z})$  beyond first . This approximation is not equivalent to the low energy approximation of effective mass type .

References

- 1) R.J.Glauber, Lecture in Colorado Summer School, Vol.1, p.315.
- 2) B.J.Malenka, Phy.Rev.95 ,522(1954).
- 3) H.D.I. Abarbanel, Lecture in Colorado Summer School, Vol 14A.

J. Haak and A. Lande  
Groningen University

and

F. Iachello

Kernfysisch Versneller Institute, Groningen, The Netherlands

Recently<sup>1</sup> we have emphasized that in consequence of the near cancellation of the isoscalar scattering lengths,  $b_0 = \frac{1}{3}(2a_3 + a_1) \approx 0$ , the finite range of the s-wave  $\pi$ -N interaction gives rise to appreciable contributions to the strong interaction shifts of  $\pi$ -mesic atoms. We consider here the related ambiguity originating in the coupling constants of the  $\pi$ -N interactions. To illustrate this, we parametrize the s-wave interaction in terms of t-channel exchanges;  $\pi\pi$ ,  $T=0$  " $\sigma$ " exchange,  $\pi\pi$ ,  $T=1$   $\rho$ -exchange, and a hard core<sup>2</sup>

$$V(r) = V_{\sigma} \frac{e^{-\mu_{\sigma} r}}{\mu_{\sigma} r} + t \cdot \tau V_{\rho} \frac{e^{-\mu_{\rho} r}}{\mu_{\rho} r} + V_{HC} \frac{e^{-\mu_{HC} r}}{\mu_{HC} r}.$$

Fixing  $\mu_{\sigma}=1.82$ ,  $\mu_{\rho}=3.78$ ,  $\mu_{HC}=9.8 \text{ fm}^{-1}$  we generate a set of phase shift equivalent potentials whose scattering lengths and effective ranges are identical within 1% (i. e. well within experimental uncertainty).

To evaluate the shifts we solve the Lippmann-Schwinger equation for each  $V(r)$  to generate the non-local  $T$ -matrix, extract a local approximation to it,  $\tilde{T}(r)\phi(r) \equiv V(r)\psi(r)$ , and fold  $\tilde{T}$  into the nuclear density to obtain the optical potential. To focus on the finite range contribution the zero range contribution is subtracted out, and the remainder is added to the optical potential:<sup>3</sup>  $b_0^{\pm} = -0.03 \mu^{-1}$ ,  $b_1 = -0.08 \mu^{-1}$ ,  $\text{Im } B_0 = 0.04 \mu^{-4}$ ,  $C_0 = 0.21 \mu^{-3}$ ,  $\text{Im } C_0 = 0.14 \mu^{-6}$ ,  $\xi = 1$ . For  $^{52}\text{Cr}$ , in the absence of the finite range contribution,  $\Delta E_{2p} = -1.72 \text{ keV}$ ,  $\Gamma_{2p} = 4.81 \text{ keV}$ . The total shift  $\Delta E_{2p}$  increases linearly with the strength of the longest range component of the  $\pi$ -nucleon interaction.

Potential	$\frac{V_{\sigma}}{\text{MeV}}$	$\frac{V_{\rho}}{\text{GeV}}$	$\frac{V_{HC}}{\text{GeV}}$	$\frac{a_3}{\text{fm}}$	$\frac{a_1}{\text{fm}}$	$\frac{\Delta E_{2p}}{\text{keV}}$	$\frac{\Gamma_{2p}}{\text{keV}}$
1	-26	2.2	14.6	.1239	-.2434	-1.97	4.79
2	-179	3.2	71.3	.1237	-.2430	-3.35	4.77
3	-301	4.0	156.9	.1240	-.2413	-4.49	4.81

<sup>1</sup>F. Iachello and A. Lande, Phys. Lett. 50B (1974) 313.

<sup>2</sup>J. Hamilton, in High Energy Physics, Vol. 1, Academic Press, N. Y. (1967) E. Burhop, ed. pp. 193-339.

<sup>3</sup>M. Krell and T. E. O. Ericson, Nucl. Phys. B11 (1969) 521.

Pion-Nucleus Multiple Scattering and Nuclear  $\Delta$ -h States\*

M. Hirata, Brown University

and F. Lenz and K. Yazaki, M.I.T.

In the standard description of pion nucleus multiple scattering, the c.m. motion of the interacting  $\pi$ -N subsystem is frozen as a consequence of the usually employed fixed scatterer approximation. We relax this approximation and include the propagation of the  $\pi$ -N system and its interaction with the residual nucleus. This results in a description of the scattering process as multiple excitations of the nuclear  $\Delta$ -h states. A systematic expansion is presented, in which the static optical potential appears as the first order term and corresponds to the closure limit for the  $\Delta$ -h state.

In solving the equation of motion of the  $\Delta$ -h states, we take into account the Fermi motion of the nucleons and the binding correction. In particular, this allows to study the possible influence of the  $\Delta$ -nucleus interaction on  $\pi$ -nucleus scattering. Non-static corrections to the  $\pi$ -N- $\Delta$  vertex are included which corresponds in the limit of no Fermi motion and no binding correction to the angle transformation of the  $\pi$ -N (33) amplitude. Higher order optical potential contributions describing the Pauli-quenching effect are contained in our description and shown to be equivalent to the Fock term in the equation of motion of the  $\Delta$ -h states. As a practical example, we calculate  $\pi$ - ${}^4\text{He}$  elastic scattering.

\* Work supported in part by ERDA.



T-S. H. Lee  
Bartol Research Foundation  
of the Franklin Institute, Swarthmore, Pa. 19081

K. Kubodera  
University of Tokyo, Tokyo, Japan and

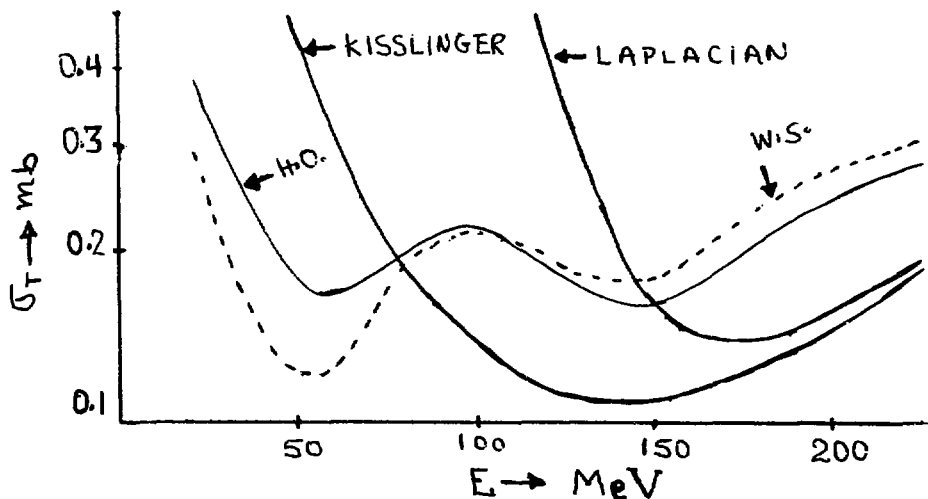
J. D. Vergados  
University of Pennsylvania, Philadelphia, Pa. 19174

## ABSTRACT

The  $^{13}\text{C}(\pi^+, \pi^0)^{13}\text{N}(\text{g.s.})$  cross section has been studied within the framework of the Distorted Wave Impulse Approximation (DWIA). The appropriate pion optical potentials and the single charge exchange transition operator were obtained from the finite  $\pi$ -n off-shell  $t$ -matrix of Londergan, Moniz and McVoy. Realistic nuclear densities were used. The various non-local effects were included exactly by performing the DW calculation in momentum space.

At energies close to the (3,3) resonance the predicted cross-section remains essentially flat exhibiting a small minimum. This minimum is less pronounced than in previous calculations<sup>1</sup> based on the Kisslinger and Laplacian models. Our predictions, however, strongly disagree with recent experimental data both in shape and in magnitude (a factor of five too small).

Harmonic oscillator (H.O) and Woods Saxon (W.S) wave functions and densities were tried. Such effects were small and unable to cure the disagreement with experiment. It seems that the problem lies with the DWIA itself. Other reaction mechanisms are currently under study.



1. N. Auerbach and J. Warsawski, Phys. Lett. 45 (1973) 171.

D. A. Sparrow

Nuclear Physics Laboratory, Department of Physics and Astrophysics  
University of Colorado, Boulder, Colorado 80302

ABSTRACT

The subject of pion scattering from nuclei has received considerable attention recently. In particular, pion charge exchange reactions are of interest because of large discrepancies between theoretical predictions and experimental results for the  ${}^{13}\text{C}(\pi^+, \pi^0){}^{13}\text{N}$  g.s. cross section.<sup>1</sup> Study of the reaction  ${}^3\text{He}(\pi^-, \pi^0){}^3\text{H}$  has been proposed<sup>2</sup> as a means to help clarify these discrepancies, since detection of the recoiling tritons would allow measurement of the angular distribution, as well as the total cross section.

The scattering is treated within the framework of the Glauber approximation, using a simple model for the scattering amplitude, which includes spin-flip. Only the leading component of the  $A=3$  wave function was retained. Reasonable agreement is obtained with the elastic scattering data at 154 MeV.

The contributions of spin-flip to the elastic scattering are generally small. For the charge exchange reaction however, at energies below around 250 MeV, the spin flip mechanism can contribute up to 50% of the total cross section as well as dramatically influencing the angular distribution. A  ${}^3\text{He}(\pi^-, {}^3\text{H})\pi^0$  experiment in which the recoiling tritons were detected to determine the angular distribution of the scattered pions would be very desirable.

1. J. Alster et al., Bull. Am. Phys. Soc. 20, 84 (1975).
2. J. M. Eisenberg and V. B. Mandelzweig, preprint.

PION ELASTIC SCATTERING FROM ALIGNED TARGETS

M. S. Iverson and E. Rost

Nuclear Physics Laboratory, Department of Physics and Astrophysics  
University of Colorado, Boulder, Colorado 80302

ABSTRACT

It was suggested<sup>1</sup> some time ago that the differences in the interactions of  $\pi^+$  and  $\pi^-$  particles with neutrons and protons can be used to investigate relative neutron and proton densities in nuclei. The use of aligned targets with  $\pi^+$  and  $\pi^-$  beams presents considerable advantages for the extraction of neutron density information. As a framework for estimating pion scattering from aligned targets we use the Kisslinger optical potential<sup>2</sup> including a deformed nucleon density distribution.<sup>3</sup> The reorientation effects are treated using the distorted wave Born approximation (DWBA) which is found to be very accurate even for the large deformation  $\beta \sim 0.33$  appropriate for  $^{165}\text{Ho}$ . The deformation effect is found to be

$$\frac{d\sigma}{d\Omega}(\text{aligned}) - \frac{d\sigma}{d\Omega}(\text{unaligned}) \sim (B_2/B_2(\text{max}) - \frac{1}{2}) \text{Re}(f^{(0)} f^{(1)*})$$

where  $f^{(0)}$  is the

elastic scattering amplitude from a spherical nucleus and  $f^{(1)}$  is the amplitude for a quadrupole transition from a spherical ground state ( $L=0$  to  $L=2$ ). This difference is linear in  $\beta$  and allows for the differentiation, in principle, of  $\beta_p$  and  $\beta_n$  deformation effects.

1. E. D. Courant, Phys. Rev. 94, 1081 (1954);  
A. Abashian, R. Cool, and J. W. Cronin, Phys. Rev. 104, 855 (1956).
2. L. S. Kisslinger, Phys. Rev. 98, 761 (1955).
3. G. W. Edwards and E. Rost, Phys. Rev. Lett. 26, 785 (1971).

Geometrical Indication of Dips in Diffraction Pattern

N. Nakamura, T. Kohmura\*) and T. Negishi\*)

Department of Physics, Tokyo University of Science, Tokyo  
 Department of Physics, Tokyo University of Education, Tokyo\*)

There exist some peaks and dips in the angular distribution for nuclear elastic scattering at intermediate energies. Two of the present authors<sup>1)</sup> pointed out that the diffraction pattern has a universal (scaling) feature almost independent of the energy or the target with the first dip at the momentum transfer squared  $q^2 \approx 0.6A^{-2/3} (\text{GeV}/c)^2$  and with the second peak at  $q^2 \approx 0.9A^{-2/3} (\text{GeV}/c)^2$ , and that this universal feature is accounted for by a geometrical picture of scattering. It was recently observed that, as the energy goes up into the high energy region, the pattern of the angular distribution gradually changes with the energy: the first dip gets deeper and the second peak higher, both being located at nearly same momentum transfers squared as in the intermediate energy region. Here, we will present some results of our present analysis on the geometrical indication of the dips.

The analysis is based on the eikonal expression for scattering, assuming the optical potential  $V(r)$  acting on the projectile. The optical potential being complex, the phase function  $\chi(b)$  in the expression consists of the real part  $\alpha\rho(b)$  and the imaginary part  $\beta\rho(b)$ .

In terms of the phase function, the real and the imaginary part of the scattering amplitude is expressed;

$$\begin{aligned} \text{Re}F(q) &= k \int e^{-\beta\rho(b)} \sin[\alpha\rho(b)] J_0(qb) b db, \\ \text{Im}F(q) &= k \int \{1 - e^{-\beta\rho(b)} \cos[\alpha\rho(b)]\} J_0(qb) b db, \end{aligned} \tag{1}$$

the integrands of which are a peaked function and a cut-off function (see Fig. 1) of  $b$  multiplied by a periodical function  $J_0(qb)b$  with a period determined by  $q$ . The zeroes of  $\text{Re}F(q)$  and  $\text{Im}F(q)$  are predictable owing to the periodicity.

Let us express the  $i$ -th zero of  $J_0(z)$  by  $\lambda_i^0$ . Zeroes of  $\text{Im}F(q)$  are predicted to be located at around  $q = \lambda_{2i}^0/R$  with the nuclear radius  $R$ , while zeroes of  $\text{Re}F(q)$  at around  $q = \lambda_{2i+1}^0/b_0$  with  $\rho(b_0) = 1/\beta$ .

A dip in the angular distribution corresponds to a zero of  $\text{Im}F(q)$ , and its depth is determined by  $\text{Re}F(q)$  (Fig. 2). Since the value of  $e^{-\beta\rho} \sin\alpha\rho$  is of the order of  $\alpha/\beta e$ , the depth of the dip in the  $\log(d\sigma/d\Omega)$  plot is predicted to be  $\log(\alpha/\beta e)^{-2}$ . The dip gets deeper with an increase of the imaginary part of the optical potential, i.e., with the energy.

Our present prediction of the first dip to be at  $q = \lambda_2^0/R$  coincides with the result of the previous work which predicted the dip at  $q = \lambda_1^2/R$ , since  $\lambda_2^0$  is nearly equal to  $\lambda_1^2$ .

References

- 1) T. Kohmura, Lett. Nuovo Cimento 8 (1973), 956.  
 T. Negishi and T. Kohmura, Prog. Theor. Phys. 51 (1974), 518.

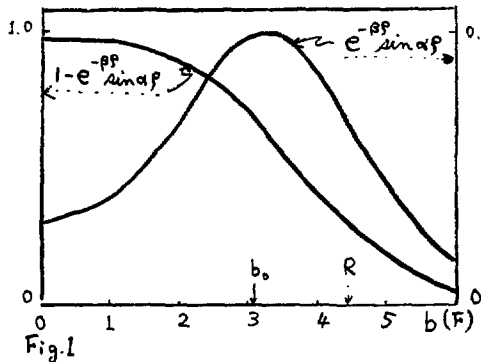


Fig.1

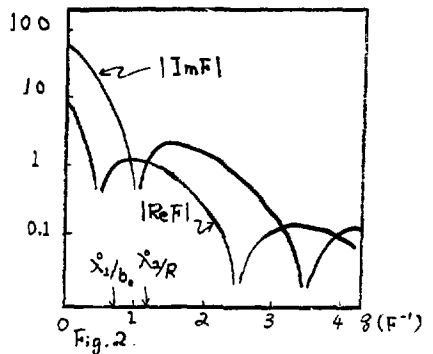


Fig.2

Pion Scattering at Resonance Energies and  
Nuclear Correlations within Nuclei

I.B.29

Tsunejiro Negishi and Toshitake Kohmura

Department of Physics, Tokyo University of Education, Tokyo

Nuclear phenomena at incident momenta of several hundred MeV/c are supposed to be sensitive to the nuclear correlations within the nucleus. Nuclear scattering at intermediate energies is, however, well reproduced by a simple nuclear model; for example by the Glauber approach. Thus, the short-ranged correlations have not manifested themselves in nuclear events yet.

The forward scattering amplitude  $F(0)$  for pion scattering from nuclei in the resonance energy region has been obtained in the experiments.<sup>1)</sup> The energy  $E_0$  at which the real part of  $F(0)$  is zero deviates from the resonance  $E_R$  for pion scattering from nucleons. Here we discuss that this deviation of the energy comes from the off-the energy-shell effect of the propagators which has an intimate relationship with the nuclear correlations in scattering process.

The Glauber approach, predicting that  $F(0)$  should be purely imaginary at the resonance energy, fails to account for the deviation of the energy.<sup>2)</sup> In its expression, the off-the energy-shell part of the Green's function do not make much contribution to the nuclear scattering amplitude. Therefore, in the Glauber expression, multiple scattering is brought about with such a probability as  $\langle 1/(kr)^A \rangle$  dully sensitive to the nuclear correlations, while in the exact scattering theory, with a probability as  $\langle e^{ikr}/kr \rangle$  sharply sensitive to the correlations at higher energies.

We formulate a correction to the Glauber expression for the nuclear scattering amplitude in order to evaluate the deviation of the energy  $E_0$  from  $E_R$ , referring to Sugar and Blankenbecler.<sup>3)</sup> The formalism is generaliz- ed to the scattering from a composite system. We have obtained the pion- nucleon potentials from the Fourier transformed of the pion-nucleon scattering amplitude in the formarism. The nuclear wave functions are used of the harmonic oscillator model.

One of our results  $R = \text{Re}F(0)/\text{Im}F(0)$  is shown in Fig. 1. The correction to the Glauber expression makes the energy  $E_0$  shifted down close to the experimental one. The present result does not, however, fit to the experi- mental data over all the energy region. This discrepancy may be explained by the nuclear short-ranged correlations, which is neglected in our present analysis. The correction terms are very sensitive to the nuclear correlations. The real part of the forward scattering amplitude, which comes dominantly from the correction terms, is a physical quantity to give some information on the nuclear correlations.

References

- 1) C. Wilkin, C. R. Cox, J. J. Domingo, K. Gabathuler, E. Pedroni, J. Rohlin, P. Schwaller and N. W. Tanner, Nuclear Phys. B62 (1973) 61.
- 2) T. F. O. Ericson and J. Hüfner, Phys. Letters 33B (1970) 601.
- 3) R. L. Sugar and R. Blankenbecler, Phys. Rev. 183 (1969) 1387.

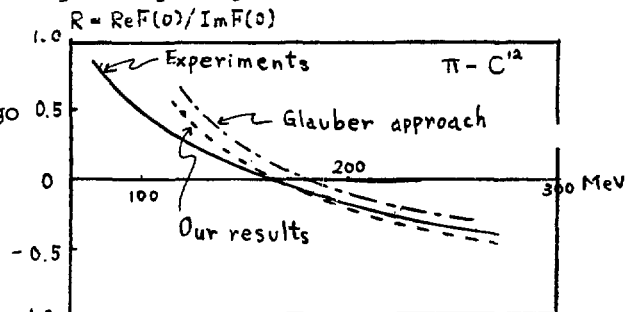


Fig. 1.

Y. Nogami and K.K. Bajaj  
 Phys. Dept., McMaster Univ., Hamilton, Ont., Canada L8S 4M1

ABSTRACT

We examine the validity of the impulse approximation for pion-nucleus scattering at medium energies by doing a model calculation in which a pion is scattered from a nucleon bound in a harmonic oscillator potential. The Hamiltonian we assume is

$$H = H_N + H_\pi + H_I \text{ where } H_N = \frac{p^2}{2m} + V(r)$$

$$H_\pi = \int d\underline{k} \omega a_{\underline{k}}^\dagger a_{\underline{k}}$$

$$H_I = - \frac{\lambda}{(2\pi)^3} \iint d\underline{k} d\underline{k}' \frac{g(\underline{k})g(\underline{k}')}{\sqrt{\omega\omega'}} P(\underline{k}, \underline{k}') a_{\underline{k}}^\dagger a_{\underline{k}'} e^{i(\underline{k}' - \underline{k}) \cdot \underline{r}}$$

$P(\underline{k}, \underline{k}')$  is a projection operator such that, when the nucleon is free ( $V=0$ ),  $H_I$  acts only in the 33-state. The "shell model potential" is

$$V(r) = \frac{1}{2} m \eta r^2 \text{ where } \eta = 41 A^{-1/3} \text{ MeV}$$

and  $m$  = nucleon mass. In the following we denote a free nucleon by  $N_f$  and a bound one by  $N_b$ .

The  $\pi N_f$  amplitude (for  $V=0$ ) is obtained exactly;  $\lambda$  and  $g(k)$  are determined such that  $\pi N_f$  data including the  $\Delta(1236)$  resonance are reproduced. For the  $\pi N_b$  amplitude, we obtain it in the orders of  $\lambda$  and  $\lambda^2$ , and then use the Padé approximant. [This is the only approximation in our model calculation.] For the  $\lambda^2$  term, we do the summation for intermediate nuclear states exactly. We find that the closure approximation which is often used for this summation is very misleading. In this respect it is of crucial importance to treat the nucleon recoil consistently. This point seems to have been overlooked in similar analyses done before.

For example, for  $A=16$  which simulates  $^{16}\text{O}$ , we find that; i) the resonance energy [where  $\text{Re}$  (forward scatt. amp.) = 0] is at  $\sim 160$  MeV of the pion kinetic energy in the  $\pi\text{-}^{16}\text{O}$  laboratory system. This is about 30 MeV lower than the corresponding energy for  $\pi N_f$ . ii) The total cross section at the resonance is  $\sim 300$  mb which is to be compared with  $\sim 200$  mb for  $\pi N_f$ . The elastic cross section is also enhanced for forward angles. It is thus clear that the impulse approximation is very poor for this model case. We are examining various other features of the model, and also the accuracy of the Padé approximant.

Hugh Burkhardt

Department of Mathematical Physics  
University of Birmingham, England

#### ABSTRACT

In the region above the inelastic threshold there is a continuum of amplitudes which give the same experimental observables. This is because the unitarity condition, which in the elastic region allows the determination of the complex scattering amplitude from the real cross-section ( and other observables if there is spin ), becomes only an inequality constraint which allows a continuum of angle dependent phase functions. In practice this ambiguity is usually serious, though it is often unrecognised because artificially restricted parametrisations are used to give a unique, but arbitrary solution.

Extra theoretical input of a dynamical nature can in principle remove the continuum ambiguity but, because numerical analytic continuation is always implied, only with data of absurd accuracy. Thus unique answers can only be found in practice by introducing model-dependent assumptions; it is important to recognise this and to ensure that these assumptions are as dynamically plausible as possible.

RENZO LEONARDI

I.N.F.N. Sezione di Bologna (Italy) and Facoltà di  
Scienze dell'Università, Trento (Italy)

We have discussed<sup>(1)</sup> some isospin effects in strength distributions of excitations carrying a unity of isospin on a target T (isovector excitations). In particular we have discussed the way in which the centroid energies split among the three available isospins  $T - 1$ , T,  $T + 1$ . The energy separation between these three energies is given in terms of an isoscalar, an isovector, and an isotensor effective potential. This last potential, not yet considered in the literature, has been proved to be systematic and significant in size. In order to illustrate the origin and the meaning of the isotensor potential we focus on excitations induced on a nucleus T by the transfer of two particles coupled to isospin  $\tau = 1$  (or two holes or one particle and one hole). If the indices 1 and 2 label the nucleons of the pair and  $\alpha, \beta$  label the nucleons of the target and one treats the interaction of the pair with the target perturbatively, it can be shown that 1) the isotensor potential emerges from second order effects and 2) it can be profitably expressed a) averaging on the isospin of the target b) on the isospin of the pair c) averaging on the isospin of both. We have in the three cases respectively:

$$\begin{aligned} \text{a) } V_{12} \text{ (tensor)} &= K_{12} \left[ 3(\vec{t}_1 \cdot \vec{T})(\vec{t}_2 \cdot \vec{T}) - T(T+1)(\vec{t}_1 \cdot \vec{t}_2) \right] \\ \text{b) } V_{\alpha\beta} \text{ (tensor)} &= K_{\alpha\beta} \left[ 3(\vec{t}_\alpha \cdot \vec{\tau})(\vec{t}_\beta \cdot \vec{\tau}) - \tau(\tau+1)(\vec{t}_\alpha \cdot \vec{t}_\beta) \right] \\ \text{c) } V \text{ (tensor)} &= V_t \left[ \frac{3}{2}(\vec{\tau} \cdot \vec{T})^2 + \frac{3}{4}(\vec{\tau} \cdot \vec{T}) - T(T+1) \right] \end{aligned}$$

In the zero range approximation ( $V_{1\alpha} \approx V_0 \delta(r_1 - r_\alpha)$ )  $K_{12}$ ,  $K_{\alpha\beta}$ ,  $V_t$  can be simply expressed in terms of the (microscopic) interaction strength  $V_0$ , the density distribution of the neutron excess pair of the target  $\rho_{en}$ , the density distribution of the transferred pair  $\rho$  and a mean energy denominator (generally negative) arising from perturbation theory to second order

$$K_{12} = \frac{V_0^2}{E} \rho_{en}(\vec{r}_1 \vec{r}_2), \quad K_{\alpha\beta} = \frac{V_0^2}{E} \rho(\vec{r}_\alpha \vec{r}_\beta), \quad V_t = \frac{V_0^2}{E} \int \rho(\vec{r} \vec{r}') \rho_{en}(\vec{r} \vec{r}') d\vec{r} d\vec{r}'$$

Isotensor effects can be measured remembering that

$$T(E_{T+1} - E_T) - (T+1)(E_T - E_{T-1}) = \text{pure isotensor effects}$$

(1) Submitted to Phys. Rev.



On the Interaction of Slow  $\pi$ -Mesons with Nuclei

G. G. Bunatian

Joint Institute for Nuclear Research

The  $\pi$ -meson-nuclei interaction is described with the help of the effective quasipotential  $V_{eff}$ . For  $\pi$ -mesic atoms not only commonly observed transitions (for them we have a satisfactory description) but also the binding energy  $E_{ne}$ , width  $\Gamma_{ne}$  and  $\Phi_{ne}$  function have been thoroughly investigated for different (ne) states of the  $\pi$ -meson (see for example fig.1). The  $E_{ne}, \Gamma_{ne}$  values depend on the form of the wavefunc-

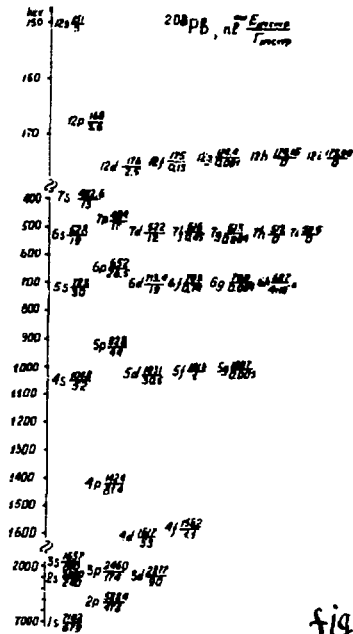


fig.1

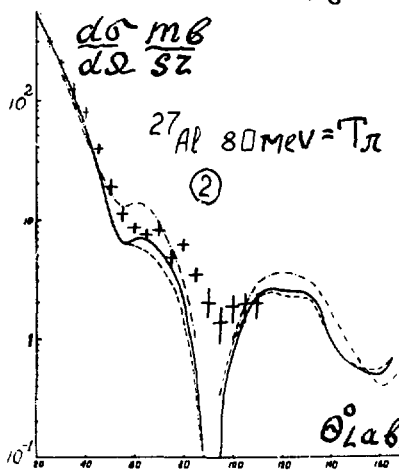


fig.2

tions which are small inside the nucleus for all states including 1S. Since the value of  $\Gamma_{ne}$ , nuclear shift in  $E_{ne}$ , is determined by the overlap of  $\Phi_{ne}$  functions with nucleus, hence it strongly depends on  $1, \Gamma_{12S} > \Gamma_{4f}, E_{4S} \approx E_{5d}$ ! We have investigated the dependence of all results on the  $V_{eff}$  parameters, in particular on nuclear density distribution (for light nuclei e.g.  $Li^6$  it is very strong). For the elastic scattering  $\pi^+, \pi^-$  on nuclei the dependence of the cross section on  $V_{eff}$  parameters has been carefully studied as well. In fig.2 the dash-point curve was obtained taking into account the Lorentz-Lorenz effect and pair absorption; the dashed curve - without considering the Lorentz-Lorenz effect, and solid curve was obtained taking into account neither Lorentz-Lorenz effect nor pair absorption. In most cases as well as in case illustrated in fig.2 the description of the experiment cannot be considered satisfactory.

I.C

## INTERMEDIATE ISOBAR CALCULATIONS

Calculation for the reaction  $K^-d \rightarrow \pi^- \Lambda p$  with two-step process

T. Ishihara, Y. Iwamura and Y. Takahashi  
Science University of Tokyo, Shinjuku-ku, Tokyo, Japan

E. Satoh  
Seikei University, Musashino-shi, Tokyo, Japan

An enhancement in the  $\Lambda p$  invariant-mass distribution near 2130 MeV has been reported from a study of the reaction  $K^-d \rightarrow \pi^- \Lambda p$  by several experimental groups. In particular, the data observed by Cline et al<sup>(1)</sup> are quite interesting; there are two peaks just below  $\Sigma N$  threshold and just above  $\Lambda N$  threshold. The physical meaning of these enhancements is not clearly understood so far partly because of the difficulties of the relativistic calculation of triangle diagram shown in fig.1.

We have applied Shapiro's model<sup>(2)</sup> to calculate the triangle diagram, here we used Hulthén type deuteron wavefunction at vertex A,  $Y_0^*(1520)$  at vertex B and Satoh's two body  $T_{\Lambda\Sigma}$  matrix<sup>(3)</sup>, in which  $\Sigma\Lambda$  conversion is explicitly taken into account, at vertex C. Then we come to conclusions;

(1) the two peaks are naturally and automatically appeared if we use the  $T_{\Lambda\Sigma}$  matrix at vertex C, (2) the positions of the two peaks are essentially depending on the  $T_{\Lambda\Sigma}$  matrix, (3) the peak just below  $\Sigma N$  threshold is due to the  $\Lambda p$  resonance (not cusp effect) which would not be able to be explained without considering  $\Sigma\Lambda$  conversion at vertex C and (4) the peak just above  $\Lambda N$  threshold is due to two-

channel final state interaction, its characteristic is included in the  $T_{\Lambda\Sigma}$  matrix. The result of our calculation is shown in fig.1 so as to compare with the experimental data by Cline et al. Calculated cross section is drawn by solid line in fig.1. The half width calculated with the parameters fitted to the cross section was estimated to be 7.1 MeV whereas Cline et al estimated to be  $\Gamma \leq 10$  MeV.

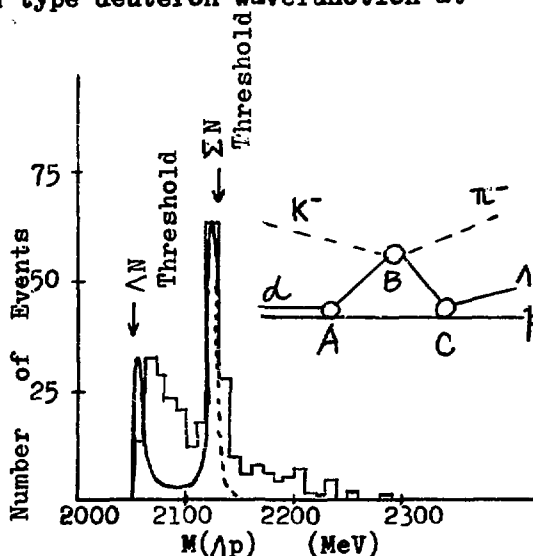


Fig. 1.  $\Lambda p$  invariant mass spectrum and triangle diagram.

1. D.Cline et al, Phys. Rev. Letters 20, 1452 (1968)
2. I. S. Shapiro, " E. Fermi " course 38, p.210 (1967)
3. E. Satoh, Nucl. Phys. B49, 489 (1972)

THE ROLE OF  $\Delta_{33}$  - ISOBARS IN PION CONDENSATION AND PION SCATTERING

G.E. Brown and W. Weise

Department of Physics, State University of New York

Stony Brook, N.Y. 11794

In an investigation of pion interactions with nuclear matter, the  $\Delta_{33}$  isobar has been introduced into a many-body description of the nuclear medium. The isobar is assumed to interact with nucleons through meson exchange mechanisms, mainly the exchange of pions and  $\rho$  mesons, supplemented by short range repulsive correlations generated by  $\omega$  mesons. Coupling constants, as far as they are not known from isobar decay, are derived from quark model considerations.

The isobar enters as an excitation channel into the pion self energy in the nuclear medium and therefore determines the response of the system to excitations carrying the quantum numbers of a pion. Two cases of interest are studied:

1. Pion condensation in dense neutron matter, which is of some relevance for neutron star dynamics. A realistic calculation of the critical density  $\rho_c$  for negative pion condensation has been carried out<sup>1</sup>, giving  $\rho_c = 2 \rho_0$  (in units of nuclear matter density,  $\rho_0 = 0.17/\text{fm}^3$ ). If isobars are not included, the critical density becomes larger than  $3 \rho_0$ . Repulsive isobar-hole correlations (mainly the Lorentz-Lorenz correction plus additional pieces due to  $\rho$  meson exchange) turn out to be extremely important. The equation of state for dense neutron matter in the presence of a pion condensate is also studied.
2. Pion scattering in nuclear matter is described in terms of the coupling of a pion to a  $T = 1$  spin-isospin mode built up by isobar-hole correlations (among which the one-pion exchange piece alone generates the conventional multiple scattering series). Self energy interactions of an isobar in the nuclear medium are estimated and found to be nearly as attractive as those of a nucleon. Neither the position nor the width of the 3.3-resonance in nuclear matter is found to undergo drastic changes due to the coupling to many-body degrees of freedom<sup>2</sup>.

## References:

1. S.-O. Backman and W. Weise, Phys. Lett. 55B, 1 (1975)
2. G.E. Brown and W. Weise, in preparation.

Leonard S. Kisslinger and Gerald A. Miller  
Carnegie-Mellon University, Pittsburgh, Pa. 15213

## ABSTRACT

The single pion production process  $(p, \pi)$  is an especially promising one for exploring new aspects of nuclear structure. The momentum transfer at the  $\pi$ -production threshold is about  $2.5 \text{ fm}^{-1}$  so that for the single nucleon mechanism one deals with high momentum components of nuclei. It has recently been shown<sup>1</sup> that by using new developments in the treatment at the pion optical potential, it is possible to calculate the known  $(p, \pi^+)$  cross sections with satisfactory agreement with experiment. Here we make use of these theoretical developments for  $(p, \pi^+)$  to study the  $(p, \pi^-)$  reaction, where quite different physics enters.

For momentum transfers of  $\geq 2 \text{ fm}^{-1}$  one can expect not only to explore the high momentum components of ordinary nuclear wave functions, but also to begin to be sensitive to meson degrees of freedom. The main point is that nuclear vertex functions for nucleon transfer drop very quickly for momentum transfer  $\geq 2 \text{ fm}^{-1}$  while the high spin and angular momentum properties for baryon resonance transfers provide relatively large high momentum components, especially at the nuclear surface.

The  $(p, \pi^-)$  should be especially promising for exploring  $\Delta^{++}$  components of nuclei because the reaction can proceed via a single  $\Delta^{++}$  transfer mechanism. In the present work we use an isobar model in which the baryon resonances are treated on the same footing as nucleons.<sup>2</sup> For the deuteron, the  $\Delta$ - $\Delta$  components have been calculated in perturbation theories and in coupled-channel calculations. However, adequate quantitative techniques for handling the many body problem have not yet been developed. Hence a qualitative model based on perturbation calculations<sup>3</sup> is used. The overall normalization is the biggest uncertainty. We observe that nuclear collective modes involving spin and isospin will play a dominant role, so that the role of baryon resonances is deeply involved with interesting nuclear structure physics.

In order to assess the utility of the  $(p, \pi^-)$  reaction in learning about  $\Delta^{++}$  components, it is necessary to evaluate the cross sections for the "ordinary nuclear" or "background" processes which compete. We consider the following terms: proton charge exchange  $(p, n)$  followed by an  $(n, \pi^-)$  reaction; emission of a  $\pi^0$   $(p, \pi^0)$  followed by a pion charge exchange reaction  $(\pi^+, \pi^-)$ . These should be the main background processes. Distorting optical potentials must be used for all of these processes.

Estimates of the cross sections at several energies are made. As the energy increases from threshold, the  $\Delta^{++}$  transfer processes stand out from the background. Even with  $\Delta$  probabilities as small as .0001, the  $\Delta$  transfer process can compete with the ordinary background charge exchange reactions at medium and high energies. Furthermore, there is strong dependence on  $N^*$  spectroscopy so that by choosing suitable nuclei one can get excellent tests of the baryon resonance models.

\*Supported in part by the National Science Foundation.

1. G. A. Miller, Nucl. Phys. A 224, 269 (1974); G. A. Miller and S. C. Phatak, Phys. Letters 51B, 129 (1974).
2. S. Jena and L. S. Kisslinger, Ann. Phys. (N.Y.) 85, 251 (1974).
3. R. Schaeffer, L. S. Kisslinger, and E. Rost, to be published.

M. Dillig, M. G. Huber

Inst. for Theor. Physics, Univ. of Erlangen-Nürnberg, Germany

The excitation of a bound nucleon into the  $N^*(1236)$  resonance has been investigated in a particle hole model<sup>1,2)</sup> for the case of light nuclei. It turns out that interesting features are expected to occur such as a collective shift of the center of gravity of the excitation spectrum and a (possible) fine structure, which might be detectable in reactions under appropriate kinematical conditions. The details of the collective excitation spectrum depend on the structure of the target nucleus and the strength of the  $N^*$ -interaction.

First steps towards a quantitative investigation of the model mentioned above have been performed:

1.  $A(\Delta N)$  interaction has been derived on the basis of a One-Boson-Exchange-Model (with the exchange of  $\pi, \eta, \omega, \rho$  mesons); a consistent set of coupling constants could be obtained from different models (especially from the quark model);
2. the binding energy of an  $N^*(1236)$  in light nuclei has been calculated, including 1<sup>st</sup> and 2<sup>nd</sup> order contributions. It turns out, that a corresponding single particle potential for a  $\Delta$  in a nucleus is comparable or somewhat stronger than the single particle potential for a nucleon.
3. The width of a bound  $N^*$  has been calculated in 1<sup>st</sup> order perturbation theory for the  $\pi N, N, \pi, NN$  channels. At least for these channels the total widths of an  $N^*$  is significantly reduced compared to  $\Gamma_{\text{free}} \approx 120$  MeV. An estimation of the  $\pi NN$  channel is in progress.
4. An estimation of collective effects resulting from the  $N\Delta$  residual interaction is under way.

The results of the calculations are compared to experimental data available for light nuclei (deuteron and  $^4\text{He}$ ). The investigation of those collective excitations of the nuclear  $(3,3)$  resonance may lead towards a better understanding of both the  $NN^*$  interaction and the properties of the nuclear many body problem.

1. M. Dillig, M. G. Huber, Phys. Lett. 48B, 417 (1974)
2. M. Dillig, M. G. Huber, "Mesonic Effects and Nuclear Structure" (Ed. K. Bleuler, Wissenschaftsverlag, Mannheim, p. 80 (1975))

E. Rost

Nuclear Physics Laboratory, Department of Physics and Astrophysics  
University of Colorado, Boulder, Colorado 80302

## ABSTRACT

In view of the current interest in nuclear isobars in a nuclear physics context, a semi-phenomenological calculation was performed considering NN\* admixtures in the deuteron for all presently accepted N\* isobars. The Reid hard core potential was used for the NN components with its intermediate range attraction modified by the presence of the NN\* components. The renormalized strength of the intermediate range attraction was treated as the eigenvalue in a coupled-channel bound state system, the deuteron binding energy being constrained to equal the measured value of 2.225 MeV. The interactions coupling the NN\* with the NN components and the diagonal NN\* interactions were generated by a generalized OPEP potential with coupling constants directly obtained in terms of experimental  $N^* \rightarrow \pi N$  widths. The results of the coupled channel calculations yield several NN\* amplitudes in the 0.1-0.3% range with a total NN\* admixture of about 1.5%. Some of the NN\* components are rather large at high momenta and thus may be observable in high momentum transfer processes.

William A. Friedman\*

University of Wisconsin, Madison, WI 53706

Recent studies of an isobar-doorway model for  $\pi$ -nucleus reactions in the (3,3) resonance region suggest an effective t-matrix appropriate for use in a multiple scattering treatment. Due to nuclear effects, this amplitude differs from the free  $\pi$ -N amplitude. Past discussion has centered on the shift in the resonance energy. We suggest that the amplitude should also have an additional width, which has a simple physical interpretation, and which can have a marked influence on the cross sections.

The additional width, designated as  $\Gamma^\downarrow$ , arises from the shortening of the life-time of the  $\Delta$ -resonance due to  $\Delta$ -N collisions. Its source is thus analogous to the atomic phenomenon of collision broadening. We estimate  $\Gamma^\downarrow$  by

$$\Gamma^\downarrow = \hbar c (P_\pi / m_\Delta c) \rho \sigma_{\Delta N}, \quad (1)$$

where  $P_\pi$  is the momentum of the incoming  $\pi$ ,  $\rho$  is the average nuclear density, and  $\sigma_{\Delta N}$  is effective  $\Delta$ -N cross section. The additional width provides a reduced amplitude at resonance, ( $t^{\text{eff}} = (\Gamma_{\pi N} / (\Gamma_{\pi N} + \Gamma^\downarrow)) t^{\text{free}}$ ).

Using the data for the  $\pi$ -d total cross section, the optical theorem, and an assumption that single scattering (with  $t^{\text{eff}}$ ) dominates the forward scattering amplitude, we estimate, for the deuteron,  $\Gamma^\downarrow \approx 16 \text{ MeV} \ll 110 \text{ MeV} = \Gamma_{\pi N}$ . With electron scattering estimates of  $\rho$ , we obtain, from Eq. (1), the value of 160 mb for  $\sigma_{\Delta N}$ . It is then possible to estimate  $\Gamma^\downarrow$  for other nuclei, e.g., 65 MeV for  $^{12}\text{C}$ , and 80 MeV for  $^{32}\text{S}$ . These values are of the same order as  $\Gamma_{\pi N}$ .

We obtain the following simple empirical relationship which fits the maxima in the measured total cross sections for nuclei with  $2 \leq A \leq 32$ :

$$\sigma_{\pi A}^{\text{max}} \sim (\alpha/A)^{1/3} (\Gamma_{\pi N} / (\Gamma_{\pi N} + \Gamma_A^\downarrow)) (k_{\pi N}^{\text{max}} / k_{\pi A}^{\text{max}})^2 A \sigma_{\pi N}^{\text{max}}. \quad (2)$$

Here, the first factor ( $\alpha \approx 1.7$ ) provides for absorption shadowing, the second involves the effect of broadening; the third is a kinematic factor necessitated by shifts in the momentum for the maxima; and the final factor is the simple single scattering result. (The widths are energy dependent; those given above are their values at the resonant energy.)

The line shape of the  $\pi$ -A resonance is determined by considerations in addition to  $\Gamma_{\pi N} + \Gamma^\downarrow$ . The absorptive shadowing varies with the energy: Off resonance,  $\sigma_{\pi A} \sim A \sigma_{\pi N}$ ; while at the resonance peak the result is given by Eq. (2). The peak is suppressed relative to the wings, giving an apparent broadening. If shadowing is not accounted for,  $\Gamma^\downarrow$  would have to be much larger to fit the data, e.g.,  $\Gamma^\downarrow \approx 200 \text{ MeV}$  for  $^{12}\text{C}$ .

Finally we note that the existence of  $\Gamma^\downarrow$  might decrease the pion absorption in multiple-scattering calculations and hence improve the agreement between theoretical and experimental total cross sections for charge-exchange reactions.

\*Supported in part by the National Science Foundation.



MODIFICATION OF THE  $\Delta$ -PROPAGATOR IN NUCLEAR MATTER\*

F. Lenz, E. J. Moniz and K. Yazaki  
Massachusetts Institute of Technology

We have studied various modifications of the  $\pi N$  3-3 resonance in nuclear matter. Our starting assumption is that of an elementary isobar coupled to the P-wave  $\pi N$  system. We calculate the isobar self-energy and fix the free parameters (the isobar bare mass and the  $\pi N \Delta$  coupling constant and interaction range) to the 3-3 scattering amplitude. With this model, we evaluate the self energy for an isobar at rest inside nuclear matter. Differences from the free self energy arise because of Pauli blocking, distortion of the pion propagator through an optical potential, and hard-core correlations. The isobar mass is defined by the zero of the real part of the  $\Delta$ -propagator, and we find an upward shift in nuclear matter (depending upon the specific model, this shift can be 10-20 Mev). Above the resonance energy, the imaginary part of the self energy is decreased. Such effects provide a correction to the  $(e, e')$  and total photoabsorption cross sections in the relevant energy region.

\* Work supported in part by the U. S. Atomic Energy Commission.

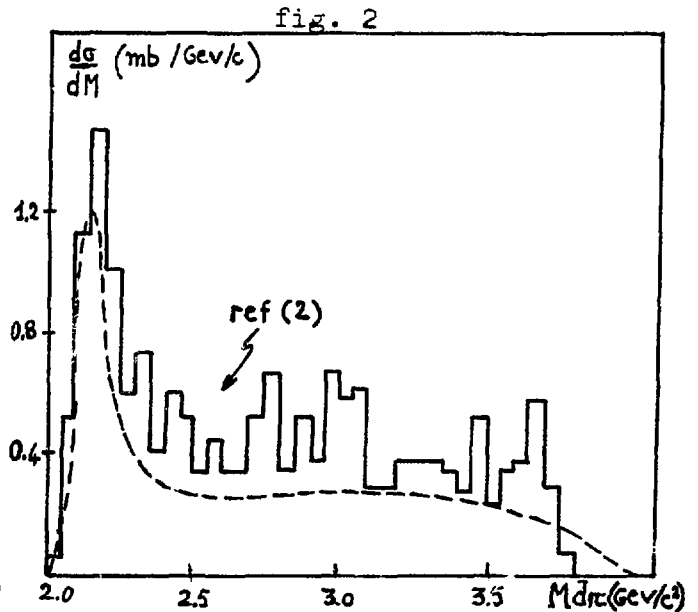
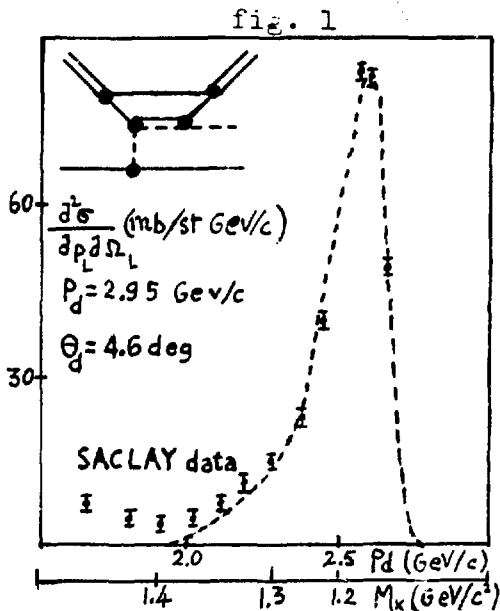
R. Baldini-Celio, F.L. Fabbri, G. La Rosa and P. Picozza  
 Laboratori Nazionali di Frascati del CNEN, Frascati, Italy

We present a calculation of the differential cross section for the process  $D+p \rightarrow D+X$  at the kinematical conditions of the Saclay-Caen-Frascati experiment<sup>(1)</sup>, where data show a very sharp peak, at small momentum transfer, corresponding at a  $M_X$  invariant mass of  $\sim 1200$  MeV, in a pure  $I=1/2$  isospin state. In this calculation the deuteron is treated following the impulse approximation and the nucleon-nucleon interaction is assumed to be dominated by one pion exchange with  $\Delta_{33}(1236)$  excitation in the deuteron according to the graph in Fig. 1. No arbitrary normalization is made and the agreement with the experimental data, as is shown in Fig. 1, is very good. This model provides also an enhancement in the  $D-\pi$  invariant mass, to be connected with the well known  $D^*(2200)$  effect, seen in many experiments. A prediction, without arbitrary normalization, is reported for the process  $\bar{p}+D \rightarrow D+\bar{n}+\pi^-$  at  $P_D=5.5$  GeV/c. In Fig. 2 is shown a comparison with experimental data<sup>(2)</sup>, normalized to the total experimental cross section, which is satisfactory, taking into account at these energies other mechanisms may contribute.

Moreover this calculation has been extended for polarized deuterons. Sizeable effects are provided. For example, in the Saclay experiment kinematical conditions, for  $\theta_D=7^\circ$ , we get at the peak:  $(d\sigma_{\perp}-d\sigma)/d\sigma \approx -15\%$  and  $(d\sigma_{\parallel}-d\sigma)/d\sigma \approx +30\%$ , being  $d\sigma$ ,  $d\sigma_{\perp}$  and  $d\sigma_{\parallel}$  the differential cross sections respectively for deuterons unpolarized and polarized with spin projection 1 and 0 normally to the scattering plane.

(1) - J. Banaigs et al., Phys. Letters 45B, 535 (1973).

(2) - H. Braun et al., CBH 73/2 (1973).



I.D

$\pi$ -NUCLEUS INTERACTIONS

F. Balestra, L. Busso, R. Garfagnini and G. Piragino.

Istituto di Fisica dell'Università, Istituto Nazionale di Fisica Nucleare, Sezione di Torino, Italy.

R. Barbini, C. Guaraldo and R. Scrimaglio

Laboratori Nazionali di Frascati del CNEN, Frascati, Italy.

F. Cannata

Istituto di Fisica dell'Università, Bologna, Italy.

Measurements and analysis have been made of the differential cross section in the process  $(\pi^{\pm}, ^{12}\text{C})$  ref. (1), and  $(\pi^{\pm}, ^{12}\text{C})$  with incident energies from 60 up to 90 MeV of the pion beam of the LEALE Laboratory of Frascati and in the angular region  $160^{\circ} \div 180^{\circ}$  laboratory angle. The experimental apparatus is described in ref. (2).

The data are compared with elastic differential cross sections calculated with the optical potential of ref. (3), in which the contribution of the nucleon momenta constitutes a longitudinal current that is non-zero and reduces by a factor (1/2) the terms containing the Laplacian of the density in the new Kisslinger potential of ref. (4), thus recovering the result of Mach, ref. (5). The cross sections calculated with the quoted potential are in better agreement with the experimental data than previous calculation with potential of ref. (4) and ref. (6).

References: (1) R. Barbini et al., Lett. Nuovo Cimento **12**, 359 (1975).

(2) F. Balestra et al., N.I.M. **119**, 347 (1974).

(3) F. Cannata et al., Phys. Rev. C **10**, 2093 (1974).

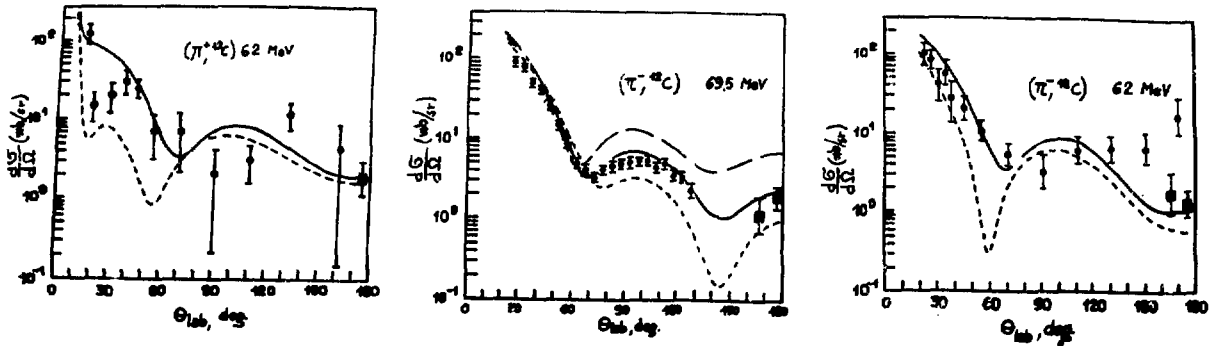
(4) S. Kisslinger and F. Tabakin, Phys. Rev. C, **9**, 188 (1974).

(5) R. Mach, Nucl. Phys. **A205**, 56 (1973).

(6) M. Ericson and T.E.O. Ericson, Ann. Phys., **36**, 323 (1966).

(7) R.M. Edelstein et al., Phys. Rev., **122**, 252 (1961).

(8) Byfield et al., Phys. Rev., **86**, 17 (1952).



$(\pi^{\pm}, ^{12}\text{C})$  elastic differential cross sections  $\frac{d^2\sigma}{d\Omega d\Omega'}$  (mb/sr)

Elastic differential cross sections at 69.5 and 62 MeV. In the figures are plotted our large angle data with 69.5 MeV  $\pi^+$  data of ref. (7) and 62 MeV  $\pi^+$  data of ref. (8). The solid curves were calculated using the optical potential of ref. (3). The long dashed curve was calculated with the potential of ref. (4). The short dashed curves were calculated with the potential of ref. (6).

Particle	Angular bin lab. syst.	Pion kinetic energy (MeV)		
		65 ± 5	75 ± 5	85 ± 5
$\pi^+$	160°-170°	2.19 ± 1.08	0.64 ± 0.27	0.70 ± 0.46
			0.22 ± 0.17	0.75 ± 0.44
$\pi^-$	170°-180°	1.40 ± 0.47	1.39 ± 0.35	0.42 ± 0.38
			1.12 ± 0.42	0.58 ± 0.32

R. Barbini, C. Guaraldo and R. Scrimaglio.  
Laboratori Nazionali di Frascati del CNEN, Frascati, Italy.

F. Balestra, L. Busso, R. Garfagnini and G. Piragino.  
Istituto di Fisica dell'Università, Istituto Nazionale di Fisica Nucleare, Sezione di Torino, Italy.

We have measured, with the pion beam of the LEALE Laboratory of Frascati, the  $(\pi^{\pm}, {}^{12}\text{C})$  backward inelastic differential cross sections, at the pion energies 60-90 MeV, in the experiment described in ref. (1). The experimental apparatus (2) consists in a magnetic spectrometer with a self shunted streamer chamber (3) for identifying scattering events, by detecting both the incident and scattered pion tracks. The resolution of the apparatus turned out to be less than 2% in the energy range considered, sufficient to clearly separate the 4.43 MeV level, the group of levels around 10 MeV and the group of levels starting at 15 MeV. As far as the 7.66 MeV level is concerned, our apparatus is fully able to separate it from the 9.63 MeV level for incident pion energies less than about 70 MeV, while it is at its resolution limits near 90 MeV. We took advantage of the redundancy of parameters measured for each event for statistically assigning each event to the inelastic channels. In tables are reported differential cross sections corresponding to excitation by negative and positive pions of the individual nuclear levels or groups of levels of  ${}^{12}\text{C}$ . Excitation of the 7.66 MeV level is of the same order of magnitude of the others. The differential cross sections for the over-all excitation of the group of levels around 15 MeV are larger than the others, according to the first data of Baker et al. (4). References: (1) R. Barbini et al., Lettere Nuovo Cimento **12**, 359 (1975).

(2) F. Balestra et al., N.I.M. **119**, 347 (1974).

(3) F. Balestra et al., N.I.M. **125**, (1975).

(4) W. Baker et al., P.R. **112**, 1763 (1958).

$(\pi^{\pm}, {}^{12}\text{C})$  INELASTIC DIFFERENTIAL CROSS SECTIONS  $\frac{d\sigma}{d\Omega} \text{ (mb/sr)}$ .

$(\pi^{\pm}, {}^{12}\text{C})$  INELASTIC DIFFERENTIAL CROSS SECTION  $\frac{d\sigma}{d\Omega} \text{ (mb/sr)}$ .

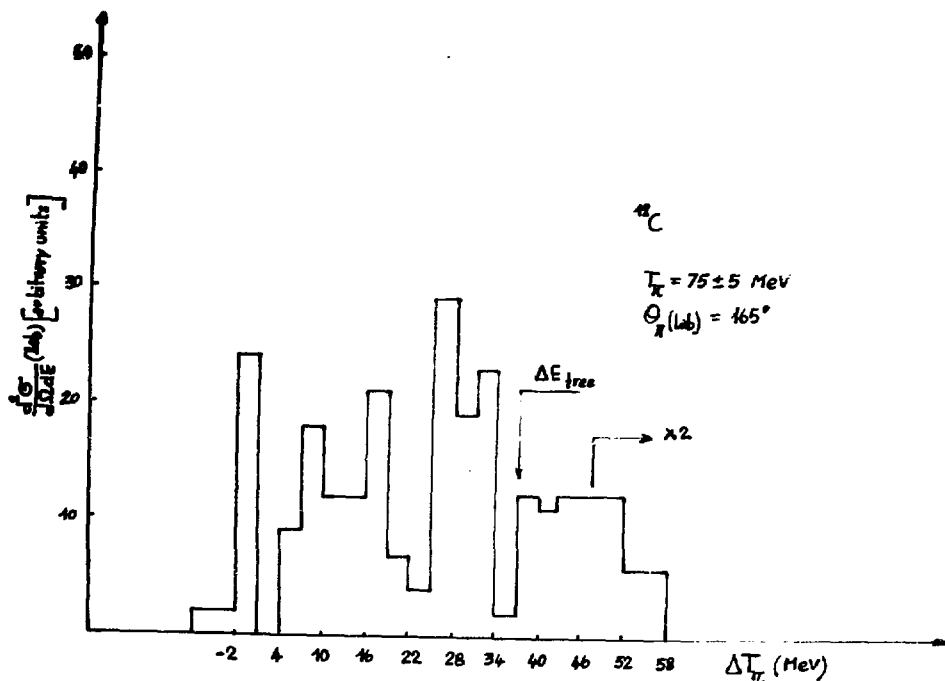
LEVEL ${}^{12}\text{C}$	Angular bin (lab. syst.)	Pion Kinetic Energy (MeV)			Level ${}^{12}\text{C}$	Angular bin (lab. syst.)	Pion Kinetic energy (MeV)		
		75 $\pm$ 5	85 $\pm$ 5	95 $\pm$ 5			65 $\pm$ 5	75 $\pm$ 5	85 $\pm$ 5
4.43 MeV	160 $^{\circ}$ - 170 $^{\circ}$	0.23 $\pm$ 0.18	0.30 $\pm$ 0.23		4.43 MeV	160 $^{\circ}$ - 170 $^{\circ}$	1.28 $\pm$ 0.75	0.47 $\pm$ 0.22	0.64 $\pm$ 0.50
	170 $^{\circ}$ - 180 $^{\circ}$	0.87 $\pm$ 0.37	0.63 $\pm$ 0.31			170 $^{\circ}$ - 180 $^{\circ}$	0.37 $\pm$ 0.25	0.61 $\pm$ 0.24	0.44 $\pm$ 0.31
7.66 MeV	160 $^{\circ}$ - 170 $^{\circ}$	1.05 $\pm$ 0.83	0.62 $\pm$ 0.37		7.66 MeV	160 $^{\circ}$ - 170 $^{\circ}$	0.40 $\pm$ 0.34	0.26 $\pm$ 0.16	0.50 $\pm$ 0.42
	170 $^{\circ}$ - 180 $^{\circ}$	0.53 $\pm$ 0.26	0.59 $\pm$ 0.30			170 $^{\circ}$ - 180 $^{\circ}$	0.34 $\pm$ 0.24	0.77 $\pm$ 0.27	0.43 $\pm$ 0.28
9.63 MeV	160 $^{\circ}$ - 170 $^{\circ}$	0.48 $\pm$ 0.32	0.73 $\pm$ 0.40		9.63 MeV	160 $^{\circ}$ - 170 $^{\circ}$	0.37 $\pm$ 0.33	0.36 $\pm$ 0.17	0.47 $\pm$ 0.37
	170 $^{\circ}$ - 180 $^{\circ}$	0.55 $\pm$ 0.26	0.99 $\pm$ 0.39			170 $^{\circ}$ - 180 $^{\circ}$	0.60 $\pm$ 0.32	0.86 $\pm$ 0.27	0.55 $\pm$ 0.30
15 MeV	160 $^{\circ}$ - 170 $^{\circ}$	0.70 $\pm$ 0.44	1.33 $\pm$ 0.56	1.78 $\pm$ 1.78	15 MeV	160 $^{\circ}$ - 170 $^{\circ}$	1.45 $\pm$ 0.69	1.22 $\pm$ 0.41	0.88 $\pm$ 0.36
	170 $^{\circ}$ - 180 $^{\circ}$	0.95 $\pm$ 0.39	1.40 $\pm$ 0.49	2.08 $\pm$ 1.13		170 $^{\circ}$ - 180 $^{\circ}$	2.21 $\pm$ 0.89	1.45 $\pm$ 0.36	1.63 $\pm$ 0.51

$(\pi^{\pm}, {}^{12}\text{C})$  BACKWARD INELASTIC SCATTERING AT INTERMEDIATE ENERGIES: VIRTUAL STATES AND QUASI-FREE SCATTERING

R. Barbini, C. Guaraldo and R. Scrimaglio  
Laboratori Nazionali di Frascati del CNEN, Frascati, Italy.

F. Balestra, L. Busso, R. Garfagnini and G. Piragino.  
Istituto di Fisica dell'Università, Istituto Nazionale di Fisica Nucleare, Sezione di Torino, Italy.

We have analyzed the energy distribution of  $\pi^{\pm}$  inelastically backward scattered from  ${}^{12}\text{C}$ , obtained for pion incident energies from 60 up to 90 MeV, in the experiment<sup>(1)</sup> performed at the LEALE Laboratory of Frascati. A typical inelastic spectrum for 75 MeV  $\pi^{-}$  at  $165^{\circ}$  laboratory angle is shown in Figure. The form of the spectrum is roughly in accord with quasi-free scattering, modified by bound and virtual states at small energy loss. At low energy loss there are binding effects: the ground state and the individual levels or group of levels of  ${}^{12}\text{C}$ . At intermediate energies, the excitation of a structure between 20 MeV and 35 MeV can be positively identified in the excitation of the electric-dipole giant resonance: the corresponding differential cross sections have been calculated. We discuss the possibility that the same excitation energy may also correspond to the kinematics of elastic scattering of the  $\pi$  meson by an  $\alpha$  particle, in the three  $\alpha$ -particle model of  ${}^{12}\text{C}$ : the corresponding differential cross sections have been calculated. The high energy loss region of the spectrum is broad peak, which resembles the form expected for quasi elastic  $\pi N$  scattering. The spectra are compared with the similar ones observed by other authors with pions and with protons. References: (1) R. Barbini et al., Let. Nuovo Cimento **12**, 359 (1975).



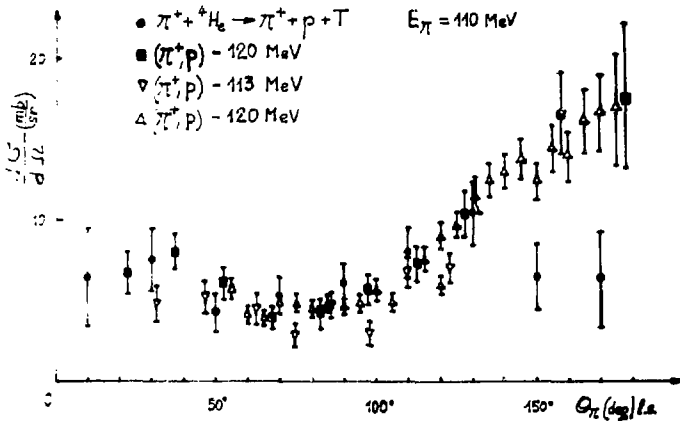
F. Balestra, L. Busso, R. Garfagnini, G. Piragino and A. Zanini.

Istituto di Fisica dell'Università, Istituto Nazionale di Fisica Nucleare, Sezione di Torino, Italy.

R. Barbini, C. Guaraldo and R. Scrimaglio.

Laboratori Nazionali di Frascati del CNEN, Frascati, Italy.

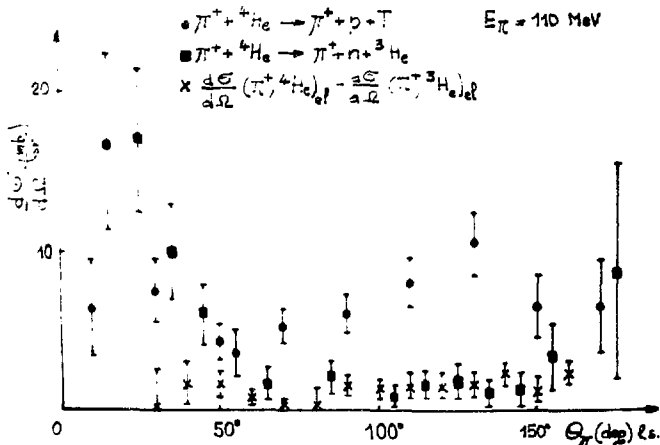
We have measured the  $(\pi^+, {}^4\text{He})$  interaction at  $110 \pm 11$  MeV with a diffusion cloud chamber filled with helium at 15 atm in a magnetic field, ref. (1), exposed to the pion beam of the LEALE Laboratory of Frascati. The value of the total inelastic (reaction and absorption) cross section is  $192 \pm 11$  mb. We have analyzed all the inelastic interactions. In Figures are reported angular behaviours of the reactions:  $\pi^+ + {}^4\text{He} \rightarrow \pi^+ + p + \text{T}$  and  $\pi^+ + {}^4\text{He} \rightarrow \pi^+ + n + {}^3\text{He}$  which represent, respectively, the 44% and the 17% of total inelastic events. A preliminary analysis of angular distributions gives some indication on a single scattering mechanism. References: (1) L. Busso et al., N.I.M., 102, 1 (1972).



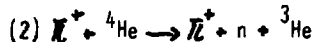
Differential cross section for the reaction



versus  $\theta_\pi$ , pion scattered angle, at 110 MeV pion energy. In the Figure are also plotted, for comparison  $(\pi, p)$  elastic differential cross sections in the same energy region (data are from CERN Report CERN-HERA 69-1, 1969).



Differential cross sections for the reactions



versus  $\theta_\pi$ , pion scattered angle, at 110 MeV pion energy. In the Figure is also plotted, for comparison with (2), the difference between the elastic differential cross sections of  $\pi^+$  on  ${}^4\text{He}$  and  ${}^3\text{He}$  at 100 MeV (Dubna-Torino collaboration).

$(\pi^+ + {}^4\text{He})$  INELASTIC SCATTERING AT 160 MeV.

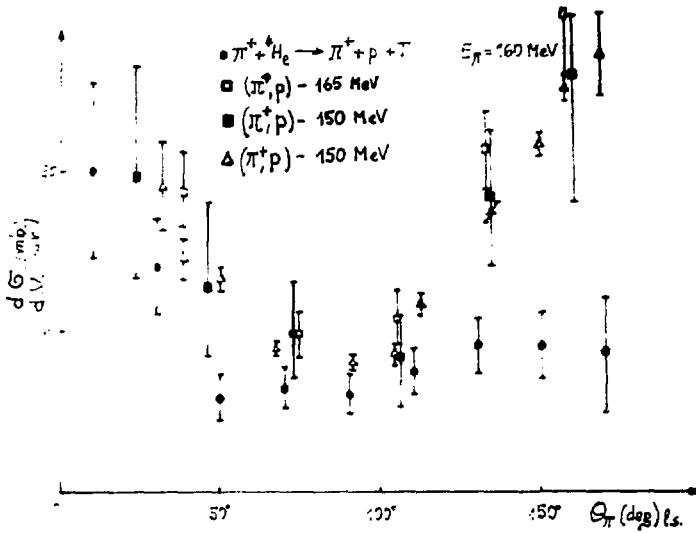
F. Balestra, L. Busso, R. Garfagnini, G. Piragino and A. Zanini.

Istituto di Fisica dell'Università, Istituto Nazionale di Fisica Nucleare, Sezione di Torino, Italy.

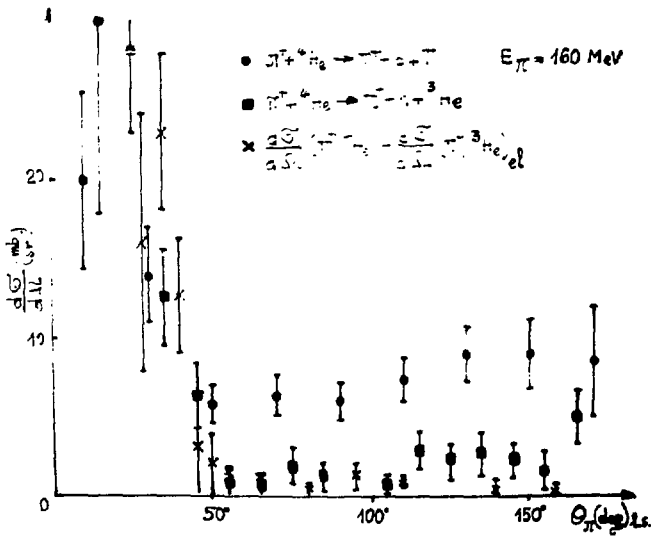
R. Barbini, C. Guaraldo and R. Scrimaglio

Laboratori Nazionali di Frascati del CNEN, Frascati, Italy.

We have measured the  $(\pi^+ + {}^4\text{He})$  interaction at  $160 \pm 18$  MeV with a diffusion cloud chamber filled with helium at 15 atm in a magnetic field<sup>(1)</sup>, exposed to the pion beam of the LEALE Laboratory of Frascati. The value of the total inelastic (reaction and absorption) cross section is  $232 \pm 11$  mb. We have analyzed all the inelastic interactions. In Figures are reported angular behaviours of the reactions:  $\pi^+ + {}^4\text{He} \rightarrow \pi^+ + p + \text{T}$  and  $\pi^+ + {}^4\text{He} \rightarrow \pi^+ + n + {}^3\text{He}$  which represent, respectively, the 44% and the 18% of total inelastic events. A preliminary analysis of angular distributions gives some indication on a single scattering mechanism. References: (1) L. Busso et al., N. I. N., 102, 1 (1972).



Differential cross section for the reaction  $\pi^+ + {}^4\text{He} \rightarrow \pi^+ + p + \text{T}$  versus  $\theta_\pi$ , pion scattered angle, at 160 MeV pion energy. In the Figure are also plotted, for comparison,  $(\pi^+, p)$  elastic differential cross sections in the same energy region (data are from Giacomelli et al., CERN-HERA 69-1, 1969).



Differential cross sections for the reactions  
 (1)  $\pi^+ + {}^4\text{He} \rightarrow \pi^+ + p + \text{T}$   
 (2)  $\pi^+ + {}^4\text{He} \rightarrow \pi^+ + n + {}^3\text{He}$   
 versus  $\theta_\pi$ , pion scattered angle, at 160 MeV pion energy. In the Figure is also plotted, for comparison with (2), the difference between the elastic differential cross section on  ${}^4\text{He}$  and  ${}^3\text{He}$  at 154 MeV (Dubna-Torino collaboration).

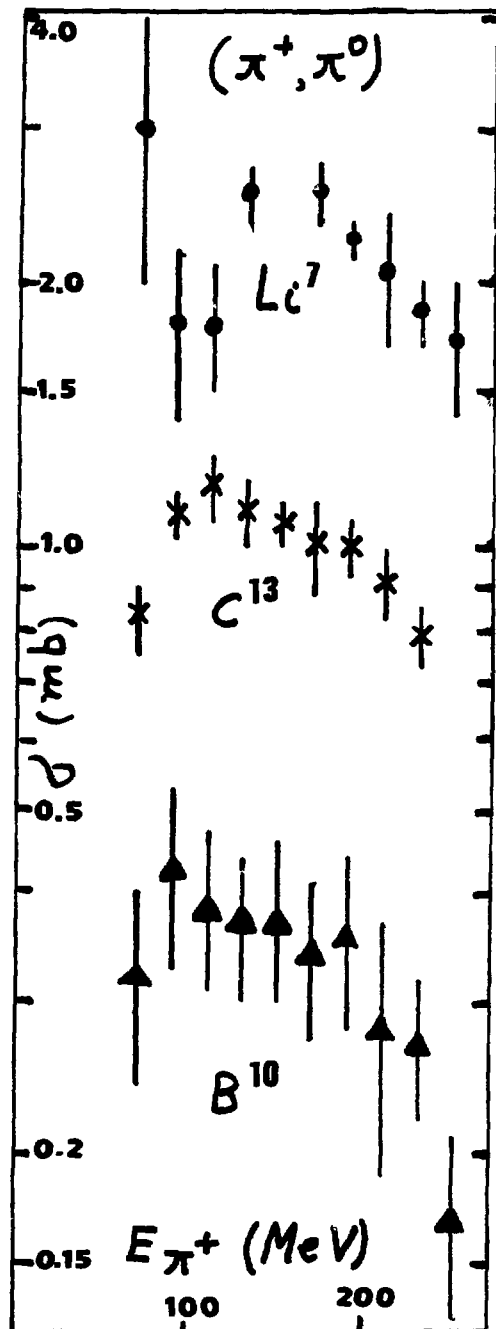


Measurements of  $\pi^\pm$  Nucleus Total Cross Sections at Energies Below 200 MeV.

G. BURLESON, and K. JOHNSON, New Mexico State Univ./LASL  
J. CALARCO, Stanford Univ.  
M. COOPER, D. HAGERMAN, H. MEYER, and R. REDWINE, LASL  
I. HALPERN, L. KNUTSON, and R. MARRS, Univ. of Washington  
M. JAKOBSON and R. JEPPESEN, Univ. of Montana

Measurements have been made of total cross sections for  $\pi^\pm$  on various nuclei, using the Low Energy Pion Channel of LAMPF. Pions were selected with either a DISC or a time-of-flight system, and standard transmission techniques were used, with both scintillation counters and wire proportional counters. The statistical precision was generally  $\sim 2-3\%$ . The data include measurements on  $^4\text{He}$  between 26 and 105 MeV, on the isotope sets ( $^{12}\text{C}$ ,  $^{13}\text{C}$ ), ( $^{16}\text{O}$ ,  $^{18}\text{O}$ ), and ( $^{40}\text{Ca}$ ,  $^{44}\text{Ca}$ ,  $^{48}\text{Ca}$ , with natural Ti) between 85 and 200 MeV, and on 18 nuclei with  $4 \leq A \leq 208$  at 85 MeV. Preliminary results indicate that the additional scattering per extra neutron is much less in the Ca isotopes than in the C or O isotopes than would be expected on the basis of an  $A^{2/3}$  dependence, and that the A dependence at 85 MeV, on the low energy side of the resonance, is generally characterized by  $\sigma \sim A^{0.8}$  with  $\sigma(\pi^-)/\sigma(\pi^+) \sim 1.4$  for all A.

The  $(\pi^+, \pi^0)$  reaction for light nuclei in the (3,3) resonance region  
 Y. Shamai, J. Alster, E. D. Arthur, D. Ashery, S. Cochavi, D. M. Drake,  
 M. A. Moinester, and A. I. Yavin  
 Tel Aviv University and LASL



We studied the reaction  $(\pi^+, \pi^0)$  on  ${}^7\text{Li}$ ,  ${}^{10}\text{B}$ , and  ${}^{13}\text{C}$  from  $E_{\pi^+} = 70$  to 250 MeV, at the LEP-channel of LAMPF. The cross sections were obtained by measuring the radioactive decay of the product nuclei following the  $(\pi^+, \pi^0)$  reaction. The cross sections are thus integrated over all angles and include the contributions of all particle bound states of the product nuclei. Thus for the reaction on  ${}^{13}\text{C}$  we measured the cross section to the isobaric analog state only, for  ${}^{10}\text{B}$  the cross section to two states which are not IAS, and for  ${}^7\text{Li}$  the cross section to one IAS and one excited IAS. The figure shows that there is a slight, broad maximum centered around 150 MeV. The errors in the figure are statistical only. At the present stage of data analysis there is still a 20% uncertainty in the absolute values of the cross sections. Our preliminary estimates for nucleon charge exchange by secondary protons in the target could lower the  $(\pi^+, \pi^0)$  cross section by 10 to 20%. The IAS transitions are much stronger than other transitions. The larger cross section in  ${}^7\text{Li}$  compared to  ${}^{13}\text{C}$  is consistent with a smaller absorption in the lighter nucleus. The results for IAS transitions do not agree with published calculations which include absorption.

Robert A. Eisenstein and Gerald A. Miller  
Carnegie-Mellon University, Pittsburgh, Pa. 15213

## ABSTRACT

We study<sup>1</sup> the reaction in which the annihilation of a pion in a collision with a nucleus results in a final state consisting of a deuteron and a residual nucleus. The present availability of good pion beams as well as a high resolution detector to measure the energy of the final deuteron, hence the final nuclear state, presents the opportunity for performing an accurate experiment.<sup>2</sup>

There are several features of this reaction which make it unique. The dominant characteristic is the high momentum transfer inherent in converting the sum of the mass and kinetic energy of the pion into the kinetic energy of the emitted high energy deuteron. Furthermore, this process presents a different kinematic situation than the more typical ( $\pi$ ,NN) reaction in which the absorption of a low energy meson results in the emission of two nucleons with approximately equal and opposite momenta. In that reaction, the high momentum components of the relative wave function of the pair are stressed. In the present case, it is the high momentum components of the center-of-mass wave function of the pair which are important.

We assume that the pion interacts with two of the target nucleons by being absorbed on either one. Thus our interaction Hamiltonian, H, is

$$H = \sqrt{\frac{4\pi}{2hE}} \frac{f}{u} i \left[ e^{ik \cdot x_1} \sigma_1 \cdot k_1 \tau_1 \cdot \phi + e^{ik \cdot x_2} \sigma_2 \cdot k_2 \tau_2 \cdot \phi \right] \quad (1)$$

where the subscripts refer to the nucleon on which the pion is absorbed. The transition rate is just the matrix element of H between the initial T=1 bound pair and the final outgoing deuteron plus two-hole state. From (1) we note that the initial state may have S=1 or S=0. In the present calculations plane waves are used to describe the motion of the incident pion and outgoing deuteron.

We have examined the reaction at incident pion energies of 50 and 100 MeV. For these energies the spin flip term of (1) is dominant. We find considerable sensitivity to both the radial and angular momentum parts of the initial di-nucleon wavefunction. Configuration mixing gives a large collective enhancement to the cross section. The kinematics of the reaction are such that there is little sensitivity to the short range behavior of the di-nucleon wavefunction.

The magnitude is about tens of microbarns and should be observable under experimental conditions at LAMPF. However, a full distorted wave calculation is needed and is presently being carried out by us and by Benz and Kerman at MIT.

## REFERENCES

1. R. A. Eisenstein and G. A. Miller, to be published May 1975, Physical Review C.
2. P. D. Barnes et al., LAMPF Proposal 140 (1973).

FORWARD ELASTIC SCATTERING AMPLITUDES FOR  $\pi^+$  FROM  $^{12}\text{C}$  AND  $^{40}\text{Ca}$ \*

M. Warneke, L. Y. Lee, B. W. Mayes,  
E. V. Hungerford, and J. C. Allred  
University of Houston, Houston, Tx. 77004

N. Gabitzsch, J. Hudomalj-Gabitzsch, D. Mann, T. Witten,  
T. Williams, G. S. Mutchler, and G. C. Phillips  
Rice University, Houston, Tx. 77001

## ABSTRACT

Elastic differential cross sections in the angular region from  $5^\circ$  to  $22^\circ$  were measured at five energies, [90-210 MeV], spanning the pion nucleon (3,3) resonance for  $\pi^+$  on  $^{12}\text{C}$  and  $^{40}\text{Ca}$ . Total cross sections were also measured for these targets at the same energies. The data were taken on the  $P^3$  channel of the Los Alamos Meson Physics Facility. Pion trajectories and momenta were calculated from a system of multi-wire proportional counters, multistrip scintillators and counters and magnets. The nuclear ( $f_S$ ) and Coulomb ( $f_C$ ) amplitudes interfere at small angles. The magnitude of the interference is proportional to the ratio of the real ( $\text{Re } f_S(0^\circ)$ ) and imaginary ( $\text{Im } f_S(0^\circ)$ ) parts of the forward elastic  $\pi$ -nucleus scattering amplitude.  $\text{Im } f_S(0^\circ)$  can be obtained from the total cross section via the optical theorem.  $\text{Re } f_S(0^\circ)$  derived from the data will be compared with the results of optical model calculations and, in the case of  $^{12}\text{C}$ , with dispersion relation calculations.

\*Supported by U.S. E.R.D.A.

Abstract

VI International Conference on High Energy Physics and Nuclear Structure  
June 8-14, 1975

I.D.10

Alpha and Multinucleon Removal from  $^{58}\text{Ni}$  and  $^{60}\text{Ni}$  by Fast Pions,\*  
H. E. JACKSON, D. G. KOVAR, I. MEYER-SCHÜTZMEISTER, J. P. SCHIFFER, S. VIGDOR, T. P. WANGLER, Argonne National Lab., R. E. SEGEL, ANL and Northwestern, R. L. BURMAN, P. A. M. GRAM, D. M. DRAKE, LASL, R. B. CLARK, Texas A & M, B. C. COOK, Iowa State, and V. G. LIND, E. N. HATCH, O. H. OTTESON, R. E. MCADAMS, Utah State.  
-As has been shown in earlier experiments, the interaction of fast pions with complex nuclei shows unexpectedly large multi-nucleon removal cross sections with indications of a favoring of the removal of one or more  $\alpha$  particles. In an effort to obtain information on the nature of the reaction mechanism responsible for these effects we have performed an extensive series of measurements for targets of  $^{58}\text{Ni}$  and  $^{60}\text{Ni}$  in which the removal cross sections were studied as a function of projectile type, charge, and energy. Measurements at LAMPF were made using beams of 200-MeV protons, 100 and 220-MeV  $\pi^+$ 's and 220-MeV  $\pi^-$ 's and at ZGS using 370-MeV  $\pi^-$  beams. A comparison of 220-MeV  $\pi^+$  and  $\pi^-$  on  $^{58}\text{Ni}$  shows striking similarities in the distribution of isotopes produced. Both the average number of nucleons removed and the average ratio of neutron removal to proton removal is independent of pion charge. There is no significant difference between data for 100-MeV  $\pi^+$  and 220-MeV  $\pi^+$ . In contrast, there is a clear energy dependence in the results for 100<sup>1</sup> and 200-MeV protons. Protons seem less effective than pions of the same energy for removing nucleons. While nuclei which could result from a removal are seen with relatively large cross sections,  $\gamma$ -rays from neighboring nuclei are also observed with substantial strength. Results for even nuclides are shown in the table below.

Production cross sections (mb) from $^{58}\text{Ni}$ Target								
Nucleus Produced \ Projectile	$^{56}\text{Fe}$	$^{54}\text{Fe}$	$^{52}\text{Cr}$	$^{50}\text{Cr}$	$^{48}\text{Ti}$	$^{46}\text{Ti}$	$^{42}\text{Ca}$	$\Sigma\sigma$ iden.
$\pi^+$ (100-MeV)	25	34	20	44	7	23	6	301
$\pi^+$ (220-MeV)	38	47	20	40	6	34	10	365
$\pi^-$ (220-MeV)	28	43	39	46	16	33	13	326
P (220-MeV)	29	44	15	26	4	9	<2	232
P (100-MeV) <sup>1</sup>	84	19	12	6	4	0.5	..	146

The lack of an energy dependence shown by the distribution of residual nuclides for pions in contrast to the obvious sensitivity to proton energy suggests that the pion rest mass contributes to these processes and that the pions are absorbed. However, the lack of dependence on the charge of the pions suggests that the pion is not absorbed.

\* Supported by the USAEC and NSF.

<sup>1</sup> C. C. Chang, N. S. Wall, and Z. Fraenkel, PRL 33, 1493 (1974).

Systematics of Fast Pion Induced Processes in Complex Nuclei, \*

R. E. SEGEL, Northwestern and Argonne National Laboratory, H. E. JACKSON, D. G. KOVAR, L. MEYER-SCHÜTZMEISTER, S. VIGDOR, and T. P. WANGLER, Argonne National Laboratory, J. P. SCHIFFER, University of Chicago and Argonne National Laboratory, V. G. LIND, E. N. HATCH, O. H. OTTESON, and R. E. MC ADAMS, Utah State, R. L. BURMAN, P. A. M. GRAM, and D. M. DRAKE, Los Alamos Scientific Laboratory and B. C. COOK, Iowa State—Ge(Li) detectors have been used to measure prompt gamma rays produced by bombarding various targets with 100-MeV  $\pi^+$ , 220 MeV  $\pi^\pm$ , 380 MeV  $\pi^-$ , and 200 MeV protons. Special care was taken to determine absolute cross sections which, in several cases, disagree with published values. The absolute incident flux was measured by integrating the current in a phototube which viewed a plastic scintillator through which the beam passed. The integrated current was calibrated at low beam intensity against the number of beam particles counted in a coincidence telescope which included a second phototube viewing the same scintillator. Dead time was measured by triggering a pulser with the scattered beam and comparing the number of triggers with the pulser peak in the spectrum. Gamma-ray energy resolution was about 3 keV. Good quality spectra were obtained in 3–6 hours. Gamma-ray lines have been identified corresponding to total cross sections between 200 and 600 mb, depending on the projectile and target nucleus. The cross section for producing nuclei differing from the target by one or more alpha particles with 220-MeV  $\pi^-$  is  $\leq 80$  mb for  $^{40}\text{Ca}$  and  $\sim 130$  mb for the Ni isotopes. The combined cross section for t,  $\alpha$ , or t +  $\alpha$  removal from  $^{27}\text{Al}$  (with 100-MeV  $\pi^+$ ) is  $\sim 65$  mb, for t and t +  $\alpha$  removal with 220-MeV  $\pi^-$  from  $^{51}\text{V}$   $\sim 105$  mb. Alpha removal from  $^{40}\text{Ar}$  (with 380 MeV  $\pi^-$ ) is  $\sim 12$  mb while with 220-MeV  $\pi^-$  no evidence was found for either t removal from  $^{93}\text{Nb}$  or  $\alpha$  removal from  $^{138}\text{Ba}$ , though for these latter two cases the limits are rather poor. For targets up to and including Ni, other even reaction products are seen with cross sections usually  $\sim 1/2$  those in the  $\alpha$  or (t+ $\alpha$ ) removal chain. Identification of transitions in odd or odd-odd nuclei is more difficult but where identification of transitions in odd nuclei has been made, these cross sections are comparable to those for adjacent even nuclei. For Al and V the centroid of product nuclei corresponds roughly to the removal of equal numbers of neutrons and protons. For S, Ca, and  $^{58}\text{Ni}$ , proton removal is slightly favored while for  $^{60}\text{Ni}$  neutron removal is somewhat stronger. Neutron removal dominates the Ar products while for  $^{93}\text{Nb}$  the most prominent lines, after inelastic scattering, correspond to  $^{88}\text{Zr}$  (p + 4n removal) with a cross section of  $\approx 100$  mb and to  $^{84}\text{Sr}$  (p +  $\alpha$  + 4n removal) with  $\approx 60$  mb. From  $^{138}\text{Ba}$ ,  $^{128}\text{Xe}$  (2p + 8n) and  $^{126}\text{Xe}$  (2p + 10n) are seen with  $\sim 85$  and  $\sim 81$  mb respectively.

\*Supported by the USAEC and NSF.

CHARGED PION SCATTERING ON  $^4\text{He}$  NUCLEI IN THE  
ENERGY RANGE FROM 68 TO 208 MeV

L.Alexandrov, T.Angelescu, I.V.Falomkin, M.M.Kulyukin,  
V.I.Lyashenko, R.Mach, A.Mihul, Nguyen Minh Kao, F.Nichitiu,  
G.B.Pontecorvo, V.K.Saricheva, M.Semergieva, Yu.A.Shcherba-  
kov, N.I.Trosheva, T.M.Troshev

Joint Institute for Nuclear Research - Dubna  
F.Balestra, L.Busso, R.Garfagnini, G.Piragino  
Istituto di Fisica dell' Università di Torino  
Istituto Nazionale di Fisica Nucleare - Sezione  
di Torino

New data on differential cross sections for elastic scattering of charged pions on the  $^4\text{He}$  nucleus are presented. Data have been obtained using a high pressure streamer chamber exposed at the JINR synrocyclotron.

Measurements have been performed at 98, 135, 145 and 156 MeV for both negative and positive pions and at 120, 174 and 208 MeV for negative pions.

An energy independent phase shift analysis has been performed for each energy and the total elastic cross section dependence on energy is given.

Total and differential elastic cross sections are compared with optical model computations using Kisslinger and Laplace potentials.

The results of an energy dependent phase shift analysis are also given.

$\pi^\pm$  ELASTIC SCATTERING ON  ${}^3\text{He}$  NUCLEI IN THE  
ENERGY RANGE FROM 68 TO 208 MeV

T. Angelescu, I.V. Falomkin, M.M. Kulyukin, V.I. Lyashenko,  
R. Mach, A. Mihai, Nguyen Minh Kao, F. Nichitiu, G.B. Pontecorvo,  
V.K. Saricheva, M. Semergieva, Yu.A. Shcherbakov,  
N.I. Trosheva, T.M. Troshev

Joint Institute for Nuclear Research - Dubna  
F. Balestra, L. Busso, R. Garfagnini, G. Piragino  
Istituto di Fisica dell' Università di Torino  
Istituto Nazionale di Fisica Nucleare - Sezione  
di Torino

Differential cross sections for the elastic scattering of both charged pions on  ${}^3\text{He}$  nuclei are given for 68, 98, 120, 135, 145 and 156 MeV. In addition  $\pi^-$   ${}^3\text{He}$  elastic scattering differential cross sections are given for 198 and 208 MeV. All the experimental data have been obtained using a high pressure streamer chamber exposed at the JINR synrocyclotron.

The differential cross sections are compared with the results of an optical model calculation using Kisslinger and Laplace potentials, taking into account the nucleus spin and isospin. Total elastic cross sections and their dependence on energy are discussed.

A phase shift analysis has been performed with the phase shift values, for high partial waves, fixed by the optical model.

The  $\pi$   ${}^3\text{He}$  coupling constant estimated according to the Chew-Low theory for  $\pi$   ${}^3\text{He}$  scattering is also presented.



PRODUCTION OF  $^{24}\text{Na}$  FROM THE IRRADIATION OF PHOSPHORUS, SULFUR AND  
CALCIUM BY 70 - MeV  $\pi^\pm$

N. Yanaki, D. Ashery, S. Cochavi and A.I. Yavin  
Department of Physics and Astronomy, Tel-Aviv University,  
Tel-Aviv, Israel; and Centre d'Etude Nucléaire de Saclay.

The secondary  $\pi^+$  and  $\pi^-$  beams from the electron linear accelerator at Saclay were used to irradiate natural targets of Phosphorus, Sulfur and Calcium at  $E_\pi = 70$  MeV. The activated targets were investigated after the irradiation with the help of a shielded Ge(Li) detector. 2754 keV and 1368 keV gamma rays from the produced  $^{24}\text{Na}$  nuclei were measured. The cross sections for the production of  $^{24}\text{Na}$  are shown in the table, where only the statistical errors are included.

It is interesting to note that the cross sections for  $\pi^-$  are larger than the respective cross sections for  $\pi^+$  by about a factor of six. This is probably caused by pion absorption, which in the case of  $\pi^-$  interaction with these target nuclei is likely to cause predominantly the emission of several alpha particles. (Absorption of  $\pi^+$  in these target nuclei can produce  $^{24}\text{Na}$  only if several protons are emitted as well).

TABLE: cross section for production of  $\text{Na}^{24}$   
with  $E_\pi = 70$  MeV.

Target	Pion Beam	Cross Section (m.b.)
Ca	$\pi^-$	$3.4 \pm 1.1$
Ca	$\pi^+$	$< 0.6$
S	$\pi^-$	$15.2 \pm 0.6$
S	$\pi^+$	$2.4 \pm 0.3$
P	$\pi^-$	$37.5 \pm 1.2$
P	$\pi^+$	$6.8 \pm 1.1$

THE REACTION  $^{16}_0(\pi^+, p)^{15}_0$  AT 70 MeV

D. Bachelier, J. L. Boyard, T. Hennino, J. C. Jourdain, P. Radvanyi and  
M. Roy-Stéphan

Institut de Physique Nucléaire, B. P. n°1. 91406, Orsay, (France)

We give here the first results of an experiment presently being performed on the  $^{16}_0(\pi^+, p)^{15}_0$  reaction with a 70 MeV pion beam of the Saclay linear electron accelerator. The simplest mechanism for such a reaction would be a neutron pick-up leading mainly to the two hole states of  $^{15}_0$ : the 6.18 MeV state  $(p3/2)^{-1}$  and the ground state  $(p1/2)^{-1}$ ; these states should then be excited with a ratio of about 2 as in ordinary medium energy  $(p, d)$  and  $(^3\text{He}, \alpha)$  reactions.

The energy of the outgoing protons (maximum energy 185 MeV) is measured with a range telescope consisting of a variable carbon absorber and of 13 plastic scintillators. This allows the coverage of 16 MeV excitation energy of the residual nucleus per measurement; the total energy resolution achieved in practice is 3.2 MeV. A  $\Delta E/\Delta x$  discrimination on the first three scintillators and a lead shielding allow a good rejection of parasite particles. The flux of incident pions is measured with a monitor telescope, at  $90^\circ$  to the beam, previously calibrated at low intensity with in-beam detectors. The  $^{16}_0$  target is a cell filled with water. The energy calibration of the range telescope has been checked with the incident pions and with the ground state protons of the  $^{12}_6(\pi^+, p)^{11}_6$  reaction at 70 MeV.

The first results have been obtained at proton angles of  $25^\circ$ ,  $35^\circ$ ,  $45^\circ$ ,  $55^\circ$  and  $105^\circ$ . The cross-section corresponding to the 6.18 level, which at  $25^\circ$  is of the order of  $40 \mu\text{b}/\text{sr}$ , decreases by a factor of only about 4.5 from  $25^\circ$  to  $55^\circ$ . It is remarkable that the ratio of the cross-sections corresponding to the 6.18 MeV and to the ground state is larger than 10 at all angles. A peak is also observed at about 11.5 MeV excitation energy, which might be the first  $T = 3/2$  state of  $^{15}_0$ .

One might possibly consider a different behaviour for the wave functions of  $3/2^-$  and  $1/2^-$  neutrons in  $^{16}_0$  at very high momenta (around  $3\text{fm}^{-1}$ ). However these results all seem in disagreement with a simple neutron pick-up model; a mechanism involving at least two nucleons of the target nucleus would seem more appropriate.

CHARGED PARTICLE EMISSION FROM NUCLEI BOMBARDED WITH 235 MEV PIONS AND 800 MEV PROTONS.† J. F. Amann, P.D. Barnes, M. Doss, S. A. Dytman, R. A. Eisenstein, J. A. Penkrot, and A. C. Thompson, CARNEGIE-MELLON UNIV., Pittsburgh, Pa. 15213.

The mechanism by which energy and momentum are transferred to a nucleus in a high energy scattering event has been studied extensively for the case of incident protons.<sup>1</sup> Particle emission spectra for outgoing p, d, t, <sup>3</sup>He, <sup>4</sup>He particles have been observed as well as Li through S ions in very energetic (5 GeV) collisions.<sup>2</sup> Although both the pre-compound model of Griffin and intra-nuclear cascade calculations give reasonable agreement with the lower energy part of the emitted proton spectra, they underestimate the higher energy proton cross sections and all the complex particle cross sections.<sup>1</sup> An attempt to calculate the inflight pion induced proton emission spectra in the intra-nuclear cascade model has been reported<sup>3</sup>, but no data was available for comparison. The observed singles gamma ray spectra induced by stopped and inflight pions and protons have been discussed in terms of the removal of one or more "α clusters". Low energy (<25 MeV) alpha emission has been observed<sup>4</sup> for 70 MeV π on Al.

We have made a direct measurement at LAMPF of the cross section at 90° for p, d, t, <sup>3</sup>He and <sup>4</sup>He emission induced by 235 MeV positive pions and 800 MeV protons from ~500 mg/cm<sup>2</sup> targets of Mg, Ni, and Ag. The detector system was a four-element telescope consisting of two Si surface barrier detectors (250 μ and 500 μ thick) followed by a dual crystal intrinsic Ge spectrometer (3 cm thick). With this system we had excellent particle identification and were able to measure proton (α particle) spectra from 20(50) MeV up to 110(400) MeV with a resolution of 1-10 MeV determined by the target thickness. The beam energy spread was ±20 MeV. The solid angle (6.5 msr), detection efficiency and effects of energy loss in the target were determined from Monte Carlo calculations. The absolute cross-section should be determined to ±20%.

For all targets with either pion or proton bombardment, the various particle emission spectra were characterized by an exponential fall-off of the type  $d^2\sigma/d\Omega dE = N_0 \exp(-bp_n^2)$ , where  $p_n$  is the momentum per nucleon. For pions the slope parameter  $b$  increases with outgoing particle mass  $A$  but is roughly independent of target mass  $A_T$ . The parameter  $N_0$  decreases rapidly with  $A_0$  but increases slowly with  $A_T$ ; e.g. Ni gives  $b \propto A_0^{3/2}$  with a much larger value of  $b$  than suggested by the proton emission calculations of Harp *et al.*<sup>3</sup> Their characterization of pion absorption is apparently not correct. Our results are similar to calculated spectra for 250 MeV proton bombardment of Ni. We are investigating whether a pick-up mechanism could explain the large number of complex particles detected.

- (1) J. M. Miller, Proc. of the Int. Conf. on Nucl. Phys., Munich, North Holland, p.597 (1973); H. Feshbach, *ibid.* p.631; K. Chen *et al.*, Phys. Rev. C4, 2234 (1971); C.K. Cline, Nucl. Phys. A193, 417 (1972).
- (2) R. Korteling and C. Toren, Phys. Rev. C7, 1611 (1973).
- (3) G. D. Harp *et al.*, Phys. Rev. C8, 581 (1973).
- (4) A. Doron *et al.*, Phys. Rev. Letters 34B, 485 (1975) and reference cited.

† Work supported through ERDA contract AT(11-1)-3244.

ELASTIC SCATTERING OF 50 MeV  $\pi^+$  FROM  $^{12}\text{C}^\dagger$ -- J. F. Amann, P. D. Barnes, M. Doss, S. A. Dytman, R. A. Eisenstein, J. Penkrot, A. C. Thompson, CARNEGIE-MELLON UNIV., Pittsburgh, Pa. 15213.

A beam from the LEP channel at LAMPF was used for this experiment. The C-MJ intrinsic Ge spectrometer<sup>1</sup> detected the scattered  $\pi$ 's. The results are shown below with the predicted angular distributions from the Kisslinger<sup>2</sup> (K) potential and the separable Londergan, McVoy, Moniz<sup>3</sup> (LMM) potential. These potentials are constructed from the free  $\pi$ -N phase shifts; the resulting minima are much deeper and further backward than the data. The local Laplacian<sup>4</sup> (LL) model (not shown) yields similar results. When the complex parameters  $b_0$  and  $b_1$  are varied in the K and LL models (holding the matter radius fixed at  $1.64F$ ), good fits are obtained. However, K violates unitarity slightly, and LL, while satisfying unitarity, produces  $\pi$ 's in some regions of the nucleus. The fits determine  $\text{Re}(b_0)$  and  $\text{Re}(b_1)$  with higher precision than  $\text{Im}(b_0)$  and  $\text{Im}(b_1)$ . (See table).

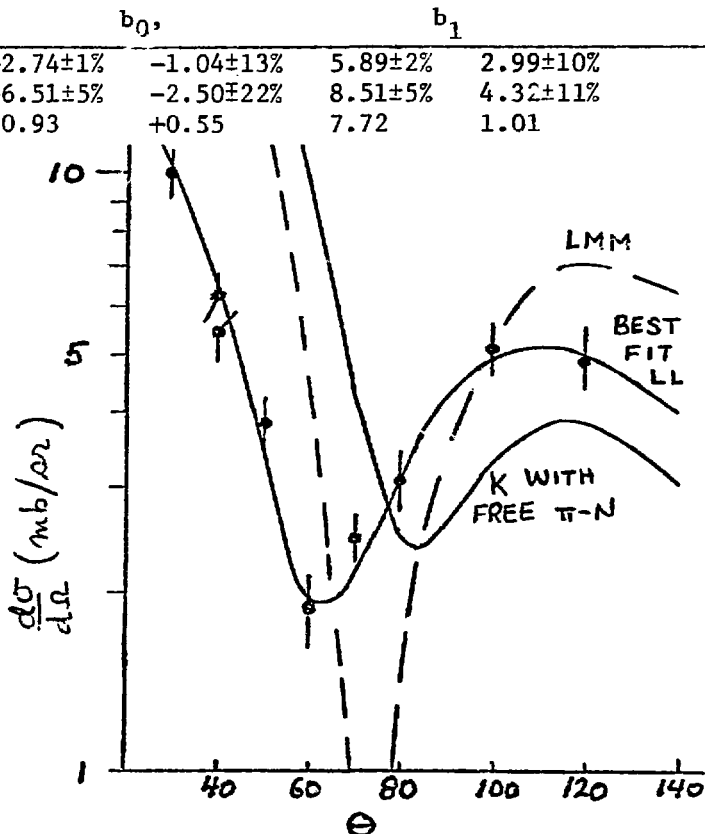
We have reexamined the 30.2 MeV  $\pi^+$ - $^{12}\text{C}$  data<sup>5</sup> and reach similar conclusions. Both K and LL (with the free  $\pi$ -N parameters) produce minima further backward and much deeper than the data. Fairly good fits can be obtained if  $b_0$  and  $b_1$  are varied; again the real parts are better determined than the imaginary. While our fit is better than ref.(5) both it and LL violate unitarity slightly.

These findings differ from analyses<sup>6</sup> at higher energies where simple K and LL models give fairly good fits to the data with no unitarity problems. Failure of these models at 30 and 50 MeV is probably due to breakdown of the simplifying assumptions made in their derivation, namely low nucleon density, no nucleon binding and no nucleon Fermi motion.

Energy	Model	$\chi^2$	$b_0$		$b_1$	
50 MeV	K	7.24	$-2.74 \pm 1\%$	$-1.04 \pm 13\%$	$5.89 \pm 2\%$	$2.99 \pm 10\%$
	LL	6.28	$-6.51 \pm 5\%$	$-2.50 \pm 22\%$	$8.51 \pm 5\%$	$4.32 \pm 11\%$
	Free $\pi$ -N values		-0.93	+0.55	7.72	1.01

1. J. Amann, *et al.*, Nucl. Inst. Meth. (to be pub.)
2. L. Kisslinger, Phys. Rev. 98 (1955) 761.
3. J. Londergan, K. McVoy, E. Moniz, Ann. Phys. 86 (1974) 147.
4. e.g. H. Lee, H. McManus, Nucl. Phys. A167 (1971) 257.
5. J. Marshall, M. Nordberg, R. Burman, Phys. Rev. C1 (1970) 1685.
6. M. Sternheim, E. Auerbach Phys. Rev. Letters 25 (1970) 1500.

† Work supported by ERDA contract AT(11-1) 3244.



RECOIL MOMENTA DISTRIBUTIONS AND  $\gamma$  RAY YIELDS  
FROM PION REACTIONS WITH C, N, Na, S, AND Ca\*

I.D.18

C. E. Stronach and C. M. Dennis  
Virginia State College, Petersburg, Va. 23803

W. J. Kossler and H. O. Funsten  
College of William and Mary, Williamsburg, Va. 23185

B. J. Lieb and W. F. Lankford  
George Mason University, Fairfax, Va. 22030

H. S. Plendl  
Florida State University, Tallahassee, Fla. 32306

The interaction of pions with a number of nuclei has been studied at the SREL<sup>1</sup> synchrocyclotron through observation of the  $\gamma$  ray spectra taken with a Ge(Li) detector in prompt coincidence with incident pions. Yields and cross sections for production of the excited states have been measured and will be presented.

By measuring the Doppler broadening of de-excitation photopeaks of states of daughter nuclei produced in pion-nucleus interactions, the recoil momentum distributions of these nuclei can be determined<sup>2</sup>. After making corrections for detector resolution and slowing down of the nuclei<sup>3</sup>, if any, the mean recoil momenta were extracted for states of daughter nuclei produced by  $\pi^-$  absorption on <sup>14</sup>N, <sup>32</sup>S, and <sup>40</sup>Ca, and those produced by the interaction of 190 MeV  $\pi^+$  with <sup>40</sup>Ca. Broadened peaks in the  $\pi^- + ^{40}\text{Ca}$  spectrum include the first excited states of <sup>36</sup>Ar (336 MeV/c) and <sup>28</sup>Si (286 MeV/c). The first excited state of <sup>28</sup>Si (87.5 mb) in the  $\pi^+ + ^{40}\text{Ca}$  spectrum displays a mean recoil momentum of 400 MeV/c.

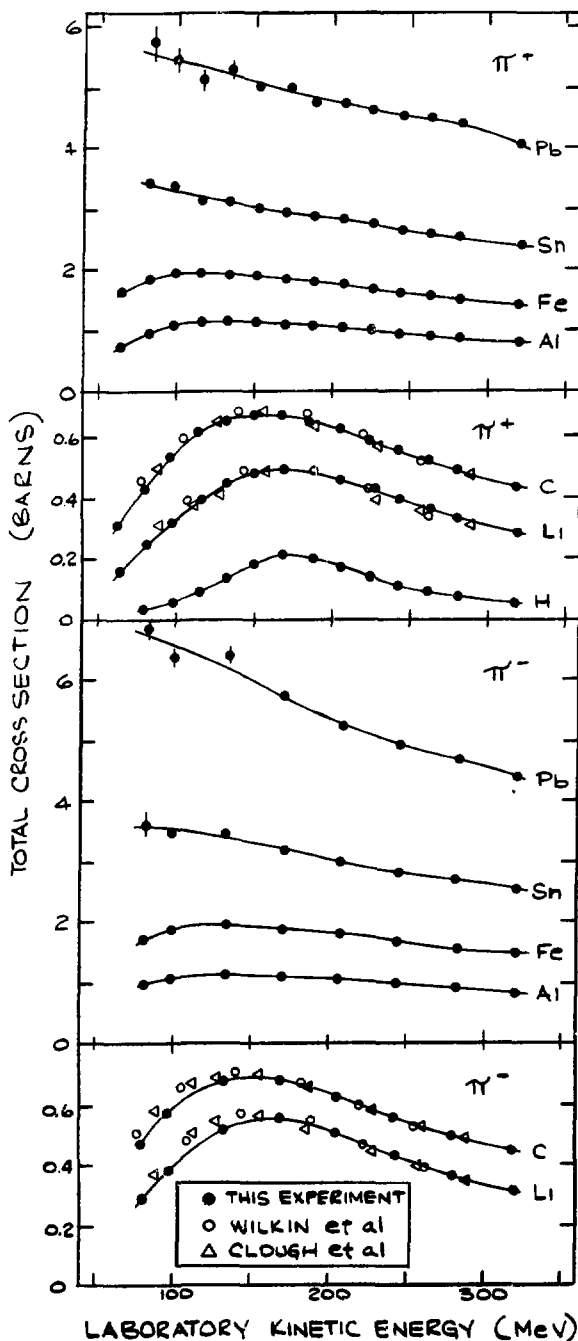
The gross features of the  $\gamma$  spectra from  $\pi^-$  absorption on <sup>32</sup>S and <sup>40</sup>Ca have been interpreted as consisting of a sum of overlapping Compton edges, for some of which the photopeaks were also observed. The theoretical Compton cross sections were used to unfold the observed spectra. After making corrections for prompt background these spectra were summed to obtain an average of about four  $\gamma$  rays per stopped  $\pi^-$ .

\* This work is supported by NASA grant NGR 47-014-006 and NSF grant NSF-GP-42001.

1. SREL is supported by NSF, NASA, and the Commonwealth of Virginia.
2. W. J. Kossler, H. O. Funsten, B. A. MacDonald, and W. F. Lankford, Phys. Rev. C4, 1551 (1971).
3. C. W. Lewis, submitted to Nuclear Instruments and Methods (1974).

\*  
 PION-NUCLEUS TOTAL CROSS SECTIONS IN THE (3,3) RESONANCE REGION

A. S. Carroll, I-H. Chiang, C. B. Dover, T. F. Kycia,  
 K. K. Li, P. O. Mazur, D. N. Michael, P. M. Mockett,\*\*  
 D. C. Rahm and R. Rubinstein\*\*\*  
 Brookhaven National Laboratory, Upton, New York 11973



Using the intense pion beam of the Brookhaven AGS, we have performed transmission measurements of total cross sections for natural targets of Li, C, Al, Fe, Sn and Pb between 160-440 MeV/c lab momentum. Most of the targets were 6" x 6" and ~ 5gr/cm<sup>2</sup> thick. A fixed four-momentum transfer from  $7 \times 10^{-4}$  to  $5 \times 10^{-3}$  GeV/c<sup>2</sup> was covered at each momentum. Considerable care was taken to determine various experimental corrections, such as multiple scattering in the target, finite spot size and pion decay.

The Coulomb and Coulomb-nuclear interference contributions, obtained from an optical model calculation, were subtracted from the data. The resulting "nuclear" cross sections are shown in the figure. The solid curves are drawn to guide the eye. For Li and C, there is good agreement with previous measurements.<sup>1</sup> A Laplacian optical potential linear in the nuclear density was used, but with a modified resonance form for the  $\pi N$  (3,3) channel. A mass dependent increase of both the elementary resonance energy and width was used.<sup>2</sup> This improves the agreement with the data, as compared to a Fermi-averaged free space amplitude, which leads to a peak position which is too low in energy.

## REFERENCES

- \* Work supported by Energy Research and Development Administration.  
 \*\* Present Address: University of Washington, Seattle, Washington 98195  
 \*\*\* Present Address: National Accelerator Laboratory, Batavia, Illinois 60510  
 1. A.S. Clough *et al.*, Nucl. Phys. **B76**, 15 (1974); C. Wilkin *et al.*, Nucl. Phys. **B62**, 61 (1973).  
 2. C.B. Dover and R.H. Lemmer, Phys. Rev. **C7**, 2312 (1973).

$\pi^-$ - ${}^4\text{He}$  SCATTERING AROUND THE  ${}^{3/2}, {}^{3/2}$  RESONANCE

F. Binon, P. Duteil, M. Gouanère, L. Hugon, J. Jansen, J.-P. Lagnaux,  
H. Palevsky, J.-P. Peigneux, M. Spighele and J.-P. Stroot

IISN (Belgium) - IPN (Orsay) Collaboration

$\pi^-$ - ${}^4\text{He}$  scattering has been measured at the CERN SC with the double achromatic spectrometer already used for  $\pi^-$ - ${}^{12}\text{C}$  scattering measurements. Results were obtained for (i) the elastic differential cross-section between  $10^\circ$  and  $180^\circ$  at 110, 150, 180, 220 and 260 MeV; (ii) the scattering at very forward angles (between  $\sim 4^\circ$  and  $20^\circ$ ) at 110, 180 and 260 MeV; (iii) the total cross-section at eleven energies between 67 and 285 MeV.

The total cross-section is maximum at about 160 MeV. The real part of the forward scattering amplitude goes through zero around 180 MeV. Two minima are observed in the angular distributions. The first one, which takes place at nearly constant angle  $\theta_{\text{cm}} \simeq 75^\circ$ , is deepest at 220 MeV. It is probably connected to the zero of the non-spin-flip  $\pi$ -N amplitude. The second one which appears for large momentum transfers, moves towards smaller angles as the pion energy increases.

A parametrization of the nuclear scattering amplitude which, among other things, takes into account explicitly the position of its zeros, as they reveal themselves by the dips in the angular distributions, has been used to fit the differential cross-sections. The resulting fits are good in the complete angular range at all energies. Starting from the fitted amplitude, it is easy to reconstruct the phase shifts. The usual ambiguities linked to this type of analysis are easily removed for the available low-energy data (around 60 MeV). Going up in energy, a continuity argument allows the selection of a set of phase shifts which show a reasonably smooth behaviour in the complex plane.

## ACTIVATION STUDIES OF PION-INDUCED REACTIONS ON C, N, O, F, Al, AND Cu

G. W. Butler, B. J. Dropesky, A. E. Norris, C. J. Orth, R. A. Williams  
 Los Alamos Scientific Laboratory, University of California  
 Los Alamos, New Mexico 87544

G. Friedlander, G. D. Harp, J. Hudis  
 Brookhaven National Laboratory, Upton, New York 11973

N. P. Jacob, Jr., S. S. Markowitz  
 Lawrence Berkeley Laboratory, University of California  
 Berkeley, California 94720

S. Kaufman  
 Argonne National Laboratory, Argonne, Illinois 60439

M. A. Yates  
 Carnegie-Mellon University, Pittsburg, Pennsylvania 15213

To establish useful techniques for monitoring pion beam intensities at LAMPF, the excitation functions for the  $^{12}\text{C}(\pi^\pm, \pi N)^{11}\text{C}$  reactions have been measured over the energy range of about 50 to 500 MeV. The excitation functions, clearly reflecting the (3,3) pion-nucleon resonance, show an upward energy shift in the resonance peak for  $\pi^-$  and a downward shift for  $\pi^+$ . The  $\sigma_{\pi^-}/\sigma_{\pi^+}$  ratio at 180 MeV is  $1.55 \pm 0.10$ . Cross sections for the neutron knock-out reactions on  $^{14}\text{N}$ ,  $^{16}\text{O}$ , and  $^{19}\text{F}$  have been measured over the same energy range. The  $\sigma_{\pi^-}/\sigma_{\pi^+}$  ratio for all three target nuclei is  $1.7 \pm 0.2$  at 180 MeV. A number of cross sections for the more complex  $\pi^\pm$  reactions on N, O, and F yielding  $^{11}\text{C}$  and  $^{13}\text{N}$  have also been measured. Some cross sections for the  $^{27}\text{Al}(\pi^\pm, \text{spallation})^{18}\text{F}$  reactions have been measured and preliminary indications are that the  $\sigma_{\pi^-}/\sigma_{\pi^+}$  ratio at 190 MeV is about 0.9. The yields of about 25 gamma-emitting products from  $\pi^\pm$ -induced spallation of copper at 190 MeV have been measured and compared with those from 349-MeV proton-induced spallation and with yields calculated with the Vegas intranuclear cascade plus evaporation codes. Interpretation of these preliminary results in terms of present models will be discussed.



## THE ELASTIC SCATTERING OF POSITIVE PIONS

I.D.22

BY CARBON AT 147 MeV\*

C. A. Bordner,\*\* P. A. M. Gram,‡ W. V. Hassenzahl,‡  
H. H. Howard,‡ T. R. King,† A. T. Oyer,† G. A. Rebka,† F. T. Shively††

We will present recent measurements of the differential cross section for  $\pi^+ - {}^{12}\text{C}$  elastic scattering at ten angles in the range  $35^\circ$  to  $85^\circ$  at an incident pion energy of 147 MeV (250 MeV/c). These data have been obtained in a "good geometry" experiment, using a double focussing spectrometer. Values of the cross section have been determined by measuring the ratio of the carbon scattering peak to the hydrogen scattering peak from the same CH target at each angle, and using the best available  $\pi$ -p scattering data.<sup>1</sup> We believe the carbon cross sections have been determined to an accuracy of 10% at most angles. They should complement the larger supply of  $\pi^- - {}^{12}\text{C}$  data already available.

---

<sup>1</sup> P. J. Bussey, J. R. Carter, D. R. Dance, D. V. Bugg, A. A. Carter, and A. M. Smith, Rutherford Lab. Preprint No. 107.

\* Supported in part by AEC Contract AT(11-1)-2197 and W-7405-ENG-36.

\*\* Colorado College, Colorado Springs, Colorado 80903.

‡ University of California, Los Alamos Scientific Laboratory, Los Alamos, New Mexico 87544.

† University of Wyoming, Laramie, Wyoming 82071 .

†† University of California, Lawrence Berkeley Laboratory, Berkeley, California 94720 .

SINGLE PROTON EMISSION FROM  $\pi^-$  ABSORPTION AT REST IN LIGHT NUCLEI

B. Coupat, P.Y. Bertin, D.B. Isabelle, G. Kawadry and P. Vernin,  
Laboratoire de Physique Corpusculaire, Université de Clermont, BP 45,  
63170 AUBIERE, France

and

A. Gérard, J. Miller, J. Morgenstern, J. Picard and B. Saghai  
DPhN/HE, Centre d'Etudes Nucléaires de Saclay, BP 2, 91190 GIF/YVETTE, France

Absorption of negative pion at rest by nuclei occurring only if at least two nucleons are involved in the capture process, is a sensitive probe to study nucleon correlation in nuclear matter<sup>1</sup>. Using the pion beam facility of the Saclay linac<sup>2</sup> we have undertaken a preliminary study of the ( $\pi^-$ , p) reaction in various light nuclei.

Two different technics were used : either a measurement of the radioactivity of the residual nucleus, or a direct detection of the emitted proton with a NaI (Tl) crystal. Due to the poor resolution of this type of spectrometer it can only be used if the residual nucleus has a large gap and large value of the nucleon separation energy (few MeV at least). Among light nuclei the only possible case is  $^{13}\text{B}$  produced in the reaction  $^{14}\text{N}(\pi^-, p)^{13}\text{B}$ . We performed this experiment and the data are presently analysed. The results will be presented at the Conference.

The activation method provides a measurement of the total probability of absorption with proton emission, as it is not possible to determine the final state of the residual nucleus. The following target nuclei have been irradiated :  $^9\text{Be}$ ,  $^{12}\text{C}$ ,  $^{16}\text{O}$ ,  $^{27}\text{Al}$ . All residual nuclei are  $\beta$ -emitters. The radioactivity is measured between beam pulses using a plastic scintillator telescope. The analysis of the raw data is performed to include all the corrections to the detection of  $\beta$  radioactivity.

The  $^{12}\text{C}$  result has already been published<sup>3</sup>. We found a probability of  $(4.5 \pm 0.8) \times 10^{-4}$  for single proton emission per pion absorbed at rest in  $^{12}\text{C}$ . We will present the corresponding result for  $^{16}\text{O}$ ,  $^{27}\text{Al}$  and eventually  $^9\text{Be}$ .

This experiment will provide the first set of data for proton emission from  $\pi^-$  absorption at rest for nuclei with A ranging from 9 to 27. We must remind that this reaction is the inverse of  $\pi^-$  production by proton which has already been observed<sup>4</sup>. To compare the two reactions it is necessary to perform measurements of the  $\pi^-$  absorption probability in flight and we have done a preliminary experiment of this type. We wish to emphasize the need for more theoretical calculations of the process ( $\pi^-$ , p).

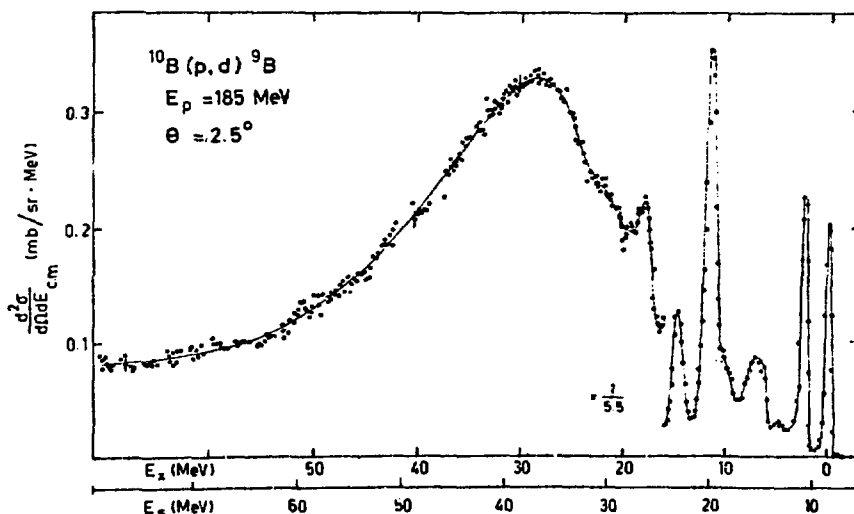
1. K. Chung, M. Danos and M.G. Huber, Phys. Lett. 29B, 265 (1969) and Z Phys. 240, 195 (1970)
2. P.Y. Bertin et al., Inter. Report C.E.A., DPhN/HE/71/3
3. B. Coupat et al., Phys. Lett. 55B, 286 (1975)
4. S. Dahlgren, P. Grafstrom, B. HÖTstad and A. Asberg, Nucl.Phys. A204, 53, (1973) and Phys. Lett. 47, 439 (1973)

## THE 1s AND 1p SHELLS OF LIGHT NUCLEI STUDIED IN (p,d) AT 185 MeV.

B. Fagerström, J. Källne, O. Sundberg and G. Tibell  
The Gustaf Werner Institute, Univ. of Uppsala, Uppsala, Sweden

Recent (p,d) measurements on  $^{12}\text{C}$ ,  $^{14}\text{N}$  and  $^{16}\text{O}$  have established the location of the  $1s_{1/2}$ ,  $1p_{3/2}$  and  $1p_{1/2}$  neutron sub-shells in the nuclei of the upper 1p-shell mass region. This has now been complemented with the corresponding information for the light nuclei and experimental results will be presented for the target nuclei  $^6,7\text{Li}$ ,  $^9\text{Be}$ ,  $^{10,11}\text{B}$  and  $^{13}\text{C}$ . Spectra were recorded at  $\theta = 2.5^\circ$  with an energy resolution of 0.6 MeV (FWHM) or better and extended to sufficiently large separation energies ( $E_s$ ) to cover the 1s pickup cross section, e.g.,  $E_s \leq 80$  MeV for  $^{13}\text{C}$ . Beyond the sharp 1p peaks in the low-energy region ( $E_s \leq 25$  MeV) a broad peak assigned to 1s-neutron pickup appeared in all spectra. One example is presented in the figure which shows the spectrum for  $^{10}\text{B}(p,d)^9\text{B}$ . This spectrum exhibits five prominent 1p peaks above  $E_s \approx 25$  MeV and superimposed on a smooth cross section a broad 1s peak at  $E_s \approx 37$  MeV. The spectroscopic strengths carried by these peaks were extracted by a DWBA analysis giving  $S(1s) = 2.0$  and  $S(1p) = 3.0$ . The agreement with the shell model prediction verifies the 1s assignment made. As in several other cases the low-energy side of the 1s peak shows some structure of unknown origin. A comparison between the present results on the 1s neutron shell and the more frequent information on the 1s proton shell shows, apart from some detailed differences, that the 1s peaks in the neutron and proton removal spectra are located in the same  $E_s$  range and that both increase in energy and width with A.

1. J. Källne and B. Fagerström, Proc. 5th Int. Conf. High Energy Phys. Nucl. Structure (Uppsala 1973) p. 369.



## FISSION OF HEAVY NUCLEI INDUCED BY STOPPED NEGATIVE PIONS

Yu.A.Batusov, D.Chultem, Dz.Ganzorig and O.Otgonsuren

Joint Institute for Nuclear Research, Dubna, USSR

Using a mica detector technique relative fission probabilities of 15 heavy nuclei from Ag to U in negative pion capture have been determined.

It is shown that for nuclei with  $(Z-I)^2/A \sim 30, \sim 25$  and  $\sim 20$  the fission probabilities are  $\sim 10^3, \sim 10^5$  and  $\geq 10^6$  times lower than for thorium and uranium isotopes.

The results are compared with statistical model calculations based on the  $\Gamma_f/\Gamma_n$  dependence of the excitation energy and of nuclear parameters ( fission barriers, neutron binding energies, nuclear density parameters and mass formula constants ).

II  
STOPPING MUONS

COULOMB CAPTURE AND X-RAY CASCADES OF MUONS IN METAL  
HALIDES.

11.1

A. Brandao d'Oliveira, H. Daniel and T. von Egidy  
Physics Department, Technical University of Munich,  
Munich, Germany.

Muonic X-ray yields have been measured for Al, AlF<sub>3</sub>, AlCl<sub>3</sub>, AlI<sub>3</sub>, KCl, KBr, KI, Cd, CdF<sub>2</sub>, CdCl<sub>2</sub>, CdBr<sub>2</sub>, CdI<sub>2</sub>, Sn, SnCl<sub>2</sub>, SnCl<sub>4</sub>, Sb, SbF<sub>3</sub>, SbF<sub>5</sub>, SbI<sub>3</sub> and SbCl<sub>5</sub>. The yields were normalized with the total intensity of the Lyman series. The capture ratios between Coulomb capture in the anion and the cation were determined for all compounds listed. Chemical effects in the intensities were observed. All observed intensities were compared with cascade calculations assuming a modified statistical population of the levels with principal quantum number  $n = 20$ . Good fits were obtained for all solid sources but not for the liquids. The capture ratios measured in the present experiment and all previous experimental values for ionic compounds were compared with the Fermi-Teller "Z-law" formula and with various modifications of this formula. It was found that a good representation of the experimental data can be obtained with one of the modifications but not the original "Z-law". The physical basis of this formula will be discussed.

II.2

RECENT EXPERIMENTAL RESULTS OF THE MESIC CHEMISTRY PROGRAM AT LAMPF\*

J. D. Knight, C. J. Orth, M. E. Schillaci, University of California, Los Alamos Scientific Laboratory, Los Alamos, NM; R. A. Naumann, Princeton University, Princeton, NJ; H. Daniel and K. Springer, Technical University of Munich, Munich, Germany; H. B. Knowles, Washington State University, Pullman, WA.

During the initial phase of experiments at LAMPF aimed at studying the effects of chemical structure on the capture of negative muons in matter, we have examined the muonic x-ray spectra of several groups of low- to medium-Z target materials, including strongly ionic to purely covalent solids, aqueous solutions of simple ions, and two metal hydrides. The observations were made using a standard muon telescope arrangement with associated fast electronics, and the muonic x rays were detected with Ge(Li) detectors. The muon channel was operated at  $130 \pm 5$  MeV/c with no measurable pion contamination and the spot size at the target was  $\sim 4$  cm x 12 cm.

Following are some results of our measurements:

1. Chemical bonding and state of aggregation - no significant spectral differences were observed between water and ice, between graphite and diamond, nor between the graphite and diamond forms of BN. The higher members of the C Lyman series are markedly more intense in various organic compounds than in diamond and graphite.

2. Z-law, solids -

a. The observation by Zinov et al.<sup>1</sup> of periodic variation of capture fraction in metal oxides is confirmed; capture fraction appears to correlate with electronegativity;

b. in crystalline alkali halides, capture probability varies more nearly as  $Z^{1/2}$  than as  $Z$ ;

c. in BN, N/B capture ratio is about 3 times Z-law;

d. in N- and O-containing organic compounds deviations from Z-law are small but appear to be real.

3. Z-law, aqueous solutions of alkali halides - capture probabilities of cations (anions) relative to oxygen in the water do not vary with changes of the anion (cation). They exhibit a smooth, monotonic dependence on  $Z$ , with the anions capturing more strongly than the cations.

4. Lyman intensity patterns, metal hydrides - relative intensities of higher members of the Lyman series of  $\text{CaH}_2$  (ionic hydrogen) and  $\text{TiH}_2$  (interstitial hydrogen) are similar.

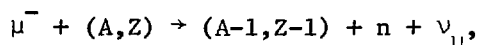
5. Charge displacement effects - no significant spectral differences were observed for N and O in para- $\text{CH}_3\text{C}_6\text{H}_4\text{NO}_2$  and para- $\text{ClC}_6\text{H}_4\text{NO}_2$ , nor for N and C in neutral and basic forms of glycine in aqueous solution.

\*Work performed under the auspices of the U. S. Atomic Energy Commission.

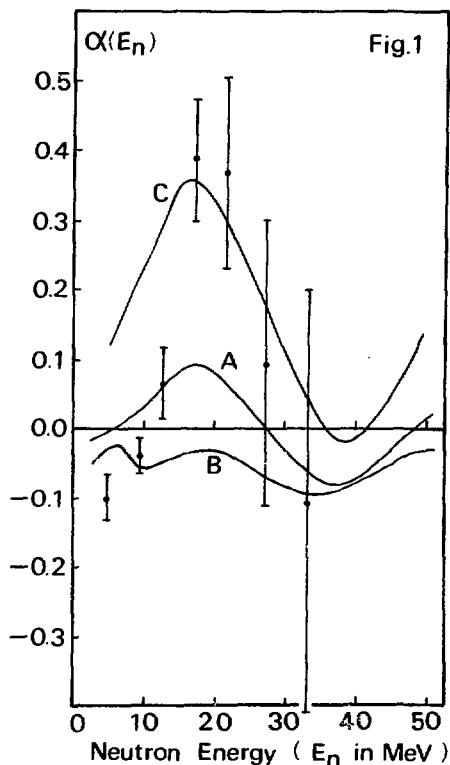
<sup>1</sup>V. G. Zinov, A. D. Konin, and A. I. Mukhin, *Sov. J. Nucl. Phys.* 2, 613 (1966).

K. Kume, N. Ohtsuka, H. Ohtsubo, and M. Morita  
Department of Physics, Osaka University, Toyonaka, Osaka 560, Japan

The high energy neutrons emitted mainly by the direct process,



have an angular distribution with respect to the muon polarization vector  $\vec{P}$ . The transition rate per unit solid angle and unit energy is expressed by  $d^2W/d\Omega dE = [N(E_n)/4\pi][1+\alpha(E_n)P \cdot k]$ ,  $k$  being the unit momentum of the emitted neutron. The asymmetry coefficient  $\alpha(E_n)$  is large and it has a strong energy dependence in muon capture by  $^{40}\text{Ca}$ ,<sup>1</sup> see, Fig.1. Among many theoretical attempt to explain this asymmetry, Bouyssy, Ngo, and Vinh Mau<sup>2</sup> noticed importance of the distortion of neutron waves due to the nuclear potential. Its effect is, however, not strong enough to produce a peak of the neutron asymmetry at the energy around 20 MeV. We show this can be explained by taking into account a realistic reaction mechanism with the effect of channel coupling. In Fig.1, the curve A shows the asymmetry  $\alpha$  in the DWBA calculation with no small component of the muon wave function. The energy dependence is relatively good, but the magnitude of  $\alpha$  is too small. If we add this small component,



$\alpha$  becomes worse, as in curve B. The asymmetry in curve C is large with a nice energy dependence, by taking into account the effect of the channel coupling in the final state. In all three cases, calculations involve the first order of the nucleon velocity terms in the effective Hamiltonian, the relativistic muon wave functions with charge distribution of the finite size nucleus, and the optical potential with no energy dependence. In curve C, we assume the Rosenfeld-type residual interaction. The energy spectrum of the emitted high energy neutrons is also investigated.

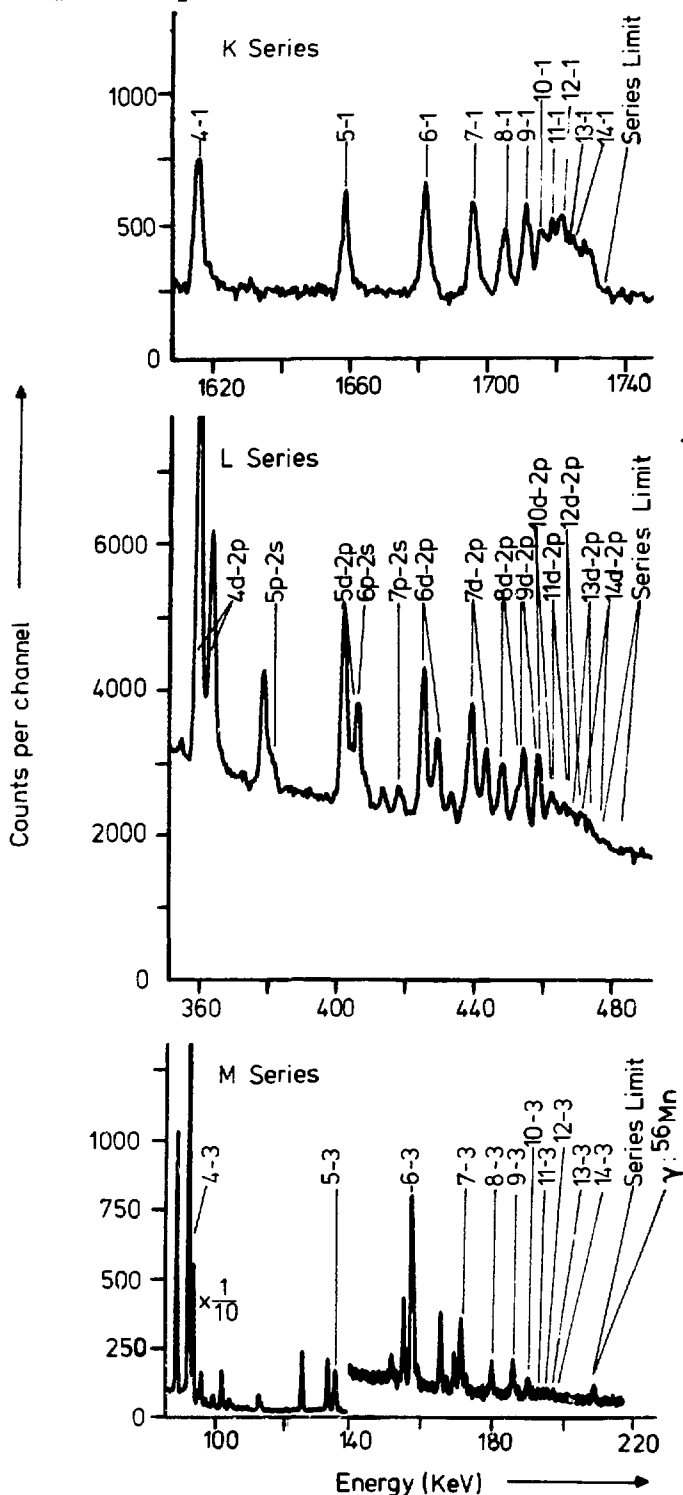
1. R. M. Sundelin and R. M. Edelstein, Phys. Rev. C 7, 1037 (1973).
2. A. Bouyssy, H. Ngo, and N. Vinh Mau, Phys. Letters 44B, 139 (1973).



MUONIC X-RAY SERIES IN METALLIC Al, Fe AND In.

R. Bergmann, H. Daniel, T. von Egidy, F. J. Hartmann, H.-J. Pfeiffer, K. Springer

Physik-Department, Technische Universität München, Munich, Germany



Muonic X-rays of metallic Al, Fe and In have been measured at the superconducting muon channel of SIN, Villigen, Switzerland. The channel was fed with pions of 150 MeV/c. Muons of 85 MeV/c were focussed on the target of typically 50 x 70 x 1 mm<sup>3</sup>. X-ray spectra were simultaneously taken with a 0.5 cm<sup>3</sup> high-resolution intrinsic Ge detector (0.25 keV fwhm at 6 keV) and a 42 cm<sup>3</sup> Ge(Li) detector (2.2 keV fwhm at 1.3 MeV) and recorded with a computer on-line and a multichannel analyzer. A typical telescope rate (123) at 10  $\mu$ A proton current was 1.5 · 10<sup>5</sup>/s. The distribution of the muon stops in the target was measured with the help of the induced radioactivity. Parts of the iron spectra are shown in fig. 1. Lines from levels with principal quantum number n up to n = 14 were observed in the K, L, M, N, and O series. The experimental intensities will be compared with computed values calculated with various initial distributions and a standard cascade program.

Fig. 1

# ATOMIC CAPTURE OF NEGATIVE MESONS; THE FUZZY FERMI-TELLER MODEL <sup>II.5</sup>

M. Leon and J. Miller

University of California  
Los Alamos Scientific Laboratory  
Los Alamos, NM 87544

A model for the atomic capture of negative mesons has been developed which, like the Fermi-Teller model,<sup>1</sup> treats the meson classically and the electron cloud in the statistical approximation. The present model allows for the inherent probabilistic nature of the response of the atomic electrons to the invading meson. Hence the average energy loss and angular momentum loss of the Fermi-Teller model are replaced by distributions of energy and angular momentum losses, and the meson slows down in discrete steps rather than continuously. Results obtained in this Fuzzy Fermi-Teller model are compared with earlier calculations, and possible applications of the model for the investigation of chemical effects in negative meson capture will be discussed.

---

<sup>1</sup>M. Leon and R. Seki, Phys. Rev. Lett. 32 (1974) 132; and, to be published.  
P. K. Haff et al., Phys. Rev. A10 (1974) 1430; and, to be published.

The  $\alpha^2(Z\alpha)^2$  contribution of vacuum polarization to level shifts  
in high Z muonic atoms.

M. K. Sundaresan  
and  
P. J. S. Watson  
Department of Physics,  
Carleton University,  
Ottawa, Canada.

## ABSTRACT

Recently results of two calculations of the  $\alpha^2(Z\alpha)^2$  vacuum polarization contribution to level shifts in high Z muonic atoms have appeared<sup>1,2</sup>. The results of these calculations are in disagreement with one another, Wilets and Rinker<sup>1</sup> claiming that the expected level shift is very small, while Chen<sup>2</sup> claims it is enough to remove the discrepancy between theory and experiment in muonic X-rays<sup>3</sup>. It is therefore necessary to ascertain what the correct value is, and we have been performing the calculation using the method due to Owen<sup>4</sup>. Results of the present calculation will be presented.

## REFERENCES

1. L. Wilets and G. A. Rinker, Jr. Phys. Rev. Letts. 34, 339, (1975)
2. Min-Yi Chen, Phys. Rev. Letts. 34, 341, (1975)
3. P. J. S. Watson and M. K. Sundaresan, Can. J. Phys. 52, 2037, (1974)
4. D. A. Owen, Phys. Rev. D8, 424, (1973)

## E2(E1) PARITY MIXING IN MUONIC ATOMS

II.7

L.M.Simons

CERN, Geneva, Switzerland

One of the most exciting discoveries in high energy physics in the last years has been the measurement of events in neutrino physics which could indicate the existence of weak neutral currents. The interest in experiments also in other fields of physics has then rapidly increased which could also demonstrate the existence of weak neutral current effects.

In muonic atoms usually it is proposed to measure parity violating effects in the  $2s-1s$   $M1(E1)$ -transition. In contrast to the effects expected there we think that a parity violating effect in other transitions like the  $3d-1s$  and the  $4f-2p$   $E2(E1)$ -transition is much easier to measure.

The main reason for this is that background problems are much less severe here and that also the possibility to reduce the background by a coincidence method is given. This and other experimental considerations will be discussed.

## EFFECTS OF NON-STATISTICAL HYPERFINE POPULATIONS IN MUON CAPTURE BY POLARIZED NUCLEI

N.C. Mukhopadhyay  
Theory Group, SIN, Villigen, Switzerland  
and

L. Hambro  
Theory Division, CERN, Geneva, Switzerland

We have examined muon capture by polarized nuclei regarding its usefulness in probing the difference between the hyperfine capture rates  $\Lambda_{\pm}$ . The capture rate  $\Lambda$  is given by

$$\Lambda = N_+ \Lambda_+ + N_- \Lambda_- \quad (1)$$

where  $N_{\pm}$  are the weights of the hyperfine population given by

$$N_{\pm} = N_{\pm}^{\text{stat}} [1 \mp \vec{a} \cdot \vec{b}], \quad N_+ = 1 - N_- \quad (2)$$

$\vec{a}, \vec{b}$  being the muon and nuclear polarizations at the instant of muon's entry in the 1S orbit,  $N_{\pm}^{\text{stat}}$  is  $\frac{I}{2I+1}$ , I being the nuclear

spin.  $N_{\pm}$  are independent of time, since  $\text{Tr}(P_{\pm} \rho_{\mu} \otimes \rho_I)$  does not change with time,  $P_{\pm}$  being the projection operators for the hyperfine states and  $\rho$ 's the density operators. If the rate  $\Lambda$  is determined for two values of polarization  $\vec{b}$ ,  $\Lambda_{\pm}$  can be separately determined by the equations

$$\Lambda_{\alpha} = [N_{\beta}^{(2)} \Lambda^{(1)} - N_{\beta}^{(1)} \Lambda^{(2)}] / [N_{\beta}^{(2)} N_{\alpha}^{(1)} - N_{\beta}^{(1)} N_{\alpha}^{(2)}] \quad (3)$$

where  $\alpha = (+, -)$ ,  $\beta = (-, +)$ , superscripts indicate the two measurements. For  $|\vec{a}| \sim \frac{1}{8}$  and  $\vec{b}$  having magnitude unity parallel and antiparallel to  $\vec{a}$ , the capture rates differ by  $\sim 30\%$  in hydrogen, deuterium,  ${}^6\text{Li}$ ,  ${}^{10}\text{B}$  targets. Adequate techniques exist to exploit the effect and determine  $\Lambda_{\pm}$  to a fair level of precision.

MIGDAL'S QUASIPARTICLE APPROACH AND ITS IMPLICATIONS OF ALLOWED MUON CAPTURE STRENGTH IN  $^{12}\text{C}$

John D. Immele

Lawrence Livermore Laboratory, Livermore, U.S.A.

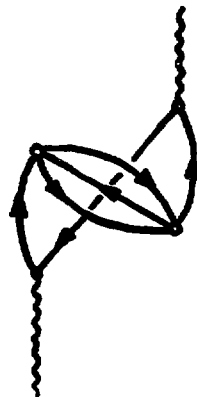
and

N.C. Mukhopadhyay, CERN, Genève, and SIN, Villigen, Switzerland

An open-shell extension of Migdal's theory of finite Fermi system is specialized to  $^{12}\text{C}$  to describe the T=1 states. The Migdal spin-spin interaction term  $g'$  has a preferred value of 0.5 to fit the rate of the process  $^{12}\text{B}(\text{g.s.})\beta^{-}^{12}\text{C}(\text{g.s.})$ . Low-lying T=1 states are well-reproduced. While the  $^{12}\text{B}(\text{g.s.})\beta^{-}^{12}\text{C}(\text{g.s.})$  weak transitions and their electromagnetic analogues are well-described, an improvement over the closed-shell RPA, the isovector M1 strength is found to be grossly overestimated. This means that the allowed muon capture strength is ill-reproduced.

A careful examination of the difficulty suggests that the trouble may lie with the neglect of the graphs of the type given in fig. 1, which is necessary to restore the Pauli principle. This however, leads to an energy-dependent p-h interaction and is thus incompatible with the basic philosophy of the Migdal approach.

Fig. 1



C. K. Hargrove, E. P. Hincks, H. Mes and R. J. McKee,  
National Research Council of Canada,

M. S. Dixit, A. L. Carter, D. Kessler and J. S. Wadden,  
Carleton University,

and

H. L. Anderson,  
University of Chicago

Muonic x-rays in the energy region 100 to 500 keV are well suited to test quantum electrodynamical (QED) effects. Discrepancies between the predictions of QED and high precision measurements of the energies of higher transitions ( $n=5\rightarrow 4$  and  $n=4\rightarrow 3$ ) in muonic atoms have been reported from two independent experiments.<sup>1,2</sup> Although much of the discrepancy was later removed by careful theoretical work (see, for example, the review by Watson and Sundaresan<sup>3</sup>) it remained at between one and two standard deviations for transitions in Ba, Pb, Tl and Hg. We have recently made new measurements of the higher lines in Cd, Ba, Pb and Bi using the SEEL synchrocyclotron and will report the progress on our comparison of experiment with theory.

\*Supported by the National Research Council of Canada and the National Science Foundation and part of the program of the Canadian Institute of Particle Physics.

<sup>1</sup>M. S. Dixit et al., Phys. Rev. Lett. 27, 878 (1971).

<sup>2</sup>H. Walter et al., Phys. Lett. B40, 197 (1972).

<sup>3</sup>P. J. S. Watson and M. K. Sundaresan, Can. J. Phys. 52, 2037 (1974).

PARTIAL MUON CAPTURE RATES IN  $^{12}\text{C}$

11.11

V. Devanathan and P.R. Subramanian  
University of Madras, Madras-600 025, India  
and

R.D. Graves and H. Überall\*  
Catholic University of America, Washington DC 20064

Partial muon capture rates to the ground state and the three lowest excited states of  $^{12}\text{B}$  have been calculated using two versions of the shell model, and the generalized Helm model<sup>1</sup>. The parameters for the latter model were obtained from an improved fit<sup>2</sup> to the inelastic electron scattering data, whereupon use of the model leads to good agreement between calculated and measured<sup>3</sup> captured rates (see Table I). In contrast, the rates calculated from the single-particle shell model (sps) give overestimates by factors of four. For the capture rate to the  $^{12}\text{B}$  ground state, we also used a configuration mixing model<sup>4</sup> (cfm) which predicts the rate correctly.

Table I  
Partial muon capture rates in  $^{12}\text{C}$  to  
the four lowest levels of  $^{12}\text{B}$  (units  $10^3 \text{ sec}^{-1}$ )

Level	Helm	sps	cfm	exper.
$1^-$	6.21	35.8	5.26	$5.74 \pm 0.80$
$2^+$	0.13	0.80	-	$0.21 \pm 0.39$
$2^-$	0.68	3.51	-	$0.37 \pm 0.57$
$1^-$	0.37	2.85	-	$0.73 \pm 0.41$

Work supported in part by the National Science Foundation.

- \* Also at Naval Research Laboratory, Washington DC 20375  
1 M. Rosen, R. Raphael, and H. Überall, Phys. Rev. 163,  
927 (1967)  
2 H. Überall et al, Phys. Rev. C6, 1911 (1972)  
3 G.H. Miller et al, Phys. Lett. 41B, 50 (1972)  
4 M. Hirooka et al, Prog. Theor. Phys. 40, 808 (1968)



CHARGE PARAMETERS, ISOTOPE SHIFTS, QUADRUPOLE MOMENTS,  
AND NUCLEAR EXCITATION IN MUONIC <sup>170,171,172,173,174,176</sup>Yb.\*

A. Zehnder and F. Boehm

California Institute of Technology, Pasadena, Ca. 91125

W. Dey, R. Engfer, H.K. Walter, and J.L. Vuilleumier

Laboratorium für Hochenergiephysik, ETH, 5234 Villigen, Switzerland

Muonic x-ray and nuclear gamma rays from six separated isotopes of ytterbium were measured simultaneously. The parameters of the deformed charge distribution, the quadrupole moments and the isotope shifts are given in Tables I and II. The analysis includes QED corrections for the monopole and the quadrupole Coulomb potential and E1 and E2 nuclear polarization.

The isotope shifts were interpreted in a model-independent way. From the static splitting of the 3d state in <sup>173</sup>Yb a nearly model-independent spectroscopic quadrupole moment was found and used for testing the assumed charge distribution.

In <sup>172</sup>Yb evidence was found for a pronounced resonance between the 3d<sub>3/2</sub>-1s<sub>1/2</sub> muonic states and a nuclear state at 6.9314 MeV. Several nuclear gamma rays were observed and the isomer shifts for the first excited 2<sup>+</sup> and 0<sup>+</sup> states were evaluated and are (73±60) eV and (-3.2±1.4) keV, respectively.

**Table I** Parameter of a deformed charge distribution  $\rho(r) = \rho_0 [1 + \exp(4 \ln 3 (r-c)/t)]^{-1}$  with  $c=c_0 (1 + \beta_2 Y_{20} + \beta_4 Y_{40})$ . The skin thickness was  $t = 2.18(2)$  for all isotopes.  $\beta_4$  was chosen to reproduce the measured or calculated hexadecapole moments. The quoted errors for  $Q_0$  are statistical. By considering the model-dependence the total error for all isotopes is 0.3b.

Yb	$c_0$ (fm)	$\beta_2$	$Q_0$ (b)
170	6.212(5)	0.322(1)	7.80(4)
171	6.214(5)	0.327(1)	7.95(4)
172	6.227(5)	0.325(1)	7.91(4)
173	6.234(5)	0.324(1)	7.92(5)
174	6.246(5)	0.320(1)	7.82(5)
176	6.271(5)	0.309(1)	7.59(5)

**Table II** The isotope shift and its equivalent radius  $R_k^{\mu ls}$  are given with  $k = 2.34$  and  $\alpha = 0.136$ . The analysis was carried out as described in ref. 1.

	$\delta E^{\mu ls}$ (keV)	$\delta R_k^{\mu ls}$ (mf)
<sup>170-172</sup> Yb	-10.64(36)	18.0(6)
<sup>170-172</sup> Yb	-5.78(37)	9.8(6)
<sup>172-174</sup> Yb	-8.75(23)	14.8(4)
<sup>174-174</sup> Yb	-5.07(40)	8.6(7)
<sup>174-176</sup> Yb	-7.86(32)	13.3(5)

REFERENCE

1. R. Engfer, H. Schneuwly, J.L. Vuilleumier, H.K. Walter, and A. Zehnder, Atomic Data & Nuclear Data Tables 14, nos. 5-6, (1974).

\* Work carried out at the CERN Synchrocyclotron, Geneva, Switzerland.

P. Vogel, P.K. Haff, V. Akylas, and A. Winther\*\*  
California Institute of Technology, Pasadena, California 91125

A comprehensive description of muon capture in all but the lightest atoms is given. After verification that the process can be calculated by classical mechanics, the frictional force derived from the stopping power of an electron gas is used in the classical equation of motion for the negative muon. The method developed allows calculation of the angular momentum and energy distribution of captured muons. Formulae, based on the statistical atomic model, are derived for the energy at which the muons are typically captured and for the capture and energy loss cross sections. The transport equation describing the combined effect of stopping and capture in a target is derived and solved. It is shown that the angular momentum distribution of the captured muons is nearly statistical. The subsequent cascade is followed classically to the electron K-shell energy, where a comparison is made with a quantum calculation. The "standard" quantum cascade calculation, expected to be accurate at the lowest muon states, is shown to be in error when applied at high ( $n = 14$ ) quantum numbers in small  $Z$  muonic atoms. The shape of the angular momentum distribution is not qualitatively changed during the cascade. In mixtures of monoatomic gases with atomic numbers  $Z_1$  and  $Z_2$  the calculated capture ratio is proportional to the relative concentration and to  $(Z_1/Z_2)^{1.15}$ . The capture ratios in cubic ionic crystals are calculated by the Monte Carlo method and the results agree well with the experimental data. In such crystals electrostatic ionic charges lead to systematic deviations from the  $Z$  law. Another approximate method of studying the capture process in a solid target is developed. Using this method with Hartree-Fock atomic densities and potentials, it is shown that the angular momentum distribution of muons in atoms near shell closure  $Z = 18$  is steeper than statistical while in the transition metal nickel it is flatter, in qualitative agreement with the experiment. As an example of capture in more complicated systems the  $SF_6$  molecule is studied.

\* Work supported in part by the U.S. AEC AT[04-3]-63 and the National Science Foundation [GP-28027].

\*\* Permanent address: Niels Bohr Institute, DK-2100, Copenhagen, Denmark.

R.J. Powers  
 California Institute of Technology, Pasadena, California 91125  
 and  
 CEN-Saclay, Gif-sur-Yvette, France 91190

P. Barreau, B. Bihoreau, J. Miller, J. Morgenstern, J. Picard, and L. Roussel  
 CEN-Saclay, Gif-sur-Yvette, France 91190

P. Bertin  
 Université de Clermont-Ferrand, Clermont-Ferrand, France

We have measured the muonic isotope shifts of the  $2p \rightarrow 1s$  transitions using separated samples of Sm with  $A = 144, 148, 149, 150, 152,$  and  $154$  at the electron Linear Accelerator at Saclay (ALS). The purpose of this experiment was to study the evolution of nuclear radius and deformation as a function of neutron number in this transitional region of the periodic table where nuclear properties vary rapidly from those associated with non-deformed, magic-in-neutron-number ( $N = 82$ ) nuclei ( $A = 144$ ) to highly deformed rotors ( $A = 152$  and  $154$ ). The absolute energies of the muonic transitions were determined relative to muonic  $^{208}\text{Pb}$ , which has been well studied previously, in order to allow the determination of the nuclear charge parameters.

The muon stopping rates (typically 20 k/s) were sufficient to allow the observation of transitions to and from the weakly populated muonic  $2s$  state in several isotopes. Initial fits of the  $^{152}\text{Sm}$  data using the  $2s_{1/2} \rightarrow 2p_{3/2}$ ,  $3d_{5/2} \rightarrow 2p_{3/2}$ ,  $2p_{3/2} \rightarrow 1s_{1/2}$ ,  $3p_{3/2} \rightarrow 1s_{1/2}$ , and  $3d_{5/2} \rightarrow 1s_{1/2}$  transition energies as well as the  $2p$  hyperfine interaction energies to a deformed Fermi distribution yield a dynamic E2 transition moment corresponding to an intrinsic moment  $Q_0 = 5.74 \pm 0.06$  b (assuming the rotational model) and a static E2 moment of the first excited state corresponding to  $Q_0 = 5.80 \pm 0.18$  b. The dependence of this analysis upon the nuclear charge model will be discussed.

\* Supported in part by the U.S. AEC AT[04-3]-63.

S. Nagamiya, K. Nagamine, O. Hashimoto and T. Yamazaki  
 Department of Physics, University of Tokyo, Hongo, Bunkyo-ku, Tokyo, Japan  
 and  
 Lawrence Berkeley Laboratory, University of California, Berkeley, CA 94720

The negative muon ( $\mu^-$ ) has been applied to study hyperfine field at the oxygen site in MnO in paramagnetic phase. This material is antiferromagnetic below  $T_N = 116$  K, where oxygen atoms play important role in superexchange interactions between  $Mn^{++}$  d-spins.

Negative muons from the 184" Cyclotron at LBL were stopped in a single crystal of MnO ( $3cm \times 4cm \times 5gr/cm^2$ ) at room temperature on which an external magnetic field (6.830 and 1.1061 kOe) was applied perpendicularly to the muon beam. Fig. 1 shows the time spectrum of decay electrons from muons. The short-lived component is due to muons bound to Mn nuclei ( $\mu^-Mn$ ), whereas the long-lived component is due to  $\mu^-O$ . We have analyzed the long-lived component to get the precession frequency and relaxation time of  $\mu^-O$  in MnO. The  $\chi^2$ -fits for this component and  $\mu^-C$  at  $H = 6.830$  kOe are plotted in Fig. 2 as a function of precession frequency. The comparison with a carbon run gave a paramagnetic shift ( $\Delta$ ) of  $\mu^-O$  in MnO,

$$\Delta \equiv \delta H/H = 1.1 \pm 0.2 \% \quad (1)$$

The relaxation time  $T_2$  of  $\mu^-O$  extrapolated to zero external magnetic field is

$$T_2 = 1.5 \pm 0.4 \text{ } \mu\text{sec} \text{ at } H = 0. \quad (2)$$

Paramagnetic MnO is one of exceptional cases where the  $^{17}O$  NMR data are available.<sup>1</sup> The present value of  $\Delta(\mu^-O)$  is about 3 times smaller than the paramagnetic shift of  $^{17}O$  ( $\Delta(^{17}O) = 3.21 \pm 0.02 \%$ ). This reduction cannot be accounted for by the reduction of 2s electron density alone. Therefore, it suggests that the polarization of local  $Mn^{++}$  d-spins is reduced due to the increase of superexchange interaction in the presence of  $\mu^-$  at the oxygen site. The relaxation time  $T_2$  can be explained if we take into account the reduction of 2s electron density as well as the enhanced local superexchange interaction.

<sup>1</sup> D.E.O'Reilly and T.Tsang, J. Chem. Phys. **40**, 734 (1964).

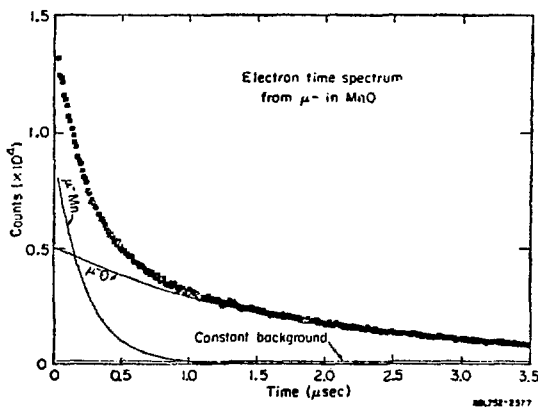


Fig. 1 Time spectrum of decay electrons.

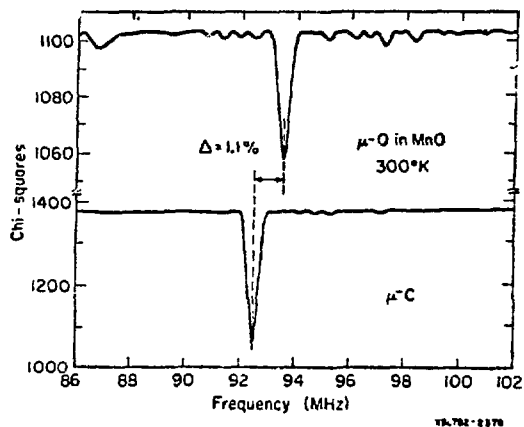


Fig. 2  $\chi^2$  vs. Larmor frequency for  $\mu^-O$  in MnO (upper) and  $\mu^-C$  (lower).

\* Work supported by JSPS (Japan), NSF and the US-AEC.

O. Hashimoto, S. Nagamiya, K. Nagamine and T. Yamazaki  
 Department of Physics, University of Tokyo, Hongo, Bunkyo-ku, Tokyo, Japan  
 and  
 Lawrence Berkeley Laboratory, University of California, Berkeley, CA 94720

We have determined lifetimes of muons bound to  $^{238}\text{U}$ ,  $^{235}\text{U}$ ,  $^{232}\text{Th}$  and  $^{239}\text{Pu}$  by observing decay electrons from ls muons in order to study systematics of muon capture rate in this region and also to see any difference between the lifetimes through the observations of decay electrons ( $\tau_e$ ) and of fission fragments ( $\tau_f$ ), as discussed by Bloom.<sup>1</sup>

Muons from the 184" Cyclotron at LBL were stopped in a metallic target, and the time distribution of  $\mu^- \rightarrow e^-$  decay was observed in the same way of the  $\mu\text{SR}$  experiment.<sup>2</sup> The results are

$$\begin{aligned} \tau_e(^{238}\text{U}) &= 81.5 \pm 3.0 \text{ nsec} & \tau_e(^{235}\text{U}) &= 78 \pm 5 \text{ nsec} \\ \tau_e(^{232}\text{Th}) &= 80.4 \pm 2.5 \text{ nsec} & \tau_e(^{239}\text{Pu}) &= 77.5 \pm 2.0 \text{ nsec}. \end{aligned}$$

The present value of  $\tau_e(^{238}\text{U})$  is closer to  $\tau_f(^{238}\text{U})$  [ $= 75.8 \pm 0.8 \text{ nsec}^3$ ] than the old value of  $\tau_e$  by Sens<sup>4</sup>, but still a little longer than  $\tau_f(^{238}\text{U})$ . The  $\tau_f$  values for the other nuclei ( $^{235}\text{U}$ ,  $^{232}\text{Th}$  and  $^{239}\text{Pu}$ ) reported by three groups<sup>3</sup> are scattered too much to be compared to the present  $\tau_e$  values.

The reduced capture rates,  $\Lambda_c / \langle \rho \rangle$ , versus  $(A - Z)/2A$  are plotted in Fig. 1 for both the fission mode and electron decay mode, where  $\Lambda_c = 1/\tau - 1/\tau_{\text{free}}$  and  $\langle \rho \rangle$  is the overlap of muon and nuclear charge densities. The straight line is extrapolated from the systematics of capture rates in lighter nuclei than  $^{209}\text{Bi}$ . In actinide region the reduced capture rate in electron decay mode is less dependent on  $(A - Z)/2A$  than in the lighter nuclei.

<sup>1</sup> S.D.Bloom, Phys. Lett. **48B**, 420 (1974).

<sup>2</sup> T. Yamazaki et al., Phys. Lett. **53B**, 117 (1974).

<sup>3</sup> J.A.Diaz et al., Nucl. Phys. **40**, 54 (1963); B.Budick et al., Phys. Rev. Lett., **24**, 674 (1970); D.Chultem et al., JINR E15-8134 (Dubna, 1974).

<sup>4</sup> J.C.Sens, Phys. Rev. **113**, 679 (1959).

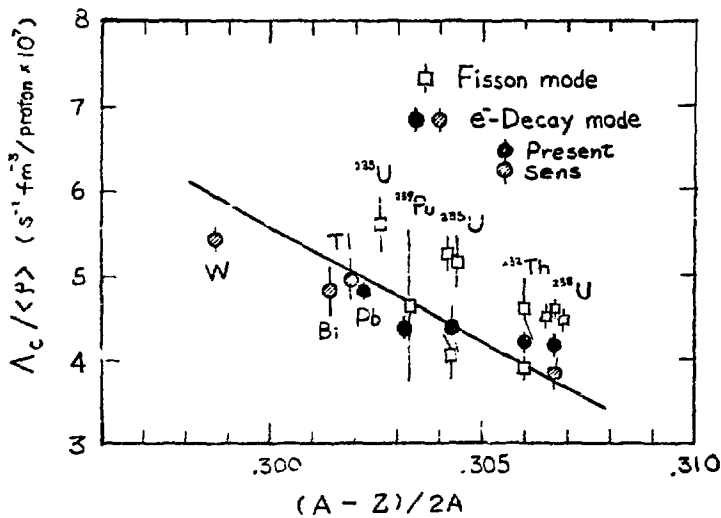


Fig. 1 Primakoff plot of  $\Lambda_c$  for heavy elements.

\* Work supported by JSPS (Japan), NSF and the US-AEC.

K. Nagamine, S. Nagamiya, O. Hashimoto, S. Kobayashi and T. Yamazaki  
 Department of Physics, University of Tokyo, Bunkyo-ku, Tokyo Japan  
 and Lawrence Berkeley Laboratory, University of California, Berkeley, Calif., U.S.A.

We have studied depolarization phenomena of negative muons in paramagnetic metals at various temperatures. The LBL facility for negative muon spin rotation was used.

Mo: A free precession was observed with almost full amplitude at RT and 18 K, which is contrary to the Dubna work.<sup>1)</sup>

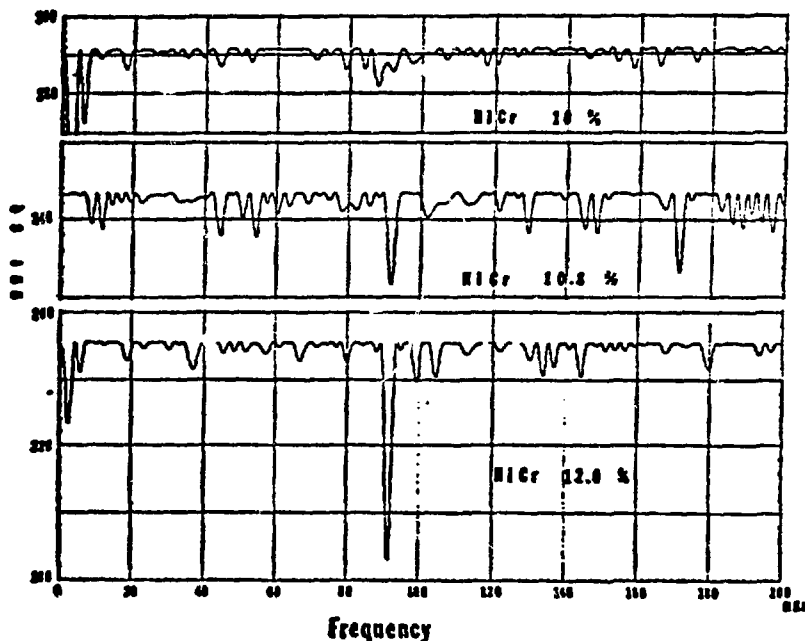
Pd: A very pure Pd sample (5 ppm Fe) was used to avoid depolarization due to iron impurities. No precession signal has been observed at any temperature (RT, 77 K and 4 K). This is very surprising in view of the known NMR data for dilute Rh in Pd host.<sup>2)</sup> If the  $\mu^-$ Pd felt the same internal field as the Rh nucleus, the  $\mu^-$ Pd would show relaxation times much longer than the  $\mu^-$  lifetime of 100 nsec. This fact indicates either 1) presence of a giant hyperfine anomaly (the hyperfine field by the  $\mu^-$ Pd is 10 times greater than that by the Rh nucleus, or 2) a fast depolarization before reaching the  $1s_{1/2}$  state of the muonic atom.

Ni and its Alloy:<sup>1/2</sup> In paramagnetic phase of Ni ( $T = 700$  K) there was no precession signal. We observed appreciable precession signal in NiCr alloy at room temperature as the Cr concentration increased toward the critical concentration (12%), where the magnetic moment of the alloy ultimately becomes zero.

\* Supported by Japan Society for the Promotion of Science, the National Science Foundation and the U.S.A.E.C.

1) A.E. Ignatenko, Nucl. Phys. 23 (1961) 75.

2) A. Narath and H.T. Weaver, Phys. Rev 3B (1971) 616.



K. Nagamine, S. Nagamiya, O. Hashimoto, N. Nishida and T. Yamazaki  
 Department of Physics, University of Tokyo, Bunkyo-ku, Tokyo, Japan  
 and Lawrence Berkeley Laboratory, University of California, Berkeley, CA94720

Metallic palladium with dilute iron impurities has interesting magnetic properties at low temperatures; the impurity spin strongly polarizes the neighbouring Pd atoms, forming a large polarized complex. The  $\mu^+$  spin rotation method was used to explore the details of this giant moment, since  $\mu^+$  stays preferentially at octahedral interstitial sites in the f.c.c. metal.

The polarized positive muons at the L.B.L. 184" cyclotron were used. A palladium metal with 150 ppm Fe impurity under 1081.1 (0.3) G applied field was cooled from 4.2 K to 0.11 K using a  $^3\text{He}$ - $^4\text{He}$  dilution refrigerator.

The time distributions at 4.2 K and 0.11 K are shown in Fig. 1, where we can see a clear difference of the damping in the precession amplitude. We found that a Gaussian type relaxation ( $A\exp(-\sigma^2 t^2)$ ) gives a better fit than an exponential type. This shows that the observed relaxation originates from the static inhomogeneity in the local interstitial fields. The results of relaxation parameter ( $\sigma$ ) and the local field ( $B_{\mu}$ ) are summarized in Table 1. The temperature dependence of  $\sigma$  does not follow that of the magnetization of the giant moment.

The observed small shift of  $B_{\mu}$  even at 0.11 K ( $+0.06 \pm 0.03\%$ ) may arise from a cancellation between the Lorentz field ( $+0.41\%$ ) and a Knight shift ( $-0.35 \pm 0.03\%$ ), which is due to the conduction electron polarization induced by the iron moment.

\* Supported by Japan Society for the Promotion of Science, the National Science foundation and U.S.A.E.C.

Table 1 Summary of  $\mu^+$ SR in PdFe Alloy (150 ppm Fe)

T (K)	$(B_{\mu} - B_{\text{ext}})/B_{\text{ext}}$ (%)	$\sigma$ ( $\mu\text{sec}^{-1}$ )
4.2	-0.02(0.02)	0.19(0.04)
0.6	+0.01(0.02)	0.32(0.04)
0.11	+0.06(0.03)	0.52(0.03)

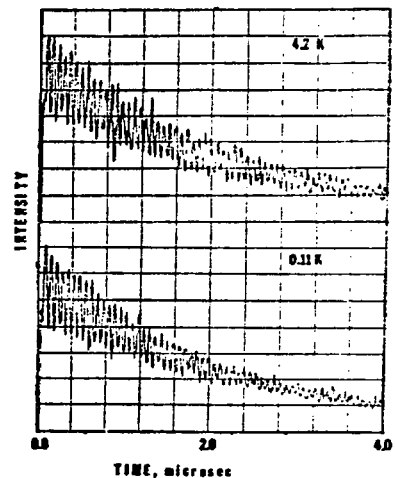


Fig. 1 Time spectrum of positive muon decay in PdFe alloy at 4.2 K and 0.11 K.

HYPERFINE FIELD ON POSITIVE MUON IN NICKEL  
IN THE TEMPERATURE RANGE OF 0.12-300 K\*

II.19

K. Nagamine, S. Nagamiya, O. Hashimoto, T. Yamazaki and B. D. Patterson  
Department of Physics, University of Tokyo, Bunkyo-ku, Tokyo, Japan  
and Lawrence Berkeley Laboratory, University of California, Berkeley, CA94720

We extended the  $\mu^+$  spin rotation experiment in a single crystal nickel<sup>1)</sup> to temperatures down to 0.12 K using a  $^3\text{He}$ - $^4\text{He}$  dilution refrigerator. The polarized  $\mu^+$  beam at the L.B.L. 184" cyclotron was used.

The local field on  $\mu^+$  at various temperatures has been determined. By subtracting the Lorentz field ( $4\pi M/3$ ), the hyperfine field ( $H_{\text{int}}$ ) can be obtained. The low temperature limit of  $H_{\text{int}}$  was obtained to be  $640.7 \pm 2.2\text{G}$ . The relative values of  $H_{\text{int}}$  normalized to the lowest temperature value are shown in Fig. 1, where we put also a relative change of the saturation magnetization ( $M$ ) and hyperfine field on Ni nuclei ( $H_n$ ) measured by NMR study<sup>2)</sup>. In contrast to the others, the  $\mu^+$  hyperfine fields<sup>n</sup> are almost temperature independent.

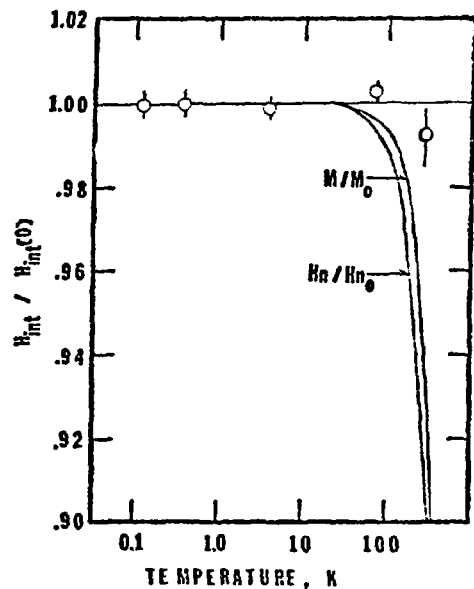
From the known hydrogen diffusion properties, we guess that the positive muon is well localized at octahedral sites below 77 K. At higher temperature, the thermal excitation of  $\mu^+$  might cause further broadening of the location. Then we expect a decrease of the hyperfine field, in contrast to the experimental tendency.

\* Supported by Japan Society for the Promotion of Science, the National Science Foundation and U.S.A.E.C.

1) M.L.G. Foy, N. Heiman, W.J. Kossler and C.E. Stronach, Phys. Rev. Lett. 30, 1064 (1973); B.D. Patterson, K.M. Crowe, F.N. Gyax, R.F. Johnson, A.M. Portis and J.H. Brewer, Phys. Lett. 46A, 453 (1974).

2) R.L. Streaver and L.H. Bennett, Phys. Rev. 131, 2000 (1963).

Fig. 1 Temperature dependence of the reduced muon hyperfine field ( $H_{\text{int}}$ ) normalized at lowest temperature.





Y.Kohyama and A.Fujii

Physics Department, Sophia University, Tokyo, Japan

A statistical method of calculating the total muon capture rate is formulated and applied to several heavy nuclei.

The assumption of the SU(4) symmetry reduces 6 conventional nuclear matrix elements into a single term

$$\int \mathbf{1} \cdot \bar{e}^{-i\mathbf{p}\cdot\mathbf{r}} = \int \psi_f^* \left( \sum_{j=1}^{\hat{A}} \tau_j^{(1)} e^{-i\nu_{fi}\cdot\mathbf{r}} \right) \psi_i \equiv M(\nu_{fi}, E_f - E_i),$$

and the total capture rate is expressed as the sum over the partial capture rates  $\sum_f \omega_{fi}$ . In the statistical treatment the final state  $f$  is regarded to distribute continuously, labeled by a continuous variable  $E = E_f - E_i$  and the sum  $\sum_f$  is replaced by an integral  $\int dE$ . The  $\nu_{fi}$ -dependence is purposely singled out, and expanded around a constant value  $\nu$  :

$$|M(\nu_{fi}, E)|^2 = |M(\nu, E)|^2 + (\nu_{fi} - \nu) \frac{d}{d\nu} |M(\nu, E)|^2.$$

$|M(\nu, E)|^2$  can be expressed as a product of the single particle strength function  $D(\nu, E)$  and the factor  $F(E)$  which manifests the exclusion principle when a nucleon jumps from the proton to neutron Fermi sea. The function  $D(\nu, E)$  is characterized by the energy weighted sum rules  $\int E^\kappa D(\nu, E) dE$  ( $\kappa = 0, 1, 2$ ), which are related to the nuclear structure parameters.

The Gaussian shape of  $D(\nu, E)$  is assumed. It yields the following total capture rate in units of  $10^6 \text{ sec}^{-1}$  (2nd row) in contrast to the experimental rate (3rd row), the last 5 of which are, however, for the natural element.

<sup>58</sup> Fe	<sup>60</sup> Fe	<sup>62</sup> Fe	<sup>64</sup> Zn	<sup>118</sup> Sm	<sup>156</sup> Gd	<sup>182</sup> W	<sup>206</sup> Pb
4.88	4.06	3.31	5.70	9.21	12.4	13.2	13.7
6.11	5.56	4.72	5.74	10.7	12.1	13.1	13.0

## Statistical Theory of Muon Capture II

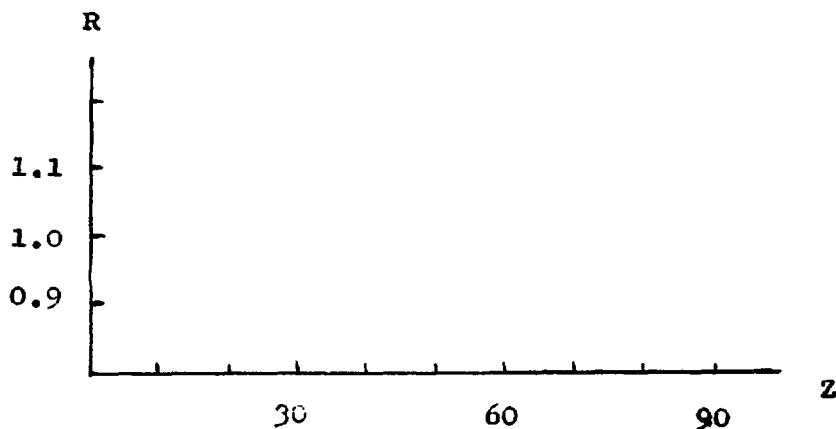
Y.Kohyama and A.Fujii

Physics Department, Sophia University, Tokyo, Japan

The statistical theory is further refined in the following points.

- 1) SU(4) symmetry is assumed only for relativistic correction terms, so that 2 nuclear matrix elements  $\int \psi \cdot \bar{\psi} e^{i\mathbf{p}\cdot\mathbf{r}}$  and  $\int \psi \cdot e^{-i\mathbf{p}\cdot\mathbf{r}}$  govern the capture rate.
- 2) The exponent  $e^{-i\mathbf{p}\cdot\mathbf{r}}$  is separated into  $\cos(\mathbf{p}\cdot\mathbf{r})$  and  $\sin(\mathbf{p}\cdot\mathbf{r})$ . The former/latter induces the nuclear transition of parity change no/yes.
- 3) The pairing effect changes the nucleon distribution near the top of the Fermi sea. This effect requires some modification of the exclusion principle factor  $F(E)$ .
- 4) The capture rate for the natural element is obtained by the weighted mean of the rates for isotopes.

A calculation is forwarded with 4 strength functions, whose shapes are assumed to be the superposition of 2 Gaussian bumps. The ratio R of the calculated and experimental capture rate is plotted as a function of Z.



D.G. Fleming, J.H. Brewer and D.M. Garner  
TRIUMF and Dept. of Chemistry, University of British Columbia

A.E. Pifer, T. Bowen and D. Delise  
Dept. of Physics, University of Arizona

K.M. Crowe  
Dept. of Physics and Lawrence Berkeley Laboratory, University of California

Studies at LBL of  $\mu^+$  depolarization in liquids have yielded a number of rate constants for chemical reactions of muonium (Mu) atoms with various reagents<sup>1</sup>. Comparison of these rate constants with those of atomic hydrogen (H) in analogous reactions has led to the direct observation of large isotopic differences, as high as a factor of  $10^4$  in some cases. Unfortunately, liquid phase results are difficult to interpret theoretically due to competing effects of diffusion and many-body collisions. In the gas phase, certain simple reactions can be characterized by reaction cross sections, for which any difference between Mu and H should agree with the quantitative theoretical predictions of dynamic isotope effects.

Recent experiments at LBL using the "Arizona" beam line, have allowed a determination of the rate constants for the reaction of Mu with added Br<sub>2</sub> and Cl<sub>2</sub> ( $\sim 5 \times 10^{-4}$  ppm.), in 1 atm. Ar moderator. A typical pair of  $\mu^+ \rightarrow e^+ \bar{\nu}_\mu \nu_e$  time histograms are shown in Figure 1. The total rate of disappearance of the Mu signal

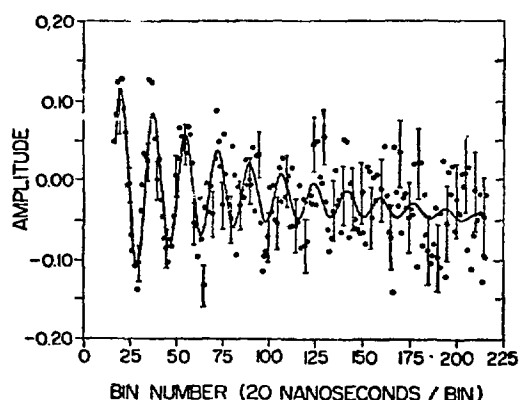
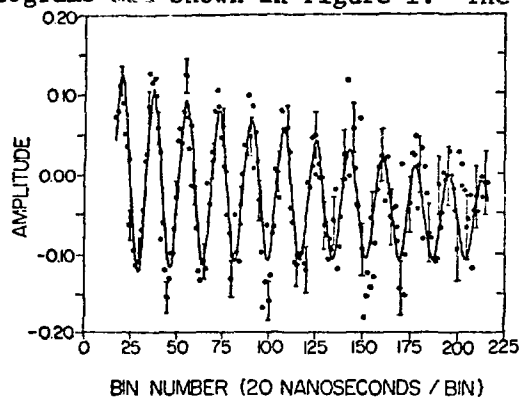
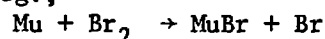


Fig. 1. (Top);  $\lambda_0$  fit of Mu precession in 1 atm. Argon. (Bottom); relaxation  $\lambda = \lambda_0 + \lambda_r$  upon addition of  $\sim 10^{-3}$  ppm. Cl<sub>2</sub>.

is composed of any "background" relaxation rate  $\lambda_0$  (top spectrum) and the rate  $\lambda_r$  of the chemical reaction of Mu atoms with added reagent ( $\lambda = \lambda_0 + \lambda_r$ ). In the absence of any spin-exchange collisions, it is the rate  $\lambda_r$  (bottom spectrum) which is of interest, since this is proportional to the thermal collision cross section of Mu atoms with added reagent, the simplest reaction of which leads to a diamagnetic bond incorporating the Mu; eg.,



The bimolecular rate constant ( $k\nu\sigma\bar{\nu}$ ) can be simply determined from the fitted value of  $\lambda_r$  for a given concentration of added Br<sub>2</sub> or Cl<sub>2</sub>. The results at 22°C are:  $k(\text{Mu}+\text{Br}_2) = (2.4 \pm 0.3) \times 10^{11}$  and  $k(\text{Mu}+\text{Cl}_2) = (6.0 \pm 0.4) \times 10^{10}$  l mole<sup>-1</sup> sec<sup>-1</sup>. The corresponding H atom rate constants<sup>2</sup> are  $\sim 3 \times 10^{10}$  and  $\sim 8 \times 10^9$ , respectively. The Mu atom rates are about a factor of ten faster in both cases; the additional factor of 3 over that expected from the difference in mean velocities is indicative of some "dynamic" enhancement in the rate.

1. J.H. Brewer, et al., Phys. Rev. **A8**, 77 (1973); *ibid*, **A9**, 495 (1974).
2. B.A. Thrush, Prog. Reaction Kinetics, **3**, 65 (1965).

NUCLEAR STRUCTURE STUDIES IN HEAVY DEFORMED  
NUCLEI USING MUONIC ATOMS\*

II.23

D. A. Close, J. J. Malanify, and J. P. Davidson<sup>†</sup>  
Nuclear Analysis Research Group  
University of California  
Los Alamos Scientific Laboratory  
Los Alamos, New Mexico 87544

Nuclear charge parameters for four nuclei in the actinide region,  $^{232}\text{Th}$ ,  $^{238}\text{U}$ ,  $^{235}\text{U}$ , and  $^{239}\text{Pu}$ , have been determined using muonic x rays. A large volume, high resolution Ge(Li) detector was used to measure transitions between circular orbits. The theoretical transition energies were obtained by numerically integrating the Dirac equation with a monopole potential derived from a Fermi charge distribution. Corrections for vacuum polarization and higher-order vacuum polarization, Lamb shift and the anomalous magnetic moment of the muon, nuclear polarization, and the screening effect of the electrons were added to the eigenvalues. A generalized least-squares fitting routine was used to minimize the  $\chi^2$  between the experimental and theoretical energies for the 3d-2p and 2p-1s transitions. The results of these analyses are shown in the following table.

Nucleus	a (fm) $\Delta a$ (fm)	c (fm) $\Delta c$ (fm)	$\beta_2$ $\Delta\beta_2$	Q (barns)
$^{232}\text{Th}$	0.471 0.002	6.998 0.003	0.253 0.001	9.62
$^{238}\text{U}$	0.472 0.003	7.048 0.004	0.280 0.001	11.14
$^{235}\text{U}$	0.471 0.003	7.024 0.004	0.269 0.001	10.59
$^{239}\text{Pu}$	0.465 0.007	7.074 0.008	0.282 0.001	11.55

The values of a, c, and  $\beta_2$  and their errors were calculated by the fitting routine which properly evaluates the error matrix. The quadrupole moments are the calculated values based on the values for a, c, and  $\beta_2$ . The data are being further analyzed to extract higher-order deformation parameters and higher-order moments of the charge distribution.

\* Work performed under the auspices of the U. S. Energy Research and Development Administration.

<sup>†</sup> On Sabbatical leave from the University of Kansas, Lawrence, KS 66045, 1974-75 academic year; presently with the Physics Division of Los Alamos Scientific Laboratory.

L. F. Mausner, R. A. Naumann, Princeton University  
 J. A. Monard, S. N. Kaplan, University of California  
 Lawrence Berkeley Laboratory

To systematically investigate the influence of chemical structure on the atomic capture of negative muons, muonic x-ray spectra have been measured for several isoelectronic and isostructural molecular series and related pure elements at the Lawrence Berkeley Laboratory 184" Cyclotron. Relative intensities were determined using an efficiency calibrated Ge(Li) detector and correcting for x-ray attenuation in the targets employed. Some of the results are summarized below.

A. Seven muonic Lyman series lines were observed from a liquid Ar target with relative intensities consistent with neighboring isoelectronic ions, but in stark contrast to the single  $K\alpha$  line previously reported for a gaseous argon target<sup>1</sup>. These results may imply a large physical state difference for muon capture in liquid or gaseous Ar.

B. The  $K\beta/K\alpha$  ratios decrease through the isoelectronic series  $S^{-2}$ ,  $Cl^{-}$ , Ar,  $K^{+}$ ,  $Ca^{+2}$ . This trend can be correlated with the maximum angular momentum ( $L_{max}$ ) of the initially captured muon at the valence radius of an atom or ion.  $L_{max} \propto r\sqrt{E}$ , where  $r$  is the atomic or ionic radius and  $E$  is the ionization potential.

C. Using the standard cascade computer code with an initial angular momentum distribution of the form  $(2L + 1) \exp(-\alpha L)$ , we obtain a good fit to these  $K\beta/K\alpha$  ratios for  $\alpha \approx 0.2-0.3$ .

D. In general, elemental  $K\beta/K\alpha$  ratios slowly decrease with increasing  $Z$ .

E. The muonic Lyman series intensity patterns from ionic solids containing the same ions are similar. The intensity ratios are similar for  $Cl^{-}$  in NaCl, KCl, and  $CaCl_2$ , for  $Ca^{+2}$  in CaS and  $CaCl_2$ , for  $Na^{+}$  in NaCl and  $NaClO_4$ , and for S in  $CaSO_4$  and  $MgSO_4$ . Conversely, differences are observed for S between CaS and  $CaSO_4$ , and for Cl in NaCl and  $NaClO_4$ .

F. We observe deviations from the Z-Law in ionic solids which appear to correlate with the effective charge on the ions.

G. Comparison of the capture ratios of NaCl vs.  $NaClO_4$ , and CaS vs.  $CaSO_4$  shows higher Z Law deviations for the oxysalts, suggesting preferential transfer of initially captured muons to the tetrahedrally coordinated oxygen from the central chlorine or sulfur atoms.

H. Muon Auger and radiative transition rates out of the  $N_{\mu} = 14$  state in the helium atom were calculated using screened hydrogenic wave functions. Comparison of the classical rotation frequency of a muon captured on this state to these transition rates, suggests that several orbits are possible before the muon deexcites. This result is consistent with the hypothesis of "mesomolecular" orbitals.

\*Work performed under the auspices of the U. S. Atomic Energy Commission

1. G. Backenstoss et. al., Phys. Lett. 36B, 422(1971)

PRECISION MEASUREMENT OF GROUND STATE MUONIUM  
HYPERFINE STRUCTURE INTERVAL  $\Delta\nu^*$

D.E. Casperson, T.W. Crane, V.W. Hughes,  
P.A. Souder, and R.D. Stambaugh, Yale Univ.,  
P.A. Thompson, Los Alamos Scientific Laboratory,  
H.F. Kaspar and H-W. Reist, Univ. of Bern,  
H. Orth and G. zu Putlitz, Univ. of Heidelberg,  
and A.B. Denison, Univ. of Wyoming

At LAMPF the hfs transition  $\Delta F=\pm 1$  in muonium has been measured at a weak magnetic field of  $<2$  mG by the microwave magnetic resonance method in low pressure krypton. The Stopped Muon Channel yielded a high purity beam of momentum 78 MeV/c and polarization 0.8. With a primary proton current of 10  $\mu$ A average and duty factor 0.05, the  $\mu^+$  instantaneous stopping rate was about  $4.5 \times 10^4$  sec $^{-1}$  in a 1.7 atm krypton target system 25 cm in length. The resonance line was observed by an "old muonium" method in which a low power oscillatory field is used and decay positrons are observed only from muonium that has lived longer than 3  $\mu$ sec, to achieve a narrow linewidth of about 220 kHz. Also the line narrowing method of separated oscillating fields was used. The data-taking time of about 600 hours was equally divided between the two methods. Proportional wire chambers as well as scintillation counters were used.

The data on the  $\Delta F=\pm 1$  weak field transition for muonium were obtained for krypton pressures ranging from 1.7 to 5.3 atm. Preliminary analysis of these data, when combined with our earlier higher pressure data<sup>1</sup>, yields  $\Delta\nu$ , as well as a and b, which are respectively the linear and quadratic hfs pressure shift coefficients:  $\Delta\nu=4463 \pm 301.1(1.6)$  kHz (0.36 ppm);  $a=-10.60(11) \times 10^{-2}$ /Torr;  $b=8.6(2.1) \times 10^{-15}$ /Torr $^2$ . The error assigned to  $\Delta\nu$  is a statistical error, which dominates systematic errors. Our  $\Delta\nu$  value agrees with the value quoted by Telegdi et al.,<sup>2</sup>  $\Delta\nu=4463 \pm 304.0(1.8)$  kHz (0.4 ppm). Using our value for  $\Delta\nu$  together with the best known value<sup>3</sup> for  $\alpha$ , we obtain a value for  $\mu_\mu/\mu_p$  and hence for the ratio of muon to electron mass:<sup>1</sup>  $\mu_\mu/\mu_p = 3.183 \pm 5(62)$  (2.0 ppm);  $m_\mu/m_e=206.769 \pm 22(41)$  (2.0 ppm).

---

\*Research (Yale Report No. COO-3075-109) supported by the U.S. Energy Research and Development Administration under Contract No. AT(11-1)3075.

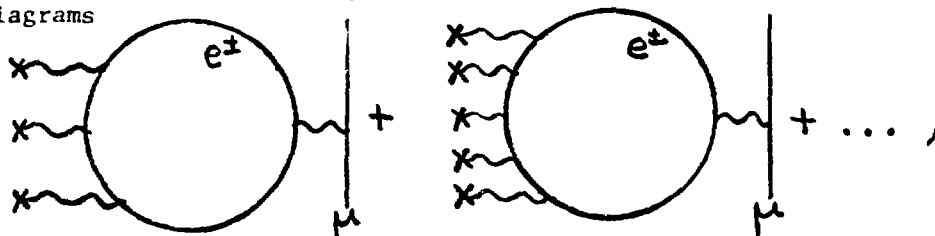
<sup>1</sup>P.A. Thompson et al., Phys. Rev. A 8, 86 (1973).

<sup>2</sup>H.G.E. Kobrak et al., Phys. Lett. 43B, 526 (1973).

<sup>3</sup>E.R. Cohen, B.N. Taylor, J. Phys. Chem. Ref. Data 2, 663 (1973).

High-Order Vacuum Polarization in Exotic Atoms, by G. A. Rinker, Jr., LASL, and L. Wilets. U. of Washington.\*

Electron-positron vacuum polarization potentials, accurate to all orders  $n \geq 3$  in  $(Z\alpha)^n$ , are calculated using realistic nuclear charge distributions for selected nuclei throughout the periodic table. These potentials are employed to determine the muonic energy shifts listed in Table I. These correspond to the diagrams



where X is a nuclear vertex with appropriate form factor. Accurate shifts for other values of Z or for other exotic particles may be interpolated by assuming that for a given level,  $\Delta E^{\alpha Z^k}$ , and for a given nucleus,  $\Delta E^{\alpha} < r_{li}^{-1} >^k$ , where k is determined in each case by fitting to nearby values. Further details concerning these results are being reported elsewhere.<sup>1</sup>

Table I. Vacuum polarization energy shifts of order  $\alpha(Z\alpha)^n$ ,  $n \geq 3$ .

Z	26	56	78	82	92	98	114
E (eV)							
1s <sub>1/2</sub>	12	151	418	492	691	839	1370
2s <sub>1/2</sub>	3	60	201	244	367	463	817
3s <sub>1/2</sub>	1	27	100	123	193	248	462
2p <sub>1/2</sub>	3	84	287	348	517	646	1110
2p <sub>3/2</sub>	3	81	277	335	500	626	1080
3p	1	34	130	160	250	322	593
3d <sub>3/2</sub>	1	38	150	186	299	390	738
3d <sub>5/2</sub>	1	36	145	180	288	374	706
4f	0	17	75	95	158	210	417
5g	0	9	41	53	89	119	245
6h	0	4	23	30	51	71	148

<sup>1</sup>G. A. Rinker, Jr. and L. Wilets, "Vacuum Polarization in Strong, Realistic Electric Fields," submitted to Phys. Rev. A. See also L. Wilets and G. A. Rinker, Jr., Phys. Rev. Lett. 34, 339 (1975); G. A. Rinker, Jr. and L. Wilets, Phys. Rev. Lett. 31, 1559 (1973).

\*Work performed under the auspices of the U.S. ERDA.

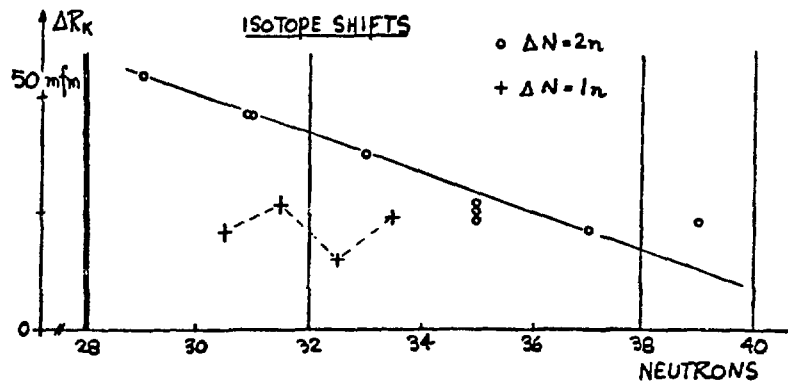
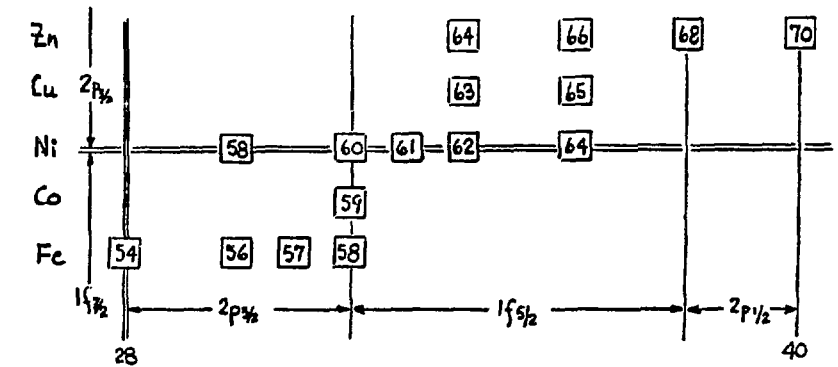
MUONIC X-RAY MEASUREMENTS OF NUCLEAR CHARGE RADII IN THE MASS-60 REGION†

E. B. Shera, E. T. Ritter††, R. B. Perkins, and L. K. Wagner†††  
 Los Alamos Scientific Laboratory, University of California, Los Alamos, NM 87544

H. D. Wohlfahrt and G. Fricke, University of Mainz, Mainz, Germany

R. M. Steffen, Purdue University, Lafayette, IN 47907

The muonic  $2p_{3/2} \rightarrow 1s_{1/2}$  and  $2p_{1/2} \rightarrow 1s_{1/2}$  transition energies for the 16 separated isotopes Fe-54,56,57,58, Co-59, Ni-58,60,61,62,64, Cu-63,65 and Zn-64,66,68,70 have been measured in the stopped-muon channel of LAMPF. Subsets of three different nuclides were measured simultaneously to extract precise values of isotope and isotone shifts. Equivalent-charge-radii differences between isotopes were determined from the Ford-Wills radial moments ( $r_{1.55}$ ) with accuracies of about  $\pm 10^{-3}$  fm. Some details of the measurements, together with results for the even Fe isotopes, appear in ref. 1. Isotope shift data for all the nuclei studied are summarized in the lower half of the figure below, in which values for the differences in charge radii,  $\Delta R_K$ , between isotopes differing by both  $\Delta n=1$  and  $\Delta n=2$  are plotted. The isotope shift values are plotted below the isotope pairs (in the upper half of the figure) to which they correspond. Two effects are readily apparent. 1) The isotope shifts between even nuclei ( $\Delta n=2$ ) form an approximately linear sequence--strikingly independent of Z--as n increases from 28 to 40. The cause of this systematic behavior is not presently understood. 2) A pronounced even-odd staggering exists for the  $\Delta n=1$  shifts. This effect, which has been observed in other optical and muonic isotope shift studies, is also evident in our isotone shift data. Detailed Hartree-Fock predictions of the nuclear charge distribution of these nuclei are presented in the following paper.



†Supported by ERDA and Deutsche Forschungsgemeinschaft.

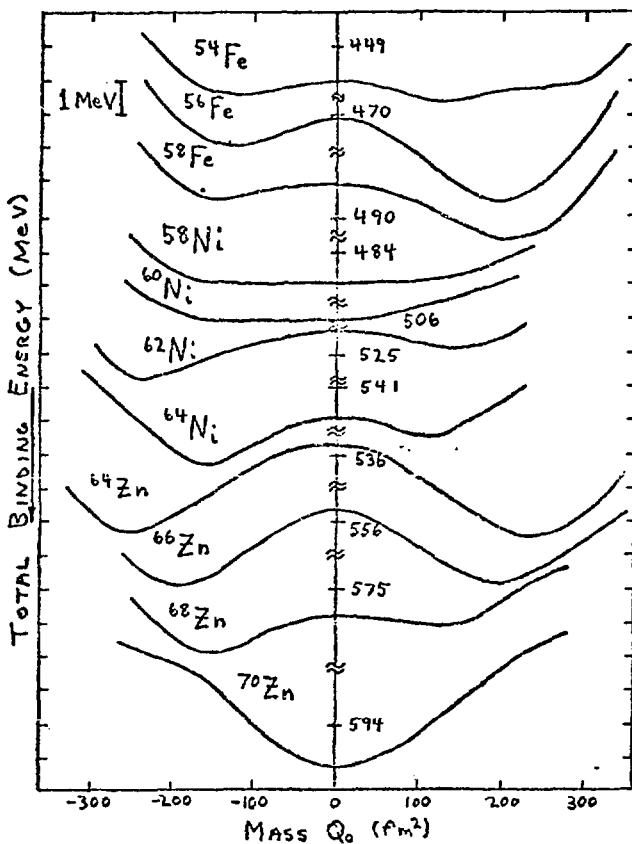
††Visitor from ERDA.

†††Also, Florida State U.

1E. B. Shera et al,  
 Phys. Rev. Lett. 34, 535  
 (1975).



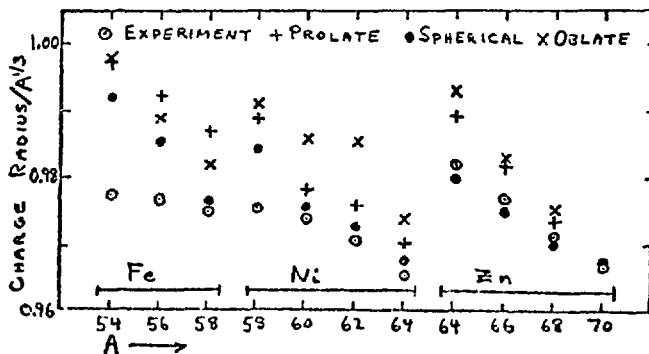
We have carried out constrained Hartree-Fock calculations for  $^{54,56,58}\text{Fe}$ ,  $^{58,60,62,64}\text{Ni}$ , and  $^{64,66,68,70}\text{Zn}$ , using a theory based on a realistic two-body interaction and a phenomenological pairing force, with a basis which allows the solutions to exhibit axially- and parity- symmetric deformations.<sup>1</sup> The energy-of-deformation curves are shown in the upper figure, as a function of the intrinsic mass quadrupole moment  $Q_0$  ( $Q_0=200\text{fm}^2$  corresponds to  $\beta\approx 0.2$ ). These curves are generally too flat to produce a definite ground-state deformation, with the exception of  $^{56,58}\text{Fe}$  and  $^{70}\text{Zn}$ . For  $^{56}\text{Fe}$ , our prediction for the charge quadrupole moment ( $+100\text{fm}^2$ ) is in agreement with a recent measurement<sup>2</sup> for the first  $2^+$  state ( $+120\text{fm}^2$ ). Although approximation of most of these nuclei by a single deformed intrinsic state is very crude, one still obtains some insight into the behavior of charge radii in this region. Shown in the lower figure are the rms radii/ $A^{1/3}$  of the constrained spherical calculations and of the prolate and oblate densities nearest the local energy minima (or the extrema of the flat central minima for  $^{58,60}\text{Ni}$ ), along with radii interpreted from a LAMPF muonic-atom experiment reported in the preceding paper. From these results one observes, for example, that the trend toward prolate deformation in the Fe isotopes reproduces much more of the experimental solutions, and that the one true spherical nucleus  $^{70}\text{Zn}$  is in excellent agreement with experiment. Evidently a better description of these nuclei will require inclusion of non-axial shapes, superposition of many nearly degenerate shapes, and polarization arising from the residual n-p interaction.



\*Work performed under the auspices of the USERDA

<sup>1</sup>E. B. Shera et al., Phys. Rev. Lett. 34, 535 (1975).

<sup>2</sup>G. Schilling et al., Phys. Rev. C1, 1400 (1970).



MICROSCOPIC CALCULATIONS OF ISOTOPIC SHIFTS IN  
DEFORMED NUCLEI

Dieter Zawischa

Institut für Theoretische Physik der TH Hannover, Germany

and

Josef Speth

Physics Department, SUNY-Stony Brook, N. Y. 11794

We used the linear response theory including pairing correlations, to calculate microscopically the change of the ms charge radii and the mesonic isotopic shifts due to the addition of one or two neutrons to an even nucleus. For the evaluation of the corresponding equation<sup>1</sup> we used single particle energies and wave functions of a deformed Woods-Saxon potential. It turns out that the static and low energy results depend very sensitively on the single particle energy scheme. Therefore the spectra of the odd mass nuclei were used to extract corrections to the theoretical s.p. energies. By this method we finally obtained one Nilsson level scheme which is used for the whole region.<sup>2</sup>

As residual interactions (particle-hole and particle-particle) density dependent zero-range forces have been used with parameters which previously have been adjusted in the lead region. A large configuration space is used so that no effective charges have to be introduced.

Some preliminary results are given in the table.

Isotope Pair	$\Delta\langle r^2 \rangle [10^{-3} \text{fm}^2]$		$\Delta E_{\mu}^{is} [\text{keV}]$	
	Theory	Exp.	Theory	Exp.
$^{157}\text{Gd}-^{156}\text{Gd}$	29.5	$21 \pm 13^a$	1.85	
$^{158}\text{Gd}-^{156}\text{Gd}$	153.0	$135 \pm 20^a$	8.63	
$^{171}\text{Yb}-^{170}\text{Yb}$	64.9	$41 \pm 10^a$	4.24	$4.86 \pm .52^b$
$^{172}\text{Yb}-^{170}\text{Yb}$	99.7	$118 \pm 16^a$	6.67	$10.64 \pm .36^b$
$^{184}\text{W}-^{182}\text{W}$	68.7	$102 \pm 12^a$	5.62	

<sup>a</sup>K. Heilig and A. Stuedel, Atomic Data and Nucl. Data Tables, in print.

<sup>b</sup>A. Zehnder, thesis (Diss. Nr. 5280), ETH, Zurich.

1. J. Meyer and J. Speth, Phys. Letters 39B (1972) 330.
2. D. Zawischa and J. Speth, Phys. Letters, in print.

Muonium and Free-Muon Precession Components in  
Noble Gases at Low Pressure\*

A. E. Pifer, T. Bowen, and D. A. DeLise

Department of Physics, University of Arizona, Tucson, Arizona 85721

and

J. H. Brewer and D. G. Fleming

TRIUMPF, University of British Columbia, Vancouver 8, B.C.

Observations on the fractions of stopped muons which precess at the free muon rate and at the muonium rate are being carried out for positive muons stopping in noble gases, particularly neon and argon, near atmospheric pressure. The muons are supplied by a 30 MeV/c beam at the LBL 184" Cyclotron. All inside surfaces of the gas target chamber are chromium plated; since chromium is anti-ferromagnetic at room temperature, muons stopping in the walls are completely depolarized and do not contribute to the precession signal. Results are very sensitive to small concentrations of impurities. Data will be presented for various target gases and impurities.

\*Work supported in part by the National Science Foundation.

S. N. Kaplan and J. A. Monard  
Lawrence Berkeley Laboratory, University of California, Berkeley, CA 94720

S. Nagamiya  
Lawrence Berkeley Laboratory, University of California, Berkeley, CA 94720  
and  
Department of Physics, University of Tokyo, Hongo, Bunkyo-ku, Tokyo, Japan

## ABSTRACT

There are a number of reported measurements of negative muon ( $\mu^-$ ) lifetime in  $^{238}\text{U}$ . All such lifetime measurements known to us have used either nuclear fission ( $\tau_f$ ) or a decay electron ( $\tau_e$ ) to signal the muon disappearance. There appears to be a significant discrepancy between  $\tau_f$  and  $\tau_e$ , as  $\tau_f = 75.8 \pm 0.8 \text{ nsec}^1$  while  $\tau_e = 81.5 \pm 3.0 \text{ nsec}^2$ . Bloom<sup>3</sup> suggests that the difference is real; that the electron measurements give the true muon lifetime,  $\tau(\mu)$ , whereas the fission measurements observe two lifetimes, one from  $\mu^-$  capture and the other from fission decay of the shape isomer which, he postulates, is copiously excited by non-radiative capture of the 2p-1s muonic transition.

It follows from Bloom's arguments and recent  $\gamma$ -decay measurements on the shape isomer<sup>4</sup> that one would expect to see  $\gamma$ -rays from the fission isomer in  $^{238}\text{U}$  following  $\mu^-$  capture. Extending Bloom's arguments to analyze the time distribution of nuclear  $\gamma$ -rays following  $\mu^-$  capture, we would expect (neglecting lifetimes of intrinsic levels) that two distinct lifetimes should be observed. The  $\gamma$ -rays from the  $\mu^-$ -capture-product levels should have the true  $\mu^-$  lifetime,  $\tau(\mu)$ . Any  $\gamma$ -rays from back decay of the shape isomer will, however, have a lifetime  $\tau = [1/\tau(\mu) + 1/\tau(i)]^{-1}$  where  $\tau(i)$  is the isomer lifetime. Furthermore, compared to electron measurements, the  $\gamma$ -ray measurements are much more free from long-lived background arising from the muons that stop in the low-Z material of surrounding counters. Because of relative capture and decay rates, such background is reduced more than a factor of 100.

Very preliminary results from the first few hours of an experimental run show no candidates for shape-isomer  $\gamma$ -rays with yields greater than 2 % of the 3d-2p X-ray yield. The present data are not yet sufficient to give lifetimes from any individual  $\gamma$ -ray peaks. However, a mean life obtained by averaging over all  $\gamma$ -ray counts in the energy range 1-2 MeV gives  $\tau(\mu) = 85 \pm 5 \text{ nsec}$  [The statistical error is about 1 %. The remainder is a conservative estimate to allow for the, as yet uncorrected, background periodicity due to muon-beam time structure.]. This result is in good agreement with electron measurements.

## REFERENCES

- <sup>1</sup> J. A. Diaz et al., Nucl. Phys. 40, 54 (1963); B. Budick et al., Phys. Rev. Lett. 24, 604 (1970); D. Chultem et al., JINR E15-8134 (Dubna, 1974).
- <sup>2</sup> O. Hashimoto et al., Contributed Paper to this Conference (1975).
- <sup>3</sup> S. D. Bloom, Phys. Lett. 48B, 420 (1974).
- <sup>4</sup> P. A. Russo, J. Pedersen and R. Vandenbosch, Nucl. Phys. A240, 170 (1975).

## PRECISE MUONIC X-RAY ENERGIES AND THE VACUUM POLARIZATION

G. Backenstoss\*, H. Koch\*\*, A. Nilsson\*\*\* and L. Tauscher\*

CERN, Geneva, Switzerland

\*University Basel, Switzerland

\*\*University Karlsruhe, Germany

\*\*\*Research Institute for Physics Stockholm, Sweden.

Considerable efforts have been made to determine X-ray energies of heavier muonic atoms with the highest possible accuracy in order to decide whether discrepancies exist to theoretically predicted energies and of which type they are. Since the transitions are chosen such that other sources of uncertainties such as finite size effect, nuclear polarization and electron screening are minimized, possible deviations are thought to be connected with quantum electrodynamical corrections, predominantly vacuum polarization.

Hence, additional information is desirable which we obtained by measuring the energy difference between the 4→3 transitions in  $\mu$ -Ba and the 5→4 transitions in  $\mu$ -Pb which are doublets interleaving each other. The components are, however, sufficiently separated that the energy difference can be determined with a high precision. Any effect depending independently on Z and the muonic state (n,  $\ell$ , j) should be detectable sensitively in this way.

We measured the X-rays from a composite Ba-Pb target simultaneously with two Ge(Li) detectors and obtained for the energy difference

$$\Delta E = E_{4f \rightarrow 3d}(\text{Ba}) - E_{5g \rightarrow 4f}(\text{Pb})$$

for the transitions between the states with  $\ell+1/2$  and those with  $\ell-1/2$  the following values ( $\Delta E_{\text{exp}}$ ) which are the averaged results of both detectors and which agree within their errors.

	$\Delta E_{\text{exp}}$ (keV)	$\Delta E_{\text{th}}$ (keV)
$\ell+1/2$	2.567±0.013	2.578
$\ell-1/2$	3.611±0.016	3.620

These data agree fully with the calculated values ( $\Delta E_{\text{th}}$ ) which include the terms of the order  $\alpha(Z\alpha)$ ,  $\alpha^2(Z\alpha)$  and  $\alpha(Z\alpha)^3$ ,<sup>5,7</sup>. In earlier work a discrepancy was reported<sup>1)</sup> for the  $\ell+1/2$  transition difference, which however was not measured directly as difference, yielding ( $\Delta E_{\text{th}} - \Delta E_{\text{exp}}$ ) = 34 eV.

A determination of the absolute energies will be attempted with a special calibration method utilizing built in calibration lines. This should yield another cross check on this important problem. The purely statistical error is expected to be of the order of 15 eV.

1) M.S. Dixit et al. Phys. Rev. Lett. 27, 878 (1971).

P.A. Souder, D.E. Casperson, T.W. Crane  
V.W. Hughes, D.C. Lu, and M.H. Yam, Yale Univ.,  
H. Orth and G. zu Putlitz, Univ. of Heidelberg,  
and H-W. Reist, Univ. of Bern

The muonic helium atom  $\alpha\mu^-e^-$  is the simple atomic system in which one of the electrons in a normal helium atom is replaced by a negative muon.<sup>1</sup> When a  $\mu^-$  is stopped in He, the muonic helium ion  $(\alpha\mu^-)^+$  in its ground 1S state is normally formed. Both electrons are lost through Auger processes, and since the ionization potential of He is higher than that of  $\alpha\mu^-e^-$ , the ion cannot capture an electron from a neighboring He atom. Thus a donor atom with a low ionization potential such as Xe must be added to form  $\alpha\mu^-e^-$ .

The method of our experimental study of the atom is the usual one for observing the Larmor precession of muonium (1.4 MHz/G) or free muons (13.6 kHz/G).<sup>2</sup> Polarized negative muons from a 100 MeV/c beam at SREL stopped in a target containing 14 atm He to which Xe could be added. Plastic scintillators detected the stopping muons and their decay electrons, and pulse height analyzers recorded the time spectra of the events. We first measured the residual polarization of  $(\alpha\mu^-)^+$  in pure He. A precession amplitude  $A_\mu = 1.24\% \pm 0.17\%$  was observed at a magnetic field of 67 G at a frequency (0.91 MHz) corresponding to free muon Larmor precession. This amplitude corresponds to a residual polarization  $P=0.06$ , which contrasts with the expected value  $P=0.17$  for  $\mu^-$  captured by atoms with spinless nuclei.<sup>3</sup> Previous experiments with He had established an upper limit on  $P$  at about this value.<sup>4</sup> Adding 0.2% Xe did not affect this amplitude, but adding 1.2% Xe resulted in a significantly smaller amplitude  $A_\mu = 0.25\% \pm 0.22\%$  suggesting that  $\alpha\mu^-e^-$  was being formed.

To provide more direct evidence, we searched for the characteristic muonic helium atom Larmor precession frequency (the same as for muonium) at several magnetic fields: 3.1G; 3.4G, 3.7G; and 4.6G. A 2% admixture of Xe in 14 atm of He was used for these data. At the expected frequency, a positive amplitude was present for each magnetic field. The average amplitude,  $A_\mu -$ , was  $0.53\% \pm 0.09\%$ . This clearly demonstrates the formation of polarized  $\alpha\mu^-e^-$  atoms and indicates that it is possible to perform precision measurements of the hyperfine structure interval  $\Delta\nu$  as has been done for muonium.<sup>5</sup> A comparison of  $\Delta\nu$  between  $\mu^+e^-$  and  $\mu^-e^-$  should yield a precise comparison of the  $\mu^+$  and  $\mu^-$  magnetic moments, serving as a test of one of the predictions of CPT invariance.

\*Research (Yale Report No. COO-3075-110) supported by the U.S. Energy Research and Development Administration under Contract AT(11-1)-3075.

1. K.N. Huang et al., Fifth International Conference on High Energy Physics and Nuclear Structure, ed. by G. Tibell, (North-Holland Pub. Co., 1973), p.312.
2. R.D. Stambaugh et al., Phys. Rev. Lett. 33, 568 (1974).
3. R.A. Mann and M.E. Rose, Phys. Rev. 121, 293 (1961).
4. D.C. Buckle et al., Phys. Rev. Lett. 20, 705 (1968); V.G. Varlamov et al., JETP Lett. 16, 224 (1972). P. Souder, et al., Abstracts, Fourth Intl. Conf. on Atomic Physics, Heidelberg, 1974, p. 32.
5. V.W. Hughes, Annu. Rev. Nucl. Sci. 16, 445 (1966).

EMISSION OF THE AUGER ELECTRONS IN  $\mu$ -MESIC ATOMS AND ESCAPE OF CHARGED PARTICLES IN  $\mu$ -MESON CAPTURE BY LIGHT (C,N,O) AND HEAVY (Ag, Br) NUCLEI.

Yu.A.Batusov, S.A.Bunyatov, L.Vizireva, G.R.Gulkanyan, F.Mirsalikhova, V.M.Sidorov, Kh.Chernev.

Joint Institute for Nuclear Research, Dubna, USSR

Abstract

The probabilities of emission of Auger electrons of  $(20 \pm 100)$  keV in  $\mu$ -mesic atoms of light (C,N,O) and heavy (Ag,Br) elements were determined to be  $\alpha^l = (1.1 \pm 0.3) \cdot 10^{-2}$  and  $\alpha^h = (31 \pm 1) \cdot 10^{-2}$ , respectively. The multiplicity was also determined and the spectrum of the Auger electrons from heavy element mesic atoms was measured.

There were obtained the relative probabilities of emission of one, two, three and four charged particles in  $\mu^-$ -meson capture by (C,N,O) and (Ag, Br) nuclei (Table I). The total yield of charged particles per one capture act is  $(7.4 \pm 1.4)\%$  for (C,N,O) and  $(2.9 \pm 0.2)\%$  for (Ag,Br) nuclei.

Table I.

The probabilities escape of charged particles per one capture act, (%)

Number of particles	Nuclei	
	C,N,O	Ag, Br
I	$W_I^l = 1.5 \pm 1.1$	$W_I^T = 2.7 \pm 0.2$
2	$W_2^l = 3.7 \pm 0.3$	$W_2^T = 0.17 \pm 0.02$
3	$W_3^l = 1.7 \pm 0.1$	$W_3^T = 0.02 \pm 0.005$
4	$W_4^l = 0.5 \pm 0.08$	$W_4^T \sim 0.001$
Total	$W^l = 7.4 \pm 1.4$	$W^T = 2.9 \pm 0.2$

## SEARCH FOR RADIATION TRANSITIONS FROM THE MESIC MOLECULAR STATES

K.Andert, V.S.Evseev, H.G.Ortlepp, V.S.Roganov, B.M.Sabirov, H.Haupt, H.Schneuwly, R.Engfer

Joint Institute for Nuclear Research, Dubna, USSR

### Abstract

By using a planar Ge(Li) diode having a high energy resolution the energy spectrum of muonic X-ray radiation from oxygen (water) has been measured by means of the pure muonic beam from the Dubna synchrocyclotron. The intensity of radiation transitions from the mesic molecular state to the ground mesoatomic state (the expected lines at K- and L-series boundaries) has been shown to be  $10^{-4}$ . These results show that the types of decays of the mesic molecular states suggested in <sup>/1,2/</sup> to explain the  $Z^{-3}$  dependence of the negative pion charge exchange rate in hydrogenous compounds and the structure of muonic X-ray spectra disagree with the experiment. The upper limit for mesic molecular states with respect to their postulated <sup>/1,2/</sup> properties has been discussed.

### References

1. S.S.Gershtein et al. Uspekhi Fiz. Nauk 97, 3 (1969).
2. L.I.Ponomarev. JINR P4-7264, Dubna (1973).



DEPENDENCE OF MUONIC X-RAY SPECTRAL STRUCTURE UPON ATOMIC  
VALENCY

K.Andert, V.S.Evseev, H-G.Ortlepp, V.S.Roganov, B.M.Sabirov,  
H.Haupt, H.Schneuwly, R.Engfer

Joint Institute for Nuclear Research, Dubna, USSR

## Abstract

It follows <sup>from</sup> the model of large mesic molecules<sup>/1/</sup> that there must be observed the dependence of muonic X-ray spectral structure upon the sign and the value of the atomic valency. The structure of the K-series of N and S compounds where these atoms have -3,0,+5 and -2,0,+6 valencies, respectively, has been investigated by using the Dubna synchrocyclotron separated muonic beam. No dependence upon the sign and the valency module has been noticed for S. For both N compounds, where the nitrogen atom has a -3, +5 valency, a considerable reduction of transition intensities from the states with a large  $n$  (with respect to the  $N_2$  case, where zero valency takes place) similar in the absolute value has been observed. The obtained results are in contradiction with the consequences on the large mesic molecule model.

## References

1. S.S.Gershtein et al. Uspekhi Fiz.Nauk 97, 3(1969),  
L.I.Ponomarev, JINR P4-7269, Dubna (1973).

STUDY OF THE REACTION  $\mu^{-12}\text{C} \rightarrow {}^4\text{He} {}^4\text{He} {}^3\text{H} n \nu$

II.37

Yu.A.Batusov, S.A.Bunyatov, L.Vizireva, G.R.Gulkanyan,  
F.Mirsalikhova, V.M.Sidorov, Kh.Chernev, R.A.Eramzhyan

Joint Institute for Nuclear Research, Dubna, USSR

Abstract

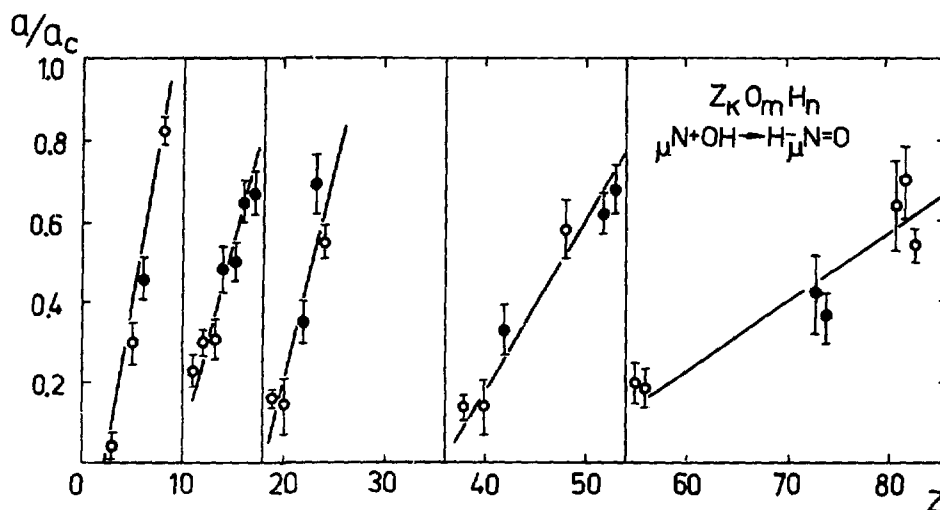
The reaction  $\mu^{-12}\text{C} \rightarrow {}^4\text{He} {}^4\text{He} {}^3\text{H} n \nu$  was investigated experimentally. The upper limit of its relative probability is determined to be  $W \lesssim 2 \cdot 10^{-2}$ . Possible mechanisms of the reaction are considered. It is shown that at the probability of  $(1.1 \pm 0.1) \cdot 10^{-2}$  per the capture act, this reaction proceeds according to the scheme predicted by the resonance mechanisms of the  $\mu^-$ -meson capture by carbon nucleus.

## NEGATIVE MUON DEPOLARIZATION IN HYDROXIDES AND ACIDS

V.I. Goldansky, V.S. Evseev, T.N. Mamedov, Yu.V. Obukhov,  
V.S. Roganov, M.V. Frontasyeva, N.I. Kholodov

Joint Institute for Nuclear Research, Dubna, USSR

The values of the residual polarization of  $\mu^-$ -mesons on oxygen contained in hydroxides ( $\circ$ ) and acids ( $\bullet$ ) have been measured by the muon spin precession method in the weak transverse magnetic field. The periodical dependence on the atomic number  $Z$  has been observed.



The obtained results are explained by the concept <sup>1/</sup> on the chemical reactions of the oxygen mesic atom  $\mu N$ . The value of the residual polarization  $a/a_c$  ( $a_c$  is the value in carbon) increases from the beginning of the period to its end due to the weakening of the bond between the group OH and the central atom  $Z$  <sup>2/</sup> and, consequently, the chemical reaction probability with forming  $H - \mu N = O$  increases. This reaction stops the depolarization caused by the paramagnetism of the free atom  $\mu N$  electron shell.

## R e f e r e n c e s

1. A.A. Dzuraev et al. Sov. JETP 66, 433 (1974).
2. G. Seaborg. Chemistry. 1963.

NEGATIVE MUON DEPOLARIZATION IN THE BENZENE AND  
CARBON TETRACHLORIDE MIXTURES

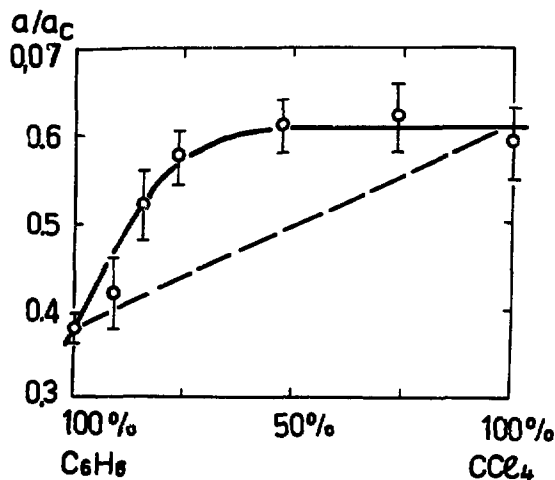
V.I.Goldansky, V.S.Evseev, T.N.Mamedov, Yu.V.Obukhov,  
V.S.Roganov, M.V.Frontasyeva, N.I.Kholodov

Joint Institute for Nuclear Research, Dubna, USSR

The values of the residual polarization  $a/a_c$  ( $a_c$  is the value in carbon) of  $\mu^-$ -mesons in  $C_6H_6$  and  $CCl_4$  mixtures at different component concentrations have been measured by the muon spin precession method in the weak transverse field.

The non-linear dependence of  $a/a_c$  on the concentration of the components has been found. It evidences for the fast chemical reaction of carbon mesic atom.

The competing acceptors method in the frame of /1/ gives the rate constant  $K = (1.9 \pm 1.2) \cdot 10^{-12} \text{ sek}^{-1} \text{ cm}^3$  which coincides in the magnitude order with that of the chemical reactions limited by diffusion /2/.



R e f e r e n c e s

1. A.A.Dzuraev et al. Sov. JETP 66, 433 (1974).
2. Advances in Radiation Chemistry. 1, 33. Wiley Intersc. 1969.

## SHIFTED ELECTRONIC X-RAYS FROM MUONIC HEAVY ATOMS

W.D.Fromm, Dz.Ganzorig, T.Krogulski, H.G.Ortlepp, S.M.Polikanov,  
B.M.Sabirov, U.Schmidt

Joint Institute for Nuclear Research, Dubna, USSR

R.Arlt

Technical University, Dresden, GDR

At the separated  $\mu^-$  beam of the Dubna synchrocyclotron muonic spectra of the elements U, Th, Pb, Ir and Ta were investigated in the low-energy region. A conventional 1234 counter telescope and two-dimensional (time-energy) registration of the Ge(Li)-detector signals were employed. The energy calibration was performed by means of radioactive standards measured in the duration of the full experiment as random coincidences.

The gamma-ray spectra associated with nuclear muon capture (delayed) show unshifted electronic X-ray groups from both Z and Z-1. The  $\gamma$ -ray spectra associated with the muonic cascade (prompt) show besides muonic transitions normal X-rays from the target material Z and electronic X-rays close to the positions of (Z-1) X-rays but shifted by some hundreds of eV to higher energy. The observed  $K_{\alpha}$ -shifts range from about 350 eV for Uranium /1/ to about 160 eV for Iridium where a similar shift was also revealed from the measurements at CERN /2/.

Vacancies in the electronic K-shell are produced by muonic Auger transitions in the muon cascade. At  $n \sim 7$  where this process mainly occurs the screening of one atomic charge unit by the muon is not yet complete /3/ and an energy shift of the X-rays has to be expected if the refilling of the electronic vacancies is sufficiently fast.

Theoretical values for the shifts basing on cascade calculations with account of the refilling process are presented. A discussion of the role of multiple vacancies in the electronic L-shell is given.

## References:

1. R.Arlt, Dz.Ganzorig, T.Krogulski, H.G.Ortlepp, S.M.Polikanov, B.M.Sabirov, W.D.Fromm, U.Schmidt, H.Schneuwly, R.Engfer. JETP Lett., 20, 635 (1974).; JINR, E6-8127(1974).
2. R.Arlt, R.Engfer, W.D.Fromm, Dz.Ganzorig, T.Krogulski, H.G.Ortlepp, S.M.Polikanov, B.M.Sabirov, H.Schneuwly, U.Schmidt; JINR E1-8504, Dubna(1974); Phys.Lett. B
3. P.Vogel. Phys.Rev. A7, 63(1973).

## STUDIES OF MUONIUM INTERACTIONS IN MONOCRYSTALLIC GERMANIUM

V.G.Firsov, G.G.Myasishceva, Yu.V.Obukhov, V.S.Roganov

Joint Institute for Nuclear Research  
Dubna, U S S R

The dependence of the amplitude and the initial phase of the residual polarization vector of positive muons upon temperature and the intensity of the external magnetic field have been studied in monocrystalline germanium. The parameters of the theory of the muonium depolarization stage have been determined within 100-200°K. The dependence of the lifetime of free muonium atoms in Ge upon temperature gives the value of the activation energy of muonium transition to the diamagnetic state to be as follows:

$$E = 0.20 \pm 0.02 \text{ eV.}$$

## References

- \* G.G.Myasischeva et al. Sov. JETP, 53,451(1967);  
D.G.Andrianov et al. Sov. JEPT 56, 1195 (1969);  
I.G.Ivanter et al. Sov. JETP 54, 559 (1968), Sov.JETP  
55, 1521 (1968); D.G.Andrianov et al. Dokl.Acad.USSR,  
201,884(1971), V.I.Kudinov et al. Sov. JETP 21,49(1975).

INVESTIGATION OF ATOMIC CAPTURE OF MUONS AND STRUCTURE  
OF MUONIC  $X$ -RAY SERIES IN MAGNESIUM OXIDES

V.N. Pokrovsky, L.I. Ponomarev, V.G. Zinov

I.A. Yutlandov

Joint Institute for Nuclear Research Dubna, USSR.

Intensities of muonic  $X$ -rays in Mg, MgO and MgO<sub>2</sub> targets were measured with Ge(Li) detector. Atomic capture of muons in the same compounds was studied with Čerenkov detectors. The results obtained are discussed in terms of present models of negative muon atomic capture.

CALCULATION OF QUASI-STATIONARY STATE CHARACTERISTICS  
OF HYDROGEN MESIC MOLECULES

L.I.Ponomarev, I.V.Puzynin, T.P.Puzynina

Joint Institute for Nuclear Research, Dubna, USSR.

The method for solving three-body problem with the Coulomb interaction developed in authors' earlier papers /1,2/ was employed to calculate the quasi-stationary levels of hydrogen mesic molecules. The energies and widths of all the quasi-stationary levels of  $pp\mu$ ,  $dd\mu$ ,  $tt\mu$ ,  $pd\mu$ ,  $pt\mu$  and  $dt\mu$  mesic molecules are found.

References:

1. A.V.Matveenko, L.I.Ponomarev, Zh.Eksp.Theor.Fiz. 59, 1597 (1970), English Transl.Soviet Phys.JETP, 32, 871 (1971)
2. L.I.Ponomarev, I.V.Puzynin, T.P. Puzynina. J.Comp.Phys. 13, 1 (1973).



II.44

THE POLARIZATION MEASUREMENT OF STOPPED MUONS BY HANLE SIGNALS

A. Possoz, L. Grenacs, J. Lehmann, D. Meda and L. Palffy  
 Institut de Physique Corpusculaire, Université Catholique de Louvain  
 Louvain-la-Neuve, Belgium

J. Julien and C. Samour  
 Centre d'Etudes Nucléaires de Saclay, Orme des Merisiers  
 Gif-sur-Yvette, France

ABSTRACT

The "dispersive" Hanle signal generated by the polarization of stopped muons in graphite is used for the measurement of the residual polarization of  $\mu^-$  in muonic  $^{12}\text{C}$ .

INTRODUCTION

When muons, polarized initially along the beam (z-axis), are subject to a transverse magnetic field  $B_x$ , the time-integrated average transverse component (y-component) of the polarization in the case of a single frequency problem is given by :

$$P_{\mu,T}(B_x) = P_{\mu} \tau_{\mu}^{-1} \int_0^{\infty} e^{-\frac{t}{\tau_{\mu}}} \sin(B_x \cdot \gamma \cdot t) dt = \frac{B_x \cdot \gamma \cdot \tau_{\mu}}{1 + (B_x \cdot \gamma \cdot \tau_{\mu})^2} P_{\mu}$$

where  $P_{\mu}$ ,  $\tau_{\mu}$  and  $\gamma$  are the residual polarization, the disappearance time and the gyromagnetic ratio of the muon. The relaxation rate  $\Lambda$  of the polarization of the muon can be taken into account by  $\tau_{\mu} \rightarrow 1/(\tau_{\mu}^{-1} + \Lambda)$ . This function of  $B_x$ , a "dispersive" Hanle signal<sup>1</sup>, can be detected with an electron counter located on the y-axis (the "absorbtive" signal can also be detected along the z-axis). We used the dispersive signal to measure  $P_{\mu}$  of  $\mu^-$  in graphite. The measurement was done at the muon-channel of ALS<sup>2</sup> with an instantaneous stop-rate  $\approx 10^6 \text{ s}^{-1}$ . In order to increase the detectable effect, the ratio of countings  $R(B_x)$  of two detectors located symmetrically, with respect to the target, on the y-axis, was measured (see figure). The results (taking  $\Lambda = 0$ <sup>3</sup>),  $P_{\mu}(\text{fd}) = + 18.0 \%$  and  $P(\text{bd}) = - 18.3 \%$  (7 % relative error) agree with those obtained using other methods<sup>3</sup>.

CONCLUSION

This signal is unaffected by the time-structure of the beam, its figure of merit at large stop-rates ( $\gg \tau_{\mu}^{-1}$ ) exceeds that of the Larmor precession method. The use of the Hanle signal(s) for muon polarization measurements at "pion factories", at least for single-frequency problems, is therefore recommended.

III

EXOTIC ATOMS AND CONDENSED NUCLEAR STATES

F. Cannata

Istituto di Fisica Nucleare, Sezione di Bologna,  
Istituto di Fisica dell'Università, Bologna, Italy

Polarizability effects have been calculated both for the Compton scattering and for the energy shifts in exotic atoms<sup>1)</sup>. The results obtained in the non relativistic quark model<sup>2)</sup> agree with those obtained by the use of effective Lagrangians<sup>3)</sup> in a pseudopotential approach; the pion and kaon electric polarizabilities ( $\alpha$ ) are respectively:  $\alpha_{\pi^{\pm}} \cong 5 \cdot 10^{-4} \text{ fm}^3$ ,  $\alpha_{K^{\pm}} \cong 3 \cdot 10^{-4} \text{ fm}^3$ . These values are still too small to be quantitatively compared with the existing experimental upper limit<sup>4)</sup>:  $\alpha_{K^-} < 2 \cdot 10^{-2} \text{ fm}^3$ .

The most relevant feature of the effective Lagrangian approach is that it gives the relation:  $\alpha = -\beta$  ( $\beta$  = magnetic polarizability) for scalar or pseudoscalar charged mesons. This leads to a picture of charged spin zero mesons as diamagnets. Furthermore the relation  $\alpha = -\beta$  gives as a consequence:  $\frac{1}{(2\pi)^2} \int \frac{\sigma(\omega)}{\omega^2} d\omega \ll \alpha$  where  $\sigma(\omega)$  is the total photoproduction cross section on the spinless target. We stress that in a non relativistic framework the polarizability is extremely sensitive to the charge of the constituents.

#### REFERENCES

- 1) F. Cannata, P. Mazzanti, unpublished.
- 2) F. Cannata, Lett. Nuovo Cimento 6, 379 (1973).
- 3) F. Cannata, P. Mazzanti and S. Zerbinì, Lett. Nuovo Cimento 10, 649 (1974).
- 4) G. Backenstoss, Phys. Lett. B43, 431 (1973).

The Lorentz-Lorenz Correction in Pionic Atoms and  
Pion Condensates\*

Gordon Baym  
Department of Physics  
University of Illinois  
Urbana, Illinois 61801

and

G. E. Brown  
NORDITA, Copenhagen  
and  
State University of New York  
Stony Brook, L.I., New York 11794

Calculation of the pion self energy including only pions and short-range repulsive correlations in intermediate states produces the Ericson-Ericson Lorentz-Lorenz correction. Extension to include  $\rho$ -mesons in intermediate states can increase this correction by more than a factor of 2, the precise amount depending upon the behavior of the two-nucleon correlation function at short distances.

The Lorentz-Lorenz correction for pions is related to the Landau Fermi liquid parameter  $g_0'$ . A numerical value for this parameter can be obtained from the position of the M 1 spin-flip resonance in  $\text{Pb}^{208}$ .

Using this datum, we find the Lorentz-Lorenz correction to be about double that found by Ericson and Ericson. This implies that the pion self energy is reduced by  $\sim 40$ - $45\%$  at nuclear-matter densities. Such a large Lorentz-Lorenz correction strongly inhibits pion condensation in neutron stars.

---

\* Research supported in part by U. S. National Science Foundation Grant NSF GP-40395 and USAEC Grant No. AT(11-1)-3001.

### Negative Pion Capture by ${}^4\text{He}$

K.KUBODERA, Dept. of Physics, Univ. of Pennsylvania, Philadelphia

Barrett et al (BMMZ)<sup>1)</sup> recently measured various correlation quantities for the particles emitted in non-radiative  $\pi^-$ -capture by  ${}^4\text{He}$ ;  $d\sigma/dp_d$ ,  $d\sigma/dp_n$ ,  $d\sigma/dp_{dn}$  and  $d\sigma/d(\cos\theta_{dn})$  for the final  $d+2n$  channel as well as  $d\sigma/dp_p$ ,  $d\sigma/dp_{pn}$ ,  $d\sigma/d(n+n \text{ missing mass})$  and  $d\sigma/d(\cos\theta_{pn})$  for the  $p+3n$  channel were measured. No absolute cross sections were determined. Though the geometry of their experiment is limited and substantial part of the phase space is cut off, the observed spectra appear to have non-trivial structures. A strong peaking observed in the angular distribution seems of significance, too.

In Ref.(2) we have shown that the zero-range two-body absorption model (Eckstein model) supplemented with final-state enhancement factors can explain all the essential features of the BMMZ data. It might also be mentioned that neither the simple final-state interaction argument nor the Eckstein model without final-state interactions can reproduce the assembly of the BMMZ data. As a typical example of comparison of the various treatments we present in the Figure below the result for  $d\sigma/dp_n$ .

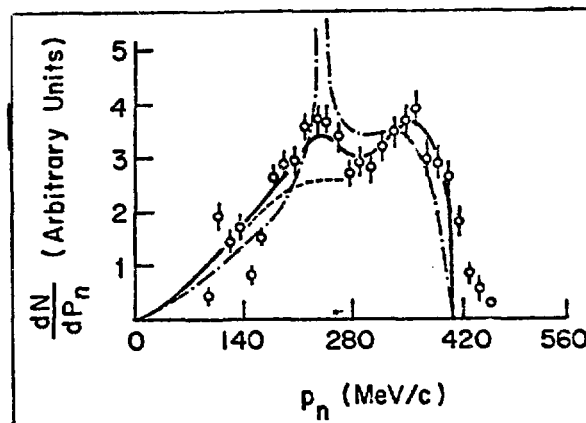
#### References :

- 1) R.Barrett et al, Nucl.Phys. A216(1973)145.
- 2) K.Kubodera, Phys.Letters B, in press.

-----  
final-state int. only

-----  
Eckstein model

-----  
Eckstein model with  
final-state interaction



A.C. PHILLIPS

Manchester University, England

F. ROIG

Universidad de Valencia, Spain.

The impulse approximation provides an accurate description of radiative pion capture in  ${}^3\text{He}$ ; the corrections to the impulse approximation are less than 12% and are comparable with those that occur in related weak interaction processes. In addition there is no indication of a three-nucleon resonance<sup>(1)</sup>. In contrast the calculations of non-radiative capture are unreliable; the 2-N absorption model predicts capture rates in  ${}^3\text{He}$  that are factor of 2 too big<sup>(2)</sup>. In view of these results and in anticipation of a new experiment<sup>(3)</sup> we present the theoretical predictions for pion capture in  ${}^3\text{H}$ . The impulse approximation and the 2-N absorption model give

$$\frac{W^{1s}(\pi^- + {}^3\text{H} \rightarrow 3n + \gamma)}{W^{1s}(\pi^- + {}^3\text{H} \rightarrow 3n)} = \frac{0.07 \times 10^{15} \text{ s}^{-1}}{(1.0 \pm 0.3) \times 10^{15} \text{ s}^{-1}} = 0.07 \pm 0.02$$

Alternatively charge independence can be used to obtain a result which is less subject to the uncertainties of the 2-N absorption model. The data on pion capture in  ${}^3\text{He}$ , an estimate for the 2p capture rate<sup>(2)</sup>, and the isospin branching ratio  $(\pi^- + {}^3\text{He} \rightarrow nnp, I=3/2) / (\pi^- + {}^3\text{He} \rightarrow nnp; I=1/2)$  calculated using the 2-N absorption model, give

$$\frac{W^{1s}(\pi^- + {}^3\text{H} \rightarrow 3n + \gamma)}{W^{1s}(\pi^- + {}^3\text{H} \rightarrow 3n)} = \frac{0.07 \times 10^{15} \text{ s}^{-1}}{(0.5 \pm 0.1) \times 10^{15} \text{ s}^{-1}} = 0.14 \pm 0.03$$

This is an upper bound since final state interactions will increase the isospin branching ratio.

1. P. Truöll et al, Phys. Rev. Lett. 32 1268 (1974) and A.C. Phillips and F. Roig, Nucl. Phys. A234 378 (1974)
2. A.C. Phillips and F. Roig, Nucl. Phys. B60 93 (1973).
3. H. Baer private communication.

M. Leon

University of California  
Los Alamos Scientific Laboratory  
Los Alamos, NM 87544

The E2 nuclear resonance effect in hadronic atoms offers a way to increase the hadronic information that can be obtained from hadronic x-ray experiments.<sup>1</sup> The effect occurs when an atomic deexcitation energy closely matches a nuclear excitation energy, so that some configuration mixing occurs. It shows up as an attenuation of some of the hadronic x-ray lines from a resonant versus a normal isotope target.

The effect was observed very clearly in pionic cadmium in a recent LAMPF experiment.<sup>2</sup> A planned LAMPF experiment will use the nuclear resonance effect to determine whether the p-wave  $\pi$ -nucleus interaction does indeed become repulsive for  $Z \geq 35$  as predicted.<sup>3</sup> The effect also appears in the kaonic molybdenum data<sup>4</sup> taken at LBL, because several of the stable Mo isotopes are resonant.

A number of promising cases for  $\pi^-$ ,  $K^-$ ,  $\bar{p}$ , and  $\Sigma^-$  atoms will be mentioned, and a spectacular and potentially very informative experiment on  $\bar{p} - {}^{100}\text{Mo}$  will be proposed.

---

<sup>1</sup>M. Leon, Phys. Lett. 50B (1974)425; *ibid.*, 53B (1974)141.

<sup>2</sup>J. N. Bradbury et al., Phys. Rev. Lett 34 (1975) 303.

<sup>3</sup>M. Ericson et al., Phys. Rev. Lett. 22 (1969) 1189.

<sup>4</sup>C. E. Wiegand and G. L. Godfrey, Phys. Rev. A 9 (1974)2282.

K. O. H. Ziock, J. Comiso, T. Meyer, and F. Schlepuetz

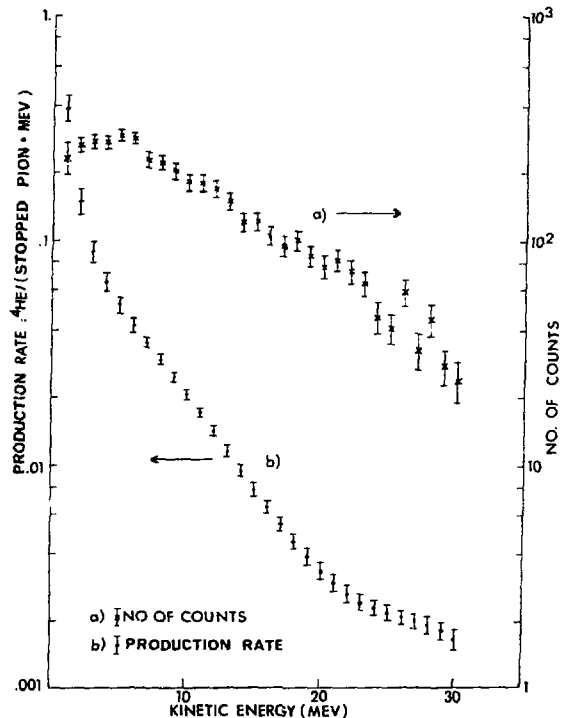
Physics Department, University of Virginia, Charlottesville, VA 22901

Indirect evidence based on the observation of  $\gamma$ -ray emission from nuclei following pion absorption indicates that the de-excitation of the residual nucleus proceeds frequently by way of  $\alpha$ -particle emission.<sup>1</sup> To provide direct evidence for this emission, we have investigated the charged particles emitted from  $^{12}\text{C}$  following pion absorption. The negative pion beam from the LAMPF biomedical channel was stopped in a 0.74 mm thick plastic scintillator. The stopping of a pion in the scintillator provided a start signal for a time of flight ( $\Delta t$ ) measurement of the secondary particles over a flight path of 60 cm from the target counter to a surface barrier detector which also measured the total energy  $E_m$  "as measured" of the secondaries. Since the target is infinitely thick for  $\alpha$ 's of less than 30 MeV, this energy must be distinguished from the energy "as produced"  $E_p$  whose determination was the object of our experiment. A scatter plot of  $E_m$  vs  $\Delta t$  clearly showed lines corresponding to masses 1, 2, 3, and 4. Lines corresponding to masses 6 and 7 were barely discernible.

While it is not possible to decide for any individual  $\alpha$ -particle whether it was produced with an energy close to  $E_m$  near the exit face or with a higher energy deeper inside the target, there is, nevertheless, sufficient information in the complete  $E_m$  spectrum to unambiguously determine the spectrum of the energies  $E_p$  with which the particles were produced in the target. As one can show, the spectrum "as produced" is given by

$$1) N(E_p) = N_o \left[ \frac{\nu(E_p)}{\left(\frac{dR}{dE}\right)_{E_p}^2} \left(\frac{d^2R}{dE^2}\right) - \frac{\left(\frac{d\nu(E)}{dE}\right)_{E_p}}{\left(\frac{dR}{dE}\right)_{E_p}} \right]$$

where  $N_o$  is the normalization factor,  $\nu(E)$  is the spectrum "as measured," and  $R = R(E)$  the range energy relation. To unfold our data, we fitted an analytic expression to the measured spectrum  $\nu(E)$  for use in Eq. 1. Figure 1 shows  $\nu(E_m)$  and  $N(E_p)$ . The production rate of  $\alpha$ -particles integrated over all energies above 0.5 MeV was found to be  $R = 1.00 \pm .07$   $\alpha$ 's/pion. The average  $\alpha$ -energy was  $4.4 \pm .3$  MeV.



<sup>1</sup>V. G. Lind et al., Phys. Rev. Lett. 32, 479 (1974).



H. Nishimura and A. Arima

Department of Physics, University of Tokyo, Hongo, Tokyo, Japan

This short note is point out two things; (1) An alpha cluster in target nuclei (call them A) competes with protons in absorbing a negative Kaon. (2) If the Kaon is absorbed by the alpha cluster, the excited states of residual nuclei (call them B) have very high spins. Because of very high values of spin, the excited states of B prefer alpha emission to neutron emission. This explains the large production rate of the nucleus missing two alpha particles. The residual nucleus C is already cool and can emit only an alpha particle.

Table 1 shows the calculated spectroscopic factors  $S_{NL}$  of the alpha cluster in  $^{58}\text{Ni}$ . The principal and angular momentum quantum numbers of the alpha cluster are N and L. The use is made of the wave functions of  $^{58}\text{Ni}$  obtained by Auerbach and Shimizu.<sup>4</sup> We assume that there exist in the nucleus B a level for each value of  $2N+L$  which contains the sum rule limit of spectroscopic factor of the alpha cluster.

Table 2 shows that (1) among many L with the same value of  $2N+L$ , the higher value of L the larger  $S_{NL}$ , and (2) the smaller  $2N+L$ , the larger  $S_{NL}$ .

The calculation of Kaon absorption widths is done under the following assumptions. (1) The alpha cluster immediately leaves the nucleus B after the Kaon absorption. (2) The widths are calculated by a formula

$$\Gamma_{\alpha} = 2WS_{NL} \int \phi_{NL}^2(R) \phi_{Knl}^2(R) R^2 dR \quad (1)$$

where W is the imaginary part of t matrix of K-alpha scattering.  $\phi_{NL}$  is a single alpha particle wave function of a Woods-Saxon potential.  $\phi_{Knl}$  is a Kaon wave function.

Several calculated values are shown in table (2). They show that Kaon absorption by the alpha cluster competes with that by the protons.

Table 1

$2N+L$	L=0	1	2	3	4	5	6	7	8	9	10	11	12
12	0.005	0.011	0.014	0.011	0.008	0.0017	0.0042						
11		0.013	0.029	0.056	0.107	0.267	0.485						
10		0.023	0.130	0.272	0.498	1.029	2.129						
9		0.280	0.739	1.429	2.646	5.04							
8		0.230	1.20	2.50	4.70	8.50							

Table 2

proton	Of 7/2	2.22eV	alpha	$2n+1=12$	0.13eV	$2n+1=9$	L=9	0.15	$2n+L=7$	0.24
	0d5/2	0.57		11	0.29		7	0.15	alpha total	
total		3.7		10, L=10	0.14	total	0.55		2.93eV	
				8	0.13	8	8	0.11		
				total	0.51	6	0.11			
						total	0.39			

Table 3 Partial width  
alpha !neutron

n=0, L=9	16keV	60eV
1, 7	14keV	100eV
2, 5	80keV	160keV
0 8	600keV	2keV
1 6	244keV	20keV
2 4	44keV	1MeV

1. R. Seki, Phys. Rev. C5 (1972) 1196, C7 (1973) 1260
2. B. . Martin and M. Sakitt, Phys. Rev. 183 (1969) 1352
3. W. A. Bardeen and E. W. Torigoe, Phys. Rev. C3 1785 (1971)
4. N. Averbach, Phys. Rev. 163 (1967) 1203  
K. Shimizu, D. Thesis Univ. of Tokyo

H. Nishimura and T. Fujita

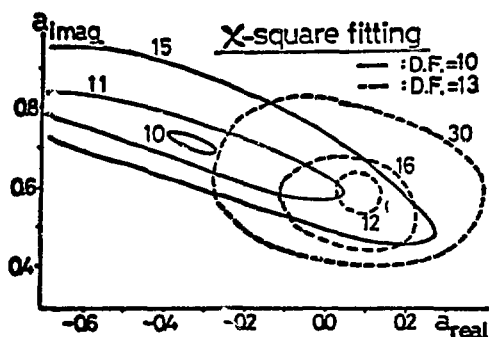
University of Tokyo, Department of Physics, Tokyo, Japan

We made an optical model analysis of recently measured x-ray transitions for several  $\bar{p}$ -atoms. The analyses<sup>(1)</sup> made so far have shown that effective optical potentials which give the best fit for the x-ray data are quite different from that predicted by the free scattering lengths<sup>(2)</sup>. Especially, the real part of the former potentials is strongly attractive whereas that of the latter is repulsive. A similar situation existing in kaonic atoms seems to be explained by taking into account  $Y_0^*(1405)$  resonance just below the  $\bar{K}$ -N threshold<sup>(3)</sup>. One might be tempted to treat the problem in  $\bar{p}$ -atoms in an analogous way. However, one knows experimentally no well established resonances near the  $\bar{p}$ -N threshold.

We point out that the all existing analyses neglected a correction from the spin-orbit force due to strong interactions, which is known to play an important role in nucleon-nucleus optical potential. We also notice that, though the  $\bar{p}$ -nucleus optical potential form factor is usually assumed to be the same as the nucleon density distribution, it might be better to use a form factor similar to nucleon-nucleus optical potential. Thus we use this new type of form factor and, treating the strength of the real and imaginary part of the potential as free parameters, perform two types of  $\chi^2$ -fitting: (1) both the energy shifts and widths of x-ray are considered; (2) only the widths are considered. For case (1), indicated by dashed line in the Figure, a  $\chi^2$ -minimum obtained when the potential has a weakly attractive real part while the imaginary part is slightly weaker than predicted by the free scattering lengths.

Thus the problem of the sign change of the real part still remains. However, if we exclude the energy shift (Case (2), shown by the solid line in Figure), the potential parameters just predicted by the free scattering lengths correspond to a  $\chi^2$ -minimum. This is a rather surprising result.

On the other hand, we have confirmed numerically that the inclusion of L.S force in the analysis of the x-ray data changes considerably the resulting energy shifts and widths. New experiments of  $\bar{p}$ -atoms including precise measurement of L.S splitting would be quite helpful and interesting.



#### References

- (1) G. Bakenstoss, et al.,  
Phys. Lett. 41B(1972)552.
- (2) R.A. Bryan and R.J.N. Phillips,  
Nucl. Phys. B5(1968)201.
- (3) W.A. Bardeen and E.W. Torigoe,  
Phys. Rev. C3(1971)1785.

Panofsky Ratio in  ${}^3\text{He}$ 

M.Mizuta, Y.Kohyama and A.Fujii

Physics Department, Sophia University, Tokyo, Japan

The charge exchange and radiative capture rate of  $\pi^-$  in  ${}^3\text{He}$  leading to  ${}^3\text{H}$  is calculated by the nuclear physics approach. The effective hamiltonian is obtained by the non-relativistic reduction of the C.G.L.N. amplitude, the trion ( ${}^3\text{He} - {}^3\text{H}$ ) wave function is assumed of the form

$$\Phi = \sqrt{P_S} \Phi_S + \sqrt{P_{S'}} \Phi_{S'} + \sqrt{P_D} \Phi_D,$$

and the Irving or Irving-Gunn type radial dependence is adopted. The initial pion orbital is either 1s or 2p state. The nuclear matrix elements allow fully analytic integration and yield the following capture rate for the choice  $P_S = 0.90$ ,  $P_{S'} = 0.02$ ,  $P_D = 0.08$ , and  $R_D = 1.2, 1.5$  where  $R_D$  is the ratio of the D state and S state radius.  $P(1s)$  is the Panofsky ratio for 1s orbital capture only and  $P$  is that with the correction due to the 2p orbital capture. In case I the Irving type is adopted for all states, and in case II the Irving-Gunn type is assumed for S state but the Irving type for the other states. The units are  $10^{15} \text{ sec}^{-1}$  for the 1s capture and  $10^{10} \text{ sec}^{-1}$  for the 2p capture.

	Case I		Case II	
$R_D =$	1.2	1.5	1.2	1.5
$W_{\pi^0}(1s)$	9.21	9.20	9.09	9.06
$W_{\gamma}(1s)$	3.34	3.32	2.91	2.84
$W_{\pi^0}(2p)$	0.285	0.276	0.236	0.218
$W_{\gamma}(2p)$	1.12	1.13	0.943	0.925
$P(1s)$	2.76	2.77	3.12	3.19
$P$	2.63	2.63	2.99	3.06

The experimental Panofsky ratio is  $2.68 \pm 0.13$ .

H. Ullrich, H.D. Engelhardt and C.W. Lewis

CERN, Geneva, Switzerland, and IEKP, University of Karlsruhe, Germany

Nuclear reactions induced by stopped  $\pi^-$  have been studied via in-beam  $\gamma$ -spectroscopy on the nuclei  $^{16}\text{O}$ ,  $^{19}\text{F}$ ,  $^{31}\text{P}$ , and  $^{40}\text{Ca}$ . A large variety of residual nuclei have been observed which correspond to the removal of up to 10 nucleons. Figure 1 shows the summed yields per stopped pion for all four target nuclei as a function of the number of removed nucleons. The distribution shows a maximum at two nucleons, as expected. However, the yields for the removal of more than two nucleons are comparable, and lie surprisingly well on a straight line in the logarithmic presentation of Fig. 1. This behaviour suggests a comparison with spallation reactions which are well described by Rudstam's empirical formula<sup>1)</sup>:  $\sigma(Z,A) \propto \exp [PA - R(Z-SA)^2]$ , where  $Z$  and  $A$  are the atomic number and mass of the residual nucleus, and the parameters  $P$ ,  $R$ , and  $S$  have been determined by Rudstam. The parameter  $P$  depends mainly on the energy of the projectile, but not on its type. The data in Fig. 1 can be fitted with  $P = 0.14$ , corresponding to 500 MeV. Also shown is a line with a slope  $P = 0.43 \pm 0.13$ , corresponding to 140 MeV ( $m_\pi c^2$ ).

The  $Z$ -dependence should have a Gaussian distribution,  $\exp [-R(Z-SA)^2]$ . The predicted distribution with  $S = 0.486$  and  $R = 2.8$  for our range of residual nuclei is shown in Fig. 2. A least-squares fit for our data gives  $R = 3.7$ .

The comparison indicates a strong similarity between reactions induced by pion absorption at rest and spallation reactions. The  $A$ -distribution of our data, however, corresponds to spallation data with 500 MeV projectile energy. This difference is most likely due to the peculiarity of the pion interaction during the first step of the nuclear reaction.

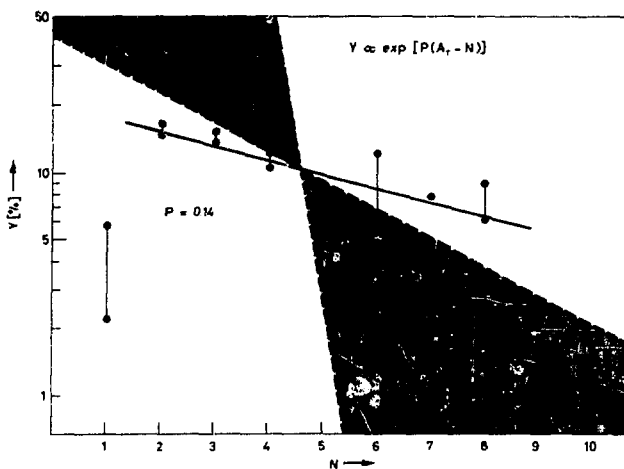


Fig. 1

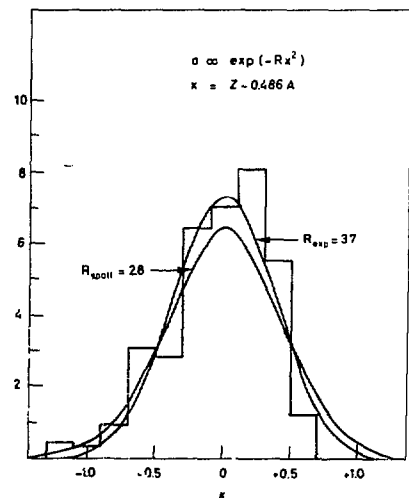


Fig. 2

1) G. Rudstam, Z. Naturforsch. 21a, 1027 (1966).

C. J. Batty, S. F. Biagi, R. A. J. Riddle, A. Roberts,  
B. L. Roberts, D. H. Worledge  
Rutherford Laboratory, Chilton, Didcot, U.K.

N. Berovic, G. J. Pyle, G. T. A. Squier  
Physics Department, University of Birmingham, U.K.

A. S. Clough, P. Coddington, R. E. Hawkins  
Physics Department, University of Surrey, U.K.

Lack of knowledge of the kaon-nucleus interaction has so far limited the usefulness of data obtained from kaonic atoms in providing nuclear structure and size information. In an attempt to provide additional data we have observed nuclear  $\gamma$ -rays in coincidence with stopping kaons. Data were taken for three thicknesses (3, 5 and 8 gm/cm<sup>2</sup>) of Aluminium in order to study the possible role of multiple interaction processes in the target. The  $\gamma$ -rays observed are used to identify the residual nucleus and thus to add information about the kaon interaction with the target.

The 1.83 MeV  $\gamma$ -ray from  $^{26}\text{Mg}$  is clearly observed but the corresponding  $\gamma$ -ray from  $^{26}\text{Al}$  at 1.81 MeV has not been observed above the statistics. We estimate the latter transition to be at least an order of magnitude weaker indicating that removal of a single proton is much more likely than single neutron removal<sup>1</sup>. Other lines observed with strengths comparable to that for  $^{26}\text{Mg}$  are from  $^{23}\text{Na}$ ,  $^{21}\text{Ne}$  and  $^{19}\text{F}$  corresponding to residual nuclei with an  $\alpha$ ,  $\alpha + d$  and  $2\alpha$  respectively less than  $^{27}\text{Al}$ . Much weaker lines are observed from  $^{24}\text{Mg}$  and  $^{22}\text{Ne}$ . The yields of all these lines vary linearly with target thickness indicating that multiple processes do not contribute significantly. The results will also be compared with similar pion experiments<sup>2</sup>.

1. P. D. Barnes et al. Phys. Rev. Lett. 29, 230, (1972).
2. D. Ashery et al. Phys. Rev. Lett. 32, 943, (1974).

C. J. Batty, S. F. Biagi, R. A. J. Riddle, A. Roberts  
B. L. Roberts, D. H. Worledge  
Rutherford Laboratory, Chilton, Didcot, U.K.

N. Berovic, G. J. Pyle, G. T. A. Squier  
Physics Department, University of Birmingham, U.K.

A. S. Clough, P. Coddington, R. E. Hawkins  
Physics Department, University of Surrey, U.K.

X rays from atoms formed by stopping  $K^-$  mesons from a separated kaon beam (momentum  $600 \text{ Mev}/c \pm 1.5\%$ ) at the Rutherford Laboratory, have been observed from targets of S, Co, Ni, Zn, Ag, Cd, In, Sn, Ho, Yb, and Ta. These targets were chosen so that the last observed X-ray transition would be measurably broadened and shifted in energy by the  $K^-$ -nucleus strong interaction. The 6h to 5g transition was experimentally resolved from the adjacent  $n = 8$  to  $n = 6$  transition by using a high resolution, large volume lithium drifted germanium detector, even though this energy difference is less than 1%. In S the 4f to 3d transition was well resolved from the adjacent  $n = 8$  to  $n = 4$  and  $n = 9$  to  $n = 4$  transitions by using a  $4 \text{ cm}^3$  high resolution Ge(Li) X-ray detector (600 eV fwhm at 122 keV). These data have been interpreted in terms of a kaon-nucleus optical potential as discussed by Seki<sup>1</sup>. The results are in general agreement with the predictions of Seki and Kunselman<sup>2</sup>.

The data from Ho, Yb, and Ta, where the 7i to 6h transitions are broadened and shifted, are more difficult to interpret since the splitting of the atomic levels due to the static quadrupole moment of the nucleus is much greater than the corresponding strong-interaction broadening. This is discussed in more detail in a companion paper.

1. R. Seki. Phys. Rev. C5, 1196, (1972).
2. R. Seki and R. Kunselman. Phys. Rev. C7, 1260, (1973).

## QUADRUPOLE HYPERFINE STRUCTURE EFFECTS IN EXOTIC ATOMS

C. J. Batty, S. F. Biagi, R. A. J. Riddle, A. Roberts,  
B. L. Roberts, D. H. Worledge  
Rutherford Laboratory, Chilton, Didcot, U.K.

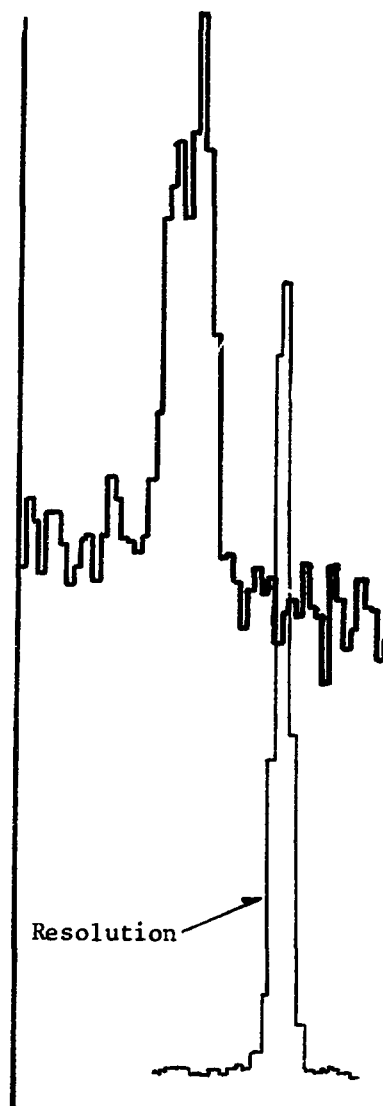
N. Berovic, G. J. Pyle, G. T. A. Squier  
Physics Department, University of Birmingham, U.K.

A. S. Clough, P. Coddington, R. E. Hawkins  
Physics Department, University of Surrey, U.K.

For nuclei with ground state quadrupole deformation the electromagnetic central force experienced by the orbiting particle can be expressed as a series multipole expansion. In exotic atoms the  $L = 2$  component causes a hyperfine splitting of the energy levels which, unlike in the atomic case, can be significant compared with the binding energy. This effect is due to the Bohr orbit of the particle being much closer to the nucleus than in normal atoms.

Observations of this splitting in pionic atoms have been reported<sup>1,2</sup>. We have obtained data for pionic and/or kaonic holmium, tantalum, ytterbium, hafnium and bismuth. The splitting is clearly visible in the holmium and tantalum data. An example is shown in the figure for the  $n = 8$  to  $n = 7$  transition in kaonic tantalum. The data have been analysed to yield quadrupole moments. The effect of the nuclear deformation on the kaon-nucleus strong interaction is being considered.

1. R. A. Carrigan et al. Phys. Lett. 25B, 193, (1967).
2. P. Ebersold et al. Phys. Lett. 53B, 48, (1974).



H. W. BAER, Case Western Reserve Univ.; J. A. BISTIRLICH, S. COOPER and K. M. CROWE, Univ. of California LBL; J. P. PERROUD, Univ. of Lausanne; R. H. SHERMAN, Los Alamos Scientific Lab.; F. T. SHIVELY, Univ. of California LBL and LASL; and P. TRUOL, Univ. of Zürich.

Radiative  $\pi^-$  capture on the isotopes of hydrogen  $^1\text{H}$ ,  $^2\text{H}$ , and  $^3\text{H}$  provide an unusually clear example for study of the nuclear force. Measurements on  $^1\text{H}$  provide a determination of the  $\pi\text{N}$  coupling strength and link  $\pi\text{N}$  scattering to photo-pion production via the Panofsky ratio. Data on  $^2\text{H}$  first determined the odd intrinsic parity of the pion and currently provides the basis for one of the most accurate values of  $a_{nn}$  (neutron 'S' scattering length). The importance of data on  $^3\text{H}$  for study of the nuclear force in a pure  $I = 3/2$ , three nucleon system at low relative momenta has long been realized, but measurements were not performed due to the great amounts of tritium required. We report here the first measurement on the  $^3\text{H}(\pi^-, \gamma)3n$  reaction. The experiment was performed at the Clinton P. Anderson Meson Physics Facility using a 5.88g liquid tritium target (with radioactivity of  $5.7 \times 10^4$  Curie), a high resolution electron-positron pair spectrometer, and a  $\pi^-$  beam of good momentum resolution and small achromatic spot size produced at the extended low-energy-pion (LEP) channel. To obtain an accurate normalization, two identical target cells filled with liquid  $^1\text{H}$  and  $^3\text{H}$  were mounted on a mobile boom, thereby allowing rapid interchange of targets. The  $^1\text{H}$  data provide calibration of the pair spectrometer detection efficiency between 50 and 150 MeV (via the Panofsky ratio), the resolution at 129.4 MeV, and the  $\pi$  stopping rates. A spectrum of  $\sim 3000$  events of the  $^3\text{H}(\pi^-, \gamma)3n$  reaction with stopped pions was obtained in an 8-day run. The spectrum shape and branching ratio will be compared to calculations<sup>1</sup> for radiative/total absorption rates from the 1s Bohr orbit which are related by charge independence to the  $^3\text{He}(\pi^-, \gamma)^3\text{H}$  data, and which use the 2N absorption model to calculate the total 1s width.

\* Research supported in part by the U. S. Atomic Energy Commission and ERDA.

<sup>1</sup> A. C. Philips, private communication (1975).



## STUDIES OF STRONG INTERACTION EFFECTS IN ANTIPROTONIC ATOMS.\*

C. Cox, M. Eckhause, J. Kane, M. Rushton, W. Vulcan, R. Welsh, COLLEGE OF WILLIAM AND MARY, Williamsburg, Va. 23185; J. Miller, R. Powers, CALIFORNIA INSTITUTE OF TECHNOLOGY, Pasadena, Cal. 91109; P. Barnes, R. Eisenstein, and R. Sutton, CARNEGIE-MELLON UNIV., Pittsburgh, Pa. 15213; W. Lam and D. Jenkins, VIRGINIA POLYTECHNIC INSTITUTE, Blacksburg, Va. 24061; T. King, R. Kunselman and P. Roberson, UNIV. OF WYOMING, Laramie, Wyo. 82070.

We have collected x-ray spectra from the antiprotonic atoms  ${}^6\text{Li}$ ,  ${}^7\text{Li}$ , C, Si, S, P, Fe, Y, Zr, Yb, and Cs. The data were collected at the Brookhaven AGS using a 750 MeV/c antiproton beam. Approximately 330 antiprotons stopped in a given target (5-8 gr/cm<sup>2</sup>) per 10<sup>12</sup> protons incident on the production target. The x-rays were observed using both planar (1 cm<sup>3</sup>) and co-axial (50 cm<sup>3</sup>) Ge(Li) detectors; resolutions were 0.6 keV at 122 keV and 1.1 keV at 279keV, respectively.

The data are being examined for evidence of strong interaction shifts and line broadenings in the atomic transitions. The results of analysis will be presented and compared to available  $\bar{p}$ - nucleus optical models.

\*Work supported by ERDA and NSF.

Fundamental Properties of  $K^-$ ,  $\bar{p}$  and  $\Sigma^-$  from Exotic Atoms \*

G. Dugan, Y. Asano, M.Y. Chen, S. Cheng, E. Hu,  
L. Lidofsky, W. Patton, C.S. Wu

Columbia University, New York, N.Y. 10027

V. Hughes, D. Lu

Yale University, New Haven, Conn. 06520

Hadrons from the low-energy separated beam of the Brookhaven AGS were stopped in Pb and U targets to form hadronic atoms. The energy spectra of the hadronic atoms were measured to high precision using Ge(Li) spectrometers. The data acquisition system was computer controlled and stabilized; the energy calibration spectrum was taken simultaneously with the data spectrum. The experimental transition energies were corrected for ADC nonlinearities and data-calibration spectrum shifts, as well as the presence of unresolved noncircular transition contaminants. Experimental energies were determined for the six circular transitions ( $n=13 \rightarrow n=12$  through  $n=8 \rightarrow n=7$ ) of the  $K^-$ -Pb atom, six circular transitions ( $n=16 \rightarrow n=15$  through  $n=11 \rightarrow n=10$ ) of the  $\bar{p}$ -Pb atom, and four circular transitions ( $n=15 \rightarrow n=14$  through  $n=11 \rightarrow n=10$ ), of the  $\Sigma^-$ -Pb atom. The energies of these transitions were computed from quantum electrodynamics, including all significant orders of vacuum polarization, electron screening and nuclear polarization. The masses of  $K^-$ ,  $\bar{p}$  and  $\Sigma^-$  were adjusted to achieve a best-fit with the experimental energies; the results were:  $m_{K^-} = 493.668 \pm 0.014$  MeV;  $m_{\bar{p}} = 938.155 \pm 0.053$  MeV;  $m_{\Sigma^-} = 1197.24 \pm 0.14$  MeV. The fine structure splitting of the transitions ( $n=11 \rightarrow n=10$ ) in  $\bar{p}$ -Pb and  $\bar{p}$ -U atoms, and the ( $n=12 \rightarrow n=11$ ) transition in  $\Sigma^-$ -Pb atoms, were analyzed to determine the magnetic moments of  $\bar{p}$  and  $\Sigma^-$ . The results were:  $\mu_{\bar{p}} = -2.790 \pm 0.021$  n.m.;

$$\mu_{\Sigma^-} = \begin{cases} -1.40^{+0.41}_{-0.28} \text{ n.m.} \\ \text{or} \\ 0.65^{+0.28}_{-0.40} \text{ n.m.} \end{cases}$$

Finally, energy shifts from the QED predictions were observed for the principal circular transitions in  $K^-$ -U and  $\bar{p}$ -U atoms. These shifts were shown to be due to the dynamic E2 effect, such as has been observed in muonic atoms.

\* Research supported in part by the National Science Foundation.

## NUCLEAR SPECTROSCOPIC QUADRUPOLE MOMENTS FROM MUONIC AND PIONIC ATOMS

W. Dey, P. Ebersold, B. Aas, R. Eichler, H.J. Leisi, W.W. Sapp and F. Scheck\*)

Laboratory for High Energy Physics, Swiss Federal Institute of Technology Zurich, c/o SIN, 5234 Villigen, Switzerland

\*) and SIN

## ABSTRACT

We have analyzed the quadrupole splitting of the 4f-3d, 5f-3d, and 5g-4f X-ray transitions in muonic  $^{175}\text{Lu}$  1). This analysis permits a precise determination of the ground state spectroscopic quadrupole moment  $Q$  2). The data were corrected for small effects of the finite nuclear size, the dynamical nuclear excitation, nuclear polarization, vacuum polarization, M1 and E4 hyperfine interaction and X-ray transitions between non-circular orbits. The results are displayed in Table I.

The quadrupole splitting of states in pionic atoms is, in addition to the electromagnetic part, also affected by the pion-nucleus interaction 3). Using a measured value for the strong-interaction shift  $\epsilon_0$ , one can extract  $Q$  in a nearly model-independent fashion from the observed quadrupole splitting (see ref. 4). We have analyzed the 5g-4f transition in pionic  $^{175}\text{Lu}$ , taking into account the small effects of the finite nuclear size and of distortions of the pionic wave function due to the strong interaction 5). The result, along with that for  $^{165}\text{Ho}$ , is shown in Table I. The strong interaction shift and width of the 4f level in  $\pi$   $^{175}\text{Lu}$  are found to be  $\epsilon_0 = 0.67(7)$  keV and  $\Gamma_0 = 0.23(7)$  keV, respectively.

Table I Ground state spectroscopic quadrupole moments of  $^{175}\text{Lu}$  and  $^{165}\text{Ho}$

Isotope	Transition	$Q(\text{b})$	Reference
$^{175}\text{Lu}$	$\mu$ 4f-3d	3.49(2)	(1)
	$\mu$ 5f-3d	3.49(5)	(1)
	$\mu$ 5g-4f	3.49(5)	(1)
	$\pi$ 5g-4f	3.47(7)	(5)
$^{165}\text{Ho}$	$\pi$ 5g-4f	3.47(11)	(4)

## REFERENCES

- 1) W. Dey, Thesis ETHZ (1975) (unpublished)
- 2) H.J. Leisi et al., J. Phys. Japan Suppl. 34, 355 (1973)
- 3) F. Scheck, Nucl. Phys. B42, 573 (1972)
- 4) P. Ebersold et al., Phys. Letters 53B, 48 (1974)
- 5) P. Ebersold, Thesis ETHZ (1975) (unpublished)

OBSERVATION OF NUCLEAR ROTATIONAL SPECTRA IN PION CAPTURE ON  
 $^{175}\text{Lu}$  AND  $^{165}\text{Ho}$ 

P. Ebersold, B. Aas, W. Dey, R. Eichler, H.J. Leisi, W.W. Sapp  
and H.K. Walter

Laboratory for High Energy Physics, Swiss Federal Institute of  
Technology Zurich, c/o SIN, 5234 Villigen, Switzerland

## ABSTRACT

In experiments designed to study X-rays of pionic atoms of  $^{175}\text{Lu}$  <sup>1)</sup> and  $^{165}\text{Ho}$  <sup>2)</sup> we have observed a large number of nuclear  $\gamma$  rays. They can be assigned to even isotopes of Yb and Dy, and corresponds to E2 transitions between the members of the ground-state rotational band. Rotational states with spins up to  $I=12^+$  have been seen. We interpret these  $\gamma$  rays as arising from the reactions



Isotopes in the final state corresponding to neutron numbers  $x = 3, 5, 7, 9$ , and 11 in the case of Lu have been observed.

From the measured intensities of the  $\gamma$  rays the following observation can be made:

- i) The E2 transition intensities within the rotational band increase as one approaches the nuclear ground state. Hence individual rotational levels are fed not only by the preceding rotational transition but also by highly excited nuclear states.
- ii) For each target nucleus the yields of the isotopes in the final state follow an evaporation-type distribution, with a maximum at  $x=7$  in the case of  $^{175}\text{Lu}$  and  $x=5$  in the case of  $^{165}\text{Ho}$ .
- iii) Comparing the intensities of the nuclear  $\gamma$  rays with the intensities of the pionic X-rays we conclude that pion capture in these nuclei is dominated by the observed capture reactions, i.e. by multiple neutron emission.

## REFERENCES

- 1) P. Ebersold, Thesis ETHZ (1975) (unpublished)  
See also abstract "Quadrupolmoments from muonic and pionic atoms", submitted to this conference.
- 2) P. Ebersold et al., Phys. Letters 53B, 48 (1974)

ISOTOPIC EFFECTS IN ANTIPROTONIC ATOMS

H. Koch<sup>\*</sup>), G. Backenstoss<sup>\*\*</sup>), P. Blüm<sup>\*</sup>), W. Fetscher<sup>\*</sup>), R. Hanelberg<sup>\*</sup>),  
 A. Nilsson<sup>†</sup>), P. Pavlopoulos<sup>††</sup>), H. Poth<sup>\*</sup>), I. Sick<sup>\*\*</sup>),  
 L. Simons<sup>††</sup>), L. Tauscher<sup>\*\*</sup>)

The measurement of strong interaction effects in antiprotonic atoms (shifts, widths, intensities of X-ray lines) yields information about the total amount of nuclear matter (protons and neutrons) present in the nuclear tail. The existing data can be analysed in terms of an optical potential, but it turns out that the *relative* amount of antiprotons absorbed on protons and neutrons cannot be deduced from the data. This number, however, is very much needed if one wants to interpret the data in terms of neutron distributions alone. A very elegant method of determining this ratio is the measurement of isotopic effects, if isotopes with known proton and neutron distributions are chosen.

We report here about the first measurement of isotopic effects on  $\bar{p}$ - $^{16}\text{O}/^{18}\text{O}$ . The experiment was performed at the CERN Proton Synchrotron with two targets of  $180\text{ g D}_2^{16}\text{O}$  and  $\text{D}_2^{18}\text{O}$ , respectively. To reduce the systematic errors to nearly zero, both targets were of exactly the same shape and were interchanged after several bursts, so that the beam distribution and the absorption corrections were identical in both targets. The water was enclosed in Ti boxes, which gave excellent calibration lines. Preliminary results are obtained for the difference of the energy shifts of the  $n = 3$  level and the ratio of the absorption widths of the  $n = 4$  level :

$$\epsilon_{16} - \epsilon_{18} = (57 \pm 50) \text{ eV}; \quad \Gamma_{16}/\Gamma_{18} = (0.74 \pm 0.15) .$$

For the comparison of the data with calculations, proton and neutron distributions derived from electron scattering, muonic atoms, and binding energy data were used. The result is that the assumption of equal antiproton absorption on the proton and neutron of the nucleus seems to be justified.

- 
- \*) Institut für Experimentelle Kernphysik, Universität and Kernforschungszentrum, Karlsruhe, Germany.  
 \*\*) Institut für Physik, Basel, Switzerland.  
 †) Research Institute for Physics, Stockholm, Sweden.  
 ††) CERN, Geneva, Switzerland.

S. Y. Lee  
Department of Physics  
National Central University  
Chung Li, Taiwan, R. O.China

The  $K^-$  nucleus optical potential have puzzled us for years (H. Koch, Messungen an Kaonischen Atomen, preprint KFK-Ext3/73-3). The widths and shifts of the kaonic atoms can not be explained by a simple multiple scattering expansion, where the first order optical potential is simply  $U^{opt} = t^{free} \cdot \rho(r)$ . There are already many recipes resolving this ambiguity. One promising resolution is taking the binding energy effect of the nucleons and the kaon into account in the optical potential (M. Alberg, E. M. Henley and L. Wilets, Phys. Rev. Lett. 30,255,1973). However the kaon interacts mainly with nucleons near the nuclear surface, the above mentioned resolution is not appearing. On the other hand, the data through the periodic table can equally fitted by the optical potential of  $U^{opt} = t^{free} \cdot \rho(r) + \alpha \frac{d\rho}{dr}$  with only one free parameter (J. Hufner, H. Schmidt and S. Y. Lee, unpublished). To find justification of this optical potential, we calculated the differential cross section for the  $K^-$  at 300 MEV/C on the oxygen target and then compared with the differential cross sections calculated from other potentials. Possible experiments are suggested to pin down this problem.

THE STUDY OF THE RELATIVE CHANGE OF THE CHARGE BY HYDROGENE ATOMS  
IN TRANSITION METAL HYDRIDES

M.F.Kost, V.I.Mikheeva, L.N.Panurets, A.A.Chertkov

Institute of General and Inorganic Chemistry, USSR Academy of  
Sciences, Moscow, U S S R

Z.V.Krumshtein, V.I.Petrukhin, V.M.Suvorov, I.Yutlandov

Joint Institute for Nuclear Research, Dubna, USSR

Abstract

The capture rate of negative pions in hydrogen is measured in hydrides of some transition and near-transition metals. These data have allowed to establish the electron density near protons shown to be almost two times larger in ionic hydrides than in metallic ones. The relative change in electron density in hydrogen atoms has been determined by moving from the 2nd group metals to the 5th group of periods IV-VI in the Periodic Table. The relative difference in the electron density of hydrogen atoms is determined by dihydride-trihydride pairs for Y, La, Ce and Er.

THE STUDY OF NEGATIVE PION TRANSFER IN  $C_m H_n + Z$  MIXTURES

V.M.Bystritsky, V.A.Vasiljev, I.Galm, V.I.Petrukhin,  
V.E.Risin, V.M.Suvorov, B.A.Khomenko

Joint Institute for Nuclear Research, Dubna, USSR

## Abstract

The  $\pi^-$ -meson transfer from hydrogen to atoms Z is studied in the mixture of  $C_m H_n + Z$  type, where  $Z = He, Ne, Ar, Kr$  and  $Xe$ . The  $\langle \Lambda_Z \rangle$  transfer rates have been measured, and the obtained  $\langle \Lambda_Z \rangle = f(Z)$  relation makes it possible to estimate the transfer contribution to the suppression of meson capture by hydrogen atoms in hydrogen compounds.



THE STUDY OF THE NEGATIVE PION TRANSFER TO CARBON IN ORGANIC  
MOLECULES

V.I.Petrukhin, V.V.Risin, I.F.Samenkova, V.M.Suvorov  
Joint Institute for Nuclear Research, Dubna, USSR

Abstract

A difference is observed between the rates of negative pion transfer to carbon atoms of organic molecules in the saturated aliaphatic series  $C_m H_n$  and the mixed gases  $H_2 + C_m H_n$ . This difference is shown to be originated in the different excitation energies of hydrogen mesoatoms formed in free hydrogen ( $H_2$ ) and in chemically bound one ( $C_m H_n$ ). Neither the grouping of atoms Z in the molecules, nor their encirclement by hydrogen atoms, nor the particular properties of the chemical bond among atoms Z seem to have any effect on the transfer process.

## NEGATIVE PION CAPTURE BY HEAVY NUCLEI

S.R.Avrarov, V.S.Butsev, D.Chultem, Yu.K.Gavrilov,  
Dz.Ganzorig, S.M.Polikanov

Joint Institute for Nuclear Research, Dubna, USSR

The stopped pion capture by Bi, Pb, Hg, Au, Pt, Ta nuclei has been investigated by using the bio-medical pion beam from the Dubna synchrocyclotron<sup>/1/</sup>. A wide distribution of the neutron multiplicity has been observed in the ( $\pi^-$ , xn) reactions. Mostly, high-spin states are excited in these reactions<sup>/2,3/</sup>:  $^{204m}\text{Pb}(9^-)$ ,  $^{202m}\text{Pb}(9^-)$ ,  $^{201m}\text{Pb}(13/2^+)$ ,  $^{199m}\text{Pb}(13/2^+)$ ,  $^{197m}\text{Pb}(13/2^+)$ ,  $^{198m}\text{Tl}(7^+)$ ,  $^{196m}\text{Tl}(7^+)$ ,  $^{193m}\text{Tl}(9/2^-)$ ,  $^{191m}\text{Tl}(9/2^-)$ ,  $^{200m}\text{Au}(12^-)$ ,  $^{198m}\text{Au}(12^-)$ ,  $^{196m}\text{Au}(12^-)$ ,  $^{194m}\text{Pt}(\geq 10)$ ,  $^{190m}\text{Pt}(\geq 12^+)$ ,  $^{190m}\text{Ir}(11^-)$ ,  $^{186m}\text{Ir}(11^-)$ ,  $^{177m}\text{Hf}(37/2^-)$

Among the products of negative pion capture the isotopes having (Z-2) and (Z-3) have been also found. These isotopes may be produced either in the radiative decay of (Z-1) nuclei or as a result of charged fragment emission. It is possible that some of them are due to the decay of new high-spin nuclear isomers.

## References

1. V.M.Abazov et al. Preprint JINR, P13-8079, Dubna, 1974.
2. V.S.Butsev et al. Abstracts of the XXV Meeting on Nuclear Spectroscopy and Nuclear Structure, Leningrad, 1975, pp. 147, 149, 150.
3. V.S.Butsev et al. Preprints JINR, E6-8535; P6-8541, Dubna, 1975.

Radiative pion capture by  ${}^6\text{Li}$

R.A.Sakaev, R.A.Eramzhyan

Joint Institute for Nuclear Research, Dubna

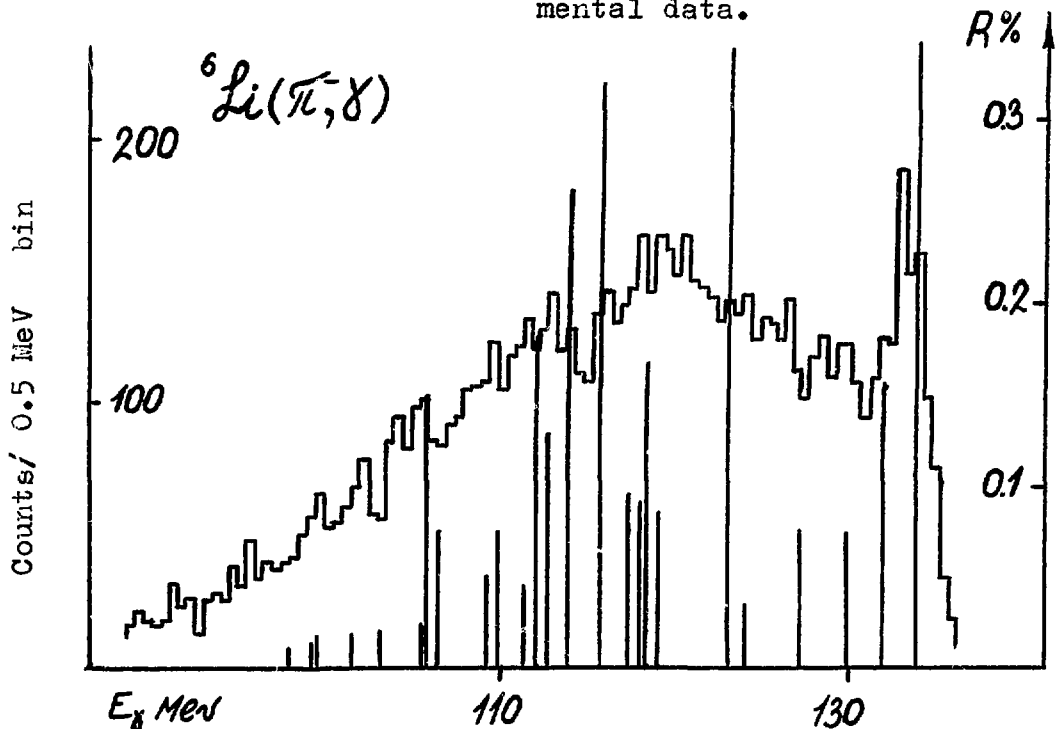
In the framework of the shell model  ${}^6\text{Li}(\pi^-, \gamma)$  process is investigated. The capture takes place from s- and from p-shell of mesoatom. Transitions to the positive and giant resonance states are considered. The pionic wave function is calculated from the Klein-Gordon equation with the Kisslinger-Erison potential. The radiative branching ratio  $R = R_s + R_p$ , where  $R_s = \lambda_{1s} \cdot \omega_s / \Gamma_{1s}$  and  $R_p = \lambda_{2p} \cdot \omega_p / \Gamma_{2p}$  and  $\omega_s = 0.4$   $\omega_p = 0.6$   $\Gamma_{1s} = 0.194 \text{ MeV}$   $\Gamma_{2p} = 0.015 \text{ eV}$  in good agreement with experimental data.

Table 1. Yield (R%) of  ${}^6\text{He}$  in radiative capture from s- and p-mesoatomic states

J $\pi$	0 $^-$	1 $^-$	2 $^-$	3 $^-$	$\Sigma R$
$R_s$ %	0.12	0.51	0.58	0.13	1.34
$R_p$ %	0.04	0.31	0.35	0.13	0.83
R %	0.16	0.82	0.93	0.26	2.17

Table 2. Yield (R%) of  ${}^6\text{He}$  in positive parity states

J $\pi$	$E^*(\text{MeV})$	$R_s$ %	$R_p$ %	R %	EXP
0 $^+$	0	0.23	0.11	0.34	0.31
0 $^+$	6.7	0.05	0.02	0.07	
2 $^+$	1.8	0.07	0.08	0.16	0.15
2 $^+$	4.2	0.03	0.05	0.07	
1 $^+$	5.1	0	0	0.01	
$\Sigma$		0.38	0.27	0.65	



S. Frankel and W. Frati  
Department of Physics  
University of Pennsylvania  
Philadelphia, Pennsylvania 19174

O. Van Dyck and R. Werbeck  
Clinton P. Anderson Meson Physics Facility  
Los Alamos, New Mexico 87544

V. Highland  
Department of Physics  
Temple University  
Philadelphia, Pennsylvania 19122

Backward ( $180^\circ$ ) elastic scattering of 800 and 600 MeV protons at LAMPF has been used as the experimental tool to search for the presence of nuclear states of very high binding, suggested by Feenberg and Primakoff and by Lee and Wick. Among the targets used were a Au foil irradiated by  $\sim 3 \times 10^{17}$  300 GeV protons at Fermi lab, and a Pt target which was for many years the internal target for the 3 GeV protons at PPA.

No evidence for condensed nuclear states was observed, and an upper limit of condensed nuclei per normal nucleus will be presented.

## Instability of Neutron Star Matter for Pion Condensation

Y. Futami, Y. Takahashi and A. Suzuki  
Science University of Tokyo, Shinjuku-ku, Tokyo, Japan

The following statement is well-known; if an approximate eigenmode satisfying the RPA equation possesses complex frequencies, then the Hartree-Fock state becomes unstable with respect to the corresponding collective oscillations.<sup>1</sup> We would like to discuss the problem of pion condensation from the viewpoint of collective oscillations. In our case, the Hartree-Fock state is neutron star matter in which all the single-particle states are filled by neutrons up to the Fermi momentum set by the total nucleon density. For simplicity, let us consider the Hamiltonian which consists of a kinetic energy of nucleons, the pion energy and the p-wave part of the  $\bar{N}$ -N interaction. In order to investigate the instability with respect to the appearance of condensed  $\pi^-$  with momentum  $\vec{k}$ , we introduce an operator

$$S_k^{(-)*} = X_{1,k}^{(-)} \phi_k^{(-)*} + X_{2,k}^{(-)} \phi_{-k}^{(+)} + S_k^{(p.h.)*}, \quad (1)$$

where  $\phi^{(\pm)}$  is the field operator for pions, X's are the coefficients, and the last term represents the particle-hole operator coupled with pion fields in the interaction Hamiltonian. From the RPA equation

$$[H, S_k^{(-)*}] = \omega S_k^{(-)*}, \quad (2)$$

we can obtain the eigenvalue equation for the energy of  $\pi^-$  in neutron star matter. These eigenfrequencies are represented by points in Fig. 1. The instability occurs at such a density that the minimum point between P and Q is raised to touch with the dotted line. Thus the instability condition is given by

$$2\omega_c = \frac{4f^2 k^2}{\Omega m_\pi^2} \sum_q \frac{\theta(q_F - q)}{(\omega_c + \epsilon_{q-k} - \epsilon_q)^2}. \quad (3)$$

Eq. (3) is the Migdal's criterion for the appearance of condensed negative pions.<sup>2</sup> Next we consider the Hamiltonian for only the  $\pi^-$  field with single momentum  $\vec{k} = -k\hat{z}$ , neglecting the

Fig. 1. Graphical analysis of the eigenvalue equation for the energy of  $\pi^-$ . The region of oblique lines represents the continuous spectra.

other pion fields. In this case, within an approximation of  $\omega + \epsilon_k \gg k v_F$ , the critical density which is determined from the instability condition similar with Eq. (3) agrees with the one obtained by use of the mean field method.<sup>3</sup>

1. K. Sawada and N. Fukuda, Prog. Theor. Phys. 25, 653 (1961).
2. A. B. Migdal, Phys. Rev. Lett. 31, 257 (1973).
3. R. F. Sawyer and D. J. Scalapino, Phys. Rev. D7, 653 (1973).

E. NYMAN and M. RHO  
Service de Physique Théorique  
Centre d'Etudes Nucléaires de Saclay  
BP n°2 - 91190 Gif-sur-Yvette  
France

We have studied the suggestion of T.D. Lee that at some density greater than that of normal nuclear matter, an abnormal state with vanishing nucleon mass and a larger binding energy could exist. The original calculation, based on the  $\sigma$ -model Lagrangian and interactions mediated by the scalar meson in semi-classical (tree) approximation, indicated that such a state could exist already at a few times the normal matter density. We consider quantum corrections to this, and have evaluated all one-loop graphs, as well as what we consider to be the most important two-loop diagram. Suitable renormalizations render the results finite. In normal nuclear matter, this set of graphs leads (in non-relativistic approximation) to the Hartree-Fock energy plus the correlation energy approximated as a sum of ring diagrams (i.e. random phase approximation).

In the tree-approximation, the  $\sigma$ -model Lagrangian leads to a three-body force which is too strong to be consistent with the conventional theory of nuclear binding energies. However when loop corrections are included, the strength of the three-body force becomes very sensitive to the parameters of the theory. We have chosen the mass of the  $\sigma$ -meson (which is an arbitrary parameter) such that the three-body force is negligibly small in normal nuclear matter. Approximating the singularities of the self-energy of the meson in medium by a single pole, we have been able to make an analytic calculation of the one- and two-loop contributions to the energy density. Our preliminary results indicate that the quantum corrections could make a qualitative change in the structure of the abnormal state.

# IV

## NUCLEON INTERACTIONS

## IV.A

### NUCLEON NUCLEUS INTERACTIONS

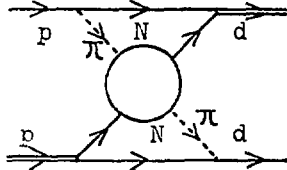


P-D elastic scattering at large angle

IV.A.1

H. Tezuka & M. Yamazaki  
 Department of Physics, Tokyo Institute of Technology

Recent experiments show that there exists a large backward peak in the differential cross section of p-d elastic scattering in the GeV region. To explain this peak, some theoretical calculations have been reported.<sup>1,2,3)</sup>

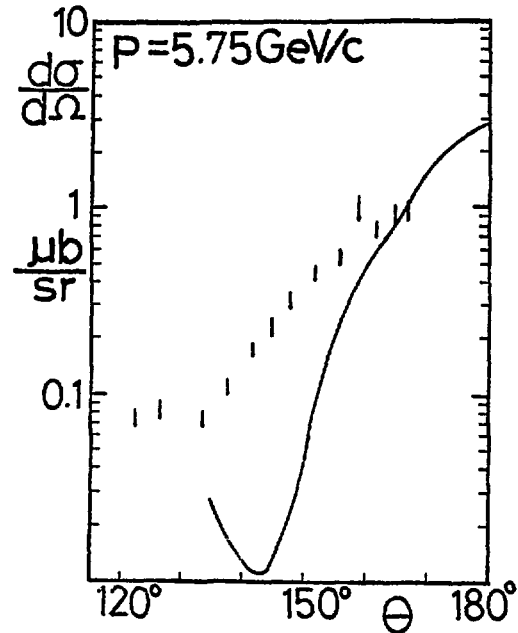
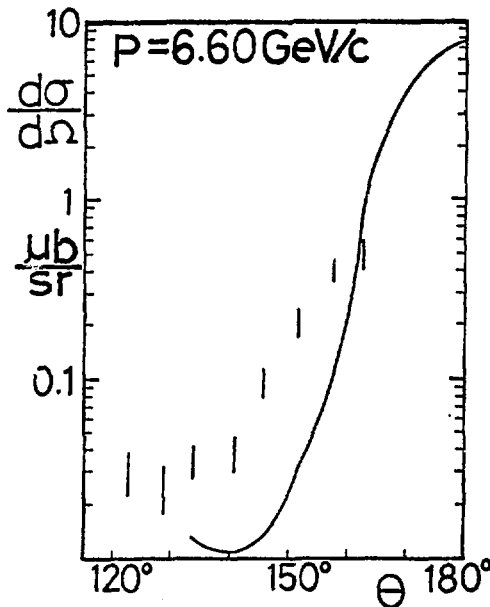


We have adopted the phenomenological model which connects the p-d differential cross section to that of  $\pi$ -N through the left Feynman graph. Then the p-d differential cross section is given by

$$\frac{d\sigma^{pd}}{d\Omega_e} = \frac{1}{3} \left[ \frac{G^2 \alpha^2}{4\pi(1-\alpha r)} \right] \frac{6m}{M^2} J^2 F(k^2)^2 \frac{1}{(k^2 - \mu^2)^2} \left( -\frac{1}{2}k^2 + \frac{1}{8}M^2 + \frac{3}{2}m^2 \right)^2 \frac{S_{\pi N}}{S_{pd}} \frac{d\sigma^{\pi N}}{d\Omega_\pi}$$

where  $J$  is a free parameter and we adopt the value of 1.03. The notations of this equation are the same as Barry's.<sup>4)</sup> Comparing with the data of Berkeley,<sup>5)</sup> we get good agreements at deuteron incident momenta 6.60 GeV/c and 5.75 GeV/c, but at 4.50 GeV/c the calculated cross section is too small compared to the experimental data. This disagreement seems to be for lack of the  $f$  meson contributions. As this effect is doubly included in our model, our calculated values are smaller than those of Craigie-Wilkin.

- 1) A.K.Kerman & L.S.Kisslinger : Phys.Rev. 180(1969)1483
- 2) N.S.Craigie & C.Wilkin : Nucl.Phys. B14(1969)477
- 3) J.S.Sharma, V.S.Bahasin & A.N.Mitra : Nucl.Phys. B35(1971)466
- 4) G.W.Barry : Ann.Phys. 73(1972)482
- 5) L.Dubal et al. : Phys.Rev. D9(1974)597

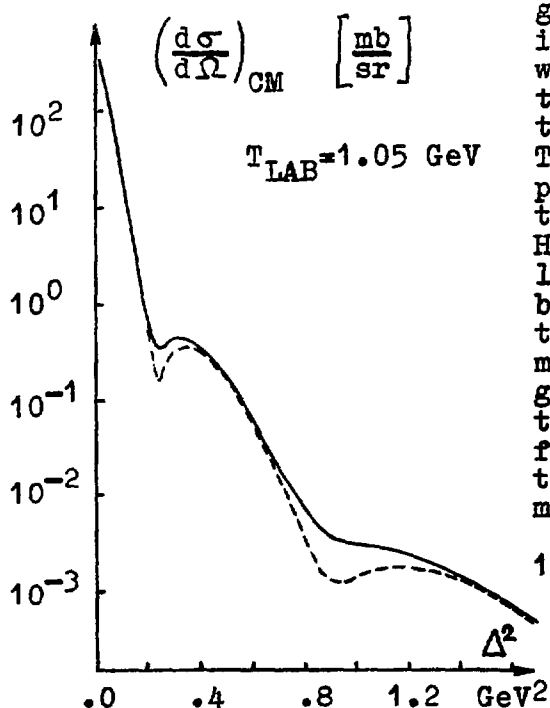


NON-EIKONAL CORRECTIONS TO THE GLAUBER MODEL IV.A.2  
AND PROTON-He<sup>4</sup> SCATTERING AT 1 GeV

M. Błeszyński and T. Jaroszewicz  
Institute of Nuclear Physics, 31-342 Kraków, Poland

A multiple scattering formula is discussed which gives the corrections to the Glauber model at medium energies, coming from the non-eikonal propagation of the projectile through the nucleus. The formula is derived from the Watson series assuming (i) the fixed scatterers approximation and (ii) the specific prescription for the off-shell continuation of the t-matrix elements for the scattering on the target nucleons /such that they depend on the momentum transfer only/, together with putting the rescattering terms /i.e. terms in which a given nucleon is struck more than once by the projectile/ equal to zero. The approximation (ii) is quite well motivated at energies of order 1 GeV /see the accompanying paper reporting the calculation based on the first order eikonal expansion/. We do not make any approximations in the free wave propagators which are left in their exact form,  $G_0(\vec{p}) = (k^2 - \vec{p}^2)^{-1}$ ,  $k$  being the initial projectile momentum.

The main effect of the non-eikonal propagation is to change the phases but not the moduli of the separate Glauber multiple scattering terms; this affects significantly the regions of the minima in the cross-section, where there is a strong interference between various multiple scattering terms. The figure below shows the comparison between the Glauber model predictions and the results obtained with the formula proposed for the proton-He<sup>4</sup> scattering at 1.05 GeV. The standard



gaussian parametrization of the individual amplitudes was used, with the slope 5 GeV<sup>-2</sup>, the real to imaginary part ratio -0.33, and the total NN cross-section 44 mb. The experimental data is not plotted here because we have used the simple gaussian form of the He<sup>4</sup> wave function /with the oscillator parameter R=1.37 fm/, this being inconsistent with the electron scattering data at large momentum transfers. Our results suggest that the non-eikonal propagation effects may be responsible for the very shallow minimum in the p-He<sup>4</sup> cross-section recently measured at Saclay<sup>1</sup>.

1. S. Baker et al., Phys. Rev. Lett. 32, 839 (1974).

Fig.1. p-He<sup>4</sup> scattering at 1.05 GeV. See the text for details.

ON THE MODIFIED KERMAN, McMANUS, AND THALER OPTICAL POTENTIAL  
AND ITS APPLICABILITY TO THE SCATTERING FROM LIGHT NUCLEI

M. Błaszynski and T. Jaroszewicz  
Institute of Nuclear Physics, 31-342 Kraków, Poland

It is claimed that the KMT optical potential in its commonly used form has to be modified in order to reproduce the correct high energy limit /i.e. the Glauber formula/. It is shown that when assuming the commonly used off-shell prescription for individual  $t$ -matrices,  $\langle \vec{k}' | t | \vec{k} \rangle = t(\vec{k} - \vec{k}')$ , it is necessary to replace the KMT potential  $V_{KMT} = V_D + V_R$  by the modified one,  $V_M = V_D$ , where  $V_D$  denotes "direct" terms and  $V_R$  - rescattering terms, i.e. the terms in which the projectile is scattered more than once from one given nucleon. For medium energies this modification is equivalent to the recently proposed prescription for the multiple scattering calculations /see the accompanying paper/. The importance of such a modification of  $V_{opt}$  is illustrated in Fig.1, where the cross-section for high energy proton- $He^4$  scattering is plotted, calculated with the usual /broken line/ and modified /solid line/ potentials obtained from the  $t$ -matrices parametrized as gaussians in the momentum transfer, continued off-shell in the above-mentioned way. These potentials are calculated to /practically/ infinite order in  $t$ . The convergence of  $V_{opt}$  is shown in Fig.2; it is seen that  $V_{opt}$  has to be taken to at least fifth order in  $t$  if the exact result is to be reproduced for larger momentum transfers.

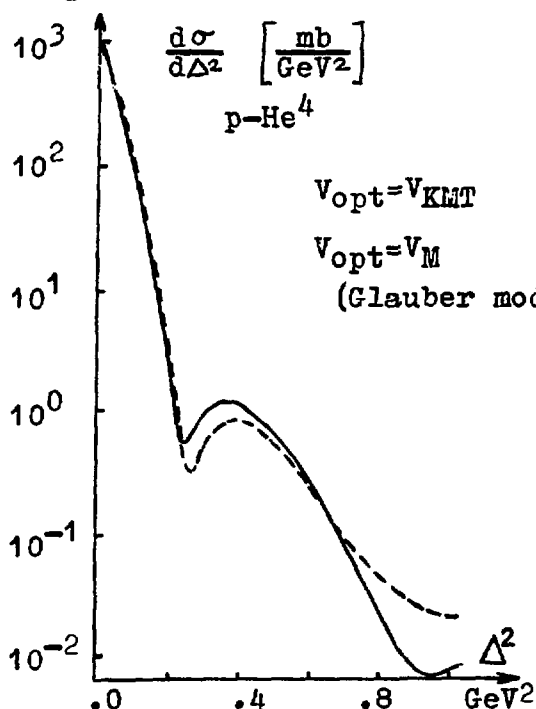


Fig.1. KMT versus the modified optical potential in the high energy p- $He^4$  scattering.

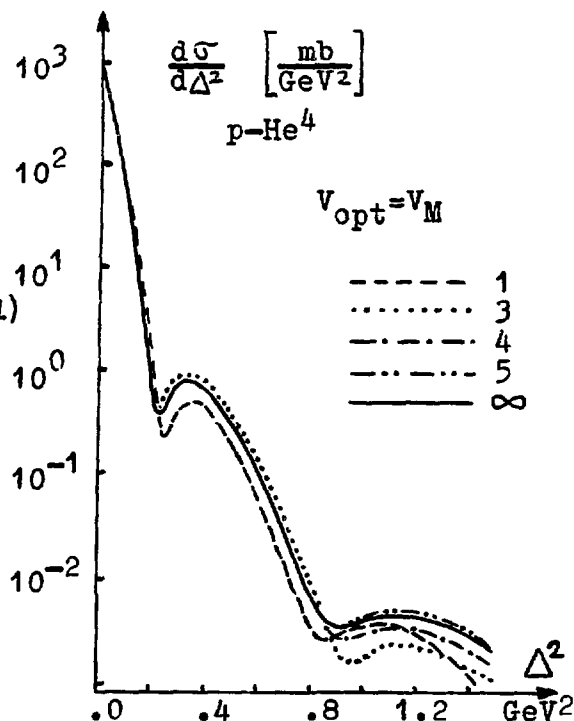


Fig.2. Convergence of  $V_{opt}$ . The numbers indicate the order to which the potential is taken.

TWO-COMPONENT MODEL OF HIGH-ENERGY HADRON SCATTERING FROM NUCLEI.

R. DYMARZ<sup>(x)</sup>, A. MAŁECKI<sup>(x)(xx)</sup> and P. PICCHI<sup>(xx)</sup>

(x) Instytut Fizyki Jadrowej, Kraków, Poland

(xx) Laboratori Nazionali del CNEN, Frascati, Italy.

We have developed a model of high-energy hadron scattering from nuclei which includes the two basic mechanisms of multiple collisions: i) in a sequence of collisions of the projectile with target sub-units all scatterings are near ly forward; ii) one scattering in the sequence occurs at a large angle and the remaining ones are forward. The Glauber model takes into account only forward scatterings. In our attempt to include both the mechanisms we treat the large-angle term in the Born approximation with waves distorted by forward scatterings along the initial and final projectile direction. Our expression for the scattering amplitude (meant as the operator acting between nuclear states) at momentum transfer  $\vec{q}$  is the following:

$$F = F_{\text{forward}} + F_{\text{large}},$$

$$F_{\text{forward}} = \frac{ip}{2\pi} \int d^2b e^{i\vec{q} \cdot \vec{b}} \left(1 - \prod_{j=1}^A (1 - \gamma_{\text{forward}}(\vec{b} - \vec{b}_j))\right),$$

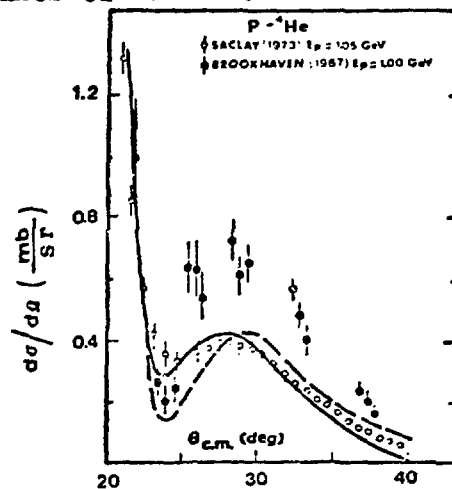
$$F_{\text{large}} = \frac{ip}{2\pi} \int d^2b e^{i\vec{q} \cdot \vec{b}} \int dz \sum_{j=1}^A f_{\text{large}}(\vec{r} - \vec{r}_j) \prod_{k(\neq j)}^A (1 - B_k - \bar{B}_k); \text{ where}$$

$$B_k = \gamma_{\text{forward}}(\vec{b}^{(i)} - \vec{b}_k^{(i)}) \theta(z^{(i)} - z_k^{(i)}), \quad \bar{B}_k = \gamma_{\text{forward}}(\vec{b}^{(f)} - \vec{b}_k^{(f)}) (1 - \theta(z^{(f)} - z_k^{(f)})),$$

$$f_{\text{large}}(\vec{r} - \vec{r}_j) = \gamma_{\text{large}}(\vec{b} - \vec{b}_j) \delta(z - z_j); \text{ the axes } Oz^{(i)}, Oz^{(f)}, Oz \text{ are directed}$$

along the initial projectile momentum, the final momentum and along the bisectrix of the scattering angle  $\theta_{\text{cm}}$ , respectively, while  $\vec{b}^{(i)}$ ,  $\vec{b}^{(f)}$ ,  $\vec{b}$  denote the projections of vectors on the planes perpendicular to these axes. The profile functions  $\gamma_{\text{forward}}$ ,  $\gamma_{\text{large}}$  are the Fourier-Bessel transforms of the two parts of the elementary amplitude which describe the elastic projectile-nucleon scattering at forward and large angles.

The application of our model to elastic  $p\text{-}^4\text{He}$  scattering at 1 GeV is presented in Figure (full line, the dashed line corresponds to only forward collisions); see also Lett. Nuovo Cimento 12, 101 (1975). The large-angle term begins to be important in the region of the minimum making the minimum appreciably shallower.



TEST OF 1 GeV NN MATRIX ON ELASTIC SCATTERING  
GLAUBER MODEL CALCULATION

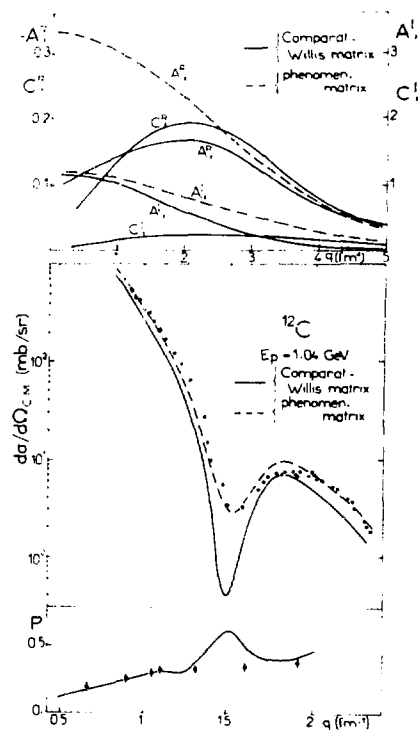
I. Brissaud, L. Bimbot, Y. Le Bornec, B. Tatischeff and N. Willis  
Institut de Physique Nucléaire, B.P. n°1, 91406, Orsay (France)

At 1 GeV, currently used phenomenological nucleon-nucleon amplitudes are restricted to central terms having a gaussian  $q$ -dependence. Recently Comparat and Willis<sup>1</sup> have obtained a complete nucleon-nucleon scattering matrix (including all A, B, ... amplitudes) by using the pp scattering phase shifts at 970 MeV<sup>2</sup> and searches on pn scattering observables. We present here results concerning differential cross section and polarization for 1 GeV protons incident on <sup>12</sup>C. The calculations are performed in the Glauber model<sup>3</sup> using this NN matrix.

In figure 1.a, we are comparing the isospin-independent terms  $A_\alpha(q)$  and  $C_\alpha(q)$  to the corresponding phenomenological amplitudes<sup>3</sup>. Cross sections and polarizations calculated to the Glauber optical limit and experimental data<sup>4</sup> are shown in figure 1.b. We see that the angular distribution

has a too pronounced minimum compared with the data. This is probably due to the very small values obtained for the real part of  $A_\alpha(q)$  at small  $q$  transfers i.e. the nuclear absorption has been underestimated. A small bump at  $q = 1.5 \text{ fm}^{-1}$  is connected to the very deep minimum of the cross section curve.

Similar conclusions can be extracted from the analysis of 1 GeV  $p + {}^{208}\text{Pb}$  scattering. We therefore tend to conclude that the Glauber approach with a realistic NN matrix need some improvements, particularly to the eikonal approximation<sup>3</sup>.



1. V. Comparat and A. Willis, annual report (1974) IPN-Orsay, France and to be published.
2. N. Hoshizaki et al., Prog. Theor. Phys. 42, 815 (1969).
3. I. Brissaud et al., Phys. Rev. C11, (1975), to be published; Phys. Lett. 48B, 319 (1974)
4. R. Bertini et al., Phys. Lett. 45B, 119 (1973); V.G. Vovchenko et al., Sov. Journ. Nucl. Phys. 16, 628 (1973).

Fig. 1.a) matrix elements.  
b) polarization and cross sections.

## Proton production in nuclei by 600 MeV protons

H. D. Orr, III

NASA, Langley Research Center, Hampton, Va. 23665

R. D. Edge

University of South Carolina, Columbia, SC 29208

T. A. Filippas

Greek Atomic Energy Commission, Athens, Greece

Abstract: The absolute differential cross sections for low-energy proton production in targets of C, Al, Ni, Cu, and Au under 600 MeV proton bombardment have been determined at several angles in the forward and backward hemispheres. A semiconductor detector telescope was used to identify the secondary protons in the energy range from 2-15 MeV. These results are compared to others at 60 MeV; an overall decrease in the cross section with increasing incident energy is found. The results are also compared with Monte Carlo calculations based on the cascade-plus-evaporation model; the predictions are found to be in fair agreement with the present experiment for light nuclei, good agreement for medium mass nuclei, but poor agreement for heavy nuclei. These results suggest the importance of nuclear structure effects in the case of light nuclei and changes in the Coulomb barrier in excited heavy nuclei.

We present a bremsstrahlung model similar in outlook to the Bair et al. model for nucleon-nucleon bremsstrahlung. We treat the nucleus and the projectile each as an elementary particle with given electric charge, magnetic moment, spin and mass. We assume the exchange of neutral mesons is responsible for the nuclear scattering. Such a model is gauge invariant and satisfies Low's low energy theorem.

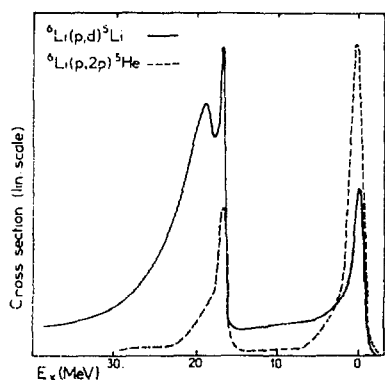
In relating bremsstrahlung to elastic scattering, the basic input parameter to be specified is  $t(q)$ , the nuclear scattering amplitude ( $q$  is the momentum transfer). This amplitude can be parameterized in several ways. At energies less than 200 MeV we will use a more or less standard optical model potential in the Schrödinger equation. At energies above 200 MeV we will use Glauber theory with the energy dependent potential used by Boridy and Fesbach. The electro-magnetic interaction is included to first order only. Thus all photons involved are real final state photons with  $k^2=0$ , where  $k$  is the four momentum of the photon. Hence no electro-magnetic form factors of the projectile or nucleus are needed. However, we sometimes use a nuclear potential plus the potential of an extended charge distribution to describe the nuclear scattering amplitude. Nuclear double scattering is neglected in the bremsstrahlung calculation. These terms have been shown to be small for non-relativistic proton-proton bremsstrahlung in the overall center of mass frame. We will present some analysis on the effect of assuming scalar meson exchange compared to pseudo-scalar meson exchange, the  $Z$ , atomic weight, projectile energy, and gamma energy systematics of the calculated cross sections, and some isotopic effects. Also a classical explanation of the differential bremsstrahlung cross section systematics is given. In general the cross section for a given gamma energy increases for higher proton energy and for larger target charge. The cross sections are generally largest when the gamma production angle is one half the proton scattering angle.

THE INDIVIDUAL NUCLEONS AND THEIR CLUSTERING IN  ${}^6\text{Li}$   
AS PROBED IN (p,d) AND (p,2p) REACTIONS.

Jan Källne

The Gustaf Werner Institute, Univ. of Uppsala, S-75121 Uppsala, Sweden

The residual states accessible by single nucleon removal from  ${}^6\text{Li}$  are discussed. It is noticed that not only residual nucleus hole-states but also states of fragmented systems are important. Events of fragmentation are taken as evidence of nucleon sub-structures (cluster) in the target nucleus which could be searched for in reactions like (p,d) and (p,2p).—The figure shows schematically two spectra for the target nucleus  ${}^6\text{Li}$  obtained with the (p,d) reaction at 185 MeV ( $\theta=2.5^\circ$ ) /1/ and the (p,2p) reaction at 100 MeV ( $\theta_1=\theta_2=35^\circ$ ) /2/. These represent the nucleon momentum situations  $q > 150$  MeV/c and  $q \ll 150$  MeV/c. The 1s nucleon removal from  ${}^6\text{Li}$  yields in both spectra the sharp peak at  $E_x=16.7$  MeV (corresponding to the  ${}^5\text{Li}/{}^5\text{He}$  state at 16.7 MeV,  $J^\pi=3/2^+$ ) and the broad peak at 19 MeV (corresponding to a fragmented system) in the (p,d) spectrum, only. The apparent differences are due to a q dependence. The 1s nucleons in  ${}^6\text{Li}$  are assumed to form an  $\alpha$  core which becomes increasingly enforced at high q. This would result in a q dependence in the partition of the 1s strength on the residual nucleus states and fragmented states as demonstrated by the spectra.— It is concluded that pickup and analogous reactions would prove useful to learn about individual nucleons forming clusters in nuclei, particularly, if simultaneous detection of the recoil products can be provided.  ${}^6\text{Li}$  just presents an exceptionally clear-



cut case where the fragmentation and thus the clustering manifested itself by a quasi-free  ${}^4\text{He}(p,d){}^3\text{He}$  peak distinguishable at high q.

/1/ J.Källne et al, Phys.Lett.52B(1974)313

/2/ R.Bhowmik et al, Nucl.Phys.A226(1974)365



PION PRODUCTION THROUGH THE REACTION  $d(p,d\pi^+)n$  AT 600 MEV\*

E. V. Hungerford, J. C. Allred, K. Koester,  
L. Y. Lee, and B. W. Mayes  
University of Houston, Houston, Tx. 77004

T. Witten, J. Hudomalj-Gabitzsch, N. Gabitzsch, T. M. Williams,  
J. Clement, G. S. Mutchler, and G. C. Phillips  
Rice University, Houston, Tx. 77001

## ABSTRACT

The production of pions through the three body process  $p + d \rightarrow d + \pi^+ + n$  is being investigated at the Space Radiation Effects Laboratory<sup>†</sup> at an incident energy of 600 MeV. The pion and deuteron were detected in coincidence with multi-wire proportional counters and the deuteron momentum was magnetically analyzed. Although isospin conservation forbids a  $\pi$ -N( $\Delta(1236)$ ) final state interaction, the  $\pi$ -d system can resonate in a  $T = 1$  state. Preliminary data show an enhancement of the cross section at a  $\pi$ -d mass of 2180 MeV with a full width at half maximum of 90 MeV. The cross section for this enhancement is a significant fraction of the inclusive pion production cross section at this angle. An experimental study of the angular distribution and a detailed momentum spectrum of the deuteron from the reaction is in process.

\*Supported by the U.S. E.R.D.A.

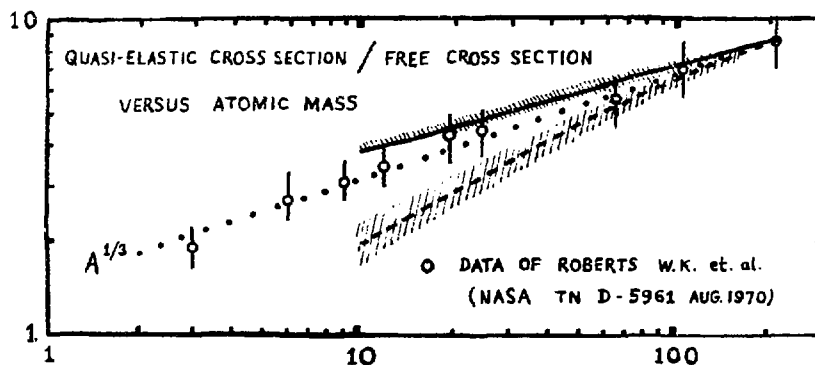
<sup>†</sup>SREL is supported by the National Aeronautics and Space Administration, the Commonwealth of Virginia, and the National Science Foundation.

A. P. Sathe and E. A. Remler

College of William and Mary, Williamsburg, Virginia 23185

## ABSTRACT

The recent development of the Wigner representation of scattering as a practical tool for treatment of complex multiparticle processes<sup>(1)</sup> has enabled us to begin analysis of inclusive production cross-sections for fragments from medium and high energy nuclear collisions.<sup>(2)</sup> Initially, to test and demonstrate this new method, we are examining data using only the simplest possible models. A number of experiments have measured quasi-elastic deuteron production by protons on nuclei; of these, the most complete set known to us are at .580 GeV<sup>(3)</sup> and 1 GeV.<sup>(4)</sup> Discussion of these has centered on two questions: the elementary production mechanism for two fast forward nucleons (e.g. to what extent it depends on initial state correlations) and, the cross-sections' dependence on Atomic Mass  $A$  (which requires understanding of multiple collisions suffered by participants in the nuclear medium before and after the elementary production). In the absence of practical theoretical methods of dealing with the latter question, explanations have been limited to noting that the data seems to go as  $A^{1/3}$ , corresponding to emanation from an 'active region' about the terminator line situated at the nuclear surface. The terminator grows as  $A^{1/3}$ . Our analysis indicates that such statements conceal a theoretically richer picture. The graph compares the .580 GeV data with two calculations based on nuclear models simplified to allow analytic expression of results. The solid line is a nucleus of uniform density throughout. The dashed line corresponds to a uniform core plus half density uniform skin. There are no free parameters except, having not as yet calculated the elementary vertex for nucleon pair production, there is an unknown overall normalization fixed to agree with data at  $^{208}\text{Pb}$ . These results indicate good agreement with data is probable at this energy using a realistic nuclear skin. Theory however implies flattening of  $A$  dependence (saturation) at higher energies in contradiction to the 1 GeV data point for  $^{208}\text{Pb}$ . More accurate data and comparison with production by other projectiles can now be analyzed in terms of nuclear surface properties.



1. E. A. Remler, Use of the Wigner Representation in Scattering Problems, College of William and Mary preprint.
2. E. A. Remler and A. P. Sathe, Quasi-Classical Scattering Theory and Bound State Production Processes, to be published in Annals of Physics.
3. W. K. Roberts et. al., unpublished report, NASA TN D-5961, (Aug. 1970).
4. R. J. Sutter et. al., Phys. Rev. Lett. 19, 1189 (1967).

$$0.13 \text{ GeV}^2/c^2 \leq -t \leq 0.55 \text{ GeV}^2/c^2$$

J. C. Fong, G. J. Igo, S. L. Verbeck, C. A. Whitten, Jr.  
University of California at Los Angeles, Los Angeles, Calif. 90024

D. L. Hendrie, V. Perez-Mendez, Y. Therrien  
Lawrence Berkeley Laboratory, Berkeley, Calif. 94720

G. W. Hoffmann  
University of Texas, Austin, Texas 78712

## ABSTRACT

At the Lawrence Berkeley Laboratory 184" synchrocyclotron an experimental technique using a gas target and a  $\Delta E$ - $E$  telescope of solid state detectors has been employed to measure the elastic scattering of 0.72 GeV protons from  ${}^4\text{He}$  in the region of four momentum transfer,  $-t$ , from 0.13 to 0.55  $\text{GeV}^2/c^2$ . With a suitably chosen collimation system the detector telescope viewed reaction

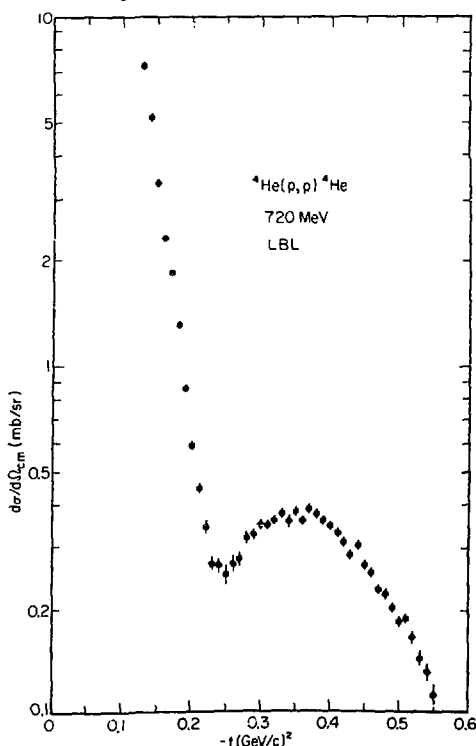


Fig. 1. Elastic scattering of protons from  ${}^4\text{He}$  at 0.72 GeV.

products from the He gas target between the angles  $\theta_{\min}$  and  $\theta_{\max}$ , such that all alpha particles within this angular range must come from elastic scattering. From the relation  $-t = 2m_{\alpha}T_{\alpha L}$  the energy of the alpha particle measures  $-t$  directly; and the energy spectrum  $dY_{\alpha}/dT_{\alpha}$  can be converted directly into an angular distribution.<sup>1</sup> The excellent particle identification provided by the  $\Delta E$ - $E$  detector telescope is very important since the yield of  ${}^3\text{He}$  particles is larger than that for  $\alpha$  particles in certain regions of the energy spectra. The intensity of the proton beam was measured and monitored by a system of ionization counters, two sets of monitor counters and beam counters; and the cross sections were measured absolutely to better than  $\pm 10\%$ . The range of  $-t$  covered in this experiment includes the interference region ( $-t \approx 0.23 \text{ GeV}^2/c^2$ ) between single and double scattering processes in multiple scattering theories where there has been disagreement between two experimental measurements at 1.0 GeV.<sup>2,3</sup> A preliminary angular distribution from the data analysis is presented in Fig. 1. The data is currently being analyzed in terms of optical model and multiple-scattering theories.<sup>4</sup> We are also currently obtaining elastic scattering data at 0.59 GeV using the same experimental technique.

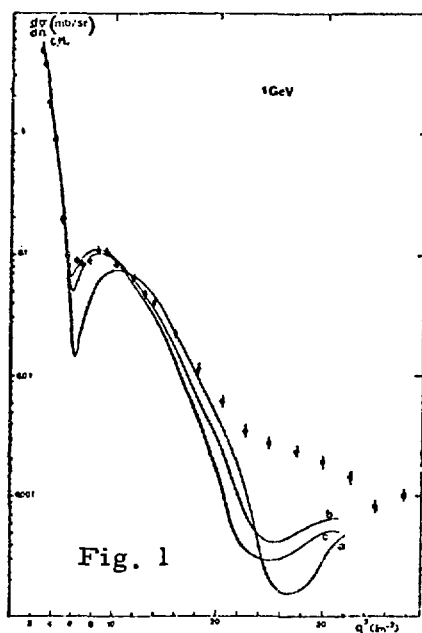
1. C. A. Whitten, Jr., Nucl. Instr. and Meth. (to be published).
2. H. Palevsky et al., Phys. Rev. Lett. 18, 1200 (1967).
3. S. D. Baker et al., Phys. Rev. Lett. 32, 839 (1974).
4. D. W. Rule and Y. Hahn, Phys. Rev. Lett. 34, 332 (1975).

p -  $^3\text{He}$  elastic scattering at intermediate energies and the NN interaction.

R. Frascaria, N. Marty, V. Comparat, M. Morlet and A. Willis.  
Institut de Physique Nucléaire, 91406, Orsay (France).

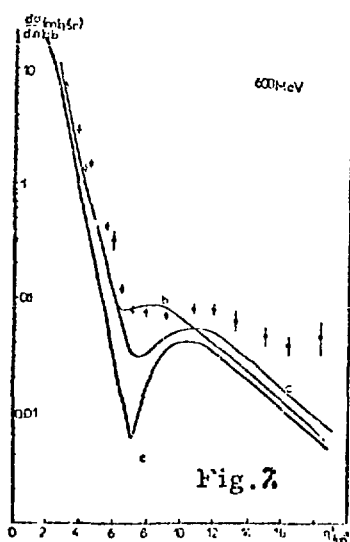
D. Legrand, D. Garreta, R. Beurtey, G. Bruge, P. Couvert, H. Catz,  
A. Chaumeaux, J. C. Faivre, Y. Terrien and R. Bertini<sup>\*</sup>.  
DPhNME, CEN-Saclay, 91190, Gif-sur-Yvette (France).

The  $^3\text{He}(p,p)^3\text{He}$  cross section was measured at 1 GeV, at the CEA Synchrotron Saturne. A liquid  $^3\text{He}$  target 2 cm thick<sup>1</sup> and the spectrometer facilities<sup>2</sup> were used. The results are given on fig. 1. The absolute uncertainty on the cross section is  $\pm 9\%$ . They are compared to calculations performed with the  $^3\text{He}$  form factor from ref. 3 which is in good agreement with the



electron scattering results. The cross sections are calculated in the Glauber formalism including the spin-isospin dependence of the NN interaction at all orders of the scattering expansion. The sensitivity to the phase shifts is illustrated in fig. 1 where three different phase shift analysis are used a) pp phases from Hoshizaki<sup>4</sup> and pn phases from ref. 5 ; b) and c) the same pn phases and pp phases from Matsuda<sup>6</sup> whose analysis is made by adding 31 new NN data (16 of them are polarization measurements). The agreement is better till  $q^2 \leq 20\text{fm}^{-2}$  with curve 1. b or 1. c.

The same calculations are performed at 600 MeV where more NN data and more systematic analysis exist. On fig. 2, a) The pp-phases are from Mc Gregor et al<sup>7</sup> and in b) and c) pp-phases from Cozzika et al<sup>8</sup>. For the three curves the pn-phases are taken from Mc Gregor<sup>9</sup>. The calculations are compared to the experimental results at 600 MeV from Boschitz et al<sup>10</sup>.



References :

1. S. Buhler, Proc. of the 8th Int. Cryog. Engeen. Conf. Berlin (May 70).
2. R. Beurtey et al., Bul. Inf. Sci. Tech. CEA n°179, 67 (1973) and Phys. Rev. Lett. Vol. 32, n°15 (1974) 839.
3. M. Fabre de la Ripelle, session d'études La Toussuire (1971)55 and Lett. Nuovo Cimento, Vol 1 n°14 (1971) 584.
4. N. Hoshizaki, Rev. Of Modern Phys. Vol 39 n°3(1967) 70D.
5. V. Comparat and A. Willis, private communication.
6. M. Matsuda and W. Watari, Lett. Nuovo Cimento Vol. 6 n°1(1973) 23.
7. M.H. Mc Gregor, A. Arndt, R.M. Wright, Phys. Rev. 169, B1149(1968)
8. G. Cozzika, Note CEA-N-1720, juillet 74.
9. M.H. Mc Gregor, A. Arndt, R.M. Wright, Phys. Rev. 173, n°5(1968)1272.
10. E. T. Boschitz, NASA TMX-52673.

<sup>\*</sup> Université de Strasbourg (France)

MEASUREMENT OF THE NEUTRON FLUX GENERATED BY THE  
LAMPF 800 MeV PROTON BEAM STOP

IV.A.13

Dennis G. Perry

The flux and spectral shape of the neutrons generated by 800 MeV protons incident on a copper beam stop have been measured at the LAMPF Radiation Effects Facility using the technique of threshold activation detectors. The detectors used were  $^{235}\text{U}$ ,  $^{238}\text{U}$ , Au and Ir. The induced activities measured were generated from the following reactions:  $^{235}\text{U}(n,f)$ ,  $^{238}\text{U}(n,f)$ ,  $^{197}\text{Au}(n,\gamma)^{198}\text{Au}$ ,  $^{197}\text{Au}(n,2n)^{196}\text{Au}$ ,  $^{197}\text{Au}(n,3n)^{195}\text{Au}$ ,  $^{197}\text{Au}(n,4n)^{194}\text{Au}$ ,  $^{191}\text{Ir}(n,\gamma)^{192}\text{Ir}$ ,  $^{191}\text{Ir}(n,2n)^{190}\text{Ir}$ ,  $^{191}\text{Ir}(n,3n)^{189}\text{Ir}$ ,  $^{193}\text{Ir}(n,n')^{193\text{m}}\text{Ir}$ . The measured spectral shape agrees well with the shape generated by a Monte Carlo calculation. The total flux measured was  $1.6 \times 10^{13}$  n/cm<sup>2</sup>-sec-mA.

## SCATTERING OF PROTONS ON HELIUM BETWEEN 348 AND 1154 MeV

E. Aslanides<sup>+</sup>, T. Bauer<sup>+</sup>, R. Bertini<sup>+</sup>, R. Beurtey,  
 A. Boudard, F. Brochard<sup>+</sup>, G. Bruge, A. Chaumeaux,  
 H. Catz, J.M. Fontaine, R. Frascaria<sup>++</sup>,  
 P. Gorodetzky<sup>+</sup>, J. Guyot, F. Hibou,  
 M. Matoba<sup>+++</sup>, Y. Terrien and J. Thirion

*CEN Saclay, BP 2, 91190, Gif-sur-Yvette, France.*

Proton elastic scattering on  ${}^4\text{He}$  has been measured at  $T_p = 348, 650, 1057$  and  $1154$  MeV. The obtained angular distributions are presented for  $|t| < 0.7$  (GeV/c)<sup>2</sup>. The deepest minimum is observed for  $t = -0.26$  at  $T_p = 650$  MeV. Glauber type calculations are in progress to fit those angular distributions.

<sup>+</sup> CRN Strasbourg

<sup>++</sup> IPN Orsay

<sup>+++</sup> On leave from the Kyoto University, Kyoto, Japan.

FROM  $^{40}\text{Ca}$ ,  $^{42}\text{Ca}$ ,  $^{44}\text{Ca}$ ,  $^{48}\text{Ca}$  and  $^{48}\text{Ti}$

G. Alkhazov<sup>†</sup>, T. Bauer, R. Beurtey, A. Boudard, G. Bruge,  
A. Chaumeaux, P. Couvert, G. Cvijanovich<sup>††</sup>, H.H. Duhm<sup>†††</sup>,  
J.M. Fontaine<sup>††††</sup>, D. Garreta., A. Kulikov<sup>†</sup>, D. Legrand,  
J.C. Lugol, J. Saudinas, J. Thirion, A. Vorobyov<sup>†</sup>,

CEN Saclay, BP 2, 91190, Gif-sur-Yvette, France.

Using the high-resolution spectrometer SPES-1, the angular distributions of 1.04 GeV protons, scattered from  $^{40}\text{Ca}$ ,  $^{42}\text{Ca}$ ,  $^{44}\text{Ca}$ ,  $^{48}\text{Ca}$  and  $^{48}\text{Ti}$  nuclei are measured in the angular range 4-19°. Here we present the elastic scattering cross sections (fig.1) which, we hope, combined with the appropriate elastic electron scattering data, may furnish an interesting information on the differences between the neutron distributions in these nuclei. The elastic cross sections for the case of  $^{40}\text{Ca}$  and  $^{48}\text{Ca}$  are in good agreement with those, obtained by Gatchina group [1]. The analysis of the data, corresponding to excitations of low-lying states, is in progress.

- † Leningrad Institute for Nuclear Physics, Gatchina., USSR  
 †† Upsala College, East Orange, New Jersey, USA  
 ††† 1, Institut für Experimentalphysik, Hamburg, Germany.  
 †††† CNRS

[1] G.D. Alkhazov et al., Physics Letters, in print.

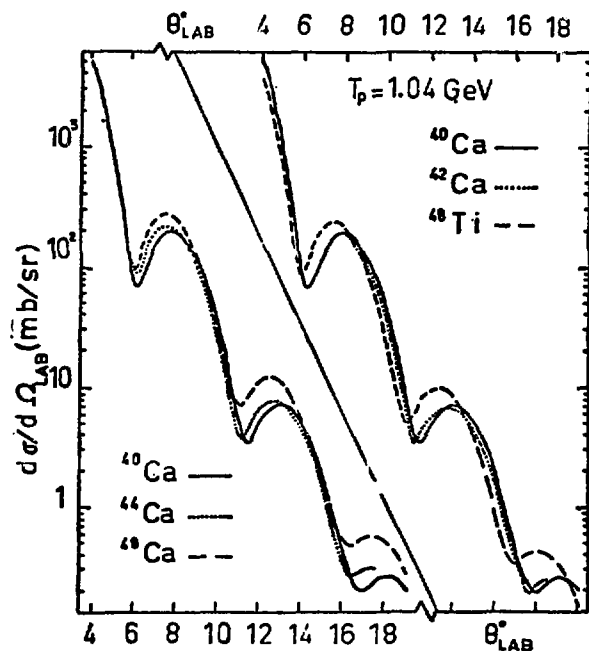


Fig. 1

The elastic cross sections (lab. system, preliminary) of 1.04 GeV proton scattering from the following targets:  $^{40}\text{Ca}$ (100%);  $^{42}\text{Ca}$ (76 %) +  $^{40}\text{Ca}$ (22 %) ;  $^{44}\text{Ca}$ (95 %) +  $^{40}\text{Ca}$ ( 5 %) ;  $^{48}\text{Ca}$ (67 %) +  $^{40}\text{Ca}$ (30 %) ;  $^{48}\text{Ti}$ (98 %)

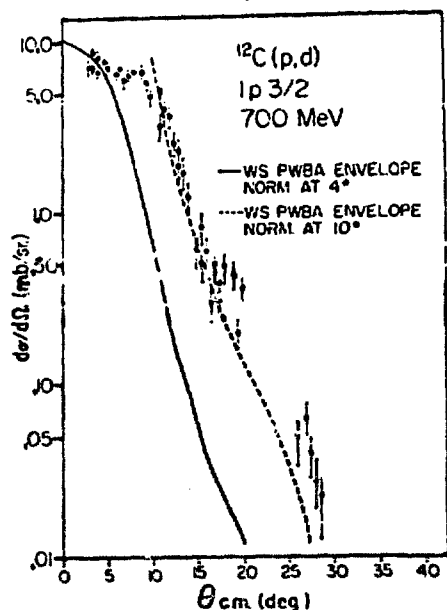
## PWBA (p,d) CALCULATIONS AT INTERMEDIATE BEAM ENERGIES

D.G. Fleming, J.W. Grabowski and E.W. Vogt  
 TRIUMF and Depts. of Chemistry and Physics, University  
 of British Columbia, Vancouver, B.C., Canada, V6T 1W5

With the advent of new high intensity and variable energy proton accelerators in the intermediate energy range, one can expect some renewed interest in direct reactions of the type (p,d), (p,t), (p,<sup>3</sup>He), etc. There are advantages and disadvantages in extending the study of pickup reactions from their traditional low energy regime. Distortion effects should be less at higher energies and the "dynamics" of the transfer process may well be more amenable to reliable calculations. On the other hand, quantum oscillations in the angular distributions become disturbingly rapid and do not reveal the orbital angular momentum of the transferred nucleon. Instead, interest centers on angular distributions averaged over such rapid oscillations.

An early motivation for our work was the hope that absolute spectroscopic factors in (p,d) reactions could be more reliably obtained, from DWBA calculations at intermediate energies, than the usual "factor of two" accuracy expected at low beam energies. Unfortunately, sources of uncertainty still remain, particularly in the choice of the deuteron optical potential. The PWBA treatment, while obviously incorrect in that it ignores all distortion effects, is nevertheless a useful tool in gaining an initial understanding of the expected momentum transfer dependence in angular distributions at intermediate energies.

The PWBA calculations can be carried out analytically for various form factors. We illustrate this radial dependence using square well, harmonic oscillator and Woods-Saxon (WS) potentials. In each case the differential cross section can essentially be factored in two parts; one part describing the rapid oscillations with angle and the other part the "envelope" of the cross section about which the oscillations occur. The latter dependence is illustrated in the accompanying Figure for a WS potential in a PWBA calculation of the <sup>12</sup>C(p,d)<sup>11</sup>C\* 1P<sub>3/2</sub> transition at 700 MeV. (Data from J. Thirion, Proc. Int. Conf. on Nucl. Phys., Munich, 1972; American Elsevier, 1973, p. 782).



There are distinct differences in calculated differential cross sections depending on the choice of form factor, but these are only apparent at angles  $\gtrsim 30^\circ$ , which is generally beyond presently available data. Calculations have also been carried out for the 185 MeV (p,d) data from Uppsala (J. Kallne et al., Gustaf Werner Institute, Preprint No. GWI-PH2/74) and, again, the envelope of the experimental cross sections are rather well reproduced. No attempt has been made to extract any spectroscopic information, only to reproduce the overall shape of the angular distributions; in this regard, the PWBA calculation is much more successful at  $\gtrsim 200$  MeV than it is at say 20 MeV.



GLAUBER CALCULATIONS FOR p-<sup>4</sup>He ELASTIC SCATTERING

J.P. Auger

Laboratoire de Physique, Faculté des Sciences d'Orléans,  
45045 Orléans Cédex, France

J.R. Gillespie\*

Institut des Sciences Nucléaires, BP 257, 38044 Grenoble, France

R.J. Lombard

Institut de Physique Nucléaire, Division de Physique Théorique  
91406 Orsay, France

The multiple scattering model of Glauber has been used to calculate p-<sup>4</sup>He scattering at 0.6, 1.0 and 20 GeV. The calculation includes spin-independent and spin-dependant amplitudes as well as the Coulomb interaction and a correction for overlapping interactions.

The nucleon-nucleon profile function is determined directly from two-particle scattering data. The <sup>4</sup>He wavefunction was taken as Gaussian. The overlapping interaction (3-body) correction for the eikonal phase function is that derived by Wallace <sup>(1)</sup> involving the nuclear density, the pair correlation function, and the interaction between the incident particle and the target nucleons. For this interaction we employed an effective potential which reproduces the spin-independent amplitude at low momentum transfer (to 1.0 fm<sup>-1</sup>).

The Coulomb interaction deepens the first minimum at 600 MeV but reduces it at 1.0 and 20 GeV. The overlap term is negligible at 0.6 and 20 GeV and provides a 20 % correction at 1 GeV.

(1) S.J. Wallace, Phys. Rev. C8, 2043 (1973).

\*On leave of absence, Dept. of Physics, Boston University.

EFFECTS OF ANTISYMMETRIZATION IN ELASTIC SCATTERING  
OF HIGH-ENERGY PROTONS FROM NUCLEI.

A. MAŁECKI<sup>(x)(o)</sup> and P. PICCHI<sup>(x)</sup>

(x) - Laboratori Nazionali del CNEN, Frascati, Italy.

(o) - Instytut Fizyki Jadrowej, Kraków, Poland.

We have studied elastic scattering of high-energy protons from nuclei taking into account the mechanism of exchange between the projectile and the target. This is equivalent to antisymmetrization between the incident proton and the ones in the target nucleus.

We considered scattering from  $^2\text{D}$  and  $^4\text{He}$  around 1 GeV using the approximation of single collisions. The nuclear wavefunctions including short-range repulsive correlations were applied. For large momentum transfers ( $q > 0.8$  GeV) the correlations are very important increasing the cross-section by several orders of magnitude.

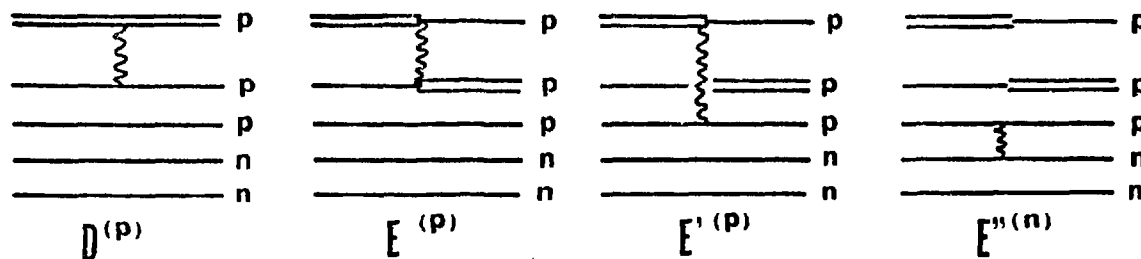
The rearrangement of protons was achieved by the two procedures: exact antisymmetrization and the so-called knockon approximation. For illustration we quote the cross-section formulas for  $^4\text{He}$  (without correlations):

$$(d\sigma/d\Omega)_{\text{exact antisym.}} = \frac{16}{9} |2D(p) + D(n) - E(p) - 2E'(p) - 2E'(n) - E''(n)|^2$$

$$(d\sigma/d\Omega)_{\text{knockon}} = |2D(p) + 2D(n) - E(p)|^2$$

while in the absence of exchange one has:  $(d\sigma/d\Omega)_{\text{direct}} = |2D(p) + 2D(n)|^2$ ;

the various amplitudes are given by the following self-explanatory diagrams:



where single lines describe bound states of nucleons, the double line - the state of free proton, and the wavy line denotes the interaction; the indices (p) and (n) correspond to the p-p and p-n interaction, respectively.

In general the effects of antisymmetrization are small for forward scattering angles, and large in the back hemisphere. We have found that the graphs  $E'$  and  $E''$  are quite important at large angles ( $\theta > 120^\circ$ ) invalidating thus the knockon approximation. The backward peaks observed in the p- $^2\text{D}$  and p- $^4\text{He}$  elastic scattering are appreciably affected by these graphs.

Currently we are studying the effects of multiple collisions and the relativistic corrections resulting from the deformation of recoiling nuclear wave function.

## INVESTIGATION OF PION AND KAON PRODUCTION ON NUCLEI

M. Dillig, M. G. Huber

Inst. for Theor. Physics, Univ. of Erlangen-Nürnberg, Germany

In the protoninduced production of  $\pi$  and K on nuclei both very large momenta ( $p \gtrsim 500$  MeV/c) and considerable angular momenta ( $l > 10 \hbar$ ) are transferred to the target nucleus even at threshold energies. Thus one may expect to investigate the nucleus under conditions which in conventional nuclear reaction at low energies are not accessible. Additionally, there are interesting phenomena expected to occur which are related to the reaction mechanisms, such as coherence effects in  $\pi$  production by complex projectiles (i. e. in  $(d, \pi)$  or  $(\alpha, \pi)$  reactions) and the formation of (real)  $N^*$  in nuclei (such as  $\Delta$ ,  $\Lambda$  and  $\Sigma$ ).

Some of those questions have been investigated in the frame of a One-Nucleon-Model (ONM) and a Two-Nucleon-Model (TNM). Those models have been applied to the  $(p, \pi^+)$  and the  $(p, \pi^-)$  reaction leading to bound excited states of the final nucleus; the calculated cross sections have been compared to experimental data at  $T_p = 156, 185$  and  $600$  MeV, respectively (Orsay, Uppsala<sup>1</sup>, CERN and Saclay<sup>2</sup>) results). From this work the following conclusions can be drawn:

1. The ONM generally leads only to a very poor description of all available data; this is mainly due to the uncertainties related to the pion nucleus optical potential, to the post-prior ambiguities and to the  $(\pi N)$  interaction;
2. in the TNM a consistent and qualitatively quite reasonable description of the various reactions can be achieved, both near threshold and above the resonance; the two particle mechanisms tend to reduce the influence of the ambiguities mentioned above;
3. the contributions of three body terms have been estimated; they become increasingly important at large values of the momentum transfer ( $\Delta p > 600$  MeV/c).

The two models have also been applied to the  $^{12}\text{C}(d, \pi^+)$  reaction at  $T_p = 185$  MeV. Preliminary results (in DWBA) indicate that the cross section for this reaction is reduced over the  $(p, \pi^+)$  values by one to two orders of magnitude. This reaction, however, seems to be particularly interesting as a further test of the assumptions entering the analysis of the  $(p, \pi)$  data.

In the frame of a similar model for the K-production the  $(p, K)$  reaction has been calculated; preliminary results indicate that cross sections of the order of  $1$  nb/sr can be expected at  $1$  GeV.

1. S. Dahlgren et al, Uppsala Report GWI-PH 1/74
2. E. Aslanides et al (private communication)

$K^+$  and  $\pi^+$  Momentum Spectra at  $0^\circ$  from  
2.5-3.1 GeV/c Protons\*

T. Bowen, D. A. DeLise, and A. E. Pifer

Department of Physics, University of Arizona, Tucson, Arizona 85721

A partially separated 0.9-1.8 GeV/c  $K^+$  beam at the Bevatron was utilized as a spectrometer (0.9% FWHM) to study the  $K^+$  and  $\pi^+$  momentum spectrum at  $0^\circ$  from carbon bombarded by protons. Most data were taken at a proton momentum of 2.5 GeV and a few points were measured at proton momentum of 2.7, 2.9 and 3.1 GeV/c. Plots of  $(d^2\sigma/d\Omega dp)_{0^\circ}$  will be presented.

\*Work supported by the National Science Foundation.

Search for Spectral Peaks from  $(p, K^+)$  and  $(p, \pi^+)$  Reactions\*

T. Bowen, D. A. DeLise, and A. E. Pifer

Department of Physics, University of Arizona, Tucson, Arizona 85721

A partially separated 0.9-1.8 GeV/c  $K^+$  beam at the Bevatron was utilized as a spectrometer (0.9% FWHM) to search near the upper end points of the  $K^+$  and  $\pi^+$  spectra from target bombardment by 2.5 GeV/c proton for spectral peaks which might be attributed to  $(p, K^+)$  and  $(p, \pi^+)$  reactions. No peaks were observed above background. The following cross section upper limits were obtained (1 nb =  $10^{-9}$  b):

Reaction	Incident Proton Momentum	Laboratory Meson Momentum	90% Confidence Upper Limit to $(\frac{d\sigma}{d\Omega})_{lab}$ at $0^\circ$
$^{12}C(p, \pi^+) ^{13}C$	2.50 GeV/c	1.704 GeV/c	20 nb/sr
$d(p, K^+) ^3H_\Lambda$	2.70	1.056	170
$^9Be(p, K^+) ^{10}Be_\Lambda$	2.50	1.418	11
$^{12}C(p, K^+) ^{13}C_\Lambda$	2.50	1.438	2.8
$^{12}C(p, K^+) ^{13}C_\Lambda$	2.70	1.635	600
$^{12}C(p, K^+) ^{13}C_\Lambda$	2.89	1.818	84
$^{56}Fe(p, K^+) ^{57}Fe_\Lambda$	2.50	1.488	9

\*Work supported by the National Science Foundation.

Characteristics of Low Z Fragments Produced in the Interaction of 800-MeV Protons with Uranium.

G. W. Butler, and D. G. Perry, University of California, Los Alamos Scientific Laboratory, Los Alamos, New Mexico 87544,  
 A. M. Poskanzer, Lawrence Berkeley Laboratory, University of California, Berkeley, California 94720,  
 J. B. Natowitz, Cyclotron Institute and Department of Chemistry, Texas A&M University, College Station, Texas,  
 F. Plasil, Oak Ridge National Laboratory, Oak Ridge, Tennessee

The energy spectra of light nuclear fragments produced by the interaction of 800-MeV protons with uranium have been determined at three laboratory angles by means of  $dE/dx-E$  measurements with silicon detector telescopes. Individual isotopes of the elements helium through boron were resolved by utilization of the power law particle identification technique. The evaporation-like energy spectra were integrated to obtain angular distributions and formation cross sections.

The experiment was done in the LAMPF Thin Target Area, which is located upstream of the first pion production target, at an average proton intensity of  $5 \mu A$ . The detectors were 4.6 m from a  $3.5 \text{ mg/cm}^2$  uranium target and they subtended a solid angle of  $10^{-6}$  sr. Two silicon detector telescopes were used to measure the energy spectra at 45, 90, and 135 deg, with one detector telescope always at 90 deg in order to normalize the individual runs.

The cross sections for the formation of the nuclides nearest the line of beta stability were the highest, with the cross sections for both the neutron-deficient and neutron-excess nuclides falling off rapidly. The angular distributions tend to be forward peaked in the laboratory frame of reference. The energy spectra have less prominent high energy portions, and the peak energies are somewhat higher than for the data from earlier experiments at proton energies of  $5.5 \text{ GeV}^1$  and  $1.0 \text{ GeV}^2$ . Also the 800 MeV formation cross sections are significantly lower, illustrating the strong energy dependence of the formation of light fragments in this region of proton bombarding energies.

<sup>1</sup>A. M. Poskanzer, G. W. Butler, and E. K. Hyde, Phys. Rev. C3, 882 (1971).  
<sup>2</sup>E. N. Volnin, A. A. Vorobyov, V. T. Grachov, D. M. Seleverstov, and E. M. Spiridenkov, Publication 101, Leningrad Institute of Nuclear Physics, June 1974.

## ELASTIC AND INELASTIC SCATTERING OF 1 GeV PROTONS BY NUCLEI

E. Boridy and H. Feshbach

Laboratory for Nuclear Science and Department of Physics  
Massachusetts Institute of Technology  
Cambridge, Massachusetts 02139

## ABSTRACT

The elastic and inelastic scattering of 1 GeV protons by nuclei has been calculated using the first order Rayleigh-Lax term in the optical potential which has been generalized so as to include the spin-spin term in the nucleon-nucleon scattering amplitude. The effect of the spin-orbit term, the dependence on the target nucleon density as well as the effect of correlations as given by the second order optical potential have been evaluated. Calculation of inelastic scattering to collective levels employs the Tassie transition potential. Comparison is made with the Saclay experimental results with target nuclei ranging from He to Pb.

## Calculation of the Reaction $pd \leftrightarrow {}^3\text{He} \gamma$ at Intermediate Energies

Harold W. Fearing

Nuclear Research Centre, University of Alberta, Edmonton, Alberta

We have calculated the cross section for the reaction  $pd \leftrightarrow {}^3\text{He} \gamma$  in the intermediate energy range using a distorted wave impulse approximation model analogous to that used previously <sup>1)</sup> with some success for the similar reactions  $pd \rightarrow t\pi^+$  and  $pd \rightarrow {}^3\text{He}\pi^0$ . Such  $(p,\gamma)$  reactions, like  $(p,\pi)$ , involve large momentum transfers and thus also give information on high momentum components of the wave functions. Furthermore distortion effects are easier to calculate than for  $(p,\pi)$ . Hence a comparison of  $(p,\gamma)$  and  $(p,\pi)$  reactions in a similar model may provide a check of the non-pionic aspects of the model and, ultimately, some insight into the proper way of handling the pion distortion.

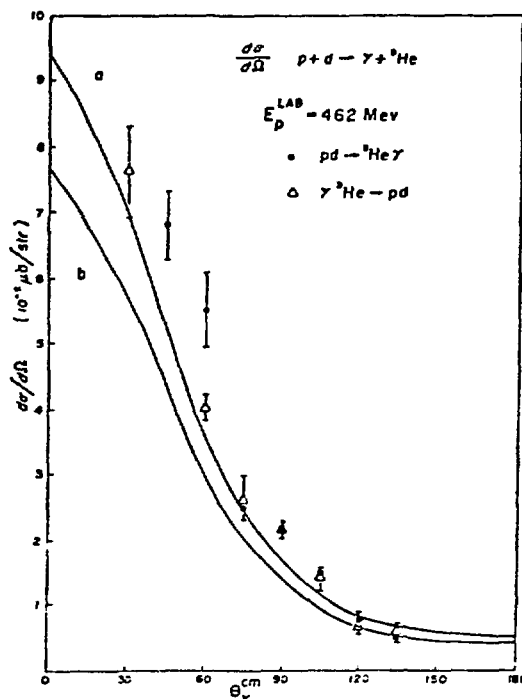
The basic physical assumption of the model is that the process is dominated in the resonance region by the two nucleon subprocess, in this case  $pn \rightarrow d\gamma$ . The cross section is then the product of the cross section for the subprocess, kinematic factors, spin factors, and a form factor. This form factor is essentially a Fourier transform involving the wave functions and distortion factors which account for the interactions of the proton as it traverses the nucleus.

In the present calculation, wave functions and other input used were the same as in the  $(p,\pi)$  calculation of Ref. (1) and in particular the deuteron D state was included. Proton distortion was put in using a Glauber formalism, and is not particularly important. There are thus no freely variable parameters. The main uncertainties are the uncertainty (here, relatively small) in overall normalization due to distortion effects, as discussed in Ref. (1), and an uncertainty of perhaps 30%, particularly at forward and backward angles, due to ambiguities in the input  $pn \rightarrow d\gamma$  data.

The figure shows a comparison of the theory with the data of Heusch, *et al.* <sup>2)</sup> The agreement for both shape and normalization is remarkable and remaining differences are well within the uncertainties of theory and experiment. The theory also seems to reproduce the energy dependence of the  $90^\circ$  cross section in the region  $E_p > 350$  MeV, although the data from various groups is not consistent. It begins to fail, however, below  $E_p = 350$  MeV where mechanisms other than the resonance begin to be important for  $pn \rightarrow d\gamma$ .

- 1) H.W. Fearing, Phys. Letters **52B** (1974) 407 and Phys. Rev. **C11** (1975) In press.
- 2) C.A. Heusch, *et al.* Univ. of Calif. Santa Cruz, Report Nos. 73/004, 73/005, 73/007 (1973)

Figure Caption: Center of mass gamma angular distribution at  $E_p^{\text{LAB}} = 462$  MeV. Curves a and b correspond respectively to the theory without and with distortion effects.





R. D. Viollier<sup>†</sup>Institute of Theoretical Physics, Department of Physics  
Stanford University, Stanford, California 94305

## ABSTRACT

Effects of long-range correlations on high-energy elastic and inelastic proton-nucleus scattering are investigated using the eikonal approximation. We treat multiple scattering of the proton in a coupled channel formalism where virtual excitations and de-excitations of the nucleus are allowed during the scattering process. This is completely equivalent to considering many-body correlations to any order. We also study effects of spin and isospin dependence of the nucleon-nucleon interaction in elastic and inelastic p+ nucleus scattering. We propose to use inelastic scattering to known nuclear states as an analyzer of the different components of the nucleon-nucleon interaction. The strong p+ nucleus interaction is treated in close analogy to electromagnetic and weak interactions where similar nuclear matrix elements occur. We calculate cross sections and polarizations using all information available from nucleon-nucleon and electron-nucleus scattering. Numerical results are compared with experimental data for elastic scattering of 1 GeV protons on  $^{12}\text{C}$  and electric excitations of the  $I^{\pi}T(E/\text{MeV}) = 2^+0(4.43)$ ,  $0^+0'(7.66)$  and  $3^-0(9.64)$  states in  $^{12}\text{C}$ . We predict the differential cross section and polarization for a magnetic transition to the  $1^+1(15.11)$  state in  $^{12}\text{C}$ .

\*Research sponsored in part by the National Science Foundation, grant MPS 073-08916.

<sup>†</sup>On leave of absence from the Department of Physics, University of Basel, Switzerland; Swiss National Science Foundation Fellow.

The Clinton P. Anderson Meson Physics Facility Radioisotope Program by IV.A.26  
H. A. O'Brien, Jr., A. E. Ogard, P. M. Grant, J. W. Barnes, and B. R. Erdal,  
University of California, Los Alamos Scientific Laboratory, Los Alamos,  
New Mexico 87544

The powerful proton beam from the LAMPF accelerator provides a unique opportunity to produce copious amounts of heretofore "rare" nuclides by spallation processes in a variety of simultaneously-irradiated targets. These nuclides are expected to be used extensively in medicine, geosciences, physics, chemistry, metallurgy, and other fields of science and engineering; in addition, they may be regarded as a by-product of the normal operation of the machine since about 50% of the beam emerges from the main experimental area.

The Isotope Production Facility, a separately-funded addition to the main LAMPF beam stop structure, provides a mechanism for remote target insertion, irradiation, and removal from the proton beam at a position immediately upstream from the main beam stop. When completed in the fall of 1975, this facility will contain nine independent target stations, each of which is capable of accommodating a single target or combination of targets up to 2.3-cm thickness.

A new program at LASL, designated the Medical Radioisotope Research Program, was established to investigate medium-energy, proton-induced spallation processes as a means of providing a new source of radioactive isotopes of demonstrated or potential value in the health sciences. The program is divided into five major areas of activity: spallation reaction research; chemistry problems; remote process development; cooperative biomedical research; and target and irradiation facility development.

The major progress to date includes the following: (1) thin-target, proton-induced cross section studies from 211 MeV to 800 MeV using a variety of target materials; (2) development of radiochemical recovery procedures for  $^{43}\text{K}$  from vanadium,  $^{82}\text{Sr}$  and  $^{88}\text{Y}$  from molybdenum, and  $^{123}\text{I}$  and  $^{127}\text{Xe}$  from lanthanum; (3) development of a fast-separation,  $^{82}\text{Sr}/^{82}\text{Rb}$  generator system for medical use; (4) three shipments of LAMPF-produced  $^{92}\text{Sr}$  to extramural collaborating researchers; and (5) a major retrofit of the Isotope Production Facility. Near-term plans for target scheduling and nuclide recovery studies will be presented.

Very intense beams of charged particles pose major technological problems in the isotope production effort, particularly problems associated with beam power density and target cooling, radiation-induced degradation of targets and target-chamber windows, and chemical interactions between radiolysis products in the coolant fluid and the target surface. Recent experiences with targets irradiated with 200-MeV protons to a fluence between 5,000 and 10,000  $\mu\text{A}\cdot\text{hr}$  will be discussed.

Gerald A. Miller  
 Carnegie-Mellon University, Pittsburgh, Pa. 15213

James E. Spencer  
 Los Alamos Scientific Laboratory, Los Alamos, N. M. 87544

ABSTRACT

Using potentials based on multiple scattering theory, a set of coupled optical equations are solved for the differential elastic, inelastic and charge-exchange cross-sections. Total reaction cross-sections and asymmetries are also computed and the sensitivity to various components such as the Coulomb, spin and isospin dependent terms are studied using an interaction of the form:

$$\begin{aligned}
 V_{\lambda}^{\text{eff}}(\mathbf{r}) = & -V_{o,\lambda}f(\mathbf{r}) - V_{so}h(\mathbf{r})\vec{\sigma}\cdot\vec{\mathbf{i}} + \frac{\hbar^2}{2u} \frac{\lambda(\lambda+1)}{r^2} - i(W_o g_o P_{<} + W'_o g'_o P_{>}) \\
 & V_{\text{Coul}}(\mathbf{r})(1/2-\tau) + \left(\frac{V_1}{A}\right)g_1(\mathbf{r})\vec{\mathbf{i}}\cdot\vec{\mathbf{i}} + \left(\frac{V_2}{A}\right)g_2(\mathbf{r})\vec{\sigma}\cdot\vec{\mathbf{i}} + \\
 & \left(\frac{V_3}{A}\right)g_3(\mathbf{r})(\vec{\mathbf{i}}\cdot\vec{\mathbf{i}})(\vec{\sigma}\cdot\vec{\mathbf{i}})
 \end{aligned}$$

where all terms are energy-dependent - particularly as one goes to lower energies. The operators  $P_{>,<}$  project onto  $T_{>}$  and  $T_{<}$  states and are retained explicitly here for contact with lower energies.

The influence of various channel coupling effects on elastic and inelastic scattering over LAMPF energies (200-800 MeV) is considered using different nuclear models. Based on what is known about the nucleon-nucleon interaction at these energies, the validity of the DWIA is assessed. The sensitivity of the results to specific forms and components of the nucleon-nucleon interaction is also considered to explore to what extent it is possible to determine this interaction from such experiments. An explicit demonstration of how and why this should be possible is given in terms of the particle-hole model which demonstrates the importance of simple nuclear states.

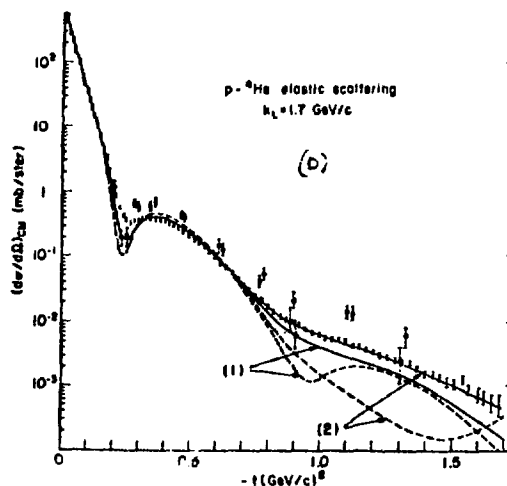
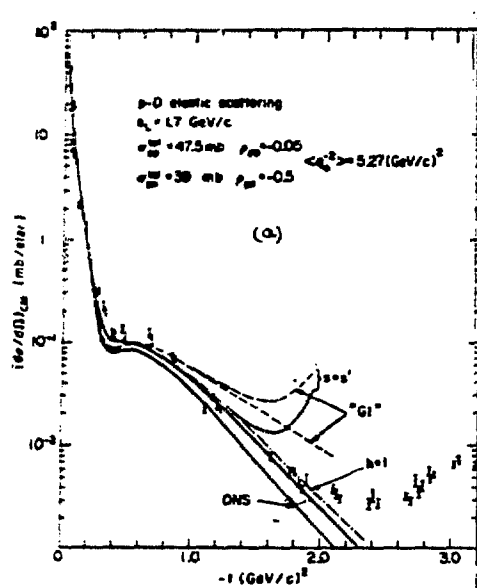
Finally, we discuss the relations of experiments with protons to those with other probes such as electrons and pions.

## Analysis of 1 GeV proton-scattering on D and He in a non-eikonal approach

A.S. Rinat (Reiner), S.A. Gurvitz and Y. Alexander  
Weizmann Institute of Science, Rehovot, Israel

We have recently formulated a theory of multiple hadron scattering on nuclei without invoking standard eikonal approximations<sup>1)</sup>. The total amplitude differs from its eikonal (Glauber limit) in a number of contributions 1) Propagator off-shell amplitudes due to retention of complete projectile propagator 2) Non-eikonal contributions to standard propagator on-shell amplitudes 3) Scattering from multiply struck nucleons (reflections). Off and on-shell propagator contributions are  $\sim \frac{1}{2} \pi$  out of phase and the former thus affect cross sections where Glauber<sup>2)</sup> theory predicts interference minima. Non-eikonal corrections grow for fixed E with t but eventually  $\rightarrow 0$  if  $E \rightarrow \infty$ .

Out of all p and  $\pi$  data on D, <sup>3</sup>He, <sup>4</sup>He analysed<sup>2)</sup> we present the 1 GeV data on D<sup>3)</sup> and <sup>4</sup>He<sup>4)</sup> together with our (—) and Glauber (---) predictions. The comparison shows the influence of 1) off-shell corrections in expected minima when no other perturbation like the D-wave admixture in  $\psi_D$  act 2) non-eikonal corrections for large t. The theory appears to account for the data out to large t values where cluster exchange overtakes scattering contributions.



- 1) S.A. Gurvitz, A.S. Rinat and Y. Alexander, submitted to Annals of Physics
- 2) S.A. Gurvitz, Y. Alexander and A.S. Rinat " " " " "
- 3) G.W. Bennett et al., Phys. Letters 19 (1967) 387.
- 4) S.D. Baker et al., Phys. Rev. Letters 32 (1974) 839.

A. Deloff

Institute for Nuclear Research, Warsaw, Poland

We have considered low energy scattering of a hadron from a complex nuclear system. The accuracy of two basic methods are examined: (i) the fixed centres approximation (FCA) and (ii) the equivalent nuclear potential method. Detailed calculations of the hadron-nucleus scattering length  $A$  have been performed for a simple soluble model yet containing all the dynamical features of a complex system. The model assumes a two body target of two identical particles in a s-wave bound state. The solution of the Faddeev equations has been compared with the results of various approximations. The considered methods are found to be reasonably accurate for small mean separations of the target constituents. For strong, attractive potentials the accuracy becomes worse as the mean separation increases. The scattering length calculated according to the FCA method shows wrong analytic behaviour as a function of the hadron-nucleon potential strength  $s$ , as there is no pole in the s-plane corresponding to the zero energy bound state. Due to the averaging procedure over the nuclear states  $A$  is always finite and passes instead through zero for some  $s$  value. Possible ways to alleviate this difficulty are considered.

ASYMMETRY MEASUREMENT OF QUASI-ELASTIC SCATTERING OF POLARIZED  
635 MEV PROTONS BY  $^{12}\text{C}$  AND  $^6\text{Li}$  NUCLEI

V.S.Nadezhdin, N.I.Petrov, V.I.Satarov

Joint Institute for Nuclear Research, Dubna, USSR

Summary

The asymmetry has been measured with a scintillation counter telescope for three values of the momentum projection of the residual nucleus to the polarized beam direction equal to  $+80;0$  and  $-80$  MeV/c. Scattering angles in c.m.s. of the incident and nuclear protons are  $57^\circ$  and  $40^\circ$  for the  $^{12}\text{C}$  nucleus and  $57^\circ$  and  $40^\circ$  for the  $^6\text{Li}$  nucleus.

Large angle pd scattering, the D form factor  
and the isobar content of the D

S.A. Gurvitz and A.S. Rinat

Weizmann Institute of Science, Rehovot, Israel

It is usually accepted that high-energy backward-angle p-D scattering is governed by baryon exchanges. Specifically the failure of simple n Regge-exchange to account for the observed cross-section has led to the assumption that the D has exotic  $N^*$  components. The observed intensity is then a measure for the  $N^*$  component in the D.<sup>1)</sup>

We have reinvestigated multiple scattering (as opposed to exchange) in pD scattering ( $k_L = 1.2, 1.7, 2.23, 2.78$  and  $3.3$  GeV/c) by means of a theory which does not use the standard eikonal approximations and which is believed to be reliable out to large  $q^2$ .<sup>2)</sup> For these large  $q^2$  one has also to consider NN amplitudes for large  $q^2$  and these are not diffractive as assumed in a standard Glauber analysis. The increase of the  $f_{NN}$  for large  $q^2$  causes the single scattering amplitude to again dominate the large  $q^2$  pD amplitude.

The corresponding cross section depends on the known NN cross section and the D body form factor, beyond the  $q^2$  range where the measured charge form factor provides information.<sup>3)</sup>

We found that a reasonable extrapolation of the D form factor may simultaneously account for all or the major portion of the large  $q^2$  pD intensity of all data. The postulated extrapolation can be tested by forthcoming d-D data from SLAC.<sup>4)</sup> If confirmed, much of the postulated evidence for  $N^*$  content of the D should be questioned.

#### References

- 1) A.K. Kerman and L. Kissinger, Phys. Rev. 180, 1435 (1969).
- 2) S.A. Gurvitz, Y. Alexander and A.S. Rinat, submitted to Annals of Physics.
- 3) A. Elias et al., Phys. Rev. 177, 2082 (1970).
- 4) J. Charpak, Communication to the Laval Conference, August 1974.

## IV.B

### NUCLEAR STRUCTURE AND HYPERNUCLEI



MOMENTUM-CUTOFF SENSITIVITY IN FADDEEV CALCULATIONS OF TRINUCLEON  
PROPERTIES

R. A. Brandenberg  
Institute of Theoretical Physics,  
University of Hannover, Hannover, Germany

and

Y. E. Kim<sup>\*</sup> and A. Tubis<sup>†</sup>  
Department of Physics, Purdue University  
W. Lafayette, Indiana 47907, USA

ABSTRACT

By increasing the cutoff  $q_{\max}$  from  $1.7 \text{ fm}^{-1}$  to  $\approx 2.8 \text{ fm}^{-1}$  in momentum-space Faddeev calculations of the trinucleon bound state of Harper et al. (HKT)<sup>1</sup>, we eliminate several discrepancies existing between the HKT results and the results of coordinate-space Faddeev calculations of Laverne and Gignoux (LG)<sup>2</sup>. Both of these calculations give complete solutions to the Faddeev equations for two-nucleon interactions in the  $^1S_0$  and  $^3S_1 - ^3D_1$  states given by the Reid soft-core potential. The calculated value of the binding energy (6.98 MeV), the minimum of the charge form factor ( $13.9 \text{ fm}^{-2}$ ) and the ratio of the experimental to theoretical charge form factor at the secondary maximum (3.5) are in good agreement with the results (7.0 MeV,  $14 \text{ fm}^{-2}$ , 3) of LG. We give a detailed comparison of results for the probabilities of wave-function components. We also give a comparison of our results with the variational results of Strayer and Sauer.<sup>3</sup> The excellent agreement between the two different Faddeev calculations and the convergence difficulties of the variational method give some support to the Faddeev formalism as the standard technique for calculating three-nucleon observables for realistic nuclear interactions.

REFERENCES

1. E. P. Harper, Y. E. Kim, and A. Tubis, Phys. Rev. Lett. 28, 1533 (1972).
2. A. Laverne and C. Gignoux, Nucl. Phys. A203, 597 (1973).
3. M. R. Strayer and P. U. Sauer, Nucl. Phys. A231, 1, 1974.

<sup>\*</sup>Supported by the U.S. National Science Foundation

<sup>†</sup>Supported by the U.S. Atomic Energy Commission.

## LIFETIME OF NUCLEAR HOLE STATES CAUSED BY PHONON-HOLE COUPLING

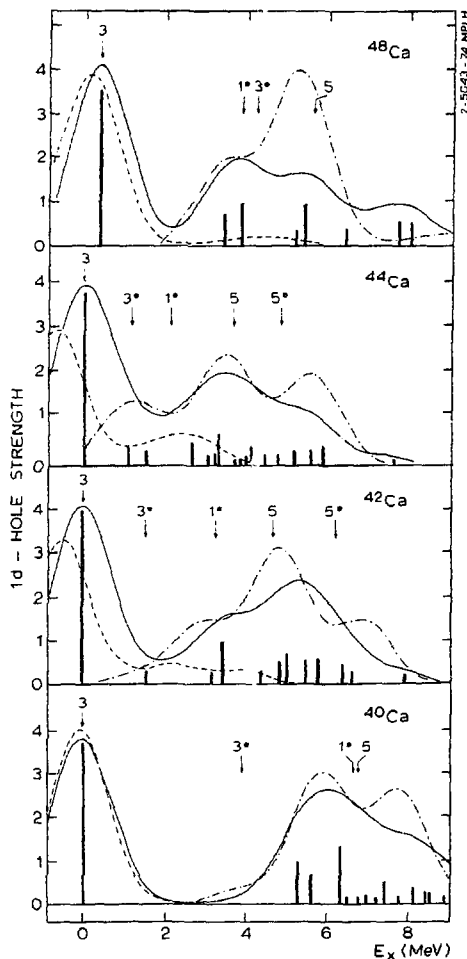
G.J. Wagner, P. Doll, K.T. Knöpfle and G. Mairle  
Max-Planck-Institut für Kernphysik, Heidelberg, Germany

A quantitative understanding of the large widths of deep nuclear hole states as produced in pick-up or knock-out reactions is still missing. We show that  $1d$  hole strength distributions in Ar and Ca isotopes are of a quasiparticle structure whose width results from phonon-hole coupling.

Spectroscopic strengths of  $\ell=2$  pick-up from  $^{36,38,40}\text{Ar}$  (Ref.<sup>1</sup>) and  $^{40,42,44,48}\text{Ca}$  (bars in Fig.1) have been obtained from  $(d,^3\text{He})$  reactions at 52 MeV. Due to the low level density the spreading widths (which vary in a seemingly unsystematic way by a factor of 2 between  $^{36}\text{Ar}$  and  $^{48}\text{Ca}$ ) could be measured independently from the much smaller escape widths. The averaged strength distributions (full line) show a quasiparticle behavior<sup>2</sup>. The

intermediate structure is related to the energies of basis states where a  $2s$ ,  $1d_{3/2}$  or  $1d_{5/2}$  hole (with spin  $j$ ) is coupled to the ground or first  $2^+$  state of the target (arrows, specified by  $2j$  and  $2j^+$ ). Configuration mixing of these basis states through standard phonon-hole interaction<sup>3</sup> yields the average strengths distributions given by dashed lines for  $1d_{3/2}$  and dashed-and-dotted lines for  $1d_{5/2}$  pick-up.

The model reproduces the measured widths within typically 10% without any parameter adjustment. This demonstrates the importance of phonon-hole coupling for the spreading widths of nuclear hole states. For deep hole states one may suspect that other collective states as e.g. giant resonances come into play.



1. P. Doll *et al.* Nucl.Phys. A230, 329 (1974)
2. C.A. Engelbrecht and H.A. Weidenmüller, Nucl.Phys. A184, 385 (1972)
3. S. Wiktor, Phys.Lett. 40B, 181 (1972)

Fig.1 Measured and calculated  $1d$  hole strength distributions in Ca isotopes. For details see text.

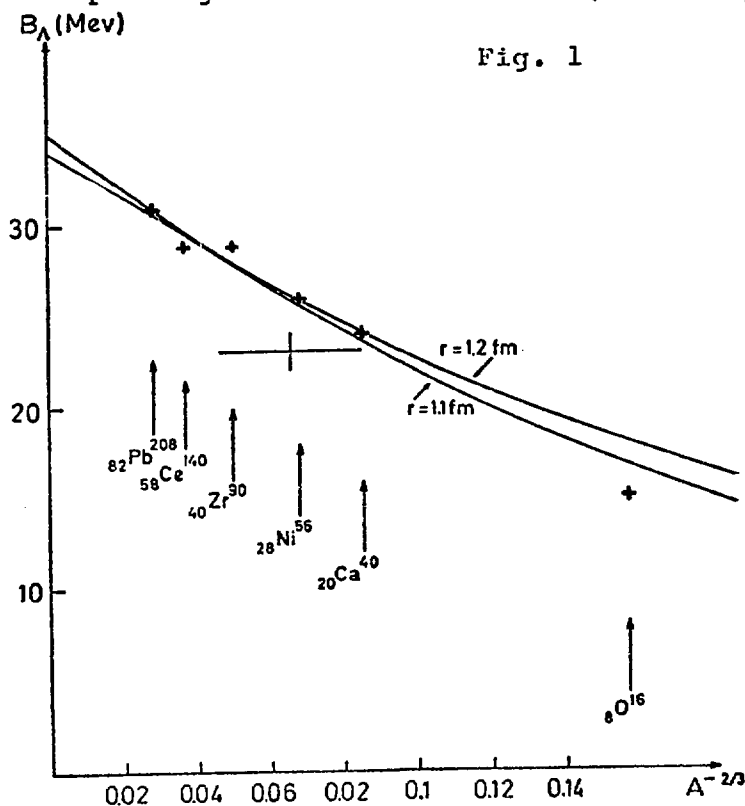
IV.B.3

SELF-CONSISTENT HYPERNUCLEI WITH THE SKYRME INTERACTION

M. Rayet  
Theoretical Nuclear Physics, Université Libre de Bruxelles,  
B 1050 Brussels, Belgium

The good saturation properties of the Skyrme interactions<sup>1)</sup> have made it possible to obtain self-consistently reasonable estimates for the binding energy  $B_\Lambda$  of the  $\Lambda$  hyperon inside various nuclei ranging from  $O^{16}$  to  $Pb^{208}$ . The  $B_\Lambda$  were obtained with a Gaussian  $\Lambda N$  force fitted to the binding energy of  ${}_\Lambda He^5$ . They are plotted on fig. 1 versus  $A^{-2/3}$  and are seen to tend to a saturation value  $D_\Lambda$  of about 35 MeV in infinite nuclear matter (the continuous lines on fig. 1 are fits of the calculated values to the binding energy in a nuclear Saxon-Wood potential with radius  $r A^{1/3}$ ). As can be expected the calculated  $B_\Lambda$  values are larger than the experimental estimate in the range  $A = 40$  to 100 (the large cross on fig. 1 which leads to an extrapolated value  $D_\Lambda$  nearer to 30 MeV), this overbinding being often ascribed to the presence in the  $\Lambda N$  force of a hard core repulsion and of p-wave suppression which were omitted here.

With a reliable self-consistent method for calculating hypernuclear binding, it becomes possible to investigate also the characteristics of the  $\Lambda$  particle motion in particle excited states. The excitation spectra of the  $\Lambda$  particle in different hypernuclei exhibit major shell excitations  $\hbar\omega_\Lambda$  which vary roughly like the corresponding nuclear excitations ( $40 A^{-1/3}$ ), rather than like the



60  $A^{-2/3}$  law suggested by Auerbach and Gal from qualitative arguments<sup>2)</sup>. This observation may have interesting consequences on the possibility of strangeness analogue resonance formation in the hypernuclear production processes which was discussed by Kerman and Lipkin<sup>3)</sup>.

- 1) see e.g.: M. Beiner, H. Flocard, N. van Giai and P. Quentin, Nucl. Phys. A238 (1975) 29
- 2) N. Auerbach and A. Gal, Phys. Lett. 48B (1974) 22
- 3) A.K. Kerman and H.J. Lipkin, Ann. of Phys. 66 (1971) 738

ON THE PRODUCTION OF HYPERNUCLEI IN  
STRANGENESS-EXCHANGE REACTIONS

G.C. Bonazzola, T. Bressani, E. Chiavassa, G. Dellacasa,  
A. Fainberg, M. Gallio, N. Mirfakhrai, A. Musso and G. Rinaudo

Istituto di Fisica Superiore dell'Università, I 10125 Torino, Italy  
Istituto Nazionale di Fisica Nucleare, Sezione di Torino

We have recently finished<sup>1)</sup> an experiment on the production of hypernuclei in the strangeness-exchange reactions:



induced by  $K^-$  of 390 MeV/c with forward emitted  $\pi^-$ . Targets of  $^{12}\text{C}$ ,  $^{16}\text{O}$  and  $^{27}\text{Al}$  were used. The experimental spectra showed a preferential production of excited hypernuclear states with cross sections of some mb/sr. Similar spectra, with better resolution, were later measured by Brückner et al.<sup>2)</sup> at 900 MeV/c. The interpretation of these hypernuclear spectra is complicated by the fact that, up to now, the theoretical predictions are at a rather qualitative stage. Better insight into the nature of these excitations could be obtained with the knowledge of the differential cross sections at different momentum transfers.

Since our spectrometer allowed the simultaneous measurement of  $\pi^-$  emitted from  $0^\circ$  to  $15^\circ$ , we are trying to obtain the relative angular distribution, without integrating over the entire solid angle as done up to now.

We could thus obtain the differential cross sections for momentum transfers from 40 to 80 MeV/c. This set of data, even in a reduced range of  $q$ , could possibly allow us to extract additional information about the nature of the hypernuclear states produced in strangeness-exchange reactions.

1) G.C. Bonazzola et al., Phys. Lett. 53B, 297 (1974); Phys. Rev. Lett. 34, 583 (1975)

2) W. Brückner et al., Phys. Lett. 55B, 107 (1975).

ON A POSSIBILITY TO RESEARCH HYPERNUCLEAR PROPERTIES  
IN THE  $K^+$  - MESON ELECTROPRODUCTION REACTIONS

V.N. Fetisov, and M.I. Kozlov

(P.N.Lebedev Physical Institute of the USSR  
Academy of Sciences, Moscow, USSR)

A study has been made of the process of hypernuclear electroproduction in the reactions  ${}^A_Z(e, e K^+) {}^A_{\Lambda}(Z-1)$  on the p-shell nuclei. It is shown that the hypernuclear levels can be investigated by means of a coincidence recording of the  $K^+$  - meson and the scattered electron in the final state. The capabilities of this method are illustrated by the cross section calculations for the reaction  ${}^7\text{Li}(e, e K^+) {}^7_{\Lambda}\text{He}$  and  ${}^9\text{Be}(e, e K^+) {}^9_{\Lambda}\text{Li}$ . Some level spectra of hypernuclei with the lowest shell configuration  $/s_{\Lambda} s^4 p^n >$  have been calculated on the basis of the shell model with the central  $\Lambda N$  - interactions.

HYPERCHARGE EXCHANGE REACTIONS ON NUCLEI

W.Brückner, M.A.Faessler, K.Kilian, U.Lynen, B.Pietrzyk, B.Povh,  
H.G.Ritter, B.Schürlein, H.Schröder and A.H.Walenta

Max-Planck-Institut für Kernphysik, Heidelberg, Germany  
Physikalisches Institut der Universität Heidelberg, Germany

The reaction  $K^- + A \longrightarrow \Lambda^A + \pi^-$  was studied on targets of  ${}^9\text{Be}$ ,  ${}^{12}\text{C}$  and  ${}^{16}\text{O}$  with  $K^-$  of 900 MeV/c using a separated beam from the CERN PS. The momenta of incoming  $K^-$  and outgoing  $\pi^-$  have been determined with a magnetic double spectrometer. Its angular acceptance was 5 msr and the energy loss of the reaction could be determined to better than 1 MeV. The double focussing property of the spectrometer was essential for the separation of the pions from the hypercharge exchange reaction from those pions originating from the decay of free  $K^-$ . In case of  ${}^{12}\text{C}$ , where an active scintillator target was used, this pion background could be further reduced, by requiring a sufficiently large pulse height in the scintillator target. The resulting spectrum of the hypernucleus  $\Lambda^{12}\text{C}$  is shown in fig. 1.

The level structures of the observed spectra will be discussed.

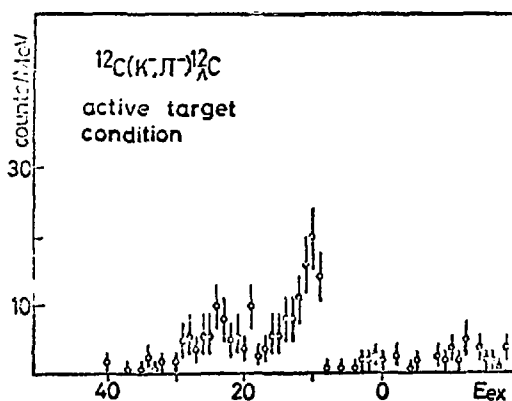


Fig. 1: Energy spectrum of the hypernucleus  $\Lambda^{12}\text{C}$ .  $E_{\text{ex}}$  is the excitation energy relative to the hypernuclear ground-state.

THE INVESTIGATION OF THE  $\gamma^-$ -TRANSITIONS  
IN LIGHT HYPERNUCLEI

M.Bedjidian<sup>x)</sup>, A.Filipkowski<sup>xx)</sup>, I.Y.Grossiord<sup>x)</sup>,  
A.Guichard<sup>x)</sup>, M.Gusakov<sup>x)</sup>, S.Majewski<sup>xx)</sup>, H.Piekarz<sup>xx)</sup>,  
J.Piekarz<sup>xx)</sup> and J.R.Pizzi<sup>x)</sup>

<sup>x)</sup>Institut de Physique Nucléaire, Université Claude Bernard  
de Lyon et Institut National de Physique Nucléaire et de  
Physique des Particules /IN2P3/ - /France/

<sup>xx)</sup>Institute of Experimental Physics, University of Warsaw  
and Institute of Nuclear Research, Warsaw

In the previous experiment [1] the  $\gamma^-$ -transitions at  $/1.09 \pm 0.01/$  MeV ascribed to the mass number 4 hypernuclei were observed in  $\gamma^-$ -spectrum induced by the  $K^-$  mesons stopped in  ${}^6\text{Li}$  and  ${}^7\text{Li}$  targets. Another line at higher energy displayed in a spectrum with  ${}^6\text{Li}$  target has not been uniquely identified as a hypernuclear transition. In the present experiment done at CERN a further investigation of the  $\gamma^-$ -transitions in light hypernuclei was continued. The  $\gamma^-$ -spectra induced by  $K^-$ -mesons stopped in  ${}^6\text{Li}$  target were obtained in coincidence with the accompanying pions. The charged pions above 40 MeV were detected in a range telescope. The pion telescope could also detect high-energy conversion electrons from  $\pi^0$  decays. In the obtained spectrum (Fig.1) two  $\gamma^-$ -lines at about 0.75 MeV and  $/1.08 \pm 0.02/$  MeV could be distinguished. The latter one obtained in coincidence with pions was strongly enhanced as compared to the background and corresponds to the previously observed 1.09 MeV hypernuclear line. The origin of 0.75 MeV line is being investigated. If it is not a background line it may tentatively be ascribed to the  $\gamma^-$ -transition in  ${}^6\text{Li}^X$  or in one of the mass-number 4 hypernuclei.

## References

- [1] A.Bamberger, M.A.Faessler, U.Lynen,  
H.Piekarz, J.Piekarz, J.Pniewski,  
B.Povh, H.G.Ritter and V.Soergel  
Nucl.Phys. **B60** 1973

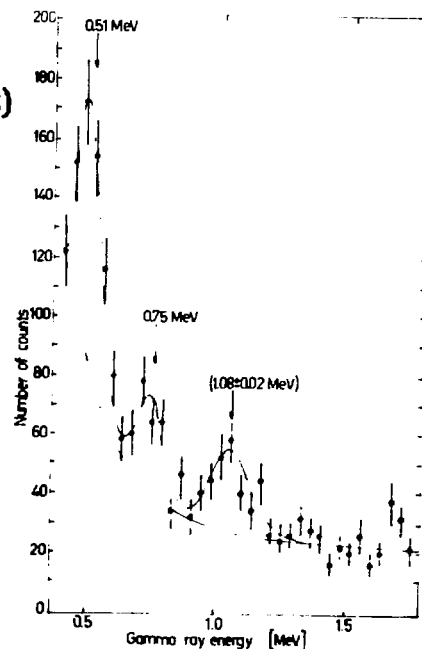


Fig.1 The  $\gamma^-$ -spectrum (in coincidence with pions) obtained for  $70.10 K^-$  stopped in  ${}^6\text{Li}$ -target.

## IV.C

### NUCLEON NUCLEON INTERACTIONS



Neutron-Proton Bremsstrahlung\*, G. E. BOHANNON and L. HELLER, Los Alamos Scientific Laboratory, and R. H. THOMPSON, Northeastern University.

We report results of a potential model calculation of neutron-proton bremsstrahlung including rescattering and exchange currents.

Brown and Franklin<sup>1</sup>, in a calculation which included the exchange current operator to lowest order in the photon momentum, have shown that exchange currents are important. Brown<sup>2</sup> has also shown that rescattering must be included.

Our calculation includes the normal one-body current operator and a two-body operator due to one-pion-exchange. We perform the calculation in momentum space because the exchange current operator is then conveniently included without an expansion in the photon momentum.

We compare our results with the experimental cross sections<sup>3,4</sup> at 130 MeV and 208 MeV.

\*Work performed under the auspices of the Energy Research and Development Administration.

1. V. R. Brown and J. Franklin in Few Particle Problems in the Nuclear Interaction, proceedings of the international conference on few particle problems in the nuclear interaction, Los Angeles, 1972, edited by I. Slaus et al. (North-Holland, 1972); V. R. Brown and J. Franklin in The Two-Body Force in Nuclei, proceedings of the Gull-Lake symposium on the two-body force in nuclei, Gull Lake, Michigan, 1971, edited by S. M. Austin and G. M. Crawley (Plenum, 1972).
2. V. R. Brown, Phys. Lett. 32B, 259 (1970).
3. F. P. Brady and J. C. Young, Phys. Rev. C 2, 1579 (1970).
4. J. A. Edgington et al., Nucl. Phys. A 218, 151 (1974).

## THREE BODY BREAK UP OF THE DEUTERON BY 800 MEV PROTONS\*

T. R. Witten, T. M. Williams, M. Furić, D. B. Mann, J.  
Hudomalj-Gabitzsch, N. D. Gabitzsch, G. S. Mutchler,  
J. M. Clement, R. D. Felder, and G. C. Phillips  
Rice University, Houston, Tx. 77001

B. W. Mayes, E. V. Hungerford, L. Y. Lee,  
M. Warneke, and J. C. Allred  
University of Houston, Houston, Tx. 77004

## ABSTRACT

The break up of the deuteron by 800 MeV protons has been studied in a kinematically complete experiment at the Los Alamos Meson Physics Facility. The angles, time-of-flight, and momentum of one proton were measured by a broad range magnetic spectrometer using multiwire proportional and scintillation counters. The angles and time-of-flight of the other coincident proton were measured. A liquid D<sub>2</sub> target was located in the external proton beam (EPB). Data were taken in two phase-space regions, corresponding to final-state interactions (FSI) and quasi-free scattering (QFS). In the FSI region momentum spectra were obtained for five angle combinations corresponding to small neutron-proton relative energies. The results will be compared to the predictions of simple FSI theory. In the QFS region momentum spectra were acquired for a number of symmetric and asymmetric angle combinations corresponding to a wide range of momentum transfer. The data will be used to determine the range of validity of the impulse approximation.

\*Work supported by the U.S. E.R.D.A.

PION PRODUCTION IN THE  ${}^1\text{H}(p, \pi^+ p)n$  REACTION AT  $E_p = 800 \text{ MEV}$ \*

J. Hudomalj-Gabitzsch, T. Witten, N. D. Gabitzsch, G. S. Mutchler, T. Williams, J. Clement, and G. C. Phillips  
Rice University, Houston, Tx. 77001

E. Hungerford, L. Y. Lee, M. Warneke,  
B. W. Mayes, and J. C. Allred  
University of Houston, Houston, Tx. 77004

## ABSTRACT

The LAMPF 800 MeV external proton beam has been used to study pion production from hydrogen in a kinematically complete experiment. The two charged particles emerging from a liquid hydrogen target were detected in coincidence with multiwire proportional counters, strobed with fast scintillator logic. A magnetic spectrometer was used to determine the momentum of the charged pion at one angle, while the proton time-of-flight was measured at a second angle. Data were collected for several pairs of angles and spectrometer field settings so that the pion-proton relative energies were near the  $\Delta^{++}(3/2, 3/2)$  resonance. A strong enhancement of the cross section has been observed indicating the formation of the  $\Delta^{++}$  resonance where expected. A comparison of the data with simple final state interaction models is in progress.

\*Supported by U.S. E.R.D.A.

STUDY OF THE REACTION  $pp \rightarrow \pi d$  AT 398, 455 AND 572 MEV

D. Aeberscher, B. Favier, G. Greeniaus\*, R. Hess, A. Junod\*\*,  
C. Lechanoine, J.-C. Niklès, D. Rapin and D.W. Werren.  
University of Geneva, Switzerland.

A B S T R A C T

An experiment to measure small angle  $pp$  elastic scattering permitted the reaction  $pp \rightarrow \pi d$  to be observed simultaneously since the deuteron is emitted in a forward cone of  $\sim 10^\circ$  in the lab. A polarized proton beam was used. Incident and outgoing particles were detected in a MWPC system. Events for  $pp \rightarrow \pi d$  were identified either by using TOF and  $dE/dX$  measurements of the deuteron, or, when possible, by observing both the  $\pi$  and  $d$  tracks. The analysis was made difficult by background due to the other inelastic channels which generally have not been sufficiently studied up to now. Results of differential cross section and  $\pi$ -production asymmetry measurements are presented.

The differential cross section is usually described by the expression

$$d\sigma/d\Omega^* = K (A + \cos^2\theta^* + B \cos^4\theta^*)$$

A non-zero B-term implies the presence of high order waves in the  $\pi d$  system. For B at 572 Mev, a good agreement is obtained with the results of C. Serre et al. ( $\pi d \rightarrow pp$ ) and S.S. Wilson et al. ( $np \rightarrow \pi^0 d$ ). At lower energy, the results seem to be incompatible with those of Wilson. The total cross sections, obtained by normalization to the  $pp$  elastic scattering, are in good agreement with previous measurements.

The  $\pi$ -production asymmetry was measured for  $0.7 \leq |\cos\theta^*| < 1$ . At 398 Mev the values are consistent with zero. At 462 Mev, the results agree with the fit given by M.G. Albrow et al. At 572 Mev the points are higher than the fit to Albrow's data at 590 Mev.

\*National Research Council Fellow at CERN,  
now at the University of Geneva.

\*\*Swiss Federal Institute of Technology, Zurich, Switzerland.

Meson Theoretical Description of the Short-Range Repulsion  
in the Nucleon-Nucleon Interaction \*

G. E. Brown and J. Durso  
NORDITA, Copenhagen

and

A. D. Jackson  
State University of New York  
Stony Brook, L.I., New York 11794

Information on the short-range behaviour of the coupling of vector mesons to nucleons can be obtained directly from the electromagnetic form factors<sup>(1)</sup>. Translation of this into the behaviour of the nucleon-nucleon interaction via vector-meson exchange<sup>(2)</sup> indicates much "softer" short-range repulsions than would arising from empirical potentials such as the Reid soft core.

It is shown, however, that the exchange of  $(\rho, \pi)$ -systems with intermediate states involving one or two  $\Delta(1230)$  isobars gives rise to considerable repulsion additional to that from  $w$ -exchange.

---

<sup>1</sup> R. Woloshyn and A. D. Jackson, Nucl.Phys., A185 (1972) 131.

<sup>2</sup> A. D. Jackson, D. O. Riska and B. Verwest, to be published

\* Work supported in part by USAEC Grant No. AT(11-1)-3001.

np Total Cross Section Between 50 and 150 MeV

D.M. Asbury and A.S. Clough, University of Surrey, England  
 J.A. Edgington, R.C. Brown and Y. Onel, Queen Mary College, London, England  
 U. von Wimmersperg, University of Birmingham, England  
 J.M. Blair, AERE, Harwell, England  
 N.M. Stewart, Bedford College, London, England

In 1973 Astbury drew attention<sup>1</sup> to correlations between the structure seen in various hadron-nucleon total cross sections, noting that 'bumps' appear whenever the c.m. momentum  $p^*$  reaches a value at which, in the  $\pi N$  system, nucleon isobar production can occur in the s-channel. Interpretations in terms of a naive quark model were postulated, and precise NN or  $\bar{N}N$  total cross section measurements were proposed as tests. Recently measurements were reported<sup>2</sup> of the  $\bar{p}p$  cross section at low energies, in which structure at  $p^* = 231$  MeV/c (corresponding to a c.m. energy in the  $\pi N$  system of 1236 MeV) was seen.

We have searched for similar structure in the np system; previous measurements<sup>3,4</sup> of the total cross section as a function of neutron energy were inconsistent, particularly near the lab energy (112 MeV) corresponding to  $p^* = 231$  MeV/c. Measurements were of the conventional attenuation type, utilizing targets of varying carbon/hydrogen ratio in the neutron time-of-flight facility of the Harwell synchrocyclotron. Two pairs of targets were used: graphite and paraffin wax, of approximate composition  $C_{20}H_{38}$ ; and decalin ( $C_{10}H_{18}$ ) and p-xylene ( $C_8H_{10}$ ), whose mass densities of carbon are identical. Excellent agreement was obtained between the two sets of results. The data, binned into intervals of a few MeV, have relative errors of less than 1%, with absolute precision of  $\sim 2\%$ . The np cross sections lie between the previous (inconsistent) measurements, and the excitation function is quite smooth with no apparent structure between 50 and 150 MeV.

References

1. A. Astbury, Rutherford Laboratory Report RPP/H/103 (1973)
2. A.S. Carroll *et al.*, Phys. Rev. Letters 32, 247 (1974)
3. P.H. Bowen *et al.*, Nucl. Phys. 22, 640 (1961)
4. D.F. Measday and J.N. Palmieri, Nucl. Phys. 85, 142 (1966)

IV.C.7 \*

Neutron Production at  $0^\circ$  from the Reaction  $pp \rightarrow n p \pi^+$  at Medium Energies. \*

G. Glass, M. E. Evans, Mahavir Jain, R. A. Kenefick, L. C. Northcliffe, TAMU,  
C. G. Cassapakis, UNM; C. W. Bjork and P. J. Riley, UTex.; B. E. Bonner and  
J. E. Simmons, LASL.

Neutron momentum spectra between 450 and 1300 MeV/c have been measured at  $0^\circ$  from the reaction  $p+p \rightarrow n+p+\pi^+$  at the incident energies 645, 764 and 798 MeV. The neutrons were detected by proton production through the charge exchange reaction in a liquid hydrogen radiator. The subsequent proton trajectories through a magnet were measured with multiwire proportional counters. At the highest two energies the momentum spectra show the general features expected from the dominant effects of the (3,3) resonance with a peak corresponding to an invariant mass in the  $p\pi$  system of 1215 MeV/c<sup>2</sup> and a width  $\approx 90$  MeV/c<sup>2</sup>. The 645 MeV data, however, peak approximately 15 MeV/c<sup>2</sup> lower and have a width  $\sim 80$  MeV/c<sup>2</sup> in the  $p\pi^+$  invariant mass primarily because of the reduced overlap between the  $\Delta^{++}$  mass distribution and phase space.

Over the energy region spanned in this experiment the assumptions inherent in the Mandelstam theory<sup>1</sup> are no longer valid. On the other hand the One Pion Exchange (OPE) or peripheral model<sup>2</sup> is not expected to fit the data in detail either because it neglects final state interactions which are expected to be important in this region. In contrast to previously published<sup>3</sup> measurements in this energy region our data have high statistical precision and should provide a stringent test of improved theories. A modified one-pion-exchange calculation<sup>4</sup> with three parameters has reproduced the observed peak positions and widths for the 764 and 798 MeV data.

Deviations occur between the calculation and experiment at the higher two energies which we attribute to an n-p final state interaction. At 645 MeV the fit is worse presumably because of the increased influence of the n-p interaction.

\*Supported in part by the U.S. ERDA.

<sup>1</sup>S. Mandelstam, Proc. Roy. Soc. A244, 491 (1958).

<sup>2</sup>E. Ferrari and E. Selleri, Nuovo Cim. 27, 1450 (1963).

<sup>3</sup>V. E. Barnes and D. V. Bugg, Phys. Rev. Letters 7, 288 (1961).

<sup>4</sup>R. C. Slansky, G. J. Stephenson, R. Gibbs, B. F. Gibson, Bulletin of APS, Ser. II 20, 83 (1975).

IV.C.8

(n,p), (n,d), and (n,t) Reactions on  $^9\text{Be}$  and  $^{12}\text{C}$  at 800 MeV.\*

P. Riley, C. Bjork, C. Newsom, U. Tex.; R. Kenefick, M. Evans, G. Glass, J. Hiebert, M. Jain, L. C. Northcliffe, TAMU; B. Bonner, J. Simmons, N. Stein, LASL; C. Cassapakis, UNM -- Preliminary measurements of charged particles induced by the LAMPF 800 MeV neutron beam have been carried out on targets of  $^{12}\text{C}$  and  $^9\text{Be}$  at  $0^\circ$ ,  $16^\circ$ , and  $24^\circ$ . A single arm magnetic spectrometer with multi-wire proportional counters to define the trajectories of the emitted protons, deuterons and tritons was used.<sup>1</sup> Particle identification was provided by a direct rest mass calculation, based on the measured momentum and time-of-flight of the charged particles. The proton momentum spectra at  $0^\circ$  from the  $^9\text{Be} + n$  and  $^{12}\text{C} + n$  reactions were compared with neutron spectra from previous  $^9\text{Be}+p$  and  $^{12}\text{C}+p$  measurements<sup>2</sup> which exhibited prominent  $^9\text{Be}$  (p,n) and  $^{12}\text{C}(p,n)$  charge-exchange peaks. The  $0^\circ$  high momentum peaks from  $^9\text{Be}+n$  and  $^{12}\text{C}+n$  have a similar structure to that observed in the corresponding 800 MeV (p,n) work. However, while the high momentum neutron yield from  $^9\text{Be}+p$  is greater than that from the  $^{12}\text{C}+p$  by about a factor of 1.7 (at 647 MeV), the high momentum proton yield from  $^9\text{Be}+n$  is slightly less than that from  $^{12}\text{C}+n$ . At  $16^\circ$  and  $24^\circ$  there is no evidence for a direct charge exchange peak, but a broad peak attributable to quasifree (n,np) scattering is observed. The deuteron momentum spectra show no evidence for the direct  $^{12}\text{C}(n,d)^{11}\text{B}$  or  $^9\text{Be}(n,d)^8\text{Li}$  reactions with the present sensitivity. The  $0^\circ$  deuteron spectra for the  $^9\text{Be}$  and  $^{12}\text{C}$  targets are similar to those we have previously observed for a deuterium target, and show both a weak quasielastic (n,nd) peak and a strong peak at the appropriate momentum for the quasifree reactions  $n+p \rightarrow d+\pi^0$  and  $n+n \rightarrow d+\pi^-$ . At  $16^\circ$  these latter quasifree deuteron peaks have disappeared, as is expected from kinematic considerations. All the deuteron momentum spectra show continua presumably due to pion production with 3-body final states. Although the absolute yield of tritons decreases with increasing angle, the triton yield relative to protons and deuterons increases. The triton momentum spectra show no particular structure.

\*Supported in part by the U. S. ERDA.

1. D. Werren, et al., LASL Report LA-5396-MS (1973).

2. C. Cassapakis, et al., Bull. of the Am. Phys. Soc. 20, 83, (1975).



MEASUREMENTS AND ANALYSIS WITH A ONE PION EXCHANGE MODEL  
 OF THE  $np \rightarrow pX$  INCLUSIVE REACTION BETWEEN 1.4 AND 1.9 GeV/c  
 AND DIFFERENTIAL CROSS SECTION MEASUREMENTS OF THE  $np \rightarrow p\Delta_{33}^0$   
 REACTION

*G. Bizard, F. Bonthonneau, J.L. Laville, F. Léfèbvres,  
 J.C. Malherbe, R. Regimbart*  
*Laboratoire de Physique Corpusculaire, Université de CAEN  
 FRANCE*

*J. Duflo, F. Plouin,  
 C.N.R.S., Département Saturne, C.E.N. SACLAY, FRANCE*

A set of 43 momentum spectra of the  $np \rightarrow pX$  inclusive reaction has been measured with a good statistical accuracy at 1.39, 1.56, 1.73 and 1.90 GeV/c (about ten spectra per incident momentum). The neutron beam was obtained by stripping a deuteron beam. The final proton has been analysed in angular range from  $0^\circ$  to  $20^\circ$  (lab.) by a magnetic spectrometer.

The  $np \rightarrow p\Delta_{33}^0$  differential cross sections  $\frac{d\sigma}{dt}$  are determined from these spectra. The whole results are analysed by a  $\pi$  exchange model with Dürr-Pilkuhn and Benecke-Dürr parametrizations.

Absolute Differential Cross Section Measurements for Proton-Proton Elastic Scattering at 647 and 800 MeV. \* H. B. Willard, P. R. Bevington, R. J. Barrett, B. D. Anderson, F. Cverna, H. W. Baer, Case Western Reserve University, Cleveland, Ohio 44106, A. N. Anderson, H. Willmes, University of Idaho, Moscow, Idaho 83543, and N. Jarmie, Los Alamos Scientific Laboratory, Los Alamos, New Mexico 87544.

Absolute differential cross sections for elastic proton-proton scattering have been measured to better than 3% accuracy at 647 and 800 MeV and center-of-mass angles from  $\sim 20^\circ$  to  $90^\circ$ . The external proton beam at LAMPF was scattered from polyethylene targets of several thicknesses from 3.5 to 19.7 mg/cm<sup>2</sup>. The scattered and recoil protons were detected by multi-wire proportional chambers (MWPC) in coincidence, with kinematic criteria of coplanarity and proper opening angle applied to distinguish elastic scattering by protons from the quasi-elastic carbon scattering background. In addition, background shapes were measured separately with carbon foils. The incident beam intensity was measured with a specially constructed 700 Kg Faraday cup capable of absolute measurements of better than 1%. At low beam intensities the beam was also monitored with an ionization chamber calibrated to about 3%. MWPC efficiencies were determined from the final data to better than 1% by requiring 3 out of 4 wire planes plus kinematics to define each event through the fourth plane. Modular electronics, designed and built at Case, encode the input data prior to processing in an MBD micro-processor and storing in a PDP 11/45 computer system which includes on-line graphics. A coincidence trigger tests each event to determine whether prescribed coincidence requirements have been met. This system is capable of handling up to 16 MWPC chambers and four logic gates (e. g. scintillators) with a resolution time as little as 49 nanoseconds for each event. Events which fail to satisfy coincidence requirements may be reset in 200 nanoseconds. All known corrections, including multiple scattering in the target and MWPC's, target thickness variations, electronic dead time, and geometric inefficiencies have been carefully analyzed and included in the quoted error. Our results, which constitute the most accurate differential cross sections measured at these energies to date, will be compared with previous data and current phase shift analyses.

\*Work supported in part by the U. S. Atomic Energy Commission

PROTON-PROTON BREMSSTRAHLUNG IN THE  
INELASTIC REGION\*

IV.C.11

B. M. K. Nefkens, O. R. Sander, D. I. Sober  
UCLA, Los Angeles, Ca. 90024

ABSTRACT

We present results from a new set of measurements of  $pp \rightarrow pp\gamma$  at an incident beam energy of 0.72 GeV. The bremsstrahlung process at so high an energy has never been explored before. The incident proton energy was chosen such that the proton-proton interaction has a large inelastic component, yet is low enough that photon emission involving virtual vector mesons is small. Furthermore,  $\sigma_t(pp)$  varies rapidly with energy in this region. Our results are compared with soft photon approximation calculations based on an extension of the Low theorem<sup>1</sup> to finite photon energies. Such calculations have proven to be successful in describing pion-proton bremsstrahlung<sup>2</sup> in the region of the  $P_{33}(1232)$  resonance. Among other things, we are interested in investigating the possibility that the structureless, monotonically decreasing photon spectrum in  $\pi^\pm p \rightarrow \pi^\pm p\gamma$  is a feature of other hadron-hadron bremsstrahlung processes.

Our results are obtained in a counter-spark chamber experiment in which all particles in the final state are detected. We measure simultaneously 16 photon angles in forward and backward directions for planar and non-planar geometry. One scattered proton is detected in the limited angular interval  $50 \pm 7^\circ$ .

---

\* Work supported in part by U.S. Atomic Energy Commission.

<sup>1</sup>F. Low, Phys. Rev. 110, 971 (1958).

<sup>2</sup>D. I. Sober et al., Phys. Rev. D, March 1, 1975.

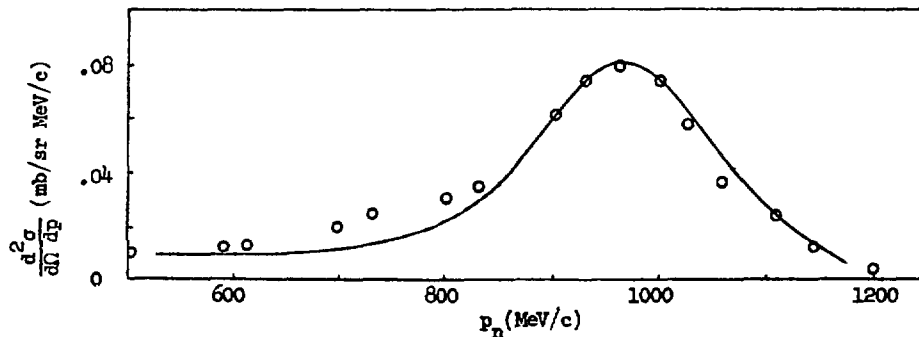
W. R. Gibbs, B. F. Gibson and G. J. Stephenson, Jr.

Theoretical Division, Los Alamos Scientific Laboratory

To analyze reactions in which a pion is produced on a heavy nucleus, it is desirable to have a description of the reaction mechanism which is compatible with our models of nuclear wave functions. To this end, we have made a model of the recently measured<sup>1</sup>  $pp \rightarrow pn\pi^+$  reaction at 764 MeV, in which the neutrons were measured at  $0^\circ$ . The model employs relativistic kinematics but uses non-relativistic representations of the pion production operator and of the pi-nucleon scattering amplitude. We have assumed the Gallilean invariant form for the production operator and taken the off-shell extension of the scattering amplitude discussed by Goplen, Gibbs and Lomon<sup>2</sup> for the  $\pi^+$ -D absorption, including the parameter values determined by them. The strong interaction in the initial state is represented by a Gaussian hole cut from the relative p-p wave function; the size of the hole defines a parameter. The curve in the figure includes the effects of the four graphs obtained by producing a  $\pi^+$  or  $\pi^0$  off either proton and scattering it from the other. In the region of interest, the process is dominated by the production of  $\pi^+$  from the incident proton, and careful treatment of the initial state is carried out only for this case. As may be seen, the one parameter fit appears to be quite good over much of the range of the data, however some caveats are in order. The deviations around 780 MeV/c are believed to arise from strong n-p final state interactions inasmuch as their relative kinetic energy becomes very small in this region. However, this suggests that the triangle diagrams must be included, and they may have a noticeable effect over the entire range. Also, the quality of the fit is very sensitive to the assumptions made about the non-relativistic reduction of the production operator, suggesting the possibility of a conspiracy of effects producing the fit to the inclusive reaction. To resolve some of these questions, it is highly desirable to have kinematically complete studies of these very interesting reactions.

\*Work done under the auspices of the U.S. ERDA.

1. G. Glass, et al., submitted to this conference; B. Bonner, et al., Laval.
2. B. Goplen, W. R. Gibbs and E. L. Lomon, Phys. Rev. Lett. 32, 1012 (1974).



SMALL ANGLE SCATTERING OF HADRONS BY DEUTERIUM AND  
EXTRACTION OF HADRON-NEUTRON AMPLITUDES\*

Girish K. Varma and Victor Franco  
Physics Department, Brooklyn College of the City University  
of New York, Brooklyn, New York 11210

When charged hadrons collide with protons and deuterons, both the Coulomb and the strong interactions contribute to the scattering amplitude. The analysis of these collisions at small angles, where the interference between the two contributions is appreciable, has become one of the important means of obtaining the real parts of the nucleon-nucleon scattering amplitudes. We have studied the problem of Coulomb-nuclear interference in high energy hadron-deuteron collisions in a formalism<sup>1</sup> which is exact within the frame work of the Glauber multiple diffraction theory. Realistic wave functions are used for the deuteron and the effects due to extended charge distributions of the incident hadron and the bound proton are explicitly included. Using the p-p measurements as input, the theoretical results are applied to the p-d elastic and elastic plus quasi-elastic measurements<sup>2</sup> between 1 and 70 GeV, to extract the ratio of real to imaginary part  $\rho_n$  and the slope parameter  $a_n$  of the proton-neutron elastic scattering amplitude. The results, shown in the table, differ significantly from those of earlier analyses. The errors for  $\rho_n$  are  $\sim \pm 0.07$ . We also derive approximate analytic expressions for hadron-deuteron elastic and elastic plus quasi-elastic scattering, which give results very close to those obtained from the more exact expressions. These approximate expressions are much more convenient for the purposes of numerical evaluation and are easily extended to include effects of charge-exchange, which are important at the lower energies, and also of quadrupole deformation of the deuteron, which are important at larger momentum-transfers.

TABLE

P (GeV/c)	1.70	2.78	6.87	8.89	10.9	11.2	15.9	19.3	20.5
$\rho_n$	-0.33	-0.10	-0.45	-0.49	-0.48	-0.29	-0.50	-0.32	-0.48
P (GeV/c)	26.5	34.8	48.9	57.2	60.8	64.8	70.2		
$\rho_n$	-0.45	-0.38	-0.33	-0.36	+0.06	-0.05	-0.25		

\* Work supported in part by the National Science Foundation.

1. V. Franco and G. K. Varma, Phys. Rev. Lett. **33**, 44 (1974).
2. N. Dalkhazhav *et al.*, Sov. J. Nucl. Phys. **8**, 196 (1969); G. G. Beznogikh *et al.*, Nucl. Phys. **B54**, 97 (1973); G. Bellettini *et al.*, Phys. Lett. **19**, 341 (1965).

R. R. Silbar, Theoretical Division, Los Alamos Scientific Laboratory\*

The momentum spectrum of the outgoing deuteron in the reaction  $nd \rightarrow d + \dots$  at  $T_n = 800$  MeV exhibits a large peak at  $p_d = 1.60$  GeV/c with a FWHM of 70 MeV/c.<sup>1</sup> This peak is considerably larger than that of backwards elastic scattering,  $nd \rightarrow dn$ , at 1.82 GeV/c. Its position is just below the maximum value of  $p_d$  associated with pion production and is close to the value of  $p_d$  that would correspond to a free  $NN \rightarrow d\pi$  reaction.

This suggests that the peak at 1.60 GeV/c is due to quasifree  $NN \rightarrow d\pi$ . To check this the following calculation was done. We assume the  $Nd \rightarrow dN\pi$  amplitude is essentially the product of the momentum space deuteron wave function  $\Psi_d$  times the  $NN \rightarrow d\pi$  amplitude. Assuming the latter is slowly varying,

$$d\sigma(Nd \rightarrow dN\pi)/dp_d d\Omega_d = \text{const} \times f(p_d) d\sigma(NN \rightarrow d\pi)/d\Omega, \quad (1)$$

where the rapidly varying  $f(p_d)$  is the phase space integral of  $|\Psi_d|^2$  over the unobserved N and  $\pi$  momenta. For a Hulthén wave function  $f(p_d)$  can be evaluated analytically. The results of this simple calculation are:

- 1) The predicted  $p_d$  spectrum indeed has a narrow peak of the right shape at 1.61 GeV/c, with FWHM = 45 MeV/c.
- 2) The predicted peak height is about twice the observed height.
- 3) The integral on  $p_d$  over the peak gives 88% of the free cross section. Experimentally this integral is about 60%.

We conclude that this quasifree reaction model is reasonably successful in explaining the data, but effects such as Glauber shadowing are perhaps also present.

---

\* Work supported by the U. S. Energy Research and Development Administration.

<sup>1</sup> IASL, UNM, Texas A & M, and U of Texas collaboration.

Abstract Submitted for the

VI INTERNATIONAL CONFERENCE ON HIGH ENERGY PHYSICS AND NUCLEAR STRUCTURE

June 9-14, 1975

IV.C.15

Energy and Angular Distribution of Neutrons Produced by 800 MeV Proton-Proton Collisions. J. PRATT, Temple University, R. BENTLEY, Los Alamos Scientific Laboratory, H. BRYANT, R. CARLINI, C. CASSAPAKIS, B. DIETERLE, C. LEAVITT, T. RUPP, D. WOLFE, University of New Mexico.--The energy spectrum of neutrons for the reaction  $p(T=800 \text{ MeV})+p \rightarrow n+p+\pi^+$  has been measured at  $0^\circ$ ,  $14^\circ$  and  $27^\circ$  laboratory angles. A neutron time-of-flight detector was used for these measurements in conjunction with the "chopped" beam at the Clinton P. Anderson Meson Physics Facility (LAMPF). The fraction of the beam used for TOF had 80 ns between short bursts ( $\sim 1$  ns in width) for the first  $\mu\text{s}$  of the spill. The remainder of the 350  $\mu\text{s}$  spill was not used. The observed width of the  $\Delta^{++}$  was 85 MeV with instrumental resolution of about 20 MeV. Preliminary results show that  $\Delta^{++}$  (1232) production predominates and that it falls off more slowly with increased 4-momentum transfer than at energies above 2 GeV.

An Exact Treatment of  $\sigma$ -Meson Decay Effects in The Exchange Contribution to Nuclear Forces.\* EARLE L. LOMON, Laboratory for Nuclear Science and Department of Physics, M.I.T.--Earlier work<sup>1</sup>

on the  $\sigma$ -meson exchange contribution to nucleon-nucleon forces has been improved by an exact summation of all pion-bubble inserts on  $\sigma$ -meson propagators. The resultant theoretical one-boson plus two-pion potential<sup>1,2</sup> is much less sensitive to uncertainties in the  $\sigma$ -meson decay rate and is very close to realistic nucleon-nucleon potentials. The implications of this approach for a reliable treatment of off-shell nucleon effects in nuclei will be discussed.

\* This work is supported in part through funds provided by ERDA under Contract AT(11-1)-3069.

1. Firooz Partovi and Earle L. Lomon, Phys. Rev. D5 1192 (1972)

2. M. Hussein Partovi and Earle L. Lomon, Phys. Rev. D2 1999 (1970)



POLARIZATION EFFECTS IN Pd BACKWARD SCATTERING

B.Z.Kopeliovich, I.K.Potashnikova

Joint Institute for Nuclear Research, Dubna, USSR

The polarization effects on the pd-backward scattering in the framework of the triangular model (see, Fig. 1) are connected with the polarization in  $pp \rightarrow d\pi^+$ . The comparison of the calculated (using data from /1 /) value of polarization with a measured one at the proton energy  $T_p = 425$  MeV is shown in Fig. 2. The disagreement is remarkable. On the other hand, in the resonant region at  $T \sim 600$  MeV, the contradiction is disappeared, as is seen from Fig. 3. If the triangular mechanism is used for  $pp \rightarrow d\pi^+$  also, then the polarization values in the pd and  $\pi^{\pm}N$  backward scattering should be connected in accordance with Fig. 4. Using the  $\pi^{\pm}p$  polarization data one can find the isotopical bounds  $p^{\max}$  and  $p^{\min}$  for the Pd-polarization. Such bounds for two energies are shown in Figs. 5 and 6. It's seen that polarization at  $\theta \sim 180^\circ$  should change a sign in the region  $T_p = 1.4 \div 1.8$  GeV.

References:

1. C.L.Dolnick, Nucl.Phys. **B22**,461(1970);
2. N.E.Booth et al.Phys.Rev., **D4**,1261(1970);
3. Yu.K.Akimov et al. Nucl.Phys. **8**,637(1958);
4. CERN-Holland Collaboration. M.Borghini et al. (1971) *Phys Lett*, **B35**, 247, 197.

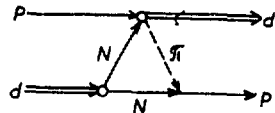


Fig 1

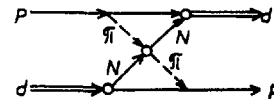


Fig 4

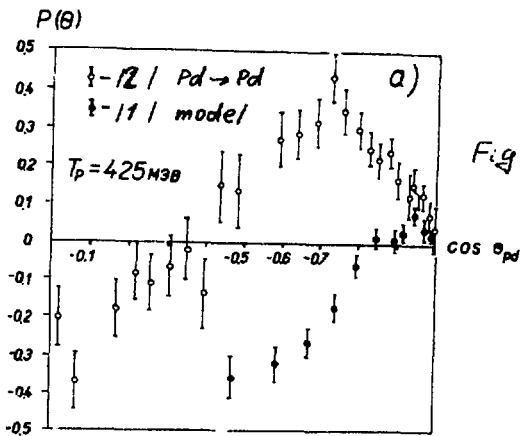


Fig 2

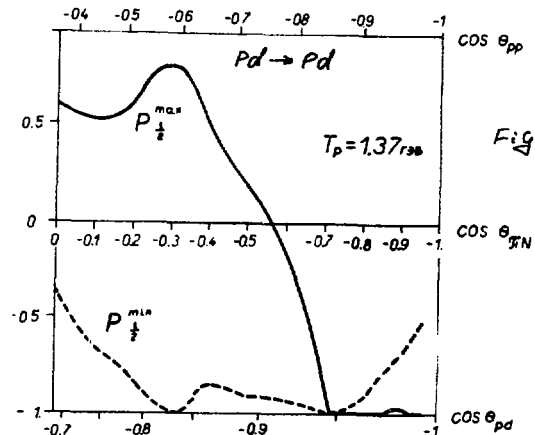


Fig 5

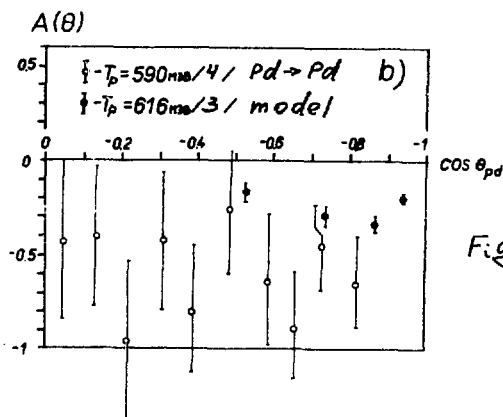


Fig 3

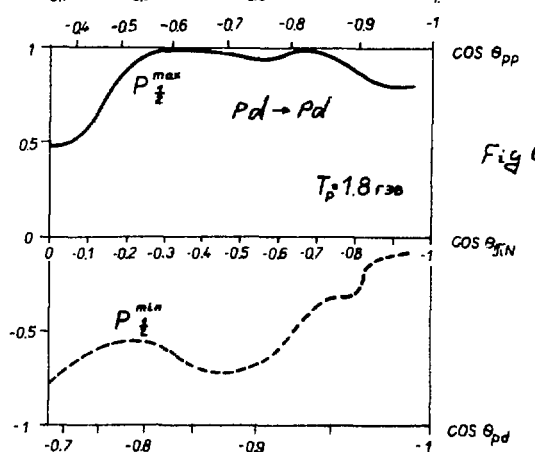


Fig 6

## CHARGE FORM FACTORS OF NUCLEI IN THE ALPHA-CLUSTER MODEL

E.V.Inopin, Phys.-Techn.Inst.Acad.of Sc.Ukr.SSR,Kharkow, USSR.

V.S. Kinchakov, Far East State Univ., Vladivostok, USSR.

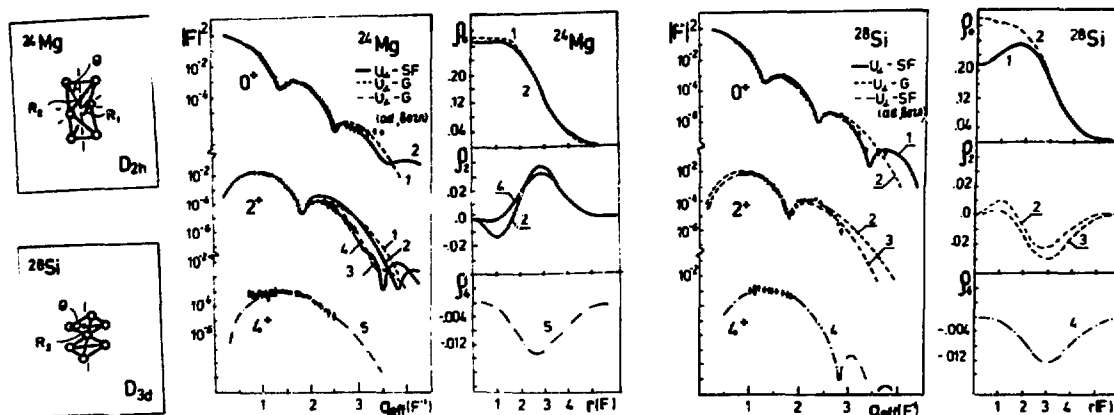
V.K.Lukyanov, Joint Inst. for Nucl.Research, Dubna, USSR.

Yu.S.Pol', The Lebedev Phys.Inst.Acad. of Sc.USSR,Moscow, USSR.

The Brink alpha-cluster model <sup>/1/</sup> has been modified <sup>/2/</sup> by an inclusion of the trial nucleon functions of the realistic exponential behaviour instead of the usually used Gaussian ones. The analysis of the p -and sd-shell 4N-nuclei form factors has been performed. It shows that in the ground state <sup>12</sup>C and <sup>20</sup>Ne are weakly clustered; <sup>16</sup>O is not clustered; <sup>24</sup>Mg approaches the  $\alpha$ -particle nucleus; <sup>28</sup>Si and <sup>32</sup>S have the  $\alpha$ -cluster nature, the  $\alpha$ -clusters in <sup>28</sup>Si being very "spreaded" especially the central one; a suggestion on the  $\alpha$ -clustering nature of <sup>40</sup>Ca does not contradict the description of its form factor. For all the nuclei it turns out that in the excited rotational states the clustering is intensified. As an example the figure gives the <sup>24</sup>Mg and <sup>28</sup>Si form factors (solid curves - the realistic trial sym. Fermi functions; dashed-Gaussian ones).

## References:

1. D.M.Brink, Int.School of Phys. "Enriko Fermi", course XXXVI (1965)
2. E.V.Inopin, V.K.Lukyanov, Yu.S.Pol', Yad.Fiz.(Sov.J.of N.P.) 19, 987 (1974)



One-Boson-Exchange Relativistic Amplitudes  
as Quantum Mechanical Potentials in Lobachevsky Space

IV.C.19

N.B.Skachkov

Joint Institute for Nuclear Research, Dubna

In author's paper (Teor.i Mat.Fiz. 22 (1975) 213; JINR preprint E2-8285 Dubna, 1974) it has been shown that Feynman matrix elements corresponding to the Born approximation to the relativistic NN scattering amplitude (OBEP) can be transformed to the three-dimensional form. In this form they look like a direct geometrical generalization of the Fourier transform of quantum-mechanical potentials obtained by change of the nonrelativistic Euclidean quantities by their analogs in Lobachevsky space. In distinction with the Foldy-Wouthuysen transformation the transition to the three-dimensional form achieved by using the Lobachevsky geometry is obtained not by expansion in  $v/c^2$  powers, but is an identical transformation.

The obtained form of OBEP makes them suitable for using in two-body relativistic equations of a quasipotential type.

## A CASCADE-EXCITON MARRIAGE MODEL

K.K.Gudima, V.D.Toneev

JOINT INSTITUTE FOR NUCLEAR RESEARCH, DUBNA, USSR

A model based on the kinetic approach to the nuclear reactions at intermediate and high energies is developed. The incident particle is supposed to initiate an intranuclear cascade which results in an excited nuclear system. A subsequent evolution of this system is described in terms of the exciton model. The condition for possible treatment of the fast particle as a cascade one is proximity of the local optical potential calculated within the intranuclear cascade model,  $W(r) = \frac{\hbar}{2} v \rho(r)$ , to the experimental one. Otherwise the particle is absorbed. The number of such absorbed ("excited") particles and that of intranuclear collisions (i.e. "holes") define the exciton number or "doorway" state. The Monte Carlo method is used to calculate both the cascade and the pre-equilibrium stage.

The cascade-exciton marriage model has turned out to give

- i) the particle angular anisotropy required at comparatively low energies due to the cascade mechanism in a far nucleus periphery,
- ii) the fast particle yield at large angles at "frontier" energies ( $E \approx 60 \text{ MeV}$ , experiment <sup>1)</sup>) due to the pre-equilibrium component.

One should note that the result of ref. <sup>1)</sup> cannot be explained within either cascade or pre-equilibrium approach only.

Reference:

- 1) F.E Bertrand, R.W Peele. Phys.Rev. C8 (1973) 1045

ON THE ROLE OF NUCLEON-NUCLEON RESONANT FORCES IN THE  
nd-INTERACTION

IV.C.21

V.N.Efimov and E.G.Tkachenko \*)

Joint Institute for Nuclear Research, Dubna, U S S R

Two-particle resonant forces can produce in a three-particle system a highly rarefied state ( a "rare gas" of three particles) provided two-particle "resonance radii" are greater enough than the potential force radii. The resulting long-range interaction in the three particle system does not then depend on details of the pairwise potentials <sup>2</sup> .

In the momentum representation the relevant one-dimensional integral equations for the S-wave nd-interaction must be cut off at large momenta, otherwise the three-nucleon doublet S-state collapsing while the obtained long-range interaction's law persisting at diminishing distances <sup>2</sup> . The cut-off parameter defined through the experimental doublet nd-scattering length, the calculated nd-scattering S-shifts expose excellent agreement with experiment <sup>3</sup> . The NN-interaction has been taken either in the zero- or effective-range approximation, the triton energy resulting in 8.22-8.68 and 9.19-10. MeV intervals, resp ., depending on the cut-off fashion <sup>3</sup> . The cut-off used does not influence quartet phase shifts <sup>4</sup> .

1. V.Efimov. Nucl.Phys. A210, 157, 1973.
2. L.H.Thomas. Phys.Rev. 47, 903, 1935.
3. V.N.Efimov, E.G.Tkachenko. JINR, E4-8414, 1974.
4. V.N.Efimov, E.G.Tkachenko. Yad.Fiz. 18, 62, 1973.

---

\*) V.G.Khlopov Radium Institute, Leningrad, USSR.

ABSTRACT

IV.C.22

Pion Production from Nuclei Bombarded by Protons of 1, 2, and 3 BeV\*. R. D. EDGE and D. H. TOMPKINS, University of South Carolina, and J. W. GLENN, Brookhaven National Laboratory. -- The differential production cross section for positive and negative pions has been found for targets of Be, C, Cu and Pb bombarded by 1-, 2- and 3- BeV protons at one or more of the angles of  $0^{\circ}$ ,  $17^{\circ}$  and  $32^{\circ}$ , using a magnetic spectrometer, and time of flight telescope. Isobar decay adequately explains the production cross section, with the possible exception of  $0^{\circ}$ . The spectral shapes show some agreement with Monte Carlo calculations of Bertini.

\*Work supported in part by the Atomic Energy Commission.

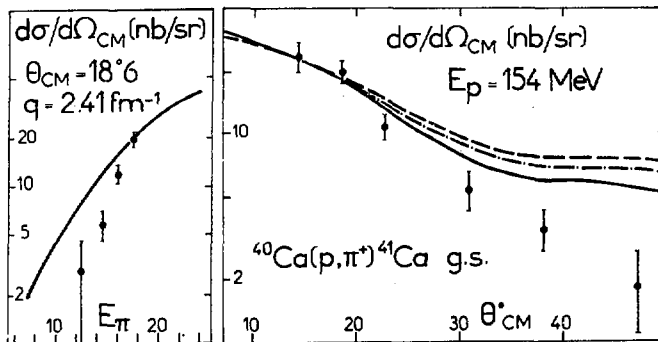
PION PRODUCTION AT THRESHOLD INDUCED BY 154 MeV PROTONS

Y. Le Bornec, B. Tatischeff, L. Bimbot, I. Brissaud, H. D. Holmgren\*,  
J. Källne, F. Reide and N. Willis.

Institut de Physique Nucléaire, B. P. n°1, 91406-Orsay (France)

Differential cross sections corresponding to  $(p, \pi^+)$  reactions at threshold ( $E_p = 154$  MeV) have been measured on several target nuclei using the proton beam of the Orsay Synchrocyclotron. The experimental set-up and measurements on a  $^{10}\text{B}$  target have been reported previously. We present below, results for the reaction  $^{40}\text{Ca}(p, \pi^+)^{41}\text{Ca}$  g. s.

In figure 1. a) the dependence of the differential cross section on the pion energy is shown. The measured variation is stronger than that predicted by phase space alone. In fact it is not possible to distinguish between the phase space factors corresponding to one  $^2$  and two nucleon mechanisms. Both account for no more than 25 % of the observed variation. The curve corresponds to a calculation in the framework of the one nucleon mechanism  $^3$  using Woods-Saxon wave function a) for the captured neutron and optical potentials for the proton and pion distorted waves. The pion optical potential has been calculated for different energies using the multiple scattering approximation and  $\pi$ -N phase shifts of Roper  $^4$ . The curve has been divided by a normalization factor : 53.



In figure 1. b) the experimental angular distribution is compared with various calculations using different pion optical potentials and single-neutron wave functions defined in table 1. In contrast to other calculations, it is found that the normalization factor remains rather stable.

Fig. 1 -  $^{40}\text{Ca}(p, \pi^+)^{41}\text{Ca}$  g. s. results

Table 1 - Parameters used for the curves in fig. 1. b), and corresponding normalization factors.

Curve	Neutron wave func.	Pion opt. pot.	norm.
—	a) $V = -52.5$ MeV $r = 1.25\text{fm}$ $a = .65\text{fm}$	MST	1/56
—	$V = -54.4$ MeV $r = 1.23\text{fm}$ $a = .7\text{fm}$	Miller II	1/50
----	$V = -54.4$ MeV $r = 1.23\text{fm}$ $a = .7\text{fm}$	Miller I	1/35
-----	$V = -53.4$ MeV $r = 1.3\text{fm}$ $a = .7\text{fm}$	Miller I	1/30

1. Y. Le Bornec et al. Phys. Lett. 49B, 434 (1974)
2. B. Hofstad et al. Physica Scripta, 9, 201 (1974)
3. "PIUCK" code of P.D. Kuntz and E. Rost (Univ. of Colorado)
4. L.D. Roper et al. Phys. Rev. 138, B 190 (1965)
5. G.A. Miller, Nucl. Phys. A224, 269 (1974)

\* On leave from the University of Maryland.

FIRST RESULTS OF  $(p, \pi^+)$  REACTIONS AT 600 MeV

IV.C.2

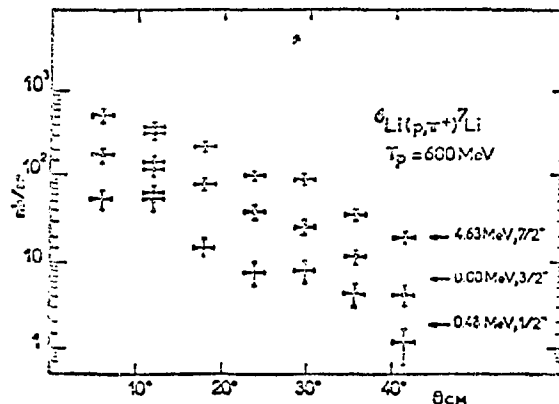
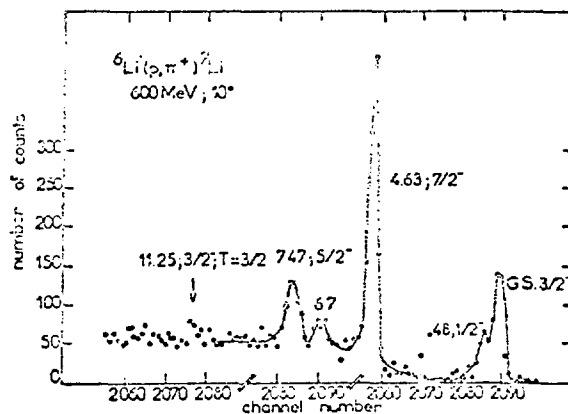
T. Bauer, R. Beurtey, A. Boudard, G. Bruge, A. Chaumeaux,  
P. Couvert, R.R. Duham, D. Garrea, M. Matoba, Y. Terrien

*Département de Physique Nucléaire  
CEA Saclay, BP 2, 91190, Gif-sur-Yvette, France.*

L. Bimbot, Y. Le Bornec, S. Tatischeff,  
*Institut de Physique Nucléaire, BP1, 91406, Orsay, France.*

E. Aslanides, R. Bertini, F. Brochard, P. Corodetzky, F. Hibou,  
*Centre de Recherche Nucléaire et Université Louis Pasteur  
67037, Strasbourg Cedex, France.*

First results of the  $(p, \pi^+)$  reaction have been obtained with 600 MeV protons on  $CD_2$ ,  ${}^6Li$  and  ${}^7Li$  targets. The experiment has been performed with the SPES I spectrometer at Saturne. The pions were identified by three Čerenkov counters located near the focal plane of the spectrometer. Energy spectra were obtained for these three targets with a 450keV energy resolution and angular distributions (from  $\theta_{lab} = 5^\circ$  to  $35^\circ$ ) for three levels of the final nucleus have been extracted for the  ${}^6Li(p, \pi^+){}^7Li$  reaction. A strong excitation of the  $7/2^-$  state of  ${}^7Li$  has been observed. Assuming a one nucleon model for the  $\pi$  production, this strong excitation may be due to a two step process as compared to a direct reaction.





V

ELECTROMAGNETIC AND WEAK INTERACTIONS

V.A

E- AND  $\gamma$ -NUCLEUS INTERACTIONS

A.E.L. DIEPERINK AND T. DE FOREST JR.

Instituut voor Kernfysisch Onderzoek, Amsterdam

Knock-out reactions of the type (e,e'p) provide an important tool for the study of single-particle aspects of nuclear structure. While the results of recent (e,e'p) experiments basically confirm the correctness of the independent particle shell model (IPSM) picture it also appears that certain features can only be explained if correlations are taken into account. Deviations from the IPSM play an important role in Koltun's binding energy sum rule <sup>1)</sup> (expressed in a shell model basis, neglecting center-of-mass effects):

$$E_A = \frac{1}{2} \left( \sum_{\alpha\beta} \rho_{\alpha\beta} T_{\alpha\beta} + \sum_{\alpha} \rho_{\alpha} \epsilon_{\alpha} \right), \quad (1)$$

where  $\rho_{\alpha}$  denotes the s.p. occupation probability and

$\epsilon_{\alpha} = - \langle \psi | a_{\alpha}^{\dagger} (H - E_A) a_{\alpha} | \psi \rangle / \rho_{\alpha}$ , the mean removal energy. A direct experimental test of (1), which holds if the hamiltonian contains no more than two-body interactions, requires the inclusion of the contributions from the normally empty states ( $\alpha > F$ ), which are difficult to identify since they occur with too little strength or above the experimental cut-off.

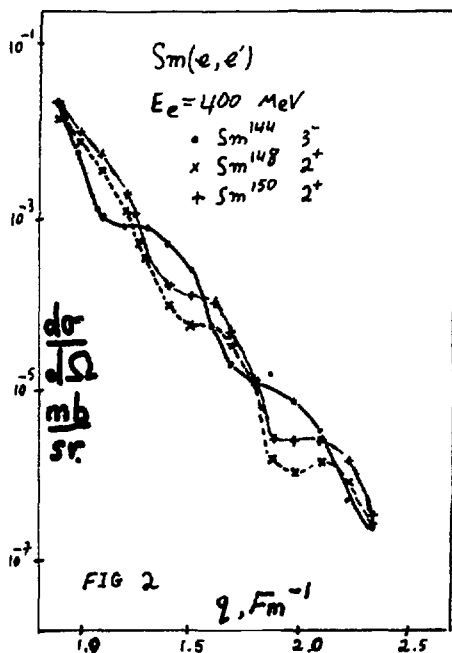
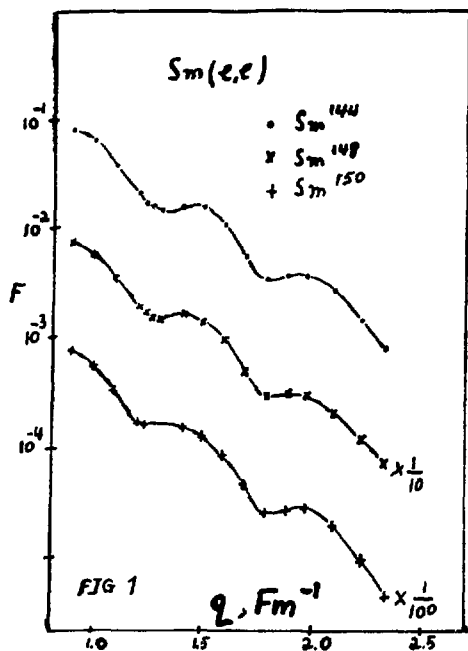
Theoretically the contribution of these states to the r.h.s. of (1) can be estimated by assuming that the strength comes from 2p2h correlations (described by the defect wave function  $\chi$ ), and that the excitation energy of the final 1p2h states can be evaluated with a free particle spectrum. Noting that the first term in (1) cancels with the contribution of the particle energy the sum  $\alpha, \beta > F$  in (1) can be expressed as

$$\frac{1}{2} \sum_{\alpha\beta > F, h_1 h_2 < F} |\langle \alpha\beta | \chi_{h_1 h_2} \rangle|^2 (\epsilon_{h_1} + \epsilon_{h_2}) = \sum_{h < F} (1 - \rho_h) \epsilon_h.$$

By using reasonable values for  $\rho_{\alpha}$  and  $\epsilon_{\alpha}$  one obtains in <sup>12</sup>C a net increase of 2-3 MeV binding energy per nucleon from the normally empty states, which is comparable to the observed discrepancy of 3 MeV. It is interesting to note that after the elimination of the explicit sum  $\alpha > F$  (1) takes on the form

$E_A = \frac{1}{2} \sum_{\alpha < F} (\rho_{\alpha} T_{\alpha} + (2 - \rho_{\alpha}) \epsilon_{\alpha})$ , i.e. the expression for the binding energy in RBHF theory.

1) D. Koltun, Phys. Rev. Lett. 28 (1972) 182



We have started a program to measure electron scattering angular distributions for all the even Samarium isotopes at 200 and 400 MeV, using the Saclay Electron Accelerator facilities. We report here results of the data obtained for  $\text{Sm}^{144,148,150}$  at 400 MeV. Energy spectra for low lying states were measured, with typical resolution of 130 keV, over the angular range of  $25^\circ$  to  $70^\circ$ , corresponding to momentum transfers between 0.9 and  $2.3 \text{ F}^{-1}$ . The measured form factors for the elastic scattering on  $\text{Sm}^{144,148,150}$  are shown in Fig. 1. Good fits were obtained with a three parameter Fermi model using the phase shift analysis program ELAS1). Figure 2 shows the angular distributions for the  $3^-$  state of  $\text{Sm}^{144}$  at 1.81 MeV, the  $2^+$  state of  $\text{Sm}^{148}$  at 0.55 MeV, and the  $2^+$  state of  $\text{Sm}^{150}$  at 0.33 MeV. In addition, we have obtained angular distributions to states in  $\text{Sm}^{144}$  at 1.66, 2.19, 2.32 MeV, corresponding to  $J^\pi = 2^+, 4^+$ , and possibly  $6^+$  states respectively. We observe also the  $(3^-, 4^+)$  doublet at 1.17 MeV in  $\text{Sm}^{148}$ , and the  $(2^+, 3^-)$  doublet at 1.06 MeV in  $\text{Sm}^{150}$ .

1. G.H. Rawitscher and C.R. Fischer, Phys. Rev. 122, 1330 (1961) and Phys. Rev. 135B, 377 (1964).

RESCATTERING EFFECTS IN THE  $\gamma + D \rightarrow p + p + \pi^-$  REACTION

V.A.3

J.M. Laget and I. Blomqvist

*Département de Physique Nucléaire*  
*CEN Saclay, BP.2, 91190, Gif-sur-Yvette, France.*

We have investigated the effects of the pion nucleon rescattering on the yield of the  $\gamma + D \rightarrow p + p + \pi^-$  reaction.

Starting from time ordered Feynman diagrams we have computed the non relativistic limits of the corresponding matrix elements (keeping terms in order  $p/m$ ). We have described the pion photoproduction vertex by the isobaric model and by the Born terms, and the pion-nucleon scattering vertex by the isobaric model.

The interesting feature of this process is that these two particles can be on their mass shell before the scattering. The singularities of these diagrams are near the physical region and the rescattering matrix element is then enhanced.

Its contribution becomes as important as the contribution of the pole diagram (spectator nucleon model) near momentum of the spectator nucleon  $P \approx 150$  MeV/c. Strong deviations from the spectator model are predicted, coming mainly from interference effects.

We have also investigated the proton-proton rescattering effects, but they are smaller than the pion nucleon rescattering ones.

A comparison to the Saclay data [1] will be presented at the conference.

---

[1] P.E. Argan et al. Communication to this conference.

THE  $D(\gamma, p\pi^-)$  AND THE  ${}^4\text{He}(\gamma, p\pi^-)$  REACTIONS  
FOR HIGH VALUES OF THE RECOIL MOMENTUM

V.A.4

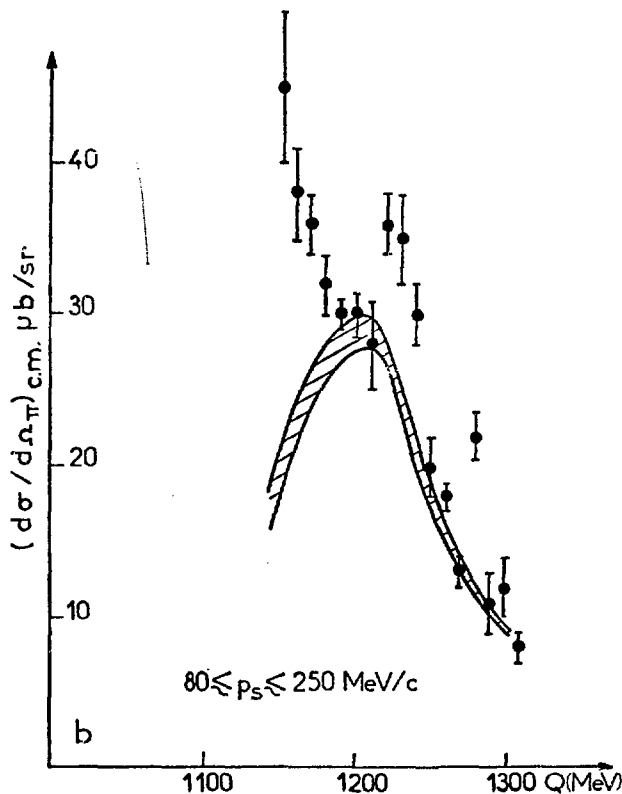
P.E. Argan, G. Audit, N. de Botton, J.L. Faure,  
J.M. Laget, J. Martin, C. Schuhl, G. Tamas

*Département de Physique Nucléaire*  
CEN Saclay, BP 2, 91190 Gif-sur-Yvette, France

In order to understand the behaviour of baryonic resonances in nuclei we have undertaken the study of the  $A(\gamma, p\pi^-)B$  reactions in the  $\Delta(1236)$  resonance region.

We have measured the  $\pi^-$  photoproduction yield on deuterium with a complete determination of the kinematics through detection of a pion and a proton in coincidence. The bremsstrahlung end point was low enough to avoid two pion emission. For low values of the undetected proton momentum ( $10 \leq p \leq 80$  MeV/c), we have deduced, in the framework of the spectator nucleon model, the values of the cross section of the elementary process  $\gamma+n \rightarrow p+\pi^-$  at  $[\theta_\pi]_{\text{c.m.}} = 90^\circ$  (dashed area in the figure), in good agreement with the previously known data [1]. But for high value of this momentum ( $80 \leq p \leq 250$  MeV/c) we have found significant deviations (experimental points in the figure) from the spectator nucleon model.

Deviations were also found in the  ${}^4\text{He}(\gamma, p\pi^-)$  reaction studied with the same methods. These results confirm departure from a model based on the distorted wave impulse approximation, we had reported earlier [2].



[1] See for instance : P. Benz  
et al. Nucl. Phys. B65 (1973)  
158.

[2] P.E. Argan et al. Phys.  
Rev. Lett. 29 (1972) 191.

$^{16}\text{O}$  FORM FACTORS INTERPRETED  
BY THE GENERALIZED HELM MODEL

V.A.5

B.A.Lamers\*, R.D. Graves, and H.Überall<sup>†</sup>  
Catholic University of America, Washington DC 20064

The generalized Helm model has proved a convenient tool for fitting<sup>1</sup> experimental electron scattering form factors by a few-parameter expressions derived from appropriate Gaussian-smeared transition densities that peak at the nuclear radius. Once fitted, the model may be used for predicting transitions to the same levels induced by other medium-energy reactions; and it is not restricted<sup>3</sup> to nuclei near closed shells. For  $^{16}\text{O}$ , we combined low<sup>2</sup> - and high<sup>3</sup> - $q$  data to obtain these fits, some of which are shown in Figs. 1 and 2 for the 14-MeV ( $1^-$ ,  $2^-$  and  $3^-$ ) and 19-MeV ( $1^-$ ,  $1^-$ ,  $2^-$  and  $4^-$ )  $T=1$  level complexes.

It is proposed to utilize this procedure for a tabulation of medium-energy properties of nuclear levels by listing the Helm-model parameters. Note that so far, conventional tables are largely restricted to static properties of nuclear levels.

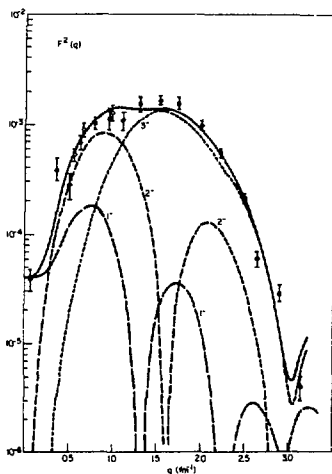
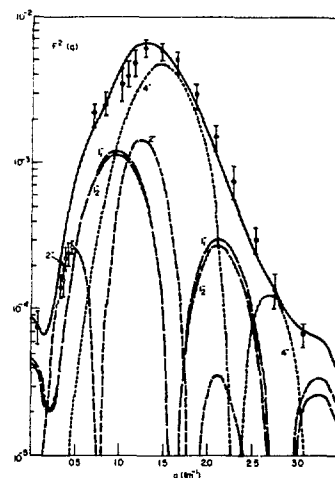


Fig. 1  
Helm-model fit  
to 14 MeV com-  
plex

Fig. 2  
Helm-model fit  
to 19 MeV com-  
plex



\* Now at Hughes Aircraft Co., Culver City Cal. 90250

<sup>†</sup> Also at the Naval Research Laboratory, Washington DC 20375

<sup>1</sup> H.Überall, B.A.Lamers, J.B. Langworthy, and F.J. Kelly, Phys. Rev. C6, 1911 (1972)

<sup>2</sup> M. Strotzel and A. Goldman, Z. Physik 233, 245 (1970)

<sup>3</sup> I. Sick et al, Phys. Rev. Letters 23, 1117 (1969)

Work supported in part by the National Science Foundation.

PION PHOTOPRODUCTION AND RADIATIVE  
PION CAPTURE IN FLIGHT FROM  $^{16}\text{O}$

V.A.6

Anton Nagl and H. Überall\*  
Catholic University of America, Washington, D.C. 20064

In Medium Energy Physics, information on nuclear level form factors gained in one nuclear reaction may be utilized in order to predict the outcome of measurements for other reactions involving the same level. We here use a phenomenological description of the  $T=1$  levels in  $^{16}\text{O}$  by the generalized Helm model,<sup>1</sup> fitted<sup>2</sup> to the measured electron scattering form factors, in order to predict angular distributions for charged pion photoproduction near threshold, and for radiative capture of charged pions in flight on an  $^{16}\text{O}$  target, with excitation of the analog levels. Fig. 1 shows differential cross sections for positive pions produced by 180 MeV photons. EL and ML levels are labeled according to a scheme shown elsewhere.<sup>3</sup> The  $\sigma,\epsilon$  interaction and plane-wave pions have been used.

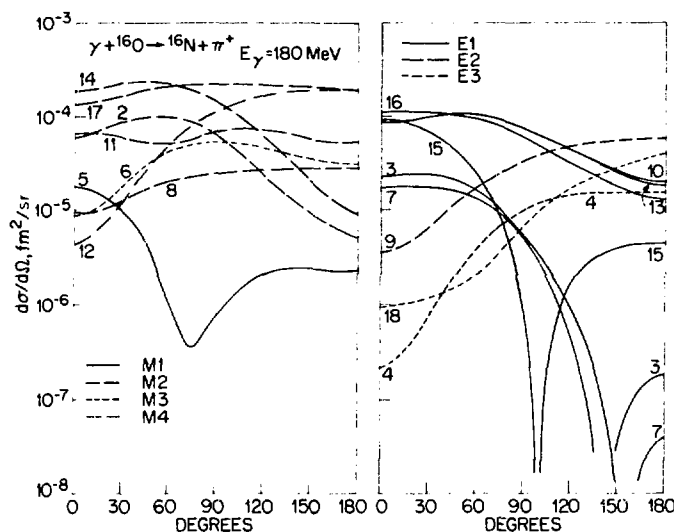


Fig. 1 Angular distributions of  $\pi^+$  produced by 180-MeV photons with excitation of  $T=1$ , ML or EL levels.

Work supported in part by the National Science Foundation.

\*Also at the Naval Research Laboratory, Washington, D.C. 20375

<sup>1</sup>M. Rosen, R. Raphael and H. Überall, Phys. Rev. **163**, 927 (1967).

<sup>2</sup>B. A. Lamers, R. D. Graves, and H. Überall, abstract, these proceedings.

<sup>3</sup>J. B. Langworthy, B. A. Lamers, and H. Überall, abstract, these proceedings.



EXPERIMENTAL STUDY OF SINGLE CHARGED PION PHOTOPRODUCTION  
FROM COMPLEX NUCLEI

K. Baba, I. Endo, M. Fujisaki, S. Kadota, Y. Sumi  
Department of Physics, Hiroshima University, Hiroshima, Japan

H. Fujii, Y. Murata  
Institute for Nuclear Study, University of Tokyo, Tokyo, Japan

S. Noguchi  
Department of Physics, University of Tokyo, Tokyo, Japan

I. Murakami  
Department of Physics, Saga University, Saga, Japan

ABSTRACT

The differential cross section  $d^2\sigma/d\Omega dp$  has been measured by a magnetic spectrometer for the processes  $C(\gamma, \pi^-)$  at a lab angle  $\theta=44.2^\circ$  and  $Cu(\gamma, \pi^\pm)$  at  $28.4^\circ$  by using the 1.3 GeV electron synchrotron at Tokyo. The initial photon energy, which covered intervals from 300 to 850 MeV for carbon and from 400 to 750 MeV for copper, was determined by a subtraction method with a 50 MeV width.

The observed pion-momentum spectra for carbon show singly-peaked distributions, the width of which is approximately proportional to the average incident photon energy  $\langle k \rangle$ . The energy spread of initial photons contributes to this width by about 50 MeV/c almost independently of  $\langle k \rangle$ . Additional broadening of the width is mainly due to the Fermi motion of target nucleon.

Values of peak momentum in these spectra are systematically smaller by about 30 MeV/c than those of pion momentum corresponding to free nucleon kinematics. A similar shift has also been observed in quasielastic scattering of electrons from nuclei and will be explained by nuclear binding effect and pion-nucleus final state interactions.

The differential cross section  $d\sigma/d\Omega$ , which is obtained by integrating the pion spectrum over  $p$ , shows an indication of enhancement due to both of the  $\Delta(1232)$  and  $N(1520)$  resonances. This fact is contrasted to our previous data for carbon at  $28.4^\circ$ , in which the  $N(1520)$  is observed, whereas the  $\Delta(1232)$  is strongly suppressed. This implies the predominance of the effect of Pauli principle inside the target nuclei. In fact, this effect suppresses a transition of nucleon to a state with small momentum transfer and consequently, the smaller  $\theta$  and  $\langle k \rangle$ , the stronger the cross section is suppressed.

The data for copper are very similar to those for carbon apart from their absolute magnitude. The  $A$ -dependence of  $d\sigma/d\Omega$  seems to be proportional to  $A$  rather than to  $A^{2/3}$  in a relatively low  $A$  region.

The coincidence measurement of the process  $C(\gamma, \pi^- p)$  is also performed parasitically. Preliminary results indicate that the separation energy distribution in this process is extended to much higher energy region compared with those observed in  $(e, e'p)$  and  $(p, 2p)$  reactions.

THRESHOLD PION PHOTOPRODUCTION FROM  $^{12}\text{C}$

V.A.8

Anton Nagl and H. Überall\*  
Catholic University of America, Washington, D.C. 20064

Charged pion photoproduction from  $^{12}\text{C}$  near threshold is now under active investigation at MIT.<sup>1</sup> This reaction proceeds to the ground states of  $^{12}\text{B}$  or  $^{12}\text{N}$ , i.e. the  $T=1$  analogs of the 15.1 MeV,  $1^+$  level in  $^{12}\text{C}$ . We described the latter by an improved version of the Helm model fitted to the inelastic  $ee'$  form factor.<sup>3</sup> The full  $\pi\text{N}$  interaction<sup>4</sup> was used in an impulse-approximation calculation, together with pion wave functions distorted by an optical potential<sup>5</sup>, in order to obtain the total cross sections shown in Figs. 1 and 2 (heavy lines). These are compared to earlier results of Koch<sup>6</sup> (light lines) who used the shell model.

This work was supported in part by the National Science Foundation.

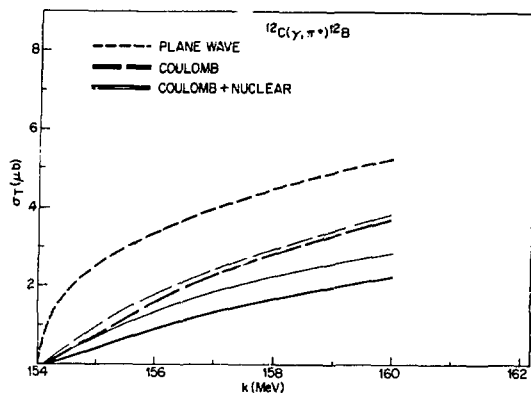


Fig. 1 Threshold  $\pi^+$  photoproduction cross section

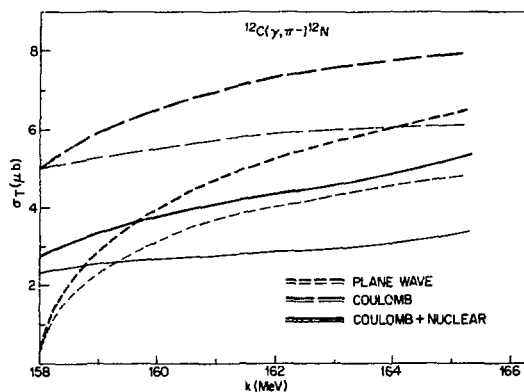


Fig. 2 Threshold  $\pi^-$  photoproduction cross section

\*Also at the Naval Research Laboratory, Washington, D.C. 20375.

<sup>1</sup>A. M. Bernstein et al, Bates Linear Accelerator Newsletter, Vol. III, No. 1, January 1975

<sup>2</sup>J. Deutsch et al., Bull. Am. Phys. Soc. 19, 1006 (1974)

<sup>3</sup>H. Überall et al., Phys. Rev. C6, 1911 (1972)

<sup>4</sup>F. A. Berends et al., Nucl. Phys. B4, 1 (1967)

<sup>5</sup>F. Cannata et al., Canad. J. Phys. 52, 1405 (1974)

<sup>6</sup>J. H. Koch and T. W. Donnelly, Nucl. Phys. B6, 478 (1973)

The  $^{11}\text{B}(\gamma, \pi^-)^{11}\text{C}$  Reaction near Threshold

E. J. Winhold, L. J. McVay, K. Min, P. Pella, D. Rowley, P. Stoler,  
S. Trentalange, and P. F. Yergin  
Rensselaer Polytechnic Institute, Troy, N.Y. 12181

K.S.R. Sastry  
University of Massachusetts, Amherst, Mass.

W. Turchinetz  
Massachusetts Institute of Technology, Cambridge, Mass.

The yield for the  $^{11}\text{B}(\gamma, \pi^-)^{11}\text{C}$  reaction has been measured at a series of energies near its 142.5 MeV threshold by the residual activity technique. Measurements were made in steps of 1 MeV to 150 MeV and in larger steps above this. The reaction was initiated by thin-radiator bremsstrahlung provided by the MIT Bates Electron Linac. Such threshold ( $\gamma, \pi^-$ ) studies are of particular interest in light of recently-reported ( $\gamma, \pi^+$ ) measurements<sup>1</sup> on several light nuclei which disagree significantly with theory.<sup>2</sup>

The cross section deduced from the experimental yield data rises abruptly within a few MeV of threshold to a value of about 12 microbarns at 150 MeV. This behavior is not inconsistent with the calculated Coulomb correction of Tzara,<sup>3</sup> which predicts a step-like threshold behavior. Our results are consistent in general with previous data for this reaction taken only at higher energies. At 160 MeV for example, the cross section is about 25 microbarns, in reasonable agreement with the lowest energy data point of Dyal and Hummel.<sup>4</sup> While the cross sections to each of the several particle-bound states of  $^{11}\text{C}$  cannot be separately deduced from the present data, there is significant strength near threshold to the ground or 2.00 MeV states, or both. The data will be compared with theoretical calculations.

\*  
Supported in part by NSF and ERDA.

<sup>1</sup>J. Deutsch et al., Phys. Rev. Lett. 33, 316 (1974)  
Bull. Am. Phys. Soc. 19, 1006 (1974)

<sup>2</sup>J. Koch and T. W. Donnelly, Nucl. Phys. B64, 478 (1973)

<sup>3</sup>C. Tzara, Nucl. Phys. B18, 246 (1970)

<sup>4</sup>P. Dyal and J. P. Hummel, Phys. Rev. 127, 2217 (1962)

V.A.10  
MEASUREMENT OF ELECTRON-DEUTERON SCATTERING AT LARGE MOMENTUM TRANSFER\*†

R. G. Arnold

The American University, Washington, D. C. 20015

ABSTRACT

We have measured the electron-deuteron elastic scattering cross-section at the Stanford Linear Accelerator Center at 8 values of the momentum transfer  $q^2$  from 1 to 6  $\text{GeV}^2$  (25 to 155  $\text{fermi}^{-2}$ ). The scattered electrons and the recoil deuterons were detected in coincidence using two high-resolution spectrometers. Elastic electron-proton coincidence measurements were also taken for each value of  $q^2$ . The deuteron cross-section is deduced from a ratio of the deuteron form factor above a  $q^2$  of 1.4  $\text{GeV}^2$  (35  $\text{fermi}^{-2}$ ) where elastic electron scattering probes the deuteron wave function near the core. It represents, we believe, the first good look at the two-nucleon system when the neutron and proton largely overlap, and gives new information on the nuclear force at small distances. Preliminary results of our measurements will be presented and compared to the predictions of the deuteron's electric form factor by the impulse approximation, meson exchange current dominance and by the quark dimensional scaling model.

---

\*Work supported by the National Science Foundation and the U.S. Energy Research and Development Administration

†Collaboration: R. G. Arnold, B. T. Chertok, E. B. Dally, A. Gregorian, C. L. Jordan, F. Martin, B. A. Mecking, W. P. Schütz and R. Zdarko

THE NEUTRON CHARGE FORM FACTOR AND  
ELECTRODISINTEGRATION OF TRITON

V.A.11

B. A. Craver<sup>\*†</sup> and Y. E. Kim<sup>†</sup>  
Purdue University, West Lafayette, Indiana 47907

ABSTRACT

We report the results of a preliminary analysis of a proposed experiment of Bertozzi<sup>1</sup> to measure the neutron charge form factor,  $F_{ch}^n(Q^2)$ , by observing the three-body electrodisintegration of  $^3\text{H}$  in which the emitted neutrons have a small relative momentum but carry off all the momentum transfer,  $Q$ , leaving the proton behind at rest (we refer to this configuration as "Bertozzi" geometry.) Neglecting final state interactions between the proton and the emitted neutrons, we estimate, in the impulse approximation, the differential cross section for charge scattering as a function of the momentum transfer for various electron scattering angles. We use the S-state triton wave function of Harper et. al.<sup>2</sup> and the  $^1S_0$  scattering state for the neutron pair, both generated from the Reid soft-core potential.<sup>3</sup> We find that for  $Q \geq 2 \text{ fm}^{-1}$ , scattering due to  $F_{ch}^n(Q^2)$  accounts for more than 75% of the cross section. This is in sharp contrast to the experiments on elastic electron-deuteron scattering, from which present knowledge of  $F_{ch}^n(Q^2)$  is obtained<sup>4</sup>, and indicates that this approach could result in a significantly more accurate determination of  $F_{ch}^n(Q^2)$ . The possibility of using geometries other than "Bertozzi" geometry, and the effects of final state interactions, exchange currents, and magnetic scattering will also be discussed.

REFERENCES

1. W. Bertozzi, private communication.
2. E. P. Harper, Y. E. Kim and A. Tubis, Phys. Rev. Lett. 28, 1533 (1972).
3. R. V. Reid, Jr., Ann. of Phys. (N.Y.) 50, 411 (1968).
4. S. Galster, H. Klein, J. Moritz, K. H. Schmidt, D. Wegener and J. Bleckwenn, Nucl. Phys. B32, 221 (1971).

<sup>†</sup>Supported by the U.S. National Science Foundation.

<sup>\*</sup>Supported by the Atomic Energy Commission.

ELECTROEXCITATION OF  $J^\pi = 6^+$  STATES IN  $^{50}\text{Cr}$  AND  $^{52}\text{Cr}$ 

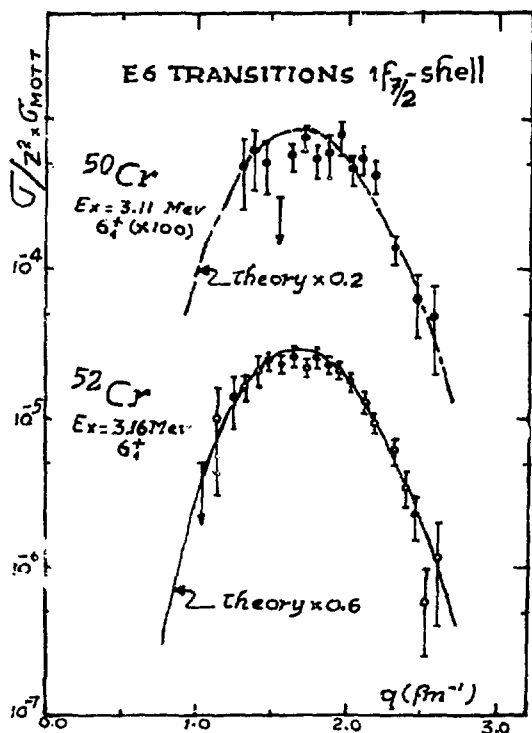
J.B. Bellicard, B. Frois, M. Huet, Ph. Leconte, A. Nakada,  
Phan Xuan Hô, S. Turck, P. de Witt Huberts\*  
- CEN Saclay - B.P. n° 2 - 91190 Gif-sur-Yvette

and

J.W. Lightbody, Jr

National Bureau of Standards Gaithersburg, Maryland U.S.A.

We have observed the  $6_1^+$  - states in  $^{50}\text{Cr}$  and  $^{52}\text{Cr}$  at  $E_x = 3.11$  and 3.16 MeV, respectively, in a study of the excitation spectrum up to 15 MeV with an overall energy-resolution of  $3.5 \cdot 10^{-4}$ , using a 400 MeV electron beam from the A.L.S. In fig. 1 are shown the E6 form-factors obtained after subtraction of the 'near-by  $2_3^+$  -state contribution assuming the  $2_1^+$  form-factor shape. Recent  $\gamma$ -decay studies of high-spin states in  $f_{7/2}$  -shell nuclei, excited in heavy-ion reactions, have given evidence for the relatively pure single-particle nature of these states<sup>1)</sup>. To test this observation D.W.B.A. form-factors were calculated using  $(f_{7/2})^n$ -space wave functions with a harmonic oscillator length-parameter  $b = 1.95$  fm. The curves shown in fig. 1 represent best fits to the data by scaling the calculated form-factors. One notes the decrease of collectivity by factors 0.2 and 0.6 for the E6 transitions in contrast to the collective nature of E2 and E4-transitions in these nuclei.



## REFERENCES

1. G. Fortuna et al., Proceedings Int. Conf. on Nucl. Structure and Spectroscopy, Amsterdam, Vol. 1, p.85, (1974)

\* on leave from Institute for Nuclear Physics Research (IKO), Amsterdam.

Fig. 1 : E6 form-factors in  $^{50}\text{Cr}$  and  $^{52}\text{Cr}$ .

V.A.13

EXTRACTION OF NUCLEAR FORM FACTOR FROM (e,e') CROSS SECTIONS

H.C. Lee and F.C. Khanna

*Atomic Energy of Canada Limited, C.R.N.L., Chalk River, Ont., KOJ 1J0, Canada*

It is shown that the equation for (e,e') in DWBA expressing the differential cross-section,  $\sigma(\theta)$ , in terms of the nuclear transition form factor,  $f_\lambda(q)$ , can be numerically inverted, at least when the transition is dominated by one multipole. Sets of "experimental"  $\{\sigma_{\text{exp}}(\theta_i)\}$  are generated as input from a known form factor and it is demonstrated that the form factor can be accurately recovered in the inversion process. In extracting the form factor from data the parametrization

$$f_\lambda(q) = f_\lambda^{(0)}(q) + \sum_{n=1}^N c_n R_{n\lambda}(qb)$$

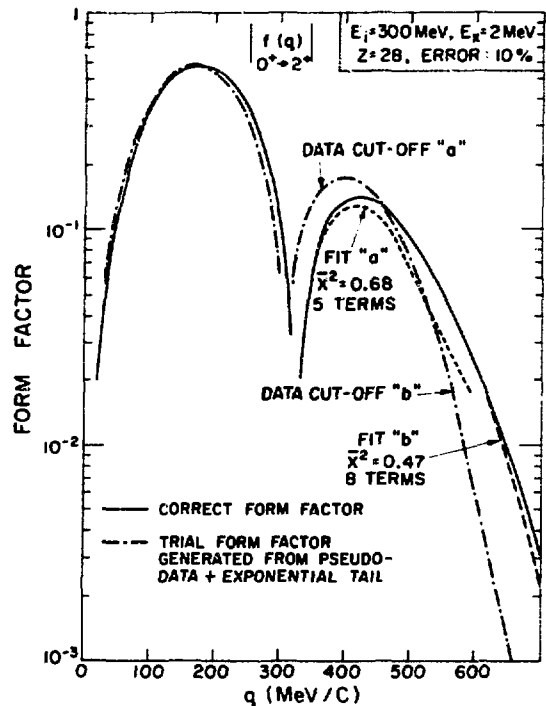
is used, where the trial form factor is given by

$$|f_\lambda^{(0)}(q(\theta))| = (\sigma_{\text{exp}}(\theta)/\sigma_{\text{Mott}}(\theta))^{1/2}$$

and  $R_{n\lambda}$  are taken to be spherical harmonic oscillator functions with the length parameter  $b$  appropriate for the scattering nucleus. The coefficients  $c_n$  are determined by the variational equation

$$\delta\chi^2 = \delta \sum_i (\sigma_{\text{exp}}(\theta_i) - \sigma_{\text{cal}}(\theta_i))^2 / \epsilon_i^2 = 0,$$

where  $\epsilon_i$  is the error. The number of terms  $N$  is roughly dictated by the maximum momentum transfer involved in the data. The figure shows results for two extractions for a  $0^+ \rightarrow 2^+$  transition in a fictitious nucleus with  $Z=28$ . In case "a" the data set corresponds to  $q(\theta)=40 \sim 360$  MeV/c in steps of 10 MeV/c with an error of 10%. In case "b" the data is extended up to  $q(\theta)=580$  MeV/c. In both cases the extracted form factors, within the range of momentum-transfer limited by the respective data set, are essentially indistinguishable from the form factor used to generate the "experimental" cross-sections.



NUCLEAR TRANSITION FORM FACTOR AND TRANSITION DENSITY  
IN INELASTIC ELECTRON SCATTERING

H.C. Lee and F.C. Khanna

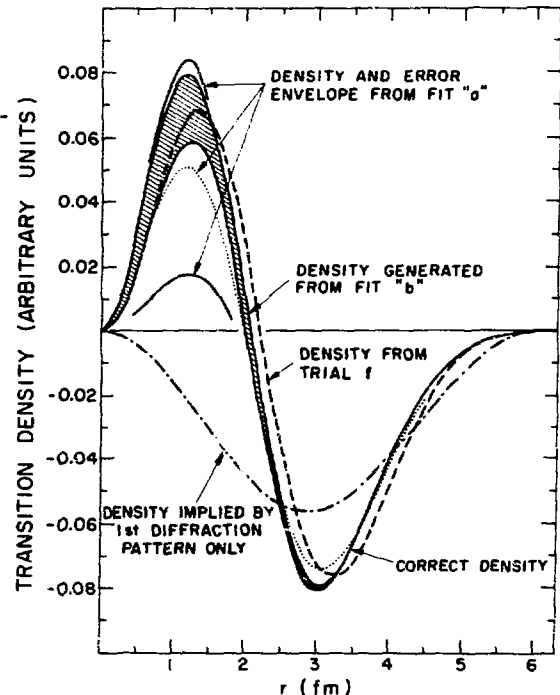
*Atomic Energy of Canada Limited, C.R.N.L., Chalk River, Ont., K0J 1J0, Canada*

Relative merits for analysing (e,e') data in the DWBA in terms of the nuclear transition form factor and the transition density are compared. It is shown that the description in terms of the form factor is overwhelmingly favored. We list a few of the reasons. (a) Four densities, the charge, the longitudinal and transverse current, and the magnetization densities, supplemented by the continuity equation which is in general difficult to implement, are needed in the density description. Only three independent form factors (Coulomb, transverse electric and magnetic) are needed in the other approach; (b) Corrections (such as two-body correlation, exchange current, etc.) to the dominant one-body term are relatively easy to calculate only for the form factor; (c) Within limits a one-to-one mapping can be made from a set of cross-sections to a section of the form factor whereas this mapping is not possible for the density. In an accompanying contribution such a mapping for the form factor is demonstrated. The figure here shows the uncertainty involved when a similar mapping is attempted for the transition density. The density  $\rho_\lambda$  and the uncertainty  $\Delta\rho_\lambda$  are written as

$$\rho_\lambda(r) \propto \int_0^\Lambda f_\lambda(q) j_\lambda(qr) q^2 dq + \int_\Lambda^\infty f_\lambda(q) j_\lambda(qr) q^2 dq$$

$$\equiv \rho_\lambda^{(\Lambda)}(r) + \Delta\rho_\lambda^{(\Lambda)}(r)$$

where  $f_\lambda$  is the form factor extracted from data,  $j_\lambda$  is the spherical Bessel function, and  $\Lambda$  is approximately the maximum momentum transfer involved in the data. In the figure  $\Lambda = 580$  MeV/c for the shaded and solid curve marked "b",  $\Lambda = 470$  MeV/c for the curve(s) marked "a" and  $\Lambda = 320$  MeV/c for the dash-dot curve. For the last case  $\Delta\rho_\lambda$  is not determined as  $f_\lambda(q)$  is assumed zero beyond  $q = 320$  MeV/c.





PION PHOTOPRODUCTION IN  $C^{12}$  JUST ABOVE THRESHOLD

V.A.15

A. M. Bernstein, N. Paras, W. Turchinets  
Massachusetts Institute of Technology, Cambridge, Massachusetts

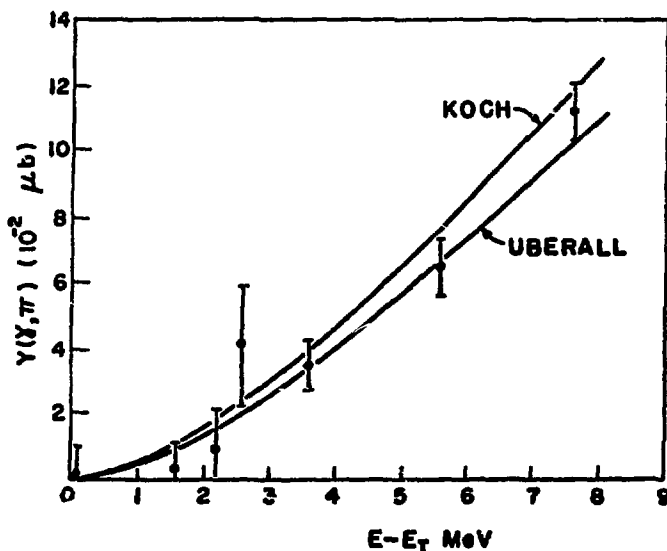
E. C. Booth, B. Chasan  
Boston University, Boston, Massachusetts \*

ABSTRACT

A bremsstrahlung beam from the Bates Linear Accelerator has been used to observe the  $C^{12}(\gamma, \pi^-)N^{12}$  reaction. The total cross section up to an energy of 12 MeV above threshold was measured by observing the energetic  $\beta^+$  rays from the decay of 11 millisecond  $N^{12}$  by counting between accelerator beam bursts. The results for the absolute yield curve are shown in the figure (plotted as a function of the energy above the pion threshold). It is in good agreement with theoretical predictions<sup>1,2</sup>. Experiments on the  $(\gamma, \pi)$  reaction near threshold indicate the need for further investigation, since the  $Li^6(\gamma, \pi^+)He^6$  experimental data<sup>3</sup> is 60% smaller than theoretical predictions<sup>1</sup> and the  $B^{11}(\gamma, \pi^-)C^{11}$  experiment<sup>4</sup> is about two times the theoretical prediction<sup>1</sup>.

\* Funded in part by ERDA contract AT(11-1)-3069, and by NSF

FIGURE



REFERENCES

1. J. Koch and W. Donnelly, Nucl. Phys. B64,478 (1973), and J. Koch, private communication.
2. H. Uberall, Private communication.
3. J. Deutsch et al, Phys. Rev. Let. 33,316 (1974).
4. J. Winhold et al, private communication.

## Renormalization of the pion photoproduction hamiltonian in nuclei

---

J. DELORME: IPN, Université de Lyon, 43 bd du 11 novembre 1918  
69621- Villeurbanne France

M. ERICSON: IPN, Université de Lyon, 43 Bd du 11 novembre 1918  
69621- Villeurbanne France

G. FALDT : Institute of theoretical physics - Lund - Suède.

---

We investigate the nuclear renormalization of the effective hamiltonian for pion photoproduction at threshold. As in the scattering case, one source of renormalization is the nuclear polarisability: the production of the pion on a nucleon first excites the nucleus which is brought back to the ground state in a second step when the pion is scattered by another nucleon. This effect is described by the effective field approach. We find that the short range and long range parts of the photoproduction interaction undergo very different renormalizations.

We show that meson exchange phenomena are responsible for a second type of renormalization. Using both kinds of many body effects i. e. nuclear polarizability and meson exchange contributions, we are able to display the link between the soft pion approach and the microscopic description of threshold pion photoproduction.

ANGULAR MOMENTUM TRANSFER IN THE  $\text{Au}^{197}(\gamma, \pi^-)\text{Hg}^{197}$  REACTION\*

Heinrich A. Medicus and Robert Smalley<sup>+</sup>  
Rensselaer Polytechnic Institute, Troy, N.N. 12181

The isomer ratio in  $\text{Hg}^{197}$  from the  $\text{Au}^{197}(\gamma, \pi^-)\text{Hg}^{197}$  reaction induced by 157-MeV bremsstrahlung from the Bates Linear Accelerator has been measured. This ratio (after corrections for contributions from secondary reactions) is  $\frac{\text{isomeric state}}{\text{ground state}} = 2.1 \pm 0.6$ . The spin of the ground state of  $\text{Au}^{197}$  is  $3/2$ , that of the ground state of  $\text{Hg}^{197}$  is  $1/2$ , and that of the isomeric state  $13/2$ . Below the isomeric state are two states with spin  $3/2$  and  $5/2$ , respectively. Thus, the observed preference for the state with high angular momentum must imply a photon absorption of relatively high multipole order for this reaction, likely of  $2^5$ -pole character. Photons of 150 MeV can easily provide an angular momentum of 5 units of  $\hbar$  to a nucleus with a radius of 8 fm, because  $kr = 6$ . At this photon energy mostly s-wave pions are emitted.

An explanation for the surprisingly high isomer ratio may be the following: The ground state of the target nucleus and the four lowest states of the product nucleus have the occupation numbers in the relevant subshells as given in the table.

State	Protons				Neutrons			
		$1h_{11/2}$	$2d_{3/2}$	$3s_{1/2}$	$1i_{13/2}$	$3p_{3/2}$	$2f_{5/2}$	$3p_{1/2}$
$\text{Au}^{197}$ ground st.	$3/2+$	12	3	0	14	4	0	0
$\text{Hg}^{197}$ ground st.	$1/2-$	12	4	0	<u>12</u>	4	0	<u>1</u>
1st exc. st.	$5/2-$	12	<u>4</u>	0	<u>12</u>	4	<u>1</u>	0
2nd exc. st.	$3/2-$	12	<u>4</u>	0	<u>14</u>	3	0	0
isomer. st.	$13/2+$	12	<u>4</u>	0	<u>13</u>	<u>4</u>	0	0

Occupation numbers that differ from those of the  $\text{Au}^{197}$  ground state are underlined.

It is thus seen that the isomeric state and the second excited state can be obtained simply by removing one neutron from a subshell and adding it as a proton to the  $2d_{3/2}$  proton subshell. The ground state and the first excited state, however, need changes in two neutron shells and therefore should be less favored.

That the second excited state (which immediately feeds the ground state) is less populated than the isomeric state may be caused by the fact that there are more  $1i_{13/2}$  neutrons available than  $3p_{3/2}$  neutrons. It also may be that the high angular momentum neutrons are closer to the nuclear surface so that the pions emitted from there are less likely being absorbed by the nucleus. A certain enhancement of the  $1i_{13/2} - 2d_{3/2}$  transition could also be due to the position of the  $1h_{11/2}$  proton subshell just below the Fermi level which may give rise to two-particle=two-hole configurations.

In addition to reaching these low lying states in Hg directly, they may also be populated by  $\gamma$  cascades from higher excited states which in our case would have to have predominantly fairly high spins.

\* Work supported by the U.S. A.E.C. and the N.S.F.

<sup>+</sup> N.S.F. Undergraduate Research Participant

${}^3\text{He}(\gamma, 2p)n^\dagger$ 

B. F. GIBSON

V.A.18

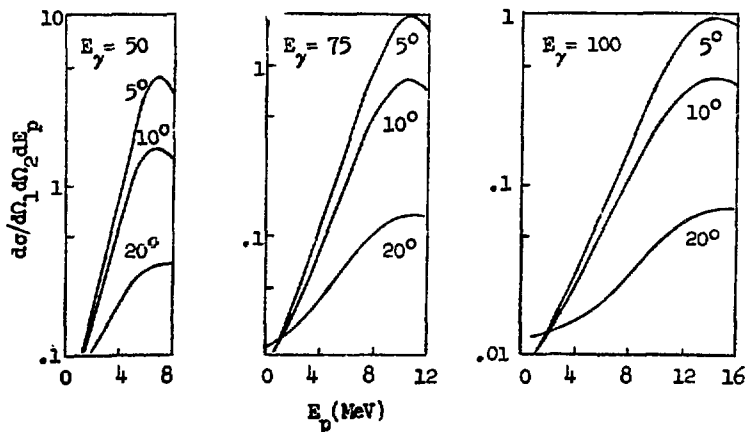
Theoretical Division, Los Alamos Scientific Laboratory  
and

D. R. LEHMAN

The George Washington University

The cross section for the photodisintegration of  ${}^3\text{He}$  leading to the 3-body final state in which both protons are detected has been calculated in the electric dipole approximation. The calculation was performed within the context of exact three-body theory. The N-N interactions were represented by s-wave, spin-dependent separable potentials. The full photodisintegration amplitudes were expressed as sums of: the plane wave Born amplitude, terms involving only a single rescattering between pairs of nucleons, and terms combining the off-shell N-d and N-p scattering amplitudes. These off-shell amplitudes were obtained by solving the corresponding integral equations using standard contour-rotation techniques.

We present here numerical results for the coplanar geometry in which the two protons are detected at angles of  $\theta_p$  where the angle is measured with respect to the perpendicular to the incident photon momentum. Calculations are shown for incident photon energies of 50, 75, and 100 MeV and for angles of  $5^\circ$ ,  $10^\circ$ , and  $20^\circ$ . The curves presented are the result of a complete calculation in which both the initial bound state and the final scattering state were generated numerically from N-N potentials fitted to the low energy singlet and triplet scattering parameters. (The triplet potential strength was reduced about 50% in the bound state calculation in order to reproduce the correct  ${}^3\text{He}$  binding energy.) The sensitivity of such a coincidence experiment to the details of the bound state can be estimated by comparing these results with those of calculations (not shown) for a model in which the bound state wave function is represented by an analytic form similar to the exact solution but where the two parameters are fitted to the binding energy and rms radius. Differences of 50 - 100% can be seen for the coincidence calculations at these energies with  $\theta_p = 5^\circ$ ; this is to be contrasted with the differences that can be seen in a similar comparison of total cross section calculations which are at most 20% in the photon energy range between 10 and 15 MeV.



<sup>†</sup>Work supported in part by the U. S. ERDA.

HOLE STRENGTH AND MOMENTUM DISTRIBUTIONS FROM  $(e, e'p)$  REACTIONS V.A. 19

M. Bernheim, A. Bussière, A. Gillebert, J. Mougey,  
M. Priou, D. Royer, I. Sick, and G. J. Wagner  
CEN Saclay, BP 2, Gif-sur-Yvette, 91190, France

ABSTRACT

Hole strengths and momentum distributions have been measured on  $^{12}\text{C}$ ,  $^{28}\text{Si}$ ,  $^{40}\text{Ca}$  and  $^{58}\text{Ni}$  using the  $(e, e'p)$  reaction at 500 MeV. The range covered is  $0 \leq E_M \leq 80$  MeV in removal energy and  $0 \leq p \leq 250$  MeV/c in recoil momentum, with an energy resolution of 1.2 MeV.

After small radiative corrections, a shell model analysis of the data has been performed, using Woods-Saxon wave functions and a partial wave expansion of the distorted outgoing proton waves. The distorted momentum distributions show an excellent agreement with the experiment. The table contains the resulting number of protons  $N$  and mean removal energy for each of the shell model states. The numbers between parenthesis are only tentative.

The complete kinematic coverage of the reaction allowed us a sum rule test<sup>1,2</sup> of the shell model picture of nuclei. As for  $^{12}\text{C}$ ,<sup>2</sup> a significant discrepancy is observed for  $^{28}\text{Si}$  and  $^{58}\text{Ni}$  which indicates that the above limits on  $E_M$  and  $p$  are not sufficient to observe all the binding energies and momentum densities of protons in those nuclei.

1. D. S. Koltun, Phys. Rev. Lett. 28, 182 (1972).
2. M. Bernheim et al., Phys. Rev. Lett. 32, 898 (1974).

Fig. 1 Sample of momentum distributions:  
2s shell in  $^{40}\text{Ca}$

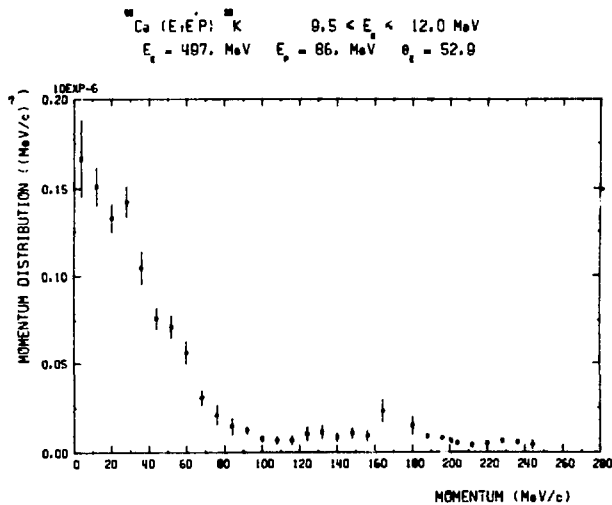


Table I Numbers of  
protons and mean  
energies (MeV) from  
DWIA analysis

	nl	N	$\langle E_{nl} \rangle$
$^{12}\text{C}$	1p	2.5	$17.5 \pm 0.4$
	1s	1.0	$38.1 \pm 1.0$
$^{28}\text{Si}$	2s	0.4	$13.8 \pm 0.5$
	1d	5.5	$16.1 \pm 0.8$
	1p	2.9	32.0
	1s	0.9	(51.)
$^{40}\text{Ca}$	2s	1.3	$11.2 \pm 0.3$
	1d	7.7	$14.9 \pm 0.8$
	1p	5.7	41.5
	1s	1.5	(56.)
$^{58}\text{Ni}$	1f	7.6	$9.3 \pm 0.3$
	2s	1.9	$14.7 \pm 0.5$
	1d	8.9	21.
	1p	6.8	45.5
	1s	1.0	(62.)

## HELIUM CHARGE FORM FACTORS AT LARGE MOMENTUM TRANSFER

Benson T. Chertok\*

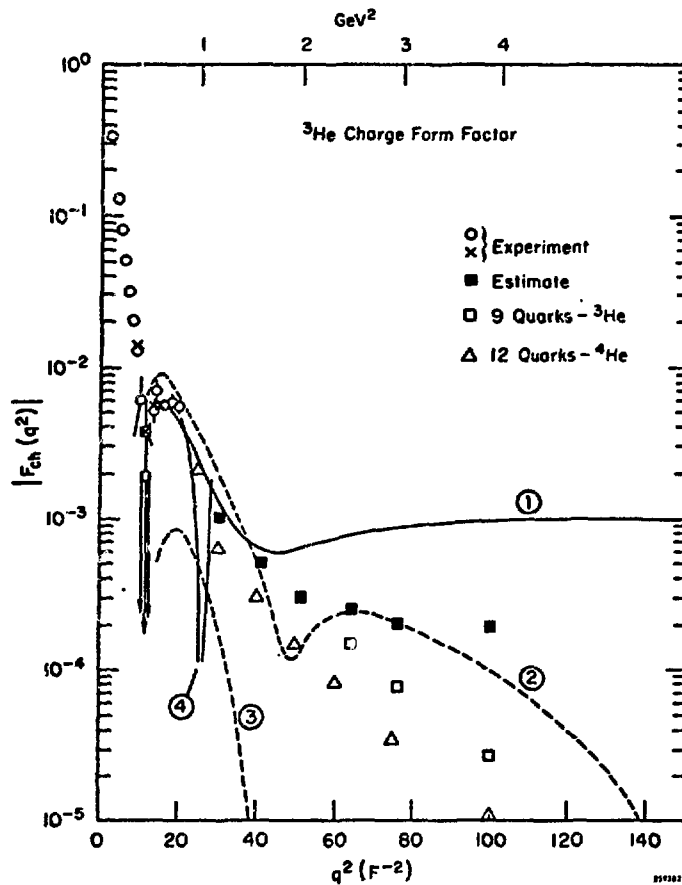
American University, Washington, D.C. and SLAC, Stanford, Ca.

## ABSTRACT

Progress in physics is often stimulated when experiment and theory are in clear disagreement. This is the situation with the elastic charge form factor of  $\text{He}^3$  where measurements at Stanford, which were confirmed at Orsay, reported a diffraction minimum at  $11.5 \text{ F}^{-2}$  followed by a secondary maximum which is approximately constant from  $13$  to  $20 \text{ F}^{-2}$ .

The figure displays the measurements ( ${}^4\text{He}$  is very similar in shape and magnitude) together with various theoretical predictions including extrapolations out to very large  $q^2$ . Calculations of Kloeet and Tjon displayed in curves 1, 2 and 3 use different N-N potentials as input to the Fadeev Equation with 1 and 2 including meson exchange current terms. Curve 3 is the Reid Soft Core prediction. Curve 4 is from Donnelly and Walecka who fit existing data by a Wood-Saxon potential and predict a second minimum at  $25 \text{ F}^{-2}$ . The quark-dimensional scaling model Brodsky and Farrar is used phenomenologically

to indicate the possible large  $q^2$ -behavior of  ${}^3\text{He}$  and  ${}^4\text{He}$ . Even with the obvious disclaimer on the reliability of these  $q^2$  extrapolations, it is clear that measurements beyond  $20 \text{ F}^{-2}$  will indicate the broad underlying features of the two bound helium nuclei. An appraisal of the predictions and other features of the large  $q^2$  region will be presented.



\*Research supported by the National Science Foundation, GP-16565.

HIGH MOMENTUM TRANSFER e-D SCATTERING AS  
A PROBE OF THE RELATIVISTIC STRUCTURE OF THE DEUTERON

V.A.21

Carl Carlson and Franz Gross  
College of William and Mary, Williamsburg, Va. 23185

A calculation of the deuteron form factors based on the relativistic impulse approximation is presented. The calculation is explicitly covariant, and uses relativistic deuteron wave functions which have recently been extracted from a new relativistic theory of nuclear forces.<sup>1</sup> At high momentum transfer the form factors differ significantly from the usual non relativistic form factors due to (a) recoil effects [previously calculated only to 1st order in  $(v/c)^2$ ] and (b) the small components of the deuteron wave function which arise because of the Dirac nature of the nucleons. Comparison of these results with the new SLAC data on e-d scattering will give a precise estimate of the size of exchange current effects, if any.

1. J. Hornstein and F. Gross, Physics Letters 47B, 205 (1973) and F. Gross, Phys. Rev. D10, 223 (1974).

CONNECTION OF MUON CAPTURE AT LARGE ENERGY TRANSFER  
TO PION ABSORPTION

J. Bernabeu, T.E.O. Ericson and C. Jarlskog \*  
CERN -- Geneva

Muon capture is usually studied for space-like momentum transfer of order 100 MeV/c. Its structure is theoretically well described inside the impulse approximation, but for fine details. In contrast, the limit of large energy-transfer of order 100 MeV, with neutrino energy close to zero, is up to now not understood, and the impulse approximation will fail badly. We take here a completely novel approach to this problem, linking it directly to the strong pion processes in a way we believe quite quantitative. In this region the  $\mu$  capture process is given symbolically by  $\Gamma_{N \rightarrow X} \propto V^2 + A^2 + A_0^2$ , where  $V_\mu$  and  $A_\mu$  are the hadronic vector and axial currents. By PCAC the axial current is linked to pion process by  $q_0 A_0 - \underline{q} \cdot \underline{A} \propto \langle X | \phi_\pi | N \rangle$ , so that in the limit  $q \rightarrow 0$  the  $A_0$  term is then, by a mass extrapolation from  $m_\pi$  to  $m_\mu$  given by the s wave  $\pi$  absorption from N to X. This is sufficient to provide a significant lower limit of  $d\Gamma_{N \rightarrow X}/dv^2|_{v \rightarrow 0}$ , expressible directly in terms of  $\text{Im } a_s$ , the s wave absorptive scattering length for pions. Apart from other terms, coming from  $\underline{V} \cdot \underline{q} A_0$ , the  $A$  term contains the p wave  $\pi$  absorption from N to X. It is a natural consequence of this picture that the muon, for this momentum transfer, behaves like a pion, leading to emission of correlated nucleon pairs, ..., as for  $\pi$  absorption. In this sense the muon becomes a strongly interacting particle.

Technically this program is carried through by the introduction of structure functions which entirely describe the hadronic tensor  $W_{\mu\nu}$  given by the expectation value of the product of two weak currents. The information given by PCAC is contained in  $q^\mu W_{\mu\nu} q^\nu$ , and this is used, as pointed out above, to express the muon absorption in terms of the absorptive  $\pi^- + N \rightarrow \pi^- + N$  amplitude near threshold but with pion mass equal  $m_\mu$ .

In addition the axial part of the tensor can be determined also for  $q^2 \approx 0$  using pion pole dominance in the amplitudes proportional to the momentum transfer. The corresponding vector contribution at  $q^2 = 0$  is provided by the total photo-absorption cross-section  $\gamma + N \rightarrow X$ , corresponding to an incident energy  $E_\gamma \simeq m_\mu/2$ . If the approach proves to be significant we will have at our disposal a unique way of learning about the off-shell behaviour of pions in hadronic matter, in particular, for a vanishing mass and a momentum of order 50 MeV/c.

\*Also at University of Göteborg, Sweden.



The  $^{16}\text{O}(\gamma, p)^{15}\text{N}$  Reaction for  $E_\gamma = 40 - 200$  MeV

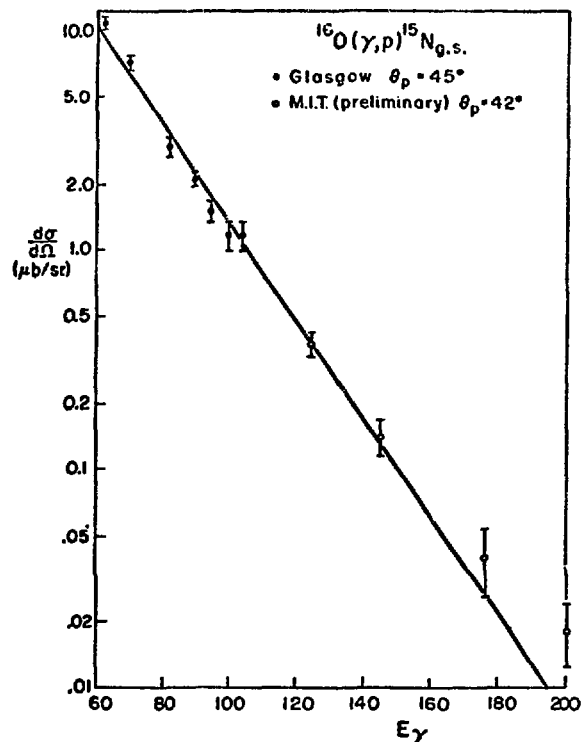
J.L. Matthews, W. Bertozzi, M.J. Leitch, C.P. Sargent and W. Turchinets  
Massachusetts Institute of Technology, Cambridge, Mass.

D.J.S. Findlay and R.O. Owens  
Glasgow University, Glasgow, Scotland

Measurements have been made of the differential cross section for the  $^{16}\text{O}(\gamma, p)^{15}\text{N}$  process at the Glasgow University 130 MeV linear accelerator (for  $E_\gamma \leq 100$  MeV) and at the M.I.T. Bates Linear Accelerator (for  $E_\gamma > 100$  MeV). Both experiments employed similar techniques: protons were detected with good resolution ( $< 1$  MeV) using a magnetic spectrometer, and the cross section for reactions leaving  $^{15}\text{N}$  in its ground state unfolded from the endpoint region of the bremsstrahlung-produced proton spectra.

The motivation for this work lies in the sensitivity of the  $(\gamma, p)$  reaction to high-momentum components in the nuclear wave function, since little momentum is carried in by the incident photon. A measurement of the angular distribution of the photoprotons essentially maps out their initial momentum distribution just as in the  $(p, 2p)$  and  $(e, e'p)$  processes, but for the region  $q > 300$  MeV/c where there are few data from the latter reactions. The fact that conventional shell models predict small amplitudes for these high momenta has led various authors to propose that short-range nucleon-nucleon correlations play an observable role in the  $(\gamma, p)$  process. However, as yet there are no theoretical calculations which can account satisfactorily for the present data below 100 MeV, and no calculations at all above 100 MeV.

A sample of the data is shown in the figure; it is seen that the cross section at  $\theta_p \approx 45^\circ$  is falling off approximately exponentially with photon energy over the range of the measurements (the line drawn through the points is arbitrary). There is no qualitative evidence for a significant enhancement of the cross section due to correlations at higher photon energies.



## A MEASUREMENT OF THE LONGITUDINAL AND TRANSVERSE $\pi^+$ ELECTROPRODUCTION CROSS SECTION.

Bardin G. - Duclos J. - Magnon A. - Michel B. (CEN-Saclay) -  
Montret J.C. (University of Clermont-Ferrand).

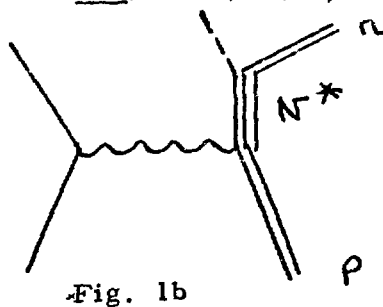
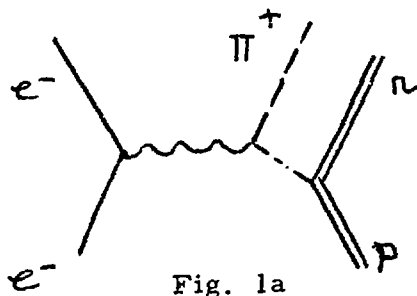
An experiment aimed at measuring the  $\pi^+$  form-factor in the space-like region has been performed at the 600 MeV electron Saclay's Linac. Owing to its high electron current and high (2%) duty cycle, we have been able to isolate the longitudinal part of the differential cross section of the electroproduction reaction  $e^-p \rightarrow e^-n\pi^+$ . Following Akerlof et al (Ref. 1) we have selected the kinematics where the  $\pi^+$  is emitted along the direction of the exchanged photon. In this circumstance, we recall that 1 - The cross section can be written as a purely electromagnetic factor time the sum of "photoproduction" cross sections by transverse and longitudinal photons =  $d^3\sigma / d\Omega_e d\Omega_\pi dE_e dE_\pi = \Gamma_{em} (d\sigma / d\Omega_\pi^T + \epsilon_\gamma d\sigma / d\Omega_\pi^L)$ ,  $\epsilon_\gamma$  being the admixture of longitudinal photon.

2 - The "pion-pole" amplitude Fig. 1a (relevant for the form-factor determination) appears only in the longitudinal component whereas the M1 excitation of the  $N^*$  Fig. 1b only shows up in the transverse part.

3 - The pion-pole contribution is maximum owing to the pole proximity. The invariant mass for the  $\pi$ -N system was chosen to be 1175 MeV. The photon  $Q^2$  was scanned from 1 to 3  $\text{fm}^{-2}$  and for each  $Q^2$  value the cross-section was measured for both a low and high  $\epsilon_\gamma$ . Unlike in the work of Ref. 1, we could go as low as  $\epsilon_\gamma = .15$ . This allow us to subtract the transverse contribution in a model-independant way. Two magnetic spectrometers associated with scintillation hodoscopes were used to detect the scattered  $e^-$  and the  $\pi^+$ . A third existing spectrometer was used for monitoring, looking at the elastic scattering from hydrogen. Until now, a sample of events from the  $Q^2 = 1 \text{ fm}^{-2}$  data point has been analysed. We find for the transverse and longitudinal  $\pi$ -N center of mass cross-sections :  $d\sigma / d\omega_\pi^T = 5.7 (1.7)$  and  $d\sigma / d\omega_\pi^L = 11.3 (3.0) \mu\text{b/strd}$ . This is a good confirmation that the pion-exchange process is dominant in our kinematics.

We hope that at the time of the conference, more precise values for  $d\sigma / d\omega_\pi^L$  versus  $Q^2$ , will be available and that from them, a value for  $\langle r_\pi^2 \rangle^{1/2}$  can be obtained.

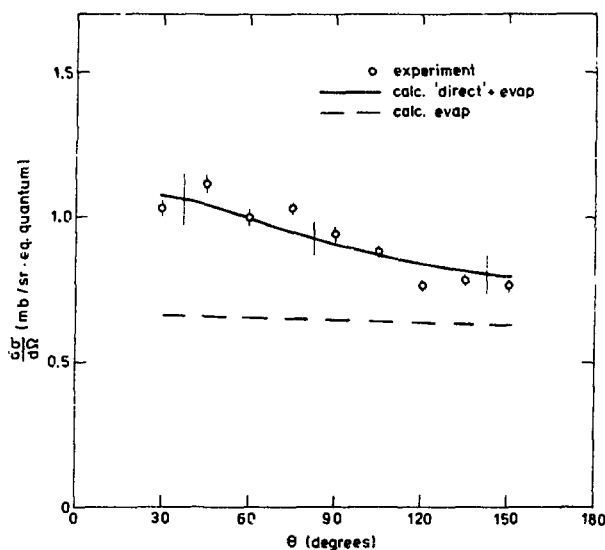
Ref. 1 - C.W. Akerlof, et al (Phys. Rev. 163, 1482, 1967).



$\alpha$ -CLUSTERING EFFECTS IN THE PHOTODISINTEGRATION OF  $^{197}\text{Au}$  AT INTERMEDIATE ENERGIES

J-O Adler, G Andersson and H-Å Gustafsson  
 Department of Physics, University of Lund, Sölvegatan 14,  
 S-223 62 LUND, Sweden.

The emission of  $\alpha$ -particles from  $^{197}\text{Au}$  irradiated by 500 MeV bremsstrahlung has recently been studied <sup>1)</sup>. A comparison with cascade-evaporation calculations showed that about 15% of the  $\alpha$ -particles must be emitted during the cascade step. As the  $\alpha$ -clustering in heavy nuclei is most important on the nuclear surface <sup>2)</sup>, we have calculated the angular and energy distributions resulting from the knock-out of surface  $\alpha$ -particles by cascade nucleons. The number of  $\alpha$ -clusters on the  $^{197}\text{Au}$  surface, defined as the region outside  $r = 7\text{fm}$ , was taken as 4 with a mean kinetic energy of 16 MeV. The height of the coulomb barrier used, 20 MeV, was taken from  $\alpha$ -scattering experiments <sup>3)</sup>. The figure shows the experimental angular distribution compared to the sum of the calculated distributions for evaporated and "directly" emitted  $\alpha$ -particles.



- 1) J-O Adler, G Andersson and H-Å Gustafsson, Nucl Phys A223, 145 (1974).
- 2) D M Brink and J J Castro, Nucl Phys A216, 109 (1973).
- 3) G Hauser et al, Nucl Phys A128, 81 (1969).

## THE NEW MESONS AS MEMBERS OF A NONET

KURT JUST

Department of Physics  
 University of Arizona  
 Tucson, Arizona 85721

In the author's theory of massless quarks without charm, the mesons  $J(3095)$  and  $\psi(3684)$  belong to a nonet which differs by a "mass parity"  $q = -1$  from that of  $\psi, \phi, \rho, K_*$ . One further member is called  $\mathcal{G}(4150)$  because it manifests itself in a broad resonance of  $e^+e^-$  annihilations above 4 GeV. Most distinctive for this proposal is that single "unusual" mesons couple extremely weakly to the photon. Since pairs of them interact normally, they decay strongly into each other and thus have large widths (except  $J$  and  $\psi$ ). While their weak interactions are negligible, they contribute to processes which one described so far by weak and electromagnetic forces only.

I Blomqvist, P Janeček and G G Jonsson  
Department of Physics, University of Lund, Sölvegatan 14,  
S-223 62 LUND, Sweden

H Dinter and K Tesch  
Deutsches Elektronensynchrotron DESY, Hamburg, Germany

The total cross sections for electro- and photoproduction of  $\pi^+$  on  $^{27}\text{Al}$  have been measured with activation method. The experiment was carried out at LINAC II at DESY ( $E_e = 130-600$  MeV). The peak cross section of the resonance is about  $15 \mu\text{b}$  which is smaller than found by Noga et al <sup>1)</sup> and by Nydahl<sup>2)</sup> ( $\approx 40 \mu\text{b}$ ) but is in agreement with the result by Walters and Hummel <sup>3)</sup>. Theoretical calculations have been performed by Janeček <sup>4)</sup> for transitions into the five lowest states of the daughter nucleus, i.e. the  $1/2^+$ ,  $3/2^+$ ,  $7/2^-$ ,  $3/2^-$  and  $5/2^-$  levels. Simple structure can be assumed for these states: one-particle harmonic oscillator states of valence nucleons were coupled to the  $^{26}\text{Mg}$  core not participating in the reaction. The contribution from the  $1/2^+$  state is very small, whereas the remaining states give about the same contribution, each with a maximum of roughly  $10 \mu\text{b}$ .

We assume contributions from higher states with more complicated structure to be small. In the calculations, no final state interactions were included, so the theoretical result is expected to give too great cross section.

The same formalism will be used for calculation of the electroproduction cross section. Then the ratio  $\sigma_q/\sigma_e$  can be calculated. This ratio is probably not very sensitive to details in the nuclear structure.

- 1) V I Noga et al, Soviet J Nucl Phys 14 (1972) 506
- 2) G Nydahl and B Forkman, Nucl Phys B7 (1968) 97
- 3) W B Walters and J P Hummel, Phys Rev 143 (1966) 833
- 4) P Janeček, Physica Scripta 7 (1973) 141 and  
Physica Scripta 10 (1974) 197.

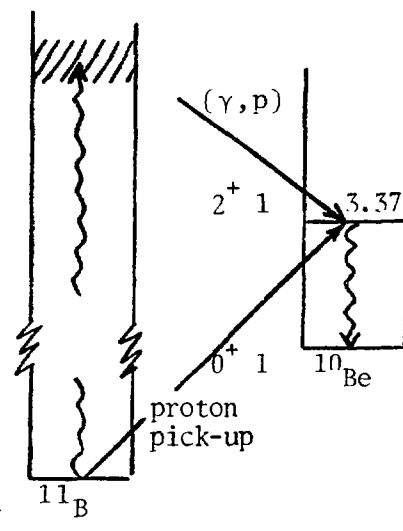
# KNOCK-OUT MECHANISMS IN $(\gamma, \text{NUCLEON})$ REACTIONS AT INTERMEDIATE ENERGIES

J-O Adler, G G Jonsson and K Lindgren

Department of Physics, University of Lund, Sölvegatan 14,  
S-223 62 LUND, Sweden

At energies above the pion production threshold, photons are absorbed mainly via excitation of a nucleon resonance. This excited state decays almost immediately into a stable nucleon and a real pion.  $(\gamma, \text{NUCLEON})$  reactions will result, if both particles leave the nucleus without further interactions. If the interaction between the resonance and the rest of the nucleus can be neglected, the  $(\gamma, \text{NUCLEON})$  reaction should give a spectroscopic factor comparable to that from the corresponding pick-up reaction. The figure shows the situation for the reaction  $^{11}\text{B}(\gamma, p)^{10}\text{Be}^x$ . From measurements of 3.37 MeV de-excitation  $\gamma$ -rays we found for the transition to the  $|2^+, 1, 3.37 \rangle$ -state in  $^{10}\text{Be}$   $\mathcal{P} = 0.9 \pm 1.2$  <sup>1)</sup> to be compared with the theoretical value  $\mathcal{P} = 1.6$  given in ref. <sup>2)</sup>.

We are currently measuring  $(\gamma, \text{NUCLEON})$  reactions on  $^{40}\text{Ca}$  leading to the  $|\frac{1}{2}^+, \frac{1}{2}, 2.48 \rangle$  and  $|\frac{1}{2}^+, \frac{1}{2}, 2.53 \rangle$ -states in  $^{39}\text{Ca}$  and  $^{39}\text{K}$  respectively. The experimental errors are here expected to be much less than for B. The same formalism will be used to interpret the results.



1) J-O Adler et al,  
Nucl Phys A239 (1975) 440.

2) S Cohen and D Kurath,  
Nucl Phys A101 (1967) 1

## ANALYSIS OF CHARGE DENSITY VARIATIONS IN NUCLEI

V.V.Burov, The Moscow State Univ., Moscow, USSR.

V.K.Lukyanov, Joint Inst. for Nucl. Research, Dubna, USSR.

Yu.S.Pol', The Lebedev Phys.Inst.Acad.of Sc.USSR,Moscow,USSR.

Three types of the trial CD-functions were used in analyzing experimental form factors<sup>/1/</sup> by the HE-method<sup>/2/</sup>

$$(O, \text{ solid}) \quad \rho_{SF} = \rho_0 \psi(rR/b) \quad \psi = (\text{sh}R/b)/(\text{ch}R/b + \text{ch}r/b)$$

$$(N, \text{ solid}) \quad \rho = \sum_{n=0}^N a_n \rho_{SF}^{(n)}(rR/b) = \rho_0 \sum_{n=0}^N a_n b^n d^n \psi / dR^n$$

$$(\text{dash}) \quad \rho_1 = \rho_{SF}(rR_0/b_0) + a_1 \rho_{SF}^{(1)}(rR_1/b_1)$$

I. For the  $\rho_{SF}$ -variant an agreement is achieved in the region of  $q$  up to  $x_0 = q_{\text{eff}} A^{1/3} \approx 7.7 F^{-1} (\pm 20 \%)$ . In details,  $x_0$  values are correlated by the nuclear shell filling:

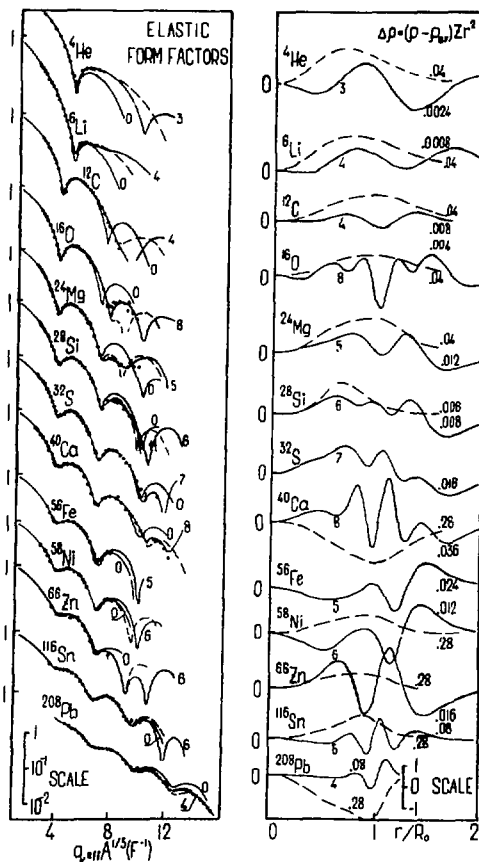
$$x_0(1s) = 5.8; \quad x_0(1p) = 6.6; \quad x_0(1d_{5/2} 2s_{1/2}) = 7.1; \quad x_0(1d_{3/2}) = 9.2.$$

II. To find an agreement at all  $q$  one needs to increase the number of parameters using the  $\rho$ -or  $\rho_1$ -functions.

III. In many cases the CD-ambiguity is found of the qualitative character, when both  $\rho_1$  with the only bump at  $r \sim R_1$  and  $\rho$  with the many oscillations give the same form factors.

1. G.C.Li, I.Sick, M.R.Yerian. Phys.Rev., 9,1861 (1974)(and refs. therein).

2. V.K.Lukyanov, I.Z.Petkov, Yu.S.Pol', transl. in Sov. Journ. of N. Phys., 9,204 (1969).



V.B

WEAK INTERACTIONS



V.B.1

A Study of Background for  
Neutrino Electron Elastic Scattering at LAMPF\*†

H. H. Chen and J. F. Lathrop  
Department of Physics  
University of California  
Irvine, California 92664

ABSTRACT

We have built a detector system to study backgrounds for neutrino electron elastic scattering at LAMPF. The detector system consists of a large liquid scintillator anti coincidence, an inert shield, a sandwich system of alternating layers of thick plastic scintillator slabs and optical thin foil spark chamber modules, and a CAMAC system interfaced to a PDP-11/05 computer. Results of this background study, conducted in situ within the LAMPF neutrino house, and also at UCI are given here. These results have led us to conclude that, at the V-A level, it is feasible to study both the cross section and the differential cross section for neutrino electron elastic scattering at LAMPF.

\*Research supported by NSF under grant No. GP 32860

†Research supported in part by the U.S. Atomic Energy Commission.

H.J. Kreuzer and C.G. Kuper\*

Theoretical Physics Institute and Department of Physics  
University of Alberta, Edmonton, Alberta T6G 2E1, Canada

It is argued that the violation of combined parity in neutral kaon decay is statistical in origin. Rather than introducing microscopic  $\hat{C}\hat{P}$  violating terms in the Hamiltonian ("superweak" theory), we show that a rigorous nonequilibrium theory can account for  $\hat{C}\hat{P}$  violation as a manifestation of the irreversibility of a decaying system.

In terms of Hagedorn's statistical model of hadronic matter, we regard the kaon as clothed by a statistical distribution of pions. On account of the strong pion-pion interaction, any fluctuation of the pion distribution away from thermal equilibrium will relax in a time  $\sim 10^{-23}$  sec. Under these conditions, we can envisage processes in which  $\hat{C}\hat{P}$  is rigorously conserved at a microscopic level, but nevertheless it is violated overall. Two or more pions are "borrowed" from the thermal bath, and subsequently returned. The total angular momentum is necessarily conserved. However, the relative angular momentum of the borrowed pions may change; the strong interactions will restore the thermal equilibrium of the bath virtually instantaneously, leaving an overall violation of  $\hat{C}\hat{P}$ .

Using the Takahashi-Umezawa formulation of statistical mechanics, a model is presented in which  $\hat{C}\hat{P}$  is violated only through nonequilibrium interactions with a heat bath.

Quite generally the theory restores the complete particle-antiparticle symmetry of the laws of physics. It predicts the same time-dependent two-pion amplitude for  $K_0$  decay as the phenomenological "superweak" theory. But, in contrast to the predictions of superweak theory, an initial  $\bar{K}_0$  will have precisely the same two-pion amplitude as a  $K_0$ . On the other hand the charge asymmetry of the leptonic decay modes does depend on the initial state. Experiments in which the initial state is  $\bar{K}_0$  can discriminate unambiguously between the statistical theory and the superweak theory.

\*On sabbatical leave from Technion -- Israel Institute of Technology, Haifa, Israel.

Asymmetry of Beta-Ray Angular Distribution in Polarized Nuclei  
and G-Parity Nonconservation

M. Morita and H. Ohtsubo

Department of Physics, Osaka University, Toyonaka, Osaka 560, Japan

An extensive search for the second class current,  $f_T$ , in

$$H = (\bar{\Psi}_p [\gamma_\lambda (f_V - f_A \gamma_5) + \sigma_{\lambda\nu} k_\nu (f_W + f_T \gamma_5) + i k_\lambda (f_S + f_P \gamma_5)] \psi_n) \\ \times (\bar{\Psi}_e \gamma_\lambda (1 + \gamma_5) \psi_\nu) / \sqrt{2} + \text{h.c.}, \quad k = k_p - k_n, \quad \sigma_{\lambda\nu} = [\gamma_\lambda, \gamma_\nu] / 2i,$$

has been done by Wilkinson and coworkers by means of the  $ft$ -value ratios, since Weinberg proposed it. The result is, however, not too clear, because of the nuclear structure. A nuclear-structure-free experiment is to measure the energy dependence of the beta-ray asymmetry in polarized nuclei, and it was, recently, performed by Sugimoto, Tanihata, and Goring at Osaka University, in the beta decays of  $^{12}\text{B}$  and  $^{12}\text{N}$ . To conclude the existence of the induced tensor in axial vector current from the result of this experiment, we have to be careful for all possible higher order effects which may affect the angular distribution of beta-rays, and there are no such formulas ever published. We have the following rule to describe the formulas correctly with inclusion of the Coulomb corrections, higher order matrices, and induced effects, by replacing

$$C_A \vec{\sigma} \rightarrow (f_A - E_0 f_T) \vec{\sigma}, \quad C_V \vec{\alpha} \times \vec{r} \rightarrow (1 + \mu_p - \mu_n) (f_V/M) \vec{\sigma} + (f_V/M) \vec{r} \times \vec{p}, \\ C_A (i f_5 \vec{r}) \rightarrow -(f_A + 2M f_T) [(1/2M) \vec{\sigma} + i(c/M) \vec{r} (\vec{\sigma} \cdot \vec{p})],$$

where  $c$  is 1 for  $f_1$  and 0 for  $f_T$ , in the published formulas, (M. Morita, Nucl. Phys. **14**, 106 (1959); M. Morita, M. Fuyuki, and S. Tsukada, Progr. Theoret. Phys. **47**, 556 (1972). The same results have been obtained by the elementary particle treatment of nuclear beta decay. We have proved that, in the Gamow-Teller transition, the asymmetry  $[W(0) - W(\pi)]/[W(0) + W(\pi)] = \mp P(p_e/E_e)(1 + \alpha_\mp E_e)$  for  $\beta^\mp$  decay does not depend on  $E_e(\text{max})$ ,  $\alpha Z/R$ , and radiative corrections. The difference,  $\alpha_- - \alpha_+$ , of the experimental values for  $^{12}\text{B}$  and  $^{12}\text{N}$  is about twice as large as the value expected from the CVC theory. The strength of the induced tensor is given by  $f_T/f_A = -(0.96 \pm 0.35) \times 10^{-3}$  (in  $\hbar = m = c = 1$ ), or equivalently,  $f_T = -(3.5 \pm 1.3) f_A / 2M$ . This value gives  $(ft)_T / (ft)_A = 1.08 \pm 0.03$  except for the Gamow-Teller matrices, in agreement with experimental data. The sign for  $f_T$  reduces the induced scalar coupling constant in the muon capture reaction effectively, in apparent disagreement with experiments.

PARITY-NONCONSERVATION AND THE PHOTON CIRCULAR POLARIZATION IN  
 $n + p \rightarrow d + \gamma$

B. A. Craver,<sup>\*†</sup> E. Fischbach<sup>\*</sup>, Y. E. Kim<sup>†</sup> and A. Tubis<sup>\*</sup>  
 Purdue University, West Lafayette, In. 47907

ABSTRACT

The photon circular polarization  $P_\gamma$  for np capture at thermal energies is calculated to all orders of the strong interactions. Several phase equivalent transformations (PET)<sup>1</sup> of the Reid soft core potential, and several different weak-interaction models<sup>2,3</sup> are used. The calculations are facilitated by the use of Green's function techniques. For a given weak-interaction model, PET of the two-nucleon interaction (which are consistent with the one-pion-exchange tail) decrease the magnitude of the calculated value of  $P_\gamma$  by a factor of  $\sim 2-4$ . This reduction appears to be due to short-range oscillations of the two-nucleon wavefunctions induced by the PET. The calculated values of  $P_\gamma$  are mostly all negative and are about 100 times smaller in magnitude than the experimental result,  $P_\gamma = -(1.3 \pm 0.45) (10)^{-6}$ , of Lobashov et al.<sup>4</sup> Thus the glaring discrepancy between theoretical and experimental results for  $P_\gamma$  seems to be mainly due to the use of the wrong dynamical treatment of the weak interactions involved and/or experimental data.

REFERENCES

1. J. P. Vary, Phys. Rev. C7, 521 (1973).
2. E. Fischbach and D. Tadic, Phys. Reports 6C, 123 (1973).
3. C. W. Kim and A. Sato, to be published in Phys. Rev. D.
4. V. M. Lobashov et. al., Nucl. Phys. A197, 241 (1972).

<sup>†</sup>Supported by the U.S. National Science Foundation.

<sup>\*</sup>Supported by the U.S. Atomic Energy Commission.

J. B. Langworthy

Naval Research Laboratory, Washington, D.C. 20375

B. A. Lamers\* and H. Uberall†

Catholic University of America, Washington, D.C. 20064

ABSTRACT

Nuclear matrix elements arising in the weak interaction (we neglect pseudo scalar and weak magnetic terms) are the same as those in electroexcitation.<sup>1</sup> B. A. Lamers, R. D. Graves and H. Uberall, in a paper submitted to this conference, have developed nuclear multipole matrix elements for 17 levels in Helm model parameters by fitting electroexcitation data. Using these parameters we calculate neutrino and antineutrino angular distributions and total cross sections for both muons and electrons. Total cross sections for the neutrino-electron reaction at low energy are shown for the levels diagramed.

This work was supported in part by the National Science Foundation.

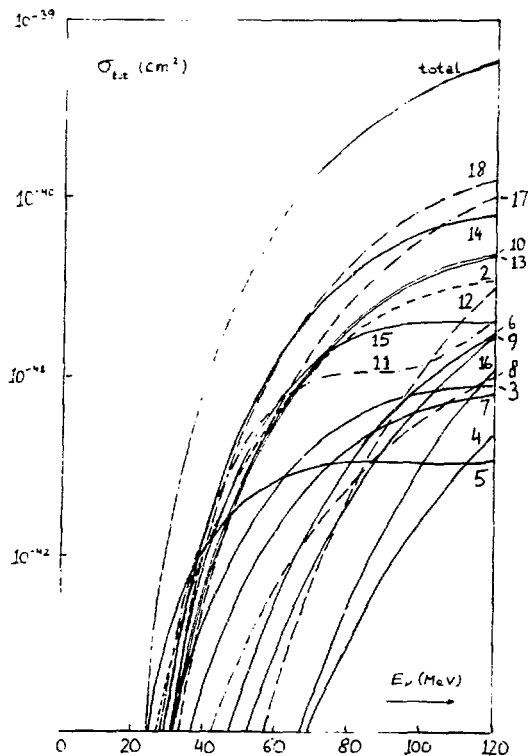
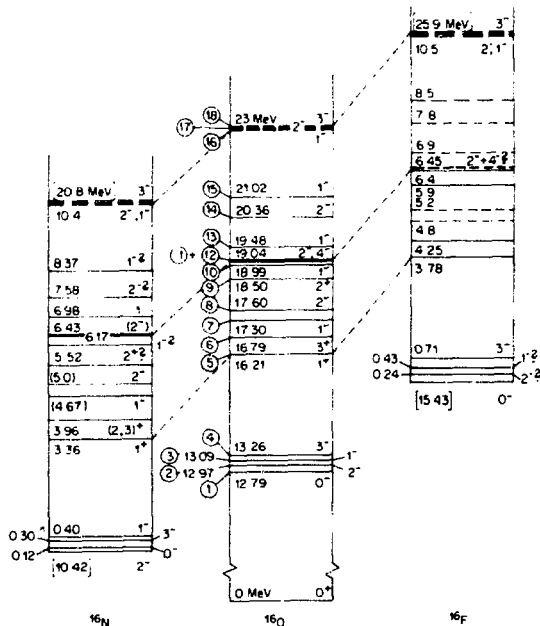


Fig. 1 Scheme of the T=1 Levels in  $^{16}\text{O}$  and their analogs

Fig. 2 Low-energy neutrino cross sections to levels of Fig. 1

\*Now at Hughes Aircraft Co., Culver City, Cal. 90250

†Also at Naval Research Laboratory, Washington, D.C. 20375

<sup>1</sup>H. Uberall, B. A. Lamers, J. B. Langworthy and F.J. Kelly, Phys. Rev. **C6**, 1911 (1972).

K. Sugimoto, I. Tanihata, and J. Göring  
 Faculty of Science, Osaka University, Toyonaka, Osaka 560, Japan

In order to investigate a possible effect due to the second-class current<sup>1)</sup>, the energy dependence of  $\beta$ -ray asymmetry has been measured for the polarized  $^{12}\text{B}$  and  $^{12}\text{N}$  decays ( $I^\pi, T, T_z; 1^+, 1, \mp 1 \rightarrow 0^+, 0, 0$ ). The asymmetry is expressed as<sup>2)</sup>

$$\mathcal{A} = \{W(0) - W(\pi)\} / \{W(0) + W(\pi)\} \cong \mp P(p/E) \{1 + \alpha_{\mp} (1 - A) E\}, \text{ and}$$

$$\alpha_{\mp} \cong \pm (2/3) \{ (\mu_p - \mu_n) / (2M |f_A|) + (1/2M) - f_T \},$$

where  $P, A, E, p, M$  and  $\mu_p - \mu_n \approx 4.7$  are the nuclear polarization and alignment, the electron energy and momentum, and the nucleon mass and transition magnetic moment, respectively. The upper sign refers to  $^{12}\text{B}$ , and the lower sign to  $^{12}\text{N}$ . The form factors  $f_A$  and  $f_T$  are of the axial vector and unknown induced-tensor.

Polarized  $^{12}\text{B}$  and  $^{12}\text{N}$  were produced through  $^{11}\text{B}(d, p)^{12}\text{B}$  and  $^{10}\text{B}(^3\text{He}, n)^{12}\text{N}$  reactions, respectively<sup>3)</sup>. The recoil nuclei were implanted, through a collimator, into a thin Al foil. The nuclear polarization ( $P \approx 13\%$  for  $^{12}\text{B}$ ,  $P \approx 25\%$  for  $^{12}\text{N}$ ) were preserved by applying a static field  $H_0 \approx 2.2\text{KG}$ . The activities were periodically produced and  $\beta$  rays, emitted from the recoil stopper, were detected by two counter telescopes located each side of the polarization at beam-off periods. At every other periods, the polarization was reversed by use of the adiabatic-fast-passage method in NMR. Energy spectra of  $\beta$  rays from both counters were accumulated for both polarization directions.

The normalized asymmetries  $\mathcal{A}^c(E)$  after necessary corrections are shown in Fig.1, where  $\mathcal{A}^c(E) = \mathcal{A}(E) / \bar{\mathcal{A}}$  and  $\bar{\mathcal{A}}$  is the energy average asymmetry. From an additional experiment, the nuclear alignments  $A$  were determined to be  $A(^{12}\text{B}) = +(0.03 \pm 0.02)$  and  $A(^{12}\text{N}) = \pm(0.03 \pm 0.03)$ .

The coefficients  $\alpha_{\mp}$  were obtained to be

$$\alpha_-(^{12}\text{B}) = +(0.31 \pm 0.06)\%/\text{MeV}, \text{ and } \alpha_+(^{12}\text{N}) = -(0.21 \pm 0.07)\%/\text{MeV}.$$

The theoretical predictions to  $\alpha_{\mp}$ , without the second-class current, are  $\alpha_{-}^{\text{CVC}} \approx +0.10\%/\text{MeV}$  and  $\alpha_{+}^{\text{CVC}} \approx -0.17\%/\text{MeV}$ . The prediction due to the weak magnetism is symmetric between a pair of mirror  $\beta$  decays, and can be compared with the present result in an amount  $(\alpha_- - \alpha_+)$ ;  $(\alpha_- - \alpha_+)_{\text{CVC}} \approx 0.27\%/\text{MeV}$  and  $(\alpha_- - \alpha_+)_{\text{exp}} = (0.52 \pm 0.09)\%/\text{MeV}$ . The experimental value is considerably larger

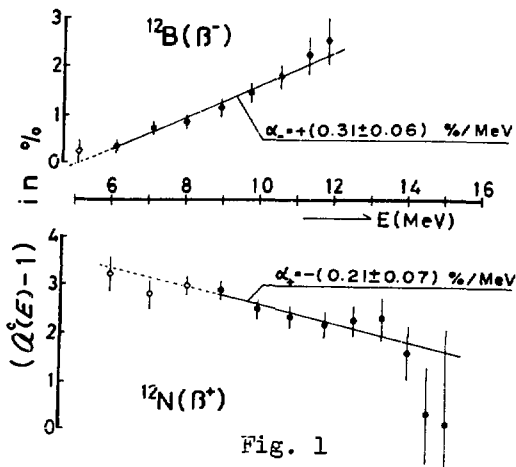


Fig. 1

than the predicted value, and in favor of the existence of the induced-tensor current of which form factor may well be comparable to the weak-magnetism term.

- 1) S. Weinberg, Phys.Rev. 112(1958)1375.
- 2) S. Nakamura, et al., Progr.Theoret. Phys. 48(1972)1899; M. Morita et al., I. Tanihata, to be published.
- 3) K. Sugimoto, et al., J.Phys.Soc.Japan 25(1968)1258; T. Minamisono, ibid., Suppl. 34(1973)324.

TESTS FOR NEUTRINO HELICITY-FLIP IN ELASTIC  $\nu_{\mu} - p$  and  $\nu_{\mu} - e$  SCATTERING\*

E. Fischbach, J. T. Gruenwald, S. P. Rosen, and H. Spivack  
 Purdue University, West Lafayette, In. 47907

and

Boris Kayser  
 National Science Foundation, Washington, D. C. 20550

## ABSTRACT

The processes  $\nu_{\mu} p \rightarrow \nu_{\mu} p$  and  $\nu_{\mu} e \rightarrow \nu_{\mu} e$  (and the corresponding anti-neutrino processes) are analyzed assuming the most general scalar (S), pseudoscalar (P), vector (V), axial-vector (A), and tensor (T) couplings. For  $\nu_{\mu} p$  scattering it is shown that measurements of the average momentum transfer  $\langle t \rangle$  and the final proton polarization  $\vec{P}$  can be used to discriminate between the neutrino helicity-preserving V,A couplings and the helicity-flipping S, P, T couplings. Furthermore, for the V,A couplings themselves, measurements of  $\vec{P}$  and  $\langle t \rangle$  can be used to establish whether or not the current is of the form suggested by gauge theories. For  $\nu_{\mu} e$  scattering the same questions can be probed by measuring the average energy  $\langle E' \rangle$  of the scattered electron. Detailed numerical results are given for  $\nu_{\mu} p$ ,  $\nu_{\mu} e$  and also for  $\bar{\nu}_e e$  elastic scattering for a number of different experimental setups. Several new experiments are suggested which could be done at LAMPF.

\* Work supported in part by the United States Energy Research and Development Administration.

Sadataka FURUI  
 Institute of Physics  
 University of Tokyo, Komaba  
 Meguro-ku, Tokyo 153, Japan

The isospin symmetry of the transition from a nucleon N to an isobar  $\Delta$  by electro-magnetic or weak currents was discussed by several authors [1,2]. The current algebra predicts that the current is iso-vector and has the odd property under the mirror operation  $U = \exp(-i\pi I_y)$  in the isospin space. The strangeness conserving weak current is iso-vector but it could include the part with the even property under the mirror operation, which is known as the second class current contribution [3]. One can naturally ask whether weak and also electro-magnetic current between the  $I = 1/2$  nucleon and the  $I = 3/2$  isobar could include the iso-tensor part which has the even property under the operation U [4].

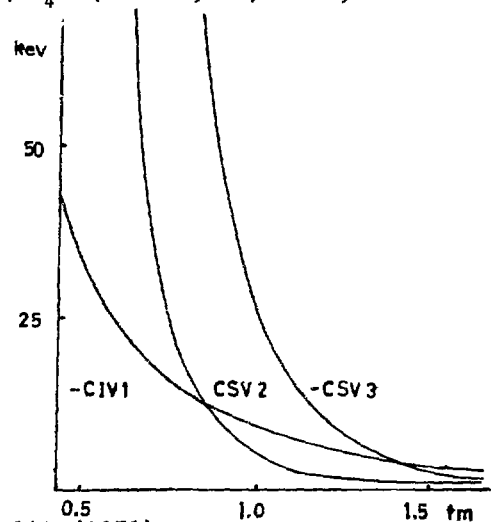
Charge symmetry violating of the nucleon-nucleon potential is thought to be due to electro-magnetic currents, and one can consider the isotensor current effect in the long range potential by the  $\pi\gamma$ -exchange mechanism. By the interference of the two iso-vector photo-production vertices one obtains the charge-independence violating potential and if there exists a mixing of the iso-tensor part in the non-Born part of the 'iso-vector' vertex, the interference can introduce the charge symmetry violating potential.

A simple static model calculation using the zero-width Chew-Low's photo-production amplitudes extrapolated to the soft-pion limit as the vertices shows that the admixture of the iso-tensor part of the order of 10% is non negligible for the charge asymmetry of the nucleon-nucleon potential of  $S_0$  states [5].

The  $\pi^0\gamma$ -exchange spherical charge symmetry violating potential is written in Figure 1. We assumed  $\xi \equiv \bar{V}_4^{(2)}(s=u=M^2, t=0) / \bar{V}_4^{(3/2)}(s=u=M^2, t=0) = 0.1$ , where the bar indicates the non-Born part. The  $\pi^\pm\gamma$ -exchange spin-spin charge independence violating potential with the Kroll-Ruderman term as the vertices is written as a comparison. Here we cut off the t integration at  $t_{\max} = (2m_\pi)^2$ . A preliminary calculation of the scattering length with the Reid potential as the reference shows that;

$$|\delta a| = \begin{cases} 0.14 \text{ fm} & \text{for } t_{\max} = (2m_\pi)^2 \\ 0.45 \text{ fm} & \text{for } t_{\max} = (3m_\pi)^2 \end{cases} \quad \xi = 0.1 \quad [6]$$

$$\begin{cases} 0.27 \text{ fm} & \text{for } t_{\max} = (2m_\pi)^2 \\ 0.88 \text{ fm} & \text{for } t_{\max} = (3m_\pi)^2 \end{cases} \quad \xi = 0.2$$



References;

- [1] A.I. Sanda and G. Shaw, Phys. Rev. D3, 243 (1971).
- [2] R.J. Oakes and H. Primakoff, Phys. Rev. D7, 275 (1973).
- [3] N. Cabibbo, Particle Symmetries (Gordon and Breach 1965) p.1.
- [4] M. Chemtob and S. Furui, Nucl. Phys. A233, 435 (1974).
- [5] S. Furui (to be published).
- [6] The computer code of Dr. Chemtob was used for this calculation.



Energy Dependence of Beta-Ray Asymmetries  
and Second Class Current

H. Ohtsubo<sup>†</sup>, K. Kubodera<sup>††</sup> and Y. Horikawa<sup>††</sup>

<sup>†</sup>Department of Physics, Osaka University, Toyonaka, Osaka, Japan

<sup>††</sup>Department of Physics, University of Tokyo, Bunkyo, Tokyo, Japan

The energy dependence of  $\beta$ -ray asymmetry, known to be important to check the possible existence of second-class currents [1], has recently been measured for  $^{12}\text{B}$  and  $^{12}\text{N}$  decays[2]. We have performed a nuclear model independent analysis of this experiment and obtained the conclusion that the experiment indicates the existence of the second-class current whose magnitude is comparable to that of the weak-magnetism: In the elementary particle treatment, the relevant matrix elements of vector and axial-vector currents are written as

$$\langle P_f : 0^+ | V_\lambda(0) | P_i : 1^+ \rangle = i\varepsilon_{\lambda\rho\sigma\kappa} q_\rho Q_\sigma \xi_\kappa (f_M^{(1)} \pm f_M^{(2)})/2M, \text{ and}$$

$$\langle P_f : 0^+ | A_\lambda(0) | P_i : 1^+ \rangle = i\xi_\lambda f_A - Q_\lambda (q_\nu \xi_\nu) (f_T^{(1)} \pm f_T^{(2)})/2M \text{ for } \beta\bar{\tau},$$

where  $f_A = f_A^{(1)} \pm f_A^{(2)}$ ,  $q = P_i - P_f$ ,  $Q = P_i + P_f$ ,  $M$  and  $\xi_\lambda$  being nuclear mass and spin-one polarization vector. The indices 1,2 denote the first- and second-class current, respectively. (The pseudo-scalar term given by PCAC can be safely neglected here.) Dropping  $f_M^{(2)}$  based upon CVC, we obtain the following expression for the  $\beta$ -ray asymmetry coefficient;

$$\mathcal{A} = \bar{\tau}(\alpha - \beta) (p_e/E_e) [(1 + \Delta) + \alpha \frac{E_e}{\bar{\tau}}] \approx \bar{\tau}(\alpha - \beta) [1 + \alpha \frac{E_e}{\bar{\tau}}] \text{ for } \beta\bar{\tau},$$

where  $\alpha_{\bar{\tau}} = 2\gamma [\pm (f_M^{(1)} - f_T^{(2)}) - f_T^{(1)}] / f_A$  and  $\Delta = \frac{2}{3} E_e (\max) \times (f_T^{(1)} \pm f_T^{(2)}) / f_A$ .

Here  $\alpha, \beta$  and  $\gamma$  are populations of the states with  $J_z = +1, -1$  and  $0$ , respectively. The Osaka experiment gives  $(\alpha_- - \alpha_+) = \bar{\tau} (0.52 \pm 0.09) \times 10^{-2} / \text{MeV}$  for  $\gamma = 0.33$ . Therefore we obtain

$$f_T^{(2)} / f_A^{(1)} = \frac{3}{4} (\alpha_+ - \alpha_-) + f_M^{(1)} / f_A^{(1)} = -(0.17 \pm 0.08) \times 10^{-2} / \text{MeV}$$

in the approximation  $f_A = f_A^{(1)}$ . The effect of Coulomb interaction for the asymmetry is found to be negligible[3]. Thus, the experiment indicates the existence of the second-class current. It might be mentioned here that a microscopic model[4] gives  $f_T^{(2)} / f_A^{(1)} = -0.3 \times 10^{-2} / \text{MeV}$  which is comparable to the experimental value.

- [1] C.W.Kim, Phys. Lett. 34B(1971)384; B.Holstein, Phys. Rev. C4(1971) 740; J.Delorme and M.Rho, Nucl. Phys. B34(1971)317.
- [2] K.Sugimoto, I.Tanihata and J.Goring, to be published.
- [3] M.Morita, Nucl.Phys. 14(1959)106; Phys. Rev. 113(1959)1584.
- [4] K.Kubodera, J.Delorme and M.Rho, Nucl.Phys. B66(1973)253.

Parity Violating Asymmetry in  $n + p \rightarrow d + \gamma$  and the Isospin Structure of the  $\Delta S = 0$  Nonleptonic Weak Interactions B. A. CRAVER,<sup>\*†</sup> Y. E. KIM<sup>†</sup> and A. TUBIS,<sup>\*</sup> Purdue University, W. Lafayette, In. 47907, P. HERCZEG,<sup>\*</sup> Los Alamos Scientific Laboratory, and P. SINGER, Technion-Israel Institute of Technology, Haifa, Israel.

In addition to the recently observed photon circular polarization for unpolarized thermal neutrons, a parity violating effect of interest in the  $n + p \rightarrow d + \gamma$  reaction is the asymmetry  $\alpha$  in the photon angular distribution with respect to an initial neutron polarization.

We calculate  $\alpha$ , using a two-nucleon strong interaction given by the Reid soft-core potential and several of its phase equivalents.<sup>1</sup> The calculations, which are exact with respect to the strong interaction, are facilitated by the use of Green's function techniques. The asymmetry can be decomposed as  $\alpha = \alpha_0 + \alpha_1$ , where  $\alpha_0$  and  $\alpha_1$  are, respectively, due to the isoscalar and isovector parts of the weak interaction. The mixing of opposite parity states in the initial n-p and the deuteron states contributes only to  $\alpha_1$  in the impulse approximation. Nonvanishing contributions to  $\alpha_0$  arise from exchange-current terms,<sup>2</sup> which could be important in models of the weak interactions, such as the Cabibbo theory, where the isovector weak coupling is much smaller than the isoscalar one.

As preliminary results, we obtain, using the parity violating potential described in Ref. 3,  $\alpha_1 \approx 5 \times 10^{-9}$  for the Cabibbo theory, and  $\alpha_1 \approx 5 \times 10^{-8}$  for theories in which the isovector coupling is larger by an order of magnitude. In both cases,  $\alpha_0 \approx 4 \times 10^{-10}$  or  $2 \times 10^{-9}$ , depending on whether the weak matrix elements are calculated in the factorization approximation or taken to be about six times larger, as suggested by another estimate.<sup>4</sup> As a consequence, observation of  $\alpha$  at the level of  $10^{-9}$  would represent evidence for the existence of a  $\Delta S = 0$ ,  $\Delta I = 1$  nonleptonic weak interaction only as long as the factorization approximation gives the correct order of magnitude for the weak matrix elements involved in  $\alpha_0$ . Detailed results will be discussed.

\*Supported by the U. S. Energy Research and Development Administration.

†Supported by the U. S. National Science Foundation.

1. J. P. Vary, Phys. Rev. C 7, 521 (1973).
2. E. M. Henley, Phys. Rev. C 7, 1344 (1973); P. Herczeg and L. Wolfenstein, Phys. Rev. D 8, 4051 (1973); P. Herczeg and P. Singer, Phys. Rev. D 11, 611 (1975) and references quoted therein.
3. E. Fischbach, D. Tadić and K. Trabert, Phys. Rev. 186, 1688 (1969).
4. B. H. J. McKellar and P. Pick, Phys. Rev. D 6, 2184 (1972).

## Pionic effects in the weak axial current for nuclei

---

J. DELORME, M. ERICSON, A. FIGUREAU and C. THEVENET  
Insitut de physique nucléaire de Lyon, Université Claude Bernard  
43 bd du 11 novembre 1918, 69621-Villeurbanne. France

---

We have established the relation between the virtual pion field in a nucleus and the weak axial current. We have shown that there is an electromagnetic analog, namely the relation between the electric field and the displacement field in dielectrics.

We have first derived the Klein-Gordon equation for the virtual pion field in a nucleus. This equation displays two kinds of modifications as compared to that for free nucleons: one is the renormalization of the pion propagator by the interaction with the nuclear medium, the other is the Lorentz-Lorenz renormalization of the pionic vertex through short range correlations.

Using P. C. A. C. we have then deduced the expression for the axial current. The analogy with electromagnetism shows that the axial current and the gradient of the pion field play the respective roles of the displacement vector and the electric field. The knowledge of the pion field thus allows the determination of the axial and pseudo-scalar coupling constants  $g_A$  and  $g_P$  renormalized by the nuclear effects. We have shown on two solvable models that they can be totally different from the nuclear matter values.

DETERMINATION OF THE AXIAL-VECTOR FORM FACTOR  
IN THE RADIATIVE DECAY OF THE PION\*

V.B.12

A. Stetz,<sup>†</sup> J. Carroll, D. Ortendahl, and V. Perez-Mendez

Lawrence Berkeley Laboratory  
University of California  
Berkeley, California 94720

and

G. Igo, N. Chirapatpimol, and M. A. Nasser

Physics Department  
University of California  
Los Angeles, California

September, 1974

ABSTRACT

The branching ratio for the decay  $\pi \rightarrow e\nu\gamma$  has been measured in a counter experiment in which the  $e^+$  was detected in a magnetic spectrometer and the gamma-ray in a lead glass hodoscope. From the measured branching ratio we determine  $\gamma$ , the ratio of the axial-vector to the vector form factor. The latter is computed using CVC and  $\tau_{\pi^0}$ , the  $\pi^0$  lifetime. Adopting a best value  $0.86 \times 10^{-16}$  seconds, we obtain  $\gamma = 0.15 \pm 0.11$  or  $\gamma = -2.07 \pm 0.11$ . A comparison between the measured values of  $\gamma$ , and various theories is made.

by

J.D. Vergados

Physics Department, University of Pa., Phila., Pa. 19174

ABSTRACT

It is well known that the two lepton mode of the double  $\beta$ -decay, if present, would indicate lepton violation.<sup>[1]</sup> If the double  $\beta$ -decay is considered as a two-step process one obtains for the two and four lepton life-times:

$$T_{1/2}^{(2)} = \frac{f_2}{\eta^2} \frac{1}{|ME|^2} \quad T_{1/2}^{(4)} = \frac{f_4}{|ME|^2} \quad (1)$$

The kinematic functions  $f_2$  and  $f_4$  are well known,<sup>[1]</sup>  $\eta$  is the degree of lepton violation and  $|ME|^2$  is the nuclear matrix element. If the two modes cannot be distinguished (e.g. in geologic ores), then

$$\frac{1}{T_{1/2}} = \left( \frac{\eta^2}{f_2} + \frac{1}{f_4} \right) |ME|^2 \quad (2)$$

in either case in order to determine  $\eta$  from the experimental life-times one needs to know  $|ME|^2$ . Transitions to ground states are considered.

We have performed shell model calculations of  $|ME|^2$  using realistic interactions in the case of  $^{48}\text{Ca}$ ,  $^{130}\text{Te}$  and  $^{128}\text{Te}$ . In the case of  $^{48}\text{Ca}$  the nuclear wave functions were obtained within the  $1f_{7/2}$  shell. For  $A=130$  and  $128$  the nuclear wave functions were of the form  $\psi_i = \varphi_i(p) \varphi_0 h_{11/2}^n$  ( $v=0$   $J=0$ );  $\psi_f = \varphi_f(p) \varphi_0 h_{11/2}^{n-2}$  ( $v=0$   $J=0$ ) +  $\alpha |dd\rangle$  where  $\varphi_i(p)$ ,  $\varphi_f(p)$  and  $\varphi_0$  are two-proton, four-proton and closed-shell neutron wave functions respectively in the orbitals  $\{2d_{5/2}, 1g_{7/2}, 2d_{3/2}, 3s_{1/2}\}_i$ .  $|dd\rangle = N \mathcal{A} Y^+ Y^+ |\psi_i\rangle$  with  $\mathcal{A}$  = anti-symmetrizer,  $N$  = Normalization,  $Y = \sum \sigma_i t+(i)$  and  $n=6$  and  $8$  for  $A=128$  and  $A=130$  respectively. The state  $|dd\rangle$  has 88 shell model components and exhausts all the sum rule.  $\alpha$  was calculated in perturbation theory and was found .015 ( $A=130$ ) and .019 ( $A=128$ ).

The results are presented in detail in the table. We simply remark that the energetically allowed transitions exhaust .36%, .02% and .04% of the sum rule for  $^{48}\text{Ca}$ ,  $^{130}\text{Te}$  and  $^{128}\text{Te}$  respectively. (The state  $|dd\rangle$  is energetically inaccessible.)

A	$f_2$ (years)	$f_4$ (years)	$T_{1/2}(\text{exp})$ (years)	$ ME ^2$	$\eta$
48	$10^{12.6}$	$10^{18.9}$	$\geq 10^{21.3}$ (ee)	$1.2 \times 10^{-2}$	$\leq 4 \times 10^{-4}$
130	$10^{13.5}$	$10^{21.5}$	$10^{21.0}$	.144	$4.0 \times 10^{-4}$
128	$10^{15.6}$	$10^{24.4}$	$10^{24.18}$	.174	$1.2 \times 10^{-4}$

[1] See e.g. H. Primakoff and S.P. Rosen, Reports on Progress in Physics, vol. XXII, 121 (1959).

SAUL BARSHAY

Centre National de la Recherche Scientifique

Centre de Recherches Nucléaires and Université

Louis Pasteur, Strasbourg, France

## Abstract

Based upon a possible quark-lepton symmetry, we suggest that the conservation of muon number may be violated by a matrix element of the order of the Fermi constant times the CP-violating parameter times the squared electric charge. We urge a renewed experimental search for the decay  $\mu^\pm \longrightarrow e^\pm e^+ e^-$  with a branching ratio of about  $4 \times 10^{-9}$ .

F. Scheck and A. Wulschlegler  
SIN, CH 5234 Villigen, and ETH Zurich

## ABSTRACT

We reanalyze the theory of radiative pion decay in the framework of gauge invariance, PCAC and current algebra<sup>1)</sup>. It has been put forward, in particular, that this process provided a counter example to Feynman's conjecture on the compensation of gradient and contact terms. A careful application of gauge invariance shows that this is in fact incorrect.

We also review some model predictions for the axial form factor in this decay: Nonrelativistic quark model; current algebra and vector dominance of the vector and axial-vector propagators. The theoretical predictions are not in very good agreement with the measured value for this form factor, unless a rather small value for the pion radius of the order of  $\langle r^2 \rangle_{\pi}^{1/2} \approx 0.5$  fm is accepted. This decay mode calls for further experimental investigation.

## REFERENCES

- <sup>1)</sup> F. Scheck and A. Wulschlegler, Nucl. Phys. B67, 504 (1973)

ELECTRON POLARIZATION IN POLARIZED MUON DECAY,  
RADIATIVE CORRECTIONS

W. E. Fischer and F. Scheck\*, SIN, CH 5234 Villigen  
\* also at ETH Zurich

## ABSTRACT

The experimental determination of the electron polarization in the decay of polarized muons is of great importance for the theory of purely leptonic interactions. We calculate the first order radiative corrections to the electron's longitudinal polarization  $P_\ell$ <sup>1)</sup>. We find the surprisingly simple analytical result for the radiative correction to  $P_\ell$  (in  $\mu^+$  decay)

$$\delta P_\ell \text{ (rad. corr.)} = \pm \frac{\alpha}{6\pi} \left( \frac{1-x}{x} \right)^2 \frac{5-2x-\cos\theta(2x+1)}{3-2x+\cos\theta(1-2x)}$$

with  $x = E/E_{\max}$ , the reduced electron energy.

This correction is about 1% at  $x = 0.5$ , about 1 % at  $x = 0.25$ . Only at very low energies does the correction increase to 10-14 %.

In conclusion, for  $x$  large enough, say  $x \gtrsim 0.1$ , any sizeable deviation from  $P_\ell = \mp 1$ , which is the expected value on the basis of the "V-A" coupling, would be a rather clean probe of the leptonic interactions.

## REFERENCES

- 1) W.E. Fischer and F. Scheck, Nucl. Phys. B83, 25 (1974)



SEARCH FOR SECOND CLASS CURRENTS IN THE  $\beta$ -DECAY OF A=12 ISOBARS

M. Steels, L. Grenacs, J. Lehmann, L. Palfy and A. Possoz  
 Institut de Physique Corpusculaire, Université Catholique de Louvain  
 Louvain-la-Neuve, Belgium

## ABSTRACT

We have measured the nuclear spin-electron correlation in the  $^{12}\text{B}(1^+) \rightarrow ^{12}\text{C}(0^+)$  Gamow-Teller beta-transition. The correlation coefficient corresponding to the alignment of the parent nucleus is measured as a function of the kinetic energy of the  $\beta^-$ -particles. This coefficient is found to be small and its implications on second class currents are discussed.

## INTRODUCTION

For an aligned nucleus the angular distribution of the emitted  $\beta$ -particles, as given by Delorme and Rho for a  $1^+ \rightarrow 0^+$  transition <sup>1</sup>, involves the  $\cos^2 \theta$  term with the following coefficient :

$$\frac{2}{3} A \alpha E = \frac{2}{3} A \frac{E}{2M} (g_A - g_V - 2Mg_M + 2Mg_T)/g_A \quad (1)$$

where A, E and M are the alignment, the kinetic energy of the electron and the nucleon mass, respectively ;  $g_A = 1.23 g_V$ ,  $g_M$  is the weak-magnetism term and  $g_T$  the second class axial-vector coupling constant. The second forbidden contributions can be taken into account by introducing a term proportional to  $(E - E_0)$  in the above paranthesis <sup>2,3</sup> ( $E_0$  is the end-point energy). The aim of the experiment is the determination of the value of the quantity in the paranthesis of equ. 1., more specifically at  $E = E_0$ .

## MEASUREMENTS

The oriented nuclei are produced by the  $^{11}\text{B}(d,p)^{12}\text{B}$  reaction. The most relevant parameters of the production are ; thickness of the production  $^{11}\text{B}$  target  $110 \mu\text{g}/\text{cm}^2$ , recoil angle of  $^{12}\text{B}$  (recoil distance)  $40 \pm 5^\circ$  (100 mm), the recoils are implanted in a  $0.8 \text{ mg}/\text{cm}^2$  thick Pd foil. The orientation of the implanted  $^{12}\text{B}$  is maintained by a static magnetic field ( $B_z = 30 \text{ G}$ ) perpendicular to the reaction plane. The  $\beta^-$ -rays from the Pd foil are counted and analyzed in their energy by two "identical" telescopes, made from plastic phosphors, located above ("Up" ;  $180^\circ$ ) and below ("Down" ;  $0^\circ$ ) the reaction plane on the axis aligned with the Pd foil. Unoriented  $^{12}\text{B}$  nuclei are obtained by the interruption of  $B_z$  during 1 ms after the implantation ("beam-on") period of 28 ms and before the counting period of 36 ms. The counting of  $\beta^-$ -particles from oriented/unoriented nuclei is alternated every 280 ms. The present experiment is done at four deuteron energies : 1.6, 2.0, 2.1 and 2.2 MeV. In these production conditions the absolute value of A of

VI

HIGH ENERGY AND HEAVY IONS

VI.A  
HIGH ENERGY COLLISIONS

In-Elastic Interactions Of 69 GeV/c Protons<sup>VI.A.1</sup>  
With Emulsion Nucleons

O.E. BADAWY, A.A. EL-NAGHY, A. HUSSEIN,  
N. METTWALLI and M.I. SHERIF,  
High Energy Experimental Laboratory  
Department Of Physics, Faculty Of Science  
University Of Cairo, CAIRO - EGYPT.

.....

In this paper the results of the study of the inelastic proton - nucleon interactions in nuclear emulsions at 69 GeV/c are presented. A total of 1887 stars were obtained through 768 meters scanned by the along the track method in a search for the inelastic interactions of protons with nucleons and nuclei of nuclear emulsions type Br-2 irradiated at the Serpukhov accelerator (USSR) with 69 GeV/c proton beam. It was found that the value of the mean free path of inelastic interactions with emulsion nucleons and nuclei ( $\lambda_{int}$ ), is nearly the same for both protons and pions in the range of energy from about 6.0 up to 300.0 GeV. At the same time the value of the mean free path can be compared with that calculated from the emulsion composition and assuming a  $A^{2/3}$  dependence of cross section on atomic weight.

The charged multiplicity distribution of the p-p and p-n interactions in our experiment together with those obtained from the results of p-p experiments both in hydrogen bubble chambers and nuclear emulsions were found to be consistent with the wang's **first** model, which reflects the cell structure of the nucleon in the energy range from 50.0 up to 303.0 GeV.

Results on the energy variation of the topological cross-section, average charged multiplicity ( $\langle n_{ch} \rangle$ ) and the two particle correlation parameter are discussed. The tendency of the ratio ( $\langle n_{ch} \rangle / D$ ) where D is the dispersion of the multiplicity distribution to approach a constant value at high energy is discussed in terms of a two-component model of high energy interactions.

The results of the different moments of the multiplicity distribution of p-p interactions is discussed to test the KNO. scaling behaviour of cross section.

A comparison of these moments with the predictions of a semi-classical composite model for p-p collisions at high energies is found to prefer the construction of a proton out of three quarks.

A study of the rapidity distribution of the emitted secondaries considered all to be pions indicates the coincidence of the distribution of the parameter  $\eta$  ( $\eta = - \ln \tan \theta_L / 2$ ) at our energy 69 GeV with that at 200 and 300 GeV in the region of target fragmentation especially for slow pions.

The angular distribution of the emitted secondaries was studied in the C.M.S. of the two colliding nucleons in case of p-p and p-n events for different multiplicities.

.....

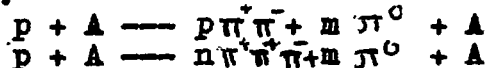
## Coherent Production Of Particles By 69 GeV/c Protons In Nuclear Emulsion

O.E.BADAWY , A.A.EL-NAGHY , A.HUSSEIN,  
N. METTWALI and M.I.SHERIF.

High Energy Experimental Laboratory  
Department of Physics, Faculty of Science  
University of Cairo, CAIRO, EGYPT.

This paper deals with an experimental study of the multiple particle production through the coherent interaction of 69 GeV/c protons with emulsion nuclei. A stack of Br-2 nuclear emulsion was exposed to 69 GeV/c protons at Surpukhov (USSR). By along the track scanning method, 768 meters of proton track were scanned and 1887 interactions were found. Out of this, 300 interactions were classified as white stars, (i.e. mainly due to p-nucleon interactions).

An over-abundance in the multiplicity distribution of these white stars was noticed at  $n_{ch} = 1$  and 3. This over-abundance is attributed to the coherent production. In the present analysis we will mainly deal with the three prong coherent events since they represent the best sample for the following coherent processes here:



where A is a target nucleus in its ground state and  $m=0,1,2,3,\dots$

Assuming a linear increase in the region of  $n_{ch} = 2, 3$  & 4 in the multiplicity distribution, a rough estimate of the number of the three prong coherent events is obtained. This lead to a value of mean free path for coherent three prong interaction of  $33.39 + 11.99 - 6.91$  meters with a corresponding cross section  $\sigma_{coh.} = 6.20 + 1.74$  mb.

A deep analysis of the parameter  $\sum \sin \theta_i$  (where  $\theta$  is the space angle of the outgoing particles relative to the incident beam direction) for both the clean and dirty events gave a  $25 \pm 6$  for the number of three prong coherent events. The corresponding mean free path is  $\lambda_3 = 30.72 \pm 10$  meters and  $\sigma_{coh.} = 6.8 \pm 1.8$  mb.

A through analysis was done for the azimuthal angular distribution of these three prong events satisfying the coherence kinematical conditions. This distribution being inconsistent with the random isotropic one, reflects the fact of the presence of coherent stars. A trial was done to separate the number of the coherent events from those due to normal p-n interactions. A number of 24 three prong stars was obtained as being due to coherent interactions. The corresponding mean free path is  $\lambda_3 = 32.0$  meters and the cross section is  $\sigma_{coh.} = 6.47$  mb.

The cross section of the three prong coherent interactions of protons with nuclei was found to increase linearly with the incident energy  $E_p$ . This energy dependence of the cross section is compared with  $P$  the optical model calculations, and with the behaviour of the coherent cross section in case of  $\pi^-$  nucleus interactions.

.....

Nuclear interactions of 200 and 300 GeV protons in emulsion.

Barcelona-Batavia-Belgrade-Bucharest-Lund-Montreal-Nancy-Ottawa  
-Paris-Rome-Strasbourg-Valencia collaboration  
(sent by I. Otterlund, Lund).

We have studied interactions in stacks of Ilford K5 emulsions irradiated to the FNAL 200 GeV and 300 GeV proton beam in 1972 and 1973. At the conference we will present results on the multiplicities of shower particles and heavy prong particles, on the correlations between shower particles and heavy prong particles, on the energy transfer between the incoming proton and the fast secondaries produced in the interactions and on single particle inclusive angular distributions.

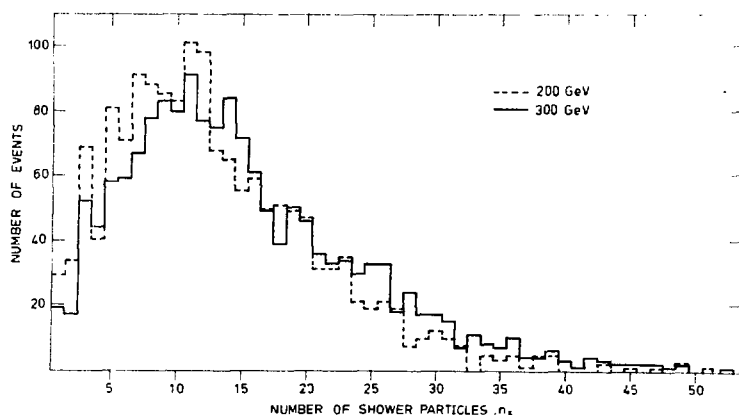
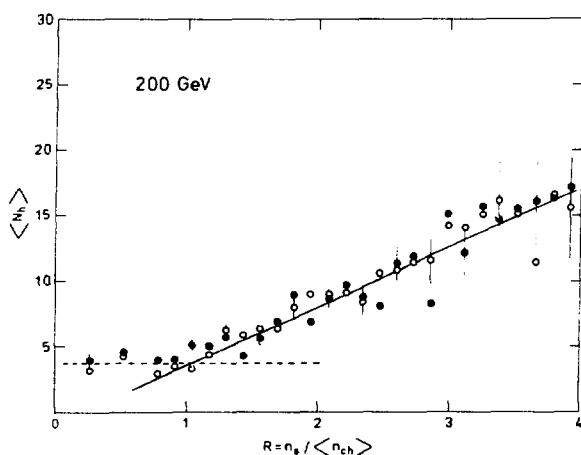


Fig. 1 shows differential  $n_s$ -distributions at 200 and 300 GeV. Fig. 2 shows the correlations between  $\langle N_h \rangle$  and

$$R = n_s (\langle n_{ch} \rangle)^{-1}$$



open circles this investigation, full circles Alma-Ata-Leningrad-Moscow-Tashkent collaboration, preprint 1974  
 $n_s$  = number of shower particles (fast moving secondaries with velocities exceeding  $0.7c$ ).  
 $N_h$  = number of heavy prong particles (heavily-ionizing slow moving particles with velocities below  $0.7c$ , mainly fragment products of the target).  $\langle n_{ch} \rangle$  = mean multiplicity in pp interactions.

For small values of  $R$  there is no evident correlation to the heavy prong multiplicity. We interpret this as a sign of single collision events of diffractive or peripheral character.

A phenomenological model for high energy proton-nucleus interactions.

B. Andersson<sup>ⓧ</sup> and I. Otterlund<sup>ⓧⓧ</sup>

ⓧ TH-Div., CERN, Switzerland

ⓧⓧ Dept. of Cosmic High Energy Physics, Univ. of Lund, Lund, Sweden.

We have developed a phenomenological model for high energy proton-nucleus interactions. In this model we describe multiplicity distributions of shower particles and heavy prong particles as a convolution of a leading particle contribution (LP-component, index 0) and one (equal and independent) contribution (index 1) from each of the repeated collisions of the impinging proton and the nucleons inside the nucleus. The total multiplicity of shower particles  $n_s$  then results as a sum of contributions from the LP-component,  $n_0$ , and from the RC-components,  $n_1$ .

$$\bar{n}_s = \bar{n}_0 + \bar{n}_1(\bar{\nu}-1) = \bar{n}_0 + \bar{n}$$

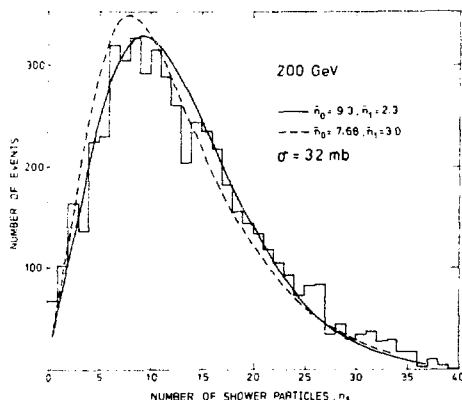
Differential  $n_s$ -distributions are given by the formulas:

$$P_s(n_s) = \sum_{\nu} \pi(\nu) P_s(n_s, \nu); \quad \pi(\nu) = \text{the probability distribution for } \nu \text{ incoherent collisions.}$$

$$P_s(n_s, \nu) = \sum_{n_0+n=n_s} P_0(n_0) P(n, \nu); \quad P_0(n_0) = \text{negative binomial distr.}$$

$$P(n, \nu) = \sum_{n_2 + \dots + n_{\nu} = n} P_1(n_2) \dots P_1(n_{\nu}); \quad P_1(n_i) = \text{Poisson distr.}$$

In Fig. 1 we compare the experimental shower particle distribution at 200 GeV (ref. 1-3) with two distributions predicted from the model. The dotted curve is valid for  $\bar{n}_0 = 7.68$ ,  $\bar{n}_1 = 3.0$  (the Gottfried EFC-model) and the solid curve for  $\bar{n}_0^0 = 9.3$  and  $\bar{n}_1 = 2.3$ . The experimental distribution is compatible with a  $\bar{n}_0^1$  value larger than the mean multiplicity in pp collisions at the same energy.



1. Barcelona-Batavia-Belgrade-Bucharest-Lund-Lyons-Montreal-Nancy-Ottawa-Paris-Rome-Strasbourg-Valencia collaboration, private communications.
2. Babecki et al. private communications.
3. Alma-Ata-Leningrad-Moscow-Tashkent collaboration, preprint 1974.

Search for Ultra-high Momentum Transfer  
Scattering of Protons by Nuclei

L.M. Lederman, and L.E. Price

Columbia University, New York, N.Y.

A search has been made for high momentum nuclei or nuclear fragments produced by a proton beam on a nuclear target. Copper and tungsten targets have been used in 300 and 400 GeV/c beams at Fermilab. The recoil nuclei are detected in dielectric track detectors made of synthetic fused silica. The insensitivity of these detectors to lightly ionizing particles makes it possible to use a very large flux of protons while looking for small numbers of recoil nuclei. The experiment is sensitive to momentum transfers up to 300 GeV/c.



CHARGED AND NEUTRAL PION PRODUCTION IN  $\pi^-$ Ne VI.A.6  
COLLISIONS AT 200 GeV/c \*

J. S. Loos, J. R. Elliott, L. R. Fortney, A. T. Goshaw,  
J. W. Lamsa, W. J. Robertson, W. D. Walker, and W. M. Yeager  
Department of Physics, Duke University, Durham, N. C. 27706

ABSTRACT

Production of charged and neutral pions in  $\pi^-$ Ne collisions have been studied in an exposure of the FNAL 30-inch bubble chamber filled with a mixture of Ne ( $\sim 30$  molar percent) and H<sub>2</sub> ( $\sim 70$  molar percent). Charged and neutral pion multiplicities are presented and compared both to  $\pi$ Ne collisions near 10 GeV/c and to  $\pi$ p collisions near 200 GeV/c. Except for the coherent  $\pi$ Ne diffractive processes, the same KNO scaling is found to apply to both  $\pi$ Ne and  $\pi$ p collisions. Preliminary measurements for the charged pion rapidity distributions will also be presented. The data support and the "energy flux" cascade models but disagree with the "independent cascade" models.

\* This work supported in part by ERDA, Grant AT-(40-1)-3065.

A STUDY OF 10.5 GeV/c  $\pi^+$  AND  $\pi^-$  WITH NEON NUCLEI \*

W. D. Walker, J. R. Elliott, L. R. Fortney, A. T. Goshaw,  
J. W. Lamsa, J. S. Loos, W. J. Robertson, W. M. Yeager  
Department of Physics, Duke University, Durham, N. C. 27706

C. R. Sun and S. Dhar  
Department of Physics, State University of New York, Albany 12222

## ABSTRACT

We report work done in the SLAC 82" bubble chamber filled with a Ne-H<sub>2</sub> mixture. Distributions of  $\pi^-$  coming from the interaction of 10.5 GeV/c  $\pi^+$  with neon nuclei will be presented. Using the fact that neon is an I = 0 nucleus, we extract the momentum, rapidity, etc. distributions of both signs of  $\pi$ 's. We have measured the spectrum of protons from these interactions up to 3.5 GeV/c. Gammas are detected in the chamber with a 25% probability. From the measurements of the momenta of the pairs, we determine the momentum and rapidity distribution of  $\pi^0$ 's. By using the momentum distribution of the charged and neutral  $\pi$ 's that are produced, we are able to make an energy balance on the  $\pi$ -Ne interactions. This analysis indicates the production of some multi-BeV neutrons.

\* This work supported in part by ERDA, Grant AT-(40-1)-3065.

p -  ${}^4\text{He}$  ELASTIC SCATTERING AT 24 GeV/c

---

J. Berthot, G. Douhet, J. Gardès, L. Méritet, M. Querrou, A. Têtefort  
and F. Vazeille  
Laboratoire de Physique Corpusculaire, Université de Clermont, BP 45,  
63170 AUBIERE (France)

and

J.P. Burq, M. Chemarin, M. Chevallier, B. Ille, M. Lambert and J.P. Marin  
Institut de Physique Nucléaire, Université Claude-Bernard, 43, bd du  
11 novembre 1918, 69621 VILLEURBANNE (France)

and

J.P. Gerber and C. Voltolini  
Centre de Recherches Nucléaires, Université Louis-Pasteur, Laboratoire  
de Physique Corpusculaire, Rue du Loess, 67037 STRASBOURG Cédex (France)

---

This experiment was using an intense extracted proton beam at CERN and a gaseous Helium target. All information is obtained from the analysis (identification, energy, angle) of the recoiling nucleus,  ${}^3\text{He}$  and  ${}^4\text{He}$ , by means of a telescope of four large area  $\Delta E - E$  semiconductor detectors.

The elastic data (about 75 000 events for  $p + {}^4\text{He} \rightarrow p + {}^4\text{He}$ ) cover the  $t$ -range from 0.03 to 0.72 (GeV/c)<sup>2</sup>, corresponding to six orders of magnitude for the cross section. The presence of a minimum and a secondary maximum allows to check the Glauber model or other approximations.

Two-step analysis of nuclear coherent  $3\pi$  production in the  $J^P=0^-$  state

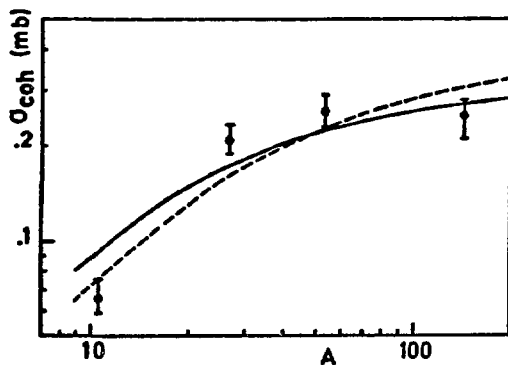
Per Osland, Universitetet i Trondheim, Trondheim, Norway

Multiple pion production on nuclear targets has been extensively studied in the last few years, one aim being to get information on how the new-born multipion state propagates through nuclear matter. The conventional analysis gives the result that  $\sigma[(3\pi)N] \approx \sigma(\pi N)$  for masses of the produced system being in the region of the  $A_1$ , whereas it is considerably smaller for higher masses (the  $A_3$  region), and also smaller for  $5\pi$  systems<sup>1)</sup>. It was recently shown<sup>2)</sup> that these cross sections might all be roughly equal, if one allows for interference between one- and two-step processes, e.g.  $\pi N \rightarrow A_3 N$  interfering with  $\pi N \rightarrow A_1 N$ , followed by  $A_1 N' \rightarrow A_3 N'$ . This result supports the idea that the final state does not develop until after the incident - now excited - pion has left the nucleus.

The  $3\pi$  data has now been partial-wave analyzed<sup>3)</sup>, and it appears that in the conventional analysis the  $J^P=0^-$  state has a much larger cross section than the dominant  $1^+$  ( $A_1$ ) state,  $\sigma[(3\pi)_{0^-} N] \approx 50$  mb. We have analyzed this  $0^-$  production in terms of interference between a direct production  $\pi N \rightarrow (3\pi)_{0^-} N$  and the two-step contribution  $\pi N \rightarrow (3\pi)_{1^+} N$  followed by  $(3\pi)_{1^+} N' \rightarrow (3\pi)_{0^-} N'$ . The  $1^+$  state is assumed to be the dominant intermediary state, since it has the same naturality, and is very strongly produced. We further assume that the  $1^+$  state has the same mass as the final  $0^-$  state.

With all cross sections equal,  $\sigma[(3\pi)_{0^-} N] = \sigma[(3\pi)_{1^+} N] = \sigma(\pi N) = 25$  mb, we have tried to fit the observed A-dependence by varying the amplitude ratio

$$R = \frac{f\{\pi \rightarrow (3\pi)_{1^+}\} f\{(3\pi)_{1^+} \rightarrow (3\pi)_{0^-}\}}{f\{\pi \rightarrow (3\pi)_{0^-}\} f_{\text{elastic}}}$$



The best fit is obtained for a rather large positive  $R$ , but no satisfactory agreement with the experimental results seems possible (see figure). This indicates that at the present energies, the  $0^-$  state does develop inside the nucleus, contrary to the  $1^+$  and  $2^-$  states.

Dashed curve:  $R = 0.4$ Solid curve:  $R = 0.8$ 1) P. Mühlemann et al, Nucl. Phys. B59 (1973) 106.2) G. Fäldt and P. Osland, Nucl. Phys. B87 (1975) 445.3) W. Beusch et al, Phys. Letters 55B (1975) 97.

## FINITE ENERGY CORRECTIONS AND MULTIPLICITY FLUCTUATIONS IN GOTTFRIED'S MODEL OF HADRON NUCLEUS INTERACTIONS

Bo Andersson  
Theory Division, CERN and  
Dept Theoretical Physics, LUND, Sweden

Appreciable corrections in the Serphukov-MAL-energy range are found in the model proposed by Gottfried. The reasons are partly that some parameters take on corrected values when contributions of the order unity cannot be neglected as compared to  $\log(s/m^2)$ . However one correction has to do with the interpretation in experiments of the predictions: the recoiling nucleon from an elementary collision will in general be experimentally classified among the heavy-prong particles and not among the showerparticles. The size of the contributions from the repeated collisions between the impinging proton and the nucleons inside the nucleus is in the model related to the outcome of lowenergetic meson-nucleon collisions

The resulting mean charged multiplicity is for 200 gev proton energy for each such contribution around 3. Therefore the neglect of the recoil nucleon is very noticeable causing corrections of the order 30%.

In particular the parameter  $\eta$  in Gottfried's formula

$$R_A = \alpha + \eta(V_A - 1)$$

will become considerably smaller,  $\eta \approx .25 - .27$  in the above-mentioned energy range. It will only rise to 1/3 for very high energies.

Here  $R_A$  is the ratio between the mean showerparticle multiplicity for proton nucleus collisions ( nuclear massnumber A) and the corresponding charged multiplicity at pp collisions of the same energy. Further  $V_A$  is the mean number of collisions as computed from a Glauber multiple scattering formula. The parameter  $\alpha$  corresponds to the "leading particle" contribution and is in Gottfried's model  $\alpha \approx 1$ .

There are in present experimental data indications that  $\alpha \approx 1.2$  and that the value value of  $\eta$  given above is quite close.

There is an appreciable broadening of the multiplicity distribution due to the relative sensitivity of the results to some of the incoming parameters, in particular to the Feynman variable x of the leading particle. This quantity is related to the inelasticity and from proton proton collisions we know that it exhibits essentially a flat distribution ( neglecting diffraction).

Some remarks are made on the difficulties with relativistic invariance for the Gottfried "slicing" procedure.

EXCITATION OF THE 15.1 MEV LEVEL OF CARBON BY BEV PROTONS AND PIONS. VI.A.11

Authors: D. Scipione, W. Mehlhop, O. Piccioni, P. Bowles, P. Caldwell, J. Sebek, R. Garland, B. Babcock, I. Kostoulas

In the course of a program of using nuclear levels to label final states of high energy interactions<sup>1</sup> we have measured the cross section for the excitation of the 15.1 Mev level of Carbon ( $J^P, I = 1^+, 1$ ) by BeV protons, and have observed an upper limit for the excitation by BeV pions. Near-elastic (without production of secondaries) excitation by protons exhibits a very marked decrease with increasing incident momentum, namely from  $183 \pm 20$  microbarns at .68 BeV/c to an upper limit of 20 microbarns at 2.0 BeV/c. It is known that excitation of C (15.1) requires flipping of both mechanical and isotopic spin of a nucleon. On the other hand, the symmetry between proton and neutron states in C, with the consequent symmetry of states with  $I_2 = +\frac{1}{2}, -\frac{1}{2}$  resp. would produce zero amplitude when the incoming protons interact with equal strength with neutrons and protons. As this is the case at 2.0 BeV/c and not at .68, a qualitative explanation in these terms seems reasonable. An adequate theoretical analysis (we know only of the work of Kawai et al<sup>2</sup> at 180 Mev kinetic energy) of our data should yield quantitative information on the degree of symmetry of the nucleonic wave functions in C, as well as on the importance of second order effects such as multiple scatterings of the incoming protons within the nucleus.

In contrast, for C (4.4) we reported before<sup>1</sup> a flat momentum dependence for the excitation cross section, both for protons (3.2 mbarns) and for pions (1.8 mbarns) up to 4 BeV/c. Of course for the C (4.4) level no flipping is expected to be involved, as confirmed by the observed recoil-gamma correlation, and diffraction scattering should be sharply preferred.

We find an upper limit of about 5 microbarns for C (15.1) excitation by 3 to 4 BeV pions. This is also consistent with the near equality of pion-proton and pion-neutron interaction. In particular, C (15.1) should not be expected to be excited by interactions mediated by a rho or by a neutral pion, because of the internal structure of C, though "macroscopically" the quantum numbers of the transition  $J^P, I = 1^+, 1$  fully allow such exchanges. The prohibition of pion or rho exchanges, if adequately strong, might of course be in itself a very useful tool for labeling high energy interactions.

<sup>1</sup>D. Scipione, W. Mehlhop, R. Garland, O. Piccioni, P. Kirk, P. Bowles, J. Sebek, S. Murty, H. Kobrak, J. Marraffino and P. Allen, Phys. Lett. 42B, 489, (1972)

G. Ascoli, T.J. Chapin, R. Cutler, L.E. Holloway, L.J. Koester, U.E. Kruse, L. J. Nodulman, T. Roberts, J. Tortora, B. Weinstein, and R.J. Wojslaw, Phys. Rev. Lett. 31, 795, (1973)

G. Ascoli, T. Chapin, L. Holloway, L. Koester, W. Kruse, L. Nodulman, and R. Wojslaw in Proceedings of the Fifth International Conference on High Energy Physics and Nuclear Structure, Uppsala, Tiber, Ed., North Holland (1973) p. 147.

W. Mehlhop, D. Scipione, O. Piccioni, P. Caldwell, J. Sebek, R. Garland, B. Babcock, P. Bowles, and I. Kostoulas, presented at the Topical Meeting on High Energy Collisions Involving Nuclei, Trieste, (1974) (to be published).

L. Koester, et al., presented at the Topical Meeting on High Energy Collisions Involving Nuclei, Trieste, (1974) (to be published)

<sup>2</sup>M. Kawai, T. Terasawa, and K. Izumo, Prog. Theor. Phys. 27, 404, (1962)

STRIPPING AND DISSOCIATION OF 6 BeV DEUTERONS AND TAGGED NEUTRON BEAMS.<sup>VI.A.12</sup>

Authors: P. Bowles, C. Leemann, W. Mehlhop, H. Grunder, O. Piccioni, R. Thomas, D. Scipione, R. Garland and J. Sebek

Short, preliminary reports of this work at LBL (Bevatron) have appeared<sup>1</sup>. We have now completed the computation of various corrections and of the expected values for some of the experimental data, on the basis of a simple model. Deuterons of 5.85 BeV/c passed through a target of various elements, at various times. Protons from the target were focused and momentum analyzed. Neutrons were detected at the end of a 383 foot pipe, within  $3 \cdot 10^{-6}$  steradian, and their momentum was measured by their time-of-flight. The neutron momentum spectrum showed an outstanding peak at half the deuteron momentum; the forward differential cross sections (Table) for neutron stripping were found to be proportional to  $A^{-.51}$  (other workers at lower energies have obtained a similar dependence<sup>2</sup>). The momentum spread was  $\pm 3.8\%$  (HWHM) with the Be target and  $\pm 3.3\%$  with U. The proton momentum spectrum was similarly narrower for U than for Be. The smaller widths<sup>3</sup> in U as well as the steepness of the A dependence, which is more than  $A^{-.33}$  which we would expect from a strong interaction phenomenon, are probably due to the importance of Coulomb dissociation for heavy elements.

We have also "tagged" the neutrons on the basis of their coincidence with protons. The proton counter, half-inch wide, selected protons within a momentum spread of  $\pm .35\%$ , and the tagged neutrons were observed to have a spread less than  $\pm .7\%$ , probably all due to experimental error. The actual spread is expected to be just equal to that of the proton detector. The A dependence of this process, (Table) after correcting for our proton solid angle, is  $A^{-1.33}$ . Thus, the Coulomb field is clearly a major contributor. In fact, using the Weizsacker-Williams method and distinguishing the different nuclear absorptions for different impact parameters, we would expect  $A^{-1.7}$ , indicating that for Uranium, only 6% of the tagged neutrons are produced by non-Coulomb interactions (86% for Be). M.L. Richardson and L. T. Kerth; Meyer; Faldt<sup>3</sup> and Lander et al<sup>4</sup> have also pointed out that Coulomb dissociation is expected to dominate for U. We also observed that about 45% of the high energy neutrons produced by U are accompanied by a tagging proton. Thus, we estimate that with a proton channel of larger, yet feasible, efficiency,  $10^6$  tagged neutrons per second could be obtained in  $3 \times 3$  square inches, at 30 feet from a  $1/8$  inches U target, accompanied by  $1.75 \cdot 10^6$  untagged neutrons. The proton counters would count  $5 \cdot 10^6$  protons. 4% of the "tagged" neutrons will be accidental coincidences between the neutron and proton channels, assuming a resolution of 4 nsec. Less intensity results in less accidentals. At BNL, for the same flux, accidentals will be 2%. It is important to note that obtaining neutron beams from protons at these high energies is very disadvantageous because of the rapid decrease of the charge exchange cross section.

TARGET	Be	C	Al	Cu	Pb	U
$\frac{d\sigma}{d\Omega}$ (0) (b/sr) untagged	$109.8^{+2.1}$	$115.8^{+3.2}$	$170.1^{+3.8}$	$295^{+8.2}$	$505.2^{+14.7}$	$579^{+16}$
$\frac{d\sigma}{d\Omega}$ (0) (b/sr) tagged	$1.7^{+.7}$		$8.9^{+1.6}$	$40.0^{+3.5}$		$174.^{+12}$

<sup>1</sup>CERN Courier 12, No. 5 (1972); C. Leemann, et al, Int. Conf. on Inst., 731 (Frascati, Italy, 1973); P. Bowles et al, Bul. of the A.P.S. 17, 1188 (1972).  
<sup>2</sup>R.L. Lander et al P.R. 137, B1228 (1965); L.M.C. Dutton et al, Nucl.Ph.A 178 488 (1972); G. Bizard et al, Nucl.Inst. and Meth. 111, 445 (1973).  
<sup>3</sup>G. Faldt, P.R. D2, 846 (1970); L.T. Richardson, Bul. of the A.P.S. 18, 1605 (1973); W.T. Meyer, Arg.Nat.Lab. Report ANL/HEP 7441 (1974).

Alexeev G.D., Zaitsev A.M., Kalinina N.A., Kruglov V.V.,  
Kuznetsov V.N., Kulikov A.V., Kuptsov A.V., Nemenov L.L.,  
Pontecorvo B.M., Khazins D.M., Churin I.N.

Joint Institute for Nuclear Research, Dubna, USSR

SEARCH FOR DELAYED HIGH ENERGY RADIATION  
FROM Pb TARGET IRRADIATED BY 45 GeV PROTONS

Search has been performed for delayed gamma-quantum or electron radiation which can appear in the decay of hypothetical long-lived particles produced in collisions of 45 GeV protons with Pb nuclei. The lifetime region from 0.1 sec to a day has been investigated. The delayed radiation effect was not observed. The values of the upper limit of the cross section for quasiradioactive nucleus production were obtained to be of the order of  $10^{-34}$  cm<sup>2</sup> for Pb nucleus.



VI.B  
HEAVY IONS

Inelastic Interactions of 17 GeV/c  $\alpha$  Particles  
with Nuclei

Dubna-Moscow-Leningrad-Koshice-Tashkent-Warsaw  
Collaboration

presented by E. Skrzypczak /University of Warsaw/

A sample of 5056 inelastic interactions of relativistic  $\alpha$  - particles /17 GeV/c / with nuclei was analysed with the emulsion techniques. Two kinds of emulsion were used /one with a standard atomic composition and another one with an increased amount of light nuclei/, which made it possible to obtain cross-sections, multiplicity and angular characteristics separately for heavy /Ag, Br/ and light /C, N, O / target nuclei. These characteristics are analysed and discussed in detail.

Stripping and fragmentation reactions were selected out of the sample of interactions for which at least one particle with  $Z = 1$  or  $Z = 2$  was emitted at a small angle  $< 3^\circ$  / with respect to the primary particle direction.

The cross section for proton - stripping reaction was obtained and the relative frequencies of inclusive reactions  ${}^4\text{He} + \text{Nucleus} \rightarrow ({}^4\text{He}, {}^3\text{He}, {}^3\text{H}, {}^2\text{H}, {}^1\text{H}) + \text{anything}$  were estimated for the standard emulsion nuclei as  $\alpha$  targets

VI.B.2

ANALYSIS OF QUASI-ELASTIC KNOCKOUT OF ALPHA PARTICLES  
FROM  $^{16}\text{O}$  AND  $^{28}\text{Si}$  BY 0.65 AND 0.85 GeV ALPHA PARTICLES

N. Chirapatpimoi, J.C. Fong, M.M. Gazzaly, G.J. Igo, A.D. Liberman,  
S.L. Verbeck, C.A. Whitten,  
*University of California, Los Angeles*

J. Arvieux, V. Perez-Mendez,  
*Lawrence Berkeley Laboratory,*

M. Matoba  
*Centre d'Etudes Nucléaires de Saclay*

and N. Chant, P. Roos  
*University of Maryland*

An analysis is in progress of quasi-elastic data taken in a coplanar geometry with angular settings  $(\theta_1, \theta_2)$  for the two arms of the detection system of  $(31^\circ, 57^\circ)$ ,  $(36^\circ, 51^\circ)$  and  $(43.5^\circ, 43.5^\circ)$ . The acceptances of the two arms are  $\Delta\Omega_1 \approx 5$  msr and  $\Delta\Omega_2 \approx 60$  msr. We are using both the plane wave impulse approximation (PWIA) and the distorted wave impulse approximation (DWIA). The measured differential cross sections  $d\sigma/d\Omega$  were obtained by integrating over  $\Delta\Omega_2$ , integrating over the momentum spectrum measured by the detector arm at  $\theta_1$ , and by summing over the excitation energy of the residual nucleus. Experimental results are : 1) at 0.85 GeV,  $d\sigma/d\Omega$  for  $^{16}\text{O}$  is 2.5 times larger than for  $^{28}\text{Si}$  at  $(\theta_1, \theta_2) = (36^\circ, 51^\circ)$ ; 2) for  $^{16}\text{O}$ ,  $d\sigma/d\Omega$  at  $(43.5^\circ, 43.5^\circ)$  at 0.65 GeV is 4 times larger than at 0.85 GeV. Using PWIA,  $d\sigma/d\Omega$  was calculated making the assumption that the off-energy shell  $\alpha$ - $\alpha$  cross section is equal to the measured on-shell  $\alpha$ - $\alpha$  cross section. This is justified because the measured variation of  $\alpha$ - $\alpha$  scattering as a function of momentum transfer at fixed incident energy, and as a function of incident energy at fixed momentum transfer is consistent with a few percent correction resulting from the use of on-shell  $\alpha$ - $\alpha$  cross sections. The wave functions for the ( $\alpha$ -cluster + residual core) system was calculated using a square well potential. A single parameter,  $N_{\text{eff}}$ , which is the effective number of alpha particles, was adjusted to bring the calculation into best agreement with  $d\sigma/d\Omega$ . Good fits were obtained for both targets ; the results for  $^{16}\text{O}$  at 0.85 GeV is shown in the figure. The values of  $N_{\text{eff}}$  are  $0.34^{+0.09}_{-0.05}$  and  $0.20 \pm 0.10$  for  $^{16}\text{O}$  and  $^{28}\text{Si}$  respectively. Fits to  $d\sigma/d\Omega$  employing DWIA will be reported. The effect of distorted waves is determined from analysis of  $\alpha$ - $^{12}\text{C}$  elastic scattering at  $T_\alpha = 104, 139, 147, 166$  and  $1370$  MeV. A straight line interpolation of the volume integrals,  $J_R$  and  $J_I$ , for real and imaginary parts of the potential plotted against  $\ln T_\alpha$  is consistent with the optical model analyses of the elastic scattering data. Values of  $J_R$  and  $J_I$  for  $200 < T_\alpha < 850$  MeV are needed in this analysis. In this interval,  $J_R$  decreases to nearly zero and  $J_I$  is constant. Thus except for the lowest energy alphas observed, the distortive effect is mainly due to attenuation.

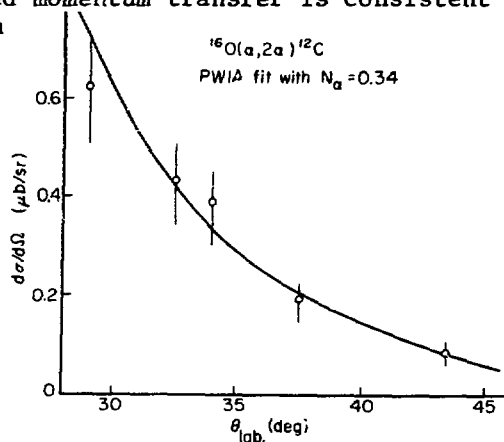


Fig. 1 Data and PWIA Analysis for the  $^{16}\text{O}(\alpha, 2\alpha)^{12}\text{C}$  Reaction at 0.85 GeV.

$^{16}\text{O}$ -Emulsion Nucleus Interactions at 0.15-0.2 and 2 GeV/n

B. Jakobsson, K. Kristiansson, R. Kullberg, B. Lindkvist  
and I. Otterlund.

Department of Physics, University of Lund, Lund, Sweden.

Emulsion stacks were exposed to the  $^{16}\text{O}$ -beam of the Berkeley Bevatron at 250 MeV/nucleon (Ilford G5) and 2.1 GeV/nucleon (Ilford K2) in 1972.

So far we have obtained about 1900 events induced by  $^{16}\text{O}$  in the energy interval 200-150 MeV/nucleon. The purpose of this investigation is to determine the fragmentation cross sections of multiply charged fragments at an energy which is one order of magnitude below the energy in a similar study made at the Berkeley Bevatron with a magnetic spectrometer. The charge of a fragment is determined by photometric measurements of the last 3.5 mm of the track.  $^{16}\text{O}$  and  $^{12}\text{C}$  tracks from the beam are used for calibration. Fragmentation cross-sections will be presented at the conference.

269 interactions have been studied at 2.0 GeV/nucleon. We have found that C-, N- and O-isotopes as well as He-isotopes in events with three He-particles (Fig. 1a) show Gaussian transverse momentum distributions and thus confirm the results found by the Heckman-group, Berkeley. On the other hand the momentum distributions of He-isotopes in reactions with one or two He-particles deviate considerably from this picture (Fig. 1b). He-isotopes with large transverse momenta are emitted. The largest emission angle observed is  $13.5^\circ$  corresponding to a momentum transfer to the He-cluster of about 700 MeV/c per nucleon.

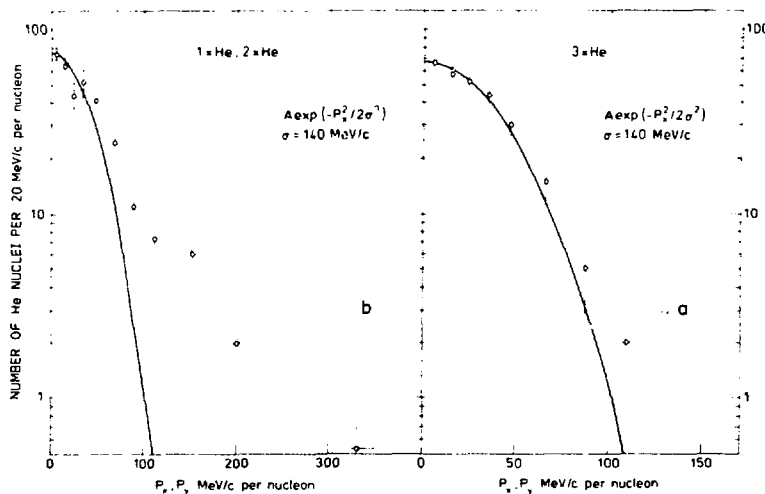


Fig. 1. Transverse momentum distribution for He-isotopes emitted from  $^{16}\text{O}$  at 2 GeV/nucleon.

PION PRODUCTION IN NUCLEUS-NUCLEUS COLLISIONS\*

VI.B.4

L. S. Schroeder  
Lawrence Berkeley Laboratory  
University of California  
Berkeley, California 94720

Current experimental and theoretical work on pion production in high-energy nucleus-nucleus collisions is reviewed. The majority of existing data are of the inclusive variety in which a single final state pion is detected. Experimental data are compared and their possible contributions to obtaining new information on nuclear structure is discussed. Various models which attempt to explain the observed single-inclusive-pion spectra either on the basis of a nucleon-nucleus interaction in which Fermi motion is included or on some type of cooperative model are examined. Other areas of interest involving pion production include tests of charge symmetry and pion multiplicities.

\*Work done under the auspices of the U. S. Energy Research and Development Administration.

## MULTIPLE-DIFFRACTION EXPANSION FOR INTERMEDIATE-ENERGY REACTIONS

C. W. Wong and S. K. Young  
Department of Physics, University of California  
Los Angeles, California 90024\*

## ABSTRACT

A multiple-diffraction expansion for heavy-ion reactions is constructed in which the leading term is Glauber's phenomenological multiple-diffraction amplitude. This is achieved with the help of a pseudopotential between elementary particles in ions which in the Glauber approximation gives the empirical elementary scattering amplitude. The leading corrections to Glauber's phenomenological amplitude include (i) a wave-spreading term of Wallace, (ii) an internal-excitation term of Hahn, (iii) a pseudopotential term which contains effects of wave spreading and zero-point motion of bound particles in ions, and (iv) a Pauli term for antisymmetrizing two clusters of identical fermions. Explicit expression for these corrections are given in the impact-parameter representation. The nature of these corrections is briefly discussed. Other corrections which have to be included in realistic calculations will be mentioned.

\* Work supported in part by the National Science Foundation.

( $\alpha, \alpha'$ ) SCATTERING ON  $^{12}\text{C}$  AT 1.37 GeV

VI.B.6

T. Bauer, R. Bertini<sup>†</sup>, A. Boudard, G. Bruge,  
H. Gatz, A. Chaumeaux, H. Duhm<sup>††</sup>, J.M. Fontaine,  
D. Garetta, V. Layly, J.C. Lugol and R. Schaeffer

*CEN Saclay, BP 8, 91190, Gif-sur-Yvette, France.*

Elastic and inelastic scattering of 1.37 GeV  $\alpha$ -particles have been measured by means of the SPES I magnetic spectrometer facility. The  $\alpha$ -particles were accelerated by the synchrotron Saturne. Angular distributions have been measured in a  $3\text{--}15^\circ$  angular range for the ground and the first three excited states in  $^{12}\text{C}$ . The energy resolution was 400-700 keV. Calculations have been performed in the framework of the Kerman, McManus and Thaler formalism. The nucleon- $\alpha$  amplitudes have been calculated from the nucleon-nucleon data at  $T = T_\alpha/4$  i.e., 350 MeV by means of the Glauber model and checked on the experimental  $p\text{--}^4\text{He}$  data at the same energy.

<sup>†</sup> CRN Strasbourg (France)

<sup>††</sup> Institut für Experimental Physik Hamburg (Germany).

Heavy Ion Collisions at ISR Energies: Possibilities for Experimental Study

H. G. Pugh

Department of Physics, University of Maryland, College Park, MD 20742

There has been great excitement generated recently by the development of heavy-ion beams in the region of 2 GeV/nucleon, particularly at the Bevalac. At the same time the strikingly original theoretical work of Lee and Wick and of Chapline, et al. has provided strong motivation for work in this area. It is the purpose of the present paper to emphasize that heavy ion studies at much higher energies are a practical possibility for the near future and to urge that these possibilities be taken seriously in the planning and development of new and existing accelerator facilities.

The basic observation is that heavy ion collisions at vastly increased energies can be obtained using existing intersecting storage ring facilities. This was suggested as a possibility by Gottfried at the last conference in this series. Fully-stripped heavy ions in the CERN ISR would provide equivalent energies of about 300 GeV/nucleon and any new storage ring facility at 400 GeV would provide an equivalent energy of about 50,000 GeV/nucleon. Studies at CERN indicate that injection of deuterons or alpha-particles could be achieved almost immediately while injection of light ions up to Carbon or Nitrogen will require only moderate development effort. Injection of fully stripped Uranium ions is at present still a dream. However, for concreteness the following remarks will be focused on fully stripped Uranium collisions;

(1) Predictions of the interactions are extremely difficult and the main difficulties lie in lack of knowledge of the strong interaction itself: the studies will therefore cast light on the nature of the strong interaction.

(2) The general behavior of the collision is dominated by its extreme relativistic nature. At 300 GeV/nucleon the entire nucleus is compressed longitudinally into about 1/50 the thickness of a proton. Many nucleons will therefore interact at once with any nucleon in the other nucleus.

(3) For many features of the interaction the thermodynamic predictions of Landau may be the most reliable. Here the Uranium nucleus is treated like a large proton since it has about the same density. Scaling from ISR results for p-p collisions then permits some predictions to be made for U-U collisions.

It is suggested that the exploratory studies should be conducted with experimental configurations that are identical to those used for studies of p-p collisions. A comparison might be made of p-p, p-H.I. and H.I.-H.I. collisions at the same GeV/nucleon. Pion multiplicities in the central region might be studied: the Landau model predicts about 600 pions produced per collision for U-U at the ISR. Inclusive distributions should be studied. Streamer chamber studies of individual events should be made. It is remarkable to consider that with 1000 or so particles emitted in each interaction, angular distributions with good statistics will be measurable for individual events.

According to this preliminary program the only important changes in the high-energy physics program would be additional work at the injector end of the facilities and devotion of a limited part of running time to heavy-ion beams. The extra effort would be most appropriate at the more complex facilities such as CERN where beams from the PS, SPS and ISR would provide a very wide range of energies and experimental setups for a relatively minor additional expenditure.



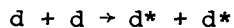
VI.B.8

Observation of Double Spectator Process in the D + D Reaction

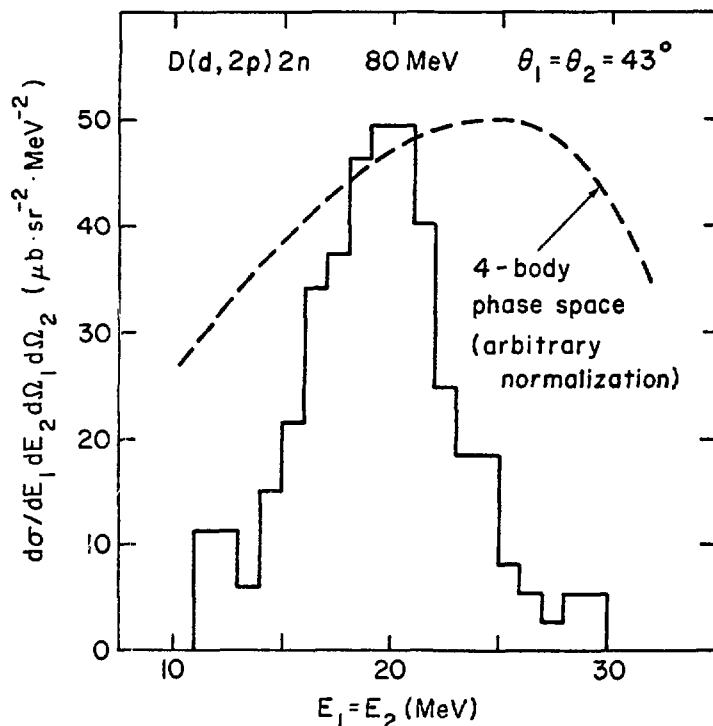
B.Th. Leemann, H.G. Pugh, N.S. Chant, C.C. Chang  
 Physics Department, University of Maryland, College Park, Md. 20742

In the d + d collision at suitably high energy an important part of the reaction may occur through collision between a single nucleon in the projectile deuteron and a single nucleon in the target deuteron. In this process the non-participating nucleons in the projectile and the target would each act as spectators and the cross-section is expected to be largest when each of the spectators has in the final state half of the initial momentum of the deuteron from which it originated.

For exploratory studies we have used the University of Maryland Cyclotron to bombard a deuterium gas target with 80 MeV deuterons. We detected outgoing proton pairs at equal angles  $\theta_1, \theta_2$  on opposite sides of the beam direction and measured their energies  $E_1, E_2$  with silicon counter telescopes. We observe a strong enhancement above four-body phase space near  $\theta_1 = \theta_2 = 43^\circ; E_1 = E_2 = 18$  MeV. The enhancement is observed both in the angular correlation and in the energy spectra. The figure shows the cross-section and four-body phase space for  $\theta_1 = \theta_2 = 43^\circ$  and for  $E_1 = E_2 = E$  plotted as a function of  $E$ . Analysis of the details of the enhancement are in progress. Apart from the double spectator process a narrow enhancement in this region of phase space might be expected to arise from the excitation of each deuteron to the  $S = 0, T = 1$  virtual state, i.e.



In this case the detected protons arise from the decay of the two virtual deuterons.



Bruce Cork  
Lawrence Berkeley Laboratory  
University of California  
Berkeley, California 94720 U.S.A.

## ABSTRACT

Nuclei with energies of several GeV/n interact with hadrons and produce fragments that encompass the fields of nuclear physics, meson physics, and particle physics. Experimental results are now available to explore problems in nuclear physics such as a) the validity of the shell model to explain the momentum distribution of fragment, b) the contribution of giant resonances to fragment production cross sections c) the effective coulomb barrier d) nuclear temperatures. A new approach to meson physics is possible by exploring the nucleon charge exchange process. Particle physics problems are explored by a) measuring the energy and target dependence of isotope production cross sections, thus determining if limiting fragmentation and target factorization are valid, b) measuring total cross sections to determine if the factorization relation

$$\sigma_{AB}^2 = \sigma_{AA} \cdot \sigma_{BB} \text{ is violated.}$$

c) determining the angular distribution of fragments that could be explained as nuclear shock waves. New experiments have been proposed to explore for abnormal matter produced by very heavy ions incident on heavy atoms.

W. Dollhopf and C. F. Perdrisat  
Physics Department, College of William and Mary  
Williamsburg, Virginia  
and  
P. Kitching and W. C. Olsen  
Nuclear Research Centre, University of Alberta  
Edmonton, Canada

In a recent experiment at the Space Radiation Effects Laboratory\* the cross section  $d^5\sigma/dT_{\alpha 1} d\Omega_{\alpha 1} d\Omega_{\alpha 2}$  has been measured<sup>1</sup> with a magnetic spectrometer-range telescope arrangement. Using an interpolated value from data at 650 MeV and 825 MeV for the elastic cross section recently obtained by Ridge e.a.,<sup>2</sup> the recoil momentum distribution  $|\phi(q)|^2$  was then calculated on the basis of the Plane Wave Impulse Approximation.

To compare the  $\alpha$ -d momentum distribution thus obtained with results from different experiments, we used the Chew-Low plot. As was shown by Ghovanlou and Prats,<sup>3</sup> with that method the data from  ${}^6\text{Li}(p, pd)$  at 156 MeV<sup>4</sup> and at 590 MeV<sup>6</sup> are compatible with each other and with the pole approximation result  $|\phi(q)|^2 = \kappa/\pi^2(q^2 + \kappa^2)^2$  for  $q \lesssim 60$  MeV/c. Here  $\kappa = (2\mu B)^{1/2}$ , where  $\mu$  is the reduced mass of the  $\alpha$ -d system and  $B = 1.47$  MeV is the separation energy for  ${}^6\text{Li} \rightarrow \alpha + d$ .

The distribution  $|\phi(q)|^2$  obtained in the present experiment is again compatible with the two results from ref. 4 and 5 and with the pole approximation. Interpreted in terms of  $\alpha$ -d clustering probability  $n_{\alpha d}$ , where  $(n_{\alpha d})^{1/2}$  is the normalization constant in the pole wave function  $\psi(r) = (n_{\alpha d})^{1/2} (\kappa/2\pi)^{1/2} \exp(-\kappa/r)r$ , the 3 experiments give  $n_{\alpha d} = 1.31, 1.07$  and  $1.00$  for ref. 4, ref. 5 and the present results, respectively.

Further comparison with low energy  $(p, p\alpha)$ <sup>6</sup> and with  $(\pi^-, 2n)$ <sup>7</sup> and  $(\pi^+, 2p)$ <sup>8</sup> experiments leads to an interesting convergence of these numerous attempts to ascertain the  $\alpha$ -d content of  ${}^6\text{Li}$ .

\* supported in parts by the National Aeronautics and Space Administration, the National Science Foundation and the Commonwealth of Virginia.

1. W. Dollhopf, e.a., Bull. Am. Phys. Soc. 19, 43 (1974).
2. R. J. Ridge, G. J. Igo, and A. D. Liberman, Bull. Am. Phys. Soc. 20, 83 (1975).
3. A. Ghovanlou and F. Prats, Phys. Rev. C 10, 1300 (1974).
4. D. Bachelier, Ph.D. thesis, U. Paris-Sud, Orsay, unpublished (1971).
5. P. Kitching, e.a., Phys. Rev. C 11, 420 (1975).
6. M. Jain, e.a., Nucl. Phys. A 153, 49 (1970).
7. H. Davies, e.a., Nucl. Phys. 78, 663 (1966).
8. E. D. Arthur, e.a., Phys. Rev. C 11, 332 (1975).

## FRAGMENTATION OF RELATIVISTIC HEAVY IONS

Herman Feshbach

Laboratory for Nuclear Science and Department of Physics  
Massachusetts Institute of Technology  
Cambridge, Massachusetts 02139

## ABSTRACT

The cross-section for fragmentation of a relativistic heavy ion projectile has been calculated. In the rest frame of the projectile, the effective time dependent potential acting on a nucleon or cluster in the projectile is assumed to arise from a Lorentz contracted target moving in a straight line with constant velocity. The excitation of the projectile to an energy  $\hbar\omega$  is shown to be produced by the component of this potential with frequency  $\omega$ . Longitudinal momentum transfer is neglected but the effect of the transverse momentum change, assumed to be small, is included. The dependence of the cross-section on the target mass number  $A_T$  is found to be approximately  $A_T^{.27}$ .

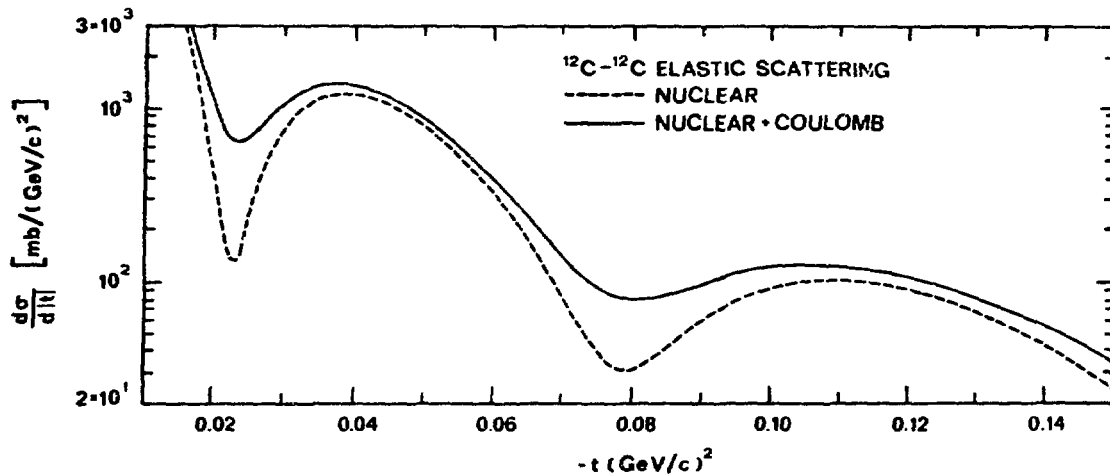
Girish K. Varma and Victor Franco  
Physics Department, Brooklyn College of the City University  
of New York, Brooklyn, New York 11210

The diffraction minima which occur in the elastic scattering intensities in high energy hadron-nucleus collisions are very sensitive to  $\rho$ , the ratios of real to imaginary parts of the hadron-nucleon forward scattering amplitudes. Hence, for simple nuclear targets, the scattering measurements near the minima can be used to estimate  $\rho$ .<sup>1</sup> However, the Coulomb effects are also significant at the minima and must be accurately included. By performing exact calculations within the diffraction theory, we have investigated the accuracy of the various approximate formulae which have been used in the past. We find that the point charge approximation<sup>2</sup> for each proton in the target is fairly accurate if the ratios  $\rho$  are different from zero. If  $\rho$  is very small, this approximation may lead to errors up to  $\sim 8\%$  near the minima. The other approximations, where the Coulomb effects are considered to originate from the nucleus as a whole, lead to much larger errors.

We have also studied the problem of incorporating the extended charge Coulomb effects in the heavy-ion collisions, in the "optical limit" of the theory. For collisions between light nuclei, the results are reduced to the evaluation of a single integral. Contrary to the belief that the Coulomb effects are important only at very small angles and near the minima, we find that they are significant even at the maxima, increasing the cross sections by  $\sim 15-20\%$ , for example, for  $^{12}\text{C}-^{12}\text{C}$  collisions at 2.1 GeV/nucleon. Our expressions can also be used to include the Coulomb effects in the Chou-Yang model where it has been suggested<sup>3</sup> that  $\rho$  can be treated as a free parameter to be determined by fitting the scattering data.

\* Work supported in part by the National Science Foundation.

1. W. Czyż, in *Advances in Nuclear Physics*, edited by M. Baranger and E. Vogt (Plenum, New York, 1971), vol. 4.
2. H. Lesniak and L. Lesniak, *Nuc. Phys.* B38, 221 (1972).
3. W. L. Wang and R. G. Lipes, *Phys. Rev.* C9, 814 (1974).

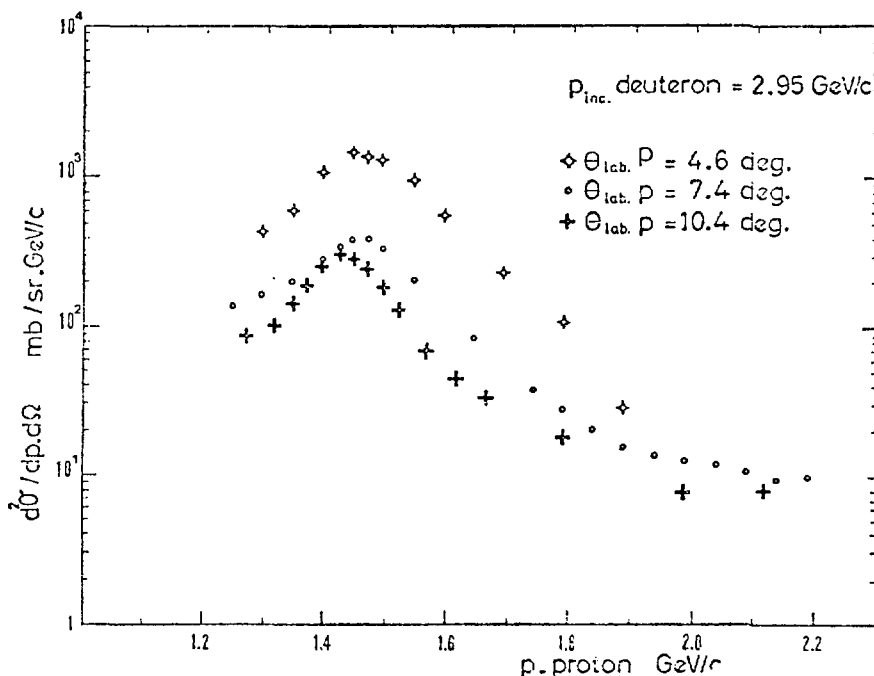


DEUTERON BREAK-UP ON PROTON AT 2.95 GeV/c

J.Banaigs, J.Berger, L.Goldzahl, L.Vu-Hai  
 CNRS et Département Saturne, CEN Saclay, France  
 M.Cottureau, C.Le Brun  
 Laboratoire de Physique Corpusculaire Université de Caen,  
 France  
 F.L.Fabbri, P.Picozza  
 Laboratori Nazionali di Frascati del CNEN, Italy

The reaction  $dp \rightarrow pX$  has been studied at the Saclay synchrotron Saturne. The use of a deuteron beam allows one to have small losses of the spectator nucleons due to favorable conditions of their observation. The aim of this experiment is to look, from the point of view of the impulse approximation, for the spectator distribution in the deuteron.

The figure shows, for three laboratory angles, the inclusive proton momentum spectra for which the possible spectator momentum in the deuteron system ranges from 120 to 450 MeV/c. These spectra include the contribution of p-p interaction and the intermixing of the d-p channels. Preliminary results of the analysis show an excess high-momentum spectators, which cannot be explained by multiple scattering only.



$^3\text{He}$  PRODUCTION FROM 6.9 GeV/c  $^4\text{He}$  BREAK UP ON HYDROGEN TARGET

J. Berger, J. Duflo, L. Goldzahl, J. Oostens\*, F. Plouin, M. Van den Bossche\*, L. Vu Hai\* - CNRS et Département Saturne Saclay, France  
 G. Bizard, C. Le Brun - Université de Caen, France  
 F. L. Fabbri, P. Picozza, L. Satta - Laboratori Nazionali di Frascati del CNEN, Italy

$^3\text{He}$  momentum spectra were taken at angles  $0^\circ < \theta_{\text{lab}} < 11^\circ$ . Their general shape is a broad peak centered roughly at  $3/4$  of the incoming momentum, suggesting a quasi two body reaction widened by Fermi motion.

Fig. 1 shows the integrated cross section as function of  $\cos\theta_{\text{lab}}$ . At small angles the slope is compatible with what is expected from knocking a neutron out of the  $^4\text{He}$ , the  $^3\text{He}$  acting as a spectator. The momentum and angle distribution thus reflects the Fermi momentum of the neutron in the  $^4\text{He}$  (Fig. 1, dotted line).

At larger angles the shift of the peak toward lower momentum is larger than predicted by the knock out kinematics (Fig. 2). The observed shift is compatible with the elastic scattering on protons of  $^3\text{He}$  at  $3/4$  of the incoming momentum suggesting the existence of a  $^3\text{He}$  component in the  $^4\text{He}$  wave function.

\* Supported by the Département Saturne.

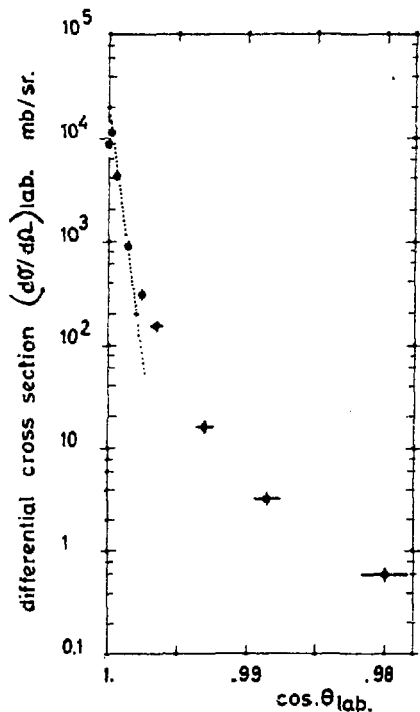


Fig. 1

dotted line - knock out calculation using a gaussian  $^4\text{He}$  wave function with a radius  $R=1.25$  Fermi.

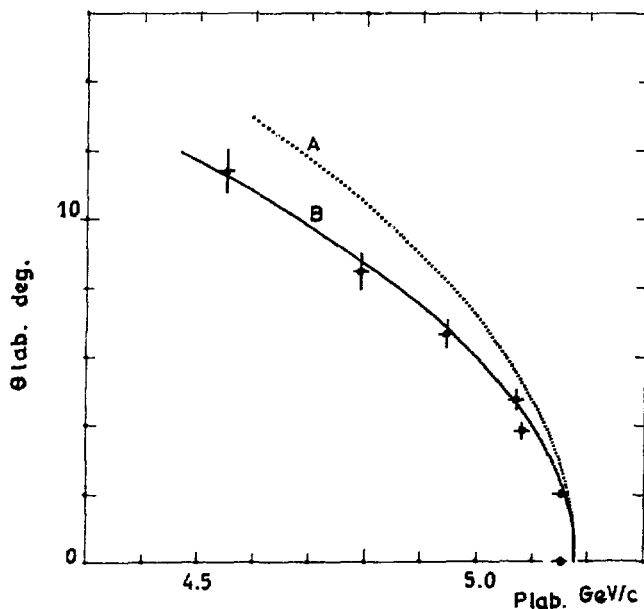


Fig. 2

Angle - momentum peak position for two hypothesis  
 A - Knock out.  
 B - Elastic  $^3\text{He}$ -p scattering.

J.Berger, J.Duflo, L.Goldzahl, F.Plouin - CNRS, Département Saturne Saclay, France  
 J.Oostens, M.Van den Bossche, L.Vu Hai - CEA, Département Saturne Saclay, France  
 G.Bizard, C.Le Brun - Laboratoire de Physique Corpusculaire Université de Caen, France  
 F.L.Fabbri, P.Picozza, L.Satta - Laboratori Nazionali di Frascati del CNEN, Italy

Existence of baryonic excited states inside nuclei have been proposed for some time<sup>1</sup>. The reaction  ${}^4\text{He} + p \rightarrow {}^3\text{He} + d$  (1) can be related to p-d backward elastic scattering (see insert in fig 2) where  $N^*$  components of the deuteron have shown to play some role<sup>2</sup>. The interest in studying (1) at higher energy than existing data, is to point out the contribution of exchanged baryonic excited states present inside  ${}^4\text{He}$  nuclei.

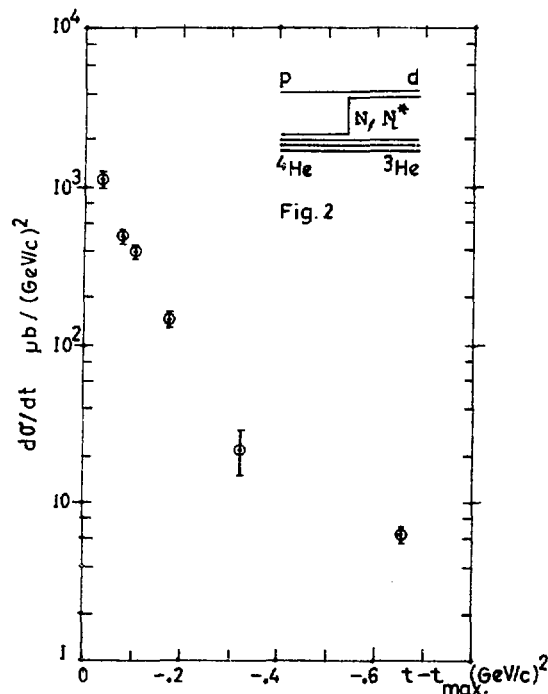
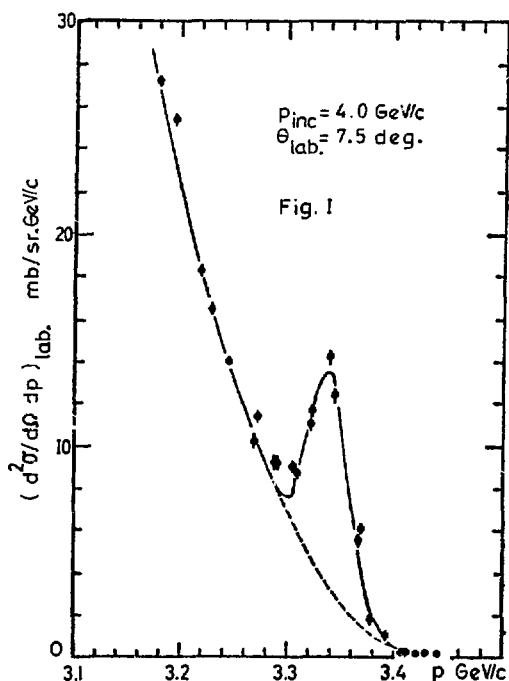
Evidence for reaction (1) appears in our data as a sharp peak at upper end of the  ${}^3\text{He}$  momentum spectrum measured with our spectrometer system. Fig 1 shows a typical peak, centered at the kinematical predicted position. The width, 30 MeV/c, is consistent with our experimental resolution ( $\Delta p/p = 1\%$  FWHM).

Cross sections presented in fig 2 have been obtained by integrating the peak with allowance for a smooth background subtraction.

<sup>1</sup> A.K.Kerman and L.S.Kislinger Phys. Rev. 180 (1969) 1483.

<sup>2</sup> L.Dubal et al Uppsala Conference (1973) p.209.

<sup>3</sup> M.Bernas et al Phys. Let. 25B (1967) 260.



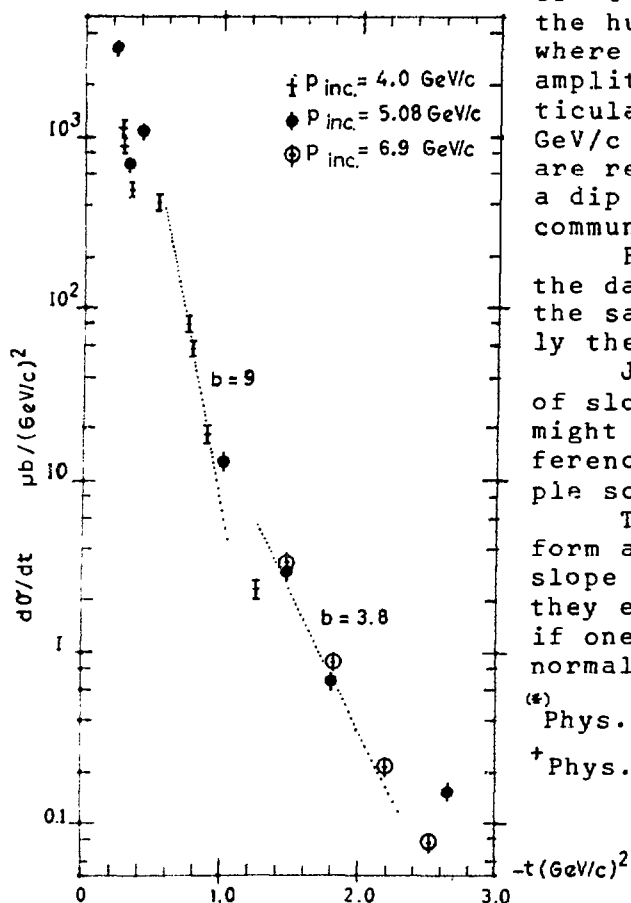


ALPHA - PROTON ELASTIC SCATTERING IN THE FORWARD HEMISPHERE  
IN THE MOMENTUM RANGE FROM 4.0 TO 6.9 GeV/c

J. Berger, J. Duflo, L. Goldzahl, F. Plouin - CNRS, Département Saturne Saclay, France  
 J. Oostens, M. Van den Bossche, L. Vu Hai - CEA, Département Saturne Saclay, France  
 G. Bizard, C. Le Brun - Laboratoire de Physique Corpusculaire Université de Caen, France  
 F. L. Fabbri, P. Picozza, L. Satta - Laboratori Nazionali di Frascati del CNEN, Italy

Exploratory measurements have been taken with the same spectrometer system used in the preceding experiments<sup>(\*)</sup>. They cover the yet unexplored region of  $-t$  in the 1. to 2.5 (GeV/c)<sup>2</sup> range, and overlap in some kinematical regions with data on p-<sup>4</sup>He reported by Saclay's SPES-1 at this conference.

Data at three incident momenta appear to show only a modest dependence in  $s$  of the invariant cross section  $d\sigma/dt$ , (see fig.).



As one considers the region of  $-t$  up to 0.6 (GeV/c)<sup>2</sup> one finds the humpy behavior at the  $-t$  value where single and double scattering amplitudes are comparable. In particular, the four points at 5.08 GeV/c (646 MeV equivalent in p-<sup>4</sup>He) are reminiscent of the existence of a dip in the SPES-1 data (private communication) at 650 MeV.

From  $-t$  between 0.6 and  $\sim 1.2$ , the data at 4.0 and 5.08 GeV/c have the same slope, and indeed practically the same values.

Just above  $-t=1.2$ , the change of slope in the 5.08 GeV/c data might be indicative of some interference between the double and triple scattering amplitudes.

The four points at 6.9 GeV/c form a straight line with the same slope as in existing data<sup>†</sup>, which they extend up to  $-t=2.5$  (GeV/c)<sup>2</sup> if one allows for appropriate cross-normalization.

<sup>(\*)</sup> Phys. Lett. **43** B, 535 (1973)

<sup>†</sup> Phys. Rev. Letters **32**, 839 (1974)

ALPHA - PROTON ELASTIC SCATTERING IN THE BACKWARD HEMISPHERE  
IN THE MOMENTUM RANGE FROM 3.2 TO 5.08 GEV/C

J. Berger, J. Duflo, L. Goldzahl, J. Oostens\*, F. Plouin, M. Van den Bossche\*, L. Vu Hai\* - CNRS et Département Saturne Saclay, France  
 G. Bizard, C. Le Brun - Laboratoire de Physique Corpusculaire  
 Université de Caen, France  
 F. L. Fabbri, P. Picozza, L. Satta - Laboratori Nazionali di  
 Frascati del CNEN, Italy

Elastic Proton- $^4\text{He}$  interaction has been studied by means of an alpha particle beam produced by the Saclay synchrotron Saturne impinging on a liquid hydrogen target. The elastically scattered alphas are momentum analysed and identified in a spectrometer system.

The very fact that an intact  $^4\text{He}$  nucleus is detected considerably alleviates the task of discriminating against inelastic reactions.

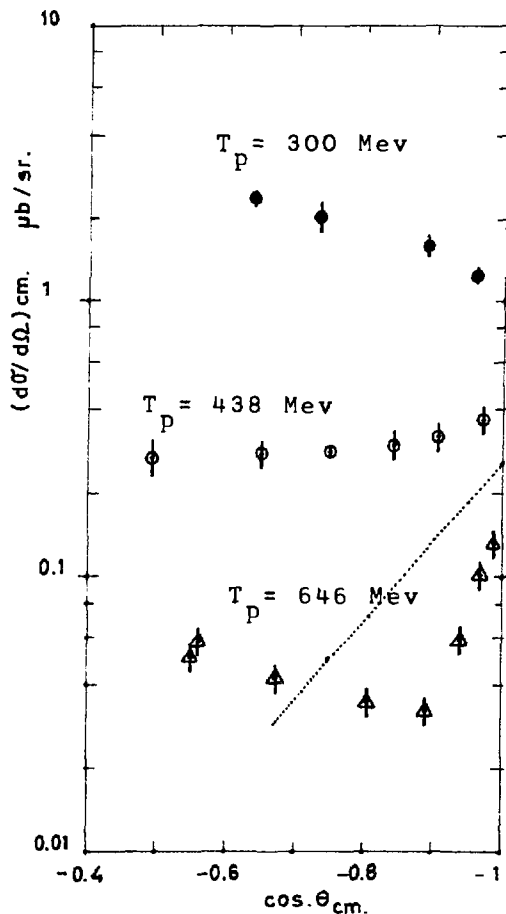
The cross sections are presented in the figure. Data have also been labeled with the proton energy corresponding to the alternate way of looking at the reaction.

The most striking feature revealed by the data is the change of shape as the incoming momentum is increased. A rise in the backward cross section appears at 4.0 and becomes much more pronounced at 5.08 GeV/c.

Such a behavior is in qualitative agreement with the one existing calculation at 5.16 GeV/c (665 MeV protons)<sup>†</sup> where a tribaryon exchange mechanism is assumed. It is shown as a dotted line in the figure.

<sup>†</sup>B.Z. Kopeliovich and I.K. Potashnikova, Sov. J. Nucl. Phys. 13 (1971) p. 592

\* Supported by the Département Saturne.



◆ -  $P_{in\alpha} = 3.2 \text{ GeV/c}$   
 ○ -  $P_{in\alpha} = 4.0 \text{ GeV/c}$   
 △ -  $P_{in\alpha} = 5.08 \text{ GeV/c}$

Dotted line - Kopeliovich and Potashnikova calculation at  $T_p = 665 \text{ MeV}$

ALPHA - PROTON INTERACTION AT 4 GEV/C

F.L.Fabrizi, P.Picozza, L.Satta - Laboratori Nazionali di Frascati del CNEN, Italy  
 J.Berger, J.Duflo, L.Goldzahl, F.Plouin - CNRS, Département Saturne Saclay, France  
 J.Oostens, M.Van den Bossche, L.Vu Hai - CEA, Département Saturne Saclay, France  
 G.Bizard, C.Le Brun - Laboratoire de Physique Corpusculaire, Université de Caen, France

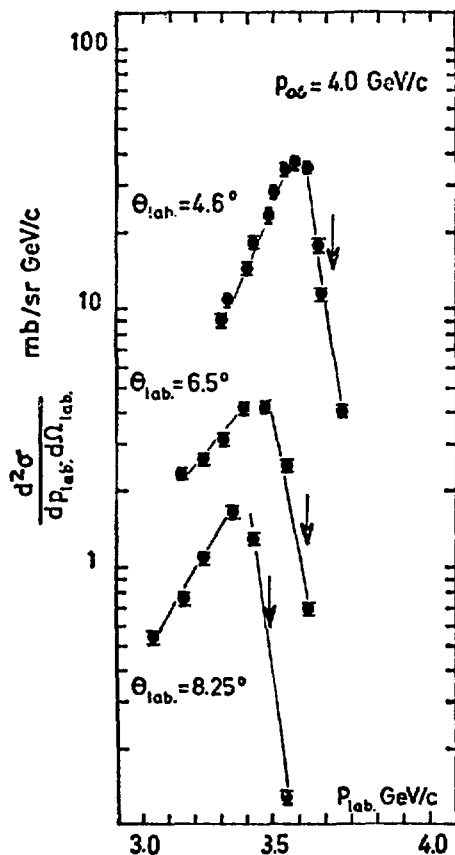
The external alpha beam of the Saclay Saturne synchrotron has been used to study the reaction  ${}^4\text{He}+p\rightarrow{}^4\text{He}+X$  where the  ${}^4\text{He}$  is detected in a magnetic spectrometer.

The use of an incident alpha beam rather than a stationary  ${}^4\text{He}$  target allows the easy detection of the intact helium nucleus, as it has momentum that gets closer to the incident one as the momentum transfer gets smaller.

Spectra corresponding to missing masses between 1050 and 1220  $\text{MeV}/c^2$  have been measured at laboratory angles  $\theta = 4.6^\circ, 6.5^\circ$  and  $8.2^\circ$ . An enhancement, 60  $\text{MeV}/c^2$  wide centered at 1130  $\text{MeV}/c^2$  is clearly seen at all angles. Its peak value decreases rapidly with the momentum transfer, ( $0.13 \leq t \leq 0.75 [\text{GeV}/c]^2$ ).

The missing object X is constrained to be in a pure  $T=1/2$  isospin state. Such an enhancement is similar to the peak observed in the  $d+p\rightarrow d+X$  reaction† where X is also constrained to be in a  $T=1/2$  state excluding the  $\Delta$ .

† Physics Letters 45 B, 535, 1973.



the arrow indicates the kinematical threshold for the coherent  $\pi$  production at each angle.

Philip J. Siemens and Jakob P. Bondorf  
The Niels Bohr Institute, Copenhagen, Denmark

Michael I. Sobel and H. A. Bethe  
NORDITA, Copenhagen, Denmark

We consider the circumstances under which matter at high densities can be produced in heavy ion collisions. We argue that laboratory energies of a few hundred MeV per nucleon will be suitable: the matter velocity will exceed the speed of sound, while the nuclear matter has sufficient stopping power to generate a shock front. A measure of the stopping power is the momentum transport length  $\lambda(p)$ ; if  $\lambda(p)$  is comparable to or exceeds the nuclear radius, the nuclei will interpenetrate instead of compressing. The hydrodynamic conservation laws can be written in the form

$$\begin{aligned} \frac{1}{2} m (\vec{v}_0 - \vec{v}_s)^2 &= \left( \frac{v-1}{v} \right)^2 \frac{1}{2} m (\vec{v}_0 \cdot \vec{n} - U)^2 \\ &= \epsilon_s - \epsilon_0 = \frac{1}{2\rho_0} \frac{v-1}{v} p_s \end{aligned}$$

where  $\epsilon_s$ ,  $p_s$ ,  $\vec{v}_s$  are the internal energy per nucleon, pressure, and mean velocity of the matter just inside the shock front,  $\rho_0$  and  $\vec{v}_0$  the internal energy and velocity of the cold, unshocked matter,  $U = Un$  is the shock front velocity, and  $v = \rho/\rho_0$  is the compression ratio. There is a maximum compression ratio given in terms of the internal energy  $\hat{\epsilon}$  and pressure  $\hat{p}$  of cold matter at density  $\rho_s$  by the expression  $v_\infty = 2 R_s + 1$  where  $R_s = \rho_s(\epsilon_s - \hat{\epsilon}) / (p_s - \hat{p})$  describes how the energy converted to heat produces a thermal pressure which resists compression.

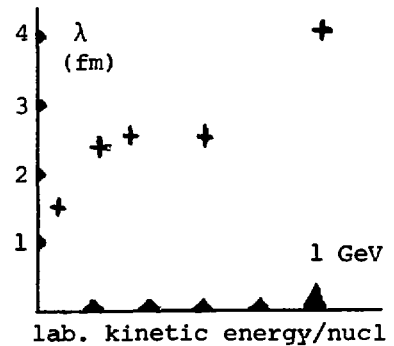


Table. Model predictions for the maximum compression

degrees of freedom	maximum compression $v_\infty$
non-relativistic point particles	4
non-relativistic translation + rotation	6
relativistic translation motion	7
massless bosons	
Landau Fermi-liquid theory	$\left[ \frac{1}{3} - \frac{\partial \ln n^*(v)}{\partial \ln v^2} \right]^{-1} + 1$

From the table, it is seen that  $v_\infty$  is determined by the kinematic character of the degrees of freedom; however,  $v_\infty$  is not a differential but an integral quantity and can become very large when phase transitions introduce new degrees of freedom. Under disintegration of the compressed matter, a mean asymptotic speed is attained

$$\langle v_{\text{asym}} \rangle = \int_{v_{\text{min}}}^v c_s(v', S) dv' / v'$$

where  $c_s(v, S)$  is the speed of sound and the specific entropy  $S$  remains constant under the decompression, as long as the fluid is dense enough to remain thermally equilibrated,  $v \geq v_{\text{min}}$ .

With laboratory energies near 1 GeV/nucleon, pions will be produced in the shock front, but the hot matter will explode long before the pion concentration reaches equilibrium (assuming the nuclear forces are repulsive at high density). We expect the number of pions to be sensitive to the details of the structure of the shock front.

R. Weiner and M. Weström  
Fachbereich Physik, Univ. Marburg, W.Germany

A theory for preequilibrium phenomena in nuclear physics is formulated in terms of propagation of temperature and heat conductivity in n.m. which is treated in the Fermi gas approximation with binary collisions. We consider peripheral collisions with momentum transfers to the target  $q \gg R^{-1}$  ( $R$  is the radius of the target). In accordance with quantum mechanics a localization of excitation near the surface of the target should then be possible. These "hot spots" define the initial condition with which we solve the equation of heat conduction.

A strong asymmetry effect in the angular distribution of evaporation products is predicted. The energy distribution obtained displays the features characteristic for preequilibrium spectra. We propose new experiments by which the propagation of "heat" in a nucleus can be investigated. They consist essentially in the measurement of  $q$  in coincidence with the evaporation products of the target.

## ON THE HIGH-MOMENTUM TAIL OF THE SPECTATOR NUCLEON

B.S.Aladashvili, V.V.Glagolev, R.M.Lebedev, M.S.Nioradze,  
I.S.Saitov, V.N.Streltsov

JINR, Dubna

B.Badełek, G.Odyniec

Warsaw University, 00-681 Warsaw

A.Sandacz, T.Siemiarczuk, J.Stepaniak, P.Zieliński

Institute for Nuclear Research, 00-681 Warsaw

Dubna-Warsaw Collaboration

An evidence has been presented recently by R.Poster et al. <sup>1)</sup> for the occurrence of the single-pion virtual state,  $|pp\pi^- \rangle$ , of the deuteron in the  $K^+d \rightarrow K^*0pp$  reaction. We report an analogous observation of the other possible virtual state,  $|pn\pi^0 \rangle$  and confirm the charge configuration seen in ref. <sup>1)</sup>.

We analyze the charge exchange and charge retention reactions

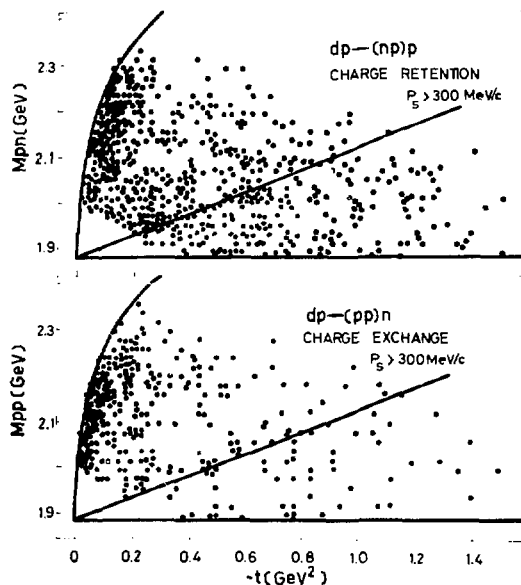


Fig. 1

The Chew-Low plot

at 3.3 GeV/c deuteron momentum (10,000 events). Fig. 1 shows the Chew-Low plot for the events with  $p_s > 300$  MeV/c. The diagonal line corresponds to the position of the events resulting from the scattering on the nucleon to be at rest. An enhancement is observed at low  $t$ -values near the kinematic boundary of the plot. The angular distributions of the spectator nucleon in the two slower nucleons rest frame (for events with  $t < 0.2$  GeV<sup>2</sup> and  $M_{2N} > 2.1$  GeV) are found to be consistent with that for the  $\pi d \rightarrow NN$  reaction at appropriate pion energy.

#### Reference

1. R.Poster et al., Phys. Rev. Lett., 33(1974)1625

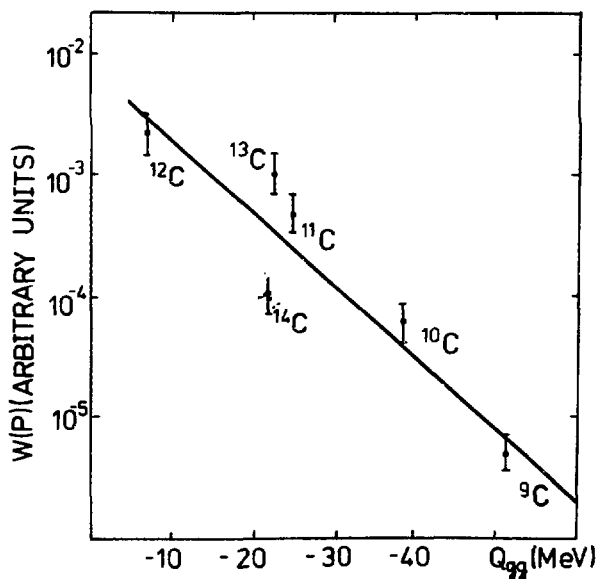
V.K.Lukyanov, A.I.Titov

Joint Institute for Nuclear Research, Dubna, USSR

A model is proposed describing the experiments of Heckman et al <sup>/1/</sup> on the fragmentation of the relativistic  $^{16}\text{O}$  on a beryllium target, where the spectra of  $^A\text{C}$ - isotopes ( $A = 9 - 15$ ) were measured. The reaction is assumed to proceed in two stages. At first the ion is excited by the peripheral collision with the target, at the second it decays statistically in flight with emitting of a fragment. The probability of the process

$$W \sim \exp(Q_{gg}/T) \exp(-p^2/2G^2)$$

One can find: I. The relative yields of fragments drop exponentially with  $-Q_{gg} = M_r - M(^{16}\text{O}) - M(^A\text{C})$ , where  $M_r$  is the mass of remaining decay products. (see Fig.) This result is in a deep analogy with the corresponding nonrelativistic reactions <sup>/2/</sup>.



II. The widths of the fragments momentum distribution have some dependence on  $T$  ( $\sim 7\text{MeV}$ ), but within experimental errors they are occurred to be one the same.

1. H.H.Heckman et al. Proc. Fifth.Int.Conf. on HEPNS in Uppsala, 1974;

2. A.G.Artukh et al. Nucl. Phys. A168 (1971) 321.

VII  
INSTRUMENTATION



B. W. Allardyce and E. G. Michaelis, CERN

After its one-year reconstruction, the CERN synchrocyclotron produced full energy protons for the first time in October 1974. There followed a phase of limited beam operation during which the r.f. system, the ion source, and the extraction system were all thoroughly tested. During this time the first beams for physics use became available, and it was clear that the design aims of the improvement programme would be achieved. Operating at one r.f. pulse in 16, time-averaged beam currents of over  $0.5 \mu\text{a}$  have been used, with extraction efficiencies greater than 70% in "short burst" mode (pulse duration 30  $\mu\text{sec}$ ), and about 50% in "long burst" mode (pulse duration 2 msec). In this latter mode, high duty cycle has been achieved, the protons emerging roughly uniformly throughout the 2 msec burst.

The proton beam has been used to produce pions and neutrons for experiments and has been transported over 60m to the new Isolde facility with an overall transmission of about 80%.

This phase of operation terminated with the start of a two-month shutdown in early April 1975 for repanelling work on the dee before this becomes too radioactive. When the SC2 starts up again in June 1975 it is hoped gradually to increase the performance towards the design aim of  $10 \mu\text{a}$  time average.

Turin, Oxford, Amsterdam, Birmingham, CERN collaboration

A spectrometer with a large solid angle and a large momentum acceptance is to be built at the SC2 at CERN; it will have an energy resolution of about 1 MeV for particles with momenta up to about 400 MeV/c. Work has started on the project, which should be operating by the autumn of 1976.

The spectrometer consists of a large magnet with a usable field volume of 1m x 2m x 0.85m. The magnetic field is homogeneous to within about 10% over this volume, in which it is intended to place planes of multi-wire chambers in front of a target, followed by arrays of multiwire and drift chambers and thin scintillators. Various geometries are possible, but the intention is to detect inside the magnet both the incident particle and the one(s) leaving the target over a large angular range. The information from the various detectors will be handled on-line by an HP computer system, which also performs some preliminary analysis. Further analysis will be done on a large computer, making use of well-established pattern recognition techniques.

The experiments of interest to such a spectrometer cover a wide range, and the initial programme will include backward scattering of pions on light nuclei; backward scattering of muons on helium; decay of  $\pi^0$  to a single lepton pair; radiative capture of  $\pi^-$  in flight by nuclei, followed by conversion of the  $\gamma$ ; electron-positron pairs by internal conversion following absorption of stopped  $\pi^-$  on light nuclei; double charge exchange ( $\pi^+$ ,  $\pi^-$ ) on nuclei; pion production experiments e.g.  $\pi^-p \rightarrow \pi^+\pi^-n$ ; nucleon knockout reactions e.g. ( $\pi^+$ ,  $\pi^+p$ ).

## STATUS OF THE SIN HIGH RESOLUTION PION SPECTROMETER (SUSI)

J.P. Egger et al<sup>1)</sup>

Physics Institute, University of Neuchâtel, Switzerland

We review briefly the status of the SIN pion spectrometer. It is a "Saclay-type" QDD system with vertical layout and has the following specifications:

Nominal momentum:	550 MeV/c for 14 KGauss
Momentum resolution:	$\Delta p/p \approx 5 * 10^{-4}$
Momentum acceptance:	$\pm 18 \%$
Solid angle:	16 msr
Incident momentum range for pions:	up to 450 MeV/c
Range of scattering angles:	0° - 140° (normal mode) 140° - 180° (with additional magnet)

Both magnets, quadrupole, frame, vacuum boxes and various equipment have arrived. The magnets were assembled and measured. The design curvatures and EFB's were obtained by adjusting the length and shape of the fieldclamp noses according to the field measurements. Raytracing is under way with analytical and measured fields as input.  $\alpha$ -tests and tune-up with pions of the spectrometer will start in a few weeks. The first experiments include elastic and inelastic pion scattering off light nuclei. Subsequent experiments will include quasielastic scattering and double charge exchange.

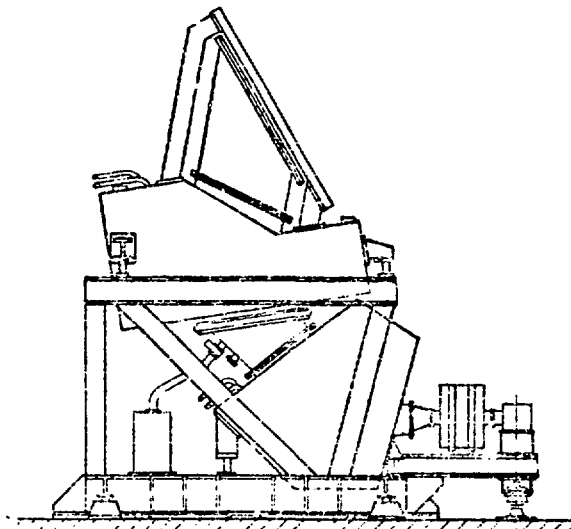


Fig. 1 SIN high resolution pion spectrometer

<sup>1)</sup> ETH-Grenoble-Heidelberg-Karlsruhe-Neuchâtel-SIN collaboration.

DOUBLE ARM SPECTROMETER SYSTEM  
FOR MEASURING ELECTRON-DEUTERON ELASTIC SCATTERING\*†

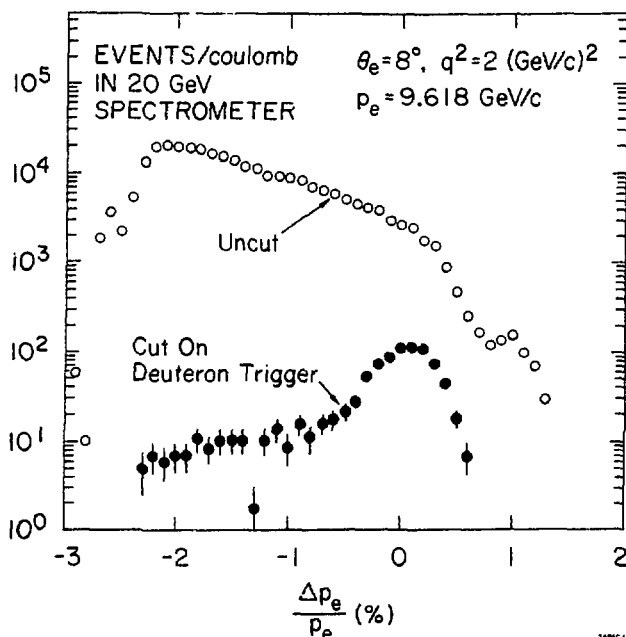
VII.4

F. Martin

Stanford Linear Accelerator Center  
Stanford, California 94305

ABSTRACT

The use of two high-precision, high-momentum spectrometers to measure elastic electron-deuteron scattering is unique in the annals of high-energy experimental physics. The existence of this equipment at SLAC has made possible the measurement of the deuteron charge form factor to a  $q^2$  of  $6.0(\text{GeV}/c)^2$  ( $\cong 154.6 f^{-2}$ ). The SLAC facility consists of three spectrometers which rotate about a common pivot point and they are capable of analyzing scattered particles from a few hundred MeV/c to 20,000 MeV/c; an electron accelerator with a momentum range from 900 MeV/c to 20,000 MeV/c and beam currents in excess of 50 mA and a computerized counting house and control system for the equipment. This paper will describe the technique of using these spectrometers in coincidence to achieve a reduction of the background by a



factor in excess of 1000 under the elastic electron-deuteron scattering peak. Shown in the Figure is a typical example of the elastic events when the electron and deuteron are identified in coincidence. The upper data plots are the electron single arm scattering data showing the tail of the quasi-elastic scattering.

\*Work supported by the National Science Foundation and the U.S. Energy Research and Development Administration.

†Collaborators: R. G. Arnold, B. T. Chertok, E. B. Dally, A. Grigorian, C.L. Jordan, F. Martin, B. A. Mecking, W. P. Schütz and R. Zdarko

A High Stopping Density  $\mu^+$  Beam\*A. E. Pifer, T. Bowen, and K. R. Kendall<sup>†</sup>

Department of Physics, University of Arizona, Tucson, Arizona 85721

A new type of  $\mu^+$  beam which utilizes muons with momentum less than 30 MeV/c which result from  $\pi^+$  decays at rest in the  $\pi^+$  production target will be described. Muons of the desired momentum are transported in vacuum by a double-focusing achromatic beam transport system having a momentum bit  $\Delta P/P = 6\%$ . Muons are identified by a three-fold coincidence of 0.127 mm thick plastic scintillator counters, one located at the intermediate focus and two near the final focus. The advantages of utilizing these low energy muons are 100% muon polarization, a small source which can be focused to a well-defined image with high density of stopping muons in a thin target, and a well defined stopping depth distribution making an anticoincidence counter unnecessary.

\*Work supported by the National Science Foundation.

<sup>†</sup>Present address: University of Victoria, Victoria, British Columbia.

## COINCIDENCE EXPERIMENTS AT INTERMEDIATE ENERGIES

J. E. Spencer and H. A. Thiessen  
Los Alamos Scientific Laboratory, Los Alamos, N. M. 87544

## ABSTRACT

This report considers the physics of coincidence experiments with proton and pion beams at LAMPF energies as well as which of the various possible measurement techniques are most relevant.

Our main conclusions concerning the physics of these reactions are:

- (1) The most probable final state multiplicity in a pion or proton reaction above 100 MeV is the three-body channels.
- (2) The most probable reaction type in these particular channels is quasi-elastic scattering of type  $(\pi, \pi'N)$  and  $(p, p'N)$ .
- (3) At energies corresponding to the basic  $(3,3)$  pion-nucleon resonance, the pion-nucleus reaction cross-section is dominated by the  $(\pi, \pi'N)$  reaction.
- (4) It is possible and worthwhile to measure two, three and some four-body inclusive and exclusive reactions in a comparatively simple way with good resolution.

Our main conclusions concerning the best means to carry out these kinds of experiments are:

- (1) Higher count rates and resolving powers are possible in a proton initiated three-body reaction with a double-arm spectrometer arrangement operating completely in an energy loss mode.
- (2) A two-arm spectrometer arrangement utilizing comparable spectrometers provides significant advantages for accurate two-body reaction studies.
- (3) A hybrid system consisting of two spectrometers and one or more solid-state counter systems are most effective from the standpoint of costs and information content from four-body final states as well as versatility for two- and three-body final states.
- (4) Significantly better detection systems are needed (and possible) to reduce the costs of these kinds of experiments.
- (5) Significantly better data acquisition systems based on more general and flexible data base structures are needed to obtain even a fraction of the information available in these experiments.

## NUCLEAR SCATTERING APPLIED TO RADIOSCOPY

J. Saudinos  
DPHN/ME, CEN Saclay, France

and

G. Charpak, F. Sauli, D. Townsend and J. Vinciarelli  
CERN, Geneva, Switzerland

We investigate the possibility of using the nuclear scattering of 500-1000 MeV protons to do radioscopy. Because the scattering angle is important, one measures the position of the interaction point and one obtains directly with only one exposure, a three-dimensional reconstruction of an object.

Elementary volumes of about  $1\text{mm}^3$  should be resolved due to the low multiple scattering effects in this incident energy range. Preliminary measurements with an incomplete set up gives a resolution of  $10\text{mm}^3$ .

We do not measure the energy of the particles and all quasi-elastic and inelastic processes are involved. In that way, the integrated cross-sections are important and the radiation doses used are compatible with human tolerances.

Because of the nuclear nature of the basis interaction, the information given by Nuclear Scattering Radioscopy is different from the one given by X-ray or particle range methods. It is much more dependent on hydrogen and light atoms concentrations. Furthermore by detecting the recoil proton, it is possible to measure the relative ratio of hydrogen concentration and carbon and oxygen concentration. Preliminary results on carbon,  $\text{CH}_2$  and eggs targets agree very well with these ideas. The last experimental results will be given.

C. Cernigoi, N. Grion, G. Pauli and M. Russi

Istituto di Fisica, Università di Trieste, Italia

Istituto Nazionale di Fisica Nucleare, Sezione di Trieste, Italia

Timing with plastic scintillator detectors is a problem of increasing importance in the field of experimental nuclear physics at medium energies. Results obtained with thin detectors of large areas are presented.

For a plastic scintillator 2 mm thick and having an area of  $800 \times 200 \text{ mm}^2$  the intrinsic time resolution has been investigated as a function of the energy dissipated within the plastic itself. A time resolution of the order of 0.7 nsec has been reached with an energy release of 1 MeV. For a plastic scintillator 10 mm thick and of  $100 \times 100 \text{ mm}^2$  area an intrinsic time resolution of the order of 0.35 nsec has been obtained for electrons at minimum ionization. With the last scintillator, time-of-flight spectra taken in negative pion beams of about 200 MeV/c have shown the possibility of determining the momentum spread of pions and muons using a path-length of 4.5 meters.



INDEX OF AUTHORS

- Aaron R I.A.3  
 Aas B III.17,.18  
 Adler J-O V.A.25,.28  
 Aebischer D IV.C.4  
 Afnan I R I.A.2  
 Akylas V II.13  
 Aladashvili B S VI.B.21  
 Alexandrov L I.D.12  
 Alexander Y IV.A.28  
 Alexeev G D VI.A.13  
 Alkhazov G IV.A.15  
 Allardyce B W VII.1  
 Allred J C I.D.9,IV.A.9,.C.2,.3  
 Alster J I.A.8,.D.7,V.A.2  
 Amman J F I.D.16,.17  
 Anderson A N IV.C.10  
 Anderson B D IV.C.10  
 Anderson H L II.10  
 Andersson B VI.A.4,.10  
 Andersson G V.A.25  
 Andert K II.35,II.36  
 Angelescu T I.D.12,.13  
 Argan P E V.A.4  
 Arima A III.7  
 Arlt R II.40  
 Arnold R G V.A.10  
 Arthur E D I.D.7  
 Arvieux J VI.B.2  
 Asano Y III.16  
 Asbury D M IV.C.6  
 Ashery D I.D.7,.14  
 Aslanides E IV.A.14,.C.24  
 Audit G V.A.4  
 Auguer J P IV.A.17  
 Avramov S R III.24  
  
 Baba K V.A.7  
 Babcock B VI.A.11  
 Bachelier D I.D.15  
 Backenstoss G II.32,III.19  
 Badawy O E VI.A.1,.2  
 Badelek B VI.B.21  
 Baer H W III.14, IV.C.10  
 Bajaj K K I.B.30  
 Baldini-Celio R I.C.8  
 Balestra F I.D.1,.2,.3,.4,.5,.12,.13  
 Ballagh H C I.A.7  
 Banaigs J VI.B.13  
 Barbini R I.D.1,.2,.3,.4,.5  
 Bardin G V.A.24  
  
 Barnes J W IV.A.26  
 Barnes P D I.D.16,.17,III.15  
 Barreau P II.14  
 Barrett R J IV.C.10  
 Barshay S V.B.14  
 Batty C J III.11,.12,.13  
 Batusov Yu A I.D.25,II.34,.37  
 Bauer T IV.A.14,.15,.C.24,VI.B.6  
 Baym G III.2  
 Bedijidian M IV.B.7  
 Bellicard J B V.A.2,.12  
 Bentley IV.C.15  
 Berger J VI.B.13,.14,.15,.16,.17  
 Bergmann R II.4  
 Bernabeu J V.A.22  
 Bernheim M V.A.19  
 Bernstein A M V.A.15  
 Berovic N III.11,.12,.13  
 Berthot J VI.A.8  
 Bertin P I.A.4,.8,.D.23,II.14  
 Bertini R IV.A.12,.14,.C.24,VI.B.6  
 Bertozzi W V.A.23  
 Bethe H A I.B.5,VI.B.19  
 Beurtey R I.A.6,IV.A.12,.14,.15,C.24  
 Bevington P R IV.C.10  
 Bhakar B S I.B.22  
 Biagi S F III.11,.12,.13  
 Bihoreau B II.14  
 Bimbot L IV.A.5,.C.23,.24  
 Binon F I.D.20  
 Bistirlich J A III.14  
 Bizard G IV.C.9,.B.14,.15,.16,.17,.18  
 Bjork C W IV.C.7,.8  
 Blair I M IV.C.6  
 Blecher M I.A.8  
 Błeszyński M I.A.1,IV.A.2,.3  
 Blomquist I V.A.3,.27  
 Blüm P III.19  
 Boehm F II.12  
 Bohannon G E I.B.16,IV.C.1  
 Bonazzola G L IV.B.4  
 Bondorf J P VI.B.19  
 Bonner B E IV.C.7,.8  
 Bonthonneau F IV.C.9  
 Booth E C V.A.15  
 Bordner C A I.A.9,.D.22  
 Boridy E IV.A.23  
 Boudard A IV.A.14,.15,.C.24,VI.B.6  
 Bowen T II.22,.30, IV.A.20,.21,VII.5  
 Bowles P VI.A.11,.12  
 Boyard J L I.D.15

Brandao d'Oliveira A II.1  
Brandenberg R A IV.B.1  
Bressani T IV.B.4  
Brewer J H II.22,.30  
Brissaud I IV.A.5,.C.23  
Brochard F IV.A.14,.C.24  
Brown G E I.C.2,III.2,IV.C.5  
Brown R C IV.C.6  
Brückner W IV.B.6  
Bruge G IV.A.12,.14,.15,.C.24,  
VI.B.6  
Bryant H IV.C.15  
Bunatian G G I.B.33  
Bunyatov S A II.34,.37  
Burkhardt H I.B.31  
Burleson G I.D.6  
Burman R L I.A.8,.D.10,.11  
Burov V V V.A.29  
Burq J P VI.A.8  
Bussiere A V.A.19  
Busso L I.D.1,.2,.3,.4,.5,.12,.13  
Butler G W I.D.21,IV.A.22  
Butsev V S III.24  
Bystritsky V M III.22

Calarco J I.D.6  
Caldwell P VI.A.11  
Cannata F I.D.1,III.1  
Carlini R IV.C.15  
Carlson C V.A.21  
Carroll A S I.D.19  
Carroll J V.B.12  
Carter A L II.10  
Casperson D E II.25,.33  
Cassapakis C G IV.C.7,.8,.15  
Catz H IV.A.12,.14,VI.B.6  
Celenza L I.B.13  
Cernigoi C VII.8  
Chang C C VI.B.8  
Chant N S VI.B.2,.8  
Charpak G VII.7  
Chasan B V.A.15  
Chaumeaux A IV.A.12,.14,.15,.C.24,  
VI.B.6  
Chemarin M VI.A.8  
Chen H H V.B.1  
Chen M Y III.16  
Cheng S III.16  
Chernev Kh II.34,.37  
Chertkov A A III.21  
Chertok B T V.A.20  
Chevallier M VI.A.8  
Chiang I H I.D.19

Chiavassa E IV.B.4  
Chirapatpimol N V.B.12,VI.B.2  
Chultem D I.D.25,III.24  
Churin I N VI.A.13  
Ciofi Degli Atti C I.B.12  
Clark R B I.D.10  
Clement J IV.A.9,.C.2,.3  
Close D A II.23  
Clough A S III.11,.12,.13,IV.C.6  
Cochavi S I.D.7,.14,V.A.2  
Coddington P III.11,.12,.13  
Comiso J III.6  
Comparat V IV.A.12  
Cook B C I.D.10,.11  
Cooper M I.D.6  
Cooper S III.14  
Cork B VI.B.9  
Cottereau M VI.B.13  
Coupat B I.A.4,.D.23  
Couvert P IV.A.12,.15,.C.24  
Cox C III.15  
Crane T W II.25,.33  
Crowe K M II.22,III.14  
Craver B A V.A.11,.B.4,.10  
Cverna F IV.C.10  
Cvijanovich G I.A.6,IV.A.15

Daniel H II.1,.2,.4  
Darden C W I.A.8  
Davidson J P II.23  
De Botton N V.A.4  
De Forest T Jr V.A.1  
Delise D II.22,.30,IV.A.20,.21  
Dellacasa G IV.B.4  
Deloff A IV.A.29  
Delorme J V.A.16,.B.11  
Denison A B II.25  
Dennis C M I.D.18  
Devanathan V II.11  
De Witt Huberts P V.A.12  
Dey W II.12,III.17,.18  
Dhar S VI.A.7  
Diepernik A E L V.A.1  
Dierlerle B IV.C.15  
Dillig M I.C.4,IV.A.19  
Dinter H V.A.27  
Dixit M S II.10  
Doll P IV.B.2  
Dollhopf W VI.B.10  
Doss M I.D.16,.17  
Douhet G VI.A.8  
Dover C B I.B.9,.D.19  
Drake D M I.D.7,.10,.11  
Dropseky B J I.D.21  
Dubal L I.A.6

Duchazeaubeneix J C I.A.6  
 Duclos J I.A.4,V.A.24  
 Duflo J IV.C.9,VI.B.14,.15,.16,.17,  
 .18  
 Dugan G III.16  
 Duhm H H I.A.6,IV.A.15,.C.24,VI.B.6  
 Durso J IV.C.5  
 Duteil P I.D.20  
 Dymarz R IV.A.4  
 Dytman S A I.D.16,.17  
  
 Ebersold P III.17,.18  
 Eckhause M III.15  
 Edge R D I.A.8,IV.A.6,.C.22  
 Edgington J A IV.C.6  
 Efimov V N IV.C.21  
 Egger J-P VII.3  
 Eichler R III.17,.18  
 Eisenstein R A I.D.8,.16,.17,III.15  
 Elliott J R VI.A.6,.7  
 El-Naghy A A VI.A.1,.2  
 Endo I V.A.7  
 Engelhardt H D III.10  
 Engfer R II.12,.35,.36  
 Eramzhyan R A II.37,III.25  
 Erdal B R IV.A.26  
 Ericson M V.A.16,.B.11  
 Ericson T E O V.A.22  
 Ernst D J I.B.7,.8  
 Evans M E IV.C.7,.8  
 Evseev V S II.35,.36,.38,.39  
  
 Fabbri F L I.C.8,VI.B.13,.14,.15,  
 .16,.17,.18  
 Faessler M A IV.B.6  
 Fagerström B I.D.24  
 Fainberg A IV.B.4  
 Faivre J C I.A.6,IV.A.12  
 Faldt G V.A.16  
 Falomkin I V I.D.12,.13  
 Faure J L V.A.4  
 Favier B IV.C.4  
 Fearing H W IV.A.24  
 Felder R D IV.C.2  
 Feshbach H IV.A.23,VI.B.11  
 Fetisov V N IV.B.5  
 Fetscher W III.19  
 Figureau A V.B.11  
 Filipkowski A IV.B.7  
 Filippas T A IV.A.6  
 Findlay D J S V.A.23  
 Firsov V G II.41  
 Fischer W E V.B.16  
 Fischbach E V.B.4,.7  
  
 Fleming D G II.22,.30,IV.A.16  
 Fong J C IV.A.11,VI.B.2  
 Fontaine J M IV.A.14,.15,VI.B.6  
 Fortney L R VI.A.6,.7  
 Franco V I.B.4,IV.C.13,VI.B.12  
 Frank J S I.A.5  
 Frankel S III.26  
 Frascaria R IV.A.12,.14  
 Frati W III.26  
 Fricke G II.27  
 Friedlander G I.D.21  
 Friedman W A I.C.6  
 Frois B V.A.12  
 Fromm W D II.40  
 Frontasyeva M V II.38,.39  
 Fujii A II.20,.21,III.9  
 Fujii H V.A.7  
 Fujisaki M V.A.7  
 Fujita T III.8  
 Funsten H O I.D.18  
 Furić M IV.C.2  
 Furui S V.B.8  
 Futami Y III.27  
  
 Gabethuler K I.A.8  
 Gabitzsch N I.D.9,IV.A.9,.C.2,.3  
 Gallio M IV.B.4  
 Galm I III.22  
 Ganzorig Dz I.D.25,II.40,III.24  
 Gardès J VI.A.8  
 Garetta D VI.B.6  
 Garfagnini R I.D.1,.2,.3,.4,.5,.12,  
 .13  
 Garland R VI.A.11,.12  
 Garner D M II.22  
 Garreta D IV.A.12,.15,.C.24  
 Gavrillov Yu K III.24  
 Gazzaly M M VI.B.2  
 Gérard A I.A.4,.D.23  
 Gerber J P VI.A.8  
 Gibbs W R I.B.17,.18,IV.C.12  
 Gibson B F I.B.17,.18,.19,IV.C.12,  
 V.A.18  
 Gillebert A V.A.19  
 Gillespie J R I.B.10,IV.A.17  
 Glagolev V V VI.B.21  
 Glass G IV.C.7,.8  
 Glenn J W IV.C.22  
 Glodis P F I.A.7  
 Goldansky V I II.38,.39  
 Goldzahl L I.A.6,VI.B.13,.14,.15,.16,  
 .17,.18  
 Göring J V.B.6  
 Gorodetzky P IV.A.14,.C.24  
 Goshaw A T VI.A.6,.7  
 Gotow K I.A.8

Gouanere M I.D.20  
 Grabowski J W IV.A.16  
 Gram P A M I.A.9,.D.10,.11,.22  
 Grant P M IV.A.26  
 Graves R D II.11,V.A.5  
 Greeniaus G IV.C.4  
 Grenacs L II.44,V.B.17  
 Grion N VII.8  
 Gross E E I.A.8  
 Gross F V.A.21  
 Grossiord I Y IV.B.7  
 Gruenwald J T V.B.7  
 Grunder H VI.A.12  
 Guaraldo C I.D.1,.2,.3,.4,.5  
 Gudima K K IV.C.20  
 Guichard A IV.B.7  
 Gulkanyan G R II.34,.37  
 Gupta M K I.B.15  
 Gurvitz S A IV.A.28,.31  
 Gusakow M IV.B.7  
 Gustafsson H-A V.A.25  
 Guyot J IV.A.14  
  
 Haak J I.B.23  
 Haddock R P I.A.7  
 Haff P K II.13  
 Hagelberg R III.19  
 Hagerman D I.D.6  
 Haik N V.A.2  
 Halpern I I.D.6  
 Hambro L II.8  
 Hargrove C K II.10  
 Harp G D I.D.21  
 Harrington D R I.B.11  
 Hartmann F J II.4  
 Hashimoto O II.15,.16,.17,.18,.19  
 Hassenzahl W V I.A.9,.D.22  
 Hatch E N I.D.10,.11  
 Haupt H II.35,.36  
 Hawkins R E III.11,.12,.13  
 Heffner R H I.A.5  
 Heller L I.B.16,IV.C.1  
 Hendrie D L IV.A.11  
 Hennino T I.D.15  
 Herczeg P V.B.10  
 Hess A T I.B.18  
 Hess R IV.C.4  
 Hibou F IV.A.14,.C.24  
 Hiebert J IV.C.8  
 Highland V III.26  
 Hincks E P II.10  
 Hirata M I.B.24  
 Ho P-X V.A.2,.12  
 Hoffman G W IV.A.11  
 Holmgren H D IV.C.23  
  
 Horikawa Y V.B.9  
 Howard H H I.A.9,.D.22  
 Hu E III.16  
 Huber M G I.C.4,IV.A.19  
 Hudis J I.D.21  
 Hudomalj-Gabitzsch J I.D.9,IV.A.9,  
 .C.2,.C.3  
 Huet M V.A.12  
 Hughes V W II.25,.33,III.16  
 Hugon L I.D.20  
 Hungerford E V I.D.9,IV.A.9,.C.2,.3  
 Hussein A VI.A.1,.2  
  
 Iachello F I.B.23  
 Igo G I IV.A.11,.B.12,.VI.B.2  
 Ille B VI.A.8  
 Immele J D II.9  
 Inopin E V IV.C.18  
 Isabelle D I.A.4,I.D.23  
 Ishihara T I.C.1  
 Iverson M S I.B.27  
 Iwamura Y I.C.1  
  
 Jackson H E I.D.10,.11  
 Jackson A D IV.C.5  
 Jacob N P Jr I.D.21  
 Jain M IV.C.7,.8  
 Jakobson M I.D.6  
 Jakobsson B VI.B.3  
 Janecek P V.A.27  
 Jansen j I.D.20  
 Jarlskog C V.A.22  
 Jarmie N IV.C.10  
 Jaroszewicz T I.A.1,IV.A.2,.3  
 Jenkins D III.15  
 Jeppesen R I.D.6  
 Johnson K I.D.6  
 Johnson M I.B.5  
 Jonsson G G V.A.27,.28  
 Jourdain J C I.D.15  
 Julien J II.44  
 Junod A IV.C.4  
 Just K V.A.26  
  
 Kadota S V.A.7  
 Kalinina N A VI.A.13  
 Kallio A I.B.12  
 Källne J I.D.24,IV.A.8,.C.23  
 Kamal A N I.B.3  
 Kane J III.15  
 Kao N M I.D.12,.13  
 Kaplan S N II.24,.31

Kaspar H F II.25  
 Kaufman S I.D.21  
 Kaufmann W B I.B.18  
 Kawadry G I.D.23  
 Kayser B V.B.7  
 Kendall K R VII.5  
 Kenefick R A IV.C.7,.8  
 Kessler D II.10  
 Khanna F C V.A.13,.14  
 Khazins D M VI.A.13  
 Kholodov N I II.38,.39  
 Khomenko B A III.22  
 Kilian K IV.B.6  
 Kim Y E IV.B.1,V.A.11,.B.4,.10  
 Kinchakov V S IV.C.18  
 King T R I.A.9,.D.22,III.15  
 Kisslinger L S I.C.3  
 Kitching P VI.B.10  
 Klare K A I.A.5  
 Knight J D II.2  
 Knöpfle K T IV.B.2  
 Knowles H B II.2  
 Knutson L I.D.6  
 Kobayashi S II.17  
 Koch H II.32,III.19  
 Koester K IV.A.9  
 Kohmura T I.B.28,.29  
 Kohyama Y II.20,.21,III.9  
 Koltun D S I.B.1  
 Kopeliovich B Z IV.C.17  
 Kossler W J I.D.18  
 Kost M F III.21  
 Kostoulas I VI.A.11  
 Kovar D G I.D.10,.11  
 Kozlov M I IV.B.5  
 Kreuzer H J V.B.2  
 Kristiansson K VI.B.3  
 Krogulski T II.40  
 Kruglov V V VI.A.13  
 Krumshstein Z V III.21  
 Kubodera K I.B.25,III.3,V.B.9  
 Kulikov A V IV.A.15,VI.A.13  
 Kullberg R VI.B.3  
 Kulyukin M M I.D.12,.13  
 Kume K II.3  
 Kunselman R III.15  
 Kuper C G V.B.2  
 Kuptsov A V VI.A.13  
 Kuznetsov V N VI.A.13  
 Kycia T F I.D.19  
  
 Laget J M V.A.3,.4  
 Lagnaux J-P I.D.20  
 Lam K C IV.A.7  
 Lam W III.15  
  
 Lambert M VI.A.8  
 Lamers B A V.A.5,.B.5  
 Lamsa J W VI.A.6,.7  
 Lande A I.B.23  
 Langworthy J B V.B.5  
 Lankford W F I.D.18  
 La Rosa G I.C.8  
 Lathrop J F V.B.1  
 Laville J L IV.C.9  
 Layly V VI.B.6  
 Leavitt C IV.C.15  
 Lebedev R M VI.B.21  
 Le Bornec Y IV.A.5,.C.23,.24  
 Le Brun C VI.B.13,.14,.15,.16,.17,  
 .18  
 Lechanoine C IV.C.4  
 Leconte P V.A.2,.12  
 Lederman L M VI.A.5  
 Lee H C V.A.13,.14  
 Lee L Y I.D.9,IV.A.9,.C.2,.3  
 Lee S Y III.20  
 Lee T-S H I.B.25  
 Leemann B Th VI.B.8  
 Leemann C VI.A.12  
 Lefebvres F IV.C.9  
 Legrand D IV.A.12,.15  
 Lehman D R V.A.18  
 Lehmann J II.44,V.B.17  
 Leisi H J III.17,.18  
 Leitch M J V.A.23  
 Lemmer R H I.B.9  
 Lenz F I.B.24,.C.7  
 Leon M II.5,III.5  
 Leonard R I.B.32  
 Leung K C I.A.7  
 Lewis C W III.10  
 Li K K I.D.19  
 Liberman A D VI.B.2  
 Lidofsky L III.16  
 Lieb B J I.D.18  
 Lightbody J W Jr V.A.12  
 Lind V G I.D.10,.11  
 Lindgren K V.A.28  
 Lindkvist B VI.B.3  
 Liu L C I.B.4,.13  
 Lombard R J IV.A.17  
 Lomon E L IV.C.16  
 Londergan J T I.B.8,.21  
 Loos J S VI.A.6,.7  
 Lu D C II.33,III.16  
 Ludemann C A I.A.8  
 Lugol J C I.A.6,IV.A.15,VI.B.6  
 Lukyanov V K IV.C.18,V.A.29,VI.B.22  
 Lyashenko V I I.D.12,.13  
 Lynen U IV.B.6

Mach R I.D.12,.13  
Magnon A I.A.4,V.A.24  
Malanify J J II.23  
Malherbe J C IV.C.9  
Mairle G IV.B.2  
Majewski S IV.B.7  
Małecki A IV.A.4,.18  
Mamedov T N II.38,.39  
Mann D B I.D.9,IV.C.2  
Marin J P VI.A.8  
Markowitz S S I.D.21  
Marks T I.A.8  
Marrs R I.D.6  
Martin F VII.4  
Martin J V.A.4  
Marty N IV.A.12  
Matoba M IV.A.14,.C.24,VI.B.2  
Matthews J L V.A.23  
Mausner L F II.24  
Mayes B W I.D.9,IV.A.9,C.2,..3  
Mazur P O I.D.19  
McAdams R E I.D.10,.11  
McKee R J II.10  
McVay L J V.A.9  
Meda D II.44  
Medicus H A V.A.17  
Melhop W VI.A.11,.12  
Méritet L VI.A.8  
Mes H II.10  
Mettwalli N VI.A.1,.2  
Meyer H I.D.6  
Meyer T III.6  
Meyer-Schützmeister L I.D.10,.11  
Michael D I.D.19  
Michaelis E G VII.1  
Michel B V.A.24  
Mihul A I.D.12,.13  
Mikheeva V I III.21  
Miller G A I.B.2,.8,.C.3,.D.8,IV.A.27  
Miller Jack I.A.4,.D.23,II.14  
Miller J II.5  
Miller J III.15  
Min K V.A.9  
Mirfakhrai N IV.B.4  
Mirsalikhova F II.34,.37  
Mischke R E I.A.5  
Mizuta M III.9  
Mockett P M I.D.19  
Moinester M A I.D.7,V.A.2  
Moir D C I.A.5  
Monard J A II.24,.31  
Moniz E J I.A.3,.B.21,.C.7  
Montret J C V.A.24  
Morgenstern J I.A.4,.D.23,II.14  
Morita M II.3,V.B.3  
Morlet M IV.A.12  
Mougey J V.A.19  
Mukhopadhyay N C II.8,.9  
Murakami A V.A.7  
Murata Y V.A.7  
Musso A IV.B.4  
Mutchler G S I.D.9,IV.A.9,.C.2,.3  
Myasishceva G G II.41  
Nadezhdin V S IV.A.30  
Nagamine K II.15,.16,.17,.18,.19  
Nagamiya S II.15,.16,.17,.18,.19,.31  
Nagarajan M A I.B.7  
Nagl A V.A.6,.8  
Nagle D E I.A.5  
Nakada A V.A.12  
Nakamura N I.B.28  
Nalcioglu O I.B.1  
Nassar M A V.B.12  
Natowitz J B IV.A.22  
Naumann R A II.2,.24  
Nefkens B M K I.A.7,IV.C.11  
Negele J W II.28  
Negishi T I.B.28,.29  
Nemenov L L VI.A.13  
Newsom C IV.C.8  
Nichitiu F I.D.12,.13  
Niklès J-C IV.C.4  
Nilsson A II.32,III.19  
Nioradze M S VI.B.21  
Nishida N II.18  
Nishimura H III.7,.8  
Nogami Y I.B.30  
Noguchi S V.A.7  
Norris A E I.D.21  
Northcliffe L C IV.C.7,.8  
Nyman E III.28  
O'Brien H A Jr IV.A.26  
Obukhov Yu V II.38,.39,.41  
Odyniec G VI.B.21  
Ogard A E IV.A.26  
Ohtsubo H II.3,V.B.3,.9  
Ohtsuka N II.3  
Olsen W C VI.B.10  
Onel Y IV.C.6  
Oostens J VI.B.14,.15,.16,.17,.18  
Orr H D IV.A.6  
Ortendahl D V.B.12  
Orth C J I.D.21,II.2  
Orth H II.25,.33  
Ortlepp H G II.35,.36,.40  
Osland P VI.A.9  
Otgonsuren O I.D.25

Otterlund I VI.A.3,.B.3  
 Otteson O H I.D.10,.11  
 Owens R O V.A.23  
 Oyer A T I.A.9,.D.22

Palevsky H I.D.20  
 Palffy L II.44,V.B.17  
 Panurets L N III.21  
 Paras N V.A.15  
 Patterson B D II.19  
 Patton W III.16  
 Pauli G VII.8  
 Pavlopoulos P III.19  
 Peigneux J P I.D.20  
 Pella P V.A.9  
 Penkrot J A I.D.16,.17  
 Perdrisat C F I.A.6,VI.B.10  
 Perez-Mendez V IV.A.11,V.B.12,  
 VI.B.2  
 Perkins R B II.27  
 Perroud J P I.A.8,III.14  
 Perry D G IV.A.13,.22  
 Petrov N I IV.A.30  
 Petrukhin V I III.21,.22,.23  
 Pfeiffer H J II.4  
 Phillips A C III.4  
 Phillips G C I.D.9,IV.A.9,.C.2,.3  
 Picard J I.A.4,I.D.23,II.14  
 Picchi P IV.A.4,.18  
 Piccioni O VI.A.11,.12  
 Picker H S I.B.14  
 Picozza P I.C.8,VI.B.13,.14,.15,  
 .16,.17,.18  
 Piekarz H IV.B.7  
 Piekarz J IV.B.7  
 Pietrzyk B IV.B.6  
 Pifer A E II.22,.30,IV.A.20,.21,  
 VII.5  
 Piragino G I.D.1,.2,.3,.4,.5,.12,  
 .13  
 Pizzi J R IV.B.7  
 Plasil F IV.A.22  
 Plendl H S I.D.18  
 Plouin F IV.C.9,VI.B.14,.15,.16,  
 .17,.18  
 Pokrovsky V N II.42  
 Pol' Yu S IV.C.18,V.A.29  
 Polikanov S M II.40,III.24  
 Ponomarev L I II.42,.43  
 Pontecorvo G B I.D.12,.13,VI.A.13  
 Poskanzer A M IV.A.22  
 Possoz A II.44,V.B.17  
 Potashnikova I K IV.C.17  
 Poth H III.19

Povh B IV.B.6  
 Powers R J I.A.4,II.14,III.15  
 Pratt J IV.C.15  
 Preedom B M I.A.8  
 Price L E VI.A.5  
 Priou M V.A.19  
 Pugh H G VI.B.7,.8  
 Puzynin I V II.43  
 Puzynina T P II.43  
 Pyle G J III.11,.12,.13

Querrou M VI.A.8

Radvanyi P I.D.15  
 Rahm D C I.D.19  
 Rapin D IV.C.14  
 Rayet M IV.B.3  
 Rebka G A I.A.9,I.D.22  
 Redwine R P I.A.8,I.D.6  
 Regimbart R IV.C.9  
 Reide F IV.C.23  
 Reist H W II.25,.33  
 Remler E A IV.A.10  
 Rho M III.28  
 Riddle R A J III.11,.12,.13  
 Riley P J IV.C.7,.8  
 Rinat A S IV.A.28,.31  
 Rinaudo G IV.B.4  
 Rinker G A Jr II.26,.28  
 Risin V III.22  
 Risin V V III.23  
 Ritter E T II.27  
 Ritter H F IV.B.6  
 Roberson P III.15  
 Roberts A III.11,.12,.13  
 Roberts B L III.11,.12,.13  
 Robertson W J Jr VI.A.6,.7  
 Rockmore F I.B.6  
 Roganov V S II.35,.36,.38,.39,.41  
 Roig F III.4  
 Roos P VI.B.2  
 Rosen S P V.B.7  
 Rost E I.B.27,I.C.5  
 Roussel L II.14  
 Rowley D V.A.9  
 Royer D V.A.19  
 Roy-Stephan M I.D.15  
 Rubinstein R I.D.19  
 Rupp T IV.C.15  
 Rushton M III.15  
 Russi M VII.8

Sabirov B M II.35,.36,.40  
 Saghai B I.D.23  
 Saitov I S VI.B.21  
 Sakaev R A III.25  
 Saltmarsh M J I.A.8  
 Samenkova I F III.23  
 Samour C II.44  
 Sandacz A VI.B.21  
 Sander O R IV.C.11  
 Sapp W W III.17,.18  
 Sargent C P V.A.23  
 Saricheva V K I.D.12,.13  
 Sastry K S R V.A.9  
 Satarov V I IV.A.30  
 Sathe A P IV.A.10  
 Satoh E I.C.1  
 Satta L VI.B.14,.15,.16,.17,.18  
 Saudinos J I.A.6, IV.A.15,VII.7  
 Sauli F VII.7  
 Schaeffer R VI.B.6  
 Scheck F III.17, V.B.15,.16  
 Schiffer J P I.D.10,.11  
 Schillaci M E II.2  
 Schlepuetz F III.6  
 Schmidt U II.40  
 Schneuwly H II.35,.36  
 Schröder H IV.B.6  
 Schroeder L S VI.B.4  
 Schuhl C V.A.4  
 Schürlein B IV.B.6  
 Scipione D VI.A.11,.12  
 Scott C K I.B.19  
 Scrimaglio R I.D.1,.2,.3,.4,.5  
 Sebek J VI.A.11,.12  
 Segel R E I.D.10,.11  
 Semergieva M I.D.12,.13  
 Shakin C M I.B.13  
 Shamaï Y I.D.7  
 Shcherbakov Yu A I.D.12,.13  
 Shera E B II.27  
 Sherif M I VI.A.1,.2  
 Sherman R H III.14  
 Shively F T I.A.9,.22,III.14  
 Sick I III.19,V.A.19  
 Sidorov V M II.34,.37  
 Siemens P J VI.B.19  
 Siemiarczuk T VI.B.21  
 Silbar R R IV.C.14  
 Simmons J E IV.C.7,.8  
 Simons L M II.7,III.19  
 Singer P V.B.10  
 Skachkov N B IV.C.19  
 Skrzypczak E VI.B.1  
 Smalley R V.A.17  
 Smith D E I.A.7  
 Sobel M I VI.B.19  
 Sober D I I.A.7,IV.C.11  
 Souder P A II.25,.33  
 Sparrow D A I.B.26  
 Spencer J E I.B.2, IV.A.27,VII.6  
 Speth J II.29  
 Spighel M I.D.20  
 Springer K II.2,.4  
 Spivak H V.B.7  
 Squier G T A III.11,.12,.13  
 Stambaugh R D II.25  
 Steffen R M II.27  
 Steels M V.B.17  
 Stein N IV.C.8  
 Stepaniak J VI.B.21  
 Stephenson G J Jr I.B. 17,.18,IV.C.12  
 Stetz A V.B.12  
 Stewart N M IV.C.6  
 Stoler P V.A.9  
 Streltsov V N VI.B.21  
 Strobel G L IV.A.7  
 Stronach C E I.D.18  
 Stroot J P I.D.20  
 Subramanian P R II.11  
 Sugimoto K V.B.6  
 Sumi Y V.A.7  
 Sun C R VI.A.7  
 Sutton R III.15  
 Sundaesan M K II.6  
 Sundberg O I.D.24  
 Suvorov V M III.21,.22,.23  
 Suzuki A III.27  
 Tabakin F I.B.16  
 Takahashi Y I.C.1,III.27  
 Tamas G V.A.4  
 Tanihata I V.B.6  
 Tatischeff B IV.C.5,.C.23,.24  
 Tauscher L II.32,III.19  
 Terrien Y IV.A.12,.14,.C.24  
 Tesch K V.A.27  
 Tezuka H IV.A.1  
 Têtefort A VI.A.8  
 Thaler R M I.B.7,.8  
 Therrien Y IV.A.11  
 Thevenet C V.B.11  
 Thiessen H A VII.6  
 Thirion J IV.A.14,.15  
 Thompson A C I.D.16,.17  
 Thompson P A II.25  
 Thompson R H IV.C.1  
 Thomas A W I.A.2  
 Thomas R VI.A.12  
 Tibell G I.D.24  
 Titov A I VI.B.22





VIII  
LATE ABSTRACTS

**YIELDS OF 25 GeV/c  $K^-$  -MESONS, ANTIPROTONS AND ANTIDEUTERONS  
FROM THE INTERACTIONS OF 70 GeV PROTONS WITH NUCLEI**

**B.Yu.Baldin, G.Chemnitz, Ya.V.Grishkevich, B.A.Khomenko,  
N.N.Khovansky, Z.V.Krumshtein, V.G.Lapshin, R.Leiste,  
Yu.P.Merekov, V.I.Petrukhin, D.Pose, A.I.Ronzhin, V.I.Rykalin,  
I.F.Samenkova, J.Schüller, G.A.Shelkov, V.I.Solianik,  
V.M.Suvorov, M.Szawlowsky, L.S.Vertogradov, N.K.Vishnevsky**

**Joint Institute for Nuclear Research, Dubna, USSR**

**Abstract**

The yields of kaons, antiprotons and antideuterons from beryllium, aluminium, copper and tungsten relative to those of pions have been measured at the Serpukhov proton synchrotron. The experiment has been performed by using the 25 GeV/c beam of negatively charged particles produced by 70 GeV protons at the internal target at angles of 0 and 10 mrad.

The relative yields  $R_{K^-, \bar{p}, \bar{d}} = \frac{d^2 \sigma_{K^-, \bar{p}, \bar{d}} / d\Omega dP}{d^2 \sigma_{\pi^-} / d\Omega dP}$  (25 GeV/c) depend weakly upon the atomic number of the target and are  $R_{K^-} \sim 3 \times 10^{-2}$ ,  $R_{\bar{p}} \sim 9 \times 10^{-3}$  and  $R_{\bar{d}} \sim (5-7) \times 10^{-7}$  in the investigated range of masses of nuclei.

THE MOMENTUM CHARACTERISTICS OF SECONDARY PARTICLES FROM  
 THE INTERACTIONS OF 50 GeV/c  $\pi^-$ -MESON WITH NUCLEI,  
 IRRADIATED UNDER A STRONG MAGNETIC FIELD

Alma-Ata- Dubna - Erevan - Leningrad - Moscow - Tashkent  
 Collaboration:

A.A.El-Naghy, R.Khoshmukhamedov, J.Salomov, K.D.Tolstov,  
 G.S.Shabratova,  
 S.A.Azimov, R.A.Bondarenko, K.G.Gulyamov, V.I.Petrov,  
 T.P.Trofimova, L.P.Tchernova, G.M.Tchernov.

A B S T R A C T

The investigations of momentum and angular characteristics of secondary particles from the interactions of 50 GeV/c  $\pi^-$ -meson with nuclei, irradiated under a strong magnetic field, were carried out. The experiment and irradiation conditions were carried out with the help of the set-up "Mamouth" in the Serpukhov accelerator. The obtained inclusive distributions were given as a function of the number of heavily ionizing particles.

This shows that, in pion-nucleus collisions, the effect of "leading particle" was noticed, but the full "Passive" assumption of primary pion after interacting with internal nucleon was found to be in contrast with the experimental results. The average transverse momentum, and fractional energy for different types of produced particles were found to be weakly dependent on nucleus dimensions.

## ON THE TOTAL BINDING ENERGY OF SPHERICAL NUCLEI

F.A. Gareev

Joint Institute for Nuclear Research, Dubna, USSR

G.M. Vagradov

Institute of Nuclear Research of the Academy of Sciences of  
the USSR, Moscow

To determine the ground state binding energy of nuclei the use is made of the many-body field theory which allows one to establish general relations between various observables and then, after some simplifications, to pass over to phenomenology. As a result, the following formula

$$E_c = \sum_n \int_{-\infty}^{+\infty} \frac{d\varepsilon}{2\pi} \frac{(\varepsilon - \frac{1}{2} \text{Re } M_{nn}(\varepsilon)) \Gamma_n(\varepsilon)}{(\varepsilon - E_n(\varepsilon))^2 + \frac{1}{4} \Gamma_n^2(\varepsilon)}, \quad (1)$$

has been found for the total binding energy of a nuclei, where  $\text{Re } M_{nn}(\varepsilon)$  is the real part of mass operator matrix element and  $\Gamma_n(\varepsilon)$  is the imaginary part, i.e., the "hole" level width. Parameters of the mass operator are defined on the basis of an optical potential and the  $\varepsilon$ -dependence of the real and imaginary parts of  $M$  is obtained<sup>1)</sup> by comparing the calculated energy spectra  $E_n(\varepsilon)$  of "hole" excitations and their widths  $\Gamma_n(\varepsilon)$  with experimental data on the reactions of quasi-elastic knocking out of nucleons<sup>2)</sup>. In understanding the mechanism of the latter much progress has been achieved in the past years<sup>3)</sup>. The total binding energies of nuclei  $O^{16}$ ,  $Ca^{40}$ , and  $Ni^{58}$  calculated by formula (1) agree with experiment within 10%. If one expands (1) in powers of  $A$  then for the total energy an expression is obtained analogous to the Weizsacker relation that once again gives evidence in favour of the proposed approach.

1. F.A. Gareev, G.M. Vagradov, JINR-preprint P4-8597, Dubna, 1975.
2. G. Jacob, Th.A.J. Maris, Rev. Mod. Phys., 45 (1973) 6.
3. V.V. Gorchakov, G.M. Vagradov, Kratkie Soobshcheniya po Fizike, v.6 (1970) 26, v.8 (1970) 66;  
D.M.E. Gross and R. Lipperheide, Nucl. Phys., A150 (1970) 449;  
D.S. Koltun, Phys. Rev, C2 (1974) 484.

DECAY CHARACTERISTICS OF THE STATES OF GIANT  
DIPOLE RESONANCE ON ISOTOPES  $^{58}\text{Ni}$  and  $^{60}\text{Ni}$

B.S. Ishkhanov, L.M. Kapitonov, V.G. Shevchenko, O.P. Shevchenko,  
V.V. Varianov

Institute of Nuclear Physics, Moscow State University  
Moscow 117234, USSR.

The semiconductor methods are used to measure the photo-  
proton spectra at several  $E_{\gamma}^{\text{max}}$  for  $^{58}\text{Ni}$  and  $^{60}\text{Ni}$  ( $^{58}\text{Ni}$  - 18.0,  
19.0, 20.0, 21.0, 22.0, 24.5, 27.0, and 32.0 MeV;  $^{60}\text{Ni}$  - 17.5, 19.5,  
22.0, 25.0, 28.0, and 32.0 MeV) with the purpose of studying the  
proton channel decay of  $^{58}\text{Ni}$  and  $^{60}\text{Ni}$  levels. The differential  
proton spectra corresponding to the decay of the levels located  
within narrow ranges of excitation energies have been obtained.  
The joint analysis of the spectra and the photoproton cross  
sections<sup>1</sup> has permitted some transitions to be identified. A con-  
siderable softening of the  $^{60}\text{Ni}$  nucleus state decay spectra has  
been found in the energy range  $E_{\gamma} \sim 20.0$  MeV as compared to the  
adjoining energies. For example, at  $E_{\gamma} = 17.5 - 19.5$  MeV  $\bar{E}^*(^{59}\text{Co})$   
 $\sim 1.0$  MeV;  $E_{\gamma} = 19.5 - 22.0$  MeV  $\sim 4.0$  MeV,  $E_{\gamma} = 22.0 - 25.0$  MeV  
 $\sim 5.0$  MeV. The share of photoproton reaction in the total photo-  
absorption cross section also increases abruptly in the energy  
range  $E_{\gamma} \sim 20.0$  MeV. Similar events has been found out for the  
 $^{58}\text{Ni}$  isotope at energies  $\sim 18$  and  $\sim 24$  MeV. It has been est-  
ablished that in case of decay of  $^{58}\text{Ni}$  and  $^{60}\text{Ni}$  nucleus level  
with equal energy  $\bar{E}^*(^{57}\text{Co})$  proves to be 2-3 MeV in excess  
of  $\bar{E}^*(^{59}\text{Co})$ . It has been shown that these events may be due  
to the shell effects during the decay of analog states of  $^{58}\text{Ni}$   
and  $^{60}\text{Ni}$  nuclei associated with certain configuration of these  
states. The difference in  $\bar{E}^*(^{57}\text{Co})$  and  $\bar{E}^*(^{59}\text{Co})$  is interpreted  
as a consequence of the greater share of  $T_{-}$  -states in the  
dipole wave function in case of  $^{58}\text{Ni}$  ( $\sim 0.8$  according to<sup>2</sup>) than  
in case of  $^{60}\text{Ni}$  ( $\sim 0.36$ ).

1. B.S. Ishkhanov, et al. Sov. Nucl. Phys. 11(1970)485

2. B. Gouliard, S. Fallieros. Can. J. Phys. 45(1967)3221.

**EXCITED STATES OF VIRTUAL CLUSTERS IN NUCLEUS  
AND QUASIELASTIC KNOCK-OUT OF CLUSTERS AT  
HIGH ENERGIES**

N.F. Golovanova, L.M. B'rn, V.G. Neudatchin, Yu.F. Smirnov,  
Yu. M. Tshuvifsky

Institute of Nuclear Physics, Moscow State University  
Moscow 117234, USSR .

Quasi-elastic knock-out of nucleon clusters from nuclei by an incident high-energy hadron is considered in the Glauber-Sitenko multiple scattering theory. An important contribution to the cross section of the process is shown to be made not only by the hadron elastic scattering on a non-excited virtual cluster but also by collisions with an excited virtual cluster, accompanied by de-excitation of this cluster. This demands the usual theory of quasi-elastic knock-out of clusters<sup>1</sup> to be changed. Firstly, the angular correlations of knocked-out cluster and scattered hadron are no longer determined by the momentum distribution of a cluster in the nucleus. They are determined by another parameter which can be called the modified momentum distribution  $F(q)$ . Secondly, meaning and values of the effective numbers of clusters  $N^{eff}$  are changed. Thirdly, the characteristics of the processes depend not only on the modulus of momentum  $q$ , which had a cluster in the nucleus, but also on its direction relative to an incident beam. The calculations have been carried out for the  $^{16}O(p,pd)^{14}N$ ,  $^{16}Li(p,pt)^3He$  and  $^{16}O(p,pd)^{12}C$  reactions. It is important that the modified momentum distribution, for instance for  $L = 0^+ \rightarrow 2^+$  transition with the nonzero angular momentum transferred to the nucleus in case of the first reaction no longer vanishes at  $q=0$  in contrast to previous theory, owing to contribution of the internal excited 2D-state of the virtual deuteron cluster. The extent to which  $N^{eff}$  changes is clear from the last reaction, where  $N^{eff}(L) = 0.75; 3.02; 3.27$  for transitions to the  $^{12}C$  nucleus lowest levels  $L = 0^+, 2^+, 4^+$  respectively. In the usual version of the theory  $N^{eff}(L) = 0.30; 1.43; 2.57$ .

V.V. Balashov, A.N. Boyarkina, J. Reiser Nucl.Phys.52,417(1964)

**EFFECTIVE HAMILTONIAN AND ANGULAR  
CORRELATIONS IN RADIATIVE PION CAPTURE**

G. Ya. Korenman and V.F. Popov

Institute of Nuclear Physics, Moscow State University  
Moscow 117234, USSR

We have investigated the influence of the effective Hamiltonian of the radiative pion capture on the following characteristics: (I) the function of angular correlation between the primary and secondary (nuclear)  $\gamma$ -quanta  $W_{\gamma\gamma}(\theta) = 1 + A_2 P_2(\cos \theta) + \dots$ ; (II) angular distribution  $W(\theta) = 1 + B_2 T_{20} P_2(\cos \theta)$  and linear polarization  $\Pi(\theta) = C_2 T_{20} \sin^2 \theta / W(\theta)$  of the primary  $\gamma$ -quanta assuming an alignment of the orbital momentum of the pion before capture. (According to the estimates<sup>1</sup> the alignment of the pion p-state  $T_{20}$  may be equal to 0.5). Some results of our calculations for the pion capture from p-orbits in  $^{12}\text{C}$  to the bound states of  $^{12}\text{B}$  are given below. Our values for the effective Hamiltonian constants (variants I, II and IV) are taken from table 8, ref.<sup>2</sup>. Nuclear matrix elements were calculated in the generalized Helium-model<sup>3</sup>.

	Transition	I	II	IV
$A_2$	$0^+ \rightarrow 1^+ \rightarrow 1^+$	+ 0.05	0.18	0.19
$B_2$	$0^+ \rightarrow 1^+$	-0.12	-0.01	-1.0
	$0^+ \rightarrow 1^-$	-0.41	-0.14	-0.12
$C_2$	$0^+ \rightarrow 1^+$	-0.44	-0.50	-0.01
	$0^+ \rightarrow 1^-$	0.30	0.43	0.44

1. G. Ya. Korenman, *Yadernaya Fizika*, **21**, No. 4 (1975)

2. G. Ya. Korenman and R. A. Eramshyan, Proc. of 8th Winter School LIYAF, part II, p. 402. Leningrad, 1973.

3. H. Uberall et al. *Phys. Rev.*, **C6**, 1911, 1972.



**TO THE THEORY OF QUASIELASTIC KNOCK-OUT OF  
NUCLEAR CLUSTERS**

V. V. Balashov and V.N. Mileev

Institute of Nuclear Physics, Moscow State University,  
Moscow 117234, USSR.

A new approach <sup>[1,2]</sup> to the consideration of the quasielastic knock-out of complex particles from nuclei based on the microscopic description of interaction of incident particles with nuclei induces one to revise the conventional ideas about the relationship between these processes and the effects of nucleon clustering in nuclei. The conception of the effective numbers of nucleon clusters in nuclei as structural characteristics of nuclei is insufficient for the description of these reactions. In these reactions an important and often dominant part is played by the mechanisms of cluster-formation in the very process of interaction between an incident particle and a nucleon group in nuclei, in which quantum numbers of internal motion of this group are changed. The contribution of these mechanisms depends on both structural peculiarities of nuclei and kind of incident particles, their energy, detection angles of scattered and knocked-out particles. A specific coherent (cumulative) effect of cluster-formation in the reactions ( $\phi, pd$ ), ( $p, p\alpha$ ) etc., as a result of subsequent collisions of an incident hadron with all nucleons of the corresponding group is of particular interest.

The paper presents results of calculations for the reactions of quasielastic knock-out of complex particles by electrons, protons and  $\pi$ -mesons for a number of nuclei.

1. V.V. Balashov and V.N. Mileev, All-Union Conf. "Nuclear Reactions at High Energies", Abstracts of contributions, p.20, Tbilisi, 1972.
2. V.V. Balashov and V.N. Mileev, Nucl.Phys. (to be published).

**TWO-STEP MECHANISM OF THE NUCLEAR  
EXCITATION IN COHERENT PARTICLE PRODUCTION**

V.V. Balashov, V.L. Korotkiĭ and V.N. Milleev

Institute of Nuclear Physics, Moscow State University  
Moscow 117234, USSR

In work<sup>1</sup> a mechanism of collective nuclear level excitation in coherent particle production (e.g.  $\pi \rightarrow 3\pi$ ) was suggested. The mechanisms of excitation of the same levels in the processes  $(\pi, \pi')$  and  $(\pi, 3\pi)$  were shown to differ. If in inelastic scattering the dominating one-step mechanism of nuclear excitation is accompanied by strong absorption of the incident and outgoing particles in nuclear matter, another mechanism is added in the coherent production. The characteristic feature of this two-step mechanism is that no excitation of the nucleus occurs during the act of particle production; the nucleus is excited either before or after the act of coherent production as a result of inelastic scattering of the incident or produced particle from the nucleus. Interference of the two mechanisms allows one to explain naturally the considerable difference between the angular distributions observed in the reactions  $^{12}\text{C}(\pi, \pi')$ ,  $^{12}\text{C}(2^+, 0)$  and  $^{12}\text{C}(\pi, 3\pi)$  ( $^{12}\text{C}(2^+, 0)$ ). The present paper intercompares our calculations of reactions  $(\pi, \pi')$  and  $(\pi, 3\pi)$  for a number of nuclei, from  $^{12}\text{C}$  to  $^{208}\text{Pb}$ . The relation between one- and two-step mechanisms is studied depending on the transition multipolarity, effective mass of produced system and atomic weight of nucleus. Experimental data on the  $(\pi, \pi'\gamma)$  and  $(\pi, 3\pi\gamma)$  reactions have been obtained with the coincidence technique. In connection, the analysis of spin density matrix and angular correlation function in the reactions  $(\pi, \pi'\gamma)$  and  $(\pi, 3\pi\gamma)$  are presented.

V.V. Balashov, V.L. Korotkiĭ and V.N. Milleev, *Phys. Lett.*

49B (1974)120

**PROPAGATION OF UNSTABLE HADRONIC SYSTEM  
THROUGH NUCLEAR MATTER IN COHERENT PRODUCTION  
PROCESSES**

V.L. Kerzhikh

Institute of Nuclear Physics, Moscow State University  
Moscow, USSR.

Propagation of compound hadron (D-system<sup>1,2</sup>) through nucleus is studied depending on the nature of interaction between hadron components. Example is considered when the states of two particles forming an hadron are described by a set of oscillator wave functions. The shape of a peak at  $m = m'$  which appears in the amplitude of D-system transitions ( $m \rightarrow m'$ ) in scattering by nucleons in a nucleus is essentially different from that in<sup>2</sup>. The calculated transitions amplitude is close to the approximation by the Gaussian dependence which have formally been used by Van Hove<sup>1</sup>. So, we have the same physical consequences as in the Van Hove model<sup>1</sup>, but, besides that, we can trace what is the dependence of the nuclear transparency on the properties of hadron produced.

For large values of  $\tau_0$  ( $\tau_0 \gg R$ ,  $R$  is the nuclear radius,  $\tau_0$  is the oscillator parameter) D-system is strongly absorbed in nucleus. In this case we have a narrow width of the amplitude peak. On the contrary, for small  $\tau_0$  ( $\tau_0 \ll R$ ) the compound hadron is weakly absorbed. This fact provides us with a possibility, in principle, to understand the various nuclear transparencies<sup>3</sup> for hadron produced in nuclei at high energies.

1. L. Van Hove, *Nucl. Phys.* **B46**(1972)75.

2. K. Góllfried, *Acta Phys. Polon.* **B3**(1972)769.

3. G. Balloni, *Proc. of the 2nd Topical meeting on HEC involving nuclei*, Trieste, 1974.

Institute for Theoretical and Experimental Physics.

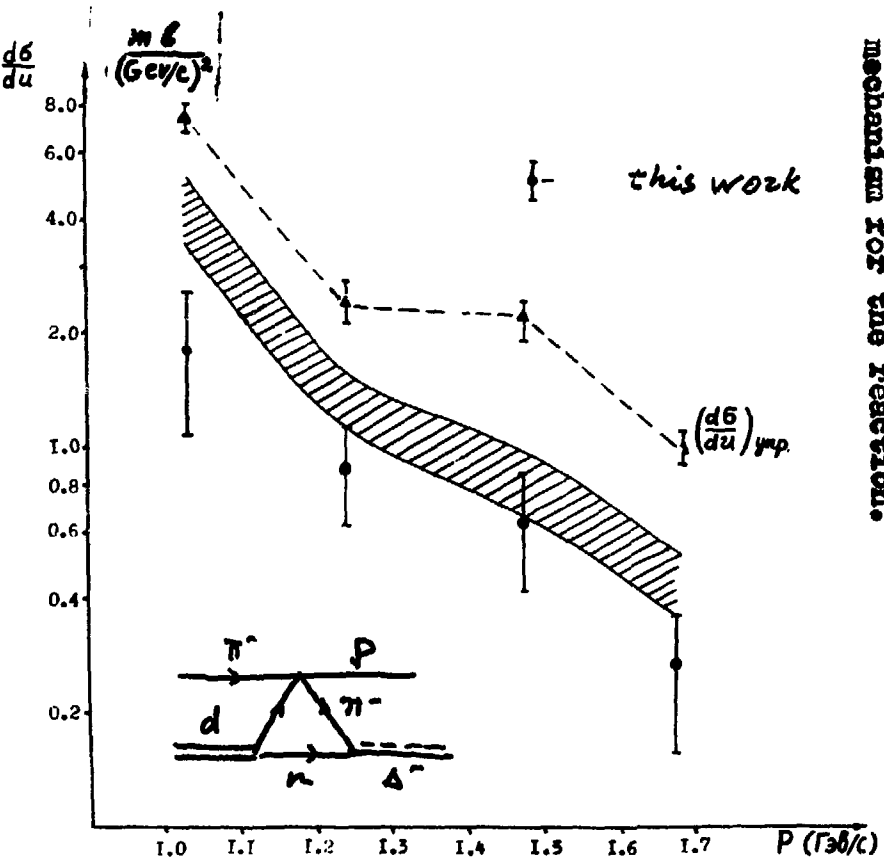
Moscow 1975.

B.M. Abramov, I.A. Dikhnovsky, V.S. Redoretz, V.V. Zishkurin,  
A.P. Krutenkova, V.V. Kulikov, I.A. Radkevich.

**Study of the isobar ( $\Delta(1236)$ ) production in the reaction  
 $\pi^- + d \rightarrow p + \Delta^-$  ( $\Delta^-$  - backward) from 1.03 to 1.68 GeV/c.**

**ABSTRACT.**

Differential cross section of backward  $\Delta^-$  ( $\Delta(1236)$ ) production in the reaction  $\pi^- + d \rightarrow p + \Delta^-$  at four incident momenta from 1.03 to 1.68 GeV/c is measured. The measured values are in good agreement with the calculations based on the triangle mechanism for the reaction.



The incident momentum dependence of isobar production differential cross section. Region of points calculated on the basis of the triangle mechanism for the reaction is shaded.  $\blacktriangle$  =  $\pi^-p$  backward elastic differential cross section integrated over the angular acceptance of the spectrometer. The curves are drawn by hand.

Institute for Theoretical and Experimental Physics.

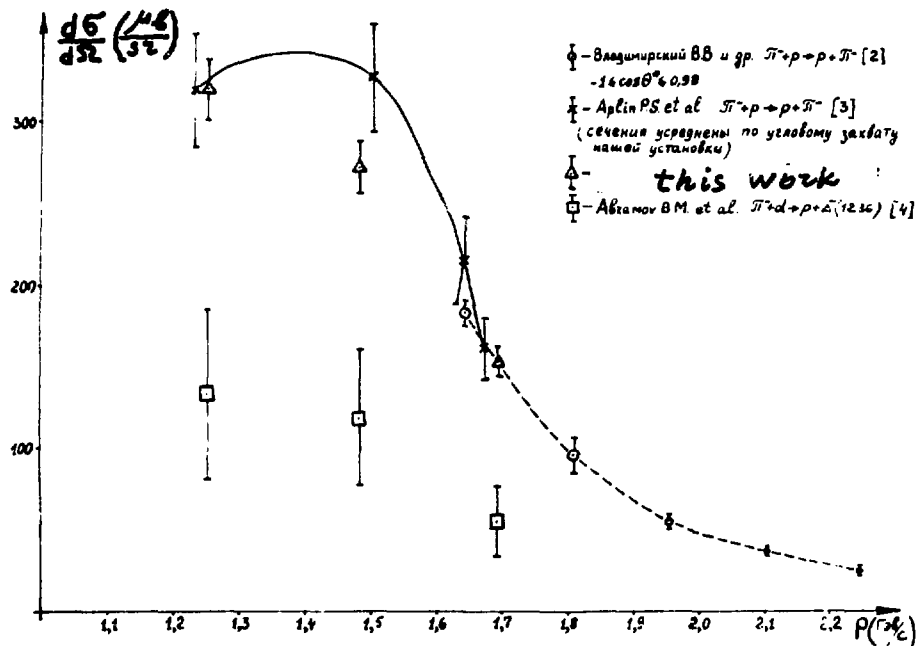
Moscow 1975.

B.M. Abranov, I.A. Dukhovskoy, V.S. Fedoretz, A.P. Krutenkova,  
V.V. Kulikov, I.A. Radkevich, V.V. Kishkurno

" Study of the reaction  $\pi^- + d \rightarrow p + \pi^- + n$  with large momentum transfer in incident momenta interval from 1,25 to 2,64 Gev/c."

ABSTRACT.

Differential cross section (DCS) for the reaction  $\pi^- + d \rightarrow p + \pi^- + n$  at c.m.s. angle nearby 180 in momenta interval from 1,25 to 2,64 Gev/c is measured. The measured values of DCS are found to be equal within statistical accuracy to DCS for  $\pi^- p$  backward elastic scattering at investigated energies.



Incident momentum dependence of  $\pi^- p$  elastic scattering, reaction  $\pi^- + d \rightarrow p + \pi^- + n$  and  $\Delta(1236)$  production differential cross section at large momentum transfer. If curves are drawn by hand.

## 1 GeV PROTON SCATTERING AND NUCLEAR SIZES

G.D. Alkhasov, S.L. Belostotsky, O.A. Domnenkov,  
 Yu.V. Dotsenko, N.P. Kuropatkin, M.A. Schuvaev,  
 and A.A. Vorobyov

Leningrad Institute of Nuclear Physics, Gatchina, USSR

The differential cross-sections of 1 GeV proton elastic scattering by  $^{11}\text{B}$ ,  $^{12,13}\text{C}$ ,  $^{28}\text{Si}$ ,  $^{32,34}\text{S}$ ,  $^{39}\text{K}$ , and  $^{40,48}\text{Ca}$  isotopes have been measured. Using Glauber multiscattering theory and MS fitting procedure, the analysis of the data provided the parameters of the matter distributions represented by fermi-functions. The proton distributions being taken from the electron scattering data, the distributions of the neutrons in the isotopes have been determined. Fig.1 compares the RMS radii of the matter and charge distributions. Fig.2 shows the proton and neutron effective distributions  $\tilde{\rho}(\vec{r})$  which take into account the finite sizes of the nucleons, the difference between neutron distributions in  $^{40}\text{Ca}$  and  $^{48}\text{Ca}$  isotopes being emphasized:

$$\langle r^2 \rangle_{m,p}^{1/2} - \langle r^2 \rangle_{n40}^{1/2} = (0.14 \pm 0.02) \text{ fm.}$$

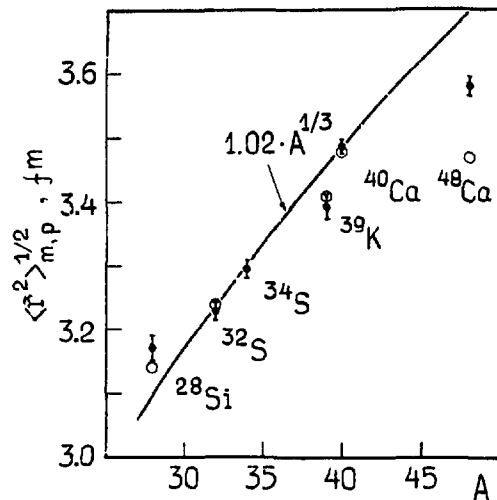


Fig.1. Nuclear sizes.  
 $\square$  - Matter RMS radii.  
 $\circ$  - charge RMS radii.

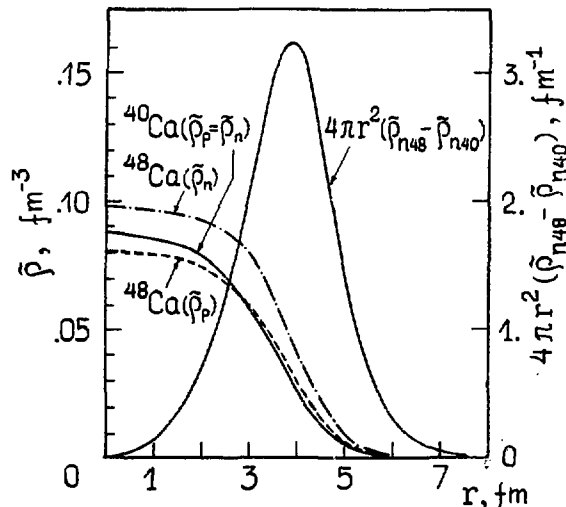


Fig.2. Distribution of the protons and neutrons in  $^{40,48}\text{Ca}$  isotopes.

**FRAGMENTS PRODUCTION IN THE INTERACTION OF 1.0 GeV PROTONS  
WITH MEDIUM AND HEAVY WEIGHT NUCLEI**

B.N.Volnii, A.A.Vorobyov and D.M.Seleverstev

Leningrad Institute of Nuclear Physics, Gatchina, USSR

The energy spectra of the fragments produced in the interaction of 1.0 GeV protons with Ti,  $^{58}\text{Ni}$ ,  $^{64}\text{Ni}$ ,  $^{112}\text{Sn}$ ,  $^{124}\text{Sn}$ , Ag, Au, and U targets have been measured at two laboratory angles -  $\theta = 60^\circ$  and  $\theta = 120^\circ$ . The isotopes of the elements from He to C were identified using a combination of the magnetic analysis and the  $\Delta E-E$  method. The yields of different isotopes and angular anisotropy parameters (P/B) have been determined.

The yields, being normalized to  $6_{\text{sec.}}$ , were found to be independent on the mass number of the target nuclei with similar values of the N/Z ratio. The  $A^{2/3}$  dependence is observed only for the yields of  $^4\text{He}$  particles. The energy spectra were analysed using the equilibrium evaporation model. The effective Coulomb barriers evaluated from this analysis proved to be  $(0.5 \pm 0.6)V_0$  for Sn and Ag targets and  $(0.7 \pm 0.8)V_0$  for Au and U, here  $V_0$  is the nominal Coulomb barrier. The nuclear temperatures were found to be about 8.5 MeV in most of the cases. However, it was only about 4 MeV when  $^4\text{He}$ -particles were emitted while in the case of  $^3\text{He}$  and  $^7\text{Be}$  emission the temperature appeared to be much higher - 11 MeV.

The conclusion is that only  $^4\text{He}$  emission could be satisfactorily explained by the evaporation mechanism while other fragments are formed, presumably, in some nonequilibrium process.

MEASUREMENTS OF  $^{12}\text{C}(\pi^{\pm}, \pi\text{N})^{11}\text{C}$  CROSS-SECTIONS  
IN THE REGION OF (3/2 3/2) RESONANCE

L. N. Batist, V. D. Vitman, V. P. Koptev, M. M. Makarov,  
A. A. Naberezhnov, V. V. Nelyubin, G. M. Obrant, V. V. Sarantsev,  
and G. V. Scherbakov

Leningrad Institute of Nuclear Physics, Gatchina, USSR

Cross-sections of  $^{12}\text{C}(\pi^-, \pi^-n)^{11}\text{C}$  and  $^{12}\text{C}(\pi^+, \pi^+n + \pi^0p)^{11}\text{C}$  reactions and their ratio for 100, 130, 150, 180, 210, 245 and 295 MeV  $\pi^{\pm}$  mesons are measured. Results are compared with calculations in the plane wave impulse approximation (PWIA).

Energy, MeV	Particle	$\sigma$ , mb	$\sigma_-/\sigma_+$
100	$\pi^-$	$41.6 \pm 3.7$	$1.20 \pm 0.08$
	$\pi^+$	$34.6 \pm 2.6$	
130	$\pi^-$	$60.2 \pm 5.0$	$1.40 \pm 0.06$
	$\pi^+$	$42.9 \pm 3.1$	
150	$\pi^-$	$65.5 \pm 4.7$	$1.47 \pm 0.05$
	$\pi^+$	$44.6 \pm 3.2$	
180	$\pi^-$	$71.0 \pm 5.0$	$1.57 \pm 0.05$
	$\pi^+$	$45.3 \pm 3.0$	
210	$\pi^-$	$74.5 \pm 5.5$	$1.74 \pm 0.08$
	$\pi^+$	$42.8 \pm 3.2$	
245	$\pi^-$	$66.5 \pm 4.7$	$1.77 \pm 0.06$
	$\pi^+$	$37.6 \pm 2.7$	
295	$\pi^-$	$52.1 \pm 3.6$	$1.70 \pm 0.04$
	$\pi^+$	$30.7 \pm 2.1$	



NOTE ON THE OPTICAL POTENTIAL FOR PION-NUCLEUS  
SCATTERING IN ( 3,3 ) RESONANCE REGION.

A.V.Stepanov.

The expression for the optical potential is derived for the description of pion-nucleus interaction in (3,3) resonance region. This potential is given in terms of pion-nucleon cross section and dynamical nuclear form factor.

THE INVESTIGATION OF MAGNETIC MOMENTS OF  $^{39}\text{K}$  AND  $^{49}\text{Ti}$  NUCLEI  
IN ELASTIC ELECTRON SCATTERING

V.P.Likhachev, N.G.Afanas'ev, A.A.Nemashkalo, G.A.Savitskiy  
and V.M.Khvastunov

The Kharkov Physical Technical Institute, Kharkov, USSR

A valuable information on nuclear magnetic moments can be obtained from data on magnetic scattering in the limited region of  $q$  or even from several  $q$  values [1,2]. In this paper we investigated the magnetic elastic electron scattering from  $^{39}\text{K}$  and  $^{49}\text{Ti}$  nuclei in the region of the second diffraction minimum of the monopole elastic cross-section. The experiments were performed at incident electron energies up to 300 Mev with the Kharkov LU-300 electron linac. The experimental installation was described in ref. [3]. Three spectra were measured for each value of the momentum transfer at different incident energies and scattering angles. Making a plot of the total formfactor against  $\frac{1}{2} + \text{tg}^2 \frac{\theta}{2}$  we could separate electric and magnetic contributions. The obtained magnetic formfactors were compared with single particle model calculations. The following magnetic moment values were obtained:

$$\mu_3(^{39}\text{K}) = (0.49 \pm 0.05) \text{ nm} \cdot \text{r}^2 ; \quad \mu_7(^{49}\text{Ti}) = (740 \pm 150) \text{ nm} \cdot \text{r}^6$$

R E F E R E N C E S

1. G.C.Li, I.Sick, J.D.Walecka and G.E.Walker, Phys.Lett. 32B, 317, 1970;
2. L.Lapikas, A.E.L.Dieperink and G.Bex, Nucl.Phys.A203, 609, 1973;
3. N.G.Afanas'ev et al, Yad.Fiz. 5, 318, 1967.

PROTON ENERGY DEPENDENCE OF THE  $(e, e'p)$  REACTION  
 CROSS SECTION FOR  ${}^2\text{H}$ ,  ${}^4\text{He}$  AND  ${}^6\text{Li}$  NUCLEI

Yu.P.Antoufiev, V.L.Agranovich, S.V.Dementiy,  
 V.S.Kuzmenko, V.I.Ogurtsov and P.V.Sorokin

(The Kharkov Physical Technical Institute, Kharkov, USSR)

A dependence of  $(e, e'p)$  reaction cross sections on the knocked out proton energy  $T_p$  was investigated to determine the role of the final state interaction (FSI). The experiments were performed at the Kharkov electron linac at incident electron energies of 800 and 1200 MeV for  $T_p = 35, 45, 56, 75, 82, 106, 125$  and 155 MeV. The apparatus was as that in the work [1]. The momentum of a recoil nucleus  $A-1$  was chosen to be  $p_N = 50$  MeV. The results of the experiments have shown that ratios of the measured cross sections to those calculated in the PWIA increase at  $T_p < 80$  MeV, being almost constant at  $T_p > 80$  MeV.

Our data for  ${}^2\text{H}$  agree with those in the  ${}^2\text{H}(p, 2p)n$  reaction [2] and the FSI calculations. The ratio dependences on  $T_p$  for  ${}^4\text{He}$  and  ${}^6\text{Li}$  are qualitatively the same.

#### References

1. Yu.P.Antoufiev et al. *Pis'ma v Zhurn. Exp. i Teor. Fiz.*, 20, 501 (1973).
2. R.D.Haraz and T.K.Lim. *Phys. Rev. Lett.*, 31, 1263 (1973).

TOTAL HADRONIC PHOTOABSORPTION CROSS-SECTIONS OF NUCLEI  
FOR PHOTONS WITH ENERGIES 150-500 MeV

V.G.Vlasenko, V.A.Goldstein, A.V.Mitrofanova, V.I.Noga,  
Yu.N.Ranyuk, V.I.Startsev, P.V.Sorokin, Yu.N.Telegin .

The Kharkov Physical Technical Institute, Kharkov, U.S.S.R.

Total hadronic photoabsorption cross-sections to the present time are measured only for photons in the energy ranges up to 150 MeV and over 1.5 GeV. We have measured the total cross-sections of a number of nuclei (C,Al,Ni,Mo,W) for photons with energies  $E = 150-500$  MeV. The measurements have been made for the virtual photons by means of the inelastic electron scattering method for the small 4-momentum transfers ( $q^2 = 0.04 - 0.1$  ( $\frac{\text{GeV}}{c}$ )<sup>2</sup>). The scattering angle was  $14^\circ$ , the initial electron energy  $E = 0.8-1.4$  GeV. The elastic and quasielastic radiation tails were subtracted from the inelastic scattering spectrum, the cross-sections in the photon points were determined by the extrapolation procedure. The statistical accuracy of the cross-sections is 10%; the cross-sections have resonant shape. They are by 30-50% higher than the sum of the free nucleon photoproton total cross-sections, that may be explained by the cluster contribution.